Rarefied Granular Gases: Correlations, Asymptotic Expansion and Hydrodynamics

A Thesis
Submitted for the Degree of
Doctor of Philosophy

by

Ramakrishna Rongali

Engineering Mechanics Unit
Jawaharlal Nehru Centre for Advanced Scientific Research
(A Deemed University)
Bangalore – 560 064

FEBRUARY 2018

DECLARATION

I hereby declare that the matter embodied in the thesis entitled "**Rarefied Granular Gases: Correlations, Asymptotic Expansion and Hydrodynamics**" is the result of investigations carried out by me at the Engineering Mechanics Unit, Jawaharlal Nehru Centre for Advanced Scientific Research, Bangalore, India under the supervision of **Prof. Meheboob Alam** and that it has not been submitted elsewhere for the award of any degree or diploma.

In keeping with the general practice in reporting scientific observations, due acknowledgment has been made whenever the work described is based on the findings of other investigators.

Ramakrishna Rongali

CERTIFICATE

I hereby certify that the matter embodied in this thesis entitled "**Rarefied Granular Gases: Correlations, Asymptotic Expansion and Hydrodynamics**" has been carried out by **Mr. Ramakrishna Rongali** at the Engineering Mechanics Unit, Jawaharlal Nehru Centre for Advanced Scientific Research, Bangalore, India under my supervision and that it has not been submitted elsewhere for the award of any degree or diploma.

Prof. Meheboob Alam
(Research Supervisor)

Acknowledgements

First, I would like to thank my Ph.D Supervisor, Prof. Meheboob Alam for his guidance and support. Without his guidance and help, this thesis would not have been a reality. His dedication towards research is a quality that I hope to emulate in my research life.

I thank all the faculty members of Engineering Mechanics Unit (EMU) (Prof. Roddam Narasimha, Prof. K. R. Sreenivas, Prof. S. Ansumali and Prof. Ganesh Subramanian) and Prof. Rama Govindarajan, for their courses. I would like to thank Prof. G. Rangarajan and Prof. Thirupathi Gudi for their ODE and PDE courses, respectively.

I especially thank, Wolfram Mathematica (a mathematical symbolic computation program) for my calculations in this thesis.

I would like to sincerely thank Dr. M. H. L. N. Reddy for helping me in writing chapters 3 and 4 of this thesis.

I am grateful to my senior, my friend and my well-wisher Sri. V. K. Naidu Rongali for his encouragement towards my higher education and for teaching SSC and Intermediate Maths.

I thank my fellow labmates: Dr. Nandu Gopan, Dr. M. H. L. N. Reddy, Sunil V Bhardwaj, Saikat Saha, Achal Mahajan, Ronak Gupta, Aghor Pratik, Prashanth, Albin, Tanumoy and all other EMUites for their advice, help and the friendly working environment in the department. I would like to express my sincere thanks to my senior labmates: Dr. Priyanka Shukla, Dr. Ujjayan Paul, Dr. Vinay Kumar Gupta and Dr. Ansari.

I thank my JNC friends (especially, cricket friends): Dr. Udumula Subba Reddy, Y. Sridhar, Dr. Yugandhar, Dr. Suresh, Dr. Nagarjun, Dr. Venky (Vancomycin), Dr. Diwakar, Dr. Murthy, Dr. Lingampally Srinivas, Dr. Pramoda, Dr. Avinash, Prem, Dhiraj, Dr. Jiaul, Dr. Umesh, Dr. Ramana Reddy, Saraiah, Deena Dayal, Dr. Gopal, Dr. Shiva Prasad, Kanwar Nain Singh, Deepthi, Ryan, Rashmi, Siddharth, Shahajhan and Arijit.

I would like to thank Dr. H. Dattu, Dr. B. Bhaskar Rao, Dr. V. Ramakrishna Reddy and Dr. N. Srinivasa Rao for their support.

I thank JNCASR and UGC for providing me the scholarship and I also thank the administration and other support staff of JNCASR for their support.

I am ever grateful to my institute, **Jawaharlal Nehru Centre for Advanced Scientific Research (JNCASR)** for providing the necessary infrastructure and financial support.

Finally, I take this opportunity to express my gratitude to my beloved parents, my sister and Almighty for their unconditional love and support.

My sincere apologies if I have forgotten to name someone (or something).

Abstract

This thesis deals with kinetic-theory analyses of "rarefied" molecular and granular gases based on Boltzmann's equation. A brief introduction about the relevance of granular materials in three possible states (gas, liquid and solid) of matter as well as related theoretical issues about rarefied gases is given in Chapter 1; the remaining thesis consists of four chapters (2, 3, 4 and 5). In each chapter, the Boltzmann equation is analysed via perturbation method to probe correlation and various rarefaction effects in molecular and granular gases.

Chapter 2 is devoted to investigate the homogeneous cooling state (HCS) of a rough granular gas by focusing on a special kind of correlation: the "orientational" or "directional" correlation between the direction of the angular velocity ($\boldsymbol{\omega}$) of a granular particle and the direction of its translational velocity ($\mathbf{c}$). The dynamical equations are derived using pseudo-Liouville operator technique, with an approximate form of the single-particle distribution function that incorporates angular correlations. To assess the effects of higher-order angular corrections, both quadratic- and quartic-order terms (in translational and rotational velocities of particles) are retained in the perturbation expansion of distribution function. It is shown that higher-order corrections can markedly affect steady-state orientational correlation when the normal restitution coefficient is moderate or small and this effect is more prominent for nearly smooth particles. The building-up of correlations during transient stage seems to be closely tied to the evolution of the ratio between the rotational and translational temperatures.

In Chapter 3, the gravity-driven Poiseuille flow of hard spheres flowing through a channel is analysed using a perturbation expansion of the velocity distribution function in powers of the strength of gravitational acceleration (the Froude number $\mathrm{Fr}_0 = g\lambda/v_{th}^2$, where λ is the mean-free path and v_{th} is the thermal velocity, both evaluated at the center of the channel) by retaining terms up to tenth-order in Fr_0. The resulting solution holds around the channel centerline since the wall-effects are not considered in the present analysis. A BGK kinetic model is adopted and the related problem for Maxwell-molecules was originally analysed by Tij & Santos (1994) by retaining terms up to sixth-order in Froude number. The present high-order expansion (for both hard spheres and Maxwell molecules) helped to assess the asymptotic nature of the perturbation expansion and the related convergence issues for the resulting hydrodynamic and rheological (stress tensor and heat flux) fields for which analytical expressions have been derived. Rarefaction effects (e.g. the bimodal shape of the temperature profile, tangential heat flux, normal stress differences, etc) are analysed using presently obtained high-order series solutions. In addition, the Shanks transformation and the Padé approximations have been used to analyse the convergence of series expansion. The present analysis indicates that the "diagonal" Padé approximation of the 10th-order solution yields accurate/converged solution for a large range of Froude number. These overall findings hold for both hard spheres and Maxwell molecules for

the present problem of gravity-driven Poiseuille flow of molecular gases.

In Chapter 4, the effect of inelastic dissipation on the gravity-driven flow of a "heated" granular gas (dubbed "granular Poiseuille flow") is studied using the same perturbation expansion of the velocity distribution function. Again a BGK-type kinetic model with heating via white-noise (that compensates for collisional cooling due to inelasticity) is employed. The complexity of the problem allowed us to determine solutions only up to fourth-order in Fr_0; the related second-order solution has been obtained previously by Tij & Santos (2004). The present fourth-order solutions are used to analyse the behaviour of (i) temperature bimodality ($\triangle T$), (ii) normal stress differences and (iii) heat fluxes as functions of the restitution coefficient (e_n) and the Froude number Fr_0. It is shown that $\triangle T$ increases with increasing dissipation at $\mathrm{Fr}_0 = 5\times10^{-3}$; for small enough values of Fr_0 ($< 4\times10^{-3}$), however, a 'non-monotonic' behaviour of $\triangle T$ with e_n [i.e. $\triangle T$ decreases with decreasing e_n for $e_n \in (1, 0.5)$, but increases for $e_n < 0.5$] is recovered. A phase-diagram is constructed in the $(\mathrm{Fr}_0, 1-e_n)$-plane that demarcates two regions by identifying a critical Froude number $\mathrm{Fr}^c \equiv \mathrm{Fr}(e_n)$, above and below which the dependence of $\triangle T$ on e_n is monotonic and non-monotonic, respectively. Similarly, the first normal-stress difference (positive $\mathcal{N}_1$) increases with increasing dissipation and the second normal-stress difference (negative $\mathcal{N}_2$) decreases with increasing dissipation at $\mathrm{Fr}_0 > \mathrm{Fr}_0^c$; the non-monotonic behaviour (similar to that of $\triangle T$) is seen at $\mathrm{Fr}_0 < \mathrm{Fr}_0^c$. Overall, it is concluded that the inelastic dissipation plays a "dual" role of decreasing (at $\mathrm{Fr}_0 < \mathrm{Fr}_0^c$) and increasing (at $\mathrm{Fr}_0 > \mathrm{Fr}_0^c$) the values of $\triangle T$, $\mathcal{N}_1$, $\mathcal{N}_2$ and tangential heat flux q_x with decreasing restitution coefficient e_n from the elastic limit. The results on temperature bimodality are compared qualitatively with recent MD simulations (Alam *et al.* 2015) and DSMC simulations (Gupta & Alam 2017) on gravity-driven granular Poiseuille flow, and the underlying differences are examined.

In Chapter 5, the derivation of 2×14-moment equations for a dilute binary granular mixture is outlined for the first time – such higher-order moment equations are deemed to be appropriate for rarefied molecular gases beyond the Navier-Stokes regime of Knudsen number ($\mathrm{Kn} > 0.01$). Instead of using the approximate kinetic models as in Chapters 3 and 4, the Boltzmann equation for a binary mixture with exact collision term is employed in this chapter to derive the extended hydrodynamic equations. The non-equilibrium distribution function in terms of 14 hydrodynamic fields is obtained following the well-known Hermite expansion around the species Maxwellian. To close the hydrodynamic equations, all source/production terms have been calculated as functions of (i) the restitution coefficient ($e_{\alpha\beta}$), (ii) the mass and size ratios of two species and (iii) the number fraction of each species. In the mono-disperse limit, the calculated source terms agree with previous work (Kremer & Marques Jr 2011). The application of the resulting of hydrodynamic equations to analyse the homogeneous cooling state of binary granular mixtures is briefly discussed in the end.

Finally, the conclusions are drawn in Chapter 6 with an overall summary and outlook of the thesis.

List of Figures

List of Tables

Contents

Chapter 1

Introduction

Granular materials are conglomerations of discrete macroscopic particles, which are ubiquitous in our daily lives, whose size can vary from 1 mm to meters to kilometres. They play an important role in applications as diverse as agriculture, mining, civil engineering, chemical, energy production, semiconductor industries, waste recycling industries and pharmaceutical manufacturing. Examples of common granular materials include sands, gravels, ores, soils, seeds, powders, food grains, fertilizers, cement, coal, capsules and pills, ice bergs, asteroids, planetary rings, and sand dunes, etc.

Granular materials show many interesting phenomena like clustering (Kudrolli *et al.* 1997), jamming (Corwin *et al.* 2005), arching phenomena (Hsiau *et al.* 1998), mixing and segregation (Ottino & Khakhar 2000), pattern formation such as sand ripples and dunes (Aranson & Tsimring (2006), Araújo *et al.* (2013)), etc. In spite of their incredible significance and applications, the mechanics of granular materials is not well understood at present. However, some notable progress has been made during last couple of decades.

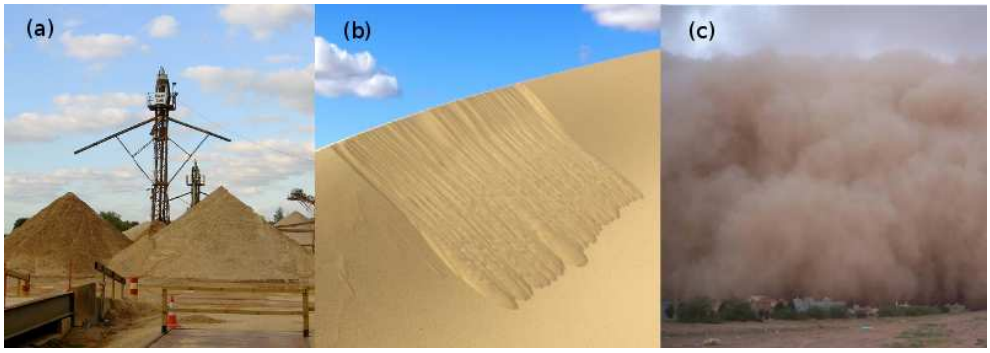

Figure 1.1: Different states of granular materials: (a) like a solid (heap of sand), (b) like a liquid (flow of sand), and (c) like a gas (dust storm). Images are taken from: http://cs.au.dk/ adc/index.php?s=dem.

Granular materials can behave like a solid, liquid, or gas [Jaeger *et al.* (1996); Campbell (1990); Goldhirsch (2003); Forterre & Pouliquen (2008); Pöschel & Luding (2001); Brilliantov & Pöschel (2004); Rao & Nott (2008)]. Fig. 1.1(a) shows sand at rest that behaves like a solid; the sand heaps are unmoving and static despite the fact that they have surface inclines and the gravitational pull attempts to turn the heap into a flat layer. Fig. 1.1(b) shows when the surface inclines exceed the angle of repose, the grains form an avalanche and flow downwards, much like a liquid. Fig. 1.1(c) shows a gaseous state when the individual grains are moving at high velocities, like inside the dust storm; the grains are interacting by inelastic collisions, much different than the interactions in molecular gases. More details can be found in the review articles cited above.

Different flow regimes can also live together in a single set up, as illustrated by the flow of beads on a pile in Fig. 1.2. The present thesis deals with the kinetic theory description of a granular gas [Jenkins & Richman (1985); Brey *et al.* (1997*a*); Sela & Goldhirsch (1998); Garzó & Dufty (1999); Brilliantov & Pöschel (2004)], with the gas being made of a collection of "inelastic" hard spheres without any interstitial fluid.

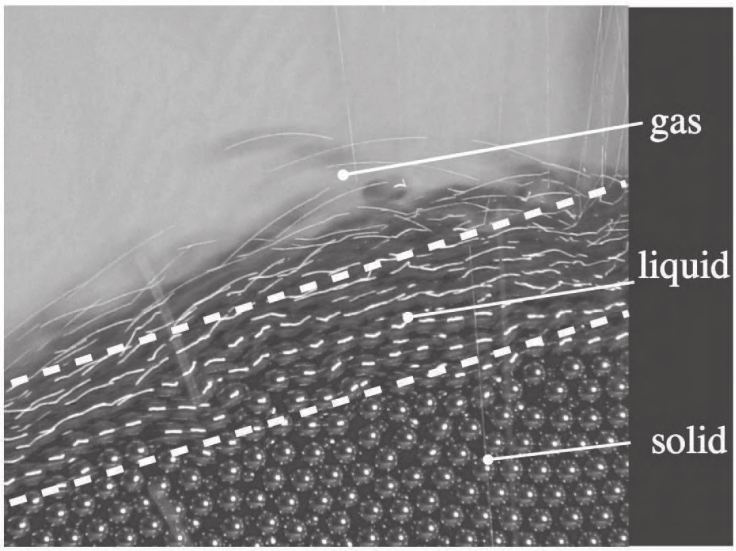

Figure 1.2: Granular materials can exhibit different states of matter in a single configuration. Image is taken from: Andreotti *et al.* (2013).

1.1 Brief Review of Kinetic Theory

One of the main objectives of the kinetic theory is to describe the macroscopic properties of gases like pressure, temperature, thermal conductivity, viscosity, etc. from microscopic quantities that are associated with the molecules which compose the gases like mass, velocity, kinetic energy, internal degrees of freedom and interaction forces between the molecules (Chapman & Cowling (1970), Kremer (2010)).

The central quantity in kinetic theory is the velocity distribution function of the gas (Chapman & Cowling (1970)). The Boltzmann equation is the central equation for the velocity distribution function, which is capable of describing processes in all flow regimes (Cercignani 1975). However, it is complicated to deal with the Boltzmann equation due to the presence of the nonlinear Boltzmann collision operator which accounts for the collisions among the gas molecules. Due to the mathematical structure of this collision operator, the Boltzmann equation becomes a nonlinear integro-differential equation and solving this equation exactly is almost impossible. For more details, one can see textbooks (Cercignani (1975), Brilliantov & Pöschel (2004), Garzó & Santos (2003), Chapman & Cowling (1970), Rao & Nott (2008), Struchtrup (2005)).

To solve the Boltzmann equation "approximately", the kinetic theory offers many "kinetic models" to replace with Boltzmann collision operator which is the main origin of difficulty in dealing with the Boltzmann equation. These kinetic models preserve the main characteristics of the collision term: (1) the conservation of mass, momentum and energy, (2) H-theorem, (3) the

velocity distribution function is a Maxwellian in equilibrium, (4) the Prandtl number (Pr), which is the dimensionless ratio of viscosity and thermal conductivity, is close to 2/3 for a monatomic gas.

One of the well-known kinetic model is Bhatnagar-Gross-Krook (BGK) model (Bhatnagar *et al.* (1954))

$$\left(\frac{\partial f}{\partial t}\right)_{\text{coll}} = -\frac{f - f_0}{\tau}, \tag{1.1}$$

where f, f_0 and τ are the single particle distribution function, the Maxwellian distribution function and relaxation time, respectively. Eq. (1.1) replaces the Boltzmann collision operator in the Boltzmann equation with a single-time relaxation model. The main drawback of BGK model is that does not predict the correct Prandtl number for a monatomic gas. Despite this drawback, the BGK model has been widely used in the literature, since it preserves other basic characteristics of the Boltzmann equation reasonably well. There exist other well-known kinetic models, e.g., (i) ES-BGK model (Ellipsoidal Statistical BGK model) proposed by Holway (1966), where the Maxwellian of the standard BGK model is replaced by an anisotropic Gaussian, (ii) S-model (Shakhov (1968)) proposed by Shakhov, etc., which produce the correct value of the Prandtl number. However, these kinetic models usually display different behaviour from the realistic one and are beyond the scope of this thesis.

For finding the approximate solutions of the Boltzmann equation, we use techniques like (i) *Chapman-Enskog expansion method* (Chapman & Cowling (1970), Ferziger & Kaper (1972), Brilliantov & Pöschel (2004)) and (ii) *Grad's moment method* (Grad (1949*b*), Grad (1958), Müller & Ruggeri (1998)). One can find details of these methods in standard textbooks (Cercignani (1969), Cercignani (1975), Truesdell & Muncaster (1980), Kogan (1969), Gombosi (1994), Struchtrup (2005), Garzó & Santos (2003), Kremer (2010)).

The Chapman-Enskog expansion method (Chapman (1918), Enskog (1917)) is based on an asymptotic expansion in terms of the Knudsen number (the ratio between the mean-free path and the macroscopic length). In this method, the velocity distribution function is expanded in terms of the Knudsen number around the Maxwellian distribution function (equilibrium distribution function). The expansion for the velocity distribution function is substituted into the Boltzmann equation and the coefficients at each order of the Knudsen number are compared on both sides of the equation, which yields (i) the Euler equations at zeroth order, (ii) the Navier-Stokes and Fourier (NSF) equations at the first order, (iii) the Burnett equations at the second order, (iv) the super-Burnett equations at the third order, and so on. The higher-order transport equations (Burnett equations) are known to be linearly unstable (Bobylev (1982), Bobylev (2006)), although there are recent works to address the instability issue (Struchtrup 2005).

In Grad's moment method (Grad 1949*b*), the velocity distribution function is expanded in terms of the orthogonal polynomials (usually Hermite polynomials) in fluctuation velocity with the equilibrium distribution function as a weight function. The unknown coefficients in the expansion are obtained by fulfilling the definition of the moments considered at that level. The moment equations emerging from Grad's moment method are always linearly stable (Bobylev 1982). Unfortunately, Grad's moment method does not tell, a priori, how many moments need to be considered for illustrating a process with a given Knudsen number. Nevertheless, it can be

stated empirically that the number of moments considered need to be increased with increasing Knudsen number (Struchtrup & Torrilhon 2003). Moreover, due to their hyperbolic nature, the renowned Grad's 13-moment equations obtained via Grad's moment method do not admit continuous shocks for flows with Mach numbers above 1.65 (Weiss (1995), Müller & Ruggeri (1998)) and do not capture the Knudsen boundary layers (Struchtrup 2002). However, by considering more moments, the Knudsen layers can be captured (Reitebuch & Weiss (1999), Struchtrup (2002)) and the smooth or continuous shock structure can be attained for high Mach numbers (Weiss 1995).

In order to overcome the shortcomings inherent in both Chapman-Enskog expansion method and Grad's moment method, Struchtrup and Torrilhon (Struchtrup & Torrilhon 2003) introduced a method, dubbed the "regularized" moment method, which regularizes Grad's 13-moment equations by means of a Chapman-Enskog expansion around a pseudo-equilibrium leading to the regularized 13-moment (R13) equations. At first, the method has been developed for Maxwell molecules along with for BGK model (Struchtrup (2005), Struchtrup & Torrilhon (2003)) and extended later to hard-sphere potential (Struchtrup & Torrilhon 2013). The regularized 13-moment equations retain the desirable qualities of both the Chapman-Enskog expansion method and Grad's moment method. The regularized 13-moment equations are linearly stable and lead to smooth shock profiles for all Mach numbers (Struchtrup & Torrilhon 2003).

1.2 Flow Regimes and Rarefaction

In kinetic theory, the key parameter is the Knudsen number (Kn), which characterises the gas rarefaction, defined as the ratio

$$\mathrm{Kn} = \frac{\lambda}{L}, \tag{1.2}$$

where λ is the molecular mean free path, which is the average distance traveled by a molecule between collisions, and L is the characteristic length of the gas flow. Based on Knudsen number (Kn), gas flows can be classified into different flow regimes (Kogan (1969), Bird (1994)) as shown in Fig. 1.3 — this classification is purely empirical.

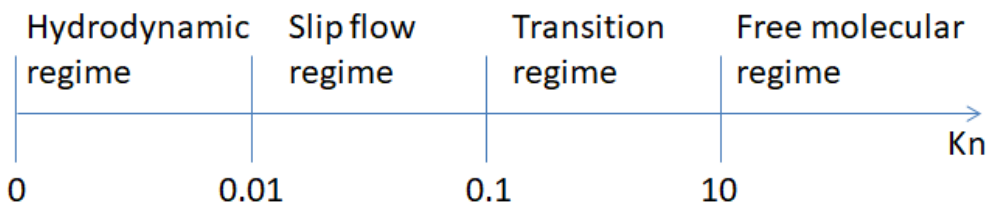

Figure 1.3: Classification of flow regimes based on Knudsen number.

In the hydrodynamic regime $\mathrm{Kn} \leq 0.01$, the continuum hypothesis is valid and the flow is well described by the Navier-Stokes-Fourier (NSF) equations. In the slip flow regime $0.01 < \mathrm{Kn} \leq 0.1$, the non-equilibrium phenomena occur near the boundary; in this regime, the flow may still be described by the NSF equations, however, they must be supplied with appropriate velocity slip (the tangential velocity of the gas near the solid surface is non-zero) and temperature jump

(the temperature of the gas near the surface is not equal to the surface temperature) boundary conditions. Higher-order hydrodynamic equations can be derived from the kinetic theory; Burnett (1936) derived the second-order approximations of stress tensor and heat flux vector from Chapman-Enskog expansion. Grad (Grad 1949*b*) derived the extended hydrodynamic equations from an Hermite expansion for 13 macroscopic quantities – density, velocity, pressure, stress tensor, and heat flux vector, namely, the Grad 13-moment equations (Grad (1949*b*), Struchtrup (2005)). Recently, Struchtrup derived the Regularized 13-moment equations (R13) by means of a Chapman-Enskog expansion around a non-equilibrium state given by Grad's distribution function (Struchtrup & Torrilhon (2003), Struchtrup (2005)).

In the transition regime $0.1 < \mathrm{Kn} \leq 10$ (see Fig. 1.3), the non-equilibrium phenomena become important in the whole system, the NSF equations are deficient for illustrating processes in this regime and a particle based analysis like DSMC (direct simulation Monte Carlo) method (Bird 1994) or the numerical solution of Boltzmann equation, is required for an accurate description of the flow. Further, the transition regime can be subdivided into two parts: (i) $0.1 < \mathrm{Kn} \leq 1$ and (ii) $1 < \mathrm{Kn} \leq 10$. In the former part of this regime ($0.1 < \mathrm{Kn} \leq 1$), processes can still be illustrated macroscopically by considering a larger set of field variables; the direct solutions of the Boltzmann equation or DSMC method are more costly in this regime. The latter part ($1 < \mathrm{Kn} \leq 10$) is occasionally indicated as the kinetic regime in which the non-equilibrium is so strong that it becomes crucial either to solve the Boltzmann equation directly or to use the DSMC method for describing a process, even though both the methods can be computationally costly.

In the free molecular regime $\mathrm{Kn} > 10$, the Boltzmann equation can be simplified due to the absence of collisions between the particles, and the flow is controlled by collisions of particles with walls. MD (Molecular Dynamics) simulations can be used to describe processes in this free molecular regime (Bird 1994).

In terms of the above empirical classification of flow regimes (Fig. 1.3), a gas is said to be *rarefied* when the Knudsen number lies in slip flow and transition regimes, i.e., when the Navier-Stokes-Fourier (NSF) equations start losing their authority. The rarefied gases display several interesting effects, such as (i) velocity slip and temperature jump (Sone *et al.* 1989), (ii) thermal creep (Ohwada *et al.* (1989*b*), Ohwada *et al.* (1989*a*), Sone (1966)), (iii) Knudsen layers (Sone (2002), Sone *et al.* (1989), Struchtrup & Torrilhon (2008)), (iv) thermal stress (Sone (1972), Sone (2002)), (v) heat flux without temperature gradients (Aoki *et al.* (2002), Todd & Evans (1997)), (vi) Knudsen-minimum or Knudsen-paradox effect (Knudsen (1909), Cercignani & Daneri (1963)), (vii) bimodality of the temperature profile (Tij & Santos (1994), Tij & Santos (2004), Mansour *et al.* (1997), Aoki *et al.* (2002)) and (viii) normal stress differences (Alam *et al.* (2015), Gupta & Alam (2017)). These effects are indicated as the non-equilibrium effects and they solely arise from rarefaction. The present thesis is devoted to analyse certain rarefaction effects in both molecular and granular gases.

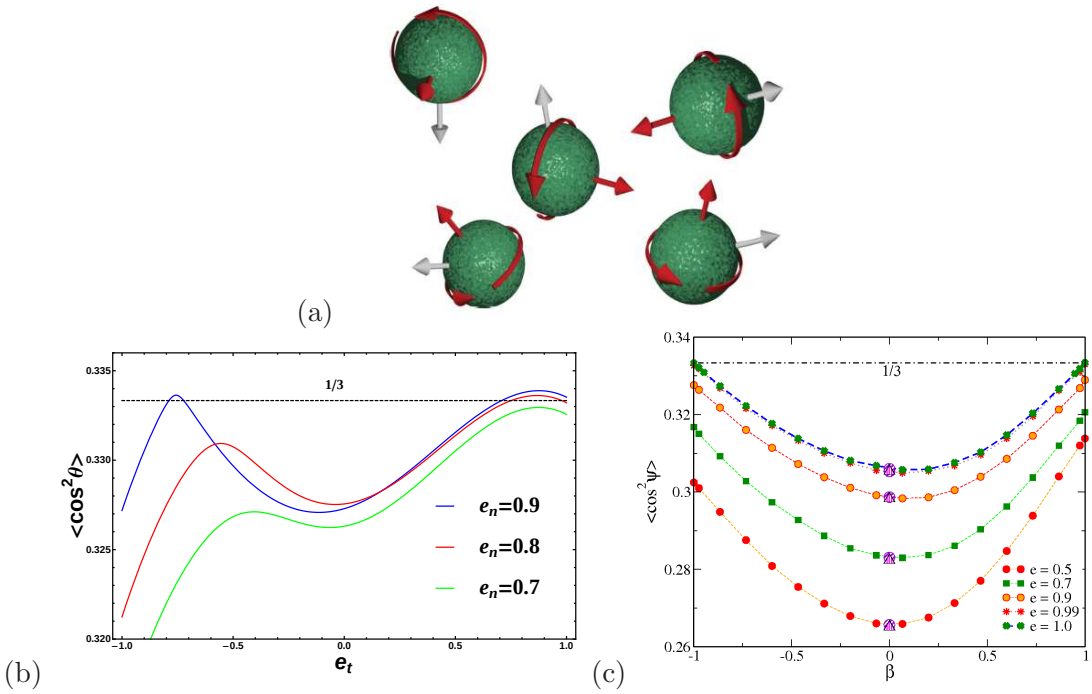

Figure 1.4: (a) Schematic of translation-rotation correlation (Brilliantov *et al.* 2007). Variations of orientaional correlation with tangential restitution coefficient in a granular gas undergoing (b) homogeneous cooling state (HCS) (Rongali & Alam 2014) and (c) uniform shear flow (Gayen & Alam 2008). These issues are discussed in Chapter 2.

1.3 Outline of Present Thesis: Some Issues in Rarefied Granular Gases

In Chapter 2, the homogeneous cooling state (HCS) of a "rough" granular gas is analysed from the pertinent Boltzmann equation, and the primary focus of this chapter is to analyse "translation-rotation" correlation (see Fig. 1.4) and its dependence on various control parameters by considering higher-order terms in perturbation expansion of the distribution fucntion. This work has been published in 'Physical Review E' (2014, vol. 89, art. no. 062201).

In Chapters 3 and 4, the acceleration-driven Poiseuille flow of a rarefied gas is analysed from the perspective of BGK-type collision models. While the Chapter 3 deals with a molecular gas, the Chapter 4 deals with a smooth "granular" gas; the underlying theoretical analysis is motivated from previous works of Tij & Santos (1994) and Tij & Santos (2004) for molecular and granular gases, respectively. In both Chapters the primary focus is to analyse various rarefaction effects [such as (i) bimodal shape of temperature profile (see Fig. 1.5), (ii) normal stress differences and (iii) tangential heat flux] from a high-order perturbation expansion of the distribution function. Another goal of this work is assess the convergence properties of such asymptotic expansions in terms of pertinent control parameters (such as Froude or Knudsen number). The latter issue is considered in detail in the latter part of Chapter 3 for the acceleration-driven Poiseuille flow of a molecular gas using (i) Shank's transformation and (ii) Padé approximation. This analysis helps to estimate the range of validity of the obtained perturbation solutions for (i) hydrodynamic fields (temperature, velcoity and pressure) and (ii) rheological quantities (normal stress differences, heat flux and related transport coefficients) in Poiseuille flow.

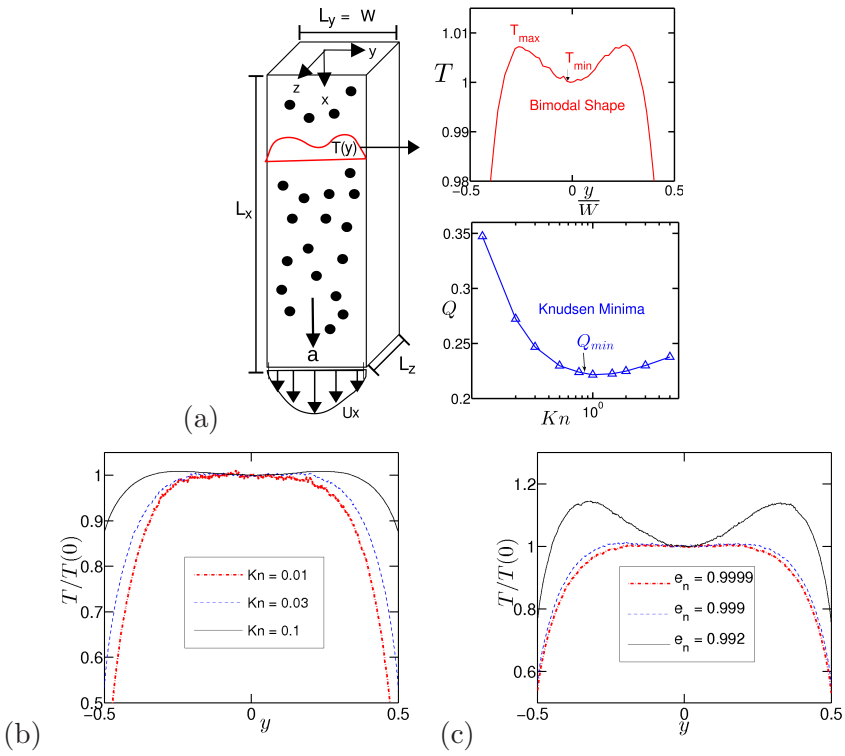

Figure 1.5: (a) Schematic of acceleration-driven Poiseuille flow. (b,c) Rarefaction effect in Poiseuille flow: (b) "Knudsen-driven" temperature bimodality and (c) "dissipation-driven" temperature bimodality; taken from Gupta & Alam (2017). Chapters 3 and 4 deal with acceleration-driven Poiseuille flow of molecular and granular gases, respectively. The right upper panel in (a) shows the bimodal nature of temperature profile, the right lower panel in (a) depicts the well-known "Knudsen-paradox" (i.e. non-monotonic variation of flow rate with Knudsen number).

Lastly, in Chapter 5, the extended hydrodynamic equations (in terms of 2×14 field variables) are derived for a binary granular mixture without any assumption about the collision term of the Boltzamnn equation – these equations are likely to be valid in the rarefied regime of binary mixtures of molecular and granular gases, and thereby complement the efforts in Chapters 2, 3 and 4. In the limit of particles having same size and density, the related 14-moment theory for a monodisperse smooth granular gas along with closed-form expressions for all source/production terms are recovered. As an application of the present theory, the homogeneous cooling state of a binary granular mixture is analysed at the end of this chapter. As a future work, appropriate boundary conditions for extended hydrodynamic fields can be derived which, along with related hydrodynamic equations, can then be used to solve boundary value problems such as acceleration-driven Poiseuille flows in the rarefied regime as suggested in Chapter 6.

Chapters 2 to 5 are largely independent and can be read as illustrated in Fig. 1.6.

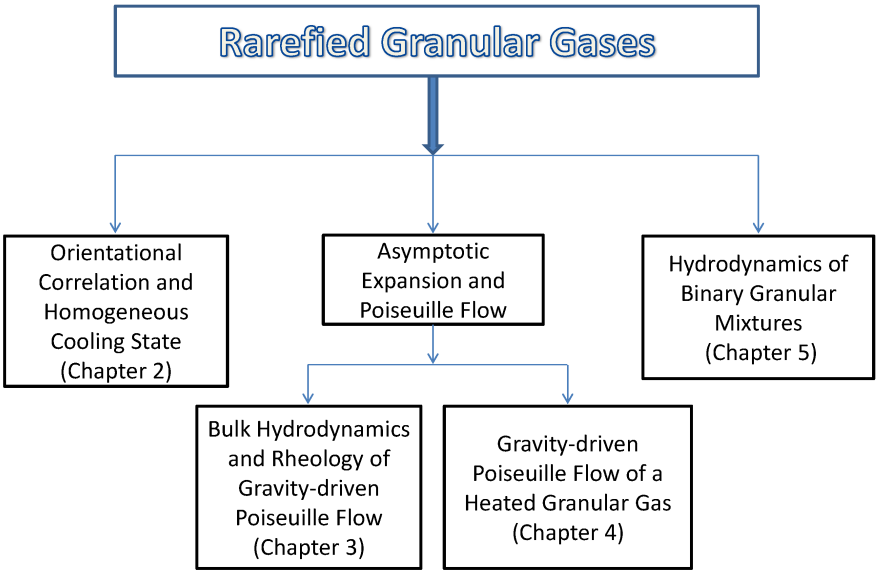

Figure 1.6: Organisation of the Thesis.

Chapter 2

Higher-Order Effects on Orientational Correlation and Relaxation Dynamics in Homogeneous Cooling State of a Rough Granular Gas[†]

2.1 Introduction

Granular materials, a collection of macroscopic particles, are ubiquitous in nature (sand storm, sand dune, avalanche, debris flows, etc.) as well as in chemical processing industries. Under strong forcing, a collection of particles move around randomly, resembling a gas but there is an important difference between a molecular gas and a granular gas [Kadanoff (1999); Goldhirsch (2003); Pöschel & Luding (2001)] since the particle-particle interactions are always dissipative. The simplest granular system is the *homogeneous cooling state* (HCS) [Haff (1983)]: this is a *spatially* homogeneous state since both the number density and the granular temperature remain homogeneous/constant in space (and the macroscopic velocity is zero), but the granular temperature decays quadratically with time due to collisional dissipation – the latter is known as Haff's (Haff 1983) cooling law. It is worth pointing out that the HCS is not only useful for theoretical analyses [Haff (1983); Goldshtein & Shapiro (1995); van Noije & Ernst (1998); Pöschel & Brilliantov (2003)], but has been realized recently in experiments [Maaß *et al.* (2008); Tatsumi *et al.* (2009)] that verified the Haff's cooling law as well as its non-Gaussian distribution function. For a theoretical understanding in the rapid flow regime (Goldhirsch 2003), the granular materials have been modelled as inelastic, smooth hard spheres via the inelastic version of well-known Boltzmann equation [Jenkins & Richman (1985); Brey *et al.* (1999*b*)]. Various facets of the HCS have been studied via theory, simulation and experiments: high-energy tails of velocity distribution function [Esipov & Pöschel (1997); van Noije & Ernst (1998); Montanero & Santos (2000); Tatsumi *et al.* (2009)], clustering of particles [Goldhirsch & Zanetti (1993); Luding & Herrmann (1999); Nie *et al.* (2002)], inelastic collapse [McNamara & Young (1996); Luding & Herrmann (1999)], correlations [Brey *et al.* (1999*a*); Pöschel & Brilliantov (2003)], etc.

In most of above mentioned theoretical studies, the collision model of macroscopic particles incorporates energy loss due to normal contact of particles, but the tangential momentum of

[†]This chapter has been published in Physical Review E (R. Rongali and M. Alam, vol. 89, 062201, 2014)

colliding particles remains unaffected since particles are assumed to be *smooth*. The real particles are inelastic as well as *rough* and *frictional*, and the study of the rough particles is therefore important. The theoretical work on rough frictional particles is relatively scarce but increasingly more attention is given to such works [Huthmann & Zippelius (1997); Alam & Nott (1997); Luding *et al.* (1998); Jenkins & Zhang (2002); Cafiero *et al.* (2002); Mitarai *et al.* (2002); Herbst *et al.* (2005); Goldhirsch *et al.* (2005); Gayen & Alam (2006); Alam (2012); Brilliantov *et al.* (2007); Gayen & Alam (2008); Kranz *et al.* (2009); Gayen & Alam (2011); Santos *et al.* (2011, 2010); Reyes & Santos (2015); Reyes *et al.* (2017)].

We investigate the HCS of a rough granular gas by focusing on a special kind of correlation: the orientational/directional correlation [Brilliantov *et al.* (2007); Kranz *et al.* (2009); Gayen & Alam (2008, 2011)] between the direction of the angular/spin velocity ($\boldsymbol{\omega}$) of a granular particle and the direction of its translational velocity ($\boldsymbol{c}$). This is given by the scalar product between $\boldsymbol{c}$ and $\boldsymbol{\omega}$ which is nothing but the cosine of the angle θ between $\boldsymbol{c}$ and $\boldsymbol{\omega}$ (appropriately averaged) and a measure of this correlation is the second moment

$$\left\langle \cos^2\theta \right\rangle = \frac{1}{N}\sum_{i=1}^{N} \frac{(\boldsymbol{c}_i\cdot\boldsymbol{\omega}_i)^2}{\boldsymbol{c}_i^2\boldsymbol{\omega}_i^2}, \tag{2.1}$$

where N is the total number of particles that constitute the granular gas. If the translational and rotational velocities are not correlated in their direction, then $\langle\cos^2\theta\rangle = \frac{1}{3}$, and $\langle\cos^2\theta\rangle \neq 1/3$ indicates that the translational and rotational velocities are correlated in direction. Brilliantov *et al.* (2007) showed for the first time that the orientational correlation can be significant in a rough granular gas undergoing homogeneous cooling, especially near the limit of smooth particles. They derived an analytical expression for orientational correlation using an expansion of the distribution function in terms of Legendre polynomials and retained terms up-to the lowest non-trivial order, quadratic in both translational and rotational velocities. The orientational correlation in the driven case of uniform shear flow was investigated by Gayen & Alam (2008, 2011) via molecular dynamics simulation. They showed that the degree of orientational correlation is much higher in a shear flow than in HCS. Moreover, the imposed shear field always leads to a preferential perpendicular alignment between the translational and rotational velocity directions in contrast to the scenario in HCS where both parallel and perpendicular alignments are possible.

In the present study of HCS, we carry out a kinetic theory analysis of a rough granular gas using the pseudo-Liouville operator technique (with molecular chaos assumption) as in the work of Brilliantov *et al.* (2007). We retain terms up-to quartic-order in both translational and rotational velocities in the Legendre expansion of distribution function. The goal is to assess how these higher-order corrections affect the steady state of orientational correlation and its relaxation for the whole range of restitution coefficients. The impact of such angular correlations on hydrodynamic fields, like the ratio between the rotational and translational temperatures, is also critically assessed.

This chapter is organized as follows. A two-parameter collision model for rough inelastic particles is described in Sec. 2.2, the pseudo-Liouville operator technique in Sec. 2.2.1, and the Legendre expansion for the single-particle distribution function in Sec. 2.2.2. The expression for

normalized 'orientational correlation', with higher-order corrections, is derived in Sec. 2.2.3. The time-evolution equations for translational and rotational temperatures and Legendre coefficients are derived in Sec. 2.2.4. An approximate expression for steady-state correlations and the effect of higher-order terms is critically assessed in Sec. 2.3.1. A qualitative comparison with simulation and the possible effects of non-Gaussian corrections are also provided in Sec. 2.3.1. The relaxation of orientational correlation and the effect of initial conditions on its transient evolution are discussed in Sec. 2.3.2. The conclusions are given in Sec. 2.4. Finally, the details of analytical calculations leading to time-evolution equations are provided in Appendix A as a Supplementary Material to this chapter at the end of this thesis.

2.2 Kinetic Theory of a Rough Granular Gas and Orientational Correlation

Ignoring Coulomb friction, the simplest collision model for rough inelastic spheres relates the post-collisional relative velocity (primed) with its pre-collisional (unprimed) counterpart via the following collision rules [Pidduck (1922); Maw *et al.* (1976)]:

$$\boldsymbol{g}' \cdot \hat{\boldsymbol{n}} = -e_n\,(\boldsymbol{g} \cdot \hat{\boldsymbol{n}}), \quad \boldsymbol{g}' \times \hat{\boldsymbol{n}} = -e_t\,(\boldsymbol{g} \times \hat{\boldsymbol{n}}), \tag{2.2}$$

where $\boldsymbol{g}$ is the relative velocity of the point of contact

$$\boldsymbol{g} = \boldsymbol{c}_1 - \boldsymbol{c}_2 + a\,\hat{\boldsymbol{n}} \times (\boldsymbol{\omega}_1 + \boldsymbol{\omega}_2), \tag{2.3}$$

Here $\boldsymbol{c}_i$ and $\boldsymbol{\omega}_i$ are the translational and rotational velocities of sphere i, respectively, a is the radius of identical spheres and $\hat{\boldsymbol{n}}$ is the unit contact vector from particle-2 to particle-1 at the point of collision. In Eq. (2.2), $e_n \in (0, 1)$ is the coefficient of normal restitution with its lower and upper limits referring to the sticky (perfectly inelastic) and the elastic collisions, respectively. The parameter e_t is a measure of particle's *surface roughness*, called the coefficient of tangential restitution, which lies between -1 (smooth) and 1 (perfectly rough). Note that the relative tangential velocity remains unchanged in a collision between smooth particles but it gets reversed in a collision between perfectly rough particles. The value of $e_t = 0$ refers to the case for which the tangential component of the post-collisional relative velocity is zero.

From the conservation laws of linear and angular momentums and the collision rule, Eq. (2.2), the post-collisional velocities can be expressed in terms of pre-collisional velocities [Brilliantov *et al.* (2007); Gayen & Alam (2008); Kranz *et al.* (2009); Gayen & Alam (2011)]:

$$\boldsymbol{c}_1' = \boldsymbol{c}_1 - \boldsymbol{\delta}, \quad \boldsymbol{\omega}_1' = \boldsymbol{\omega}_1 + \frac{1}{qa}(\hat{\boldsymbol{n}} \times \boldsymbol{\delta}), \tag{2.4}$$

$$\boldsymbol{c}_2' = \boldsymbol{c}_2 + \boldsymbol{\delta}, \quad \boldsymbol{\omega}_2' = \boldsymbol{\omega}_2 + \frac{1}{qa}(\hat{\boldsymbol{n}} \times \boldsymbol{\delta}), \tag{2.5}$$

where

$$\boldsymbol{\delta} = \eta_t \boldsymbol{g} + (\eta_n - \eta_t)(\hat{\boldsymbol{n}} \cdot \boldsymbol{g})\hat{\boldsymbol{n}}, \tag{2.6}$$

$$\eta_n = \frac{1+e_n}{2}, \quad \eta_t = \frac{q}{2}\left(\frac{1+e_t}{1+q}\right), \tag{2.7}$$

and q is the dimensionless moment of inertia of a sphere

$$q = \frac{\mathcal{I}}{ma^2}. \tag{2.8}$$

The numerical values of $q = 2/5$ and $2/3$ represent a homogeneous sphere of uniform mass distribution, and a sphere with its mass being concentrated in the outer shell, respectively; $q \to 0$ corresponds to a sphere with its mass being concentrated towards its center.

2.2.1 Pseudo-Liouville Operator and Boltzmann Equation

Our starting point is the mesoscopic description of a dilute granular gas in terms of Liouville equation. The original formalism of the pseudo-Liouville operator for a hard-sphere potential is due to Ernst *et al.* (1969) and this has been extended to inelastic granular gases [Huthmann & Zippelius (1997); Brilliantov & Pöschel (2004); Herbst *et al.* (2005); Brilliantov *et al.* (2007); Kranz *et al.* (2009)]. We follow this approach to derive evolution equations which is briefly outlined below for the sake of completeness.

The evolution of a dynamical variable $\chi(t) = \chi(\boldsymbol{r}_i(t), \boldsymbol{c}_i(t), \boldsymbol{\omega}_i(t))$ is governed by the Liouville equation

$$\partial_t \chi(t) = \mathcal{L}\chi(t), \tag{2.9}$$

where the pseudo-Liouville operator $\mathcal{L}$ for hard spheres can be decomposed as

$$\mathcal{L} = \mathcal{L}_0 + \mathcal{L}_1. \tag{2.10}$$

The first term $\mathcal{L}_0 = \mathcal{L}_0^{\mathrm{tr}} + \mathcal{L}_0^{\mathrm{rot}}$ describes the free streaming of translational and rotational motion of particles. The second term in Eq. (2.10) represents the interaction of the particles:

$$\mathcal{L}_1 = \sum_{i<j} \mathcal{L}_{ij}, \tag{2.11}$$

where $\mathcal{L}_{ij}$ is the binary collision operator as given by [Ernst *et al.* (1969); Brilliantov & Pöschel (2004); Kranz *et al.* (2009)]:

$$\mathcal{L}_{ij} = -(\hat{\boldsymbol{n}}_{ij} \cdot \boldsymbol{c}_{ij})\Theta(-\hat{\boldsymbol{n}}_{ij} \cdot \boldsymbol{c}_{ij})\delta(r_{ij} - 2a)(\mathcal{B}_{ij} - 1), \tag{2.12}$$

with $\Theta(\cdot)$ and $\delta(\cdot)$ being the Heaviside and delta functions, respectively. The operator $\mathcal{B}_{ij}$ is defined such that it replaces the pre-collisional quantities by their post-collisional counterparts, satisfying the collision rules, Eqs. (2.4) and (2.5). For example,

$$\mathcal{B}_{12}\boldsymbol{c}_1 = \boldsymbol{c}_1', \quad \mathcal{B}_{12}\boldsymbol{c}_2 = \boldsymbol{c}_2', \quad \mathcal{B}_{12}\boldsymbol{c}_k = \boldsymbol{c}_k, \quad k \neq 1, 2 \tag{2.13}$$

where $\boldsymbol{c}_1'$ and $\boldsymbol{c}_2'$ are given by Eqs. (2.4) and (2.5).

Let us define the ensemble average of a dynamical variable via

$$\langle \chi \rangle = \int \mathrm{d}\Gamma \rho_N(0)\chi(t) = \int \mathrm{d}\Gamma \rho_N(t)\chi(0), \tag{2.14}$$

where $\rho_N(t)$ is the N-particle distribution function and $d\Gamma = \prod_i (d^3 r_i d^3 c_i d^3 \omega_i)$ is the phase-space volume. By differentiating Eq. (2.14) and with the aid of Eq. (2.9), we obtain the following master equation:

$$\frac{\mathrm{d}}{\mathrm{d}t}\langle \chi \rangle = \langle \mathcal{L}\chi \rangle \equiv \int \mathrm{d}\Gamma \rho_N(t)\mathcal{L}\chi(0). \tag{2.15}$$

To make further progress, we assume that the molecular chaos assumption holds and therefore the N-particle distribution function can be factorized into

$$\rho_N(t) = g_N(\boldsymbol{r}_1, \ldots, \boldsymbol{r}_N) \prod_i f(\boldsymbol{c}_i, \boldsymbol{\omega}_i, t), \tag{2.16}$$

where $f(\boldsymbol{c}, \boldsymbol{\omega}, t)$ is the single-particle distribution function and $g_N(\boldsymbol{r}_1, \ldots, \boldsymbol{r}_N)$ is the N-particle correlation function of a hard-sphere system. The master equation (2.15) will be used later to derive the time-evolution equations for hydrodynamic fields (granular temperatures) and other related variables which is the major focus of this chapter.

The connection of the pseudo-Liouville operator to the Boltzmann equation is now made clear via the single particle distribution function $f(\boldsymbol{c}, \boldsymbol{\omega}, t)$ in Eq. (2.16). The Boltzmann equation for the HCS of a granular gas reads:

$$\frac{\partial}{\partial t} f(\boldsymbol{c}, \boldsymbol{\omega}, t) = J(f, f), \tag{2.17}$$

where $J(f, f)$ is the collision integral that accounts for the change of the distribution function $f(\boldsymbol{c}, \boldsymbol{\omega}, t)$ in binary inelastic collisions. We do not solve Eq. (2.17) exactly, rather an ansatz is made to obtain an approximate expression for $f(\boldsymbol{c}, \boldsymbol{\omega}, t)$ as discussed in Sec. 2.2.2. The resulting approximate solution $f(\boldsymbol{c}, \boldsymbol{\omega}, t)$ will be subsequently used in conjunction with the master equation (2.15) and Eq. (2.16) to derive time evolution equations for hydrodynamic fields (two temperatures) as well as the related time-dependent coefficients of the distribution function as detailed in Sec. 2.2.4. It may be noted that the interaction term of the pseudo-Liouville operator ($\mathcal{L}_{ij}$) can be formally tied to the collision operator of the Boltzmann equation (see Chapter 13 in Brilliantov & Pöschel (2004)). Therefore, with molecular chaos assumption, the present formalism of pseudo-Liouville operator is equivalent to the Boltzmann-Enskog equation.

2.2.2 Ansatz for Distribution Function: Legendre Expansion

The homogeneous cooling state (HCS) of a granular gas is devoid of any spatial inhomogeneity, and hence the distribution function $f(\boldsymbol{c}, \boldsymbol{\omega})$ would depend on the magnitudes of $\boldsymbol{c}$ and $\boldsymbol{\omega}$ and the angle θ between $\boldsymbol{c}$ and $\boldsymbol{\omega}$. There is a scaling solution [Goldshtein & Shapiro (1995); Pöschel & Luding (2001); Brilliantov & Pöschel (2004)] to the inelastic Boltzmann equation for HCS that can be modelled via a Sonine polynomial expansion around the Maxwellian; such non-Gaussian

corrections might affect the leading-order behavior of the orientational correlation in the HCS of a rough granular gas as demonstrated in a recent work (Reyes *et al.* 2014).

Incorporating non-Gaussian corrections to the distribution function would make the analysis of higher-order effects on orientational correlation extremely complicated, but can be followed up in a future work, see the discussion in Sec. 2.3.1. As in the work of Brilliantov *et al.* (2007) and Kranz *et al.* (2009), we use an approximate form for the distribution function by focusing only on the angular-dependence of $f(\boldsymbol{c},\boldsymbol{\omega})$ via $\cos\theta$ in this chapter. With the above assumption, we expand f around a product of two Maxwellian in terms of Legendre polynomials $P_l(\cos\theta)$

$$f(\boldsymbol{c},\boldsymbol{\omega},t) \propto \exp\left(-\frac{m\boldsymbol{c}^2}{2T(t)}\right)\exp\left(-\frac{\mathcal{I}\boldsymbol{\omega}^2}{2R(t)}\right)\sum_{n=0}^{\infty}\sum_{p=0}^{\infty}\sum_{l=0}^{\infty} b_{npl}(t)\boldsymbol{c}^{2n}\boldsymbol{\omega}^{2p}P_l(\cos\theta), \tag{2.18}$$

where $b_{npl}(t)$ are time-dependent expansion coefficients and the distribution function must be normalized according to $\int\int d\boldsymbol{c}d\boldsymbol{\omega}f(\boldsymbol{c},\boldsymbol{\omega},t)=1$ as well as to reproduce temperatures from their definition. For a N-particle system with translational and rotational degrees of freedom, there are two temperatures: the translational and rotational temperatures as defined via

$$T(t)=\frac{1}{3}\langle m\boldsymbol{c}^2\rangle \quad \text{and} \quad R(t)=\frac{1}{3}\langle\mathcal{I}\boldsymbol{\omega}^2\rangle. \tag{2.19}$$

For the present system of homogeneous cooling state (HCS) it is known that both temperatures decay with time but their ratio

$$R_T(t)=\frac{R(t)}{T(t)} \tag{2.20}$$

remains time-invariant after a transient period, and the value of R_T depends on two restitution coefficients (e_n and e_t) and the moment of inertia (q). It is also known that $R_T\neq 1$, i.e., the energy is unequally partitioned between translational and rotational modes in a granular gas.

In Eq. (2.18) it is straightforward to verify that the terms for odd $l=1,3,\ldots$ vanish due to symmetry. Therefore, the approximate distribution function, with at most quartic-order corrections in $\boldsymbol{c}$ and $\boldsymbol{\omega}$, is given by:

$$\begin{aligned} f(\boldsymbol{c},\boldsymbol{\omega},t) \;\propto\; & \exp\left(-\frac{m\boldsymbol{c}^2}{2T(t)}\right)\exp\left(-\frac{\mathcal{I}\boldsymbol{\omega}^2}{2R(t)}\right)\Big[1+b_{112}(t)\boldsymbol{c}^2\boldsymbol{\omega}^2P_2(\cos\theta)+\underline{b_{122}(t)\boldsymbol{c}^2\boldsymbol{\omega}^4}P_2(\cos\theta) \\ & +\underline{b_{212}(t)\boldsymbol{c}^4\boldsymbol{\omega}^2}P_2(\cos\theta)\Big]. \end{aligned} \tag{2.21}$$

The leading-order correction in above equation is quadratic in both $\boldsymbol{c}$ and $\boldsymbol{\omega}$ which has been considered by Brilliantov *et al.* (2007). In this chapter we focus on the effects of higher-order corrections (underlined terms in Eq. (2.21)) on the orientational correlation as well as on the relaxation dynamics of two temperatures. Note that

$$P_2(\cos\theta)=\frac{3}{2}\left(\cos^2\theta-\frac{1}{3}\right), \tag{2.22}$$

and therefore $\cos^2\theta=\frac{1}{3}$ corresponds to the distribution function being given by the product of two Maxwellian.

2.2.3 Higher-order Corrections to Orientational Correlation

The leading-order measure of the correlation between the axis of rotation of a granular particle and the direction of its translational velocity is $\langle \cos^2\theta \rangle$ which can be appropriately normalized to yield a definition of *orientational correlation* [Brilliantov *et al.* (2007); Gayen & Alam (2008)]

$$\Psi_\theta = \langle \cos^2\theta \rangle - \frac{1}{3}. \tag{2.23}$$

Note that the first moment of $\cos\theta$ vanishes due to symmetry. A null value for Ψ_θ indicates that the angular and linear velocities are not correlated in direction; however, $\Psi_\theta < 0$ or > 0 represents the angular and linear velocities being preferably perpendicular or parallel, respectively.

From the definition of ensemble average (2.14) and Eq. (2.16), we obtain an expression for $\langle \cos^2\theta \rangle$ in terms of Legendre polynomials:

$$\begin{aligned}
\Psi_\theta &= \langle \cos^2\theta \rangle - \frac{1}{3} \\
&= \frac{1}{3}\int_c\int_\omega [P_0(\cos\theta) + 2P_2(\cos\theta)][P_0(\cos\theta) + b_{112}(t)\boldsymbol{c}^2\boldsymbol{\omega}^2 P_2(\cos\theta) \\
&\quad + b_{122}(t)\boldsymbol{c}^2\boldsymbol{\omega}^4 P_2(\cos\theta) + b_{212}(t)\boldsymbol{c}^4\boldsymbol{\omega}^2 P_2(\cos\theta)] - \frac{1}{3},
\end{aligned} \tag{2.24}$$

where the integrations over $\boldsymbol{c}$ and $\boldsymbol{\omega}$ are defined via

$$\left.\begin{aligned}
\int_c &= \left(\tfrac{m}{2\pi T}\right)^{\frac{3}{2}} \int d^3c \exp\left(-\tfrac{m\boldsymbol{c}^2}{2T}\right) \\
\int_\omega &= \left(\tfrac{\mathcal{I}}{2\pi R}\right)^{\frac{3}{2}} \int d^3\omega \exp\left(-\tfrac{\mathcal{I}\boldsymbol{\omega}^2}{2R}\right).
\end{aligned}\right\} \tag{2.25}$$

Eq. (2.24) can be simplified by changing into spherical coordinates and using the orthogonality relation for Legendre polynomials, resulting in

$$\begin{aligned}
\Psi_\theta(t) &= b_{112}(t)\left(\frac{6T(t)R(t)}{5qm^2a^2}\right) + b_{122}(t)\left(\frac{6T(t)R^2(t)}{q^2m^3a^4}\right) + b_{212}(t)\left(\frac{6T^2(t)R(t)}{qm^3a^2}\right) \\
&\equiv \Psi_\theta^{11}(t) + \Psi_\theta^{12}(t) + \Psi_\theta^{21}(t).
\end{aligned} \tag{2.26}$$

While $\Psi_\theta^{11}(t)$ is the leading-order expression for orientational correlation [Brilliantov *et al.* (2007); Gayen & Alam (2008); Kranz *et al.* (2009); Gayen & Alam (2011)], the last two terms, $\Psi_\theta^{12}(t)$ and $\Psi_\theta^{21}(t)$, in Eq. (2.26) represent its next higher-order corrections. Clearly, Ψ_θ depends on time via its dependence on two temperatures [$T(t)$ and $R(t)$] and the three Legendre coefficients [$b_{112}(t)$, $b_{122}(t)$ and $b_{212}(t)$]. To evaluate (2.26) we need to derive evolution equations for the above five dynamical variables which is considered below.

2.2.4 Evolution Equations for Translational and Rotational Temperatures and the Legendre Coefficients

The time evolution equations for translational and rotational temperatures and the related Legendre coefficients have been derived by applying the master equation (2.15) and using Eqs. (2.16) and (2.21); the detailed derivation of these equations is documented in Supplementary

Material to this chapter as Appendix A at the end of this thesis. To illustrate the underlying calculation, we consider the evolution equation for translational temperature $T(t) = \langle m\boldsymbol{c}^2/3\rangle$:

$$\frac{\mathrm{d}T}{\mathrm{d}t} = \langle \mathcal{L}\chi \rangle \tag{2.27}$$

which is obtained by putting $\chi = m\boldsymbol{c}^2/3$ into the master equation (2.15). Neglecting quadratic nonlinear terms in $b_{npl}(t)$ [Eqs. (A.14) and (A.17) of Appendix A in Supplementary Material to Chapter 2], the right-hand side of Eq. (2.27) can be decomposed into four parts:

$$\langle \mathcal{L}\chi \rangle = \langle (\mathcal{B}_{12}-1)\chi \rangle^{(0)} + b_{112}(t)\langle (\mathcal{B}_{12}-1)\chi \rangle^{(1)} + b_{122}(t)\langle (\mathcal{B}_{12}-1)\chi \rangle^{(2)} + b_{212}(t)\langle (\mathcal{B}_{12}-1)\chi \rangle^{(3)}, \tag{2.28}$$

with $\chi = m\boldsymbol{c}^2/3$ and it is straightforward to verify that

$$\frac{1}{4}(\mathcal{B}_{12}-1)\boldsymbol{c}^2 = \eta_t(\eta_t-1)(\hat{\boldsymbol{n}}\times\boldsymbol{v})^2+\eta_n(\eta_n-1)(\hat{\boldsymbol{n}}\cdot\boldsymbol{v})^2+\eta_t^2a^2(\hat{\boldsymbol{n}}\times\boldsymbol{\Omega})^2+\eta_t(2\eta_t-1)a((\hat{\boldsymbol{n}}\times\boldsymbol{\Omega})\cdot\boldsymbol{v}). \tag{2.29}$$

Four types of averages in Eq. (2.28), denoted by superscripts 0, 1, 2 and 3, have integral expressions (see Appendix A of Supplementary Material to Chapter 2) which, for any function $\mathcal{F}$, take following forms:

$$\langle \mathcal{F} \rangle^{(0)} = \sqrt{2}\,\nu \int_v\int_V\int_\omega\int_\Omega (\hat{\boldsymbol{n}}\cdot\boldsymbol{v})\Theta(-\hat{\boldsymbol{n}}\cdot\boldsymbol{v})\,\mathcal{F} \tag{2.30}$$

$$\begin{aligned}\langle \mathcal{F} \rangle^{(1)} = \frac{3\sqrt{2}}{4}\,\nu \int_v\int_V\int_\omega\int_\Omega (\hat{\boldsymbol{n}}\cdot\boldsymbol{v})\Theta(-\hat{\boldsymbol{n}}\cdot\boldsymbol{v})\Big[&(\boldsymbol{v}\cdot\boldsymbol{\omega})^2+(\boldsymbol{v}\cdot\boldsymbol{\Omega})^2+(\boldsymbol{V}\cdot\boldsymbol{\omega})^2+(\boldsymbol{V}\cdot\boldsymbol{\Omega})^2\\ &-\frac{1}{3}(\boldsymbol{v}^2+\boldsymbol{V}^2)(\boldsymbol{\omega}^2+\boldsymbol{\Omega}^2)+2(\boldsymbol{v}\cdot\boldsymbol{\Omega})(\boldsymbol{V}\cdot\boldsymbol{\omega})+2(\boldsymbol{v}\cdot\boldsymbol{\omega})(\boldsymbol{V}\cdot\boldsymbol{\Omega})-\frac{4}{3}(\boldsymbol{v}\cdot\boldsymbol{V})(\boldsymbol{\omega}\cdot\boldsymbol{\Omega})\Big]\,\mathcal{F}\end{aligned} \tag{2.31}$$

$$\begin{aligned}\langle \mathcal{F} \rangle^{(2)} = \frac{3\sqrt{2}}{8}\,\nu \int_v\int_V\int_\omega\int_\Omega (\hat{\boldsymbol{n}}\cdot\boldsymbol{v})\Theta(-\hat{\boldsymbol{n}}\cdot\boldsymbol{v})\Big[&(\boldsymbol{\omega}^2+\boldsymbol{\Omega}^2)\Big((\boldsymbol{v}\cdot\boldsymbol{\omega})^2+(\boldsymbol{v}\cdot\boldsymbol{\Omega})^2+(\boldsymbol{V}\cdot\boldsymbol{\omega})^2+(\boldsymbol{V}\cdot\boldsymbol{\Omega})^2\\ &-\frac{1}{3}(\boldsymbol{v}^2+\boldsymbol{V}^2)(\boldsymbol{\omega}^2+\boldsymbol{\Omega}^2)+2(\boldsymbol{v}\cdot\boldsymbol{\Omega})(\boldsymbol{V}\cdot\boldsymbol{\omega})+2(\boldsymbol{v}\cdot\boldsymbol{\omega})(\boldsymbol{V}\cdot\boldsymbol{\Omega})\Big)+4(\boldsymbol{\omega}\cdot\boldsymbol{\Omega})\Big((\boldsymbol{v}\cdot\boldsymbol{\omega})(\boldsymbol{v}\cdot\boldsymbol{\Omega})+(\boldsymbol{V}\cdot\boldsymbol{\Omega})(\boldsymbol{V}\cdot\boldsymbol{\omega})\\ &+(\boldsymbol{v}\cdot\boldsymbol{\omega})(\boldsymbol{V}\cdot\boldsymbol{\omega})+(\boldsymbol{v}\cdot\boldsymbol{\Omega})(\boldsymbol{V}\cdot\boldsymbol{\Omega})-\frac{1}{3}(\boldsymbol{v}^2+\boldsymbol{V}^2)(\boldsymbol{\omega}\cdot\boldsymbol{\Omega})-\frac{2}{3}(\boldsymbol{\omega}^2+\boldsymbol{\Omega}^2)(\boldsymbol{v}\cdot\boldsymbol{V})\Big)\Big]\,\mathcal{F}\end{aligned} \tag{2.32}$$

$$\begin{aligned}\langle \mathcal{F} \rangle^{(3)} = \frac{3\sqrt{2}}{8}\,\nu \int_v\int_V\int_\omega\int_\Omega (\hat{\boldsymbol{n}}\cdot\boldsymbol{v})\Theta(-\hat{\boldsymbol{n}}\cdot\boldsymbol{v})\Big[&(\boldsymbol{v}^2+\boldsymbol{V}^2)\Big((\boldsymbol{v}\cdot\boldsymbol{\omega})^2+(\boldsymbol{v}\cdot\boldsymbol{\Omega})^2+(\boldsymbol{V}\cdot\boldsymbol{\omega})^2+(\boldsymbol{V}\cdot\boldsymbol{\Omega})^2\\ &-\frac{1}{3}(\boldsymbol{v}^2+\boldsymbol{V}^2)(\boldsymbol{\omega}^2+\boldsymbol{\Omega}^2)+2(\boldsymbol{v}\cdot\boldsymbol{\Omega})(\boldsymbol{V}\cdot\boldsymbol{\omega})+2(\boldsymbol{v}\cdot\boldsymbol{\omega})(\boldsymbol{V}\cdot\boldsymbol{\Omega})\Big)+4(\boldsymbol{v}\cdot\boldsymbol{V})\Big((\boldsymbol{v}\cdot\boldsymbol{\omega})(\boldsymbol{v}\cdot\boldsymbol{\Omega})+(\boldsymbol{V}\cdot\boldsymbol{\Omega})(\boldsymbol{V}\cdot\boldsymbol{\omega})\\ &+(\boldsymbol{v}\cdot\boldsymbol{\omega})(\boldsymbol{V}\cdot\boldsymbol{\omega})+(\boldsymbol{v}\cdot\boldsymbol{\Omega})(\boldsymbol{V}\cdot\boldsymbol{\Omega})-\frac{2}{3}(\boldsymbol{v}^2+\boldsymbol{V}^2)(\boldsymbol{\omega}\cdot\boldsymbol{\Omega})-\frac{1}{3}(\boldsymbol{\omega}^2+\boldsymbol{\Omega}^2)(\boldsymbol{v}\cdot\boldsymbol{V})\Big)\Big]\,\mathcal{F}\end{aligned} \tag{2.33}$$

where we have introduced new integration variables:

$$\begin{aligned}\boldsymbol{v} &\equiv \frac{\boldsymbol{c}_1-\boldsymbol{c}_2}{\sqrt{2}} = \frac{\boldsymbol{c}_{12}}{\sqrt{2}}, \quad \boldsymbol{V} \equiv \frac{(\boldsymbol{c}_1+\boldsymbol{c}_2)}{\sqrt{2}},\\ \boldsymbol{\omega} &\equiv \frac{\boldsymbol{\omega}_1-\boldsymbol{\omega}_2}{\sqrt{2}} = \frac{\boldsymbol{\omega}_{12}}{\sqrt{2}}, \quad \boldsymbol{\Omega} \equiv \frac{(\boldsymbol{\omega}_1+\boldsymbol{\omega}_2)}{\sqrt{2}}.\end{aligned} \tag{2.34}$$

In Eqs. (2.30)-(2.33), $\Theta(\cdot)$ is the Heaviside function and $\nu = -8\pi n a^2 g_2(2a)$, with n being the number density of particles and $g_2(2a)$ is the contact value of the pair correlation function (i.e. the radial distribution function). The remaining task to obtain the complete temperature equation (2.27) is to carry out the above integrations by using $\mathcal{F} = (\mathcal{B}_{12}-1)\boldsymbol{c}^2$ via Eq. (2.29). We have made extensive use of the "Mathematica" software to complete this calculation (see

Appendix A of Supplementary Material to Chapter 2), leading to five differential equations for $T(t)$, $R(t)$, $b_{112}(t)$, $b_{122}(t)$ and $b_{212}(t)$ which are written down as Eqs. (A.46), (A.47), (A.48), (A.49), and (A.50), respectively, in Appendix A of Supplementary Material to Chapter 2. As a check, we have verified that the lowest-order equations for $T(t)$, $R(t)$ and $b_{112}(t)$ (Kranz *et al.* 2009) are recovered (see Appendix A), barring a few minor mistakes, from Eqs. (A.79)-(A.81) in the appropriate limit by setting all terms originating from higher-order Legendre coefficients (b_{122} and b_{212}) to zero.

To put the dynamical equations (A.46–A.50) in dimensionless form, we introduce rescaled Legendre coefficients

$$\left.\begin{aligned} x(\tau) &= b_{112}(\tau)\left(\frac{T(\tau)R(\tau)}{qm^2a^2}\right) \\ y(\tau) &= b_{122}(\tau)\left(\frac{T(\tau)R^2(\tau)}{q^2m^3a^4}\right) \\ z(\tau) &= b_{212}(\tau)\left(\frac{T^2(\tau)R(\tau)}{qm^3a^2}\right) \end{aligned}\right\}, \tag{2.35}$$

and a dimensionless time τ via

$$\frac{\mathrm{d}}{\mathrm{d}\tau} = \tau_f \frac{\mathrm{d}}{\mathrm{d}t}, \tag{2.36}$$

where τ_f is the mean-free time given by

$$\tau_f^{-1} = 16\left(\frac{\pi T}{m}\right)^{1/2} na^2 g_2(2a). \tag{2.37}$$

Note that the rescaled/dimensionless time τ measures time in terms of the average number of collisions that each particle has encountered. With these scaling, the equations (see Appendix A of Supplementary Material to Chapter 2) for $T(\tau)$ [Eq. (A.66)], $R(\tau)$ [Eq. (A.67)], $b_{112}(\tau)$ [Eq. (A.68)], $b_{122}(\tau)$ [Eq. (A.69)] and $b_{212}(\tau)$ [Eq. (A.70)] are transformed into a reduced set of

four equations for $R_T(\tau) = R(\tau)/T(\tau)$, $x(\tau)$, $y(\tau)$ and $z(\tau)$:

$$\frac{3}{4}\frac{\mathrm{d}R_T}{\mathrm{d}\tau} = \alpha_1 R_T + \alpha_2 - (\alpha_2 R_T + \alpha_3)\Big(1 - \frac{x}{2} - \frac{7}{2}y - \frac{13}{4}z\Big)R_T, \tag{2.38}$$

$$\begin{aligned}\frac{\mathrm{d}x}{\mathrm{d}\tau} &= \Big[A_{31}R_T^2 + A_{32}R_T + A_{33}R_T^{-1} + A_{34} + \frac{4}{3}\Big(\alpha_2 R_T^{-1} - \alpha_1 + (\alpha_2 R_T - \alpha_3)\Big(1 - \frac{x}{2} - \frac{7}{2}y - \frac{13}{4}z\Big)\Big)\Big]x(\tau)\\ &+\Big(A_{11}R_T^2 + A_{12}R_T + A_{13}R_T^{-1} + A_{14}\Big)y(\tau) + \Big(A_{21}R_T^2 + A_{22}R_T + A_{23}R_T^{-1} + A_{24}\Big)z(\tau)\\ &+\Big(A_{01}R_T^2 + A_{02}R_T + A_{03}R_T^{-2} + A_{04} + A_{05}R_T^{-1}\Big) + \Big(-\frac{70}{3}\alpha_2 R_T + 28\alpha_3\Big)x(\tau)y(\tau)\\ &+\Big(-\frac{55}{2}\alpha_2 R_T + \frac{137}{6}\alpha_3\Big)x(\tau)z(\tau) + \Big(-\frac{1519}{6}\alpha_2 R_T + \frac{1505}{6}\alpha_3\Big)y(\tau)z(\tau) + \Big(-\alpha_2 R_T + \alpha_3\Big)x^2(\tau)\\ &+\Big(-\frac{343}{3}\alpha_2 R_T + 147\alpha_3\Big)y^2(\tau) + \Big(-\frac{273}{2}\alpha_2 R_T + \frac{637}{6}\alpha_3\Big)z^2(\tau),\end{aligned} \tag{2.39}$$

$$\begin{aligned}\frac{\mathrm{d}y}{\mathrm{d}\tau} &= \Big(B_{31}R_T + B_{32} + B_{33}R_T^{-1}\Big)x(\tau) + \Big[B_{11}R_T + B_{12} + B_{13}R_T^{-1}\\ &+\frac{4}{3}\Big(2\alpha_2 R_T^{-1} - \alpha_1 + (\alpha_2 R_T - 2\alpha_3)\Big(1 - \frac{x}{2} - \frac{7}{2}y - \frac{13}{4}z\Big)\Big)\Big]y(\tau) + \Big(B_{21}R_T + B_{22} + B_{23}R_T^{-1}\Big)z(\tau)\\ &+\Big(B_{01}R_T + B_{02} + B_{03}R_T^{-1} + B_{04}R_T^{-2}\Big) + \Big(\frac{4}{3}\alpha_2 R_T - \frac{22}{3}\alpha_3\Big)x(\tau)y(\tau) - \frac{9}{2}\alpha_3 x(\tau)z(\tau)\\ &+\Big(\frac{26}{3}\alpha_2 R_T - \frac{293}{6}\alpha_3\Big)y(\tau)z(\tau) - \frac{1}{3}\alpha_3 x^2(\tau) + \Big(\frac{28}{3}\alpha_2 R_T - 35\alpha_3\Big)y^2(\tau) - \frac{91}{6}\alpha_3 z^2(\tau),\end{aligned} \tag{2.40}$$

$$\begin{aligned}\frac{\mathrm{d}z}{\mathrm{d}\tau} &= \Big(C_{31}R_T^2 + C_{32}R_T + C_{33}\Big)x(\tau) + \Big(C_{11}R_T^2 + C_{12}R_T + C_{13}\Big)y(\tau)\\ &+\Big[C_{21}R_T^{-1} + C_{22}R_T^2 + C_{23}R_T + C_{24} + \frac{4}{3}\Big(\alpha_2 R_T^{-1} - 2\alpha_1 + (2\alpha_2 R_T - \alpha_3)\Big(1 - \frac{x}{2} - \frac{7}{2}y - \frac{13}{4}z\Big)\Big)\Big]z(\tau)\\ &+\Big(C_{01}R_T^2 + C_{02}R_T + C_{03} + C_{04}R_T^{-1}\Big) + \frac{14}{3}\alpha_2 R_T x(\tau)y(\tau) + \Big(\frac{43}{6}\alpha_2 R_T - \frac{4}{3}\alpha_3\Big)x(\tau)z(\tau)\\ &+\Big(\frac{301}{6}\alpha_2 R_T - \frac{28}{3}\alpha_3\Big)y(\tau)z(\tau) + \frac{1}{3}\alpha_2 R_T x^2(\tau) + \frac{49}{3}\alpha_2 R_T y^2(\tau) + \Big(\frac{65}{2}\alpha_2 R_T - \frac{26}{3}\alpha_3\Big)z^2(\tau),\end{aligned} \tag{2.41}$$

where

$$\alpha_1 \equiv \eta_n(1-\eta_n) + \eta_t(1-\eta_t), \quad \alpha_2 \equiv \frac{\eta_t^2}{q}, \quad \alpha_3 \equiv \frac{\eta_t}{q}\Big(1 - \frac{\eta_t}{q}\Big), \tag{2.42}$$

and the explicit expressions for the dimensionless coefficients A_{ij}, B_{ij} and C_{ij} are given in Appendix A of Supplementary Material to Chapter 2. The above set of coupled differential equations must be solved to yield information on (i) the relaxation dynamics of each field, (ii) the orientational correlation Ψ_θ and (iii) the temperature ratio $R_T(\tau) = R(\tau)/T(\tau)$ which are discussed in the next section. The nonlinear terms of $x(\tau)$, $y(\tau)$ and $z(\tau)$ in Eq. (2.39)-(2.41) have been neglected in the following analysis to stay tuned with our original assumption of neglecting quadratic-order terms in b_{npl} to derive dynamical equations (see Appendix A). We have verified from numerical simulation of Eqs. (2.38)-(2.41) that these nonlinear terms in Eqs. (2.39)-(2.41) do not noticeably affect the temporal dynamics and steady states of correlation and temperature ratio.

2.3 Results and Discussion: Assessment of Higher-order Corrections

2.3.1 Steady State for Orientational Correlation and Temperature Ratio

In terms of the rescaled Legendre coefficients (2.35), the expression for orientational correlation (2.26) is

$$\begin{aligned}\Psi_\theta(\tau) &\equiv \left(\langle\cos^2\theta\rangle_\tau - \frac{1}{3}\right) = \frac{6}{5}x(\tau) + 6y(\tau) + 6z(\tau) \\ &\equiv \Psi_\theta^{11}(\tau) + \Psi_\theta^{12}(\tau) + \Psi_\theta^{21}(\tau).\end{aligned} \tag{2.43}$$

The steady state orientational correlation is calculated from

$$\Psi_\theta^\infty = \lim_{\tau\to\infty}\left(\frac{6}{5}x(\tau) + 6y(\tau) + 6z(\tau)\right), \tag{2.44}$$

after evaluating the steady-state values of $x(\infty)$, $y(\infty)$ and $z(\infty)$.

To obtain approximate analytical expression for the stationary solutions of (2.38)-(2.41) we use the iteration scheme of Kranz *et al.* (2009): the zeroth-order approximation of the temperature ratio $R_T^{(0)}$ is calculated by neglecting correlations ($x = 0$, $y = 0$ and $z = 0$) as

$$R_T^{(0)}(\infty) = \frac{\alpha_1 - \alpha_3}{2\alpha_2} + \sqrt{1 + \frac{(\alpha_1 - \alpha_3)^2}{4\alpha_2^2}} = R_T^{(0)}. \tag{2.45}$$

The approximate values of x_∞, y_∞ and z_∞ are subsequently calculated by inserting the above steady-state temperature into Eqs. (2.39)-(2.41) and solving the resulting steady linear equations to yield:

$$x_\infty^{(0)} = \left[\frac{K_0(L_1M_2 - L_2M_1) + K_1(L_2M_0 - L_0M_2) + K_2(L_0M_1 - L_1M_0)}{K_1(L_3M_2 - L_2M_3) + K_2(L_1M_3 - L_3M_1) + K_3(L_2M_1 - L_1M_2)}\right], \tag{2.46}$$

$$y_\infty^{(0)} = \left[\frac{K_0(L_2M_3 - L_3M_2) + K_2(L_3M_0 - L_0M_3) + K_3(L_0M_2 - L_2M_0)}{K_1(L_3M_2 - L_2M_3) + K_2(L_1M_3 - L_3M_1) + K_3(L_2M_1 - L_1M_2)}\right], \tag{2.47}$$

$$z_\infty^{(0)} = \left[\frac{K_0(L_3M_1 - L_1M_3) + K_1(L_0M_3 - L_3M_0) + K_3(L_1M_0 - L_0M_1)}{K_1(L_3M_2 - L_2M_3) + K_2(L_1M_3 - L_3M_1) + K_3(L_2M_1 - L_1M_2)}\right], \tag{2.48}$$

where

$$\left.\begin{aligned}
K_0 &= A_{01}{R_T^{(0)}}^2 + A_{02}R_T^{(0)} + A_{03}/{R_T^{(0)}}^2 + A_{04} + A_{05}/R_T^{(0)} \\
K_1 &= A_{11}{R_T^{(0)}}^2 + A_{12}R_T^{(0)} + A_{13}/R_T^{(0)} + A_{14} \\
K_2 &= A_{21}{R_T^{(0)}}^2 + A_{22}R_T^{(0)} + A_{23}/R_T^{(0)} + A_{24} \\
K_3 &= A_{31}{R_T^{(0)}}^2 + \left(A_{32} + \tfrac{4\alpha_2}{3}\right)R_T^{(0)} + \left(A_{33} + \tfrac{4\alpha_2}{3}\right)/R_T^{(0)} + \left(A_{34} - \tfrac{4}{3}(\alpha_1+\alpha_3)\right) \\
L_0 &= B_{01}R_T^{(0)} + B_{02} + B_{03}/R_T^{(0)} + B_{04}/{R_T^{(0)}}^2 \\
L_1 &= \left(B_{11} + \tfrac{4\alpha_2}{3}\right)R_T^{(0)} + \left(B_{12} - \tfrac{4}{3}(\alpha_1+2\alpha_3)\right) + \left(B_{13} + \tfrac{8\alpha_2}{3}\right)/R_T^{(0)} \\
L_2 &= B_{21}R_T^{(0)} + B_{22} + B_{23}/R_T^{(0)} \\
L_3 &= B_{31}R_T^{(0)} + B_{32} + B_{33}/R_T^{(0)} \\
M_0 &= C_{01}{R_T^{(0)}}^2 + C_{02}R_T^{(0)} + C_{03} + C_{04}/R_T^{(0)} \\
M_1 &= C_{11}{R_T^{(0)}}^2 + C_{12}R_T^{(0)} + C_{13} \\
M_2 &= \left(C_{21} + \tfrac{4\alpha_2}{3}\right){R_T^{(0)}}^{-1} + C_{22}{R_T^{(0)}}^2 + \left(C_{23} + \tfrac{8\alpha_2}{3}\right)R_T^{(0)} + \left(C_{24} - \tfrac{4}{3}(2\alpha_1+\alpha_3)\right) \\
M_3 &= C_{31}{R_T^{(0)}}^2 + C_{32}R_T^{(0)} + C_{33}
\end{aligned}\right\}, \tag{2.49}$$

Inserting solutions (2.46)-(2.48) into Eq. (2.44), we obtain an expression for steady state orientational correlation:

$$\begin{aligned}
\Psi_\theta^\infty &\approx \frac{6}{5}\left[\frac{-K_2L_1M_0 + K_1L_2M_0 + K_2L_0M_1 - K_0L_2M_1 - K_1L_0M_2 + K_0L_1M_2}{K_3L_2M_1 - K_2L_3M_1 - K_3L_1M_2 + K_1L_3M_2 + K_2L_1M_3 - K_1L_2M_3}\right] \\
&\quad +6\left[\frac{-K_3L_2M_0 + K_2L_3M_0 + K_3L_0M_2 - K_0L_3M_2 - K_2L_0M_3 + K_0L_2M_3}{K_3L_2M_1 - K_2L_3M_1 - K_3L_1M_2 + K_1L_3M_2 + K_2L_1M_3 - K_1L_2M_3}\right] \\
&\quad +6\left[\frac{K_3L_1M_0 - K_1L_3M_0 - K_3L_0M_1 + K_0L_3M_1 + K_1L_0M_3 - K_0L_1M_3}{K_3L_2M_1 - K_2L_3M_1 - K_3L_1M_2 + K_1L_3M_2 + K_2L_1M_3 - K_1L_2M_3}\right] \qquad (2.50) \\
&= \Psi_\theta^{11} + \Psi_\theta^{12} + \Psi_\theta^{21} \equiv \Psi_\theta^H. \qquad (2.51)
\end{aligned}$$

The expression of Brilliantov *et al.* (2007) follows from the above by setting the higher-order corrections ($\Psi_\theta^{12} = 0 = \Psi_\theta^{21}$) to zero and evaluating Ψ_θ^{11} for $y(\tau) = 0 = z(\tau)$:

$$\Psi_\theta^L = \Psi_\theta^{11}(y=0=z) = -\frac{6}{5}\left(\frac{A_{L0} + B_{L0}R_T^{(0)} + C_{L0}/R_T^{(0)}}{A_{L1} + B_{L1}R_T^{(0)} + 40\alpha_2/R_T^{(0)} - 40\alpha_3}\right), \tag{2.52}$$

with the superscript L on Ψ_θ^L indicating the lowest-order analysis (that predicts orientational correlation). The expressions for A_{L0}, A_{L1}, B_{L0}, B_{L1} and C_{L0} are given in Appendix A of Supplementary Material to Chapter 2. This amounts to solving the coupled system of equations for $R_T(\tau)$ and $x(\tau)$, Eqs. (2.38)-(2.39), by removing all terms originating from higher-order Legendre coefficients b_{122} and b_{212} [see Eqs. (A.88, A.89) in Appendix A of Supplementary Material to Chapter 2]. In the following we shall compare Ψ_θ^L with the leading contribution Ψ^{11} (first term in Eq. (2.51)) of our higher-order analysis.

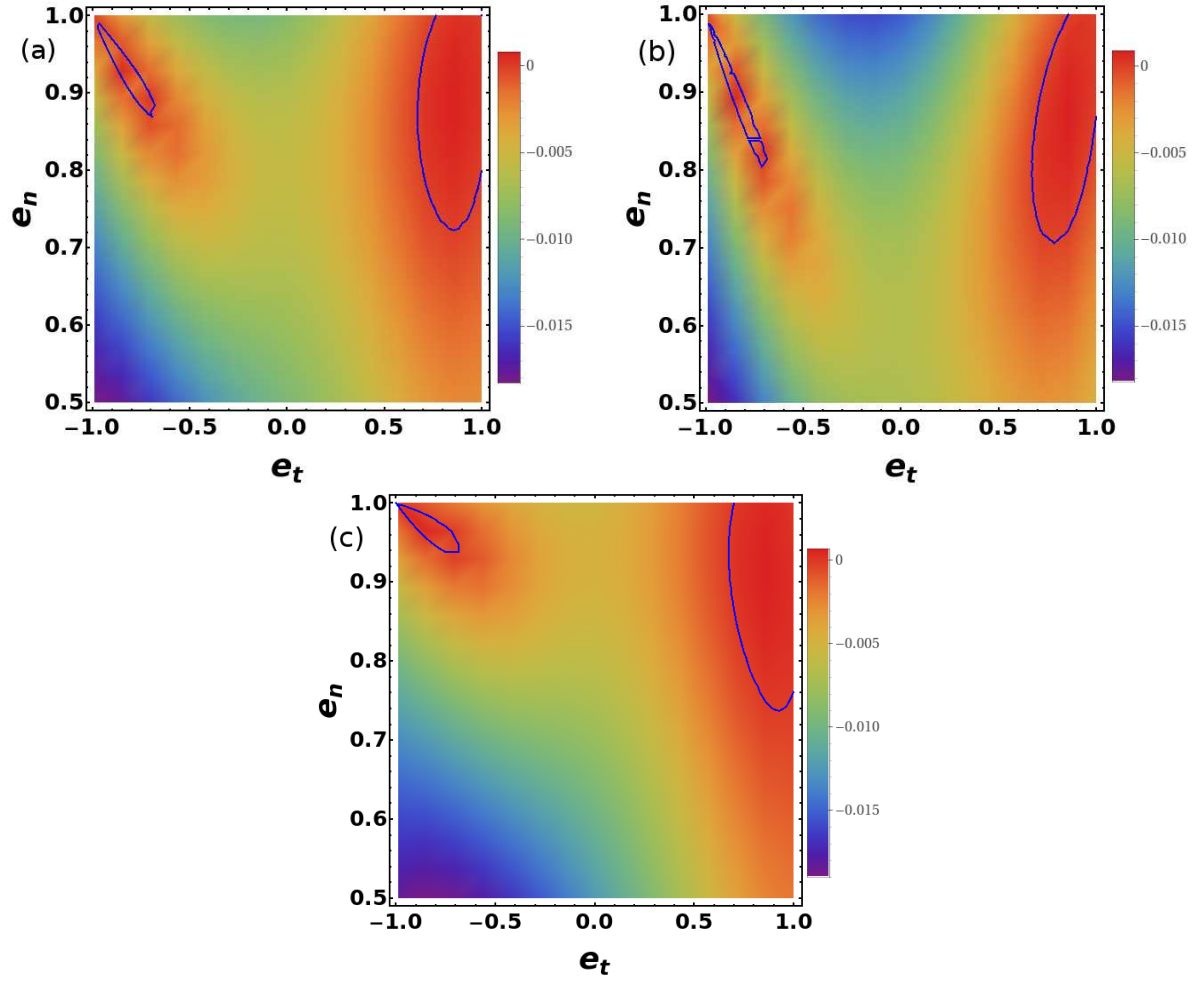

Figure 2.1: Steady total orientational correlation in the (e_n, e_t)-plane for for (a) $q = \frac{2}{5}$ (i.e. homogeneous spheres), (b) $q = \frac{1}{5}$, and (c) $q = \frac{2}{3}$ (i.e. spheres with mass-concentrated on it outer shell). Thick blue lines in each panel corresponds to parameter values of (e_n, e_t) at which orientational correlation vanishes and they demarcate the regions of positive and negative correlations; see text for details.

Numerical results on steady orientation correlation

Let us first analyze total correlation, Eq. (2.51), which depends on three parameters: the moment of inertia, q, of particles and the restitution coefficients (e_n, e_t). The total correlation $\Psi_\theta^H = \Psi_\theta^{11} + \Psi_\theta^{12} + \Psi_\theta^{21}$ as a function of two restitution coefficients (e_n, e_t) is displayed as color-maps in Figs. 2.1(a,b,c); each panel corresponds to a different value of the moment of inertia q. It is clear that the particle inertia has noticeable effects on the magnitude of Ψ_θ for $e_t \sim 0$ that corresponds to maximum dissipation at a given value of e_n. The regions enclosed by the blue lines correspond to positive correlations ($\Psi_\theta > 0$) and outside it to negative correlations ($\Psi_\theta < 0$). The region of positive correlation for nearly smooth particles ($e_t \sim -1$) is markedly affected by the moment of inertia, but the one for rough particles ($e_t \sim 1$) is less affected by changes in q. Recall that a positive/negative value of Ψ_θ implies a scenario of spinning rough particles (Brilliantov *et al.* 2007) behaving like "rifled" bullets (i.e. $\boldsymbol{c} \parallel \boldsymbol{\omega}$), or, "sliced" tennis balls (i.e. $\boldsymbol{c} \perp \boldsymbol{\omega}$), respectively. For most parameter values of (e_n, e_t), we find $\Psi_\theta < 0$ and therefore the directions of translational and rotational velocities of particles in the HCS of a rough granular gas tend to remain perpendicular like a sliced tennis ball. This conclusion mirrors that of Brilliantov *et al.* (2007) who considered only lowest-order correlation $\Psi^L \equiv \Psi^{11}(y = z = 0)$. This calls for a close scrutiny of higher-order correction terms.

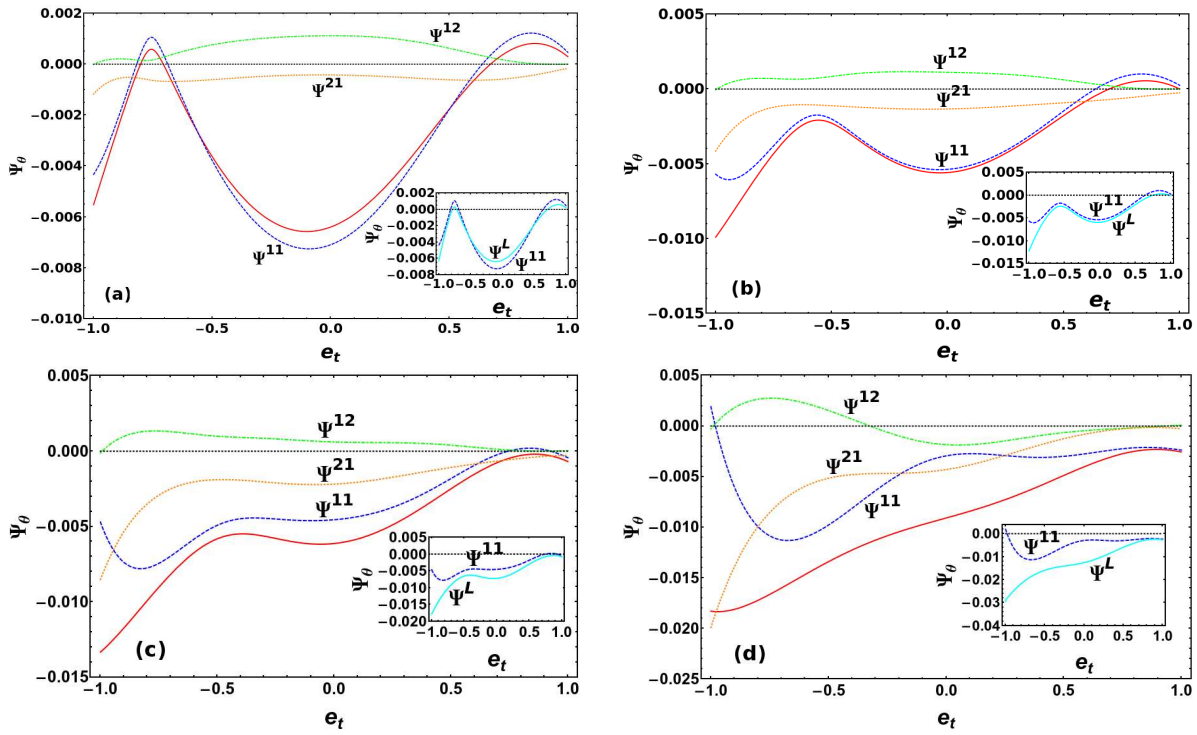

Figure 2.2: Effect of higher-order terms on the steady-state Ψ_θ as a function of tangential restitution coefficient e_t for the case of homogeneous spheres $q = \frac{2}{5}$: (a) $e_n = 0.9$, (b) $e_n = 0.8$, (c) $e_n = 0.7$ and (d) $e_n = 0.5$. While the blue dashed, green dot-dashed and orange dotted lines represent Ψ_θ^{11}, Ψ_θ^{12} and Ψ_θ^{21}, respectively, the red solid line represents total correlation $\Psi_\theta^H = \Psi_\theta^{11} + \Psi_\theta^{12} + \Psi_\theta^{21}$. The inset in each panel shows the variations of Ψ_θ^{11} (blue dashed line) and $\Psi_\theta^L \equiv \Psi^{11}(y = z = 0)$ (cyan solid line), see text for details. The horizontal black dotted line in each panel is a reference for zero correlation.

Now we analyze individual contributions of the leading term ($\Psi_\theta^{11} \propto b_{112}\langle \boldsymbol{c}^2\boldsymbol{\omega}^2\rangle$) and its next two higher-order terms ($\Psi_\theta^{12} \propto b_{122}\langle \boldsymbol{c}^2\boldsymbol{\omega}^4\rangle$ and $\Psi_\theta^{21} \propto b_{212}\langle \boldsymbol{c}^4\boldsymbol{\omega}^2\rangle$) to total correlation Ψ_θ^H,

focusing on the case of homogeneous spheres ($q = 2/5$) in Fig. 2.1(a). Fig. 2.2 shows the variations of steady Ψ_θ^H (red solid line), Ψ_θ^{11} (blue dashed line), Ψ_θ^{12} (green dot-dashed line), Ψ_θ^{21} (orange dotted line), with tangential restitution coefficient $e_t \in (-1, 1)$ for four values of the normal restitution coefficient ($e_n = 0.9$, 0.8, 0.7 and 0.5). In the quasi-elastic limit ($e_n \sim 1$, panel a), it is clear that the higher-order terms (Ψ^{12} and Ψ^{21}) have similar magnitude but of opposite sign and hence they cancel each other, leading to the total correlation being given approximately by its leading-order term (Ψ^{11}). However, with decreasing e_n (panels b, c and d), both Ψ^{12} and Ψ^{21} acquire different magnitudes and may have different signs depending on the value of the tangential restitution coefficient (e_t); for example, Ψ^{12} undergo a sign-change at $e_t \approx -0.3$ for $e_n = 0.5$ in panel d. Hence the total correlation differs noticeably from its leading correlation for highly inelastic systems ($e_n < 0.7$) due to the prominence of higher-order terms. This observation is also reflected in the insets in Fig. 2.2 where we have compared the leading-order contribution Ψ_θ^{11} (blue dashed line, first term of Eq. (2.51)) with the lowest-order correlation Ψ_θ^L (cyan solid line; this is same as that given by Brilliantov *et al.* (2007)) for the whole range of $e_t \in (-1, 1)$. We observe that Ψ_θ^L follows closely Ψ_θ^{11} at $e_n = 0.9$ (panel a) and $e_n = 0.8$ (panel b, except near $e_t \sim -1$), but Ψ_θ^L can differ significantly from Ψ_θ^{11} at $e_n = 0.7$ (panel c) and 0.5 (panel d) for a large range of tangential restitution coefficient $e_t < 0.5$. In all cases, the difference between Ψ_θ^L and Ψ_θ^{11} is very large near the smooth limit ($e_t \to -1$). The latter effect is presumably due to the strong coupling effect (that increases with increasing dissipation) among Ψ_θ^{11}, Ψ_θ^{12}, Ψ_θ^{21} and R_T via Eqs. (2.38)-(2.41) in our higher-order analysis.

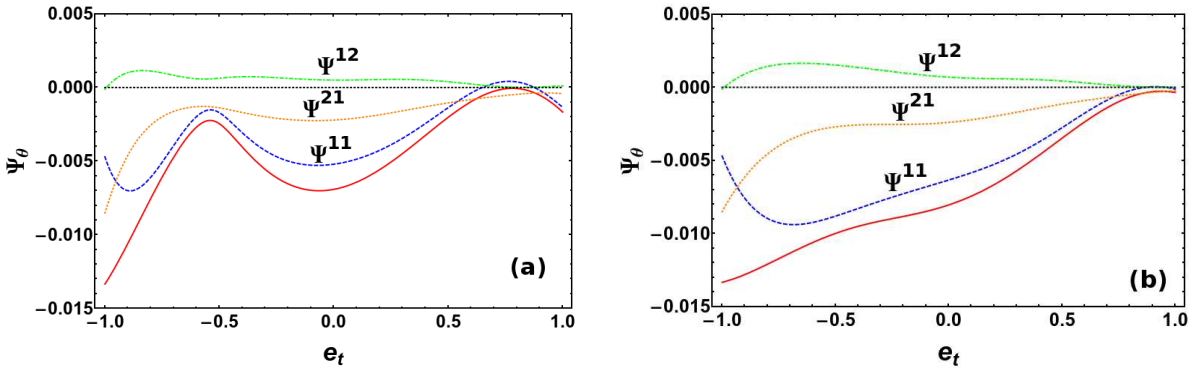

Figure 2.3: Same as Fig. 2.2(c), but for different values of the moment of inertia: (a) $q = 1/5$ and (b) $q = 2/3$. The red line corresponds to total correlation $\Psi_\theta = \Psi_\theta^{11} + \Psi_\theta^{12} + \Psi_\theta^{21}$, and other colored lines are marked. The horizontal black dotted line in each panel is a reference for zero correlation.

The effects of moment of inertia (q) on steady-state values of Ψ_θ, Ψ_θ^{11}, Ψ_θ^{12} and Ψ_θ^{21} can be ascertained from Figs. 2.3(a) and 2.3(b) for $q = 1/5$ and $q = 2/3$, respectively. The normal restitution coefficient is set to $e_n = 0.7$ as in Fig. 2.2(c) for which $q = 2/5$. Recall that $q = 2/5$ and 2/3 correspond to a homogeneous sphere (i.e. the mass is homogeneously distributed), and a sphere with its mass concentrated at its outer shell, respectively; $q \to 0$ represents a sphere with its mass concentrated near its centre. Comparing Figs. 2.3(a) and 2.3(b) with Fig. 2.2(c), we find that the moment of inertia has a noticeable effect on the leading-order correlation (Ψ^{11}, blue dashed lines); in particular, $\Psi^{11} > 0$ for a small range of e_t (near the perfectly rough limit of $e_t \sim 1$) for $q = 1/5$ but it becomes negative for increasing values of $q = 2/5$ and 2/3. Among

two higher-order corrections, the variations of Ψ^{12} (> 0) and Ψ^{21} (< 0) with e_t remain similar even if q is different, only the respective magnitude increases slightly with increasing q (compare green and orange lines in panels a and b). In all cases, the contribution of Ψ^{12} (this term is proportional to $\langle \boldsymbol{c}^2\boldsymbol{\omega}^4\rangle$ in Legendre expansion, Eqs. (2.21) and (2.26)) to total correlation is the least for this parameter combination.

Implications of present higher-order analysis and non-Gaussian corrections

Here we attempt a qualitative comparison between the predictions of our higher-order theory with previous direct simulation Monte Carlo (DSMC) data of Brilliantov *et al.* (2007) as given in their Fig. 2 for steady correlation; note that their tangential restitution coefficient should be replaced by $-e_t$ to match our definition (Eq. (2.2)). Focusing on the data for $e_n = 0.9$, we find that the curve representing our higher-order prediction for orientational correlation [Ψ^{11}, see the inset in Fig. 2.2(a)] lies above the lower-order theory of Brilliantov *et al.* (2007) in the limit of perfectly rough particles ($e_t \to 1$) at which there is positive correlation for a range of e_t. The DSMC data (blue squares in Fig. 2 of Brilliantov *et al.* (2007)) also indicates larger positive correlations (compared to their theory) in agreement with present higher-order analysis. Focusing on the limit of perfectly smooth particles ($e_t \to -1$), the curve representing our prediction as well as the DSMC data lie above the predictions of Brilliantov *et al.* (2007) as seen in the inset of Fig. 2.2(a). For intermediate values of $e_t \in (-0.5, 0.5)$, our prediction indicates a larger negative correlation than that of Brilliantov *et al.* and this is also in qualitative agreement with their simulation (although the DSMC data can differ from our theory by more than 50% at $e_t \sim 0$). The above features of qualitative comparison between our theory and previous simulation (Brilliantov *et al.* 2007) also hold at a higher dissipation of $e_n = 0.8$, although the quantitative disagreement worsens with further decreasing e_n. This in turn suggests that other effects like non-Gaussian corrections [Pöschel & Luding (2001); Brilliantov & Pöschel (2004)] are likely to be important in predicting orientational correlation which might provide a fair comparison of the simulation data with a complete higher-order theory.

The recent work of Reyes *et al.* (2014) clarified that the non-Gaussian Sonine corrections (incorporating only lowest-order Legendre term) have important effects on orientational correlation as well as on hydrodynamics. Their theoretical predictions agree well with particle simulation in the perfectly rough limit up-to a tangential restitution coefficient of $e_t \geq -0.5$, however, the non-convergence issue remains near the perfectly smooth limit ($e_t \sim -1$) as in the present study. The interaction between higher-order angular corrections and the above non-Gaussian Sonine corrections remains unexplored and is recommended for a future work.

2.3.2 Relaxation to Steady-state: Orientational Correlation and the Role of Temperature Ratio

In this section we present results on the time evolution of orientational correlation $\Psi_\theta(\tau)$, Eq. (2.43), and temperature ratio $R_T(\tau)$. The differential equations (2.38)-(2.41) are integrated in time with specified initial conditions on $x(0), y(0), z(0)$ and $R_T(0)$. At large enough time ($\tau \to \infty$), all four fields reach a steady state from which one can calculate steady values of the

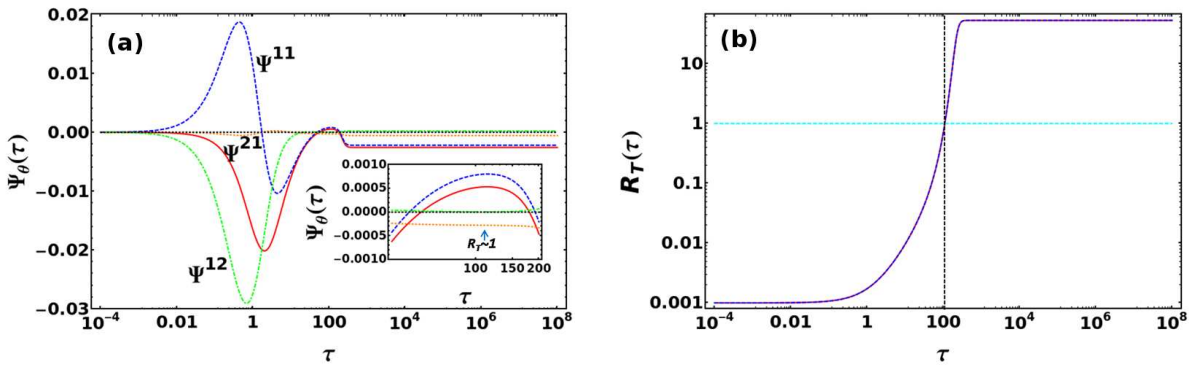

Figure 2.4: Relaxation of (a) orientational correlation $\Psi_\theta(\tau)$ and (b) temperature ratio $R_T(\tau)$ for $q = \frac{2}{5}$, $e_n = 0.9$ and $e_t = -0.9$. Initial conditions are of vanishing correlations $[x(0) = y(0) = z(0) = 0]$ and $R_T(0) = 0.001$. The blue dashed, green dot-dashed and orange dotted lines represent Ψ_θ^{11}, Ψ_θ^{12} and Ψ_θ^{21}, respectively, the red solid line represents total correlation $\Psi_\theta^H = \Psi_\theta^{11} + \Psi_\theta^{12} + \Psi_\theta^{21}$. The black dotted horizontal line in panel a is a reference for zero correlation; the arrow in its inset locates the time τ at which $R_T \approx 1$.

orientational correlation which has been checked with the approximate solution, Eqs. (2.46)-(2.48), given in the previous section. Here our focus is to understand how correlation builds up during the transient stage and the related driving factors that decide the final steady state.

First we solve equations (2.38)-(2.41) numerically with initial conditions of $x(0) = y(0) = z(0) = 0$ and $R_T(0) = 0.001$; this corresponds to an "unbiased" initial condition of zero correlation $[\Psi(0) \equiv \Psi^{11}(0) + \Psi^{12}(0) + \Psi^{21}(0) = 6x(0)/5 + 6y(0) + 6z(0) = 0]$. Starting from such an initial state of zero correlation, Fig. 2.4(a) shows the time-evolution of Ψ^{11} (blue dashed line), Ψ^{12} (green dot-dashed line), Ψ^{21} (orange dotted line) and the total correlation Ψ (red line). The parameter values are as in Fig. 2.2(a) with $e_t = -0.9$ (i.e. nearly smooth particles). Recall from Eq. (2.36) that the dimensionless time τ measures time in terms of the average number of collisions that each particle has encountered. It is seen from Fig. 2.4(a) that the steady state (constancy of Ψ) is reached after about 500 collisions. [For perfectly smooth particles $e_t = -1$, the translational and rotational degrees of freedom are decoupled from each other and hence the closer the value of e_t is to -1, the larger the time to reach a steady state.] It is noteworthy that although the final state is characterized by a negative value of $\Psi^\infty \approx -0.004$, the total correlation and its components can become positive and negative during their transient evolution.

The corresponding evolution of temperature ratio $R_T(\tau)$ is shown in Fig. 2.4(b). Note that two curves for $R_T(\tau)$ with and without higher-order corrections are indistinguishable from each other, implying that such higher-order "angular" corrections do not have noticeable effect on the steady state of $R_T(\tau \to \infty)$ as well as on its transient evolution. Physically, the relaxation of $R_T(\tau)$ is tied to the transfer of energy from translational to rotational degrees of freedom and vice versa upon inter-particle collisions. Another point to note in Fig. 2.4(b) is that the time to reach the steady state for $R_T(\tau)$ is almost the same as that for orientational correlation Ψ_θ. Comparing Fig. 2.4(a) and Fig. 2.4(b), we find that when the temperature ratio, during its transient evolution, becomes close to unity (i.e. the energy is equally partitioned between translational and rotational motions) at $\tau \sim 100$, correlations become very small (close to zero)

[see the inset in Fig. 2.4(a)] – this was pointed out by Brilliantov *et al.* (2007) and seems to persist even with higher-order corrections. It takes little longer to reach the final state of energy non-equipartition $R_T^{\infty} \sim 50$, and the correlations also evolve during this final transient-stage to eventually reach its steady negative value at $\tau \sim 200$.

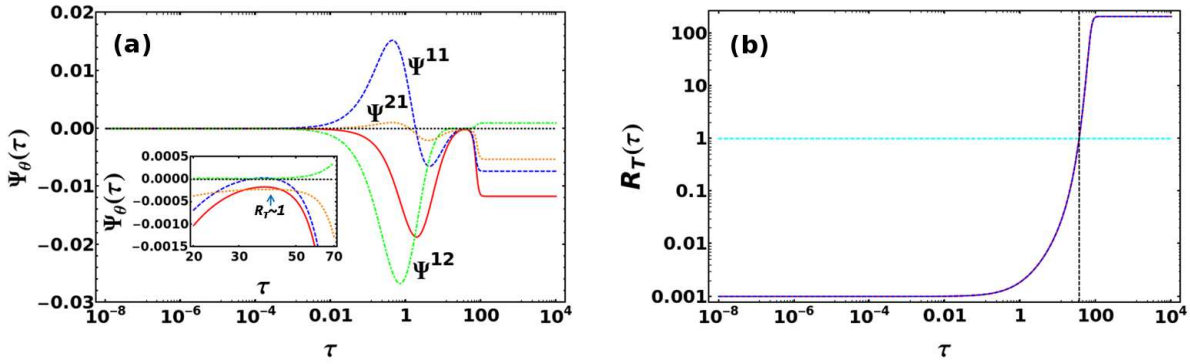

Figure 2.5: Same as Fig. 2.4 but for $e_n = 0.7$. The arrow in the inset of panel *a* locates the time τ at which $R_T \approx 1$.

The above overall features of orientational correlation and temperature ratio hold at other values of e_n too, see Fig. 2.5 which is an analog of Fig. 2.4 for $e_n = 0.7$. With increasing dissipation, the time to reach steady state decreases ($\tau \sim 100$) as expected. More importantly, the building-up of orientational correlation and its possible connection with the evolution of $R_T(\tau)$ seems to hold for this case too as found from a comparison of the time-scale in the inset of Fig. 2.5(a) with that at $R_T = 1$ in Fig. 2.5(b).

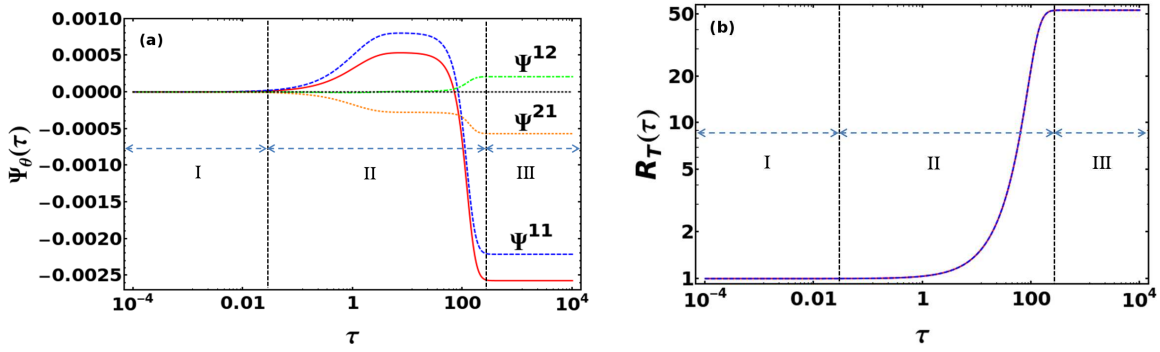

Figure 2.6: Same as Fig. 2.4 but with different initial condition on temperature ratio: $R_T(0) = 1$. Other parameters are same as in Fig. 2.4.

To verify the above connection, we solve equations (2.38)-(2.41) with zero initial correlation [$x(0) = y(0) = z(0) = 0$], but the initial temperature-ratio is now set to $R_T(0) = 1$ that corresponds to equipartition of energy at the initial state of the granular gas. The results are shown in Fig. 2.6(a,b), with identical parameters as in Fig. 2.4. We find three stages over which temporal evolution occurs: (I) almost nothing happens up-to a small time of $\tau \equiv \tau_{\rm I} \sim 0.01$, with nearly zero correlation and energy equipartition; (II) correlations develop slowly beyond some time $\tau = \tau_{\rm II} > 0.02$ as the temperature ratio increases departing from its initial state of

equipartition; (III) the steady state is reached beyond a larger time $\tau = \tau_{\rm III} \sim 200$. It is clear that the relaxation of all fields occurs during stage-II and $\tau = \tau_{\rm III}$ can be equated with relaxation time. Interestingly, however, the total correlation (Ψ^H, red line) and its leading contribution (Ψ^{11}, blue dashed line) go from a positive value to negative at $\tau \sim 100$ when the energy is strongly non-equipartitioned ($R_T \sim 20$). Therefore, the occurrence of energy equipartition ($R_T(\tau) = 1$) and negligible/zero orientational correlation ($\Psi(\tau) \sim 0$) simultaneously during transient evolution depends on the initial state of the granular gas.

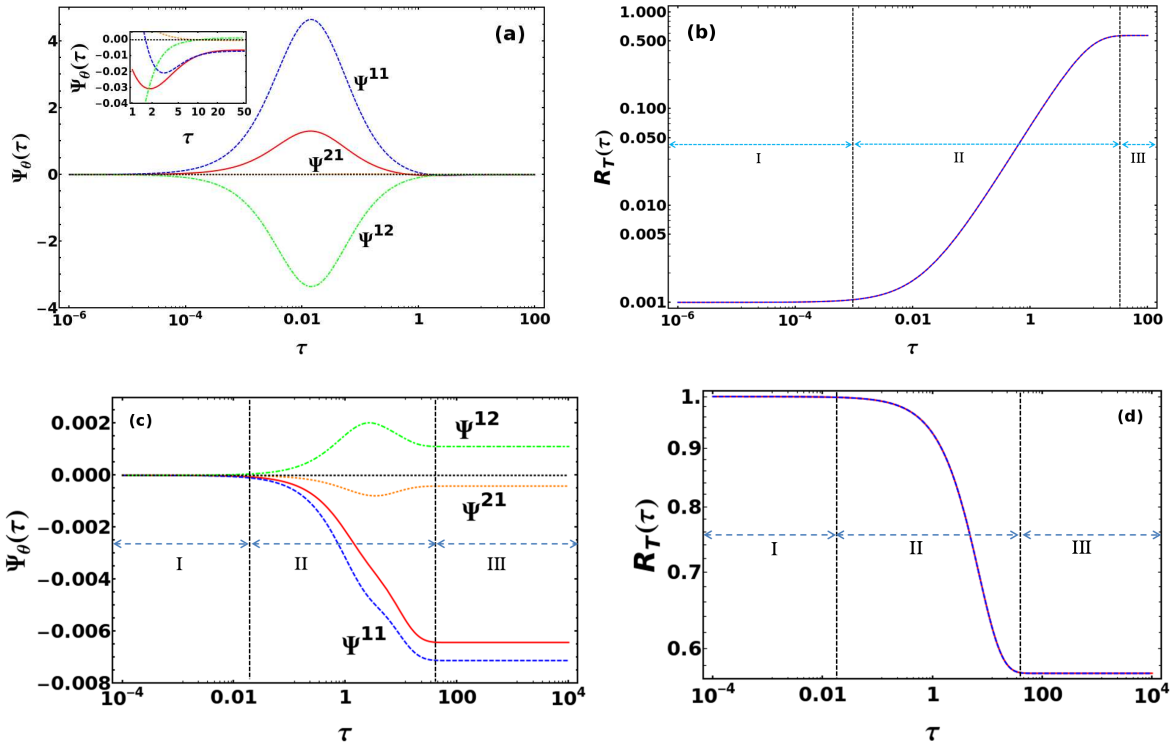

Figure 2.7: Relaxation of (a,c) orientational correlation $\Psi_\theta(\tau)$ and (b,d) temperature ratio $R_T(\tau)$ for $e_t = 0$; other parameters as in Fig. 2.4. Initial conditions are of vanishing correlation [$x(0) = y(0) = z(0) = 0$], with $R_T(0) = 0.001$ (panels a, b) and $R_T(0) = 1$ (panels c, d).

The above findings also hold when the particles are made rougher (i.e. for larger values of e_t). A set of representative results on the temporal evolution of $\Psi(\tau)$ and $R_T(\tau)$ is shown in Figs. 2.7(a,b) for a larger value of the tangential restitution coefficient $e_t = 0$, with other parameters as well as initial conditions [$x(0) = y(0) = z(0) = 0$ and $R_T(0) = 0.001$] are same as in Fig. 2.4. Panel b and the inset of panel a indicate that the system reaches a steady state at $\tau \sim 20$ which is much smaller than the relaxation time for $e_t = -0.9$ ($\tau \sim 200$, Fig. 2.4) – this is expected since R_T relaxes at a faster rate due to the strong coupling between translational and rotational motions at $e_t = 0$ than the case of nearly smooth particles $e_t = -0.9$. It is noteworthy from the inset of Fig. 2.7(a) that the total and leading correlations (Ψ^{11} and Ψ^H) decreases from positive to negative values at $\tau \sim 1$ when the system is strongly non-equipartitioned ($R_T \sim 0.1$). For this case, the final temperature ratio is $R_T \sim 0.6 < 1$. With identical parameters as in Fig. 2.7(a,b) but with an initial condition of $R_T(0) = 1$ (equipartition), the results on the relaxation of correlations and temperature ratio are displayed in Fig. 2.7(c,d). It is observed that R_T

decreases monotonically to its final state of $R_T \sim 0.6$ and the correlations also follow three distinct temporal-stages [I, II and III as marked in Fig. 2.7(c)]; the relaxation of all fields occur during the stage-II of their temporal evolutions, irrespective of initial conditions. Comparing orientational correlations in Figs. 2.7(a,c), we find that Ψ^{11}, Ψ^{12}, Ψ^{21} and Ψ^{H} have opposite signs and vastly different magnitudes, depending on initial conditions, during the stage-II of their evolution, but they all settle to the same final steady state in stage-III [see the inset of Fig. 2.7(a) and Fig. 2.7(c)]. It is clear from these figures that the relaxation time ($\tau = \tau_{\rm III} \sim 25$ and ~ 45 in Fig. 2.7(a,b) and Fig. 2.7(c,d), respectively) depends crucially on the initial condition.

2.4 Summary and Conclusions

The orientational/directional correlation between translational and rotational velocities, defined as the mean-square of the cosine of the angle between translational and rotational velocity of particles, was analyzed for the homogeneous cooling state (HCS) of a rough granular gas in an effort to assess certain higher-order effects on the related dynamical fields. A two parameter collision model in terms of normal ($0 \le e_n \le 1$) and tangential ($-1 \le e_t \le 1$) restitution coefficients was used to account for the energy loss due to inelasticity and roughness, respectively, of particles. Ignoring non-Gaussian corrections, an approximate form for the single-particle velocity distribution function was chosen by incorporating angular correlation in terms of Legendre polynomials. The evolution equations for the translational and spin temperatures and the first three Legendre coefficients were derived starting from the pseudo-Liouville operator with molecular chaos assumption. This coupled set of differential equations was solved to calculate orientational correlation as a function of normal and tangential restitution coefficients and the moment of inertia of particles. The effects of quadratic- and quartic-order terms (in both translational and rotational velocities of particles) in the Legendre expansion were critically assessed on the steady state of correlations and the related relaxation dynamics.

We found that the leading-order contribution (Ψ^{11}) to steady-state orientational correlation can differ noticeably from the analysis of Brilliantov *et al.* (2007) that incorporates only the lowest-order term and this effect is more prominent for nearly smooth particles ($e_t \sim -1$). The deviation increases with decreasing normal restitution coefficient ($e_n < 0.9$), especially for $e_t < 0.5$. This is due to the strong coupling effect (that increases with dissipation) among Ψ^{11}, Ψ^{12}, Ψ^{21} and R_T via Eqs. (2.38)-(2.41) in our higher-order analysis. In comparison to its value for the lowest-order analysis (Brilliantov *et al.* 2007), the total orientational correlation ($\Psi^{H} = \sum_{i,j=1,2} \Psi^{ij}$), including higher-order corrections, increases/decreases for quasi-elastic ($e_n \sim 1$) or dissipative ($e_n < 0.9$) collisions, respectively. The transient dynamics of correlations is strongly affected by the higher-order terms. In particular we found that the time evolution of the leading-order correlation $\Psi^{11}(\tau)$ can differ from that of $\Psi^{L}(\tau)$ (Brilliantov *et al.* 2007) not only in magnitude but also in its sign during the transient phase [compare Figs. 2.4(a) and 2.6(a) as well as Figs. 2.7(a) and 2.7(c)] even in the quasi-elastic limit ($e_n \sim 1$). We showed that the simultaneous occurrence of energy equipartition ($R_T(\tau) = 1$) and negligible/zero orientational correlation ($\Psi^{ij}(\tau) \sim 0$) during their transient evolution depends on the initial state of the granular gas.

The higher-order correlations (Ψ^{12} and Ψ^{21}) are found to have similar magnitude but of

opposite sign in the quasi-elastic limit ($e_n \to 1$) and hence they cancel each other, leading to the total correlation being given by its leading-order value (Ψ^{11}) as seen in the inset of Fig. 2.2(a) for $e_n = 0.9$. This suggests that higher-order "angular" corrections may be neglected in developing a hydrodynamic theory for a rough granular gas in the quasi-elastic limit but they should be retained for very dissipative particles.

A recent work (Reyes *et al.* 2014) indicates non-Gaussian corrections may have important bearing on orientational correlation as well as on hydrodynamics. In a future work non-Gaussian corrections [Pöschel & Luding (2001); Brilliantov & Pöschel (2004)] to distribution function, including the present quartic-order angular terms, should be analyzed. As clarified in Sec. 2.3.1, such an analysis is also required to make a fair comparison with results from particle simulations. Within the present setup, however, this is a formidable analytical task and is beyond the scope of this chapter. Another direction of research would be to analyze the same problem with a more realistic collision model that includes Coulomb/sliding friction [Jenkins & Zhang (2002); Goldhirsch *et al.* (2005); Gayen & Alam (2011)]; simulations on shear flow (Gayen & Alam 2011) clarified that Coulomb friction has non-trivial effects on orientational correlation and temperature ratio.

An important issue (not considered in this chapter) is the "asymptotic" nature of the adopted expansion [Eq. (2.18)] whose convergence properties need to be checked in a future work via Shanks transformation or Padé approximation. This issue is discussed in detail in the latter part of Chapter 3 that deals with a similar asymptotic expansion technique to analyse acceleration-driven Poiseuille flow.

Chapter 3

Bulk Hydrodynamics and Rheology of Acceleration-Driven Poiseuille Flow via BGK Kinetic Model

3.1 Introduction

Poiseuille flow, one of the well-known classical problems in fluid dynamics, was first studied by Jean Léonard Marie Poiseuille (Poiseuille 1847) and Gotthilf Heinrich Ludwig Hagen (Hagen 1839) in the 19th century. Poiseuille flow of a gas through a channel/pipe can be generated by the action of uniform pressure gradient or uniform body force (e.g., gravity), and has gotten much consideration from both computational (Mansour *et al.* (1997), Travis *et al.* (1997), Todd & Evans (1997), Risso & Cordero (1998), Alam *et al.* (2015)) and theoretical (Alaoui & Santos (1992), Tij & Santos (1994), Tij *et al.* (1998), Risso & Cordero (1998), Uribe & Garcia (1999), Hess & Mansour (1999), Tij & Santos (2001), Aoki *et al.* (2002), Sabbane *et al.* (2003), Tij & Santos (2004), Pareschi *et al.* (2006)) points of view.

In this chapter, the gravity-driven Poiseuille flow of hard spheres is analysed for a dilute molecular gas in the framework of kinetic theory by using a perturbation expansion of the velocity distribution function in powers of the strength of gravitational acceleration by retaining terms up to tenth-order. The Boltzmann collision operator is approximated by a BGK kinetic model by retaining terms up to tenth-order in Froude number. Using the high-order expansion for hard spheres, analytical expressions have been derived for the hydrodynamic fields and their fluxes (pressure tensor and heat flux vector) which are used to assess the asymptotic nature of the perturbation expansion, and the related convergence issues constitute the main focus of the present work. It must be noted that the original work of Tij & Santos (1994) analysed the same acceleration-driven Poiseuille flow by focusing on Maxwell molecules (in contrast to a hard-sphere gas in the present work)– we have also extended their calculations for Maxwell molecules up to tenth-order (in dimensionless gravity) which are briefly discussed at the end of this chapter (Section 3.7).

Rarefaction effects such as (i) the bimodal shape of the temperature profile, (ii) tangential heat flux, (iii) normal stress differences are analysed in detail using presently obtained high-order series solutions. It must be noted that the bimodality of the temperature profile was originally predicted by Tij & Santos (1994) and later confirmed numerically by Mansour *et al.* (1997). It is found that the temperature bimodality shows oscillating behaviour for Froude numbers greater than 10^{-3} which indicates the divergent nature of the series expansion. Subsequently, the Shanks transformation and the Padé approximations have been used to further analyse the convergence of the adopted series expansion. One goal of this analysis is to estimate the range

of validity of asymptotic series solutions in terms of Knudsen or Froude numbers.

3.2 Kinetic Theory Description: Boltzmann equation

In kinetic theory description, the state of the molecular gas is specified by a single particle distribution function $f(\boldsymbol{x}, \boldsymbol{c}; t)$ which characterizes the spatial and velocity distribution of individual particles. In other words, all the relevant physical knowledge about the gas is contained in $f(\boldsymbol{x}, \boldsymbol{c}; t)$. The time evolution of single-particle distribution $f(\boldsymbol{x}, \boldsymbol{c}; t)$ obeys the Boltzmann equation which is the master equation in the kinetic theory of rarefied gases derived by Ludwig Boltzmann in 1872. Here, we consider a dilute molecular gas composed of smooth hard spheres of diameter σ, and mass m. The Boltzmann equation for one-particle velocity distribution function $f(\boldsymbol{x}, \boldsymbol{c}; t)$ in the dilute regime reads

$$\left(\partial_t + \boldsymbol{c} \cdot \boldsymbol{\nabla} + \boldsymbol{g} \cdot \frac{\partial}{\partial \boldsymbol{c}}\right) f = J[f, f], \tag{3.1}$$

where $\boldsymbol{g}$ is the acceleration due to an external force and $J[f, f]$ is the Boltzmann collision operator, which measures the rate of change of f due to binary collisions. For hard-sphere molecules, the explicit form of collision operator is given by

$$J[f, f] \;=\; \sigma^2 \int d\boldsymbol{c}_1 \int d\hat{\boldsymbol{\sigma}}\; \Theta(\boldsymbol{c}_{01} \cdot \hat{\boldsymbol{\sigma}})(\boldsymbol{c}_{01} \cdot \hat{\boldsymbol{\sigma}})\; [f(\boldsymbol{c}'')f(\boldsymbol{c}_1'') - f(\boldsymbol{c})f(\boldsymbol{c}_1)]. \tag{3.2}$$

In Eq. (3.2), Θ represents the Heaviside step function, $\hat{\boldsymbol{\sigma}}$ is a unit vector directed along the center of the particle without index to the particle with index 1 at contact, $\boldsymbol{c}_{01} = \boldsymbol{c} - \boldsymbol{c}_1$ is the relative velocity, and the pre-collisional velocities $\boldsymbol{c}''$ and $\boldsymbol{c}_1''$ are given in terms of post-collisional velocities $\boldsymbol{c}$ and $\boldsymbol{c}_1$ by

$$\boldsymbol{c}'' = \boldsymbol{c} - (\boldsymbol{c}_{01} \cdot \hat{\boldsymbol{\sigma}})\hat{\boldsymbol{\sigma}},\;\; \boldsymbol{c}_1'' = \boldsymbol{c}_1 + (\boldsymbol{c}_{01} \cdot \hat{\boldsymbol{\sigma}})\hat{\boldsymbol{\sigma}}. \tag{3.3}$$

To determine the macroscopic state of a dilute gas it is sufficient to have the knowledge of single-particle distribution function f. The macroscopic field variables, namely, the number density n, the flow velocity $\boldsymbol{u}$, and the temperature T are defined via the zeroth, first and second moments of the distribution function, respectively, and are given by

$$\begin{pmatrix} n(\boldsymbol{x}, t) \\ n(\boldsymbol{x}, t)\; \boldsymbol{u}(\boldsymbol{x}, t) \\ n(\boldsymbol{x}, t)\; k_B\; T(\boldsymbol{x}, t) \end{pmatrix} = \int d\boldsymbol{c} \begin{pmatrix} 1 \\ \boldsymbol{c} \\ \frac{m}{3} C^2 \end{pmatrix} f(\boldsymbol{x}, \boldsymbol{c}; t), \tag{3.4}$$

where $\boldsymbol{C} = \boldsymbol{c} - \boldsymbol{u}$ is the peculiar velocity and k_B is the Boltzmann constant which is set to one. The macroscopic transport equations for the local densities of mass, momentum, and energy follow directly from Eq. (3.1) by taking velocity moments:

$$D_t n + n \boldsymbol{\nabla} \cdot \boldsymbol{u} = 0, \tag{3.5}$$

$$D_t \boldsymbol{u} + \frac{1}{mn} \boldsymbol{\nabla} \cdot \boldsymbol{P} = \boldsymbol{g}, \tag{3.6}$$

$$D_t T + \frac{2}{3n} (\boldsymbol{\nabla} \cdot \boldsymbol{q} + \boldsymbol{P} : \boldsymbol{\nabla} \boldsymbol{u}) = 0, \tag{3.7}$$

where $D_t \equiv \partial_t + \boldsymbol{u} \cdot \boldsymbol{\nabla}$ is the material time derivative,

$$\boldsymbol{P}(\boldsymbol{x}, t) = m \int d\boldsymbol{c}\, \boldsymbol{C}\boldsymbol{C} f(\boldsymbol{x}, \boldsymbol{c}; t) \tag{3.8}$$

is the pressure or stress tensor, and

$$\boldsymbol{q}(\boldsymbol{x}, t) = \frac{m}{2} \int d\boldsymbol{c}\, C^2 \boldsymbol{C} f(\boldsymbol{x}, \boldsymbol{c}; t) \tag{3.9}$$

is the heat flux vector.

3.3 Gravity-driven Poiseuille Flow of a Molecular Gas

The Poiseuille flow of a molecular gas corresponds to a steady flow along a long channel or tube of constant cross-section driven by an imposed pressure difference across the ends of the channel/tube. During the last few decades, this problem has been analyzed by replacing pressure differences by a constant external field, namely, the gravitational acceleration (g), and the same effects are obtained like earlier [Tij & Santos (1994, 2004); Alaoui & Santos (1992); Aoki *et al.* (2002)]. Here we consider the "acceleration-driven" Poiseuille flow confined in a planar channel geometry. We assume that the molecular gas, composed of hard-sphere particles, is enclosed between two infinite parallel plates normal to the y-axis, which are at stationary – the schematic geometry of the present problem is shown in Fig. 3.1. A constant external force per unit mass (e.g., gravity) $\boldsymbol{g} = -g\hat{\boldsymbol{x}}$ is applied along a direction $\hat{\boldsymbol{x}}$ parallel to the plates. Our analysis is restricted in the bulk of the channel around its mid-plane ($y = 0$) since we do not incorporate wall-effects in the present analysis.

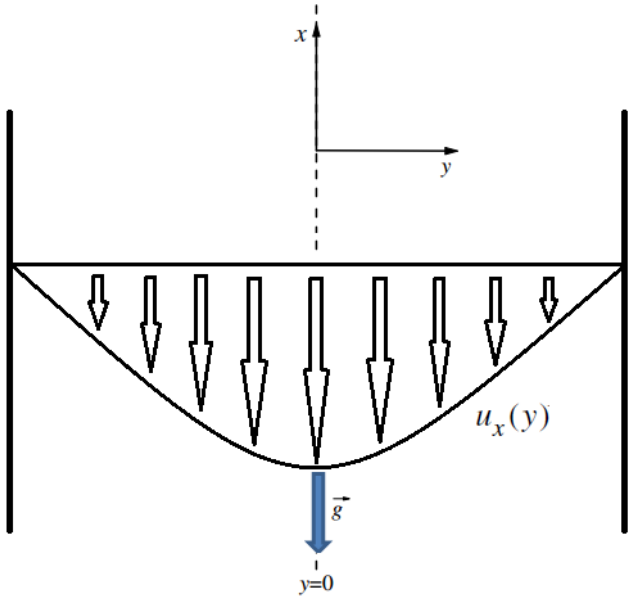

Figure 3.1: Schematic of the gravity-driven planar Poiseuille flow.

A steady fully developed flow can be expected in which the physical/hydrodynamic quantities

depend only on the coordinate y and the flow velocity is parallel to the x-axis, $\boldsymbol{u} = u_x(y)\hat{\boldsymbol{x}}$. For the present steady flow configuration, the Boltzmann equation (3.1) takes the following form

$$\left(- g\frac{\partial}{\partial c_x} + c_y\frac{\partial}{\partial y}\right) f = J[f, f]. \tag{3.10}$$

Similarly, under the steady $[\partial/\partial t(\cdot) = 0]$ and fully developed $[\partial/\partial y(\cdot) \neq 0$, but $\partial/\partial x(\cdot) = 0 = \partial/\partial z(\cdot)]$ flow conditions, the basic conservation equations for momentum (Eq. (3.6)) and energy (Eq. (3.7)), reduce to

$$\frac{\partial P_{yy}}{\partial y} = 0, \tag{3.11}$$

$$\frac{\partial P_{yx}}{\partial y} = -\rho g, \tag{3.12}$$

$$P_{yx}\frac{\partial u_x}{\partial y} + \frac{\partial q_y}{\partial y} = 0, \tag{3.13}$$

where $\rho = mn$ is the mass density.

3.4 Kinetic Model and Solution via Perturbation Expansion

Any attempt to solve the Boltzmann equation analytically for a particular flow problem will encounter difficulties with the Boltzmann collision operator $J[f, f]$. Due to the mathematical complexity of the Boltzmann collision operator $J[f, f]$ and to avoid the intricacy in the perturbation analysis, here we employ the simple well-known kinetic model called Bhatnagar-Gross-Krook (BGK) kinetic model [Bhatnagar *et al.* (1954)] of the Boltzmann equation. In BGK kinetic model the detailed Boltzmann collision term $J[f, f]$ is replaced by a single-time relaxation term of the form

$$J[f, f] \to -\nu(f - f_l), \tag{3.14}$$

where ν is the collision frequency and f_l is the local Maxwellian distribution which are given by,

$$\nu = n\sigma^2\sqrt{\frac{T}{m}}\frac{4\Omega_3}{5\sqrt{\pi}}, \quad \Omega_3 = \frac{2\pi^{3/2}}{\Gamma(3/2)}, \tag{3.15}$$

$$f_l(\boldsymbol{x}, \boldsymbol{c}; t) = n(\boldsymbol{x}, t)\left[\frac{m}{2\pi T(\boldsymbol{x}, t)}\right]^{3/2} \exp\left[- \frac{m(\boldsymbol{c} - \boldsymbol{u}(\boldsymbol{x}, t))^2}{2T(\boldsymbol{x}, t)}\right]. \tag{3.16}$$

The Navier-Stokes transport coefficients (i.e. shear viscosity (η), thermal conductivity (κ) and Dufour coefficient (μ)) derived from the BGK kinetic model (3.14) are (Santos 2003):

$$\eta = \frac{p}{\nu}, \quad \kappa = \frac{5}{2}\frac{p}{m\nu}, \quad \mu = 0. \tag{3.17}$$

With the help of BGK kinetic model (3.14), the kinetic equation (3.10) reads

$$\left(- g\frac{\partial}{\partial c_x} + c_y\frac{\partial}{\partial y}\right) f = -\nu(f - f_l). \tag{3.18}$$

We express the non-equilibrium distribution function f as

$$f = f_l(1+\Phi), \tag{3.19}$$

where Φ is the deviation from the local equilibrium distribution. The subsequent analysis in this section closely follows the original work of Tij & Santos (1994).

Using the above expansion (3.19) for f, Eq. (3.18) becomes (for derivation, see Sec. §B.1)

$$\begin{aligned}(1+\Phi)\left[C_y\tilde{\partial}_y \log f_l - \left(g + C_y\frac{\partial u_x}{\partial y}\right)\frac{\partial}{\partial C_x}\log f_l\right] \;=\; \\ \left(g + C_y\frac{\partial u_x}{\partial y}\right)\frac{\partial}{\partial C_x}\Phi - C_y\tilde{\partial}_y\Phi - \nu\Phi,\end{aligned} \tag{3.20}$$

where the operator $\tilde{\partial}_y$ is defined via

$$\tilde{\partial}_y \equiv \frac{\partial}{\partial y} + (\frac{\partial u_x}{\partial y})\frac{\partial}{\partial C_x} \tag{3.21}$$

with respect to y at constant $\boldsymbol{C}$. Since we are interested about the solution of Eq. (3.20) in the "bulk" region (around the centerline of the channel, see Fig. 3.1), it is convenient to consider the state at the channel center $y = 0$ as a reference state. Using this reference state, the following dimensionless quantities are introduced:

$$\boldsymbol{C}^* = \frac{\boldsymbol{C}}{c_0}, \quad y^* = \frac{y\nu_0}{c_0}, \quad f_l^* = \frac{f_l c_0^3}{n_0}, \tag{3.22}$$

$$p^* = \frac{p}{p_0}, \quad \boldsymbol{u}^* = \frac{\boldsymbol{u}}{c_0}, \quad T^* = \frac{T}{T_0}, \quad g^* = \frac{g}{\nu_0 c_0}, \tag{3.23}$$

$$\nu^* = \frac{\nu}{\nu_0}, \quad \boldsymbol{P}^* = \frac{\boldsymbol{P}}{p_0}, \quad \boldsymbol{q}^* = \frac{\boldsymbol{q}}{p_0 c_0}, \tag{3.24}$$

where the subscript 0 denotes quantities evaluated at $y = 0$. In particular,

$$c_0 = \sqrt{\frac{2T_0}{m}} \tag{3.25}$$

is the thermal velocity (c_{th}) at $y = 0$. Note that the dimensionless quantities y^* and g^* measure (i) the distance in units of a nominal mean free path and (ii) the strength of the gravity field on a particle moving with the thermal velocity along a distance of the order of the mean free path, respectively. In terms of non-dimensionlized units, the kinetic equation (3.20) becomes

$$(1+\Phi)\left[C_y^*\tilde{\partial}_{y^*}\log f_l^* + \frac{2C_x^*}{T^*}\left(g^* + C_y^*\frac{\partial u_x^*}{\partial y^*}\right)\right] \;=\; \left(g^* + C_y^*\frac{\partial u_x^*}{\partial y^*}\right)\frac{\partial}{\partial C_x^*}\Phi - C_y^*\tilde{\partial}_{y^*}\Phi - \nu^*\Phi,$$

In terms of particle velocity this can be written as

$$\begin{aligned}(1+\Phi)\left[c_y^*\tilde{\partial}_{y^*}\log f_l^* + \frac{2(c_x^* - u_x^*)}{T^*}\left(g^* + c_y^*\frac{\partial u_x^*}{\partial y^*}\right)\right] \;=\; \\ \left(g^* + c_y^*\frac{\partial u_x^*}{\partial y^*}\right)\frac{\partial}{\partial c_x^*}\Phi - c_y^*\tilde{\partial}_{y^*}\Phi - \nu^*\Phi,\end{aligned} \tag{3.26}$$

where

$$\tilde{\partial}_{y^*} \log f_l^* = \frac{\partial \log p^*}{\partial y^*} + \left(\frac{{C^*}^2}{T^*} - \frac{5}{2}\right)\frac{\partial \log T^*}{\partial y^*}. \tag{3.27}$$

Our main aim is to solve Eq. (3.26) to high-orders in g^* and get the associated hydrodynamic profiles at each order. Here, all the quantities will be understood to be expressed in dimensionless units and, for simplicity, the asterisks will be dropped in the subsequent analysis.

3.4.1 Perturbation Expansion

The perturbation expansion of Φ in powers of external force field $g = g^*$ is

$$\Phi = \sum_{i=1}^{10} \Phi^{(i)} g^i + O(g^{11}), \tag{3.28}$$

In the absence of gravity, the solution of Eq. (3.18) is $f = f_l$ with uniform $n, \boldsymbol{u}$, and T. The expansions for the hydrodynamic field variables have the forms

$$p = 1 + \sum_{i=1}^{5} p^{(2i)} g^{2i} + O(g^{12}), \tag{3.29}$$

$$u_x = \sum_{i=1}^{5} u^{(2i-1)} g^{2i-1} + O(g^{11}), \tag{3.30}$$

$$T = 1 + \sum_{i=1}^{5} T^{(2i)} g^{2i} + O(g^{12}). \tag{3.31}$$

Due to the symmetry of the problem, p and T are even functions of g, while u_x is an odd function of g. Further, without loss of generality, we assume that $u_0 = 0$, i.e., we are performing a Galilean transformation to a reference frame moving with the fluid at $y = 0$.

Since the collision frequency for the hard-sphere molecules (Cercignani (1988), Chapman & Cowling (1970)) is $\nu = pT^{-1/2}$, we can write

$$\begin{aligned}
\nu &= 1 + \left(p^{(2)} - \frac{1}{2}T^{(2)}\right)g^2 + \left(p^{(4)} - \frac{p^{(2)}T^{(2)}}{2} + \frac{3}{8}{T^{(2)}}^2 - \frac{T^{(4)}}{2}\right)g^4 \\
&\quad + \left(p^{(6)} - \frac{p^{(4)}T^{(2)}}{2} + \frac{3p^{(2)}{T^{(2)}}^2}{8} - \frac{5{T^{(2)}}^3}{16} - \frac{p^{(2)}T^{(4)}}{2} + \frac{3T^{(2)}T^{(4)}}{4} - \frac{T^{(6)}}{2}\right)g^6 \\
&\quad + \left(p^{(8)} - \frac{p^{(6)}T^{(2)}}{2} + \frac{3p^{(4)}{T^{(2)}}^2}{8} - \frac{5p^{(2)}{T^{(2)}}^3}{16} + \frac{35{T^{(2)}}^4}{128} - \frac{p^{(4)}T^{(4)}}{2} + \frac{3p^{(2)}T^{(2)}T^{(4)}}{4}\right. \\
&\quad \left. - \frac{15{T^{(2)}}^2T^{(4)}}{16} + \frac{3{T^{(4)}}^2}{8} - \frac{p^{(2)}T^{(6)}}{2} + \frac{3T^{(2)}T^{(6)}}{4} - \frac{T^{(8)}}{2}\right)g^8 + O(g^{10}), \\
&= 1 + \nu^{(2)}g^2 + \nu^{(4)}g^4 + \nu^{(6)}g^6 + \nu^{(8)}g^8 + O(g^{10}),
\end{aligned} \tag{3.32}$$

where

$$\nu^{(2)} = p^{(2)} - \frac{1}{2}T^{(2)}, \tag{3.33}$$

$$\nu^{(4)} = p^{(4)} - \frac{p^{(2)}T^{(2)}}{2} + \frac{3}{8}T^{(2)^2} - \frac{T^{(4)}}{2}, \tag{3.34}$$

$$\nu^{(6)} = p^{(6)} - \frac{p^{(4)}T^{(2)}}{2} + \frac{3p^{(2)}T^{(2)^2}}{8} - \frac{5T^{(2)^3}}{16} - \frac{p^{(2)}T^{(4)}}{2} + \frac{3T^{(2)}T^{(4)}}{4} - \frac{T^{(6)}}{2}, \tag{3.35}$$

$$\begin{aligned}\nu^{(8)} \;=\; & p^{(8)} - \frac{p^{(6)}T^{(2)}}{2} + \frac{3p^{(4)}T^{(2)^2}}{8} - \frac{5p^{(2)}T^{(2)^3}}{16} + \frac{35T^{(2)^4}}{128} - \frac{p^{(4)}T^{(4)}}{2} + \frac{3p^{(2)}T^{(2)}T^{(4)}}{4} \\ & - \frac{15T^{(2)^2}T^{(4)}}{16} + \frac{3T^{(4)^2}}{8} - \frac{p^{(2)}T^{(6)}}{2} + \frac{3T^{(2)}T^{(6)}}{4} - \frac{T^{(8)}}{2}.\end{aligned} \tag{3.36}$$

In order to solve Eq. (3.26) at each order, one needs to satisfy the following consistency conditions

$$\int d\boldsymbol{C} f_l \Phi = 0, \tag{3.37}$$

$$\int d\boldsymbol{C} C_y f_l \Phi = 0, \tag{3.38}$$

$$\int d\boldsymbol{C} C_x f_l \Phi = 0, \tag{3.39}$$

$$\int d\boldsymbol{C} C^2 f_l \Phi = 0. \tag{3.40}$$

To solve Eq. (3.26), we are going to adopt a heuristic procedure followed in previous works of Tij and Santos [Tij & Santos (1994, 2004)]. The solution method of Tij and Santos to Eq. (3.26) is as follows: (i) guess the hydrodynamic profiles and then (ii) verify the consistency of assumed solutions using consistency conditions [Eq. (3.37) - Eq. (3.40)].

3.4.2 Solution procedure at odd-order in g

The equation (3.26), at odd-order in g yields

$$(1 - \mathscr{A})\Phi^{(2i-1)} = \text{known function of} \, u^{(2i-1)} \equiv \phi^{(2i-1)}, \tag{3.41}$$

where $\mathscr{A}$ is the operator

$$\mathscr{A} = -c_y \frac{\partial}{\partial y}. \tag{3.42}$$

At this order, the expression for $\phi^{(2i-1)}$ depends only on velocity due to the symmetry of the problem and its space dependence occurs through $u^{(2i-1)}$, which remains unknown so far. In order to solve the governing equation at odd-order in g [Eq. (3.41)], using the method of Tij and Santos [Tij & Santos (1994, 2004)], firstly, we guess the velocity profile. Next, the formal solution to Eq. (3.41) is $\Phi^{(2i-1)} = \sum_{k=0}^{\infty} \mathscr{A}^k \phi^{(2i-1)}$ and the functional structure of $\mathscr{A}^k \phi^{(2i-1)}$ persists to be the same for any k. This suggests the form of the trial function for $\Phi^{(2i-1)}$. Later, one can find the precise form of $\Phi^{(2i-1)}$ by inserting its trial form into Eq. (3.41) and verifying the consistency conditions [Eq. (3.37) - Eq. (3.40)]. Once the expression for $\Phi^{(2i-1)}$ is known explicitly, one can obtain the associated hydrodynamic profiles at odd orders.

3.4.3 Solution procedure at even-order in g

The equation (3.26) at even-order in g yields

$$(1-\mathscr{A})\Phi^{(2i)} = \text{known function of}\, p^{(2i)}\ \&\ T^{(2i)} \equiv \phi^{(2i)}, \tag{3.43}$$

At this order, the expression for $\phi^{(2i)}$ depends on pressure p and temperature T as these are even functions of g and its space dependence occurs through $p^{(2i)}$ and $T^{(2i)}$, which remains unknown so far. In order to solve the governing equation at even-order in g [Eq. (3.43)], we use the same heuristic procedure used by Tij and Santos [Tij & Santos (1994, 2004)]. First, we guess the pressure and temperature profiles; secondly, the form of trial function for $\Phi^{(2i)}$ is to be assumed. With above assumptions, we get the explicit expression for $\Phi^{(2i)}$ from which one can find the expressions for the associated hydrodynamic profiles at even orders.

3.4.4 Solution at first-order in g

At first-order in g, Eq. (3.26) yields

$$(1-\mathscr{A})\Phi^{(1)} = -2c_x\left(1 + c_y\frac{\partial u^{(1)}}{\partial y}\right) \equiv \phi^{(1)}. \tag{3.44}$$

The function $\phi^{(1)}$ has a known velocity dependence. Its space dependence occurs through $u^{(1)}$, which remains unknown so far. In order to solve the governing equation (3.44), we follow the procedure discussed in §3.4.2. In the process of solving Eq. (3.44), firstly, we guess that the first-order velocity profile is parabolic:

$$u^{(1)}(y) = u_2^{(1)} y^2. \tag{3.45}$$

Next, we note that the formal solution to Eq. (3.44) is $\Phi^{(1)} = \sum_{k=0}^{\infty}\mathscr{A}^k\phi^{(1)}$ and that the functional structure of $\mathscr{A}^k\phi^{(1)}$ remains the same for any k. Consequently, the solution to Eq. (3.44) must have the following trial structure,

$$\Phi^{(1)}(y,\boldsymbol{c}) = c_x\,(a_0 \,+\, a_1\,c_y^2 \,+\, a_2\,c_y\,y), \tag{3.46}$$

where a_0, a_1, a_2 are the coefficients, which are obtained by insertion of Eq. (3.46) into Eq. (3.44) and the explicit values of these coefficients are

$$\left.\begin{array}{rcl} a_0 &=& -2, \\ a_1 &=& 4\,u_2^{(1)}, \\ a_2 &=& -4\,u_2^{(1)}. \end{array}\right\} \tag{3.47}$$

Now substituting Eq. (3.46) into the consistency condition (3.39), we can determine the coefficient $u_2^{(1)}$ to be

$$u_2^{(1)} = 1. \tag{3.48}$$

The other consistency conditions (3.37), (3.38), and (3.40) are verified through symmetry. Fi-

nally, we get the explicit form of $\Phi^{(1)}$ to be

$$\Phi^{(1)}(y,\boldsymbol{c}) = 2\,c_x\,(2\,c_y^2\;-\;2\,c_y\,y-\;1). \tag{3.49}$$

With the help of Eq. (3.49), we can find the "non-zero" components of the fluxes to first-order in g which are given by

$$P_{yx}^{(1)}(y) = -2\,y, \tag{3.50}$$

$$q_x^{(1)}(y) = 1. \tag{3.51}$$

3.4.5 Solution at second-order in g

To second-order in g, Eq. (3.26) yields an equation for $\Phi^{(2)}$ as follows

$$\begin{aligned}(1-\mathscr{A})\Phi^{(2)} \;=\; & \left[\frac{\partial}{\partial c_x} - 2c_x\left(1+c_y\frac{\partial u^{(1)}}{\partial y}\right)\right]\Phi^{(1)} - c_y\left[\frac{\partial p^{(2)}}{\partial y} + \left(c^2-\frac{5}{2}\right)\frac{\partial T^{(2)}}{\partial y}\right] \\ & +2u^{(1)}\left(1+c_y\frac{\partial u^{(1)}}{\partial y}\right) \equiv \phi^{(2)}.\end{aligned} \tag{3.52}$$

From the above expression, we see that the function $\phi^{(2)}$ has a known dependence on pressure and temperature; its space dependence occurs through $p^{(2)}$ and $T^{(2)}$, which are unknown so far. Here, the governing equation (3.52) is solved using the procedure discussed in §3.4.3. In the process of solving Eq. (3.52), we guess the pressure and temperature profiles:

$$p^{(2)}(y) = p_2^{(2)}y^2, \tag{3.53}$$

$$T^{(2)}(y) = T_2^{(2)}y^2 + T_4^{(2)}y^4. \tag{3.54}$$

The structure of $\mathscr{A}^k\phi^{(2)}$ suggests the trial function of the form

$$\begin{aligned}\Phi^{(2)}(y,\boldsymbol{c}) \;=\; & b_0 + b_1c_y^2 + b_2c_yy + b_3y^2 + b_4c_y^4 + b_5c_y^3y + b_6c_y^2y^2 + b_7c_yy^3 \\ & +c_x^2\big(b_8 + b_9c_y^2 + b_{10}c_yy + b_{11}y^2 + b_{12}c_y^4 + b_{13}c_y^3y + b_{14}c_y^2y^2\big) \\ & +c^2\big(b_{15} + b_{16}c_y^2 + b_{17}c_yy + b_{18}y^2 + b_{19}c_y^4 + b_{20}c_y^3y \\ & +b_{21}c_y^2y^2 + b_{22}c_yy^3\big).\end{aligned} \tag{3.55}$$

Insertion of Eq. (3.55) into Eq. (3.52) allows one to get the coefficients b_i's in terms of $p_2^{(2)}, T_2^{(2)}$, and $T_4^{(2)}$. Here, the consistency condition (3.39) is verified via symmetry, while the consistency condition (3.38) is identically fulfilled irrespective of the values of $p_2^{(2)}, T_2^{(2)}$, and $T_4^{(2)}$. The other consistency conditions (3.37) and (3.40) yield

$$p_2^{(2)} = \frac{24}{5}, \quad T_2^{(2)} = \frac{76}{25}, \quad T_4^{(2)} = -\frac{4}{15}. \tag{3.56}$$

Substituting values of $p_2^{(2)}, T_2^{(2)}$, and $T_4^{(2)}$ into the expressions of the coefficients b_i's, we get

$$\begin{aligned} &b_0 = -2, \quad b_1 = \frac{32}{5}, \quad b_2 = -\frac{12}{5}, \quad b_3 = 2, \quad b_4 = -8, \quad b_5 = 8, \quad b_6 = -4, \quad b_7 = \frac{4}{3}, \\ &b_8 = 4, \quad b_9 = -24, \quad b_{10} = 16, \quad b_{11} = 0, b_{12} = 48, \quad b_{13} = -48, \quad b_{14} = 16, \quad b_{15} = 0, \\ &b_{16} = \frac{152}{25}, \quad b_{17} = -\frac{152}{25}, \quad b_{18} = 0, \quad b_{19} = -\frac{32}{5}, \quad b_{20} = \frac{32}{5}, \quad b_{21} = -\frac{16}{5}, \quad b_{22} = \frac{16}{15}. \end{aligned} \tag{3.57}$$

If we substitute the values of $b_i, p_2^{(2)}, T_2^{(2)}$, and $T_4^{(2)}$ into the solution (3.55), we get the explicit functional form of $\Phi^{(2)}$ as:

$$\begin{aligned} \Phi^{(2)}(y, \boldsymbol{c}) \quad = \quad & -\frac{2}{75}(240c_y^6 - 240c_y^5 y - 75(-1 + 2c_x^2 + y^2) - 8c_y^3 y(9 + 30c_z^2 - 195c_x^2 + 5y^2) \\ & +24c_y^4(3 + 10c_z^2 - 65c_x^2 + 5y^2) - 2c_y y(5(-9 + 5y^2) + 2c_z^2(-57 + 10y^2) \\ & +2c_x^2(93 + 10y^2)) + 6c_y^2(5(-8 + 5y^2) - 16c_x^2(-7 + 5y^2) \\ & +c_z^2(-38 + 20y^2))). \end{aligned} \tag{3.58}$$

Now, using this form of $\Phi^{(2)}$, we can calculate the second-order contributions to the flux fields which are given by

$$P_{yy}^{(2)} = -\frac{612}{25}, \tag{3.59}$$

$$P_{xx}^{(2)}(y) = \frac{656}{25} + \frac{56}{5}y^2, \tag{3.60}$$

$$q_y^{(2)}(y) = \frac{4}{3}y^3. \tag{3.61}$$

Note that other flux terms [$P_{xy}^{(2)}$ and $q_x^{(2)}$] at second-order are zero.

3.4.6 Solution at third-order in g

The equation for $\Phi^{(3)}$ which yields from equation (3.26) is

$$\begin{aligned} (1 - \mathscr{A})\Phi^{(3)} \quad = \quad & \left[\frac{\partial}{\partial c_x} - 2c_x\left(1 + c_y\frac{\partial u^{(1)}}{\partial y}\right)\right]\Phi^{(2)} + \left[2u^{(1)}\left(1 + c_y\frac{\partial u^{(1)}}{\partial y}\right) - \left(p^{(2)} - \frac{T^{(2)}}{2}\right)\right. \\ & \left. -c_y\left(\frac{\partial p^{(2)}}{\partial y} + \left(c^2 - \frac{5}{2}\right)\frac{\partial T^{(2)}}{\partial y}\right)\right]\Phi^{(1)} \\ & +2c_x\left[T^{(2)} + u^{(1)}c_y\frac{\partial T^{(2)}}{\partial y} + c_y\left(T^{(2)}\frac{\partial u^{(1)}}{\partial y} - \frac{\partial u^{(3)}}{\partial y}\right)\right] \equiv \phi^{(3)}. \end{aligned} \tag{3.62}$$

Following the solution procedure at odd-order in g [see §3.4.2], we guess the velocity profile to be

$$u^{(3)}(y) = u_2^{(3)}y^2 + u_4^{(3)}y^4 + u_6^{(3)}y^6. \tag{3.63}$$

Next, the structure of $\mathscr{A}^k\phi^{(3)}$ suggests the trial function to be

$$\begin{aligned}\Phi^{(3)}(y,\boldsymbol{c}) &= c_x\big(c_0c_y^8+c_1c_x^2+c_2+c_3c_y y^5+c_y^6(c_4c_x^2+c_5)+c_z^2(c_6c_y^6+c_7c_y^2+c_8c_y^4+c_9)\\
&+c_y^2(c_{10}c_x^2+c_{11})+c_y^4(c_{12}c_x^2+c_{13})+y^2(c_{14}c_y^6+c_{15}+c_{16}c_x^2+c_y^4(c_{17}c_x^2+c_{18})\\
&+c_z^2(c_{19}c_y^4+c_{20}c_y^2+c_{21})+c_y^2(c_{22}c_x^2+c_{23}))+y(c_{24}c_y^7+c_y^3(c_{25}c_x^2+c_{26})\\
&+c_z^2(c_{27}c_y^5+c_{28}c_y+c_{29}c_y^3)+c_y^5(c_{30}c_x^2+c_{31})+c_y(c_{32}c_x^2+c_{33}))\\
&+y^3(c_{34}c_y^5+c_z^2(c_{35}c_y+c_{36}c_y^3)+c_y^3(c_{37}c_x^2+c_{38})+c_y(c_{39}c_x^2+c_{40}))\\
&+y^4(c_{41}c_y^4+c_{42}c_x^2+c_{43}+c_y^2(c_{44}c_x^2+c_{45})+c_z^2(c_{46}c_y^2+c_{47}))\big).\end{aligned}\tag{3.64}$$

The unknown coefficients c_i's in the above equation (3.64) can be obtained in terms of $u_2^{(3)}, u_4^{(3)}$ and $u_6^{(3)}$ by substituting Eq. (3.64) into Eq. (3.62). By using consistency conditions, we found the values of $u_2^{(3)}, u_4^{(3)}$ and $u_6^{(3)}$ to be

$$u_2^{(3)}=\frac{10904}{25},\quad u_4^{(3)}=\frac{43}{5},\quad u_6^{(3)}=\frac{14}{225}.\tag{3.65}$$

Using $u_2^{(3)}, u_4^{(3)}$ and $u_6^{(3)}$ into the expressions of the coefficients c_i's, we get the explicit values of the coefficients c_i's:

$$\begin{aligned}&c_0=-384,\quad c_1=-8,\quad c_2=12,\quad c_3=-\frac{256}{75},\quad c_4=576,\quad c_5=\frac{3168}{25},\quad c_6=-384,\\
&c_7=-\frac{912}{25},\quad c_8=\frac{5248}{25},\quad c_9=0,\quad c_{10}=\frac{1488}{25},\quad c_{11}=\frac{42096}{25},\quad c_{12}=-\frac{6752}{25},\\
&c_{13}=\frac{12336}{25},\quad c_{14}=-\frac{896}{5},\quad c_{15}=\frac{116}{25},\quad c_{16}=0,\quad c_{17}=\frac{1024}{5},\quad c_{18}=\frac{1056}{25},\\
&c_{19}=-\frac{896}{5},\quad c_{20}=\frac{1696}{25},\quad c_{21}=0,\quad c_{22}=-\frac{704}{25},\quad c_{23}=\frac{4104}{25},\quad c_{24}=384,\\
&c_{25}=\frac{4672}{25},\quad c_{26}=-\frac{2032}{5},\quad c_{27}=384,\quad c_{28}=\frac{608}{25},\quad c_{29}=-\frac{4928}{25},\quad c_{30}=-576,\\
&c_{31}=-\frac{2848}{25},\quad c_{32}=-\frac{592}{25},\quad c_{33}=-\frac{43312}{25},\quad c_{34}=\frac{256}{5},\quad c_{35}=-\frac{64}{15},\quad c_{36}=\frac{256}{5},\\
&c_{37}=-\frac{64}{5},\quad c_{38}=-\frac{32}{5},\quad c_{39}=-\frac{64}{15},\quad c_{40}=-\frac{3712}{75},\quad c_{41}=-\frac{128}{15},\quad c_{42}=0,\\
&c_{43}=-\frac{4}{15},\quad c_{44}=-\frac{128}{15},\quad c_{45}=\frac{88}{15},\quad c_{46}=-\frac{128}{15},\quad c_{47}=0.\end{aligned}\tag{3.66}$$

Substituting the values of c_i's, $u_2^{(3)}, u_4^{(3)}$, and $u_6^{(3)}$ into the solution (3.64), we obtain the explicit functional form of $\Phi^{(3)}$ as

$$\begin{aligned}\Phi^{(3)}(y,\boldsymbol{c}) &= \frac{4}{75}c_x(225-7200c_y^8-150c_x^2+7200c_y^7y+87y^2-5y^4+24c_y^5y(-89+300c_z^2\\
&-450c_x^2+40y^2)-24c_y^6(-99+300c_z^2-450c_x^2+140y^2)-12c_y^3y(635+10y^2\\
&+c_z^2(308-80y^2)+4c_x^2(-73+5y^2))-4c_yy(8121+232y^2+16y^4\\
&+2c_z^2(-57+10y^2)+c_x^2(111+20y^2))-4c_y^4(-2313-198y^2+40y^4\\
&+c_x^2(1266-960y^2)+24c_z^2(-41+35y^2))-2c_y^2(-15786-1539y^2-55y^4\\
&+c_z^2(342-636y^2+80y^4)+c_x^2(-558+264y^2+80y^4))).\end{aligned}\tag{3.67}$$

Finally, the above expression of $\Phi^{(3)}$ [Eq. (3.67)] is used to calculate third-order contributions to the fluxes. The expressions for flux fields at third-order in g are given by

$$P_{yx}^{(3)} = -\frac{8y^3\left(11+y^2\right)}{75}, \tag{3.68}$$

$$q_x^{(3)} = -\frac{42018}{25} - \frac{3158}{25}y^2 - \frac{114}{15}y^4, \tag{3.69}$$

$$P_{xx}^{(3)} = 0 = P_{yy}^{(3)} = q_y^{(3)}. \tag{3.70}$$

3.4.7 Solution at fourth-order in g

Up to fourth-order in g, Eq. (3.26) for $\Phi^{(4)}$ is given by

$$\begin{aligned}(1-\mathscr{A})\Phi^{(4)} \;=\; & \left[\frac{\partial}{\partial c_x} - 2c_x\left(1+c_y\frac{\partial u^{(1)}}{\partial y}\right)\right]\Phi^{(3)} + \left[2u^{(1)}\left(1+c_y\frac{\partial u^{(1)}}{\partial y}\right) - \left(p^{(2)} - \frac{T^{(2)}}{2}\right)\right. \\ & \left. -c_y\left(\frac{\partial p^{(2)}}{\partial y} + \left(c^2-\frac{5}{2}\right)\frac{\partial T^{(2)}}{\partial y}\right)\right]\Phi^{(2)} \\ & + \left[2c_x\left(T^{(2)} + c_y\left(u^{(1)}\frac{\partial T^{(2)}}{\partial y} + \frac{\partial u^{(1)}}{\partial y}T^{(2)} - \frac{\partial u^{(3)}}{\partial y}\right)\right)\right]\Phi^{(1)} \\ & + \left[\left(2u^{(3)} - 2T^{(2)}u^{(1)}\right)\left(1+c_y\frac{\partial u^{(1)}}{\partial y}\right) + 2c_y u^{(1)}\frac{\partial u^{(3)}}{\partial y} - c_y\left(\frac{\partial}{\partial y}\left(p^{(4)} - \frac{{p^{(2)}}^2}{2}\right)\right.\right. \\ & \left.\left. + \left(\frac{\partial}{\partial y}\left(T^{(4)} - \frac{{T^{(2)}}^2}{2}\right)\right)\left(c^2-\frac{5}{2}\right) + \frac{\partial T^{(2)}}{\partial y}\left({u^{(1)}}^2 - T^{(2)}c^2\right)\right)\right] \equiv \phi^{(4)}. \end{aligned} \tag{3.71}$$

To obtain the solution at this fourth-order in g, we follow the procedure presented in §3.4.3. As a first step in the procedure, the pressure and temperature profiles are taken as

$$p^{(4)}(y) = p_2^{(4)}y^2 + p_4^{(4)}y^4 + p_6^{(4)}y^6, \tag{3.72}$$

$$T^{(4)}(y) = T_2^{(4)}y^2 + T_4^{(4)}y^4 + T_6^{(4)}y^6 + T_8^{(4)}y^8. \tag{3.73}$$

With the help of the trial form of $\Phi^{(4)}$, we solve the equation (3.71) which allows to represent unknown coefficients in the trail function $\Phi^{(4)}$ in terms of $p_2^{(4)}, p_4^{(4)}, p_6^{(4)}, T_2^{(4)}, T_4^{(4)}, T_6^{(4)}$ and $T_8^{(4)}$. Further by using trail function $\Phi^{(4)}$ and consistency conditions, we found the values of $p_2^{(4)}, p_4^{(4)}, p_6^{(4)}, T_2^{(4)}, T_4^{(4)}, T_6^{(4)}$ and $T_8^{(4)}$. The explicit values of these are

$$p_2^{(4)} = -\frac{2523696}{125}, \quad p_4^{(4)} = -\frac{15008}{125}, \quad p_6^{(4)} = \frac{64}{125}, \tag{3.74}$$

$$T_2^{(4)} = -\frac{199914896}{3125}, \quad T_4^{(4)} = -\frac{1287016}{1875}, \quad T_6^{(4)} = -\frac{34768}{5625}, \quad T_8^{(4)} = -\frac{248}{7875}. \tag{3.75}$$

Finally, the explicit expression of $\Phi^{(4)}$ can be obtained by substituting the values of $p_2^{(4)}, p_4^{(4)}, p_6^{(4)}$, $T_2^{(4)}, T_4^{(4)}, T_6^{(4)}$ and $T_8^{(4)}$ into the trail solution. The exact expression of $\Phi^{(4)}$ is given by (B.18), which is provided in Appendix B as a supplementary material to this chapter. From the explicit

form of $\Phi^{(4)}$ (B.18), one can calculate fourth-order contributions to the fluxes as given by

$$P_{yy}^{(4)} = \frac{1171581312}{3125}, \tag{3.76}$$

$$P_{xx}^{(4)} = \frac{16\left(-200059248 - 23078925y^2 - 132150y^4 + 700y^6\right)}{9375}, \tag{3.77}$$

$$q_y^{(4)} = \frac{8y^3\left(190820 + 4669y^2 + 45y^4\right)}{2625}. \tag{3.78}$$

3.4.8 Solution at fifth-order in g

The governing equation for $\Phi^{(5)}$ can be obtained from the equation (3.26) and is given by Eq. (B.4) of Appendix B. The final solution to Eq. (B.4) is obtained by following the procedure discussed in §3.4.2. The explicit functional form of $\Phi^{(5)}$ is given by the equation (B.19) in Appendix B. At fifth-order in g, the velocity profile is given by

$$u^{(5)}(y) = u_2^{(5)}y^2 + u_4^{(5)}y^4 + u_6^{(5)}y^6 + u_8^{(5)}y^8 + u_{10}^{(5)}y^{10}, \tag{3.79}$$

where

$$\begin{aligned} u_2^{(5)} &= -\frac{86923879504}{3125}, \quad u_4^{(5)} = -\frac{24094924}{125}, \\ u_6^{(5)} &= -\frac{7375666}{28125}, \quad u_8^{(5)} = \frac{12643}{5625}, \quad u_{10}^{(5)} = \frac{4318}{354375}. \end{aligned} \tag{3.80}$$

Further, with the help of solution $\Phi^{(5)}$ [see Eq. (B.19)], fifth-order contributions to the flux fields are calculated and are given by

$$P_{yx}^{(5)} = -\frac{16y^3\left(3232431468 + 24850287y^2 + 200970y^4 + 2525y^6\right)}{1771875}, \tag{3.81}$$

$$q_x^{(5)} = \frac{2\left(22886907186402 + 969620988042y^2 + 6897708825y^4 + 9292990y^6 - 117225y^8\right)}{196875} \tag{3.82}$$

3.4.9 Solution at sixth-order in g

The governing equation for $\Phi^{(6)}$ and its solution is given by Eq. (B.7) and Eq. (B.20), respectively, and are presented in supplementary material to this Chapter as Appendix B. At this order, the guessed pressure and temperature profiles are given by

$$p^{(6)}(y) = p_2^{(6)}y^2 + p_4^{(6)}y^4 + p_6^{(6)}y^6 + p_8^{(6)}y^8 + p_{10}^{(6)}y^{10}, \tag{3.83}$$

$$T^{(6)}(y) = T_2^{(6)}y^2 + T_4^{(6)}y^4 + T_6^{(6)}y^6 + T_8^{(6)}y^8 + T_{10}^{(6)}y^{10} + T_{12}^{(6)}y^{12}, \tag{3.84}$$

where $p_2^{(6)}, p_4^{(6)}, p_6^{(6)}, p_8^{(6)}, p_{10}^{(6)}, T_2^{(6)}, T_4^{(6)}, T_6^{(6)}, T_8^{(6)}, T_{10}^{(6)}$ and $T_{12}^{(6)}$ are coefficients which are found to be

$$\begin{aligned}
&p_2^{(6)} = \frac{411361184764608}{78125}, \quad p_4^{(6)} = \frac{454326281344}{15625}, \quad p_6^{(6)} = \frac{1829361664}{46875}, \\
&p_8^{(6)} = -\frac{1497344}{65625}, \quad p_{10}^{(6)} = \frac{72704}{590625}, \quad T_2^{(6)} = \frac{13020804044172544}{390625}, \\
&T_4^{(6)} = \frac{46777257631904}{234375}, \quad T_6^{(6)} = \frac{331901290208}{703125}, \quad T_8^{(6)} = \frac{336461248}{984375}, \\
&T_{10}^{(6)} = -\frac{15320864}{8859375}, \quad T_{12}^{(6)} = -\frac{58336}{8353125}.
\end{aligned} \tag{3.85}$$

Using the explicit form of the solution $\Phi^{(6)}$ [see Eq. (B.20)], one can calculate sixth-order contributions to the fluxes as

$$P_{yy}^{(6)} = -\frac{54407785846698048}{390625}, \tag{3.86}$$

$$\begin{aligned}
P_{xx}^{(6)} = \frac{1}{31640625}(64(&56200132723253796 + 4836534074286615y^2 + 27118423310850y^4 \\
&+36375055200y^6 - 19660500y^8 + 142000y^{10})),
\end{aligned} \tag{3.87}$$

$$\begin{aligned}
q_y^{(6)} = \frac{1}{97453125}(8y^3(&-451786863722040 - 3612280404348y^2 \\
&-4463258085y^4 + 59147550y^6 + 364475y^8)).
\end{aligned} \tag{3.88}$$

3.4.10 Solution at seventh-order in g

At this order, the velocity profile has the following form

$$u^{(7)}(y) = u_2^{(7)}y^2 + u_4^{(7)}y^4 + u_6^{(7)}y^6 + u_8^{(7)}y^8 + u_{10}^{(7)}y^{10} + u_{12}^{(7)}y^{12} + u_{14}^{(7)}y^{14}, \tag{3.89}$$

with the coefficients being given by

$$\begin{aligned}
&u_2^{(7)} = \frac{9343350030025987616}{390625}, \quad u_4^{(7)} = \frac{9569536879895536}{78125}, \quad u_6^{(7)} = \frac{51061147798576}{234375}, \\
&u_8^{(7)} = \frac{16727973311}{234375}, \quad u_{10}^{(7)} = -\frac{4387076308}{44296875}, \quad u_{12}^{(7)} = \frac{75344042}{97453125}, \quad u_{14}^{(7)} = \frac{17320532}{5320940625}.
\end{aligned} \tag{3.90}$$

The equation for $\Phi^{(7)}$ [see Eq. (B.10)] and its solution [see Eq. (B.21)] are provided in supplementary material to this Chapter as Appendix B. The solution $\Phi^{(7)}$ [see Eq. (B.21)] is used to calculate seventh-order contributions to the fluxes and are given by

$$\begin{aligned}
P_{yx}^{(7)} = -\frac{1}{95016796875}(64y^3(&-27780372862376816682 - 10126806640385935 5y^2 \\
&-171697654151595y^4 - 13331496750y^6 + 1332929325y^8 + 9762625y^{10})),
\end{aligned} \tag{3.91}$$

$$\begin{aligned}
q_x^{(7)} = -\frac{1}{2436328125}(4(&1808791379063941987236 06 + 5904121206140205562206y^2 \\
&+3129940462324387981 5y^4 + 59544686214211275y^6 + 34918128065700y^8 \\
&-7262186525y^{10} + 182975125y^{12})).
\end{aligned} \tag{3.92}$$

3.4.11 Solution at eighth-order in g

The equation for $\Phi^{(8)}$ and its explicit functional form is given by Eq. (B.11) and Eq. (B.22), respectively, and are supplemented in Appendix B. At eighth-order, the guessed pressure and temperature profiles are given by

$$p^{(8)}(y) = p_2^{(8)}y^2 + p_4^{(8)}y^4 + p_6^{(8)}y^6 + p_8^{(8)}y^8 + p_{10}^{(8)}y^{10} + p_{12}^{(8)}y^{12} + p_{14}^{(8)}y^{14}, \tag{3.93}$$

$$T^{(8)}(y) = T_2^{(8)}y^2 + T_4^{(8)}y^4 + T_6^{(8)}y^6 + T_8^{(8)}y^8 + T_{10}^{(8)}y^{10} + T_{12}^{(8)}y^{12} + T_{14}^{(8)}y^{14} + T_{16}^{(8)}y^{16}, \tag{3.94}$$

where the exact values of the coefficients are found to be

$$\begin{aligned}
p_2^{(8)} &= -\frac{20522182018749716378112}{1953125}, \quad p_4^{(8)} = -\frac{93272512626802130688}{1953125}, \\
p_6^{(8)} &= -\frac{419407979683606016}{5859375}, \quad p_8^{(8)} = -\frac{11147570290176}{390625}, \\
p_{10}^{(8)} &= \frac{1099283708416}{73828125}, \quad p_{12}^{(8)} = -\frac{2759714816}{487265625}, \quad p_{14}^{(8)} = \frac{15794176}{422296875}, \\
T_2^{(8)} &= -\frac{50788211998323271096989 44}{48828125}, \quad T_4^{(8)} = -\frac{14018830651456092177664}{29296875}, \\
T_6^{(8)} &= -\frac{25046647240246208512}{29296875}, \quad T_8^{(8)} = -\frac{87073445793927904}{123046875}, \\
T_{10}^{(8)} &= -\frac{55260934228096}{369140625}, \quad T_{12}^{(8)} = \frac{866422291648}{7308984375}, \\
T_{14}^{(8)} &= -\frac{78026114176}{133023515625}, \quad T_{16}^{(8)} = -\frac{781138912}{399070546875}.
\end{aligned} \tag{3.95}$$

From exact expression of $\Phi^{(8)}$ [see Eq. (B.22)], we calculated eighth order contributions to the fluxes and their expressions are given by

$$P_{yy}^{(8)} = \frac{17608275005174335193309568}{48828125}, \tag{3.96}$$

$$\begin{aligned}
P_{xx}^{(8)} = \frac{1}{3959033203125}(256(&-41973997864694577067514468 34 \\
&-29027913642095668678147770 0y^2 - 13408353372499198194831 75y^4 \\
&-20320005596619042814 50y^6 - 808536891662106750y^8 \\
&+431401588153250y^{10} - 136702345000y^{12} + 1349600000y^{14})),
\end{aligned} \tag{3.97}$$

$$\begin{aligned}
q_y^{(8)} = \frac{1}{475083984375}(16y^3(&94696020473067137736612 0 + 55968277393593857532 24y^2 \\
&+10486930261732224300y^4 + 2793669136712025y^6 - 5342987784225y^8 \\
&+54528649375y^{10} + 249034125y^{12})).
\end{aligned} \tag{3.98}$$

3.4.12 Solution at ninth-order in g

At this order, the evolution equation for $\Phi^{(9)}$ [see Eq. (B.14)] is solved using the procedure discussed in §3.4.2 and the final expression of the solution to Eq. (B.14) is given by Eq. (B.23). Further, the ninth-order velocity profile is given by

$$u^{(9)}(y) = u_2^{(9)}y^2 + u_4^{(9)}y^4 + u_6^{(9)}y^6 + u_8^{(9)}y^8 + u_{10}^{(9)}y^{10} + u_{12}^{(9)}y^{12} + u_{14}^{(9)}y^{14} + u_{16}^{(9)}y^{16} + u_{18}^{(9)}y^{18}, \tag{3.99}$$

with the following coefficients

$$\begin{aligned}
u_2^{(9)} &= -\frac{5414207592454643614382232256}{48828125}, \quad u_4^{(9)} = -\frac{891522170407886911336576}{1953125}, \\
u_6^{(9)} &= -\frac{313558215178258344363904}{439453125}, \quad u_8^{(9)} = -\frac{30378435693258921724}{68359375}, \\
u_{10}^{(9)} &= -\frac{32371969246115594}{1845703125}, \quad u_{12}^{(9)} = \frac{1948966097535356}{36544921875}, \quad u_{14}^{(9)} = -\frac{23005805338052}{665117578125}, \\
u_{16}^{(9)} &= \frac{587172218459}{1995352734375}, \quad u_{18}^{(9)} = \frac{8795102606}{8722541953125}.
\end{aligned} \tag{3.100}$$

From the solution $\Phi^{(9)}$ [see Eq. (B.23)], the ninth-order contributions to the flux fields are calculated as

$$\begin{aligned}
P_{yx}^{(9)} = &-\frac{1}{4240124560546875}(64y^3(4130009452307700346338633243564 \\
&+1141609423993056014267268597 6y^2 + 145225411156050315782491 80y^4 \\
&+85667094041450365694 25y^6 - 64967445655486920 0y^8 \\
&-1128753705077250y^{10} + 27547383108500y^{12} + 143797125625y^{14})), \qquad (3.101) \\
q_x^{(9)} = &-\frac{1}{83139697265625}(2(-7544540357915304538669909 6450560456 \\
&-1992130611750963230740187251833576y^2 - 8559268783442575644937459468500y^4 \\
&-1373592773566495245163053654 0y^6 - 9656649102706846618853475y^8 \\
&-1720564336894141338600y^{10} + 995759329843164250y^{12} + 9269158652500y^{14} \\
&+3799241923125y^{16})). \qquad (3.102)
\end{aligned}$$

3.4.13 Solution at tenth-order in g

At tenth-order in g, the equation for $\Phi^{(10)}$ is given by Eq. (B.15) which is solved using the procedure discussed in §3.4.3. The final expression of the tenth-order solution to Eq. (B.15) is given by Eq. (B.24). Further, at this order the pressure and temperature profiles take the following forms:

$$\begin{aligned}
p^{(10)}(y) = &\, p_2^{(10)}y^2 + p_4^{(10)}y^4 + p_6^{(10)}y^6 + p_8^{(10)}y^8 + p_{10}^{(10)}y^{10} + p_{12}^{(10)}y^{12} + p_{14}^{(10)}y^{14} \\
&+ p_{16}^{(10)}y^{16} + p_{18}^{(10)}y^{18}, \qquad (3.103) \\
T^{(10)}(y) = &\, T_2^{(10)}y^2 + T_4^{(10)}y^4 + T_6^{(10)}y^6 + T_8^{(10)}y^8 + T_{10}^{(10)}y^{10} + T_{12}^{(10)}y^{12} + T_{14}^{(10)}y^{14} \\
&+ T_{16}^{(10)}y^{16} + T_{18}^{(10)}y^{18} + T_{20}^{(10)}y^{20}, \qquad (3.104)
\end{aligned}$$

where the values of $p_{2i}^{(10)}, T_{2i}^{(10)}$ are given by

$$
\begin{aligned}
p_2^{(10)} &= \frac{113251757688507070506558281966592}{1220703125},\\
p_4^{(10)} &= \frac{85642636505370496881216320512}{244140625},\\
p_6^{(10)} &= \frac{14036633437299047026131968}{29296875}, \quad p_8^{(10)} = \frac{277656831584064485113856}{1025390625},\\
p_{10}^{(10)} &= \frac{60988701666748066816}{1845703125}, \quad p_{12}^{(10)} = -\frac{201660239003930624}{12181640625},\\
p_{14}^{(10)} &= \frac{593294960562176}{100775390625}, \quad p_{16}^{(10)} = -\frac{91824406528}{60465234375}, \quad p_{18}^{(10)} = \frac{1294979301376}{101762989453125},\\
T_2^{(10)} &= \frac{77528942340420325905278080702435 84}{6103515625},\\
T_4^{(10)} &= \frac{17513439090077050598310116094464}{3662109375},\\
T_6^{(10)} &= \frac{77261800700646361310524657664}{10986328125}, \quad T_8^{(10)} = \frac{26215444286938718576174336}{5126953125},\\
T_{10}^{(10)} &= \frac{247558659876164499220864}{138427734375}, \quad T_{12}^{(10)} = \frac{70842143334073921664}{913623046875},\\
T_{14}^{(10)} &= -\frac{1472896959755461888}{16627939453125}, \quad T_{16}^{(10)} = \frac{1958963253962752}{49883818359375},\\
T_{18}^{(10)} &= -\frac{333960912335488}{1526444841796875}, \quad T_{20}^{(10)} = -\frac{18003468073088}{29002451994140625}.
\end{aligned}
\tag{3.105}
$$

From the tenth-order solution $\Phi^{(10)}$ [see Eq. (B.24)], the contributions to the flux fields are found to be

$$
P_{yy}^{(10)} = -\frac{24002728357534086810943888543143168}{6103515625}, \tag{3.106}
$$

$$
\begin{aligned}
P_{xx}^{(10)} = \frac{1}{4770140130615234375}&(1024(1299205030631778240924027740397 3832985469\\
&+750053975841262009377815716659124241415y^2\\
&+28760902154404628045232755738586458 25y^4\\
&+39748173363313183363449866437676 25y^6 + 22650429817362567692670978780 00y^8\\
&+27383375422100207725027312 5y^{10} - 14087037764839754373750 0y^{12}\\
&+51190491255642787500y^{14} - 9093697940250000y^{16} + 138318712000000y^{18}))
\end{aligned}
\tag{3.107}
$$

$$
\begin{aligned}
q_y^{(10)} = \frac{1}{3625306499267578125}&(8y^3(-669974595355637294895736632445742 16480\\
&-31965784403134422605743721577932 6976y^2\\
&-53166826020631498458079525720992 0y^4\\
&-33372171078665511575390527620 0y^6 + 65838870349664473199092 5y^8\\
&+44079593129730246973500y^{10} - 31418042241907865250y^{12}\\
&+33277671083252250 0y^{14} + 1210056152628125y^{16})).
\end{aligned}
\tag{3.108}
$$

Note that the spatial structure of the hydrodynamic profiles and their fluxes can be summarized as follows,

$u^{(2i-1)}(y) = y^2\mathcal{P}_{2i-2}(y^2), \quad p^{(2i)}(y) = y^2\mathcal{P}_{2i-2}(y^2), \quad T^{(2i)}(y) = y^2\mathcal{P}_{2i-1}(y^2),$

$P_{yx}^{(2i-1)}(y) = y^3\mathcal{P}_{2i-3}(y^2), \quad P_{yy}^{(2i)}(y) = \text{const}, \quad P_{xx}^{(2i)}(y) = \mathcal{P}_{2i-1}(y^2),$
$q_x^{(2i-1)}(y) = \mathcal{P}_{2i-2}(y^2), \quad q_y^{(2i)}(y) = y^3\mathcal{P}_{2i-2}(y^2),$
where $\mathcal{P}_j(y^2)$ denotes a generic polynomial of degree j in y^2.

3.5 Results and Discussion: Hydrodynamics and Rheology

In this section we present the main results obtained from the kinetic theory description by retaining terms up to tenth-order in the (dimensionless) gravity field. The final expressions for hydrodynamic fields, namely, pressure, temperature and velocity are written in terms of real units and they are given by

$$
\begin{aligned}
p(y) &= p_0\Bigg[1 + p_2^{(2)}\frac{1}{4}\left(\frac{mg}{T_0}\right)^2 y^2 + p_2^{(4)}\left(\frac{m^5\eta_0^2 g^4}{8\rho_0^2 T_0^5}\right)y^2 + p_4^{(4)}\frac{1}{16}\left(\frac{mg}{T_0}\right)^4 y^4 + p_6^{(4)}\left(\frac{m^3\rho_0^2 g^4}{32\eta_0^2 T_0^3}\right)y^6 \\
&+p_2^{(6)}\left(\frac{g^6 m^8\eta_0^4}{16\rho_0^4 T_0^8}\right)y^2 + p_4^{(6)}\left(\frac{g^6 m^7\eta_0^2}{32\rho_0^2 T_0^7}\right)y^4 + p_6^{(6)}\left(\frac{g^6 m^6}{64 T_0^6}\right)y^6 + p_8^{(6)}\left(\frac{g^6 m^5\rho_0^2}{128\eta_0^2 T_0^5}\right)y^8 \\
&+p_{10}^{(6)}\left(\frac{g^6 m^4\rho_0^4}{256\eta_0^4 T_0^4}\right)y^{10} + p_2^{(8)}\left(\frac{g^8 m^{11}\eta_0^6}{32\rho_0^6 T_0^{11}}\right)y^2 + p_4^{(8)}\left(\frac{g^8 m^{10}\eta_0^4}{64\rho_0^4 T_0^{10}}\right)y^4 + p_6^{(8)}\left(\frac{g^8 m^9\eta_0^2}{128\rho_0^2 T_0^9}\right)y^6 \\
&+p_8^{(8)}\left(\frac{g^8 m^8}{256 T_0^8}\right)y^8 + p_{10}^{(8)}\left(\frac{g^8 m^7\rho_0^2}{512\eta_0^2 T_0^7}\right)y^{10} + p_{12}^{(8)}\left(\frac{g^8 m^6\rho_0^4}{1024\eta_0^4 T_0^6}\right)y^{12} + p_{14}^{(8)}\left(\frac{g^8 m^5\rho_0^6}{2048\eta_0^6 T_0^5}\right)y^{14} \\
&+p_2^{(10)}\left(\frac{g^{10} m^{14}\eta_0^8}{64\rho_0^8 T_0^{14}}\right)y^2 + p_4^{(10)}\left(\frac{g^{10} m^{13}\eta_0^6}{128\rho_0^6 T_0^{13}}\right)y^4 + p_6^{(10)}\left(\frac{g^{10} m^{12}\eta_0^4}{256\rho_0^4 T_0^{12}}\right)y^6 \\
&+p_8^{(10)}\left(\frac{g^{10} m^{11}\eta_0^2}{512\rho_0^2 T_0^{11}}\right)y^8 + p_{10}^{(10)}\left(\frac{g^{10} m^{10}}{1024 T_0^{10}}\right)y^{10} + p_{12}^{(10)}\left(\frac{g^{10} m^9\rho_0^2}{2048\eta_0^2 T_0^9}\right)y^{12} \\
&+p_{14}^{(10)}\left(\frac{g^{10} m^8\rho_0^4}{4096\eta_0^4 T_0^8}\right)y^{14} + p_{16}^{(10)}\left(\frac{g^{10} m^7\rho_0^6}{8192\eta_0^6 T_0^7}\right)y^{16} + p_{18}^{(10)}\left(\frac{g^{10} m^6\rho_0^8}{16384\eta_0^8 T_0^6}\right)y^{18}\Bigg] \\
&+O(g^{12}),
\end{aligned}
\tag{3.109}
$$

$$
\begin{aligned}
u_x(y) &= u_0 + \left(\frac{\rho_0 g}{2\eta_0}\right)y^2 + u_2^{(3)}\left(\frac{m^3\eta_0 g^3}{4\rho_0 T_0^3}\right)y^2 + u_4^{(3)}\left(\frac{m^2\rho_0 g^3}{8\eta_0 T_0^2}\right)y^4 + u_6^{(3)}\left(\frac{m\rho_0^3 g^3}{16\eta_0^3 T_0}\right)y^6 \\
&+u_2^{(5)}\left(\frac{g^5 m^6\eta_0^3}{8\rho_0^3 T_0^6}\right)y^2 + u_4^{(5)}\left(\frac{g^5 m^5\eta_0}{16\rho_0 T_0^5}\right)y^4 + u_6^{(5)}\left(\frac{g^5 m^4\rho_0}{32\eta_0 T_0^4}\right)y^6 + u_8^{(5)}\left(\frac{g^5 m^3\rho_0^3}{64\eta_0^3 T_0^3}\right)y^8 \\
&+u_{10}^{(5)}\left(\frac{g^5 m^2\rho_0^5}{128\eta_0^5 T_0^2}\right)y^{10} + u_2^{(7)}\left(\frac{g^7 m^9\eta_0^5}{16\rho_0^5 T_0^9}\right)y^2 + u_4^{(7)}\left(\frac{g^7 m^8\eta_0^3}{32\rho_0^3 T_0^8}\right)y^4 + u_6^{(7)}\left(\frac{g^7 m^7\eta_0}{64\rho_0 T_0^7}\right)y^6 \\
&+u_8^{(7)}\left(\frac{g^7 m^6\rho_0}{128\eta_0 T_0^6}\right)y^8 + u_{10}^{(7)}\left(\frac{g^7 m^5\rho_0^3}{256\eta_0^3 T_0^5}\right)y^{10} + u_{12}^{(7)}\left(\frac{g^7 m^4\rho_0^5}{512\eta_0^5 T_0^4}\right)y^{12} \\
&+u_{14}^{(7)}\left(\frac{g^7 m^3\rho_0^7}{1024\eta_0^7 T_0^3}\right)y^{14} + u_2^{(9)}\left(\frac{g^9 m^{12}\eta_0^7}{32\rho_0^7 T_0^{12}}\right)y^2 + u_4^{(9)}\left(\frac{g^9 m^{11}\eta_0^5}{64\rho_0^5 T_0^{11}}\right)y^4 \\
&+u_6^{(9)}\left(\frac{g^9 m^{10}\eta_0^3}{128\rho_0^3 T_0^{10}}\right)y^6 + u_8^{(9)}\left(\frac{g^9 m^9\eta_0}{256\rho_0 T_0^9}\right)y^8 + u_{10}^{(9)}\left(\frac{g^9 m^8\rho_0}{512\eta_0 T_0^8}\right)y^{10} \\
&+u_{12}^{(9)}\left(\frac{g^9 m^7\rho_0^3}{1024\eta_0^3 T_0^7}\right)y^{12} + u_{14}^{(9)}\left(\frac{g^9 m^6\rho_0^5}{2048\eta_0^5 T_0^6}\right)y^{14} + u_{16}^{(9)}\left(\frac{g^9 m^5\rho_0^7}{4096\eta_0^7 T_0^5}\right)y^{16} \\
&+u_{18}^{(9)}\left(\frac{g^9 m^4\rho_0^9}{8192\eta_0^9 T_0^4}\right)y^{18} + O(g^{11}),
\end{aligned}
\tag{3.110}
$$

$$
\begin{aligned}
T(y) \;=\; & T_0\Bigg[1+T_4^{(2)}\left(\frac{m\rho_0^2g^2}{8\eta_0^2T_0}\right)y^4+T_2^{(2)}\frac{1}{4}\left(\frac{mg}{T_0}\right)^2y^2+T_2^{(4)}\left(\frac{m^5\eta_0^2g^4}{8\rho_0^2T_0^5}\right)y^2+T_4^{(4)}\frac{1}{16}\left(\frac{mg}{T_0}\right)^4y^4\\
&+T_6^{(4)}\left(\frac{m^3\rho_0^2g^4}{32\eta_0^2T_0^3}\right)y^6+T_8^{(4)}\left(\frac{m^2\rho_0^4g^4}{64\eta_0^4T_0^2}\right)y^8+T_2^{(6)}\left(\frac{g^6m^8\eta_0^4}{16\rho_0^4T_0^8}\right)y^2+T_4^{(6)}\left(\frac{g^6m^7\eta_0^2}{32\rho_0^2T_0^7}\right)y^4\\
&+T_6^{(6)}\left(\frac{g^6m^6}{64T_0^6}\right)y^6+T_8^{(6)}\left(\frac{g^6m^5\rho_0^2}{128\eta_0^2T_0^5}\right)y^8+T_{10}^{(6)}\left(\frac{g^6m^4\rho_0^4}{256\eta_0^4T_0^4}\right)y^{10}+T_{12}^{(6)}\left(\frac{g^6m^3\rho_0^6}{512\eta_0^6T_0^3}\right)y^{12}\\
&+T_2^{(8)}\left(\frac{g^8m^{11}\eta_0^6}{32\rho_0^6T_0^{11}}\right)y^2+T_4^{(8)}\left(\frac{g^8m^{10}\eta_0^4}{64\rho_0^4T_0^{10}}\right)y^4+T_6^{(8)}\left(\frac{g^8m^9\eta_0^2}{128\rho_0^2T_0^9}\right)y^6+T_8^{(8)}\left(\frac{g^8m^8}{256T_0^8}\right)y^8\\
&+T_{10}^{(8)}\left(\frac{g^8m^7\rho_0^2}{512\eta_0^2T_0^7}\right)y^{10}+T_{12}^{(8)}\left(\frac{g^8m^6\rho_0^4}{1024\eta_0^4T_0^6}\right)y^{12}+T_{14}^{(8)}\left(\frac{g^8m^5\rho_0^6}{2048\eta_0^6T_0^5}\right)y^{14}\\
&+T_{16}^{(8)}\left(\frac{g^8m^4\rho_0^8}{4096\eta_0^8T_0^4}\right)y^{16}+T_2^{(10)}\left(\frac{g^{10}m^{14}\eta_0^8}{64\rho_0^8T_0^{14}}\right)y^2+T_4^{(10)}\left(\frac{g^{10}m^{13}\eta_0^6}{128\rho_0^6T_0^{13}}\right)y^4\\
&+T_6^{(10)}\left(\frac{g^{10}m^{12}\eta_0^4}{256\rho_0^4T_0^{12}}\right)y^6+T_8^{(10)}\left(\frac{g^{10}m^{11}\eta_0^2}{512\rho_0^2T_0^{11}}\right)y^8+T_{10}^{(10)}\left(\frac{g^{10}m^{10}}{1024T_0^{10}}\right)y^{10}\\
&+T_{12}^{(10)}\left(\frac{g^{10}m^9\rho_0^2}{2048\eta_0^2T_0^9}\right)y^{12}+T_{14}^{(10)}\left(\frac{g^{10}m^8\rho_0^4}{4096\eta_0^4T_0^8}\right)y^{14}+T_{16}^{(10)}\left(\frac{g^{10}m^7\rho_0^6}{8192\eta_0^6T_0^7}\right)y^{16}\\
&+T_{18}^{(10)}\left(\frac{g^{10}m^6\rho_0^8}{16384\eta_0^8T_0^6}\right)y^{18}+T_{20}^{(10)}\left(\frac{g^{10}m^5\rho_0^{10}}{32768\eta_0^{10}T_0^5}\right)y^{20}\Bigg]+O(g^{12}).
\end{aligned}
\tag{3.111}
$$

The coefficients $p_i^{(j)}, u_i^{(j)}$ and $T_i^{(j)}$ can be found in Section 3.4.

3.5.1 Temperature Profile and its Bimodal Shape

To analyze the characteristics of temperature profile (3.111) in gravity-driven Poiseuille flow, we scale the y-coordinate in terms of the centreline mean free path λ_0, which is defined as the average distance traveled by a molecule/particle between two successive collisions:

$$\lambda_0 = \frac{1}{(\pi\sqrt{2}n_0\sigma^2)}. \tag{3.112}$$

In terms of the 'centreline' thermal velocity (c_0) and the collision frequency (ν_0), the centreline mean-free-path is given by

$$\lambda_0 = \frac{8}{5\sqrt{\pi}}\frac{c_0}{\nu_0}. \tag{3.113}$$

Now we introduce a dimensionless number, namely, the Froude number (Fr), which is defined as the ratio of external (gravitational) and inertial forces: it measures the influence of gravity on the current flow field. The Froude number at the channel centreline is given by

$$\mathrm{Fr}_0 = \frac{g\lambda_0}{c_0^2}, \tag{3.114}$$

which can be tied to the Knudsen number via the following relation (Gupta & Alam 2017)

$$\mathrm{Fr}_0 = \widehat{g}\ \mathrm{Kn}_0\left(\frac{T_w}{T_0}\right), \tag{3.115}$$

where $\mathrm{Kn}_0 = \lambda_0/W$ is the centreline Knudsen number, W is the characteristic width of channel and dimensionless parameter $\widehat{g}$ defined via

$$\widehat{g} = \frac{gW}{\frac{2k_BT_w}{m}},$$

where T_w is the wall-temperature (which is fixed at 1 for thermal-walls), m is the mass of a particle and k_B is the Boltzmann constant (set to unity in simulations).

With introduced centreline mean free path (λ_0) and Froude number (Fr_0), Eq. (3.111) becomes

$$\begin{aligned}
\frac{T(y)}{T_0} &= 1+\mathrm{Fr}_0^2\left(\frac{y}{\lambda_0}\right)^2\left[A_2^{3D}+A_4^{3D}\left(\frac{y}{\lambda_0}\right)^2\right] \\
&\quad +\mathrm{Fr}_0^4\left(\frac{y}{\lambda_0}\right)^2\left[B_2^{3D}+B_4^{3D}\left(\frac{y}{\lambda_0}\right)^2+B_6^{3D}\left(\frac{y}{\lambda_0}\right)^4+B_8^{3D}\left(\frac{y}{\lambda_0}\right)^6\right] \\
&\quad +\mathrm{Fr}_0^6\left(\frac{y}{\lambda_0}\right)^2\left[C_2^{3D}+C_4^{3D}\left(\frac{y}{\lambda_0}\right)^2+C_6^{3D}\left(\frac{y}{\lambda_0}\right)^4+C_8^{3D}\left(\frac{y}{\lambda_0}\right)^6\right. \\
&\quad \left.+C_{10}^{3D}\left(\frac{y}{\lambda_0}\right)^8+C_{12}^{3D}\left(\frac{y}{\lambda_0}\right)^{10}\right]+\mathrm{Fr}_0^8\left(\frac{y}{\lambda_0}\right)^2\left[D_2^{3D}+D_4^{3D}\left(\frac{y}{\lambda_0}\right)^2\right. \\
&\quad +D_6^{3D}\left(\frac{y}{\lambda_0}\right)^4+D_8^{3D}\left(\frac{y}{\lambda_0}\right)^6+D_{10}^{3D}\left(\frac{y}{\lambda_0}\right)^8+D_{12}^{3D}\left(\frac{y}{\lambda_0}\right)^{10} \\
&\quad \left.+D_{14}^{3D}\left(\frac{y}{\lambda_0}\right)^{12}+D_{16}^{3D}\left(\frac{y}{\lambda_0}\right)^{14}\right]+\mathrm{Fr}_0^{10}\left(\frac{y}{\lambda_0}\right)^2\left[E_2^{3D}+E_4^{3D}\left(\frac{y}{\lambda_0}\right)^2\right. \\
&\quad +E_6^{3D}\left(\frac{y}{\lambda_0}\right)^4+E_8^{3D}\left(\frac{y}{\lambda_0}\right)^6+E_{10}^{3D}\left(\frac{y}{\lambda_0}\right)^8+E_{12}^{3D}\left(\frac{y}{\lambda_0}\right)^{10} \\
&\quad \left.+E_{14}^{3D}\left(\frac{y}{\lambda_0}\right)^{12}+E_{16}^{3D}\left(\frac{y}{\lambda_0}\right)^{14}+E_{18}^{3D}\left(\frac{y}{\lambda_0}\right)^{16}+E_{20}^{3D}\left(\frac{y}{\lambda_0}\right)^{18}\right]+O(g^{12}), \\
&= 1+\frac{T^{(\mathrm{II})}}{T_0}+\frac{T^{(\mathrm{IV})}}{T_0}+\frac{T^{(\mathrm{VI})}}{T_0}+\frac{T^{(\mathrm{VIII})}}{T_0}+\frac{T^{(\mathrm{X})}}{T_0}+O(g^{12}),
\end{aligned} \tag{3.116}$$

where

$$\frac{T^{(\mathrm{II})}}{T_0} = \mathrm{Fr}_0^2\left(\frac{y}{\lambda_0}\right)^2\left[A_2^{3D} + A_4^{3D}\left(\frac{y}{\lambda_0}\right)^2\right], \tag{3.117}$$

$$\frac{T^{(\mathrm{IV})}}{T_0} = \mathrm{Fr}_0^4\left(\frac{y}{\lambda_0}\right)^2\left[B_2^{3D} + B_4^{3D}\left(\frac{y}{\lambda_0}\right)^2 + B_6^{3D}\left(\frac{y}{\lambda_0}\right)^4 + B_8^{3D}\left(\frac{y}{\lambda_0}\right)^6\right], \tag{3.118}$$

$$\begin{aligned}\frac{T^{(\mathrm{VI})}}{T_0} = \mathrm{Fr}_0^6\left(\frac{y}{\lambda_0}\right)^2\Bigg[&C_2^{3D} + C_4^{3D}\left(\frac{y}{\lambda_0}\right)^2 + C_6^{3D}\left(\frac{y}{\lambda_0}\right)^4 + C_8^{3D}\left(\frac{y}{\lambda_0}\right)^6 \\ &+C_{10}^{3D}\left(\frac{y}{\lambda_0}\right)^8 + C_{12}^{3D}\left(\frac{y}{\lambda_0}\right)^{10}\Bigg],\end{aligned} \tag{3.119}$$

$$\begin{aligned}\frac{T^{(\mathrm{VIII})}}{T_0} = \mathrm{Fr}_0^8\left(\frac{y}{\lambda_0}\right)^2\Bigg[&D_2^{3D} + D_4^{3D}\left(\frac{y}{\lambda_0}\right)^2 + D_6^{3D}\left(\frac{y}{\lambda_0}\right)^4 + D_8^{3D}\left(\frac{y}{\lambda_0}\right)^6 \\ &+D_{10}^{3D}\left(\frac{y}{\lambda_0}\right)^8 + D_{12}^{3D}\left(\frac{y}{\lambda_0}\right)^{10} + D_{14}^{3D}\left(\frac{y}{\lambda_0}\right)^{12} + D_{16}^{3D}\left(\frac{y}{\lambda_0}\right)^{14}\Bigg],\end{aligned} \tag{3.120}$$

$$\begin{aligned}\frac{T^{(\mathrm{X})}}{T_0} = \mathrm{Fr}_0^{10}\left(\frac{y}{\lambda_0}\right)^2\Bigg[&E_2^{3D} + E_4^{3D}\left(\frac{y}{\lambda_0}\right)^2 + E_6^{3D}\left(\frac{y}{\lambda_0}\right)^4 + E_8^{3D}\left(\frac{y}{\lambda_0}\right)^6 \\ &+E_{10}^{3D}\left(\frac{y}{\lambda_0}\right)^8 + E_{12}^{3D}\left(\frac{y}{\lambda_0}\right)^{10} + E_{14}^{3D}\left(\frac{y}{\lambda_0}\right)^{12} + E_{16}^{3D}\left(\frac{y}{\lambda_0}\right)^{14} \\ &+E_{18}^{3D}\left(\frac{y}{\lambda_0}\right)^{16} + E_{20}^{3D}\left(\frac{y}{\lambda_0}\right)^{18}\Bigg],\end{aligned} \tag{3.121}$$

$$
\begin{aligned}
&A_2^{3D} = \frac{76}{25}, \quad A_4^{3D} = -\frac{256}{375\pi}, \quad B_2^{3D} = -\frac{12494681\pi}{500},\\
&B_4^{3D} = -\frac{1287016}{1875}, \quad B_6^{3D} = -\frac{2225152}{140625\pi}, \quad B_8^{3D} = -\frac{1015808}{4921875\pi^2},\\
&C_2^{3D} = \frac{50862515797549\pi^2}{10000}, \quad C_4^{3D} = \frac{1461789300997\pi}{18750},\\
&C_6^{3D} = \frac{331901290208}{703125}, \quad C_8^{3D} = \frac{21533519872}{24609375\pi},\\
&C_{10}^{3D} = -\frac{62754258944}{5537109375\pi^2}, \quad C_{12}^{3D} = -\frac{15292432384}{130517578125\pi^3},\\
&D_2^{3D} = -\frac{396782906236900555445 23\pi^3}{6400000},\\
&D_4^{3D} = -\frac{5476105723225036006 9\pi^2}{750000},\\
&D_6^{3D} = -\frac{391353863128847008\pi}{1171875}, \quad D_8^{3D} = -\frac{87073445793927904}{123046875},\\
&D_{10}^{3D} = -\frac{3536699790598144}{9228515625\pi}, \quad D_{12}^{3D} = \frac{3548865706590208}{4568115234375\pi^2},\\
&D_{14}^{3D} = -\frac{20454077674553344}{2078492431640625\pi^3}, \quad D_{16}^{3D} = -\frac{13105336252628992}{155886932373046875\pi^4},\\
&E_2^{3D} = \frac{3028474310172668980674925027 4389\pi^4}{1024000000},\\
&E_4^{3D} = \frac{3420593572280673944982444549 7\pi^3}{120000000},\\
&E_6^{3D} = \frac{1886274431168124055432730 9\pi^2}{17578125}, \quad E_8^{3D} = \frac{4096163169834174777527 24\pi}{205078125},\\
&E_{10}^{3D} = \frac{247558659876164499220864}{138427734375}, \quad E_{12}^{3D} = \frac{4533897173380730986496}{22840576171875\pi},\\
&E_{10}^{3D} = \frac{247558659876164499220864}{138427734375}, \quad E_{12}^{3D} = \frac{4533897173380730986496}{22840576171875\pi},\\
&E_{14}^{3D} = -\frac{6032985947158371893248}{10392462158203125\pi^2}, \quad E_{16}^{3D} = \frac{513530463246811660288}{779434661865234375\pi^3},\\
&E_{18}^{3D} = -\frac{5602934361809546641408}{5962675163269042968 75\pi^4}, \quad E_{20}^{3D} = -\frac{1933107664712327443 2512}{2832270702552795410156 25\pi^5}.
\end{aligned}
\tag{3.122}
$$

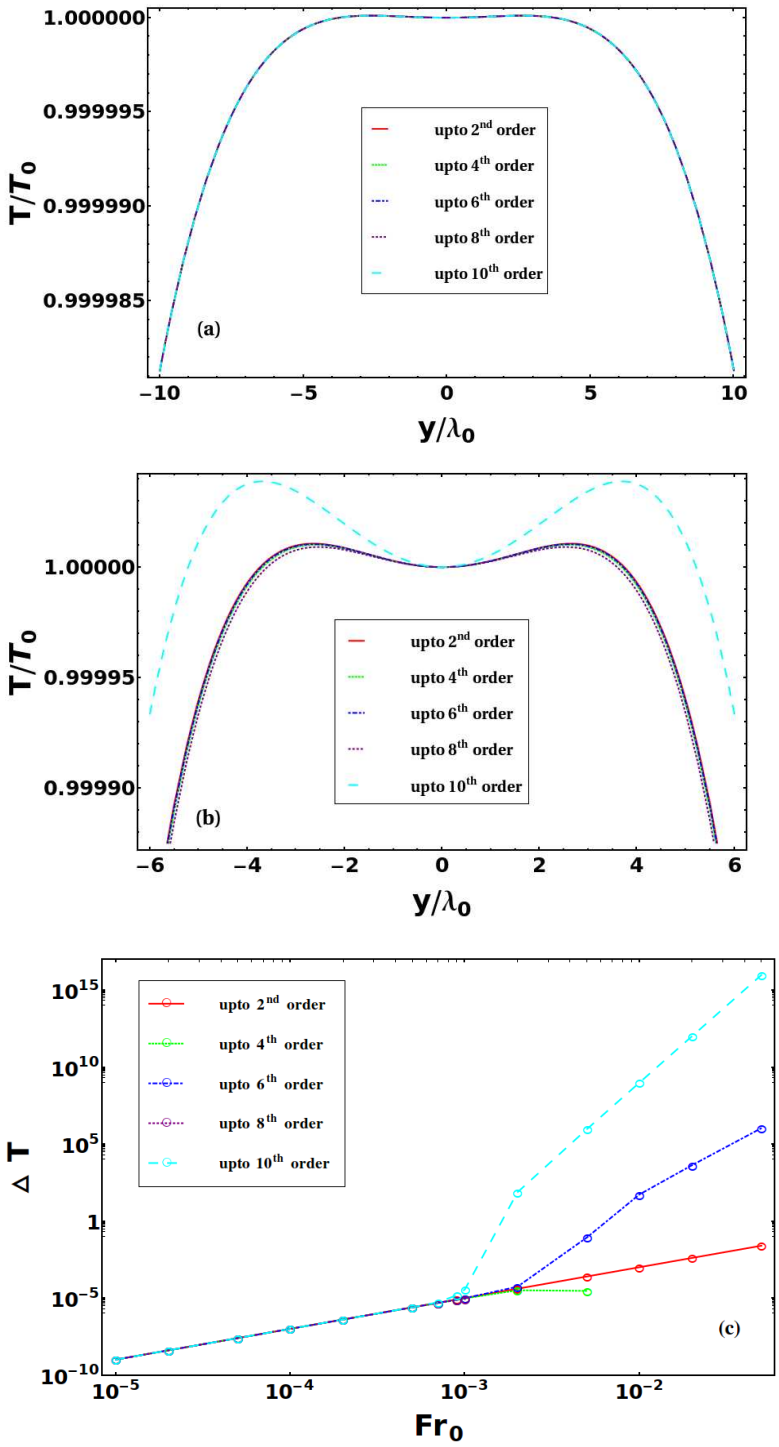

Figure 3.2: Temperature profiles for (a) $\mathrm{Fr}_0 = 10^{-4}$, (b) $\mathrm{Fr}_0 = 10^{-3}$, and (c) $\Delta T (= T_{\max}/T_0 - 1)$ with Fr_0 as predicted by kinetic theory description. The red solid, green tiny dashed, blue dot-dashed, purple dotted and cyan large dashed lines represent the 2^{nd} order, 4^{th} order, 6^{th} order, 8^{th} order and 10^{th} order series solutions, respectively.

Figs. 3.2(a) and 3.2(b) display the temperature profiles $T(y)$ [solution of Eq. (3.116)] for the cases of $\mathrm{Fr}_0 = 10^{-4}$ and $\mathrm{Fr}_0 = 10^{-3}$, respectively. The dimensionless temperature T/T_0 is plotted against y/λ_0, where λ_0 is the centreline mean free path. One can notice that the temperature profile $T(y)$ has a local minimum at the channel centreline (i.e. at $y = 0$) and it is

surrounded by two maxima on either side of it at the some distance of few mean free paths from the channel centreline – such bimodal-shape of the temperature profile is a characteristic feature of the rarefaction of the gas (called the temperature bimodality). Further, it can be observed that the variations between different orders solutions of temperature profiles are negligible for the case of $\mathrm{Fr}_0 = 10^{-4}$ (panel a), but the deviations are noticeable at higher values of Froude numbers (panel b).

To quantify the degree of the temperature bimodality (such as in Fig. 3.2), we introduce a new variable $\triangle T$, which is defined as the relative difference between the maxima and minimum of temperature and is given by

$$\triangle T = \frac{T_{\max} - T_0}{T_0}. \tag{3.123}$$

It is well-known from literature that the Navier-Stokes model predicts zero value for $\triangle T$, whereas the present solutions predict non-zero values for the same, which is evident from Fig. 3.2(c). From Figs. 3.2(a) and 3.2(b), it is evident that as Fr_0 increases from 10^{-4} to 10^{-3}, the degree of bimodality ($\triangle T$) increases. Further, if we go beyond $\mathrm{Fr}_0 > 10^{-3}$, the temperature bimodality show oscillating behaviour as it is evident from a comparison between 4th-order and 6th-order solution for $\triangle T$ in Fig. 3.2(c). Such oscillating nature of solution (with the perturbation parameter) is a clear signal of the divergent nature of the adopted series expansion – this issue will be further discussed in the context of rheological quantities in the following sections. It is worth noting at this point that the DSMC simulations (Gupta & Alam 2017) of gravity-driven Poiseuille flow of a molecular gas suggest that the temperature bimodality $\triangle T$ should increase with increasing gravitational strength (Fr_0) as well as Knudsen number.

3.5.2 Pressure Tensor and Normal Stress Differences

The expressions for three non-zero components of the pressure tensor P_{ij} up to tenth-order in g, expressed in real units are given by

$$\begin{aligned}
P_{xx} &= p_0\Bigg[1+\frac{656}{25}\left(\frac{\rho_0\eta_0^2g^2}{2p_0^3}\right)+\frac{56}{5}y^2\left(\frac{1}{4}\left(\frac{mg}{T_0}\right)^2\right)+\frac{448y^6}{375}\left(\frac{\rho_0^5g^4}{32\eta_0^2p_0^3}\right)\\
&-\frac{28192y^4}{125}\left(\frac{1}{16}\left(\frac{mg}{T_0}\right)^4\right)-\frac{1066982656}{3125}\left(\frac{\rho_0^2\eta_0^4g^4}{4p_0^6}\right)-\frac{4923504y^2}{125}\left(\frac{\rho_0^3\eta_0^2g^4}{8p_0^5}\right)\\
&+\frac{44405043139361024}{390625}\left(\frac{\rho_0^3\eta_0^6g^6}{8p_0^9}\right)+\frac{764291804331712y^2}{78125}\left(\frac{g^6\rho_0^4\eta_0^4}{16p_0^8}\right)\\
&+\frac{2571228284288y^4}{46875}\left(\frac{g^6\rho_0^5\eta_0^2}{32p_0^7}\right)+\frac{10346682368y^6}{140625}\left(\frac{g^6\rho_0^6}{64p_0^6}\right)\\
&-\frac{1118464y^8}{28125}\left(\frac{g^6\rho_0^7}{128p_0^5\eta_0^2}\right)+\frac{72704y^{10}}{253125}\left(\frac{g^6\rho_0^8}{256p_0^4\eta_0^4}\right)\\
&-\frac{1325260351174974621586278 4}{48828125}\left(\frac{\rho_0^4\eta_0^8g^8}{16p_0^{12}}\right)-\frac{3666035639608041924300 8y^2}{1953125}\left(\frac{g^8\rho_0^5\eta_0^6}{32p_0^{11}}\right)\\
&-\frac{16933873353115007155 2y^4}{1953125}\left(\frac{g^8\rho_0^6\eta_0^4}{64p_0^{10}}\right)-\frac{256628380643281408y^6}{1953125}\left(\frac{g^8\rho_0^7\eta_0^2}{128p_0^9}\right)\\
&-\frac{428874269392384y^8}{8203125}\left(\frac{g^8\rho_0^8}{256p_0^8}\right)+\frac{6178394772992y^{10}}{221484375}\left(\frac{g^8\rho_0^9}{512p_0^7\eta_0^2}\right)\\
&-\frac{4307175424y^{12}}{487265625}\left(\frac{g^8\rho_0^{10}}{1024p_0^6\eta_0^4}\right)+\frac{15794176y^{14}}{180984375}\left(\frac{g^8\rho_0^{11}}{2048p_0^5\eta_0^6}\right)\\
&+\frac{17022626629631787148863457964739584}{6103515625}\left(\frac{g^{10}\eta_0^{10}\rho_0^5}{32p_0^{15}}\right)\\
&+\frac{19654925099247632713280382037708 8y^2}{1220703125}\left(\frac{g^{10}\eta_0^8\rho_0^6}{64p_0^{14}}\right)\\
&+\frac{15073405270536128472674845388 8y^4}{244140625}\left(\frac{g^{10}\eta_0^6\rho_0^7}{128p_0^{13}}\right)\\
&+\frac{12499058395016149067601612 8y^6}{146484375}\left(\frac{g^{10}\eta_0^4\rho_0^8}{256p_0^{12}}\right)\\
&+\frac{49857972002938333469344y^8}{1025390625}\left(\frac{g^{10}\eta_0^2\rho_0^9}{512p_0^{11}}\right)+\frac{574058092053752832y^{10}}{9765625}\left(\frac{g^{10}\rho_0^{10}}{1024p_0^{10}}\right)\\
&-\frac{1105135515521724416y^{12}}{36544921875}\left(\frac{g^{10}\rho_0^{11}}{2048p_0^9\eta_0^2}\right)+\frac{36544880554790912y^{14}}{3325587890625}\left(\frac{g^{10}\rho_0^{12}}{4096p_0^8\eta_0^4}\right)\\
&-\frac{7226703872y^{16}}{3701953125}\left(\frac{g^{10}\rho_0^{13}}{8192p_0^7\eta_0^6}\right)+\frac{1294979301376y^{18}}{43612709765625}\left(\frac{g^{10}\rho_0^{14}}{16384p_0^6\eta_0^8}\right)\Bigg]+O(g^{12}), \quad (3.124)
\end{aligned}$$

$$\begin{aligned}
P_{yy} &= p_0\Bigg[1-\frac{612}{25}\left(\frac{\rho_0\eta_0^2g^2}{2p_0^3}\right)+\frac{1171581312}{3125}\left(\frac{\rho_0^2\eta_0^4g^4}{4p_0^6}\right)-\frac{54407785846698048}{390625}\left(\frac{\rho_0^3\eta_0^6g^6}{8p_0^9}\right)\\
&+\frac{17608275005174335193309568}{48828125}\left(\frac{\rho_0^4\eta_0^8g^8}{16p_0^{12}}\right)\\
&-\frac{24002728357534086810943888543143168}{6103515625}\left(\frac{\rho_0^5\eta_0^{10}g^{10}}{32p_0^{15}}\right)\Bigg]+O(g^{12}), \quad (3.125)
\end{aligned}$$

$$
\begin{aligned}
P_{yx} \;=\; & -\rho_0 g y - \frac{88y^3}{75}\left(\frac{\rho_0^3 g^3}{8p_0^2}\right) - \frac{8y^5}{75}\left(\frac{\rho_0^4 g^3}{16\eta_0^2 p_0}\right) - \frac{273644992y^3}{9375}\left(\frac{g^5\rho_0^4\eta_0^2}{16p_0^5}\right) \\
& - \frac{2103728y^5}{9375}\left(\frac{g^5\rho_0^5}{32p_0^4}\right) - \frac{10208y^7}{5625}\left(\frac{g^5\rho_0^6}{64p_0^3\eta_0^2}\right) - \frac{1616y^9}{70875}\left(\frac{g^5\rho_0^7}{128p_0^2\eta_0^4}\right) \\
& + \frac{21927996240699008y^3}{1171875}\left(\frac{g^7\rho_0^5\eta_0^4}{32p_0^8}\right) + \frac{15986868069824y^5}{234375}\left(\frac{g^7\rho_0^6\eta_0^2}{64p_0^7}\right) \\
& + \frac{569212632256y^7}{4921875}\left(\frac{g^7\rho_0^7}{128p_0^6}\right) + \frac{15910784y^9}{1771875}\left(\frac{g^7\rho_0^8}{256p_0^5\eta_0^2}\right) \\
& - \frac{12499264y^{11}}{13921875}\left(\frac{g^7\rho_0^9}{512p_0^4\eta_0^4}\right) - \frac{4998464y^{13}}{760134375}\left(\frac{g^7\rho_0^{10}}{1024p_0^3\eta_0^6}\right) \\
& - \frac{913153329872716840049228 8y^3}{146484375}\left(\frac{g^9\rho_0^6\eta_0^6}{64p_0^{11}}\right) \\
& - \frac{252412121321136880593 92y^5}{146484375}\left(\frac{g^9\rho_0^7\eta_0^4}{128p_0^{10}}\right) - \frac{1498449313776229452 8y^7}{68359375}\left(\frac{g^9\rho_0^8\eta_0^2}{256p_0^9}\right) \\
& - \frac{15910578945100864y^9}{123046875}\left(\frac{g^9\rho_0^9}{512p_0^8}\right) + \frac{5688315014144y^{11}}{580078125}\left(\frac{g^9\rho_0^{10}}{1024p_0^7\eta_0^2}\right) \\
& + \frac{1618828843136y^{13}}{95016796875}\left(\frac{g^9\rho_0^{11}}{2048p_0^6\eta_0^4}\right) - \frac{829662361856y^{15}}{1995352734375}\left(\frac{g^9\rho_0^{12}}{4096p_0^5\eta_0^6}\right) \\
& - \frac{14724825664y^{17}}{6784199296875}\left(\frac{g^9\rho_0^{13}}{8192p_0^4\eta_0^8}\right) + O(g^{11}),
\end{aligned}
\tag{3.126}
$$

The normal stress differences (NSD's) are one signature of a non-Newtonian (rarefied) fluid; the normal stress differences are zero (Sela & Goldhirsch (1998), Alam & Luding (2005)) in a Newtonian fluid. To characterize the normal stress differences in the Poiseuille flow, the first and second normal stress differences are defined via:

$$
\mathcal{N}_1(y) = \frac{P_{xx} - P_{yy}}{p}, \quad \mathcal{N}_2(y) = \frac{P_{yy} - P_{zz}}{p}. \tag{3.127}
$$

Since $P_{zz} = 3p - P_{yy} - P_{xx}$, we can write

$$
\mathcal{N}_1(y) = \frac{P_{xx} - P_{yy}}{p}, \quad \text{and} \quad \mathcal{N}_2(y) = \frac{P_{xx} + 2P_{yy}}{p} - 3. \tag{3.128}
$$

In the remainder of this section, we analyse numerical results for the two normal stress differences.

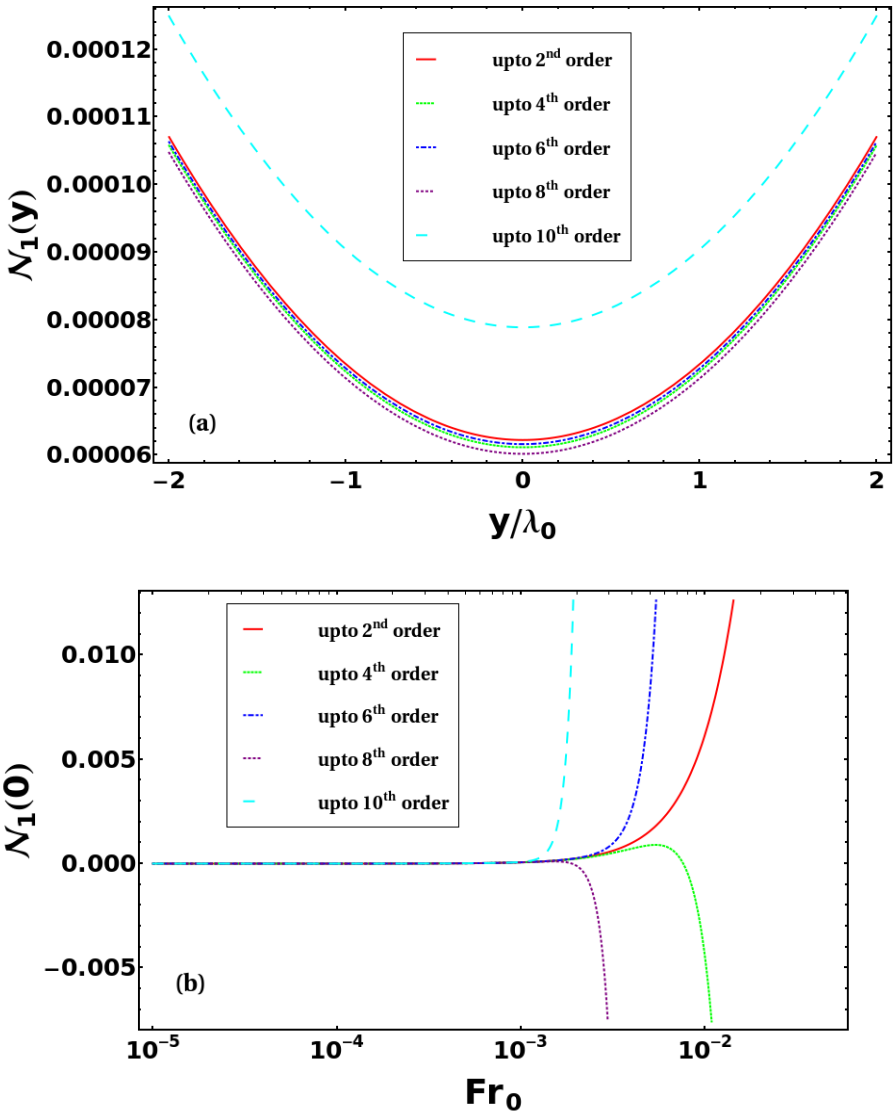

Figure 3.3: (a) First normal stress difference profiles for $\mathrm{Fr}_0 = 10^{-3}$, and (b) $\mathcal{N}_1$ evaluated at channel centreline ($y = 0$), with Fr_0 as predicted by kinetic theory approach. In both panels (a) and (b), the red solid, green tiny dashed, blue dot-dashed, purple dotted and cyan large dashed lines indicates the solution of 2^{nd} order, 4^{th} order, 6^{th} order, 8^{th} order and 10^{th} order series solutions, respectively.

Fig. 3.3(a) shows the transverse profiles of first normal stress difference for $\mathrm{Fr}_0 = 10^{-3}$. From this figure, one can observe that first normal stress difference attains its minimum at $y = 0$ and increases as one moves away from the channel centreline. Fig. 3.3(b) displays the first normal stress difference evaluated at the channel centreline ($y = 0$) against Froude number. From Figs. 3.3(a) and 3.3(b), we find that for Froude number less than 10^{-3}, the variations of the solutions among all orders are very small – this indicates a convergent series solution for $\mathcal{N}_1$ at $\mathrm{Fr}_0 \leq 10^{-3}$. For Froude number greater than 10^{-3}, the solutions for $\mathcal{N}_1$ indicate the divergent nature of the series expansion in g as evident from Fig. 3.3(b). From Fig. 3.3(b), it is evident that the solution via second, sixth and tenth order in g diverges upward whereas the solution via fourth and eighth order in g diverges downward for Fr_0 greater than 10^{-3}. Overall, Fig. 3.3(b) suggests that all order solutions are valid only for $\mathrm{Fr}_0 \leq 10^{-3}$.

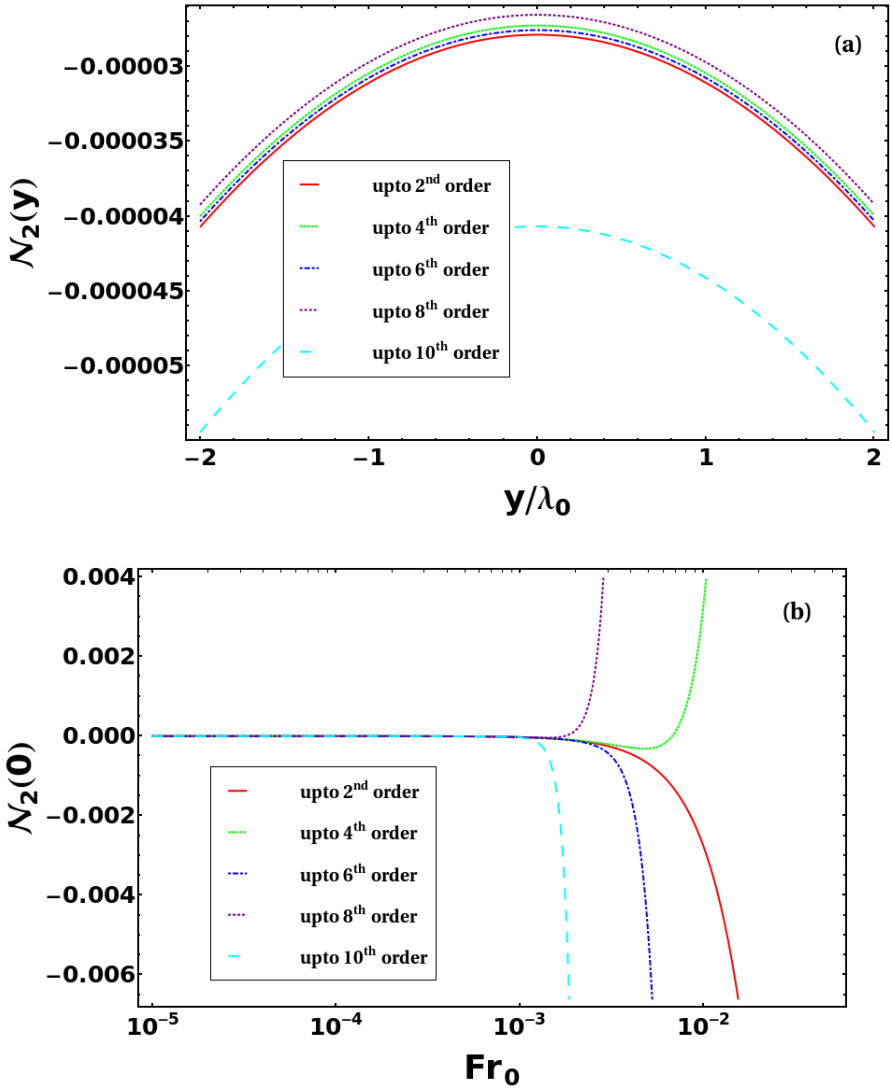

Figure 3.4: (a) Second normal stress difference profiles for $\mathrm{Fr}_0 = 10^{-3}$, and (b) $\mathcal{N}_2$ evaluated at channel centreline($y = 0$), with Fr_0 as predicted by kinetic theory approach. In both panels (a) and (b), the red solid, green tiny dashed, blue dot-dashed, purple dotted and cyan large dashed lines represent the 2^{nd} order, 4^{th} order, 6^{th} order, 8^{th} order and 10^{th} order series solutions, respectively.

The second normal stress difference profiles as predicted by the present kinetic model for $\mathrm{Fr}_0 = 10^{-3}$ are presented in Fig. 3.4(a) which shows that second normal stress difference approaches its maximum at $y = 0$ and decreases away from the channel centreline. Fig. 3.4(b) shows the second normal stress difference evaluated at the channel centreline ($y = 0$) against Froude number. From Figs. 3.4(a) and 3.4(b), we find that for Froude number less than 10^{-3}, the variation of the solutions of all orders is very small, indicating converged solution for $\mathcal{N}_2$ for $\mathrm{Fr}_0 \leq 10^{-3}$. However, the solutions for $\mathcal{N}_2$ for $\mathrm{Fr}_0 > 10^{-3}$ indicates the divergent nature of the series expansion in g as evident from Fig. 3.4(b). It is seen in Fig. 3.4(b) that the solutions from second, sixth and tenth order in g show downward divergence whereas the fourth and eighth order solutions show upward divergence for $\mathrm{Fr}_0 > 10^{-3}$ which is opposite as compared to the related behaviour of $\mathcal{N}_1$ (see Fig. 3.3(b)). Overall, Fig. 3.4(b) suggests that all order solutions

are converged and valid only for $\mathrm{Fr}_0 \leq 10^{-3}$.

3.5.3 Tangential and Normal Heat Flux Components

The tangential/longitudinal component of heat flux (q_x) and the normal/transverse component of heat flux (q_y) up to tenth-order in g, expressed in real units, are given by

$$
\begin{aligned}
q_x \;=\;& \eta_0 g - \frac{38y^4}{5}\left(\frac{\rho_0^3 g^3}{8\eta_0 p_0}\right) - \frac{42018}{25}\left(\frac{\rho_0 \eta_0^3 g^3}{2p_0^3}\right) - \frac{3158y^2}{25}\left(\frac{\rho_0^2 \eta_0 g^3}{4p_0^2}\right) \\
&+ \frac{726568482108}{3125}\left(\frac{g^5\rho_0^2\eta_0^5}{4p_0^6}\right) + \frac{30781618668y^2}{3125}\left(\frac{g^5\rho_0^3\eta_0^3}{8p_0^5}\right) + \frac{26276986y^4}{375}\left(\frac{g^5\rho_0^4\eta_0}{16p_0^4}\right) \\
&+ \frac{531028y^6}{5625}\left(\frac{g^5\rho_0^5}{32p_0^3\eta_0}\right) - \frac{1042y^8}{875}\left(\frac{g^5\rho_0^6}{64p_0^2\eta_0^3}\right) - \frac{116003936447903927352}{390625}\left(\frac{g^7\rho_0^3\eta_0^7}{8p_0^9}\right) \\
&- \frac{3786513520051438552y^2}{390625}\left(\frac{g^7\rho_0^4\eta_0^5}{16p_0^8}\right) - \frac{12044022943047188y^4}{234375}\left(\frac{g^7\rho_0^5\eta_0^3}{32p_0^7}\right) \\
&- \frac{13747690900828y^6}{140625}\left(\frac{g^7\rho_0^6\eta_0}{64p_0^6}\right) - \frac{56433338288y^8}{984375}\left(\frac{g^7\rho_0^7}{128p_0^5\eta_0}\right) \\
&+ \frac{105631804y^{10}}{8859375}\left(\frac{g^7\rho_0^8}{256p_0^4\eta_0^3}\right) - \frac{5855204y^{12}}{19490625}\left(\frac{g^7\rho_0^9}{512p_0^3\eta_0^5}\right) \\
&+ \frac{8861849917179005049823673 8512}{48828125}\left(\frac{g^9\rho_0^4\eta_0^9}{16p_0^{12}}\right) \\
&+ \frac{2339965280752126451726036752y^2}{48828125}\left(\frac{g^9\rho_0^5\eta_0^7}{32p_0^{11}}\right) \\
&+ \frac{8043003471254272495229 6y^4}{390625}\left(\frac{g^9\rho_0^6\eta_0^5}{64p_0^{10}}\right) + \frac{9680568275227384574248y^6}{29296875}\left(\frac{g^9\rho_0^7\eta_0^3}{128p_0^9}\right) \\
&+ \frac{9527903309240731238y^8}{41015625}\left(\frac{g^9\rho_0^8\eta_0}{256p_0^8}\right) + \frac{45835879770739696y^{10}}{1107421875}\left(\frac{g^9\rho_0^9}{512p_0^7\eta_0}\right) \\
&- \frac{175078563488908y^{12}}{7308984375}\left(\frac{g^9\rho_0^{10}}{1024p_0^6\eta_0^3}\right) - \frac{29661307688y^{14}}{133023515625}\left(\frac{g^9\rho_0^{11}}{2048p_0^5\eta_0^5}\right) \\
&- \frac{368411338y^{16}}{4031015625}\left(\frac{g^9\rho_0^{12}}{4096p_0^4\eta_0^7}\right) + O(g^{11}),
\end{aligned}
\tag{3.129}
$$

$$
\begin{aligned}
q_y \;=\;& \frac{\rho_0^2 g^2 y^3}{3\eta_0} + \frac{24y^7}{175}\left(\frac{\rho_0^5 g^4}{32\eta_0^3 p_0}\right) + \frac{5336y^5}{375}\left(\frac{\rho_0^4 g^4}{16\eta_0 p_0^2}\right) + \frac{43616y^3}{75}\left(\frac{\rho_0^3\eta_0 g^4}{8p_0^3}\right) \\
& - \frac{347695518016y^3}{9375}\left(\frac{g^6\rho_0^4\eta_0^3}{16p_0^6}\right) - \frac{13900068896y^5}{46875}\left(\frac{g^6\rho_0^5\eta_0}{32p_0^5}\right) - \frac{24044488y^7}{65625}\left(\frac{g^6\rho_0^6}{64p_0^4\eta_0}\right) \\
& + \frac{9104y^9}{1875}\left(\frac{g^6\rho_0^7}{128p_0^3\eta_0^3}\right) + \frac{116632y^{11}}{3898125}\left(\frac{g^6\rho_0^8}{256p_0^2\eta_0^5}\right) + \frac{3737340012010395046 4y^3}{1171875}\left(\frac{g^8\rho_0^5\eta_0^5}{32p_0^9}\right) \\
& + \frac{368147259447343488y^5}{1953125}\left(\frac{g^8\rho_0^6\eta_0^3}{64p_0^8}\right) + \frac{82776918976192y^7}{234375}\left(\frac{g^8\rho_0^7\eta_0}{128p_0^7}\right) \\
& + \frac{4167711532624y^9}{44296875}\left(\frac{g^8\rho_0^8}{256p_0^6\eta_0}\right) - \frac{12525685648y^{11}}{69609375}\left(\frac{g^8\rho_0^9}{512p_0^5\eta_0^3}\right) \\
& + \frac{1395933424y^{13}}{760134375}\left(\frac{g^8\rho_0^{10}}{1024p_0^4\eta_0^5}\right) + \frac{10625456y^{15}}{1266890625}\left(\frac{g^8\rho_0^{11}}{2048p_0^3\eta_0^7}\right) \\
& - \frac{2165683036981857445 7528929024y^3}{146484375}\left(\frac{g^{10}\rho_0^6\eta_0^7}{64p_0^{12}}\right) \\
& - \frac{5166446423908045877 62130944y^5}{732421875}\left(\frac{g^{10}\rho_0^7\eta_0^5}{128p_0^{11}}\right) \\
& - \frac{4010089627719339792 01024y^7}{341796875}\left(\frac{g^{10}\rho_0^8\eta_0^3}{256p_0^{10}}\right) - \frac{4077676993790509343168y^9}{5537109375}\left(\frac{g^{10}\rho_0^9\eta_0}{512p_0^9}\right) \\
& + \frac{88491878732748712y^{11}}{60908203125}\left(\frac{g^{10}\rho_0^{10}}{1024p_0^8\eta_0}\right) + \frac{1400358670643104y^{13}}{14396484375}\left(\frac{g^{10}\rho_0^{11}}{2048p_0^7\eta_0^3}\right) \\
& - \frac{32937813545008y^{15}}{475083984375}\left(\frac{g^{10}\rho_0^{12}}{4096p_0^6\eta_0^5}\right) + \frac{307525947488y^{17}}{418777734375}\left(\frac{g^{10}\rho_0^{13}}{8192p_0^5\eta_0^7}\right) \\
& + \frac{281613068248y^{19}}{105463461796875}\left(\frac{g^{10}\rho_0^{14}}{16384p_0^4\eta_0^9}\right) + O(g^{12}).
\end{aligned}
\tag{3.130}
$$

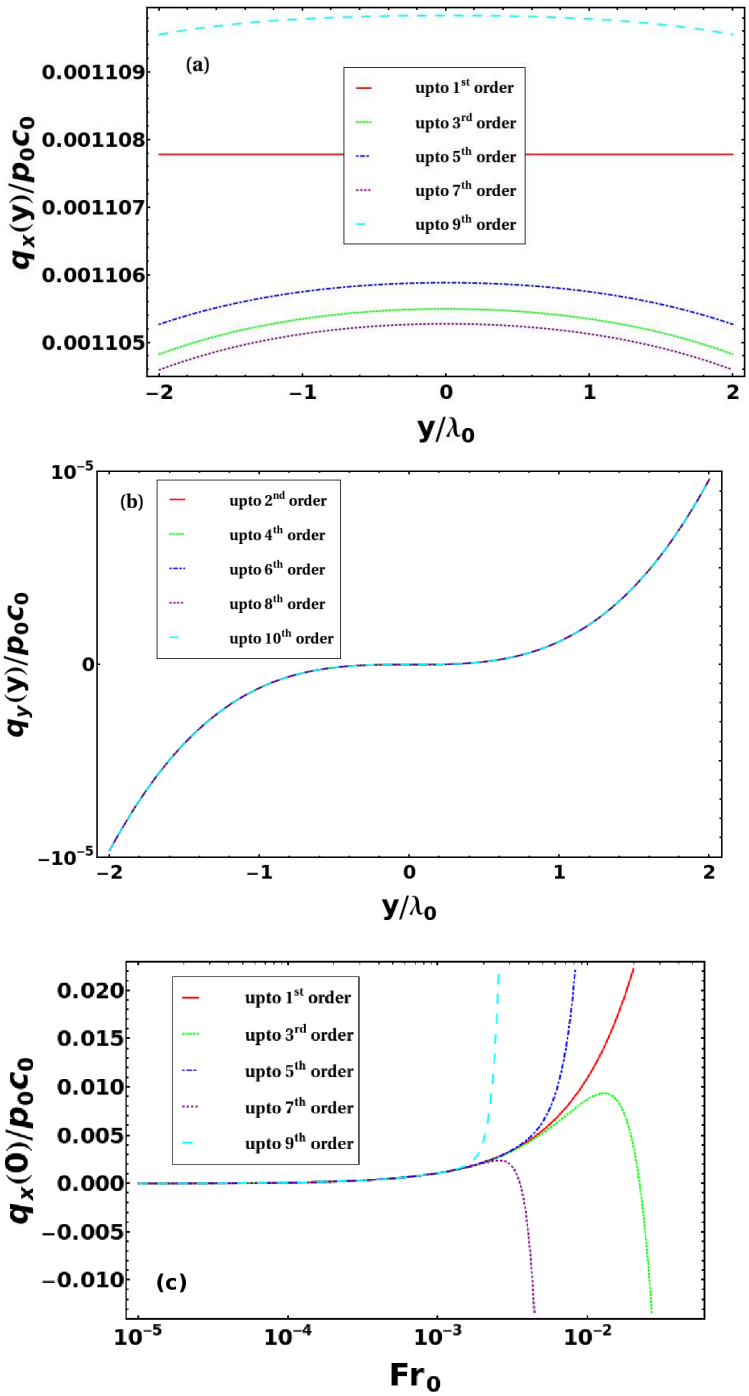

Figure 3.5: Profiles of dimensionless (a) x-component of heat flux ($q_x^* = q_x/p_0c_0$), and (b) y-component of heat flux ($q_y^* = q_y/p_0c_0$) for $\mathrm{Fr}_0 = 10^{-3}$ (c) x-component of heat flux ($q_x^* = q_x/p_0c_0$) evaluated at channel centreline ($y = 0$), with Fr_0 as predicted by kinetic theory approach. In all panels, the red solid, green tiny dashed, blue dot-dashed, purple dotted and cyan large dashed lines represents the solutions of respective orders.

The profiles of dimensionless tangential component of heat flux for $\mathrm{Fr}_0 = 10^{-3}$ are presented in Fig. 3.5(a). Note that according to Navier-Stokes model, the tangential component of heat flux (q_x) is zero, but it is different from zero according to the kinetic theory description (Kogan (1969); Tij & Santos (1994)). All series solutions discussed here predict a non-zero value for

the tangential heat flux, which is evident from Fig. 3.5(a). Further from Fig. 3.5(a), one can conclude that the solutions via $3^{\text{rd}}, 5^{\text{th}}, 7^{\text{th}}$ and 9^{th} orders in g for tangential heat flux predicts maximum at $y = 0$, whereas the first-order solution predicts a nearly constant value across the channel width. The profiles of dimensionless normal/transverse component of heat flux for the value of $\text{Fr}_0 = 10^{-3}$ are presented in Fig. 3.5(b). Fig. 3.5(b) indicates that the variation between the solutions of different orders in g for normal heat flux profile for the value of $\text{Fr}_0 = 10^{-3}$ is almost negligible.

Fig. 3.5(c) displays tangential heat flux evaluated at $y = 0$ against Froude number. It is evident from Fig. 3.5(c) that the adopted perturbation series solution (up to tenth-order in g) agree well among themselves for $\text{Fr}_0 < 10^{-3}$ and for Froude number greater than 10^{-3}, all series solutions show oscillating behaviour. Clearly, similar to the perturbation solutions of $\triangle T$, $\mathcal{N}_1$ and $\mathcal{N}_2$, the behaviour of $q_x(0)$ suggest asymptotic nature of its series solution.

3.5.4 Summary on Hydrodynamic and Rheological Fields: Convergence Issues of Perturbation Solutions

Overall it must be noted here that the perturbation series expansion of temperature bimodality, first and second normal stress difference and the tangential heat flux up to tenth-order in g agree well among themselves for $\text{Fr}_0 \leq 10^{-3}$, beyond which the series solutions of $\triangle T$, $\mathcal{N}_1$, $\mathcal{N}_2$ and q_x show oscillating behaviour, which indicates the divergent nature of each series solution. Further, it is evident from Figs. 3.2(c), 3.3(b), 3.4(b) and 3.5(c) that the series is divergent but asymptotic. Similar characteristic features have been reported for the perturbation solution of Boltzmann equation in the literature [Santos *et al.* (1986); Santos (2008); Brilliantov & Pöschel (2006)].

For example, in Santos (2008), the convergence of the Chapman-Enskog (CE) series expansion for a sheared granular gas has been analysed by considering full CE series of the shear stress. The CE series expansion of shear stress can be written in the dimensionless form as

$$\frac{P_{xy}}{nT} = -\mu\, F(\mu^2), \quad F(z) = \sum_{k=0}^{\infty} c_k\, z^k. \tag{3.131}$$

In order to analyze the CE expansion, we consider the scaled viscosity $F(z)$ as a function of scaled shear rate or uniformity parameter μ [Santos (2008)]. Elimination of time dependence with the help of the energy balance and stress balance equations in favour of $z \equiv \mu^2$ yields a single second-order ODE for the scaled viscosity function $F(z)$ which is given by

$$\begin{aligned} 1 - \left(1 + \frac{2}{d} zF\right)^2 F = \frac{1}{2}\left(\epsilon - \frac{2}{d} zF\right) \times \Bigg\{ z\frac{\partial}{\partial z}\left[\left(\epsilon - \frac{2}{d} zF\right)\left(F + 2z\frac{\partial F}{\partial z}\right)\right] \\ + \left(1 + \frac{2}{d} zF\right)\left(F + 2z\frac{\partial F}{\partial z}\right) + 2z\frac{\partial}{\partial z}\left[\left(1 + \frac{2}{d} zF\right) F\right] \Bigg\}, \end{aligned} \tag{3.132}$$

where d is the dimensionality of the problem.

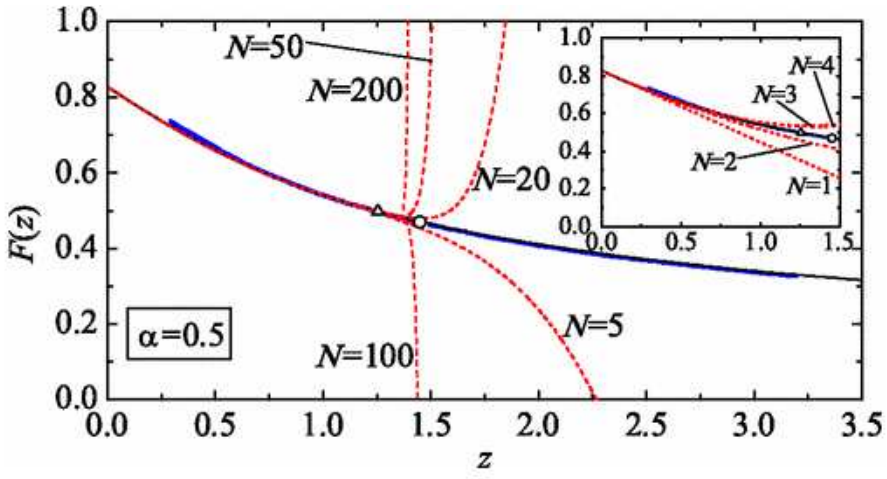

Figure 3.6: Scaled viscosity function $F(z)$ for $\alpha = 0.5$ and $d = 3$. Taken from Santos (2008).

The convergent nature of the series presented in Eq. (3.131) for a sheared granular gas with restitution coefficient $\alpha = 0.5$ is shown in Fig. 3.6, which shows the comparison of numerical solution of Eq. (3.132) with the truncated Chapman-Enskog series

$$F_N(z) = \sum_{k=0}^{N} c_k \, z^k. \tag{3.133}$$

The truncated CE series at different orders agree well among themselves and also with the numerical solution of Eq. (3.132) for $z < z_s$ (where $z_s \sim 1.5$ is a singular point), which is evident from Fig. 3.6. It is seen that for $z > z_s$ the CE expansion becomes useless as different order truncated CE series shows oscillating behaviour, which indicates the diverging nature of truncated CE expansion.

To improve the region of convergence of the adopted series expansion (3.28) for the present problem of gravity-driven Poiseuille flow, we apply some convergence acceleration methods to the current series solutions.

3.6 Acceleration of Series Convergence: Shanks Transformation and Padé Approximation

Analytical results for all hydrodynamic and flux fields obtained from different order series expansion in g, which are discussed in §3.5, suggested that all series solutions for Froude number less than 10^{-3} are convergent, but for Froude number greater than 10^{-3} they show oscillating behaviour, which indicates the diverging nature of the selected series expansion [See. Eq. (3.28)].

We need to put effort on further analysing the convergence of the adopted series expansion. In the process of finding radius of convergence of the present series expansion, initially, we tried to use Domb-Sykes plot method (Bender & Orszag 1999) and this method did not yield the radius of convergence in the present case as we know only first few coefficients of the series expansion. In the following we discuss about two widely used convergence acceleration methods, namely, (i) Shanks transformation and (ii) Padé approximation to improve the radius/region of convergence

of the series expansion (3.28) with first ten known coefficients that we have calculated in Section 3.4.

3.6.1 Shanks Transformation

Shanks (Shanks (1955)) has suggested a non-linear transformation to accelerate the convergence of slowly convergent and divergent series. The Shanks transformation provides an excellent convergence acceleration technique for infinite-series of oscillating partial sums and alternating series [Bender & Orszag (1999)].

For any given series

$$S = \sum_{n=1}^{\infty} a_n, \tag{3.134}$$

one can construct the sequence of partial sum (S_N); for example, the N^{th} partial sum of above series is

$$S_N = \sum_{n=1}^{N} a_n. \tag{3.135}$$

Suppose that, for sufficiently large N, the N^{th} term of the sequence (S_N) takes the following form:

$$S_N = S + \epsilon\, b^N, \tag{3.136}$$

where $|b| < 1$, so that as $N \to \infty$ we have $S_N \to S$; here, the term $\epsilon\, b^N$ is of transient (oscillatory) nature. It is clear that any term of the sequence $\{S_N\}$ depends on three parameters S, ϵ and b. Therefore, S can be determined from three consecutive terms of the sequence $\{S_N\}$ [Bender & Orszag (1999)], say S_{N-1}, S_N, S_{N+1}:

$$\begin{aligned} S_{N-1} &= S + \epsilon\, b^{N-1}, \\ S_N &= S + \epsilon\, b^N, \\ S_{N+1} &= S + \epsilon\, b^{N+1}. \end{aligned} \tag{3.137}$$

On solving the system of equations (3.137), we get

$$b = \frac{S_{N+1} - S}{S_N - S} = \frac{S_N - S}{S_{N-1} - S}. \tag{3.138}$$

Further solving Eq. (3.138) for S gives the sequence transformation $(S_N) \to (e_1(S_N))$, which is the nonlinear transformation called Shanks transformation

$$e_1(S_N) = \frac{\begin{vmatrix} S_N & S_{N+1} \\ \Delta S_N & \Delta S_{N+1} \end{vmatrix}}{\begin{vmatrix} 1 & 1 \\ \Delta S_N & \Delta S_{N+1} \end{vmatrix}} = \frac{S_{N+1}S_{N-1} - S_N^2}{S_{N+1} + S_{N-1} - 2S_N}, \tag{3.139}$$

where $\Delta S_N = S_N - S_{N-1}$ and $e_1(S_N)$ is an estimate for the limit S, based on the $N-1, N$, and $N+1$ partial sums.

The sequence generated from Shanks transformation, i.e. $e_1(S_N)$, often converges more

rapidly than the sequence of partial sums S_N. One can generate a new sequence $(e_1^2(S_N))$ by iterating the original Shanks transformation, i.e, by treating the sequence $e_1(S_N)$ as a sequence of partial sums:

$$e_1^2(S_N) = \frac{e_1(S_{N+1})e_1(S_{N-1}) - e_1(S_N)^2}{e_1(S_{N+1}) + e_1(S_{N-1}) - 2e_1(S_N)}, \tag{3.140}$$

which converges even more rapidly than the convergence of (S_N) and $e_1(S_N)$. If more number of terms in the series expansion is known, one can further iterate Shanks transformation to obtain new sequences $e_1^3(S_N) = e_1(e_1^2(S_N)), e_1^4(S_N) = e_1(e_1^3(S_N)), \cdots$ and so on, which can give the better approximation to the convergence of the series. The first and second iterations of Shanks transformation to the series with known first five terms are presented in Table 3.1.

Table 3.1: First and second iteration of Shanks transformation to the series

N	S_N	$e_1(S_N)$	$e_1^2(S_N)$
1	S_1		
2	S_2	$e_1(S_2) = \frac{S_3S_1 - S_2^2}{S_3 + S_1 - 2S_2}$	
3	S_3	$e_1(S_3) = \frac{S_4S_2 - S_3^2}{S_4 + S_2 - 2S_3}$	$e_1^2(S_3) = \frac{e_1(S_4)e_1(S_2) - e_1(S_3)^2}{e_1(S_4) + e_1(S_2) - 2e_1(S_3)}$
4	S_4	$e_1(S_4) = \frac{S_5S_3 - S_4^2}{S_5 + S_3 - 2S_4}$	
5	S_5		

To illustrate the advantage of Shanks transformation in improving convergence of a series, we apply this transformation to conditionally convergent series [Bender & Orszag (1999)]

$$\sum_{N=1}^{\infty} (-1)^{N+1} \frac{1}{N} = 1 - \frac{1}{2} + \frac{1}{3} - \frac{1}{4} + \frac{1}{5} - \frac{1}{6} + \cdots, \tag{3.141}$$

which converge very slowly to $\ln 2 = 0.69314718$, which means that one has to consider thousands of partial sums to obtain the limit of $\ln 2$ accurate to four decimal places. Here, the Shanks transformation (3.139) is applied to first seven partial sums of the series (3.141)

$$\begin{aligned} &S_1 = 1, \quad S_2 = \frac{1}{2} = 0.5, \quad S_3 = \frac{5}{6} \approx 0.833333, \quad S_4 = \frac{7}{12} \approx 0.583333, \\ &S_5 = \frac{47}{60} \approx 0.783333, \quad S_6 = \frac{37}{60} \approx 0.616666, \quad S_7 = \frac{319}{420} \approx 0.759523. \end{aligned} \tag{3.142}$$

All these partial sums oscillate around the limit of the series. The iterated Shanks transformations of the sequence of partial sums (S_N): $e_1(S_N)$, $e_1^2(S_N)$ and $e_1^3(S_N)$, gives very accurate approximation to the exact limit of $\ln 2$ up to three, four and five decimal places, respectively, after a relatively small number of terms, which is evident from the Table 3.2.

Application of Shanks Transformation to Present Work

Here we apply Shanks transformation to accelerate the convergence of series expansion for $\mathcal{N}_1(0)$, $\mathcal{N}_2(0)$ and $q_x(0)$. First five partial sums of perturbation series expansion of $\mathcal{N}_1(0)$ [first NSD at

Table 3.2: Iterated Shanks transformation of the series (3.141)

N	S_N	$e_1(S_N)$	$e_1^2(S_N)$	$e_1^3(S_N)$
1	1	–	–	–
2	0.5	0.7	–	–
3	0.833333	0.690476	0.693277	–
4	0.583333	0.694444	0.693105	0.693148
5	0.783333	0.692424	0.693163	–
6	0.616666	0.693589	–	–
7	0.759523	–	–	–

channel centreline ($y = 0$)] are given by

$$S_1 = \frac{317\mathrm{Fr}_0^2\pi}{16}, \quad S_2 = \frac{317\mathrm{Fr}_0^2\pi}{16} - \frac{17488781\mathrm{Fr}_0^4\pi^2}{160}, \tag{3.143}$$

$$S_3 = \frac{317\mathrm{Fr}_0^2\pi}{16} - \frac{17488781\mathrm{Fr}_0^4\pi^2}{160} + \frac{1543950452907173\mathrm{Fr}_0^6\pi^3}{102400}, \tag{3.144}$$

$$S_4 = \frac{317\mathrm{Fr}_0^2\pi}{16} - \frac{17488781\mathrm{Fr}_0^4\pi^2}{160} + \frac{1543950452907173\mathrm{Fr}_0^6\pi^3}{102400} - \frac{24110061341346938600915 9\mathrm{Fr}_0^8\pi^4}{16384000}, \tag{3.145}$$

$$S_5 = \frac{317\mathrm{Fr}_0^2\pi}{16} - \frac{17488781\mathrm{Fr}_0^4\pi^2}{160} + \frac{1543950452907173\mathrm{Fr}_0^6\pi^3}{102400} - \frac{24110061341346938600915 9\mathrm{Fr}_0^8\pi^4}{16384000} + \frac{160255292918616695155497447296417\mathrm{Fr}_0^{10}\pi^5}{2621440000}. \tag{3.146}$$

Based on above partial sums, the expressions for Shanks and iterated Shanks transformations for the centreline first normal stress difference are

$$e_1(S_2) = \frac{\mathrm{Fr}_0^2\pi\left(3548123889280 + 469857416076152337\mathrm{Fr}_0^2\pi\right)}{179085117440 + 24703207246514768\mathrm{Fr}_0^2\pi} \equiv \mathcal{N}_1^{(2)}(0), \tag{3.147}$$

$$\begin{aligned} e_1(S_3) = {} & \frac{\mathrm{Fr}_0^2\pi}{640\left(247032072465147680 + 24110061341346938600915 9\mathrm{Fr}_0^2\pi\right)} \\ & \times(3132366678858072582400 + 30398746188215154229634238 00\mathrm{Fr}_0^2\pi \\ & -1448244030678304953686722812878 7\mathrm{Fr}_0^4\pi^2) \equiv \mathcal{N}_1^{(3)}(0), \end{aligned} \tag{3.148}$$

$$\begin{aligned} e_1(S_4) = {} & \mathrm{Fr}_0^2\pi(391315939594597352268305423360 0 \\ & +162347081478304739544380135875332240 00\mathrm{Fr}_0^2\pi \\ & -867074518920178362390710594384028895456 08\mathrm{Fr}_0^4\pi^2 \\ & +946483631470593532624480535183611813369423059 3\mathrm{Fr}_0^6\pi^3) \\ & \times(5120(385760981461551017614654 40 \\ & +160255292918616695155497447296417\mathrm{Fr}_0^2\pi))^{-1} \equiv \mathcal{N}_1^{(4)}(0), \end{aligned} \tag{3.149}$$

$$
\begin{aligned}
e_1^2(S_3) \;=\; & (\mathrm{Fr}_0^2\pi(11257831860507076865721454070465786823472726665741129724957 \\
& 83256087618811625088579096989440000 + 99363302160269420074618149456 36 \\
& 56672074836893606459146521065180586077099947588399651366364364203200\mathrm{Fr}_0^2\pi \\
& +91522450499447095218574329245825828538602703299699900131979494138767 92 \\
& 62756762091760514373944648498956755\mathrm{Fr}_0^4\pi^2 + 51693750905046831931465402654 6 \\
& 20982918975931589584850838700960502716097047809736224383934081818254431 1 \\
& 26051149\mathrm{Fr}_0^6\pi^3))(10\left(247032072465147680 + 24110061341346938600915 9\mathrm{Fr}_0^2\pi\right) \\
& \times(23001816611557015088655390309008624935989848975799054209221235637478 43 \\
& 840 + 18069483982884321754007925032515446546934797251691881340942784126 79 \\
& 4059860703272\mathrm{Fr}_0^2\pi + 11744202405504237541981222699386172471091623865310183 \\
& 69705555747830665831116493177217\mathrm{Fr}_0^4\pi^2))^{-1} \equiv \mathcal{N}_1^{(23)}(0). \qquad (3.150)
\end{aligned}
$$

The numerical results based on these Shanks transformation, along with related Padé approximations, will be compared and discussed in the Section §3.6.3.

3.6.2 Padé Approximation

The objective of approximation/summation theory is to represent a given function by a convergent expression, which is the limit of a convergent series and the limit of convergent integral in Euler and Borel summation methods, respectively. The main drawback of these two methods, Euler and Borel summation, is that all terms in a power series representation of a function must be known which is not possible in almost all realistic perturbation problems. Therefore, a summation method is needed which only requires a finite number of terms of a divergent series as input. Padé approximation (Padé 1892) is a well-known summation method having a key property: *extracting the information from the power series expansion with only a few known terms*, introduced by Padé in 1892. The main idea of Padé approximation is to replace a power series representation of a function by a sequence of rational functions [Bender & Orszag (1999), Baker, G. A. Jr & Graves-Morris (1996), Pozzi (1994)], that means that a Padé approximant of a function is the ratio of two polynomials, which are constructed from the coefficients of the Taylor series expansion of a function.

For a given power series $\sum_{n=0}^{\infty} a_n x^n$, the Padé approximation/summation is defined as [Bender & Orszag (1999), Baker, G. A. Jr & Graves-Morris (1996), Pozzi (1994)]

$$
P_M^N(x) = \frac{Q_M(x)}{D_N(x)} \equiv P[M,N], \qquad (3.151)
$$

where

$$
Q_M(x) = \sum_{n=0}^{M} A_n x^n, \quad D_N(x) = \sum_{n=0}^{N} B_n x^n. \qquad (3.152)
$$

Notice that there are $M+1$ numerator coefficients and $N+1$ denominator coefficients in Eq. (3.151); for definiteness, we take $B_0 = 1$. So there are $M+1$ independent numerator coefficients

and N independent denominator coefficients, a total $(M+N+1)$ unknown coefficients in Eq. (3.151). Consequently, we can write the given power series in terms of Padé summation as

$$\sum_{n=0}^{\infty} a_n x^n = \frac{A_0 + A_1 x + A_2 x^2 + \cdots + A_M x^M}{1 + B_1 x + B_2 x^2 + \cdots + B_N x^N} + O(x^{M+N+1}). \tag{3.153}$$

To find this $(M+N+1)$ unknown coefficients in Eq. (3.151), we compare the first $(M+N+1)$ terms of the power series $\sum_{n=0}^{\infty} a_n x^n$ with the first $(M+N+1)$ terms in the Taylor series expansion of $P_M^N(x)$.

The emerging rational function $P[M,N] \equiv P_M^N(x)$, given by (3.153), is called a Padé approximant to given power series. If $M = N$, then $P[M,M]$ is called a "diagonal" Padé approximant. To construct a Padé approximant $P[M,N]$, one just needs to know the first $(M+N+1)$ terms in the power series representation of a function and it involves only algebraic operations. Due to this reason, the Padé summation is more convenient for computational purposes than Borel summation method, which requires one to integrate the analytic continuation of a function defined by a power series over an infinite range.

The advantage of Padé approximation is illustrated here by considering the Maclaurin series expansion of $\tan^{-1}(x)$ up to x^{10}. The expression of $\tan^{-1}(x)$ using Maclaurin series is

$$\tan^{-1}(x) \approx x - \frac{x^3}{3} + \frac{x^5}{5} - \frac{x^7}{7} + \frac{x^9}{9}. \tag{3.154}$$

The Padé summation of (3.154) is given by

$$x - \frac{x^3}{3} + \frac{x^5}{5} - \frac{x^7}{7} + \frac{x^9}{9} = \frac{A_0 + A_1 x + A_2 x^2 + A_3 x^3 + A_4 x^4 + A_5 x^5}{1 + B_1 x + B_2 x^2 + B_3 x^3 + B_4 x^4 + B_5 x^5} + O(x^{10}). \tag{3.155}$$

By equating corresponding coefficients, we get

$$A_0 = 0, \quad A_1 = 1, \quad A_2 = B_1, \quad A_3 = -\frac{1}{3} + B_2, \quad A_4 = -\frac{B_1}{3} + B_3, \tag{3.156}$$

$$A_5 = \frac{1}{5} - \frac{B_2}{3} + B_4, \quad \frac{B_1}{5} - \frac{B_3}{3} = 0, \quad -\frac{1}{7} + \frac{B_2}{5} - \frac{B_4}{3} = 0, \tag{3.157}$$

$$-\frac{B_1}{7} + \frac{B_3}{5} - \frac{B_5}{3} = 0, \quad \frac{1}{9} - \frac{B_2}{7} + \frac{B_4}{5} = 0, \quad \frac{B_1}{9} - \frac{B_3}{7} + \frac{B_5}{5} = 0. \tag{3.158}$$

One should solve above equations to obtain the values of unknown coefficients in the Padé summation [Eq. (3.155)]:

$$A_0 = 0, \quad A_1 = 1, \quad A_2 = 0, \quad A_3 = \frac{7}{9}, \quad A_4 = 0, \quad A_5 = \frac{64}{945}, \tag{3.159}$$

$$B_1 = 0, \quad B_2 = \frac{10}{9}, \quad B_3 = 0, \quad B_4 = \frac{5}{21}, \quad B_5 = 0. \tag{3.160}$$

The diagonal Padé approximations $P[5,5]$ and $P[4,4]$ of Eq. (3.154) are given by

$$P[5,5] = \frac{x + \frac{7}{9}x^3 + \frac{64}{945}x^5}{1 + \frac{10}{9}x^2 + \frac{5}{21}x^4}, \tag{3.161}$$

$$P[4,4] = \frac{x + \frac{11x^3}{21}}{1 + \frac{6x^2}{7} + \frac{3x^4}{35}}. \tag{3.162}$$

Table 3.3: Diagonal Padé approximation versus Maclaurin series for $\tan^{-1}(x)$

x	Exact value	$P[5,5]$	Error	$P[4,4]$	Error	Maclaurin	Error
0.2	0.19740	0.19740	0.00000	0.19740	0.00000	0.19740	0.00000
0.4	0.38051	0.38051	0.00000	0.38050	0.00001	0.38051	0.00000
0.6	0.54042	0.54042	0.00000	0.54040	0.00002	0.54067	-0.00025
0.8	0.67474	0.67477	-0.00003	0.67450	0.00024	0.67982	-0.00508
1	0.78540	0.78558	-0.00018	0.78431	0.00109	0.83492	-0.04952

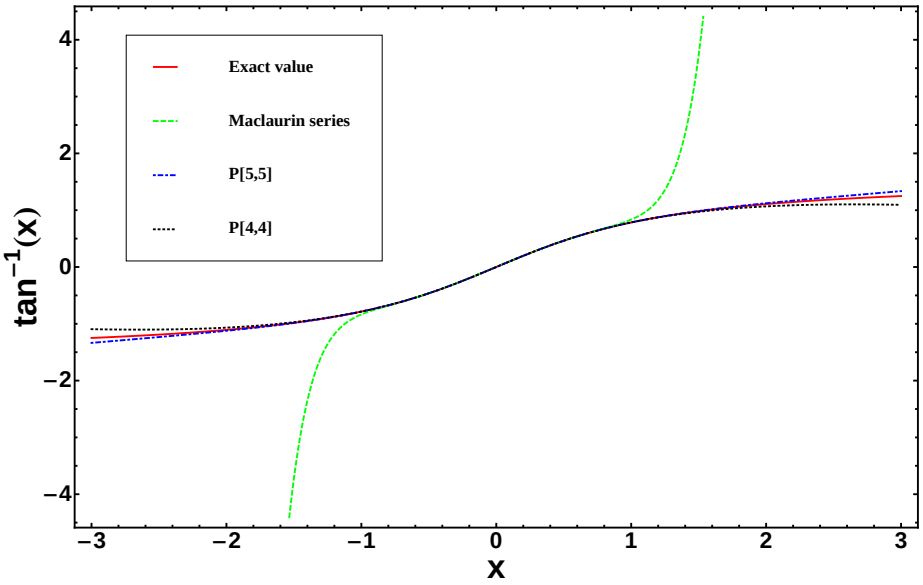

Figure 3.7: Diagonal Padé approximants versus Maclaurin series for $\tan^{-1}(x)$

Table 3.3 and Fig. 3.7 show the convergence of diagonal Padé approximants $P[5,5]$ and $P[4,4]$ in comparison to Maclaurin series expansion of $\tan^{-1}(x)$ up to x^{10}. It is evident from Fig. 3.7 that the Maclaurin series solution diverges as one moves away from $x = 0$, whereas the diagonal Padé approximants still approximate the exact value of $\tan^{-1}(x)$ accurately. Further, it is noticed that higher diagonal Padé approximants converges more accurately to the exact value, which can be seen from Fig. 3.7.

3.6.3 Applications of Padé Approximation and Shanks Transformation to Present Work

Here we use Padé approximation to assess the convergence of series expansions of $\mathcal{N}_1(0)$, $\mathcal{N}_2(0)$ and $q_x(0)$ – a comparison with related results using Shanks transformation will also be presented. The final expressions of diagonal Padé approximants $P[3,3]$ and $P[5,5]$ of $\mathcal{N}_1(0)$ are given by

$$P[3,3] = \frac{317\mathrm{Fr}_0^2\pi}{16\left(1+\frac{17488781\mathrm{Fr}_0^2\pi}{3170}\right)} \equiv \mathcal{N}_1^{[3,3]}(0), \tag{3.163}$$

$$P[5,5] = \frac{\frac{317\mathrm{Fr}_0^2\pi}{16} + \frac{7986510206314934135424744821\mathrm{Fr}_0^4\pi^2}{400944995051649994240}}{1+\frac{5066457698035859038272373\mathrm{Fr}_0^2\pi}{5011812438145624928} + \frac{48274801022610165122890760429 29\mathrm{Fr}_0^4\pi^2}{1002362487629124985600}} \equiv \mathcal{N}_1^{[5,5]}(0). \tag{3.164}$$

The diagonal Padé approximations $P[3,3]$ and $P[5,5]$ for $\mathcal{N}_2(0)$ are given by

$$P[3,3] = -\frac{71\mathrm{Fr}_0^2\pi}{8\left(1+\frac{2492539\mathrm{Fr}_0^2\pi}{355}\right)} \equiv \mathcal{N}_2^{[3,3]}(0), \tag{3.165}$$

$$P[5,5] = \frac{-\frac{71\mathrm{Fr}_0^2\pi}{8} - \frac{1423094921606684239236305 87\mathrm{Fr}_0^4\pi^2}{14565227044986433280}}{1+\frac{4034284565408605912934 17\mathrm{Fr}_0^2\pi}{364130676124660832} + \frac{4858649159978336537687047287 01\mathrm{Fr}_0^4\pi^2}{72826135224932166400}} \equiv \mathcal{N}_2^{[5,5]}(0). \tag{3.166}$$

The diagonal Padé approximations $P[2,2]$ and $P[4,4]$ for $q_x(0)$ are given by

$$P[2,2] = \frac{5\mathrm{Fr}_0\sqrt{\pi}}{8\left(1+\frac{10581\mathrm{Fr}_0^2\pi}{16}\right)} \equiv q_x^{[2,2]}(0), \tag{3.167}$$

$$P[4,4] = \frac{\frac{5\mathrm{Fr}_0\sqrt{\pi}}{8} + \frac{1284575736483764263\mathrm{Fr}_0^3\pi^{3/2}}{3950193422848}}{1+\frac{1286208431663731243\mathrm{Fr}_0^2\pi}{2468870889280} + \frac{1216350442993762731861 9\mathrm{Fr}_0^4\pi^2}{39501934228480}} \equiv q_x^{[4,4]}(0). \tag{3.168}$$

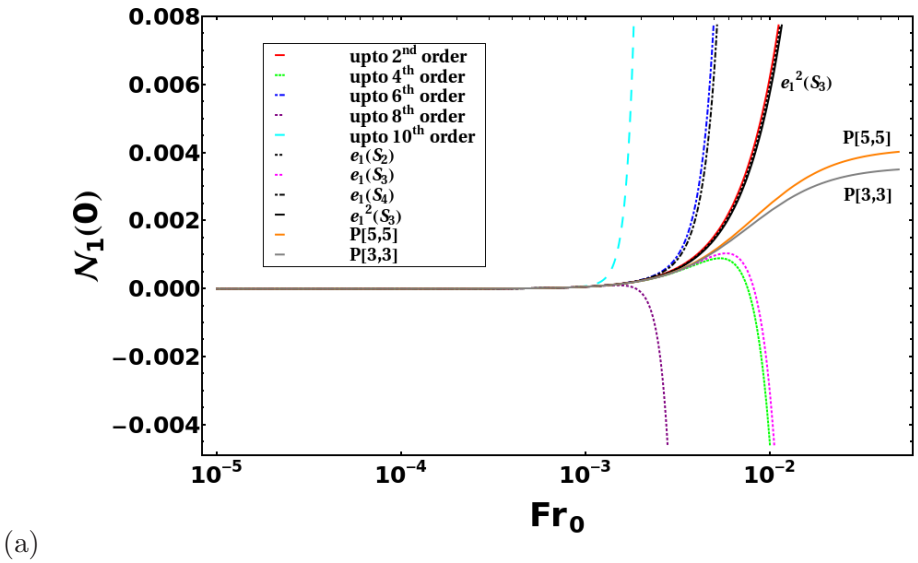

(a)

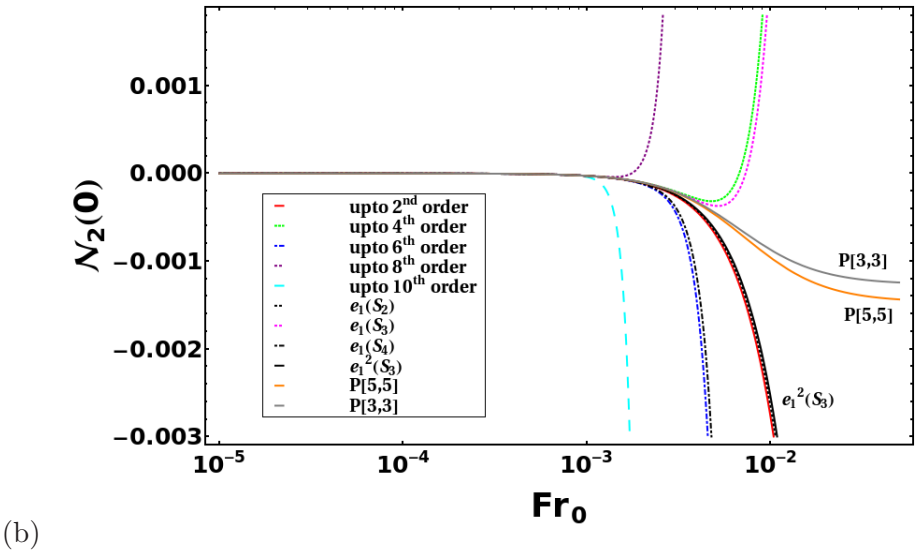

(b)

Figure 3.8: Different series solutions behaviour for (a) first normal stress difference and (b) second normal stress difference both evaluated at channel centreline ($y = 0$), with Fr_0 as predicted by kinetic model description. The red solid, green tiny dashed, blue dot-dashed, purple dotted, cyan large dashed, black dotted, magenta dotted, black dot-dashed, black solid, orange solid and grey solid lines in each panel represent the 2nd order, 4th order, 6th order, 8th order, 10th order, $e_1(S_2)$, $e_1(S_3)$, $e_1(S_4)$, $e_1^2(S_3)$, $P[5,5]$, and $P[3,3]$, respectively.

Figs. 3.8(a) and 3.8(b) display the "Padé-approximated" first and second normal stress differences evaluated at $y = 0$ (channel centreline) against Froude number. From Section 3.5.2, we know that for Fr_0 greater than 10^{-3}, all solutions for both $\mathcal{N}_1$ and $\mathcal{N}_2$ predicted by the different order series expansions display oscillating behaviour (see Figs. 3.3b and 3.4b) which indicated the diverging nature of the respective series solution. From Fig. 3.8, one can observe that the solutions obtained by applying Shanks transformation to the 10th-order series solution shows the convergent behaviour up to $\mathrm{Fr}_0 \approx 5 \times 10^{-3}$, but 8th and 10th-order series solution diverges for $\mathrm{Fr}_0 \approx 5 \times 10^{-3}$.

In contrast, the solutions using Padé approximation to the 10th-order series solution extends the convergent solution from $\mathrm{Fr}_0 = 10^{-3}$ to $\mathrm{Fr}_0 \approx 5 \times 10^{-2}$ which is evident from both panels in

Fig. 3.8. Overall, Fig. 3.8 confirms that the Padé approximation is the best approximation to the 10th-order series solution (of normal stress differences) as compared to the approximation based on Shanks transformation.

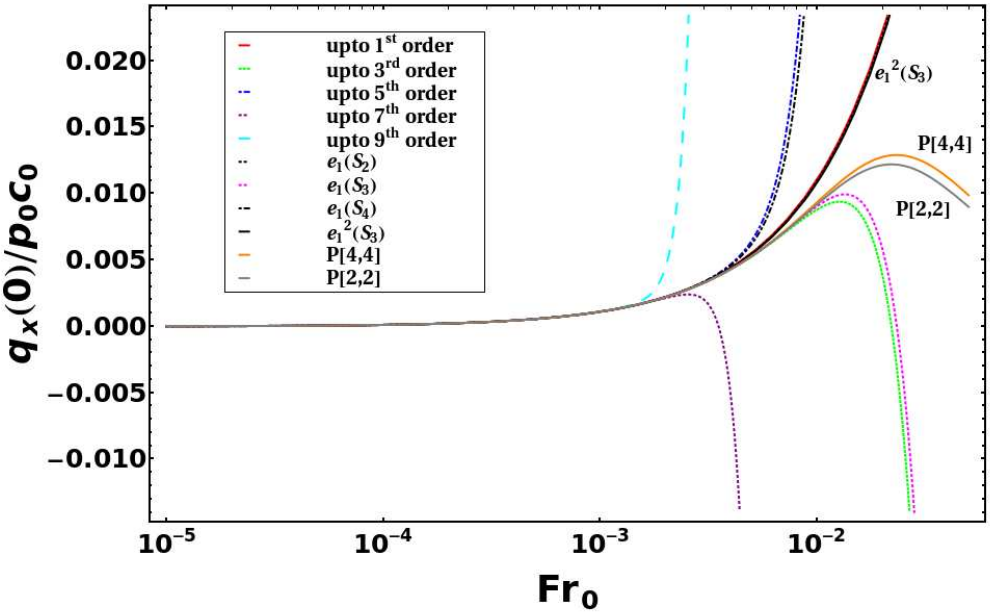

Figure 3.9: Variations of $q_x(0)/(p_0 c_0)$ evaluated at $y = 0$ with Fr_0 as predicted by kinetic model. The red solid, green tiny dashed, blue dot-dashed, purple dotted, cyan large dashed, black dotted, magenta dotted, black dot-dashed, black solid, orange solid and grey solid lines represent the 1st order, 3rd order, 5th order, 7th order, 9th order, $e_1(S_2)$, $e_1(S_3)$, $e_1(S_4)$, $e_1^2(S_3)$, $P[4,4]$, and $P[2,2]$, respectively.

Fig. 3.9 displays the x-component of the heat flux evaluated at $y = 0$ (channel centreline) against the Froude number. Recall from Fig. 3.5(c) that, for Froude number greater than 10^{-3}, the high-order series solutions show oscillating behaviour which indicates the divergent nature of the series expansion. One can observe from Fig. 3.9 that the solutions obtained by applying Shanks transformation to the 10th-order series solution shows convergent behaviour up to $\mathrm{Fr}_0 \approx 5 \times 10^{-3}$ but 8th and 10th-order series solution diverges for $\mathrm{Fr}_0 \approx 5 \times 10^{-3}$. On the other hand, the solutions using Padé approximation to the 10th-order series solution extend the convergent solution from $\mathrm{Fr}_0 = 10^{-3}$ to $\mathrm{Fr}_0 \approx 5 \times 10^{-2}$ which is evident from Fig. 3.9.

Overall, Figs. 3.8 and 3.9 confirm that the Padé approximation provides the best approximation to the 10th-order series solution (for heat flux as well as normal stress differences) as it extended the range of convergence of the respective series solutions from $\mathrm{Fr}_0 = 10^{-3}$ to $\mathrm{Fr}_0 \approx 10^{-1}$.

3.7 Results for Maxwell Molecules

The Maxwell gas is a special gas composed of molecules which repel each other in the physical space, with a force inversely proportional to the fifth power of distance between them [McCormack & Williams (1972); Pulvirenti & Toscani (1996)]. The main difference between a

hard-sphere gas and a Maxwell gas is that the collision kernel is independent of relative velocity of particles in case of Maxwell molecules whereas for hard-sphere molecules it is proportional to relative velocity of particles. Here we present a brief summary of the results for the gravity-driven Poiseuille flow for a gas of Maxwell molecules (Maxwellian gas). Note that the related results up to sixth-order in dimensionless gravity were determined by Tij & Santos (1994) – however they did not analyse the convergence issues as we discuss below.

The gravity-driven Poiseuille flow of Maxwell molecules is analysed in the context of kinetic theory [§3.2] using a BGK kinetic model of the Boltzmann equation and the solution is obtained via a similar perturbation expansion in power of the force field up to tenth-order. The solution procedure is the same as in the case of hard-sphere molecules discussed in §3.4. The geometry of the present problem is also the same as in Fig. 3.1 with hard-sphere particles being replaced by Maxwell molecules. The equation for collision frequency ν for Maxwell molecules differs from Eq. (3.32) and is given by

$$\begin{aligned}\nu &= 1+(p^{(2)}-T^{(2)})g^2+(p^{(4)}-p^{(2)}T^{(2)}+{T^{(2)}}^2-T^{(4)})g^4\\ &\quad+(p^{(6)}-p^{(4)}T^{(2)}+p^{(2)}{T^{(2)}}^2-{T^{(2)}}^3-p^{(2)}T^{(4)}+2T^{(2)}T^{(4)}-T^{(6)})g^6\\ &\quad+(p^{(8)}-p^{(6)}T^{(2)}+p^{(4)}{T^{(2)}}^2-p^{(2)}{T^{(2)}}^3+{T^{(2)}}^4-p^{(4)}T^{(4)}+2p^{(2)}T^{(2)}T^{(4)}\\ &\quad-3{T^{(2)}}^2T^{(4)}+{T^{(4)}}^2-p^{(2)}T^{(6)}+2T^{(2)}T^{(6)}-T^{(8)})g^8+O(g^{10}),\end{aligned} \tag{3.169}$$

since, for Maxwell molecules, the collision frequency (ν) is $\nu = pT^{-1} \propto n$, which is independent of temperature [Garzó *et al.* (1989); Tij & Santos (1994)]. Finally, by following the solution procedure discussed in §3.4, we obtain hydrodynamic and flux fields. The explicit expressions of hydrodynamic and flux fields for the case of Maxwell molecules are omitted.

3.7.1 Comparison with Tij and Santos (1994)

In Tij & Santos (1994), the dimensionless scaled space variable s is defined as

$$s(y) = \frac{1}{c_0}\int_0^y \nu(y')dy'. \tag{3.170}$$

The above relationship can be inverted to yield

$$y^*(s) = \int_0^s \frac{ds'}{\nu^*(s')}, \quad y^* \equiv \frac{y\nu_0}{c_0}. \tag{3.171}$$

Since $\nu^* = \frac{p^*}{T^*}$ for Maxwell molecules and we substitute $p^*(= 1 + p^{(2)}{g^*}^2 + \cdots)$ and $T^*(= 1 + T^{(2)}{g^*}^2 + \cdots)$, into above equations; after integration, we get a relation between s and y^*.

$$s = y^* + {g^*}^2{y^*}^3\left(\frac{11}{75}+\frac{1}{150}{y^*}^2\right)+\cdots. \tag{3.172}$$

Substitute the above expression (3.172) into the Eqs. (45)-(47) and (75)-(80) of Tij & Santos (1994) and converting the resulted expressions into real units, we obtain

$$p(y) = p_0\left[1+\frac{6}{5}\left(\frac{mg}{T_0}\right)^2 y^2\right]+O(g^4), \tag{3.173}$$

$$u_x(y) = u_0 + \left(\frac{\rho_0 g}{2\eta_0}\right)y^2 + \frac{2737}{25}\left(\frac{m^3\eta_0 g^3}{\rho_0 T_0^3}\right)y^2 + \frac{76}{75}\left(\frac{m^2\rho_0 g^3}{\eta_0 T_0^2}\right)y^4 + \frac{1}{150}\left(\frac{m\rho_0^3 g^3}{\eta_0^3 T_0}\right)y^6 + O(g^5), \tag{3.174}$$

$$T(y) = T_0\left[1 - \frac{1}{30}\left(\frac{m\rho_0^2 g^2}{\eta_0^2 T_0}\right)y^4 + \frac{19}{25}\left(\frac{mg}{T_0}\right)^2 y^2\right] + O(g^4), \tag{3.175}$$

$$P_{xx}(y) = p_0\left[1 + \frac{328}{25}\left(\frac{\rho_0\eta_0^2 g^2}{p_0^3}\right) + \frac{14}{5}y^2\left(\frac{mg}{T_0}\right)^2\right] + O(g^4), \tag{3.176}$$

$$P_{yy}(y) = p_0\left[1 - \frac{306}{25}\left(\frac{\rho_0\eta_0^2 g^2}{p_0^3}\right)\right] + O(g^4), \tag{3.177}$$

$$P_{zz}(y) = p_0\left[1 - \frac{22}{25}\left(\frac{\rho_0\eta_0^2 g^2}{p_0^3}\right) + \frac{4}{5}y^2\left(\frac{mg}{T_0}\right)^2\right] + O(g^4), \tag{3.178}$$

$$P_{yx}(y) = -\rho_0 g y - \frac{11y^3}{75}\left(\frac{\rho_0^3 g^3}{p_0^2}\right) - \frac{y^5}{150}\left(\frac{\rho_0^4 g^3}{\eta_0^2 p_0}\right) + O(g^5), \tag{3.179}$$

$$q_x(y) = \eta_0 g - \frac{21162}{25}\left(\frac{\rho_0\eta_0^3 g^3}{p_0^3}\right) - \frac{159y^2}{5}\left(\frac{\rho_0^2\eta_0 g^3}{p_0^2}\right) - \frac{29y^4}{30}\left(\frac{\rho_0^3 g^3}{\eta_0 p_0}\right) + O(g^5), \tag{3.180}$$

$$q_y(y) = \frac{\rho_0^2 g^2 y^3}{3\eta_0} + O(g^4). \tag{3.181}$$

Here $-g = \frac{F}{m}$ as in Tij & Santos (1994). We have checked that the above results of Tij & Santos (1994) are same as present results for Maxwell molecules up to third-order in g.

3.7.2 Extension of Tij and Santos (1994)

Now we discuss presently obtained higher-order solutions for Maxwell molecules on (i) temperature, (ii) first and second normal stress differences and (iii) the tangential heat flux profiles of gravity-driven Poiseuille flow of a Maxwell gas.

Fig. 3.10(a) displays the dimensionless temperature T/T_0 vs y/λ_0, where λ_0 is the centreline mean free path for $\mathrm{Fr}_0 = 10^{-3}$. One can observe that the temperature bimodality, i.e, temperature profile $T(y)$ has a local minimum at the channel centreline (i.e. at $y = 0$) which is surrounded by two maxima. The bimodal nature of temperature profile is clearly visualized from the tenth-order series solution which is evident from Fig. 3.10(a). The degree of bimodality $\triangle T$ increases as Fr_0 increases from 10^{-4} to 10^{-3} and shows oscillating nature for Froude number beyond $\mathrm{Fr}_0 > 10^{-3}$. Overall, these results on the temperature profiles resemble the results on temperature profiles for a hard-sphere gas undergoing Poiseuille flow (Fig. 3.2) which are discussed in §3.5.1.

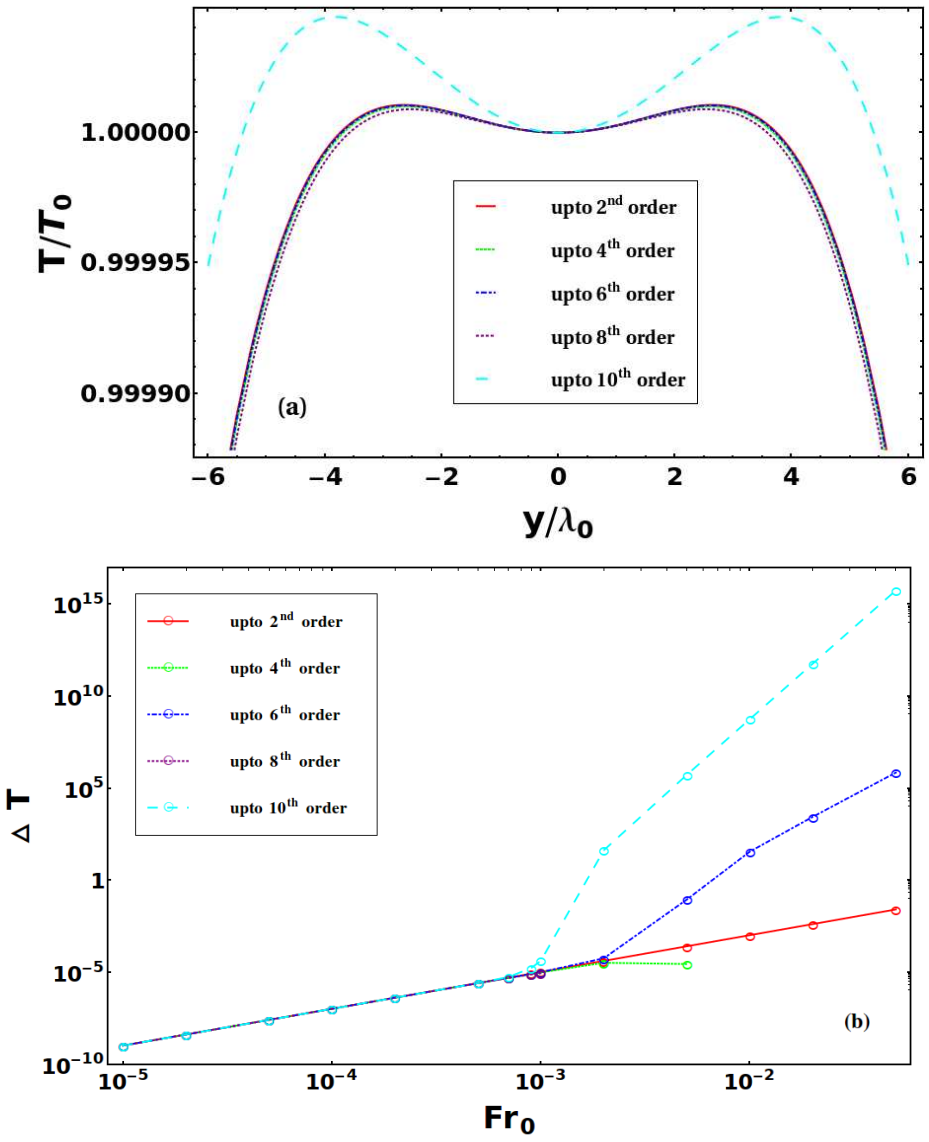

Figure 3.10: Temperature profiles for Maxwell molecules for (a) $\mathrm{Fr}_0 = 10^{-3}$, and (b) $\Delta T (= T_{\max}/T_0 - 1)$ with Fr_0 as predicted by kinetic model. The red solid, green tiny dashed, blue dot-dashed, purple dotted and cyan large dashed lines represent the solutions of 2^{nd} order, 4^{th} order, 6^{th} order, 8^{th} order and 10^{th} order, respectively.

The profiles of first normal stress difference for $\mathrm{Fr}_0 = 10^{-3}$ using different series solutions are presented in Fig. 3.11(a): $\mathcal{N}_1(y)$ has a minimum at the channel centreline. The profiles of $\mathcal{N}_1(0)$ in Fig. 3.11(b) indicates a convergent nature of series solution at $\mathrm{Fr}_0 < 10^{-3}$; however, for $\mathrm{Fr}_0 > 10^{-3}$ the solutions for $\mathcal{N}_1$ shows the divergent nature of the series expansion in g which is evident from Fig. 3.11(b). Similar kind of behaviour for $\mathcal{N}_1$ was reported in §3.5.2 (Fig. 3.4) for a hard-sphere gas.

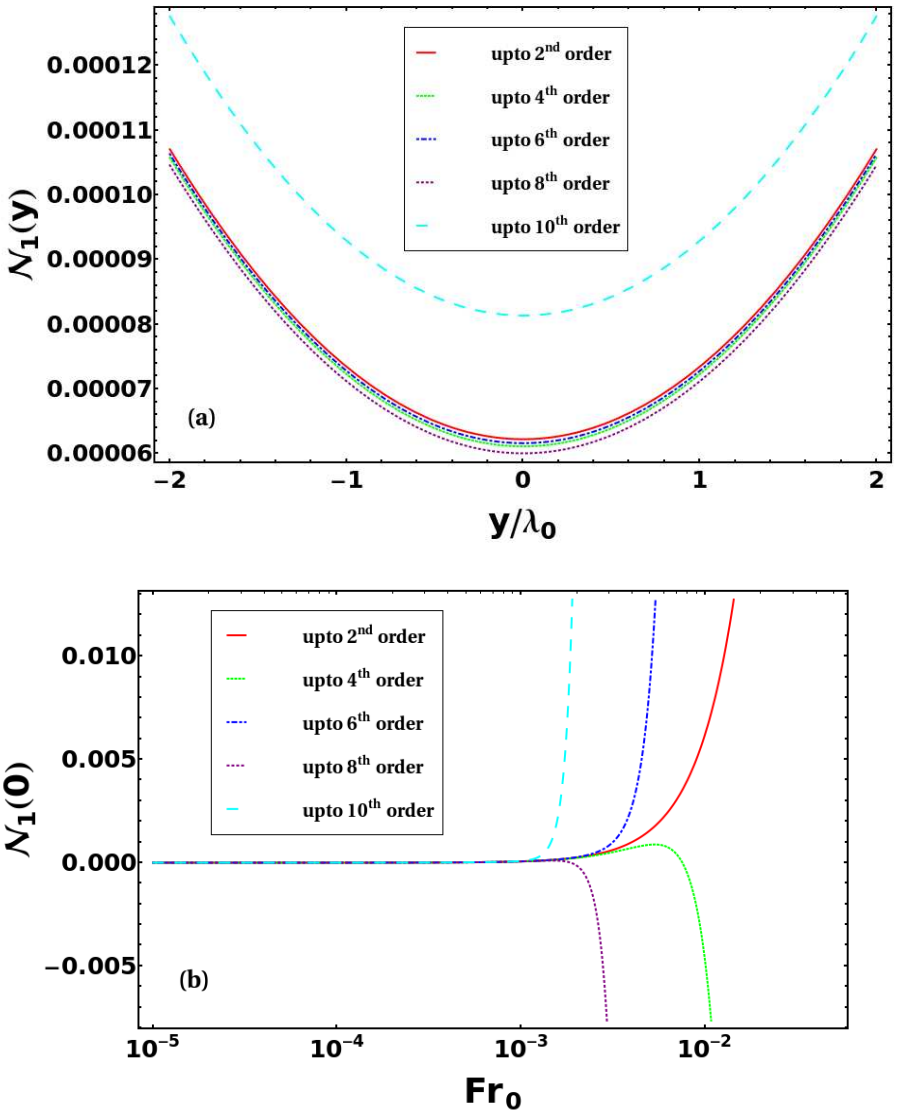

Figure 3.11: (a) Transverse profiles of the first normal stress difference for a Maxwell gas for $\mathrm{Fr}_0 = 10^{-3}$, and (b) $\mathcal{N}_1$ evaluated at channel centreline ($y = 0$), with Fr_0. In both panels (a) and (b), the red solid, green tiny dashed, blue dot-dashed, purple dotted and cyan large dashed lines indicate the solutions of 2^{nd} order, 4^{th} order, 6^{th} order, 8^{th} order and 10^{th} order, respectively.

The second normal stress difference profiles for a Maxwell gas as predicted by the present kinetic model for $\mathrm{Fr}_0 = 10^{-3}$ are presented in Fig. 3.12(a). We notice that second normal stress difference is maximum at $y = 0$, i.e at the channel centreline. Fig. 3.12(b) shows the second normal stress difference evaluated at the channel centreline ($y = 0$), against Froude number. Results for $\mathcal{N}_2$ shows that convergent series expansion for Fr_0 less than 10^{-3} and divergent solutions for $\mathrm{Fr}_0 > 10^{-3}$ as evident from Fig. 3.12(b). Same kind of behaviour is for $\mathcal{N}_2$ is presented in §3.5.2 for hard-sphere gas.

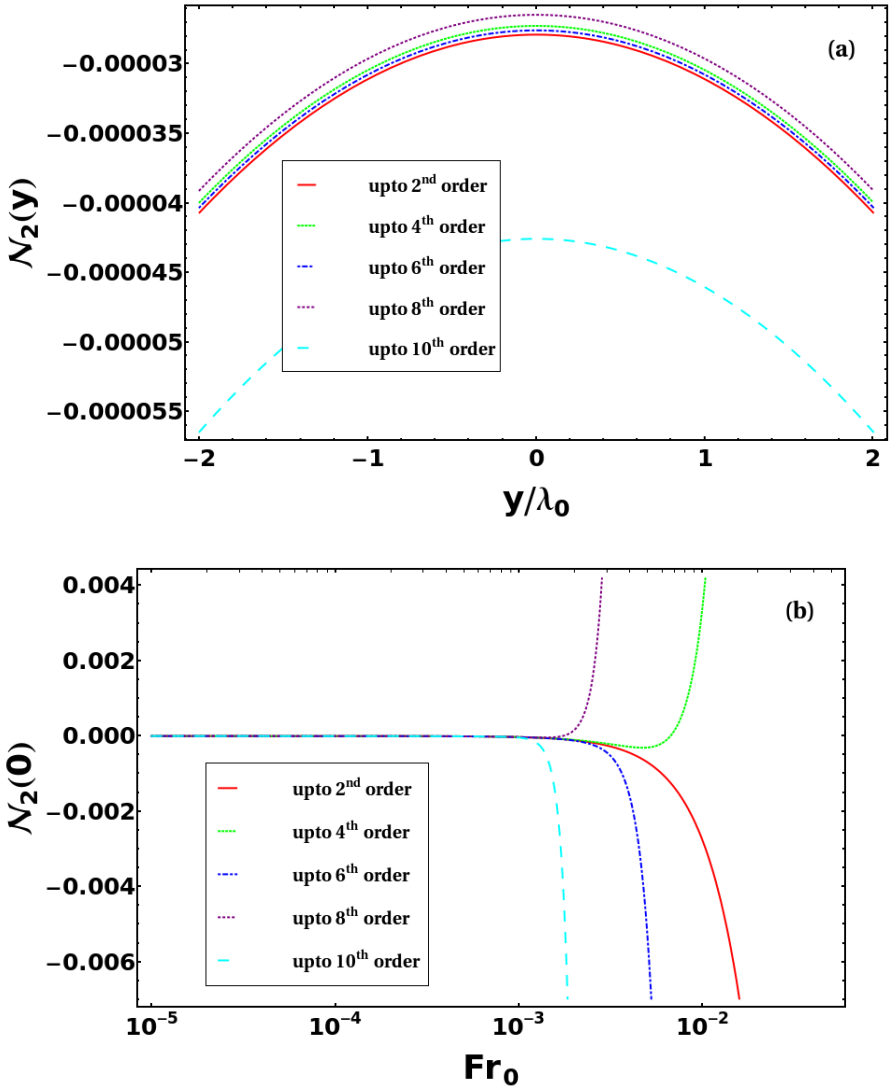

Figure 3.12: (a) Transverse profiles of the second normal stress difference for a Maxwell gas for $\mathrm{Fr}_0 = 10^{-3}$, and (b) $\mathcal{N}_2$ evaluated at channel centreline ($y = 0$), with Fr_0 as predicted by kinetic theory description. In both panels (a) and (b), the red solid, green tiny dashed, blue dot-dashed, purple dotted and cyan large dashed lines represent the solutions of 2^{nd} order, 4^{th} order, 6^{th} order, 8^{th} order and 10^{th} order, respectively.

Based on above results for a Maxwell gas undergoing Poiseuille flow, it should be noted that the perturbation series solutions for temperature bimodality, first and second normal stress difference and the longitudinal component of heat flux vector (not shown) up to tenth-order in g agree well among themselves for $\mathrm{Fr}_0 \leq 10^{-3}$, beyond which, adopted series expansion of $\triangle T$, $\mathcal{N}_1$, $\mathcal{N}_2$ and q_x shows oscillating behaviour, indicating the divergent nature of each solution. We apply convergence acceleration methods, namely Shanks transformation and Padé approximation, which are discussed in §3.6 to the adopted perturbation series expansion of temperature bimodality, first and second normal stress difference and the longitudinal component of heat flux vector to improve the range of convergence of the series.

For Maxwell molecules, the convergence acceleration of (i) the first and second normal stress differences and (ii) the tangential heat flux, all evaluated at $y = 0$, are shown in Fig. 3.13

and Fig. 3.14, respectively. It is evident from both figures that the solutions obtained by applying Shanks transformation to the 10th-order series solution shows a convergent behaviour up to $\mathrm{Fr}_0 \approx 5 \times 10^{-3}$ but 8th and 10th-order series solution diverges for $\mathrm{Fr}_0 \approx 5 \times 10^{-3}$. The solutions using Padé approximation to the 10th-order series solution further extends the convergent solution from $\mathrm{Fr}_0 = 10^{-3}$ to $\mathrm{Fr}_0 \approx 10^{-2}$ as compared to Shanks transformation, which is evident from Fig. 3.13 and Fig. 3.14.

On the whole, Fig. 3.13 and Fig. 3.14 suggest that the Padé approximation is the best approximation to the present 10th-order series solution as it extended the range of convergence of the series from $\mathrm{Fr}_0 = 10^{-3}$ to $\mathrm{Fr}_0 \approx 10^{-1}$. This overall conclusion also holds for a hard-sphere gas undergoing acceleration-driven Poiseuille flow as discussed in Section 3.6.

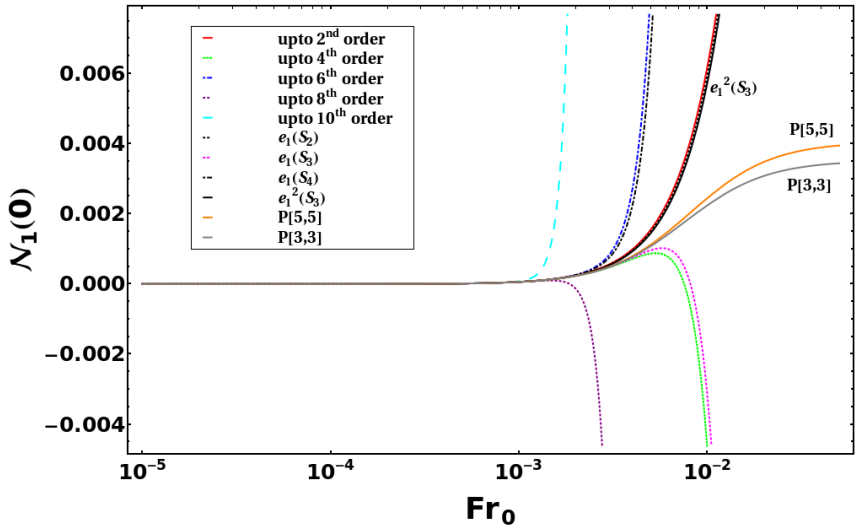

(a)

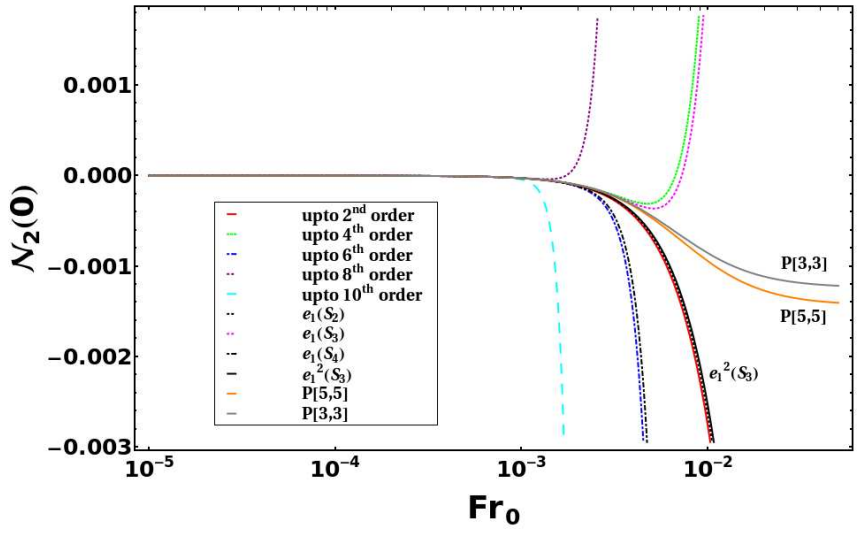

(b)

Figure 3.13: Different series solutions behaviour for (a) first normal stress difference and (b) second normal stress difference both evaluated at channel centreline ($y = 0$), with Fr_0 as predicted by kinetic theory description. The red solid, green tiny dashed, blue dot-dashed, purple dotted, cyan large dashed, black dotted, magenta dotted, black dot-dashed, black solid, orange solid and grey solid lines in each panel represent the 2nd order, 4th order, 6th order, 8th order, 10th order, $e_1(S_2)$, $e_1(S_3)$, $e_1(S_4)$, $e_1^2(S_3)$, $P[5,5]$, and $P[3,3]$, respectively.

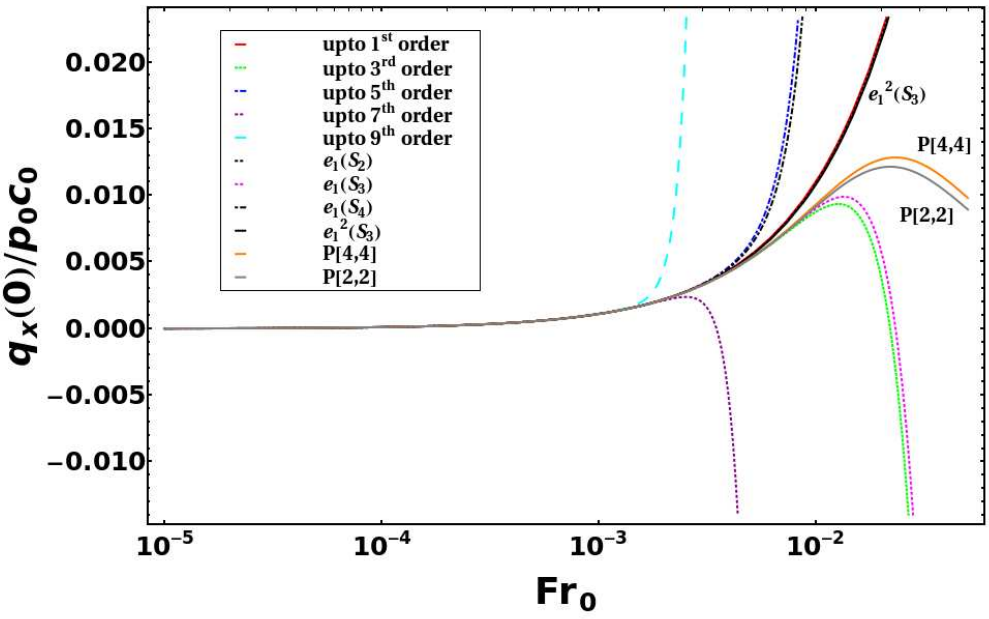

Figure 3.14: Variations of $q_x(0)/(p_0 c_0)$, evaluated at channel centreline ($y = 0$), with Fr_0 as predicted for a Maxwell gas undergoing Poiseuille flow. The red solid, green tiny dashed, blue dot-dashed, purple dotted, cyan large dashed, black dotted, magenta dotted, black dot-dashed, black solid, orange solid and grey solid lines represent the 1st order, 3rd order, 5th order, 7th order, 9th order, $e_1(S_2)$, $e_1(S_3)$, $e_1(S_4)$, $e_1^2(S_3)$, $P[4,4]$, and $P[2,2]$, respectively.

3.8 Summary and Discussion

The gravity-driven Poiseuille flow of both hard-sphere and Maxwell gases flowing through a channel is analysed using a perturbation expansion of the velocity distribution function in powers of the strength of gravitational acceleration (the Froude number $\mathrm{Fr}_0 = g\lambda/v_{th}^2$, where λ is the mean-free path and v_{th} is the thermal velocity, both evaluated at the center of the channel) by retaining terms up to tenth-order in Fr_0. The resulting solution holds only around the channel centerline since the wall-effects are not considered in the present analysis. A BGK kinetic model is adopted and the related problem for Maxwell-molecules was originally analysed by Tij & Santos (1994) by retaining terms up to sixth-order in Froude number as discussed in Section 3.7.

The present high-order expansion (for both hard spheres and Maxwell molecules) helped to assess the asymptotic nature of the perturbation expansion and the related convergence issues for the resulting hydrodynamic and rheological (stress tensor and heat flux) fields for which analytical expressions have been derived. Rarefaction effects (e.g. the bimodal shape of the temperature profile, tangential heat flux, normal stress differences, etc) are analysed using presently obtained high-order series solutions. It is found that the temperature bimodality [$\triangle T = (T_{\max}/T_0 - 1)$, where T_0 is the temperature at the channel centerline and $T_{\max}$ is the maximum temperature that occurs away from the channel center] and all transport coefficients show oscillating behaviour for Froude number greater than 10^{-3} and blindly adding further higher-order terms does not help to obtain converged solution – both indicates the divergent nature of the adopted series

expansion. Subsequently, the Shanks transformation and the Padé approximations have been used to further analyse the convergence of series expansion. The present analysis indicates that the "diagonal" Padé approximation of the 10th-order series solution yields accurate/converged solution for a much larger range of Froude numbers up to $\mathrm{Fr}_0 \approx 10^{-1}$. These overall findings hold for both hard spheres and Maxwell molecules for the present problem of gravity-driven Poiseuille flow of molecular gases.

The recent DSMC simulations of Gupta & Alam (2017) indicates that $\triangle T, \mathcal{N}_1(0), |\mathcal{N}_2(0)|$ and $q_x(0)$ increase with increasing Knudsen number and Froude number for a molecular gas undergoing acceleration-driven Poiseuille flow. Our Padé-approximated solutions for $\mathcal{N}_1(0), |\mathcal{N}_2(0)|$ and $q_x(0)$ show similar increasing trend with increasing Fr_0 as seen in Fig. 3.8 and Fig. 3.9. Therefore, we may conclude that the present series solution must be Padé-approximated (by retaining a large number of terms) to make it useful at larger values of Froude number. Recall from Eq. (3.115), the Knudsen number is proportional to the Froude number – therefore, our Padé-approximated solution is likely to be valid at large Knudsen number too. The simulation results for the acceleration-driven Poiseuille flow of both molecular and granular gases are briefly discussed in Section 4.7 of Chapter 4.

Appendix 3A. Profiles of $u_x(y)$, $p(y)$ and $P_{yx}(y)$ for hard spheres

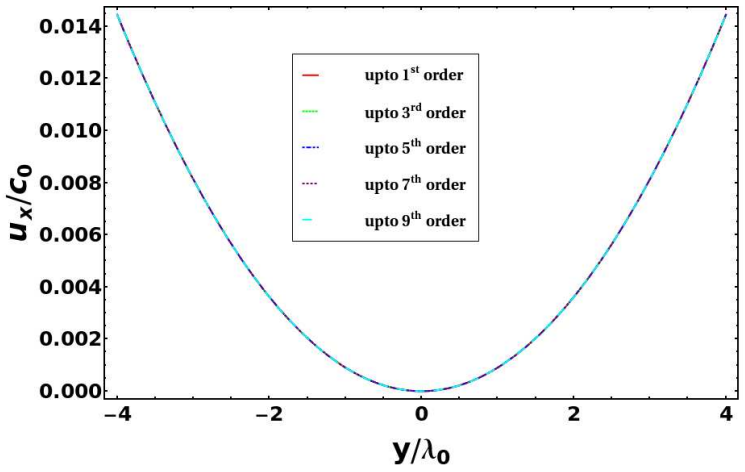

(a)

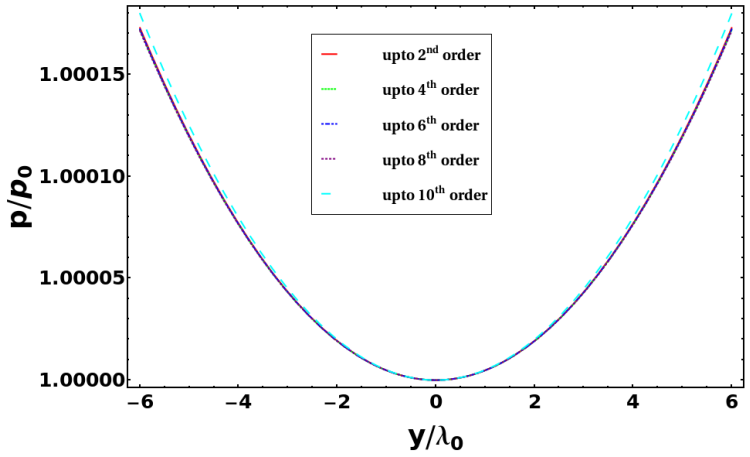

(b)

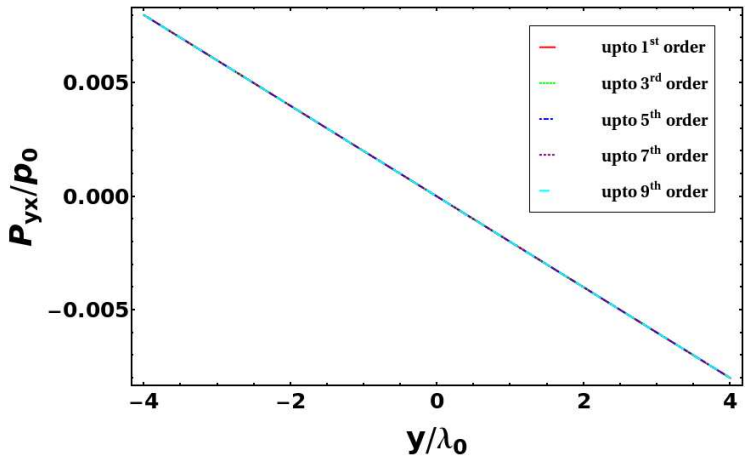

(c)

Figure 3.15: Profiles of $u_x(y)$, $p(y)$ and $P_{yx}(y)$ for $\mathrm{Fr}_0 = 10^{-3}$.

Appendix 3B. Comparison of results between hard spheres and Maxwell molecules up to third-order

To compare, first we substitute the coefficients $p_i^{(j)}, u_i^{(j)}$ and $T_i^{(j)}$ (can be found in Section 3.4) in the Eqs. (3.109)-(3.111), we get

$$p(y) = p_0\left[1 + \frac{6}{5}\left(\frac{mg}{T_0}\right)^2 y^2\right] + O(g^4),$$

$$u_x(y) = u_0 + \left(\frac{\rho_0 g}{2\eta_0}\right)y^2 + \frac{2726}{25}\left(\frac{m^3\eta_0 g^3}{\rho_0 T_0^3}\right)y^2 + \frac{43}{40}\left(\frac{m^2\rho_0 g^3}{\eta_0 T_0^2}\right)y^4 + \frac{7}{1800}\left(\frac{m\rho_0^3 g^3}{\eta_0^3 T_0}\right)y^6 + O(g^5),$$

$$T(y) = T_0\left[1 - \frac{1}{30}\left(\frac{m\rho_0^2 g^2}{\eta_0^2 T_0}\right)y^4 + \frac{19}{25}\left(\frac{mg}{T_0}\right)^2 y^2\right] + O(g^4).$$

Up-to second-order in g, the above expressions for hard spheres are identical with the corresponding expressions [Eqs. (3.173)-(3.175)] for Maxwell molecules, while those to third order they are numerically close. Similar argument holds for the components of pressure tensor and heat flux as well.

Chapter 4

Acceleration-Driven Poiseuille Flow of a Heated Granular Gas: Temperature Bimodality and Non-Newtonian Behaviour

4.1 Introduction

In this chapter, we analyse hydrodynamics and rheology for the gravity-driven Poiseuille flow of a "heated" granular gas using the tools of kinetic theory (Boltzmann equation with a BGK-type kinetic model) based on a perturbation expansion of the velocity distribution function in powers of the gravity strength g [Tij & Santos (1994, 2001); Tij *et al.* (1998); Sabbane *et al.* (2003); Tij & Santos (2004); Pareschi *et al.* (2006)]. A BGK-like kinetic model with heating via white-noise, which compensates for collisional cooling due to inelasticity, is employed as in the work of Tij and Santos (2004).

Aiming for a solution of the flow in the bulk region, the effect of gravity is incorporated perturbatively around a 'uniform' state (of constant temperature and density). In the process of finding the analytical solution, the distribution function and all hydrodynamic and rheological fields are expanded in power-series in gravitational acceleration g, with the base state representing their respective values at the channel centreline. Due to the complexity of the problem, the analytical expressions have been derived for the hydrodynamic fields and their fluxes (pressure tensor and heat flux vector) up to "fourth-order" in the gravity field g. Finally, the present fourth-order solution is used to analyse the certain rarefaction and/or non-Newtonian effects (such as the bimodal shape of the temperature profile, normal stress differences, and tangential heat flux) in granular Poiseuille flow. The present chapter is a direct extension of the work of Tij & Santos (2004) (who determined the second-order perturbative solution of the same problem) – one motivation of the present work is to understand certain differences between (i) the theoretical work of Tij & Santos (2004) and (ii) the MD simulation work of Alam *et al.* (2015) and the DSMC simulation of Gupta & Alam (2017). A qualitative comparison of present solutions with the simulation data is discussed at the end of this chapter with reference to (i) the bimodal shape of the temperature profile and (ii) the first normal stress difference in granular Poiseuille flow.

4.2 Boltzmann Equation for a Heated Granular Gas

In order to understand the macroscopic behaviour of dilute granular gases, the kinetic theory approach has been developed for granular gases by many authors [Haff (1983); Jenkins & Richman (1985); Sela & Goldhirsch (1998); Brey *et al.* (1999*b*); Tij & Santos (2004); Alaoui & Santos (1992); Pareschi *et al.* (2006)]. Here, we consider a granular gas composed of smooth inelastic hard spheres of mass m and diameter σ, which interact via binary collisions. The velocities of two spheres before and after collisions are given by $(\boldsymbol{c}, \boldsymbol{c}_1)$ and $(\boldsymbol{c}', \boldsymbol{c}_1')$, respectively. The geometry of the collision is fully specified by a unit vector $\hat{\boldsymbol{\sigma}}$ directed along the centers of the two spheres which are participated in a collision. The collisions in a granular gas are inelastic, unlike in a molecular gas, and are characterized by the relation:

$$(\boldsymbol{c}_{01} \cdot \hat{\boldsymbol{\sigma}}) = -e_n(\boldsymbol{c}_{01}' \cdot \hat{\boldsymbol{\sigma}}), \tag{4.1}$$

where $\boldsymbol{c}_{01} = \boldsymbol{c} - \boldsymbol{c}_1$ and $\boldsymbol{c}_{01}' = \boldsymbol{c}' - \boldsymbol{c}_1'$ denote the relative velocities before and after a collision, respectively, and e_n is the coefficient of normal restitution. Note that $e_n \in [0, 1]$, with $e_n = 1$ and 0 representing perfectly elastic and sticky collisions, respectively. The binary collision between two granular spherical particles leads to the following collision rule:

$$\boldsymbol{c}' = \boldsymbol{c} - \frac{1+e_n}{2}(\boldsymbol{c}_{01} \cdot \hat{\boldsymbol{\sigma}})\hat{\boldsymbol{\sigma}}, \qquad \boldsymbol{c}_1' = \boldsymbol{c}_1 + \frac{1+e_n}{2}(\boldsymbol{c}_{01} \cdot \hat{\boldsymbol{\sigma}})\hat{\boldsymbol{\sigma}}. \tag{4.2}$$

According to kinetic theory description the state of the granular gas or the relevant information about the systems is conveyed via a single particle distribution function $f(\boldsymbol{x}, \boldsymbol{c}; t)$. In the low density regime, temporal evolution of $f(\boldsymbol{x}, \boldsymbol{c}; t)$ is governed by the non-linear inelastic Boltzmann equation [Tij & Santos (2004)]

$$\left(\partial_t + \boldsymbol{c} \cdot \boldsymbol{\nabla} + \boldsymbol{g} \cdot \frac{\partial}{\partial \boldsymbol{c}} + \mathscr{F}\right) f = J[f, f], \tag{4.3}$$

where $\boldsymbol{g}$ is the acceleration due to an external force, $\mathscr{F}$ is the operator representing the action of a given heating mechanism to compensate for the collisional energy loss, and $J[f, f]$ is the Boltzmann collision integral, which calculates the rate of change of f through binary inelastic collisions. Its explicit form for granular gas is

$$J[f, f] \;=\; \sigma^2 \int d\boldsymbol{c}_1 \int d\hat{\boldsymbol{\sigma}}\; \Theta(\boldsymbol{c}_{01} \cdot \hat{\boldsymbol{\sigma}})(\boldsymbol{c}_{01} \cdot \hat{\boldsymbol{\sigma}})[e_n^{-2} f(\boldsymbol{c}'')f(\boldsymbol{c}_1'') - f(\boldsymbol{c})f(\boldsymbol{c}_1)], \tag{4.4}$$

where Θ represents the Heaviside step function, and the double primed velocities $(\boldsymbol{c}'', \boldsymbol{c}_1'')$ denotes the pre-collisional velocities for the restituting/inverse collision which leads to $(\boldsymbol{c}, \boldsymbol{c}_1)$ following an inelastic binary collision given by

$$\boldsymbol{c}'' = \boldsymbol{c} - \frac{1+e_n}{2e_n}(\boldsymbol{c}_{01} \cdot \hat{\boldsymbol{\sigma}})\hat{\boldsymbol{\sigma}}, \;\; \boldsymbol{c}_1'' = \boldsymbol{c}_1 + \frac{1+e_n}{2e_n}(\boldsymbol{c}_{01} \cdot \hat{\boldsymbol{\sigma}})\hat{\boldsymbol{\sigma}}. \tag{4.5}$$

The macroscopic field variables, namely, the number density n, the flow velocity $\boldsymbol{u}$, and the *granular* temperature T are defined via the zeroth, first and second moments of the distribution

function

$$\begin{pmatrix} n(\boldsymbol{x},t) \\ n(\boldsymbol{x},t)\boldsymbol{u}(\boldsymbol{x},t) \\ n(\boldsymbol{x},t)k_BT(\boldsymbol{x},t) \end{pmatrix} = \int d\boldsymbol{c} \begin{pmatrix} 1 \\ \boldsymbol{c} \\ \frac{m}{3}C^2 \end{pmatrix} f(\boldsymbol{x},\boldsymbol{c};t), \tag{4.6}$$

where

$$\boldsymbol{C} = \boldsymbol{c} - \boldsymbol{u}$$

is the peculiar velocity and k_B is the Boltzmann's constant which is set to one. The macroscopic balance equations for mass, momentum, and granular energy follow directly from Eq. (4.3) by taking velocity moments:

$$D_t n + n\boldsymbol{\nabla}\cdot\boldsymbol{u} = 0, \tag{4.7}$$

$$D_t \boldsymbol{u} + \frac{1}{mn}\boldsymbol{\nabla}\cdot\boldsymbol{P} = \boldsymbol{g}, \tag{4.8}$$

$$D_t T + \frac{2}{3n}(\boldsymbol{\nabla}\cdot\boldsymbol{q} + \boldsymbol{P}:\boldsymbol{\nabla}\boldsymbol{u}) = -(\zeta-\gamma)T, \tag{4.9}$$

where $D_t \equiv \partial_t + \boldsymbol{u}\cdot\boldsymbol{\nabla}$ is the material time derivative, $\boldsymbol{P}(\boldsymbol{x},t)$ and $\boldsymbol{q}(\boldsymbol{x},t)$ represents the full pressure tensor and the heat flux, respectively and these are defined as

$$\boldsymbol{P}(\boldsymbol{x},t) = m\int d\boldsymbol{c}\; \boldsymbol{C}\boldsymbol{C} f(\boldsymbol{x},\boldsymbol{c};t), \tag{4.10}$$

$$\boldsymbol{q}(\boldsymbol{x},t) = \frac{m}{2}\int d\boldsymbol{c}\; C^2\boldsymbol{C} f(\boldsymbol{x},\boldsymbol{c};t). \tag{4.11}$$

The first two equations, (4.7) and (4.8) correspond to mass and momentum conservation laws, which are same for the general fluid. The last equation (4.9) represents the energy balance equation for a granular gas. The cooling rate $\zeta(\boldsymbol{x},t)$ on the right hand side of Eq. (4.9) provides the rate of energy loss due to inelastic/dissipative collisions and $\gamma(\boldsymbol{x},t)$ represents the heating rate associated with the external driving $\mathscr{F}$; the expressions for these are given by

$$\zeta(\boldsymbol{x},t) = -\frac{m}{3n(\boldsymbol{x},t)T(\boldsymbol{x},t)}\int d\boldsymbol{c}\; C^2 J[f,f], \tag{4.12}$$

$$\gamma(\boldsymbol{x},t) = -\frac{m}{3n(\boldsymbol{x},t)T(\boldsymbol{x},t)}\int d\boldsymbol{c}\; C^2 \mathscr{F} f(\boldsymbol{x},\boldsymbol{c};t). \tag{4.13}$$

Here it has been assumed that the external heating mechanism $\mathscr{F}$ does not alter the mass and momentum balance laws which means that the action of $\mathscr{F}$ preserves the local number density and momentum density, i.e.,

$$\int d\boldsymbol{c}\mathscr{F} f(\boldsymbol{x},\boldsymbol{c};t) = \int d\boldsymbol{c}\; \boldsymbol{c}\mathscr{F} f(\boldsymbol{x},\boldsymbol{c};t) = 0. \tag{4.14}$$

From the expression (4.12), it is clear that the cooling rate is a complicated nonlinear functional of f. By using collision rule and dimensional analysis, it is straightforward to see that

$$\zeta \propto n(1-e_n^2)\sqrt{T},$$

with an unknown proportionality constant. To find an acceptable estimate of ζ, one can replace

the actual velocity distribution function f by its local Maxwellian approximation f_l in Eq. (4.12). The local Maxwellian is given by

$$f_l(\boldsymbol{x},\boldsymbol{c};t) = n(\boldsymbol{x},t)\left[\frac{m}{2\pi T(\boldsymbol{x},t)}\right]^{3/2}\exp\left[-\frac{m(\boldsymbol{c}-\boldsymbol{u}(\boldsymbol{x},t))^2}{2T(\boldsymbol{x},t)}\right]. \tag{4.15}$$

Using Eq. (4.15), the estimated result for ζ is [Tij & Santos (2004)]

$$\zeta_l(\boldsymbol{x},t) = \nu(\boldsymbol{x},t)\frac{5}{12}(1-e_n^2), \tag{4.16}$$

with ν being an effective collision frequency, given by

$$\nu = \frac{16}{5}n\sigma^2\sqrt{\frac{\pi T}{m}}, \tag{4.17}$$

which is independent of the coefficient of restitution e_n. From (4.16), it is clear that if the collisions are elastic, the cooling rate ζ vanishes and no external energy needs to be injected into the system, i.e, $\gamma = 0$. On the contrary, if the collisions are inelastic, one has non-vanishing cooling rate (i.e, $\zeta > 0$) for which we assume that the heating rate associated with the external driving compensates for the collisional cooling locally, i.e, $\gamma = \zeta$, such that a steady state can be achieved. Overall, the macroscopic balance equations for a molecular gas of hard spheres is same as Eq. (4.7) - Eq. (4.9) in the limit of vanishing ζ and γ.

4.3 Gravity-driven Poiseuille Flow of a Heated Granular Gas

Here we consider the granular Poiseuille flow in which the granular gas is confined between two infinite parallel plates normal to the y-axis – the schematic of the present flow configuration is shown in Fig. 4.1. The flow is driven by a constant external force, namely the gravitational acceleration– a constant gravitational force per unit mass $\boldsymbol{g} = -g\hat{\boldsymbol{x}}$ is applied along the direction $\hat{\boldsymbol{x}}$ parallel to the plates.

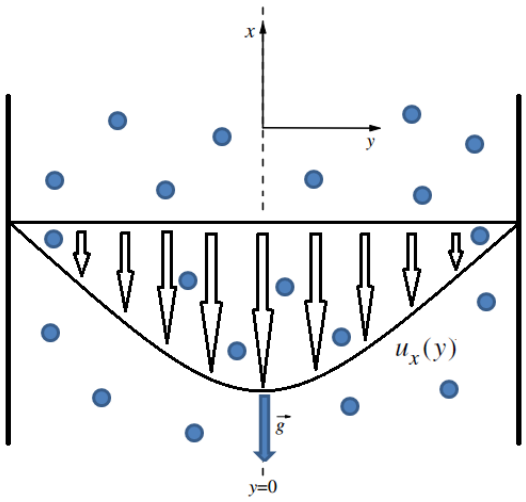

Figure 4.1: Schematic of the gravity-driven planar granular Poiseuille flow.

Like in laboratory experiments and computer simulations, we will assume that an external energy source, originated from some sort of driving (for example, boundary vibrations, external thermostats, etc.), is injected into the system to counter balance the internal energy sink ζ, so that a steady state is achieved even in the absence of gravity field. At theoretical level, this kind of "heating" mechanism through the boundaries is complicated to handle due to inevitable boundary effects– these complications are avoided by assuming a bulk heating mechanism, which acts on all particles simultaneously. The most common type of bulk driving mechanism for dissipative/inelastic particles contains a stochastic force in the form of Gaussian white-noise. For more details on the Gaussian white-noise, the reader is referred to Tij & Santos (2004) and van Noije & Ernst (1998). The operator $\mathscr{F}$ associated with the Gaussian white-noise appearing in the Boltzmann equation (4.3) is given by [van Noije & Ernst (1998); Tij & Santos (2004)]

$$\mathscr{F} = -\frac{\xi^2}{2}\left(\frac{\partial}{\partial \boldsymbol{c}}\right)^2, \tag{4.18}$$

where, ξ^2 represents the strength of the correlation and the term $\frac{\xi^2}{2}$ acts as a diffusion coefficient in velocity space. The external heating operator (4.18) satisfies the properties listed in Eq. (4.14). Further, insertion of Eq. (4.18) into Eq. (4.13) shows that the heating rate γ is

$$\gamma = \frac{m\xi^2}{T}. \tag{4.19}$$

We assume that the white-noise driving mechanism exactly balances the collisional energy loss locally– this implies that at every point,

$$\gamma = \zeta \quad \Longrightarrow \quad \xi = \sqrt{\zeta T/m},$$

which defines the spatial dependence of the heating rate γ.

By considering the above white-noise excitation mechanism, a steady state can be expected in which the physical quantities depend on the coordinate y only and the flow velocity is parallel to the x-axis,

$$\boldsymbol{u} = u_x(y)\hat{\boldsymbol{x}}.$$

In this stationary laminar state, the Boltzmann equation (4.3) becomes

$$\left(-\frac{\zeta T}{2m}\frac{\partial^2}{\partial \boldsymbol{c}^2} - g\frac{\partial}{\partial c_x} + c_y\frac{\partial}{\partial y}\right) f = J[f,f]. \tag{4.20}$$

The appropriate boundary conditions describing the nature of interaction of the particles with the plates/walls need to be supplemented to the Boltzmann equation (4.20) in order to solve the complete problem of granular Poiseuille flow. However, we are mainly interested to find the solution to (4.20) in the bulk region of the system, which is sufficiently far away from the plates. Therefore, our main aim is to find the "normal" solution[†] to (4.20). Similarly, under the steady and fully developed flow conditions, the balance equations for momentum and energy, Eqs. (4.8)

[†] "normal" solutions refer to specific solution of Eq. (4.20) in which the spatial-dependence of the distribution function occurs via hydrodynamic fields.

and (4.9), reduce to

$$\frac{\partial P_{yy}}{\partial y} = 0, \tag{4.21}$$

$$\frac{\partial P_{yx}}{\partial y} = -\rho g, \tag{4.22}$$

$$P_{yx}\frac{\partial u_x}{\partial y} + \frac{\partial q_y}{\partial y} = 0, \tag{4.23}$$

where $\rho = mn$ is the mass density. Note that the inelasticity does not appear explicitly in the balance equations (4.21)-(4.23). Eq. (4.21) implies that the normal stress P_{yy} is uniform throughout the system. Further, it must be noted that neither the longitudinal component of the heat flux q_x nor the two normal stresses P_{xx} and P_{zz} appear explicitly in the hydrodynamic equations (4.21)-(4.23).

4.4 BGK-like Kinetic Model and Perturbation Solution

It is evident that all the mathematical difficulties manifested in the Boltzmann equation for elastic hard spheres are due to collision operator $J[f, f]$. These difficulties are further increased in the inelastic hard spheres case. In order to get explicit results with a fair amount of effort, researchers [Brey *et al.* (1999*b*); Tij & Santos (2004); Santos & Astillero (2005)] have extended the BGK kinetic model (3.14) to the territory of inelastic/dissipative collisions. The analysis in this section closely follows the work of Tij & Santos (2004).

Due to the mathematical intricacy of the Boltzmann collision operator, especially in the case of inelastic collisions, we simplify our analysis by replacing the collision operator $J[f, f]$ [see Eq. (4.4)] by a BGK-like kinetic model [Brey *et al.* (1999*b*); Santos & Astillero (2005)]:

$$J[f, f] \to -\beta(e_n)\nu(f - f_l) + \frac{\zeta_l}{2}\frac{\partial}{\partial \boldsymbol{c}} \cdot [(\boldsymbol{c} - \boldsymbol{u})f], \tag{4.24}$$

where ν is the collision frequency [see Eq. (4.17)], f_l is the local Maxwellian distribution which is given in Eq. (4.15), ζ_l is the associated cooling rate [see Eq. (4.16)], and $\beta(e_n)$ is a dimensionless function of the coefficient of restitution which can be chosen freely to optimize the agreement between the present description and the Boltzmann description. The current form of kinetic model presented in Eq. (4.24) differs from the original formulation of the model kinetic equation [Brey *et al.* (1999*b*)] in that the exact local homogeneous cooling state of the Boltzmann equation is replaced by local Maxwellian f_l (4.15) and the exact cooling rate ζ (4.12) is approximated by ζ_l (4.16). A simple choice for the parameter β is $\beta(e_n) = (1+e_n)/2$ [Tij & Santos (2004); Santos & Astillero (2005)]. An excellent quantitative agreement between the Boltzmann equation and the current kinetic model (4.24) has been noted in literature [Brey *et al.* (1997*b*, 1999*b*); Montanero *et al.* (1999); Tij *et al.* (2001); Tij & Santos (2004); Santos & Astillero (2005)] for the simple shear, Poiseuille and Couette flows.

The first term on the right-hand side of (4.24) describes a single-time collisional relaxation towards the local equilibrium with a collision rate $\beta\nu$, on the other hand the second term describes the dominant collisional cooling effects, which can be treated simply as an effective "drag" force that produces the same rate of energy loss as that yield by the inelastic collisions [Tij

& Santos (2004)]. The NS transport coefficients (i.e. shear viscosity (η), thermal conductivity (κ) and Dufour coefficient (μ)) derived from the present BGK-like kinetic model (4.24) in the case of white-noise heating are (Santos 2003)

$$\eta = \frac{p}{\beta\nu + \zeta_l}, \tag{4.25}$$

$$\kappa = \frac{5}{2}\frac{p}{m(\beta\nu + \frac{3}{2}\zeta_l)}, \tag{4.26}$$

$$\mu = 0. \tag{4.27}$$

Where ν is the collision frequency given in Eq. (4.17). The correct choice for a dimensionless function $\beta(e_n)$, which makes the shear viscosity (4.25) agree well with the approximate Boltzmann results is

$$\beta = \frac{1}{6}(1+e_n)(2+e_n), \tag{4.28}$$

while the correct thermal conductivity (κ) is reproduced with the kinetic model (4.24) with the following choice for $\beta(e_n)$

$$\beta = (1+e_n)\frac{(19-3e_n)}{48}. \tag{4.29}$$

Here, we will take $\beta = \frac{1}{6}(1+e_n)(2+e_n)$ which makes the BGK shear viscosity (η) agree with that obtained from the Boltzmann equation [Santos & Astillero (2005), Brey *et al.* (1999*b*)].

The inability of the BGK model to reproduce simultaneously different transport coefficients (shear viscosity (η) and thermal conductivity(κ)) is known for molecular gases and consequently the Prandtl number is not correct – this is the price to be paid for the inclusion of a single collision frequency in BGK model. In particular, the BGK model yields $\mathrm{Pr} = 1$ for the Prandtl number $\mathrm{Pr} = 5\eta/2m\kappa$ in the elastic limit, while its correct value is $\mathrm{Pr} = 2/3$ [Santos & Astillero (2005), Brey *et al.* (1999*b*), Kremer (2010)] that follows from Boltzmann equation.

By making use of the present kinetic model (4.24), the Boltzmann kinetic equation (4.20) to describe the stationary Poiseuille flow is modified to [Tij & Santos (2004)]

$$\left(-g\frac{\partial}{\partial c_x} + c_y\frac{\partial}{\partial y}\right)f = -\beta\nu(f - f_l) + \frac{\zeta_l}{2}\frac{\partial}{\partial \boldsymbol{c}}\cdot\left(\boldsymbol{C} + \frac{T}{m}\frac{\partial}{\partial \boldsymbol{c}}\right)f, \tag{4.30}$$

where the heating rate γ associated with the external driving mechanism is assumed to be equal to ζ_l, as discussed earlier in §4.2. As our main focus is on the deviations from the local equilibrium distribution, let us express the non-equilibrium distribution function f in terms of perturbative expansion as

$$f = f_l(1+\Phi), \tag{4.31}$$

where the term Φ represents the deviation from the local equilibrium distribution f_l. With the presence of the above perturbation expansion (4.31) for f, Eq. (4.30) becomes (for derivation, see Sec. §C.1)

$$\begin{aligned}(1+\Phi)\left[C_y\tilde{\partial}_y \log f_l - \left(g + C_y\frac{\partial u_x}{\partial y}\right)\frac{\partial}{\partial C_x}\log f_l\right] &= \left(g + C_y\frac{\partial u_x}{\partial y}\right)\frac{\partial}{\partial C_x}\Phi \\ -C_y\tilde{\partial}_y\Phi - (\nu' - \zeta_l)\Phi \; &+ \frac{\zeta_l}{2}\left[\left(\frac{T}{m}\frac{\partial}{\partial \boldsymbol{C}} - \boldsymbol{C}\right)\cdot\frac{\partial}{\partial \boldsymbol{C}}\Phi\right],\end{aligned} \tag{4.32}$$

where the operator

$$\tilde{\partial}_y \equiv \frac{\partial}{\partial y} + (\frac{\partial u_x}{\partial y})\frac{\partial}{\partial C_x}$$

is with respect to y at constant peculiar velocity $\boldsymbol{C}$. Further, we have introduced a modified collision frequency

$$\nu' \equiv \beta\nu + \zeta_l$$

in Eq. (4.32) in the view of Eq. (4.25). According to Eq. (4.25), ν' is the effective collision frequency associated with the shear viscosity of a heated granular gas in the present kinetic model (Tij & Santos 2004).

Since we are interested in finding the normal solution of Eq. (4.32), which is valid in the bulk region, it is convenient to take the state at the channel centreline, i.e, the mid-point $y = 0$ as a reference state. Using this reference state, the following dimensionless quantities are used:

$$\boldsymbol{C}^* = \frac{\boldsymbol{C}}{c_0}, \quad y^* = \frac{y\nu_0'}{c_0}, \quad f_l^* = \frac{f_l c_0^3}{n_0}, \tag{4.33}$$

$$p^* = \frac{p}{p_0}, \quad \boldsymbol{u}^* = \frac{\boldsymbol{u}}{c_0}, \quad T^* = \frac{T}{T_0}, \quad g^* = \frac{g}{\nu_0' c_0}, \tag{4.34}$$

$$\nu'^* = \frac{\nu'}{\nu_0'}, \quad \boldsymbol{P}^* = \frac{\boldsymbol{P}}{p_0}, \quad \boldsymbol{q}^* = \frac{\boldsymbol{q}}{p_0 c_0}, \tag{4.35}$$

where the subscript 0 denotes quantities evaluated at $y = 0$; for example,

$$c_0 = \sqrt{\frac{2T_0}{m}} \tag{4.36}$$

is the thermal velocity c_{th} at the channel centreline $y = 0$. Here, the reduced quantity y^* measures distance in units of a nominal mean free path, while g^* measures the strength of the gravity field on a particle moving with the thermal velocity along a distance of the order of the mean free path. Furthermore, it is advisable by a larger directness in the calculations originating from the kinetic model (4.24), the choice on the time unit $1/\nu_0$ which is independent of e_n is replaced by $1/\nu'$ which depends on e_n. In terms of the above reduced units, the kinetic equation (4.32) becomes

$$(1+\Phi)\left[C_y^*\tilde{\partial}_{y^*}\log f_l^* + \frac{2C_x^*}{T^*}\left(g^* + C_y^*\frac{\partial u_x^*}{\partial y^*}\right)\right] = \left(g^* + C_y^*\frac{\partial u_x^*}{\partial y^*}\right)\frac{\partial}{\partial C_x^*}\Phi$$
$$-C_y^*\tilde{\partial}_{y^*}\Phi - \nu'^*(1-\zeta_0^*)\Phi + \zeta_0^*\frac{\nu'^*}{2}\left[\left(\frac{1}{2}T^*\frac{\partial}{\partial \boldsymbol{C}^*} - \boldsymbol{C}^*\right)\cdot\frac{\partial}{\partial \boldsymbol{C}^*}\Phi\right],$$

In terms of particle velocity this can be written as

$$(1+\Phi)\left[c_y^*\tilde{\partial}_{y^*}\log f_l^* + \frac{2(c_x^*-u_x^*)}{T^*}\left(g^* + c_y^*\frac{\partial u_x^*}{\partial y^*}\right)\right] = \left(g^* + c_y^*\frac{\partial u_x^*}{\partial y^*}\right)\frac{\partial}{\partial c_x^*}\Phi$$
$$-c_y^*\tilde{\partial}_{y^*}\Phi - \nu'^*(1-\zeta_0^*)\Phi + \zeta_0^*\frac{\nu'^*}{2}\left[\left(\frac{1}{2}T^*\frac{\partial}{\partial \boldsymbol{c}^*} - \boldsymbol{C}^*\right)\cdot\frac{\partial}{\partial \boldsymbol{c}^*}\Phi\right], \tag{4.37}$$

where

$$\tilde{\partial}_{y^*}\log f_l^* = \frac{\partial \log p^*}{\partial y^*} + \left(\frac{C^{*2}}{T^*} - \frac{5}{2}\right)\frac{\partial \log T^*}{\partial y^*}. \tag{4.38}$$

On the right-hand side of Eq. (4.37), we have expressed cooling rate ζ_l in terms of effective collision frequency ν' as $\zeta_l = \zeta_0^* \nu'$ [Tij & Santos (2004)], where [see Eq. (4.16)]

$$\zeta_0^* = \frac{\frac{5}{12}(1-e_n^2)}{\beta(e_n) + \frac{5}{12}(1-e_n^2)} \tag{4.39}$$

which is purely a number that only depends on the coefficient of restitution e_n and it represents the cooling rate at any given point in units of the modified collision frequency ν' at that same point.

Our main purpose is to solve Eq. (4.37) to fourth-order in g^* and get the associated hydrodynamic profiles at each order considered. Here, all the quantities will be understood to be expressed in dimensionless units and for simplicity, the asterisks will be discarded. The expansion of Φ in powers of gravity force field g is

$$\Phi = \Phi^{(1)} g + \Phi^{(2)} g^2 + \Phi^{(3)} g^3 + \Phi^{(4)} g^4 + O(g^5), \tag{4.40}$$

In the absence of gravity, the solution of Eq. (4.30) is $f = f_l$ with uniform $n, \boldsymbol{u}$, and T. The expansions for the hydrodynamic field variables have the forms

$$p = 1 + p^{(2)} g^2 + p^{(4)} g^4 + O(g^6), \tag{4.41}$$

$$u_x = u^{(1)} g + u^{(3)} g^3 + O(g^5), \tag{4.42}$$

$$T = 1 + T^{(2)} g^2 + T^{(4)} g^4 + O(g^6). \tag{4.43}$$

Due to the symmetry of the problem, p and T are even functions of g, while u_x is an odd function of g. Further, without loss of generality, we assume that $u_0 = 0$, i.e., we are performing a Galilean transformation to a reference frame moving with the fluid at $y = 0$. Since for the hard-sphere molecules, the effective collision frequency [Cercignani (1988); Chapman & Cowling (1970)) is $\nu' = pT^{-1/2}$, we have

$$\nu' = 1 + \left(p^{(2)} - \frac{1}{2}T^{(2)}\right) g^2 + \left(p^{(4)} - \frac{p^{(2)}T^{(2)}}{2} + \frac{3}{8}T^{(2)^2} - \frac{T^{(4)}}{2}\right) g^4 + O(g^6). \tag{4.44}$$

Note that only $\nu' = 1$ is required in the evaluation of first and second order deviations $\Phi^{(1)}$ and $\Phi^{(2)}$, while $\nu' = 1 + \left(p^{(2)} - \frac{1}{2}T^{(2)}\right) g^2$ is needed in the evaluation of other higher-order deviations $\Phi^{(3)}$ and $\Phi^{(4)}$.

In order to solve Eq. (4.37) at each order, one needs satisfy the following consistency conditions associated with the different order deviations from the equilibrium

$$\int d\boldsymbol{C} f_l \Phi = 0, \tag{4.45}$$

$$\int d\boldsymbol{C} C_y f_l \Phi = 0, \tag{4.46}$$

$$\int d\boldsymbol{C} C_x f_l \Phi = 0, \tag{4.47}$$

$$\int d\boldsymbol{C} C^2 f_l \Phi = 0. \tag{4.48}$$

To solve Eq. (4.37), we are going to take up a heuristic procedure followed in previous works of Tij and Santos [Tij & Santos (1994, 2004)]. The solution technique of Tij and Santos to Eq. (4.37) is as follows: (i) guess the hydrodynamic profiles and then (ii) verify their consistency using consistency conditions [Eq. (4.45) - Eq. (4.48)].

4.4.1 Solution at first-order in g

At first-order in g, the kinetic equation (4.37) yields

$$(1-\mathscr{A})\Phi^{(1)} = -\frac{2}{1-\zeta_0^*} c_x \left(1 + c_y \frac{\partial u^{(1)}}{\partial y}\right) \equiv \phi^{(1)}, \tag{4.49}$$

where the operator $\mathscr{A}$ is defined as

$$\mathscr{A} = \frac{\zeta_0^*}{2(1-\zeta_0^*)} \left[\left(\frac{1}{2}\frac{\partial}{\partial \boldsymbol{c}} - \boldsymbol{c}\right) \cdot \frac{\partial}{\partial \boldsymbol{c}}\right] - \frac{1}{1-\zeta_0^*} c_y \frac{\partial}{\partial y}. \tag{4.50}$$

At this order, the expression for $\phi^{(1)}$ depends only on velocity due to the symmetry of the problem and its space dependence occurs through $u^{(1)}$, which is unknown so far. In order to solve the governing equation at this order in g [Eq. (4.49)], we follow an heuristic procedure of Tij and Santos [(Tij & Santos 1994, 2004)] to construct solution – the detailed solution procedure is discussed in §3.4.2 and §3.4.4. In the process of solving Eq. (4.49), we guess that the first-order velocity profile is parabolic:

$$u^{(1)}(y) = u_2^{(1)} y^2. \tag{4.51}$$

Next, we note that the formal solution to Eq. (4.49) is $\Phi^{(1)} = \sum_{k=0}^{\infty} \mathscr{A}^k \phi^{(1)}$ and that the functional structure of $\mathscr{A}^k \phi^{(1)}$ remains the same for any k. Consequently, the solution to Eq. (4.49) must have the following trial structure,

$$\Phi^{(1)}(y, \boldsymbol{c}) = c_x (a_0 + a_1 c_y^2 + a_2 c_y y). \tag{4.52}$$

where a_0, a_1, a_2 are the coefficients, which are obtained by insertion of Eq. (4.52) into Eq. (4.49). Finally, one can identify the coefficients a_0, a_1, a_2 to be

$$\left.\begin{aligned} a_0 &= \frac{4(-2-\zeta_0^* + 2u_2^{(1)}\zeta_0^*)}{(4-\zeta_0^{*2})} \\ a_1 &= \frac{8u_2^{(1)}}{2+\zeta_0^*} \\ a_2 &= -4u_2^{(1)} \end{aligned}\right\}. \tag{4.53}$$

The coefficient $u_2^{(1)}$ is determined by using the consistency condition (4.47) and the trial form $\Phi^{(1)}$ (4.52) and the result is

$$u_2^{(1)} = 1. \tag{4.54}$$

The other consistency conditions (4.45), (4.46), and (4.48) are verified by symmetry. At this stage, we know the explicit form of $\Phi^{(1)}$, through which one can access the non-zero components

of the fluxes to first-order in g. The final expressions for the fluxes are given by

$$P_{yx}^{(1)}(y) = -2y, \tag{4.55}$$

$$q_x^{(1)}(y) = \frac{2}{2+\zeta_0^*}. \tag{4.56}$$

The expressions for P_{yx} and the longitudinal heat flux component q_x obtained here exactly coincide with the results of Tij & Santos [Tij & Santos (2004)] at this order.

4.4.2 Solution at second-order in g

At second-order in g, the governing equation for $\Phi^{(2)}$ is

$$\begin{aligned}(1-\mathscr{A})\Phi^{(2)} &= \frac{1}{1-\zeta_0^*}\left[\left(1+\frac{\zeta_0^*}{2}u^{(1)}\right)\frac{\partial}{\partial c_x} - 2c_x\left(1+c_y\frac{\partial u^{(1)}}{\partial y}\right)\right]\Phi^{(1)} \\ &\quad -\frac{c_y}{1-\zeta_0^*}\left[\frac{\partial p^{(2)}}{\partial y}+\left(c^2-\frac{5}{2}\right)\frac{\partial T^{(2)}}{\partial y}\right] \\ &\quad +\frac{1}{1-\zeta_0^*}2u^{(1)}\left(1+c_y\frac{\partial u^{(1)}}{\partial y}\right) \equiv \phi^{(2)}.\end{aligned} \tag{4.57}$$

The expression for $\phi^{(2)}$ depends on pressure p and temperature T as these are even functions of g and its space dependence occurs through $p^{(2)}$ and $T^{(2)}$, which are unknown so far. In order to solve Eq. (4.57), we use the same procedure which is discussed in §3.4.3 and §3.4.5. As a first step in the process of obtaining solution to Eq. (4.57), firstly, we guess the pressure and temperature profiles to be

$$p^{(2)}(y) = p_2^{(2)}y^2, \tag{4.58}$$

$$T^{(2)}(y) = T_2^{(2)}y^2 + T_4^{(2)}y^4. \tag{4.59}$$

The structure of $\mathscr{A}^k\phi^{(2)}$ suggests the trial function of the form

$$\begin{aligned}\Phi^{(2)}(y,\boldsymbol{c}) &= b_0 + b_1c_y^2 + b_2c_yy + b_3y^2 + b_4c_y^4 + b_5c_y^3y \\ &\quad + b_6c_y^2y^2 + b_7c_yy^3 + c_x^2\big(b_8 + b_9c_y^2 + b_{10}c_yy \\ &\quad + b_{11}y^2 + b_{12}c_y^4 + b_{13}c_y^3y + b_{14}c_y^2y^2\big) \\ &\quad + c^2\big(b_{15} + b_{16}c_y^2 + b_{17}c_yy + b_{18}y^2 + b_{19}c_y^4 \\ &\quad + b_{20}c_y^3y + b_{21}c_y^2y^2 + b_{22}c_yy^3\big).\end{aligned} \tag{4.60}$$

Insertion of Eq. (4.60) into Eq. (4.57) allows one to get the coefficients b_i's in terms of $p_2^{(2)}, T_2^{(2)}$, and $T_4^{(2)}$. Here, the consistency condition (4.47) is verified due to symmetry, while the consistency condition (4.46) is identically fulfilled irrespective of the values of $p_2^{(2)}, T_2^{(2)}$, and $T_4^{(2)}$. The other two consistency conditions (4.45) and (4.48) yield

$$p_2^{(2)} = \frac{24}{5}, \tag{4.61}$$

$$T_2^{(2)} = \frac{4}{25}\frac{38+43\zeta_0^*+17\zeta_0^{*2}}{(1+\zeta_0^*)(2+\zeta_0^*)}, \tag{4.62}$$

$$T_4^{(2)} = -\frac{2}{15}(2+\zeta_0^*). \tag{4.63}$$

Appendix C provides the supplementary material to this chapter and contains the exact expressions of the coefficients b_i's as functions of ζ_0^* [see §C.2]. With this, we know the explicit form of $\Phi^{(2)}$ which is used to calculate the second-order contributions to the fluxes as

$$P_{xx}^{(2)} = \frac{32}{25}\frac{82+67\zeta_0^*+8\zeta_0^{*2}}{(1+\zeta_0^*)(2+\zeta_0^*)^2} + \frac{56}{5}y^2, \tag{4.64}$$

$$P_{yy}^{(2)} = -\frac{24}{25}\frac{102+87\zeta_0^*+13\zeta_0^{*2}}{(1+\zeta_0^*)(2+\zeta_0^*)^2}, \tag{4.65}$$

$$q_y^{(2)} = \frac{4}{3}y^3. \tag{4.66}$$

The present results for flux contributions are same as those obtained by Tij & Santos [Tij & Santos (2004)] at second-order. The solutions at third- and fourth-orders are new contributions of this chapter as discussed in following two subsections.

4.4.3 Solution at third-order in g

The equation for $\Phi^{(3)}$ which yields from the kinetic equation (4.37) is

$$\begin{aligned}(1-\mathscr{A})\Phi^{(3)} = &\frac{1}{1-\zeta_0^*}\left[\left(1+\frac{\zeta_0^*}{2}u^{(1)}\right)\frac{\partial}{\partial c_x} - 2c_x\left(1+c_y\frac{\partial u^{(1)}}{\partial y}\right)\right]\Phi^{(2)}\\ &+\frac{1}{1-\zeta_0^*}\left[\left(p^{(2)}+\frac{T^{(2)}}{2}\right)\frac{\zeta_0^*}{4}\frac{\partial^2}{\partial c^2} - \left(p^{(2)}-\frac{T^{(2)}}{2}\right)(1-\zeta_0^*)\right.\\ &-\frac{1}{2}\left(p^{(2)}-\frac{T^{(2)}}{2}\right)\zeta_0^*\left(\boldsymbol{c}\cdot\frac{\partial}{\partial \boldsymbol{c}}\right) + 2u^{(1)}\left(1+c_y\frac{\partial u^{(1)}}{\partial y}\right)\\ &\left.-c_y\left(\frac{\partial p^{(2)}}{\partial y}+\left(c^2-\frac{5}{2}\right)\frac{\partial T^{(2)}}{\partial y}\right)\right]\Phi^{(1)}\\ &+\frac{1}{1-\zeta_0^*}2c_x\left[T^{(2)}+u^{(1)}c_y\frac{\partial T^{(2)}}{\partial y}+c_y\left(T^{(2)}\frac{\partial u^{(1)}}{\partial y}-\frac{\partial u^{(3)}}{\partial y}\right)\right] \equiv \phi^{(3)}.\end{aligned} \tag{4.67}$$

Following the same solution procedure as discussed in §3.4.2 and §3.4.6 , we first guess the velocity profile

$$u^{(3)}(y) = u_2^{(3)}y^2 + u_4^{(3)}y^4 + u_6^{(3)}y^6. \tag{4.68}$$

As a next step in the solution procedure, a trial form of $\Phi^{(3)}$ need to be assumed – the structure of $\mathscr{A}^k\phi^{(3)}$ suggests the trial function to be of the form

$$\begin{aligned}\Phi^{(3)}(y,\boldsymbol{c}) &= c_x\big(c_0c_y^8+c_1c_x^2+c_2+c_3c_y y^5+c_y^6(c_4c_x^2+c_5)+c_z^2(c_6c_y^6+c_7c_y^2+c_8c_y^4+c_9)\\
&+c_y^2(c_{10}c_x^2+c_{11})+c_y^4(c_{12}c_x^2+c_{13})+y^2(c_{14}c_y^6+c_{15}+c_{16}c_x^2+c_y^4(c_{17}c_x^2+c_{18})\\
&+c_z^2(c_{19}c_y^4+c_{20}c_y^2+c_{21})+c_y^2(c_{22}c_x^2+c_{23}))+y(c_{24}c_y^7+c_y^3(c_{25}c_x^2+c_{26})\\
&+c_z^2(c_{27}c_y^5+c_{28}c_y+c_{29}c_y^3)+c_y^5(c_{30}c_x^2+c_{31})+c_y(c_{32}c_x^2+c_{33}))\\
&+y^3(c_{34}c_y^5+c_z^2(c_{35}c_y+c_{36}c_y^3)+c_y^3(c_{37}c_x^2+c_{38})+c_y(c_{39}c_x^2+c_{40}))\\
&+y^4(c_{41}c_y^4+c_{42}c_x^2+c_{43}+c_y^2(c_{44}c_x^2+c_{45})+c_z^2(c_{46}c_y^2+c_{47}))\big). \qquad (4.69)\end{aligned}$$

The unknown coefficients c_i's in equation (4.69) can be obtained in terms of $u_2^{(3)}, u_4^{(3)}$ and $u_6^{(3)}$ by inserting Eq. (4.69) into Eq. (4.67). Using consistency conditions, the expressions for $u_2^{(3)}, u_4^{(3)}$ and $u_6^{(3)}$ are found to be

$$u_2^{(3)} = \frac{16(10904+\zeta_0^*(30784+\zeta_0^*(29442+\zeta_0^*(10706+(799-165\zeta_0^*)\zeta_0^*))))}{25(1+\zeta_0^*)^2(2+\zeta_0^*)^3(2+3\zeta_0^*)}, \qquad (4.70)$$

$$u_4^{(3)} = \frac{1}{15}\left(83-\frac{12}{1+\zeta_0^*}+\frac{116}{2+\zeta_0^*}\right), \qquad (4.71)$$

$$u_6^{(3)} = \frac{7(2+\zeta_0^*)}{225}. \qquad (4.72)$$

By substituting the values of $u_2^{(3)}, u_4^{(3)}$ and $u_6^{(3)}$ back into the expressions of the coefficients c_i's, we get the explicit values for the coefficients c_i's and are supplemented in §C.3 of Appendix C.

Finally, the explicit form of $\Phi^{(3)}$ is used to determine the third-order contributions to the fluxes as

$$P_{yx}^{(3)} = -\frac{4y^3\left(44+94\zeta_0^*+26\zeta_0^{*2}+y^2(1+\zeta_0^*)(2+\zeta_0^*)^2\right)}{75\left(2+3\zeta_0^*+\zeta_0^{*2}\right)}, \qquad (4.73)$$

$$\begin{aligned}q_x^{(3)} = &-\frac{2y^4\left(2+3\zeta_0^*+\zeta_0^{*2}\right)^3\left(114+257\zeta_0^*+58\zeta_0^{*2}\right)}{15(1+\zeta_0^*)^3(2+\zeta_0^*)^4(1+2\zeta_0^*)}\\
&-\frac{1}{25(1+\zeta_0^*)^3(2+\zeta_0^*)^4(1+2\zeta_0^*)(2+3\zeta_0^*)^2}\Big(8(336144+1690880\zeta_0^*+3427496\zeta_0^{*2}\\
&+3545632\zeta_0^{*3}+1930569\zeta_0^{*4}+495020\zeta_0^{*5}+35069\zeta_0^{*6}-942\zeta_0^{*7}+1152\zeta_0^{*8})\Big)\\
&+\frac{1}{25(1+\zeta_0^*)^3(2+\zeta_0^*)^4(1+2\zeta_0^*)(2+3\zeta_0^*)^2}\Big(4y^2(-50528-367408\zeta_0^*-1102144\zeta_0^{*2}\\
&-1768792\zeta_0^{*3}-1631470\zeta_0^{*4}-839947\zeta_0^{*5}-186671\zeta_0^{*6}+22797\zeta_0^{*7}+20613\zeta_0^{*8}\\
&+3150\zeta_0^{*9})\Big). \qquad (4.74)\end{aligned}$$

Note that other flux terms $[P_{xx}^{(3)}, P_{yy}^{(3)}$ and $q_y^{(3)}]$ are zero at third-order.

4.4.4 Solution at fourth-order in g

The kinetic equation (4.37) up to fourth-order in g yields the equation for $\Phi^{(4)}$:

$$
\begin{aligned}
(1-\mathscr{A})\Phi^{(4)} \;=\; & \frac{1}{1-\zeta_0^*}\left[\left(1+\frac{\zeta_0^*}{2}u^{(1)}\right)\frac{\partial}{\partial c_x}-2c_x\left(1+c_y\frac{\partial u^{(1)}}{\partial y}\right)\right]\Phi^{(3)}\\
&+\frac{1}{1-\zeta_0^*}\left[\left(p^{(2)}+\frac{T^{(2)}}{2}\right)\frac{\zeta_0^*}{4}\frac{\partial^2}{\partial c^2}-\left(p^{(2)}-\frac{T^{(2)}}{2}\right)(1-\zeta_0^*)\right.\\
&-\frac{1}{2}\left(p^{(2)}-\frac{T^{(2)}}{2}\right)\zeta_0^*\left(\boldsymbol{c}\cdot\frac{\partial}{\partial \boldsymbol{c}}\right)+2u^{(1)}\left(1+c_y\frac{\partial u^{(1)}}{\partial y}\right)\\
&\left.-c_y\left(\frac{\partial p^{(2)}}{\partial y}+\left(c^2-\frac{5}{2}\right)\frac{\partial T^{(2)}}{\partial y}\right)\right]\Phi^{(2)}\\
&+\frac{1}{1-\zeta_0^*}\left[\left(\left(p^{(2)}-\frac{T^{(2)}}{2}\right)u^{(1)}+u^{(3)}\right)\frac{\zeta_0^*}{2}\frac{\partial}{\partial c_x}\right.\\
&\left.+2c_x\left(T^{(2)}+c_y\left(u^{(1)}\frac{\partial T^{(2)}}{\partial y}+\frac{\partial u^{(1)}}{\partial y}T^{(2)}-\frac{\partial u^{(3)}}{\partial y}\right)\right)\right]\Phi^{(1)}\\
&+\frac{1}{1-\zeta_0^*}\left[\left(2u^{(3)}-2T^{(2)}u^{(1)}\right)\left(1+c_y\frac{\partial u^{(1)}}{\partial y}\right)+2c_yu^{(1)}\frac{\partial u^{(3)}}{\partial y}\right.\\
&-c_y\left(\frac{\partial}{\partial y}\left(p^{(4)}-\frac{{p^{(2)}}^2}{2}\right)+\left(\frac{\partial}{\partial y}\left(T^{(4)}-\frac{{T^{(2)}}^2}{2}\right)\right)\left(c^2-\frac{5}{2}\right)\right.\\
&\left.\left.+\frac{\partial T^{(2)}}{\partial y}\left({u^{(1)}}^2-T^{(2)}c^2\right)\right)\right]\equiv\phi^{(4)}.
\end{aligned}
\tag{4.75}
$$

To determine the solution at this order we follow the same procedure presented in §3.4.3 and §3.4.7. The pressure and temperature profiles are guessed as

$$
p^{(4)}(y)=p_2^{(4)}y^2+p_4^{(4)}y^4+p_6^{(4)}y^6, \tag{4.76}
$$

$$
T^{(4)}(y)=T_2^{(4)}y^2+T_4^{(4)}y^4+T_6^{(4)}y^6+T_8^{(4)}y^8. \tag{4.77}
$$

The structure of $\mathscr{A}^k\phi^{(4)}$ suggests a trial function of the form:

$$\begin{aligned}
\Phi^{(4)}(y,\boldsymbol{c}) &= d_0c_y^{12}+d_1c_x^4+d_2+d_3c_x^2+c_y^2(d_4c_x^4+d_5+d_6c_x^2)+c_y^4(d_7c_x^4+d_8c_x^2+d_9)\\
&+c_z^4(d_{10}c_y^8+d_{11}c_y^4+d_{12}+d_{13}c_y^2+d_{14}c_y^6)+c_y^6(d_{15}c_x^4+d_{16}+d_{17}c_x^2)\\
&+c_y^{10}(d_{18}c_x^2+d_{19})+c_y^8(d_{20}c_x^4+d_{21}c_x^2+d_{22})+y^7\big(d_{23}c_y^3+d_{24}c_z^2c_y\\
&+c_y(d_{25}+d_{26}c_x^2)\big)+c_z^2(d_{27}c_y^{10}+d_{28}c_x^2+d_{29}+c_y^4(d_{30}c_x^2+d_{31})+c_y^2(d_{32}c_x^2+d_{33})\\
&+c_y^6(d_{34}c_x^2+d_{35})+c_y^8(d_{36}c_x^2+d_{37}))+y^2\big(d_{38}c_x^4+d_{39}c_x^2+d_{40}+d_{41}c_y^{10}\\
&+c_y^2(d_{42}c_x^4+d_{43}+d_{44}c_x^2)+c_y^4(d_{45}c_x^2+d_{46}c_x^4+d_{47})+c_z^4(d_{48}c_y^4+d_{49}c_y^2+d_{50}\\
&+d_{51}c_y^6)+c_y^8(d_{52}c_x^2+d_{53})+c_y^6(d_{54}c_x^4+d_{55}c_x^2+d_{56})+c_z^2(d_{57}c_x^2+d_{58}+d_{59}c_y^8\\
&+c_y^4(d_{60}+d_{61}c_x^2)+c_y^2(d_{62}c_x^2+d_{63})+c_y^6(d_{64}c_x^2+d_{65}))\big)+y^3\big(d_{66}c_y^9+c_y(d_{67}\\
&+d_{68}c_x^2+d_{69}c_x^4)+c_z^4(d_{70}c_y+d_{71}c_y^3+d_{72}c_y^5)+c_y^5(d_{73}c_x^4+d_{74}c_x^2+d_{75})\\
&+c_y^7(d_{76}+d_{77}c_x^2)+c_y^3(d_{78}c_x^4+d_{79}+d_{80}c_x^2)+c_z^2(d_{81}c_y^7+c_y(d_{82}+d_{83}c_x^2)\\
&+c_y^5(d_{84}c_x^2+d_{85})+c_y^3(d_{86}c_x^2+d_{87}))\big)+y^5\big(d_{88}c_y^7+c_z^4(d_{89}c_y+d_{90}c_y^3)\\
&+c_y^5(d_{91}c_x^2+d_{92})+c_y^3(d_{93}c_x^4+d_{94}c_x^2+d_{95})+c_y(d_{96}c_x^4+d_{97}+d_{98}c_x^2)\\
&+c_z^2(d_{99}c_y^5+c_y^3(d_{100}c_x^2+d_{101})+c_y(d_{102}c_x^2+d_{103}))\big)+y\big(d_{104}c_y^{11}\\
&+c_y(d_{105}c_x^4+d_{106}+d_{107}c_x^2)+c_z^4(d_{108}c_y^7+d_{109}c_y+d_{110}c_y^3+d_{111}c_y^5)\\
&+c_y^5(d_{112}c_x^4+d_{113}c_x^2+d_{114})+c_y^7(d_{115}c_x^4+d_{116}+d_{117}c_x^2)+c_y^3(d_{118}c_x^4\\
&+d_{119}c_x^2+d_{120})+c_y^9(d_{121}c_x^2+d_{122})+c_z^2(d_{123}c_y^9+c_y(d_{124}c_x^2+d_{125})\\
&+c_y^5(d_{126}c_x^2+d_{127})+c_y^3(d_{128}c_x^2+d_{129})+c_y^7(d_{130}c_x^2+d_{131}))\big)+y^6\big(d_{132}c_x^2\\
&+d_{133}c_x^4+d_{134}+d_{135}c_y^6+c_z^4(d_{136}c_y^2+d_{137})+c_y^4(d_{138}c_x^2+d_{139})+c_y^2(d_{140}c_x^4\\
&+d_{141}c_x^2+d_{142})+c_z^2(d_{143}c_y^4+d_{144}+d_{145}c_x^2+c_y^2(d_{146}c_x^2+d_{147}))\big)+y^4\big(d_{148}\\
&+d_{149}c_x^4+d_{150}c_x^2+d_{151}c_y^8+c_z^4(d_{152}c_y^4+d_{153}c_y^2+d_{154})+c_y^6(d_{155}c_x^2+d_{156})\\
&+c_y^4(d_{157}c_x^4+d_{158}+d_{159}c_x^2)+c_y^2(d_{160}c_x^4+d_{161}c_x^2+d_{162})+c_z^2(d_{163}c_x^2+d_{164}\\
&+d_{165}c_y^6+c_y^4(d_{166}c_x^2+d_{167})+c_y^2(d_{168}c_x^2+d_{169}))\big). \qquad (4.78)
\end{aligned}$$

Using the trial form of $\Phi^{(4)}$ (4.78), we solve the equation (4.75) which allows to express unknown coefficients d_i's in the trial function $\Phi^{(4)}$ in terms of $p_2^{(4)},p_4^{(4)},p_6^{(4)},T_2^{(4)},T_4^{(4)},T_6^{(4)}$ and $T_8^{(4)}$. Later, by using trial function $\Phi^{(4)}$ and consistency conditions, one can find the values of $p_2^{(4)},p_4^{(4)},p_6^{(4)},T_2^{(4)},T_4^{(4)},T_6^{(4)}$ and $T_8^{(4)}$. The explicit expressions of these are

$$\begin{aligned}
p_2^{(4)} &= \frac{1}{625(1+\zeta_0^*)^3(2+\zeta_0^*)^4(1+2\zeta_0^*)(2+3\zeta_0^*)^2}\Big(96(-8412320+\zeta_0^*(-55869712\\
&+\zeta_0^*(-151604336+\zeta_0^*(-217466256+\zeta_0^*(-177155550+\zeta_0^*(-80683559\\
&+\zeta_0^*(-17862719+9\zeta_0^*(-84451+\zeta_0^*(31625+2454\zeta_0^*)))))))))\Big), \qquad (4.79)\\
p_4^{(4)} &= \frac{32(-1876+\zeta_0^*(-1704+\zeta_0^*(-127+53\zeta_0^*)))}{125(1+\zeta_0^*)(2+\zeta_0^*)^2}, \qquad (4.80)\\
p_6^{(4)} &= \frac{32(2+\zeta_0^*)}{125}, \qquad (4.81)
\end{aligned}$$

$$
\begin{aligned}
T_2^{(4)} &= \frac{1}{3125(1+\zeta_0^*)^4(2+\zeta_0^*)^4(1+2\zeta_0^*)^2(2+3\zeta_0^*)^3(2+5\zeta_0^*)}\Big(32(-1599319168 \\
&+\zeta_0^*(-16962443840+\zeta_0^*(-80336432416+\zeta_0^*(-224669350416+\zeta_0^*(-412962839352 \\
&+\zeta_0^*(-524178620364+\zeta_0^*(-467685587414+\zeta_0^*(-290769190027+\zeta_0^*(-120744935798 \\
&+3\zeta_0^*(-9970960822+3\zeta_0^*(-313866280+3\zeta_0^*(17035559 \\
&+12\zeta_0^*(392957+20005\zeta_0^*)))))))))))\Big), \qquad (4.82)\\
T_4^{(4)} &= \frac{1}{1875(1+\zeta_0^*)^3(2+\zeta_0^*)^3(1+2\zeta_0^*)(2+3\zeta_0^*)^2}\Big(8(-5148064+\zeta_0^*(-32818512 \\
&+\zeta_0^*(-89374032+\zeta_0^*(-136566880+\zeta_0^*(-128589078+\zeta_0^*(-75796543 \\
&+\zeta_0^*(-26372423+\zeta_0^*(-4378435+3\zeta_0^*(-9301+18690\zeta_0^*)))))))))\Big), \qquad (4.83)\\
T_6^{(4)} &= -\frac{8(8692+\zeta_0^*(11868+\zeta_0^*(5579+759\zeta_0^*)))}{5625(1+\zeta_0^*)(2+\zeta_0^*)}, \qquad (4.84)\\
T_8^{(4)} &= -\frac{62(2+\zeta_0^*)^2}{7875}. \qquad (4.85)
\end{aligned}
$$

Finally, the expression of $\Phi^{(4)}$ can be obtained by finding the unknown coefficients d_i's for which one has to make use of the values of $p_2^{(4)}, p_4^{(4)}, p_6^{(4)}, T_2^{(4)}, T_4^{(4)}, T_6^{(4)}$ and $T_8^{(4)}$. The detailed expressions of these coefficients d_i's as functions of ζ_0^* are presented in §C.4 of Appendix C. Having found the exact form of $\Phi^{(4)}$, we can calculate fourth-order contributions to the fluxes as

$$
\begin{aligned}
P_{xx}^{(4)} &= \frac{224}{375}y^6(2+\zeta_0^*)+\frac{32y^4}{375(1+\zeta_0^*)^4(2+\zeta_0^*)^5(2+3\zeta_0^*)^3(2+5\zeta_0^*)}(4+12\zeta_0^*+11\zeta_0^{*2} \\
&+3\zeta_0^{*3})^3\left(-21144-70636\zeta_0^*-43978\zeta_0^{*2}+2137\zeta_0^{*3}+2455\zeta_0^{*4}\right) \\
&+\frac{1}{3125(1+\zeta_0^*)^4(2+\zeta_0^*)^5(1+2\zeta_0^*)^2(2+3\zeta_0^*)^3(2+5\zeta_0^*)}\Big(512(-1066982656 \\
&-11957194240\zeta_0^*-58644859232\zeta_0^{*2}-165729887792\zeta_0^{*3}-298651532384\zeta_0^{*4} \\
&-358002977288\zeta_0^{*5}-287936971998\zeta_0^{*6}-151710315739\zeta_0^{*7}-48209843396\zeta_0^{*8} \\
&-6708938562\zeta_0^{*9}+779555905\zeta_0^{*10}+433209456\zeta_0^{*11}+57182436\zeta_0^{*12}+2568240\zeta_0^{*13})\Big) \\
&+\frac{1}{625(1+\zeta_0^*)^4(2+\zeta_0^*)^5(1+2\zeta_0^*)^2(2+3\zeta_0^*)^3(2+5\zeta_0^*)}\Big(32y^2(-393880320 \\
&-5561605632\zeta_0^*-34942366336\zeta_0^{*2}-129006012416\zeta_0^{*3}-311212453440\zeta_0^{*4} \\
&-515641881312\zeta_0^{*5}-599613703128\zeta_0^{*6}-490133164848\zeta_0^{*7}-276196369025\zeta_0^{*8} \\
&-101648368600\zeta_0^{*9}-21034331946\zeta_0^{*10}-954252636\zeta_0^{*11} \\
&+548620335\zeta_0^{*12}+105666444\zeta_0^{*13}+4864860\zeta_0^{*14})\Big), \qquad (4.86)
\end{aligned}
$$

$$
\begin{aligned}
P_{yy}^{(4)} &= -\frac{1}{3125(1+\zeta_0^*)^4(2+\zeta_0^*)^5(1+2\zeta_0^*)^2(2+3\zeta_0^*)^3(2+5\zeta_0^*)}\Big(384(-1562108416 \\
&-17537832640\zeta_0^* - 86542601952{\zeta_0^*}^2 - 247386118112{\zeta_0^*}^3 - 454210757024{\zeta_0^*}^4 \\
&-560679708268{\zeta_0^*}^5 - 472406095078{\zeta_0^*}^6 - 269146497804{\zeta_0^*}^7 - 99542188931{\zeta_0^*}^8 \\
&-21415804832{\zeta_0^*}^9 - 1710159795{\zeta_0^*}^{10} + 250281216{\zeta_0^*}^{11} + 61806996{\zeta_0^*}^{12} \\
&+3518640{\zeta_0^*}^{13})\Big),
\end{aligned} \tag{4.87}
$$

$$
\begin{aligned}
q_y^{(4)} &= \frac{12}{175}y^7(2+\zeta_0^*) + \frac{8y^5\left(2668+10388\zeta_0^*+14179{\zeta_0^*}^2+7782{\zeta_0^*}^3+1323{\zeta_0^*}^4\right)}{375(1+\zeta_0^*)^2(2+\zeta_0^*)(2+3\zeta_0^*)} \\
&-\frac{64y^3\left(-10904-30784\zeta_0^*-29442{\zeta_0^*}^2-10706{\zeta_0^*}^3-799{\zeta_0^*}^4+165{\zeta_0^*}^5\right)}{75(1+\zeta_0^*)^2(2+\zeta_0^*)^3(2+3\zeta_0^*)}.
\end{aligned} \tag{4.88}
$$

Note that other flux terms [$P_{xy}^{(4)}$ and $q_x^{(4)}$] are zero at this order.

Another point we want to make it here that, when particularized to elastic collisions ($\zeta_0^* = 0$) all the above results are consistent with those of Chapter 3.

4.5 Results on Hydrodynamics and the Bimodal Temperature Profile

Here we discuss the analytical results obtained via the kinetic model up to fourth-order in the gravity field. The hydrodynamic profiles derived at first, second, third and fourth order in g are presented in §4.4 and these results at each order are combined to obtain a single expression for each hydrodynamic field and are expressed in real units as

$$
\begin{aligned}
T(y) &= T_0\Bigg[\underline{1+T_4^{(2)}\left(\frac{m\rho_0^2g^2}{8\eta_0^2T_0}\right)y^4+T_2^{(2)}\frac{1}{4}\left(\frac{mg}{T_0}\right)^2y^2}+T_2^{(4)}\left(\frac{m^5\eta_0^2g^4}{8\rho_0^2T_0^5}\right)y^2 \\
&+T_4^{(4)}\frac{1}{16}\left(\frac{mg}{T_0}\right)^4y^4+T_6^{(4)}\left(\frac{m^3\rho_0^2g^4}{32\eta_0^2T_0^3}\right)y^6+T_8^{(4)}\left(\frac{m^2\rho_0^4g^4}{64\eta_0^4T_0^2}\right)y^8\Bigg]+O(g^6),
\end{aligned} \tag{4.89}
$$

$$
\begin{aligned}
p(y) &= p_0\Bigg[\underline{1+p_2^{(2)}\frac{1}{4}\left(\frac{mg}{T_0}\right)^2y^2}+p_2^{(4)}\left(\frac{m^5\eta_0^2g^4}{8\rho_0^2T_0^5}\right)y^2+p_4^{(4)}\frac{1}{16}\left(\frac{mg}{T_0}\right)^4y^4+p_6^{(4)}\left(\frac{m^3\rho_0^2g^4}{32\eta_0^2T_0^3}\right)y^6\Bigg] \\
&+O(g^6),
\end{aligned} \tag{4.90}
$$

$$
\begin{aligned}
u_x(y) &= \underline{u_0+\left(\frac{\rho_0 g}{2\eta_0}\right)y^2}+u_2^{(3)}\left(\frac{m^3\eta_0g^3}{4\rho_0T_0^3}\right)y^2+u_4^{(3)}\left(\frac{m^2\rho_0g^3}{8\eta_0T_0^2}\right)y^4+u_6^{(3)}\left(\frac{m\rho_0^3g^3}{16\eta_0^3T_0}\right)y^6 \\
&+O(g^5).
\end{aligned} \tag{4.91}
$$

The underlined terms in the expressions of pressure, velocity and temperature profiles correspond to results up to "second-order" in the gravity field as obtained previously by Tij & Santos (2004). In the remainder of this section, we focus on analysing the characteristics of the temperature profile based on (i) second-order and (ii) fourth-order solutions.

In order to explore the temperature profile (4.89) in detail, let us scale the y-coordinate in terms of the centreline mean-free-path λ_0, which is defined as the average distance traveled

by a molecule/particle between two successive collisions. The centreline mean free path λ_0 is $\lambda_0 = 1/(\pi\sqrt{2}n_0\sigma^2)$ which can be rewritten in terms of thermal velocity (c_0) and the collision frequency (ν_0) as

$$\lambda_0 = \frac{8}{5\sqrt{\pi}}\frac{c_0}{\nu_0}. \tag{4.92}$$

We also introduce Froude number (Fr) which is a dimensionless number, defined as the ratio of external (gravitational) and inertial forces and it measures the influence of gravity on the current flow field. The Froude number at the channel centreline is

$$\mathrm{Fr}_0 = \frac{g\lambda_0}{c_0^2}$$

as defined earlier in Eq. (3.114).

The expression for the temperature profile (4.89) in terms of centreline mean free path λ_0 and the centreline Froude number Fr_0 becomes

$$\begin{aligned}\frac{T(y)}{T_0} &= \underline{1+\mathrm{Fr}_0^2\left(\frac{y}{\lambda_0}\right)^2\left[A_2^{3D}(e_n)+A_4^{3D}(e_n)\left(\frac{y}{\lambda_0}\right)^2\right]+\mathrm{Fr}_0^4\left(\frac{y}{\lambda_0}\right)^2\left[B_2^{3D}(e_n)+B_4^{3D}(e_n)\left(\frac{y}{\lambda_0}\right)^2\right.}\\ &\quad \left.+B_6^{3D}(e_n)\left(\frac{y}{\lambda_0}\right)^4+B_8^{3D}(e_n)\left(\frac{y}{\lambda_0}\right)^6\right]+O(g^6),\end{aligned} \tag{4.93}$$

where

$$A_2^{3D}(e_n) = \frac{4\left(2719-2741e_n+706e_n^2\right)}{25(7-4e_n)(23-11e_n)}, \tag{4.94}$$

$$A_4^{3D}(e_n) = -\frac{8(3-e_n)(1+e_n)^2(23-11e_n)}{1125\pi}, \tag{4.95}$$

$$\begin{aligned}B_2^{3D}(e_n) = \frac{25}{4\left(-3-2e_n+e_n^2\right)^2}\Bigg(&-\frac{33267022075095579}{46981321887500}+\frac{511377408}{169(19-13e_n)^2}\\ &-\frac{497664000}{14641(23-11e_n)^4}+\frac{2189749248}{73205(23-11e_n)^2}-\frac{15390720}{49(11-7e_n)^2}-\frac{23085}{(7-4e_n)^4}\\ &-\frac{50053887}{100(7-4e_n)^2}+\frac{20977461}{100(-7+4e_n)^3}+\frac{2127452263}{2500(-7+4e_n)}+\frac{3686400}{49(-11+7e_n)^3}\\ &-\frac{928213632}{875(-11+7e_n)}-\frac{648843264}{14641(-23+11e_n)^3}+\frac{1566633408}{1830125(-23+11e_n)}\\ &-\frac{127918424064}{21125(-19+13e_n)}+\frac{392000000}{31(-43+31e_n)}\Bigg)\pi,\end{aligned} \tag{4.96}$$

$$\begin{aligned}B_4^{3D}(e_n) = &-\frac{247750795519}{3179426250}-\frac{1060608}{1331(23-11e_n)^2}+\frac{102400}{49(11-7e_n)^2}+\frac{96183}{50(7-4e_n)^2}\\ &-\frac{405}{2(-7+4e_n)^3}-\frac{750619}{250(-7+4e_n)}+\frac{776448}{1225(-11+7e_n)}-\frac{829440}{1331(-23+11e_n)^3}\\ &+\frac{635968}{33275(-23+11e_n)}+\frac{700416}{65(-19+13e_n)},\end{aligned} \tag{4.97}$$

$$B_6^{3D}(e_n) = -\frac{32(-3+e_n)(1+e_n)^2\left(-2082193+2926828e_n-1371221e_n^2+213674e_n^3\right)}{140625\left(161-169e_n+44e_n^2\right)\pi}, \tag{4.98}$$

$$B_8^{3D}(e_n) = -\frac{992(23-11e_n)^2(-3+e_n)^2(1+e_n)^4}{44296875\pi^2}. \tag{4.99}$$

4.5.1 Temperature Profile up to second-order in g

Here we discuss the temperature profiles predicted by Tij & Santos (2004) who used the same kinetic model by retaining terms up to second-order in g. Fig. 4.2 shows the temperature profiles $T(y)$ [solution of underlined terms in Eq. (4.93)] as predicted by the kinetic theory description for a granular gas ($e_n = 0.5$ and $e_n = 0.8$), as well as for an elastic gas ($e_n = 1$) for the two values of Froude number (a) $\mathrm{Fr}_0 = 10^{-3}$ and (b) $\mathrm{Fr}_0 = 5 \times 10^{-3}$, respectively. In each panel, the dimensionless temperature $T(y)/T_0$ is plotted against y/λ_0, where T_0 and λ_0 are the centreline temperature and mean free path, respectively.

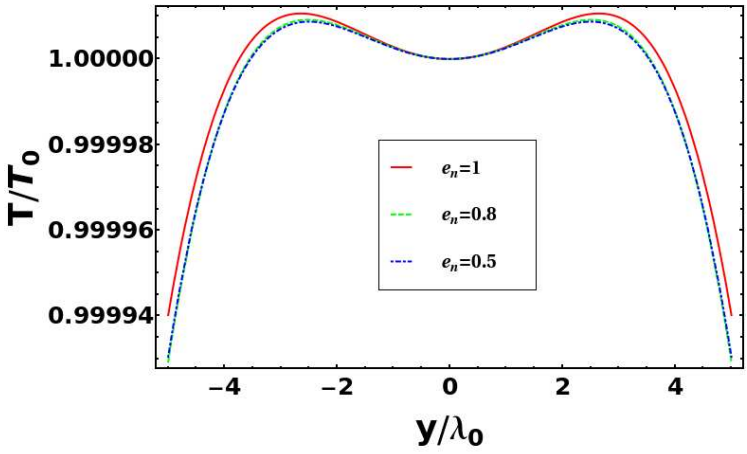

(a)

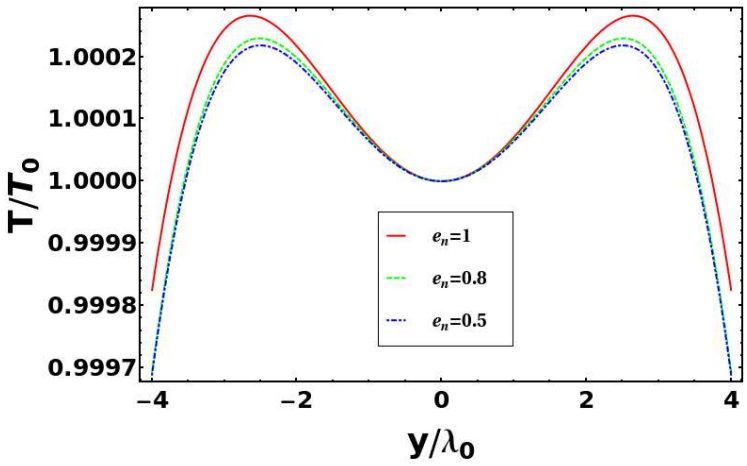

(b)

Figure 4.2: Temperature profiles for (a) $\mathrm{Fr}_0 = 10^{-3}$ and (b) $\mathrm{Fr}_0 = 5 \times 10^{-3}$ as predicted by the kinetic-model up to second-order in g; $e_n = 1$ (red solid line), $e_n = 0.8$ (green dashed line) and $e_n = 0.5$ (blue dash dotted line).

From Figs. 4.2(a) and 4.2(b), it is clear that the temperature profile is of "bimodal" shape: $T(y)/T_0$ has a local minimum at the channel centreline (at $y = 0$) and it is surrounded by two symmetric maxima on either side of it. This unique feature is present in molecular (elastic) gases (as discussed in Chapter 3, see Fig. 3.2) as well as in granular gases as evident from Fig. 4.2(a) and Fig. 4.2(b). Further, we notice that the location of two symmetric maxima of temperature shifts towards the channel centreline with increasing dissipation (i.e. with decreasing restitution

coefficient e_n). The location $y_{\max}$ of two symmetric temperature maxima is given by

$$y_{\max} = \pm\lambda_0 \sqrt{-\frac{A_2^{3D}(e_n)}{2A_4^{3D}(e_n)}}, \tag{4.100}$$

for results up to second-order in the gravity field g. The occurrence of symmetric maxima of temperature profiles on either side of channel centreline, which is known as temperature bimodality, is one of the major characteristics of rarefaction in Poiseuille flow (Tij & Santos 1994, 2004). It has been confirmed recently via (i) MD simulations (Alam *et al.* (2015)) and (ii) DSMC simulations (Gupta & Alam (2017)) of granular Poiseuille flow that the inelastic dissipation can also be responsible for the appearance of the bimodal temperature profile (in the continuum limit of zero Knudsen number).

To quantify the degree of temperature bimodality, we define the relative value of the maximum temperature as $\triangle T = \frac{T_{\max}-T_0}{T_0}$, dubbed *excess temperature*, and the expression for it at this second-order in g is

$$\Delta T \;=\; \frac{T_{\max}-T_0}{T_0} = -\frac{A_2^{3D^2}(e_n)}{4A_4^{3D}(e_n)}\mathrm{Fr}_0^2 + O(g^4), \tag{4.101}$$

where A_2^{3D} and A_4^{3D} are sole functions of e_n as given in Eqns. (4.94) and (4.95), respectively. It therefore follow that the 'scaled' excess temperature, defined via

$$\frac{\Delta T}{\mathrm{Fr}_0^2} = -\frac{A_2^{3D^2}(e_n)}{4A_4^{3D}(e_n)}, \tag{4.102}$$

is independent of the Froude number at second-order in g.

Fig. 4.3 shows the dependence of degree of temperature bimodality ΔT on the restitution coefficient e_n for two values of Froude numbers $\mathrm{Fr}_0 = 10^{-3}$ and $\mathrm{Fr}_0 = 5\times10^{-3}$. We recall that from Fig. 4.2(a) and Fig. 4.2(b) that as dissipation [$\sim (1-e_n)$] increases from zero, the value of temperature maximum decreases. However, an opposite behaviour is found at higher dissipation rates (i.e, for $e_n \lesssim 0.5$) which is evident from Fig. 4.3(a,b). Further, we see from Fig. 4.3(a,b) that the excess temperature $\triangle T$ attains its minimum at a restitution coefficient $e_n \approxeq 0.56$ for both values of Froude numbers. Fig. 4.3(c) shows the variation of scaled excess temperature $\Delta T/\mathrm{Fr}_0^2$ [Eq. (4.102)] with e_n, which does not depend on Fr_0 at second-order. Overall, from Figs. 4.2 and 4.3 we conclude following points: (i) the temperature bimodality is present in both elastic and inelastic gases undergoing acceleration-driven Poiseuille flow, (ii) the value of maximum temperature shows non-monotonic behaviour with respect to e_n, and (iii) the location of the temperature maxima $y_{\max}$ moves towards the center of the channel as the restitution coefficient e_n decreases from 1 to 0.5 and away from the channel center for $e_n < 0.56$. The variation of $|y_{\max}|/\lambda_0$ with e_n is also found to be non-monotonic as shown in Fig. 4.4. Above findings are similar to that of results obtained by Tij & Santos [Tij & Santos (2004)].

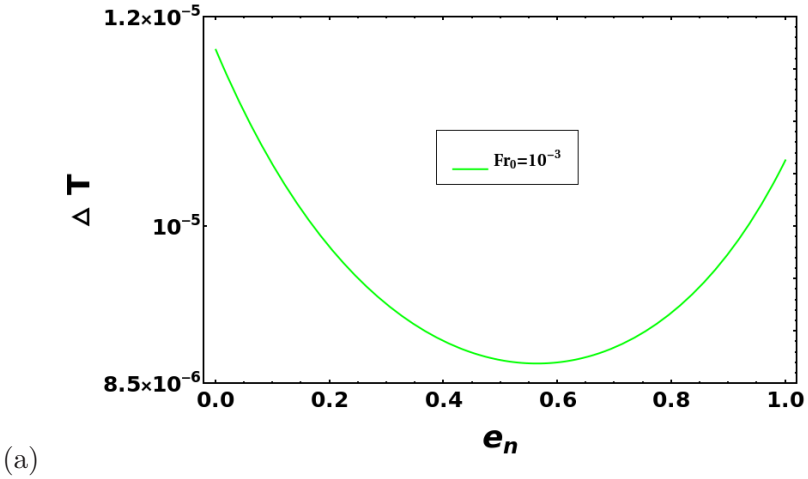

(a)

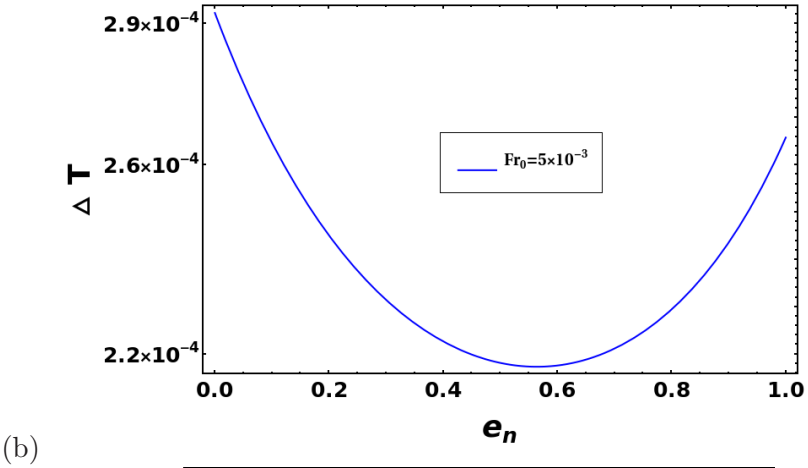

(b)

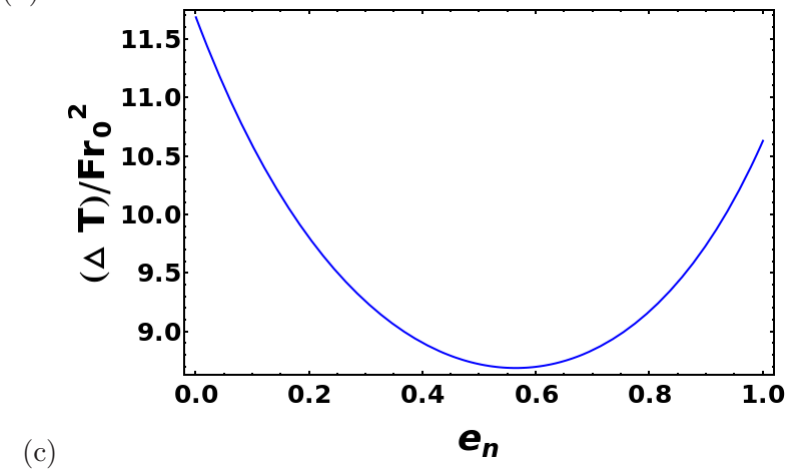

(c)

Figure 4.3: Plots of $\Delta T(= T_{\max}/T_0 - 1)$ vs. e_n for two different values of Froude numbers: (a) $\mathrm{Fr}_0 = 10^{-3}$, (b) $\mathrm{Fr}_0 = 5 \times 10^{-3}$. (c) Plot of $\Delta T/\mathrm{Fr}_0^2$ [Eq. (4.102)] with e_n.

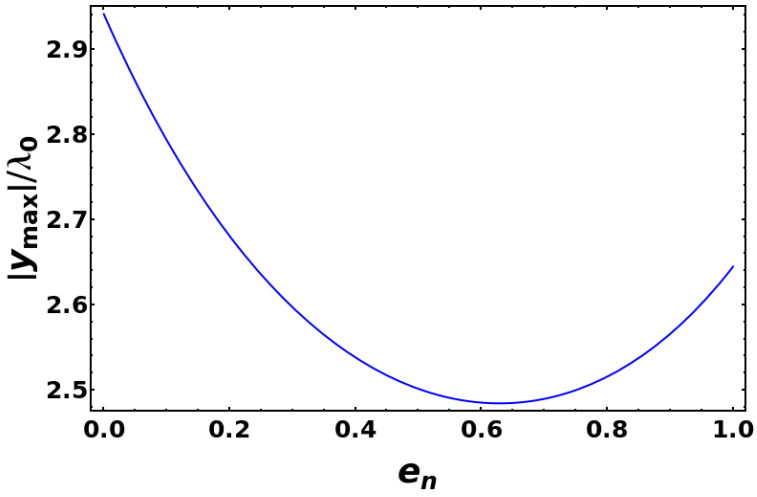

Figure 4.4: Plot of $|y_{\max}|/\lambda_0$ vs. e_n as predicted by the kinetic-model up to second-order in g.

4.5.2 Temperature Profile up to fourth-order in g

Here we examine the temperature profiles by retaining terms up to "fourth-order" in the gravitational acceleration and make a comparison with corresponding second-order solution. Fig. 4.5 displays the temperature profiles [solution of Eq. (4.93)] at Froude numbers of (a) $\mathrm{Fr}_0 = 10^{-3}$ and (b) $\mathrm{Fr}_0 = 5 \times 10^{-3}$ for a dissipative gas with $e_n = 0.5$ and $e_n = 0.8$, as well as for a non-dissipative molecular gas. The quantity $T(y)/T_0$ is plotted against y/λ_0, with λ_0 being the centreline mean free path, in each panel of Fig. 4.5. It is seen from Fig. 4.5(a) that for both molecular (elastic) and granular gases, the temperature profile $T(y)/T_0$ exhibits bimodal nature with a local minimum at the channel centreline (at $y = 0$) and the location of two symmetric maxima of temperature shifts towards the channel centreline as we increase dissipation. The value of the maximum temperature decreases with increasing dissipation as it is evident from Fig. 4.5(a). It is seen that at this value of Froude number, the temperature profiles obtained from the fourth-order solution are qualitatively similar to those obtained from the solution at second-order in g [see §4.5.1]. Overall, we can say that the temperature profiles obtained from both fourth and second-order solutions (in gravity field) predict qualitatively similar features at $\mathrm{Fr}_0 = 10^{-3}$.

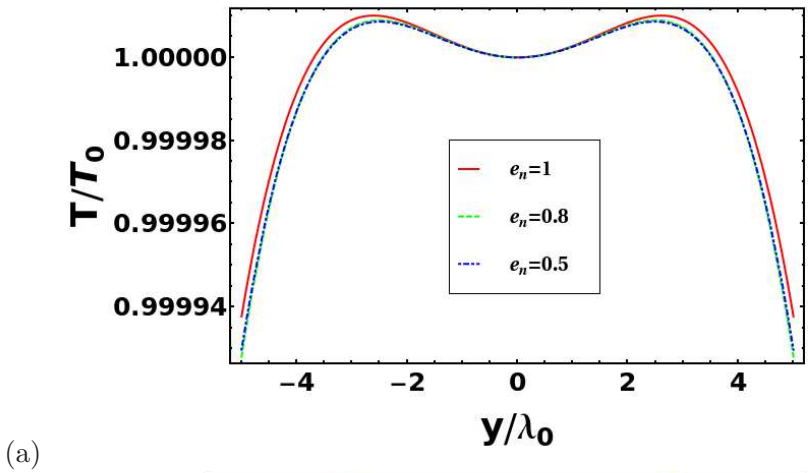

(a)

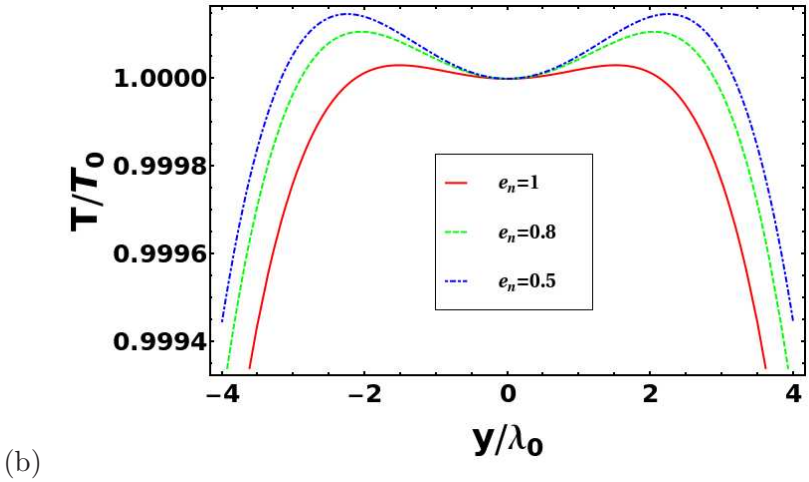

(b)

Figure 4.5: Temperature profiles for (a) $\mathrm{Fr}_0 = 10^{-3}$ and (b) $\mathrm{Fr}_0 = 5 \times 10^{-3}$ with $e_n = 1$ (red solid line), $e_n = 0.8$ (green dashed line) and $e_n = 0.5$ (blue dash dotted line), as predicted by the kinetic-model up to "fourth-order" in g.

Temperature profiles [solution of Eq. (4.93)] for a Froude number of $\mathrm{Fr}_0 = 5 \times 10^{-3}$ for a molecular gas $e_n = 1$ and inelastic gases with $e_n = 0.5$ and $e_n = 0.8$ are presented in Fig. 4.5(b). Like in the case of $\mathrm{Fr}_0 = 10^{-3}$ (Fig. 4.5(a)), the temperature bimodality is observed at $\mathrm{Fr}_0 = 5 \times 10^{-3}$; however, one finds noticeable differences in the temperature profiles obtained from the fourth-order solution in comparison to the results obtained at $\mathrm{Fr}_0 = 10^{-3}$. The differences are as follows: (i) as inelasticity increases, the value of the temperature maximum $T_{\max}$ decreases at $\mathrm{Fr}_0 = 10^{-3}$ whereas the opposite trend is observed at $\mathrm{Fr}_0 = 5 \times 10^{-3}$, i.e, the value of maximum temperature $T_{\max}$ increases with increasing inelasticity, and (ii) the spatial location of two symmetric maxima of temperature moves away from the channel centreline with increasing dissipation [see Fig. 4.5(b)] for $\mathrm{Fr}_0 = 5 \times 10^{-3}$, while exactly opposite behaviour is detected for $\mathrm{Fr}_0 = 10^{-3}$. These findings at $\mathrm{Fr}_0 = 5 \times 10^{-3}$ [Fig. 4.5(b)] resemble the simulation results reported by Alam *et al.* (2015) and Gupta & Alam (2017) who found that the maximum temperature $T_{\max}$ increases with decreasing e_n.

For the fourth-order solution in g, the spatial location $y_{\max}$ of two symmetric temperature

maxima is given by

$$y_{\max} = \pm\lambda_0\Bigg[\sqrt{\Bigg(- \frac{B_6^{3D}}{4B_8^{3D}} - \frac{(2\ 2^{1/3}A_4^{3D})}{(k_1+\sqrt{(k_1^2+4k_2^3)})^{1/3}} - \frac{(2\ 2^{1/3}B_4^{3D}\mathrm{Fr}_0^2)}{(k_1+\sqrt{(k_1^2+4k_2^3)})^{1/3}} + \frac{(3B_6^{3D^2}\mathrm{Fr}_0^2)}{(2\ 2^{2/3}B_8^{3D}(k_1+\sqrt{(k_1^2+4k_2^3)})^{1/3})} + \frac{1}{12\ 2^{1/3}B_8^{3D}\mathrm{Fr}_0^2}(k_1+\sqrt{(k_1^2+4k_2^3)})^{1/3}\Bigg)\Bigg], \tag{4.103}$$

and the expression for the excess temperature ΔT is given by

$$\begin{aligned}
\Delta T &= \frac{T_{\max}-T_0}{T_0} = \frac{1}{\left(12B_8^{3D}h_1^{1/3}\right)}\Bigg((-8\ 3^{2/3}A_4^{3D}B_8^{3D}\mathrm{Fr}_0^2 + 3\ 3^{2/3}B_6^{3D^2}\mathrm{Fr}_0^4 \\
&-8\ 3^{2/3}B_4^{3D}B_8^{3D}\mathrm{Fr}_0^4 - 3B_6^{3D}\mathrm{Fr}_0^2h_1^{1/3} + 3^{1/3}h_1^{2/3}) \\
&\times\Bigg(A_2^{3D} + \frac{1}{(12B_8^{3D}\mathrm{Fr}_0^2h_1^{1/3})}(A_4^{3D}(-8\ 3^{2/3}A_4^{3D}B_8^{3D}\mathrm{Fr}_0^2 + 3\ 3^{2/3}B_6^{3D^2}\mathrm{Fr}_0^4 \\
&-8\ 3^{2/3}B_4^{3D}B_8^{3D}\mathrm{Fr}_0^4 - 3B_6^{3D}\mathrm{Fr}_0^2h_1^{1/3} + 3^{1/3}h_1^{2/3})) + \frac{1}{1728}\mathrm{Fr}_0^2\Bigg(1728B_2^{3D} \\
&+\frac{1}{(B_8^{3D^2}\mathrm{Fr}_0^4h_1^{2/3})}(12B_6^{3D}(8\ 3^{2/3}A_4^{3D}B_8^{3D}\mathrm{Fr}_0^2 - 3\ 3^{2/3}B_6^{3D^2}\mathrm{Fr}_0^4 + 8\ 3^{2/3}B_4^{3D}B_8^{3D}\mathrm{Fr}_0^4 \\
&+3B_6^{3D}\mathrm{Fr}_0^2h_1^{1/3} - 3^{1/3}h_1^{2/3})^2) - \frac{1}{(B_8^{3D^2}\mathrm{Fr}_0^6h_1)}(8\ 3^{2/3}A_4^{3D}B_8^{3D}\mathrm{Fr}_0^2 - 3\ 3^{2/3}B_6^{3D^2}\mathrm{Fr}_0^4 \\
&+8\ 3^{2/3}B_4^{3D}B_8^{3D}\mathrm{Fr}_0^4 + 3B_6^{3D}\mathrm{Fr}_0^2h_1^{1/3} - 3^{1/3}h_1^{2/3})^3 \\
&+\frac{1}{(B_8^{3D}\mathrm{Fr}_0^2h_1^{1/3})}(144B_4^{3D}(-8\ 3^{2/3}A_4^{3D}B_8^{3D}\mathrm{Fr}_0^2 + 3\ 3^{2/3}B_6^{3D^2}\mathrm{Fr}_0^4 \\
&-8\ 3^{2/3}B_4^{3D}B_8^{3D}\mathrm{Fr}_0^4 - 3B_6^{3D}\mathrm{Fr}_0^2h_1^{1/3} + 3^{1/3}h_1^{2/3}))\Bigg)\Bigg)\Bigg) + O(g^6),
\end{aligned} \tag{4.104}$$

where

$$\begin{aligned}
k_1 &= 216A_4^{3D}B_6^{3D}B_8^{3D}\mathrm{Fr}_0^4 - 432A_2^{3D}B_8^{3D^2}\mathrm{Fr}_0^4 - 54B_6^{3D^3}\mathrm{Fr}_0^6 + 216B_4^{3D}B_6^{3D}B_8^{3D}\mathrm{Fr}_0^6 \\
&\quad -432B_2^{3D}B_8^{3D^2}\mathrm{Fr}_0^6, \qquad (4.105)\\
k_2 &= (-9B_6^{3D^2}\mathrm{Fr}_0^4 + 24B_8^{3D}\mathrm{Fr}_0^2(A_4^{3D} + B_4^{3D}\mathrm{Fr}_0^2)), \qquad (4.106)\\
h_1 &= 36A_4^{3D}B_6^{3D}B_8^{3D}\mathrm{Fr}_0^4 - 72A_2^{3D}B_8^{3D^2}\mathrm{Fr}_0^4 - 9B_6^{3D^3}\mathrm{Fr}_0^6 + 36B_4^{3D}B_6^{3D}B_8^{3D}\mathrm{Fr}_0^6 \\
&\quad -72B_2^{3D}B_8^{3D^2}\mathrm{Fr}_0^6 + \frac{1}{3}\sqrt{\Bigg(729\mathrm{Fr}_0^8(-4A_4^{3D}B_6^{3D}B_8^{3D} + 8A_2^{3D}B_8^{3D^2} \\
&\quad +(B_6^{3D^3} - 4B_4^{3D}B_6^{3D}B_8^{3D} + 8B_2^{3D}B_8^{3D^2})\mathrm{Fr}_0^2)^2 \\
&\quad + \left(-9B_6^{3D^2}\mathrm{Fr}_0^4 + 24B_8^{3D}\mathrm{Fr}_0^2\left(A_4^{3D} + B_4^{3D}\mathrm{Fr}_0^2\right)\right)^3\Bigg)}. \qquad (4.107)
\end{aligned}$$

It is easy to verify that the rescaled temperature bimodality, $\Delta T/\mathrm{Fr}_0^2$, does depend on the Froude number (unlike the second-order solution in Eq. (4.101)) along with restitution coefficient.

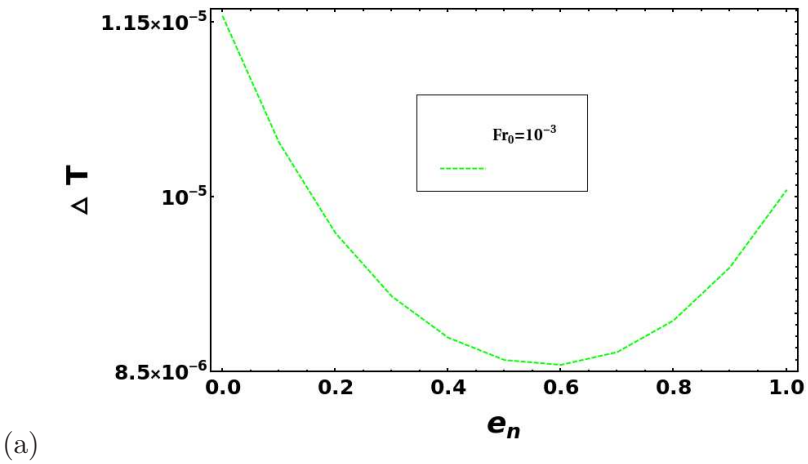

(a)

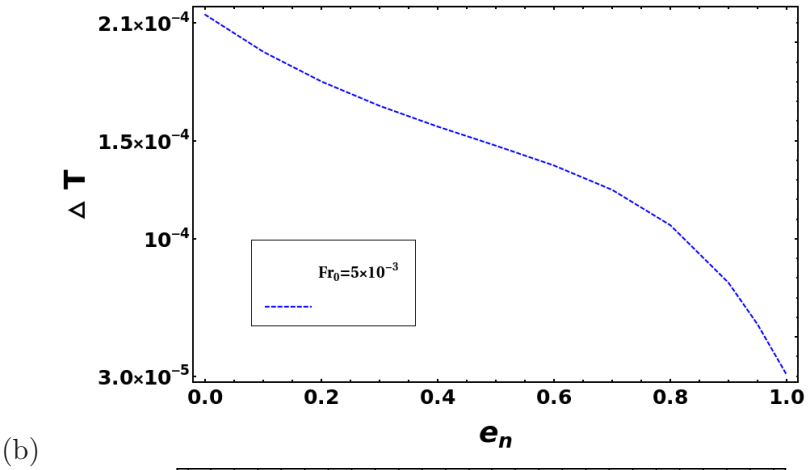

(b)

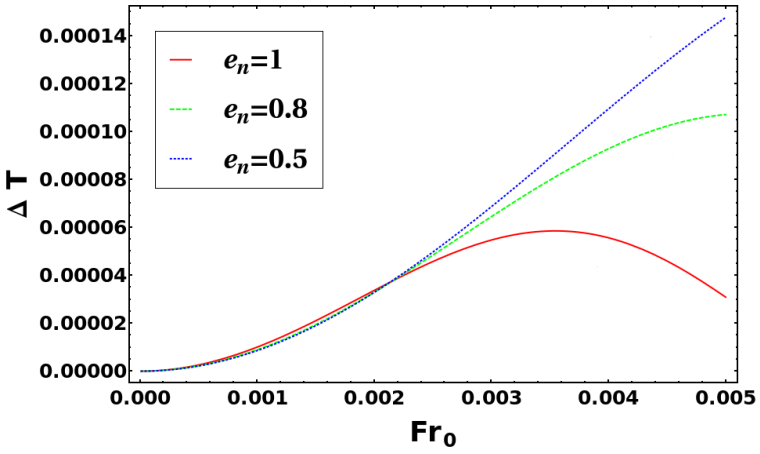

(c)

Figure 4.6: (a,b) Plots of $\Delta T(= T_{\max}/T_0 - 1)$ vs. e_n for two values of Froude numbers: (a) $\mathrm{Fr}_0 = 10^{-3}$, (b) $\mathrm{Fr}_0 = 5 \times 10^{-3}$. (c) Variation of ΔT with Fr_0 for different e_n.

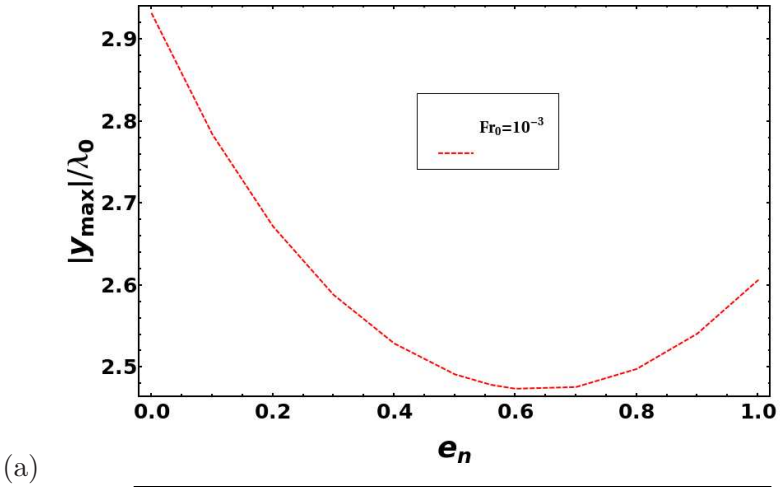

(a)

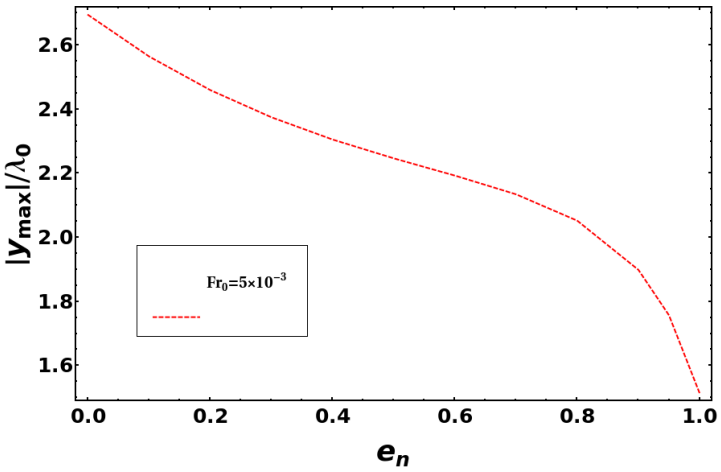

(b)

Figure 4.7: Plots of $|y_{\max}|/\lambda_0$ vs. e_n for two values of Froude numbers: (a) $\mathrm{Fr}_0 = 10^{-3}$ and (b) $\mathrm{Fr}_0 = 5 \times 10^{-3}$.

To understand the dependence of temperature bimodality ΔT (excess temperature) on the restitution coefficient e_n from the fourth-order solution [Eq. (4.104)], we present the plots of ΔT for two values of Froude numbers $\mathrm{Fr}_0 = 10^{-3}$ and $\mathrm{Fr}_0 = 5 \times 10^{-3}$ in Fig. 4.6(a,b). From Fig. 4.6(a), the excess temperature ΔT is found to have a non-monotonic dependence on the restitution coefficient e_n; ΔT has a minimum around a restitution coefficient of $e_n \approx 0.56$ and shows increasing trend as we go towards the two extreme limits of the restitution coefficient from $e_n = 0.56$. These findings are similar to the result obtained from the second-order solution at any Froude number (see Fig. 4.3(a)). On the other hand, ΔT increases with increasing dissipation at a Froude number $\mathrm{Fr}_0 = 5 \times 10^{-3}$, which is evident from Fig. 4.6(b). Fig. 4.6(c) shows the variation of ΔT with Fr_0 for different values of e_n. Overall, Fig. 4.6 confirms that as we increase Fr_0 from 10^{-3} to 5×10^{-3}, the variation of the excess temperature ΔT switches from non-monotonic to monotonic nature with respect to increasing dissipation (i.e. with decreasing restitution coefficient). Similar behaviour is also found for the location of the temperature maxima, $|y_{\max}|/\lambda_0$, see Fig. 4.7.

The above transition from "non-monotonic" to "monotonic" dependence of ΔT on restitution coefficient as a function of Froude number Fr_0 is illustrated in Fig. 4.8. The red-colored region at small Fr_0 in the lower left corner of Fig. 4.8(b) corresponds to region where ΔT decreases

with increasing dissipation. Fig. 4.8(b) confirms that there is a critical Froude number

$$\mathrm{Fr}_0^c \equiv \mathrm{Fr}_0(e_n) \tag{4.108}$$

that depends on e_n, below which ΔT varies non-monotonically with e_n but ΔT increases monotonically with increasing dissipation at $\mathrm{Fr}_0 > \mathrm{Fr}_0^c$. In other words, the inelasticity plays a "dual" role of increasing and decreasing ΔT at $\mathrm{Fr}_0 > \mathrm{Fr}_0^c$ and $\mathrm{Fr}_0 < \mathrm{Fr}_0^c$, respectively.

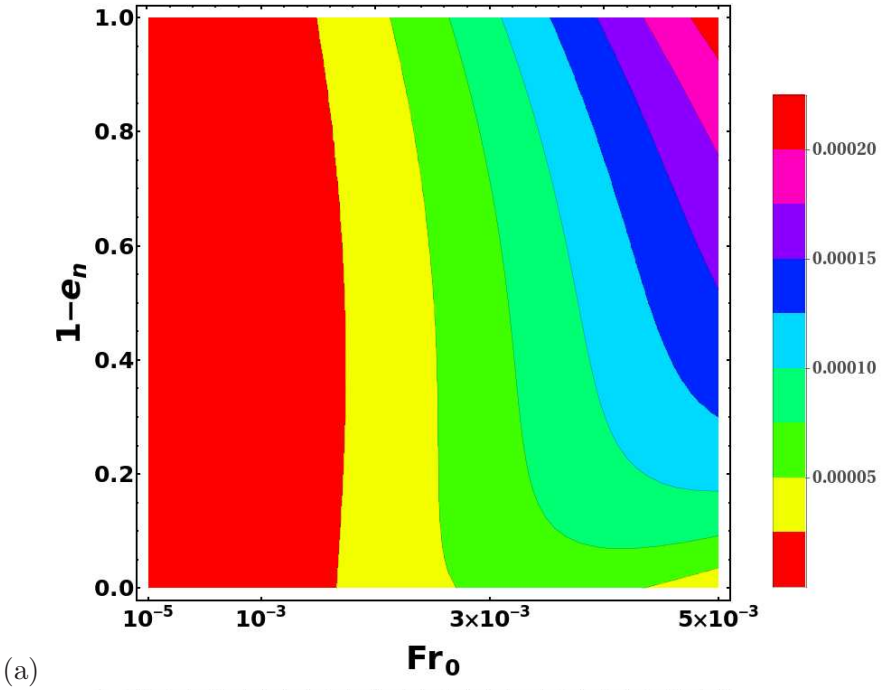

(a)

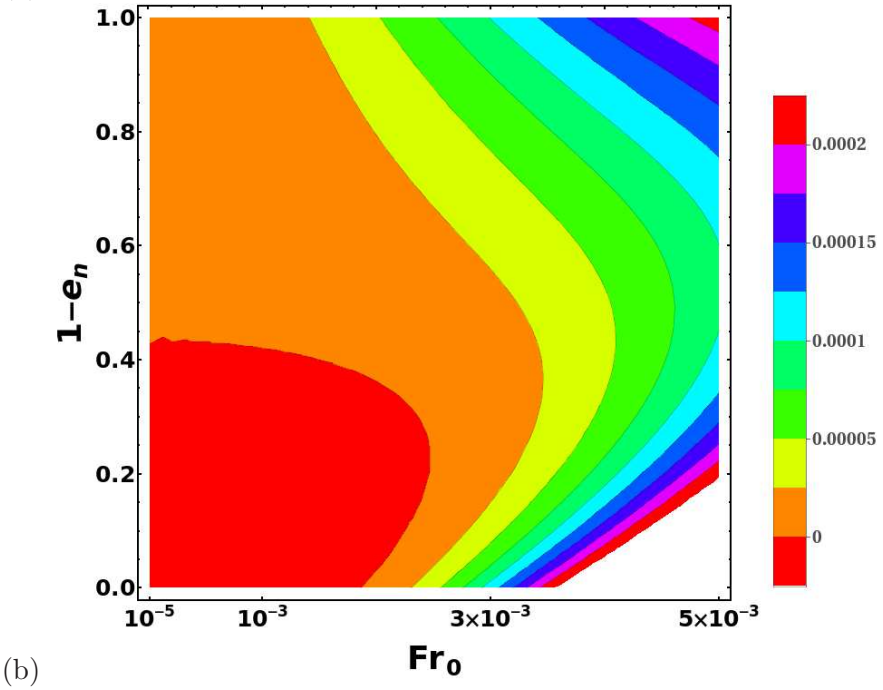

(b)

Figure 4.8: Contour plots of (a) ΔT and (b) derivative of ΔT w.r.to e_n, i.e. $d\Delta T/de_n$, in $(\mathrm{Fr}_0, 1 - e_n)$-plane.

4.6 Results on Rheology: Pressure Tensor and Heat Flux Vector

4.6.1 Pressure Tensor and the Normal Stress Differences

The expressions for the elements of the pressure tensor and the components of the heat flux up to fourth-order are given by Eqs. (4.55)-(4.56), (4.64)-(4.66), (4.73)-(4.74) and (4.86)-(4.88). In real units, the expressions for the components of pressure tensor are given by

$$
\begin{aligned}
P_{xx} &= p_0\Bigg[1+\frac{32}{25}\frac{82+67\zeta_0^*+8\zeta_0^{*2}}{(1+\zeta_0^*)(2+\zeta_0^*)^2}\left(\frac{\rho_0\eta_0^2g^2}{2p_0^3}\right)+\frac{56}{5}y^2\left(\frac{1}{4}\left(\frac{mg}{T_0}\right)^2\right)+\frac{224}{375}y^6(2+\zeta_0^*)\left(\frac{\rho_0^5g^4}{32\eta_0^2p_0^3}\right)\\
&+\frac{32y^4}{375(1+\zeta_0^*)^4(2+\zeta_0^*)^5(2+3\zeta_0^*)^3(2+5\zeta_0^*)}\left(4+12\zeta_0^*+11\zeta_0^{*2}+3\zeta_0^{*3}\right)^3(-21144\\
&-70636\zeta_0^*-43978\zeta_0^{*2}+2137\zeta_0^{*3}+2455\zeta_0^{*4})\left(\frac{1}{16}\left(\frac{mg}{T_0}\right)^4\right)\\
&+\frac{1}{3125(1+\zeta_0^*)^4(2+\zeta_0^*)^5(1+2\zeta_0^*)^2(2+3\zeta_0^*)^3(2+5\zeta_0^*)}\Bigg(512(-1066982656\\
&-11957194240\zeta_0^*-58644859232\zeta_0^{*2}-165729887792\zeta_0^{*3}-298651532384\zeta_0^{*4}\\
&-358002977288\zeta_0^{*5}-287936971998\zeta_0^{*6}-151710315739\zeta_0^{*7}-48209843396\zeta_0^{*8}\\
&-6708938562\zeta_0^{*9}+779555905\zeta_0^{*10}+433209456\zeta_0^{*11}\\
&+57182436\zeta_0^{*12}+2568240\zeta_0^{*13})\Bigg)\left(\frac{\rho_0^2\eta_0^4g^4}{4p_0^6}\right)\\
&+\frac{1}{625(1+\zeta_0^*)^4(2+\zeta_0^*)^5(1+2\zeta_0^*)^2(2+3\zeta_0^*)^3(2+5\zeta_0^*)}\Bigg(32y^2(-393880320\\
&-5561605632\zeta_0^*-34942366336\zeta_0^{*2}-129006012416\zeta_0^{*3}-311212453440\zeta_0^{*4}\\
&-515641881312\zeta_0^{*5}-599613703128\zeta_0^{*6}-490133164848\zeta_0^{*7}-276196369025\zeta_0^{*8}\\
&-101648368600\zeta_0^{*9}-21034331946\zeta_0^{*10}-954252636\zeta_0^{*11}\\
&+548620335\zeta_0^{*12}+105666444\zeta_0^{*13}+4864860\zeta_0^{*14})\Bigg)\left(\frac{\rho_0^3\eta_0^2g^4}{8p_0^5}\right)\Bigg]+O(g^6),
\end{aligned}
\tag{4.109}
$$

$$
\begin{aligned}
P_{yy} &= p_0\Bigg[1-\frac{24}{25}\frac{102+87\zeta_0^*+13\zeta_0^{*2}}{(1+\zeta_0^*)(2+\zeta_0^*)^2}\left(\frac{\rho_0\eta_0^2g^2}{2p_0^3}\right)\\
&-\frac{1}{3125(1+\zeta_0^*)^4(2+\zeta_0^*)^5(1+2\zeta_0^*)^2(2+3\zeta_0^*)^3(2+5\zeta_0^*)}\Bigg(384(-1562108416\\
&-17537832640\zeta_0^*-86542601952\zeta_0^{*2}-247386118112\zeta_0^{*3}-454210757024\zeta_0^{*4}\\
&-560679708268\zeta_0^{*5}-472406095078\zeta_0^{*6}-269146497804\zeta_0^{*7}-99542188931\zeta_0^{*8}\\
&-21415804832\zeta_0^{*9}-1710159795\zeta_0^{*10}+250281216\zeta_0^{*11}\\
&+61806996\zeta_0^{*12}+3518640\zeta_0^{*13})\Bigg)\left(\frac{\rho_0^2\eta_0^4g^4}{4p_0^6}\right)\Bigg]+O(g^6),
\end{aligned}
\tag{4.110}
$$

$$
\begin{aligned}
P_{yx} &= -\rho_0 gy-\frac{4y^3\left(44+94\zeta_0^*+26\zeta_0^{*2}\right)}{75\left(2+3\zeta_0^*+\zeta_0^{*2}\right)}\left(\frac{\rho_0^3g^3}{8p_0^2}\right)-\frac{4y^5(1+\zeta_0^*)(2+\zeta_0^*)^2}{75\left(2+3\zeta_0^*+\zeta_0^{*2}\right)}\left(\frac{\rho_0^4g^3}{16\eta_0^2p_0}\right)\\
&+O(g^5).
\end{aligned}
\tag{4.111}
$$

The expression for mean pressure is

$$p(y) = \underline{p_0\left[1+p_2^{(2)}\frac{1}{4}\left(\frac{mg}{T_0}\right)^2 y^2 + p_2^{(4)}\left(\frac{m^5\eta_0^2 g^4}{8\rho_0^2 T_0^5}\right)y^2 + p_4^{(4)}\frac{1}{16}\left(\frac{mg}{T_0}\right)^4 y^4 + p_6^{(4)}\left(\frac{m^3\rho_0^2 g^4}{32\eta_0^2 T_0^3}\right)y^6\right]} + O(g^6) \tag{4.112}$$

which is same as in Eq. (4.90). The underlined terms in the above equations represent the solution of respective fluxes up to second-order in gravity field g. From Eq. (4.112), Eq. (4.109) and Eq. (4.110), it is easy to verify that $P_{yy} < p < P_{xx}$, which means that normal stresses are small along the normal direction and large along the direction of the flow, leading to 'non-zero' normal stress differences as discussed below.

Normal Stress Differences (NSD's) at fourth-order

In order to characterize the normal stress differences, we present numerical results on first and second normal-stress differences $\mathcal{N}_1$ and $\mathcal{N}_2$, which are defined in §3.5.2 [see Eq. (3.128)]:

$$\mathcal{N}_1 = \frac{P_{xx}-P_{yy}}{p} \quad \text{and} \quad \mathcal{N}_2 = \frac{P_{yy}-P_{zz}}{p} \equiv \frac{P_{xx}+2P_{yy}}{p} - 3. \tag{4.113}$$

where p is the mean pressure. Recall that the Navier-Stokes description predicts zero value for both first and second normal stress differences.

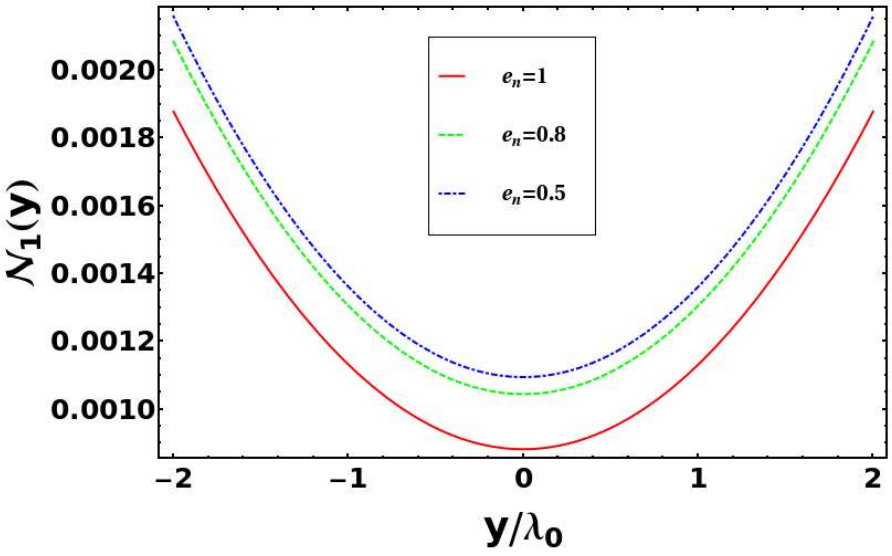

Figure 4.9: Profiles of the first normal-stress difference $\mathcal{N}_1$ for $\mathrm{Fr}_0 = 5\times10^{-3}$ and $e_n = 0.5$, $e_n = 0.8$, and $e_n = 1$, as predicted by the "fourth-order" solution of the kinetic model.

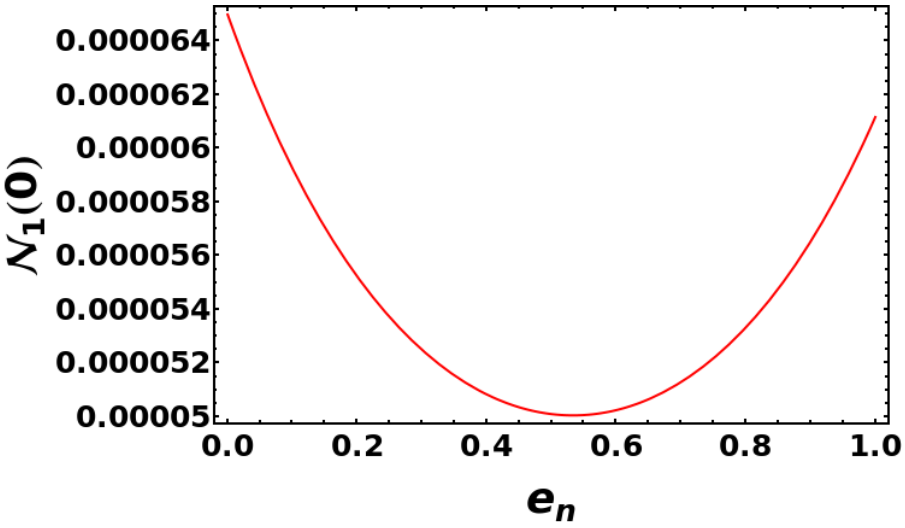

(a)

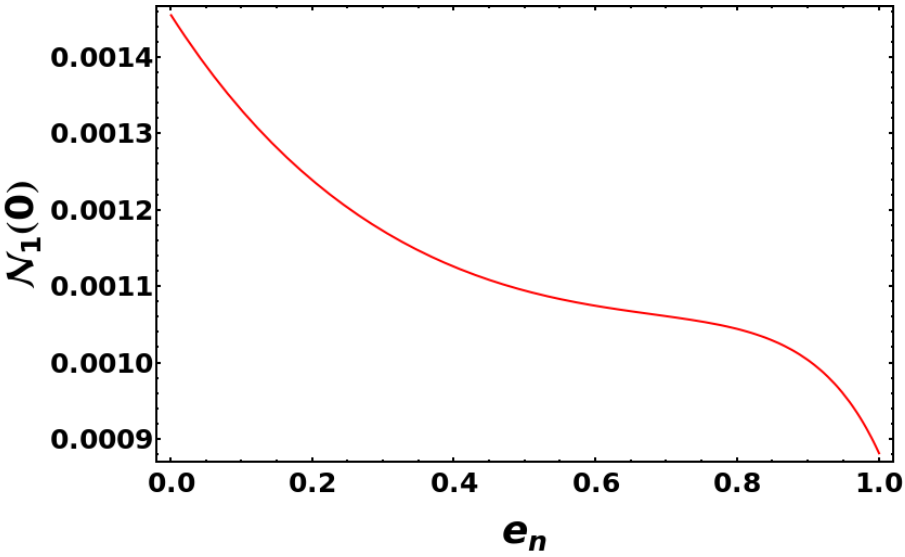

(b)

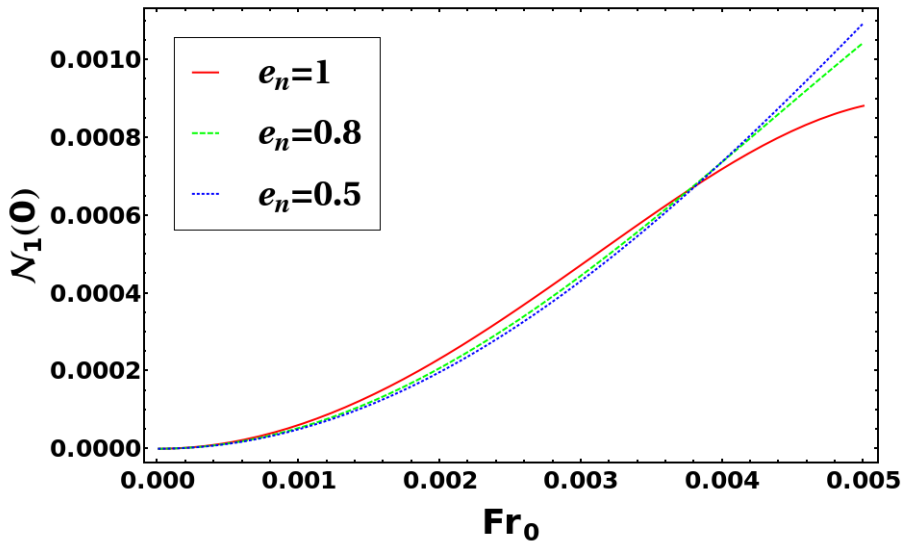

(c)

Figure 4.10: (a,b) First normal-stress difference $\mathcal{N}_1$ evaluated at channel centreline ($y = 0$) against e_n for (a) $\mathrm{Fr}_0 = 10^{-3}$, (b) $\mathrm{Fr}_0 = 5 \times 10^{-3}$. (c) Variation of $\mathcal{N}_1(0)$ with Fr_0.

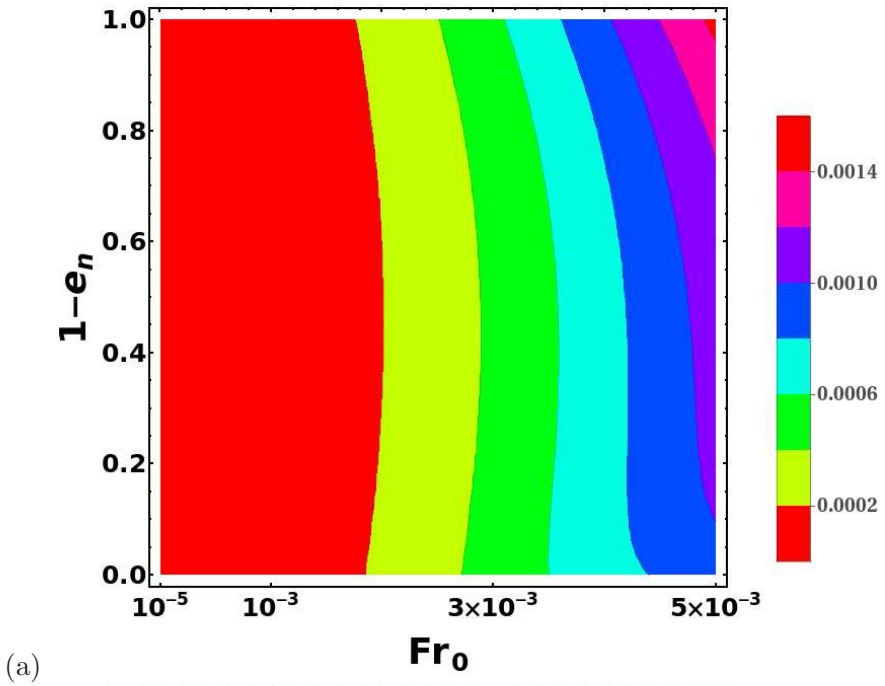

(a)

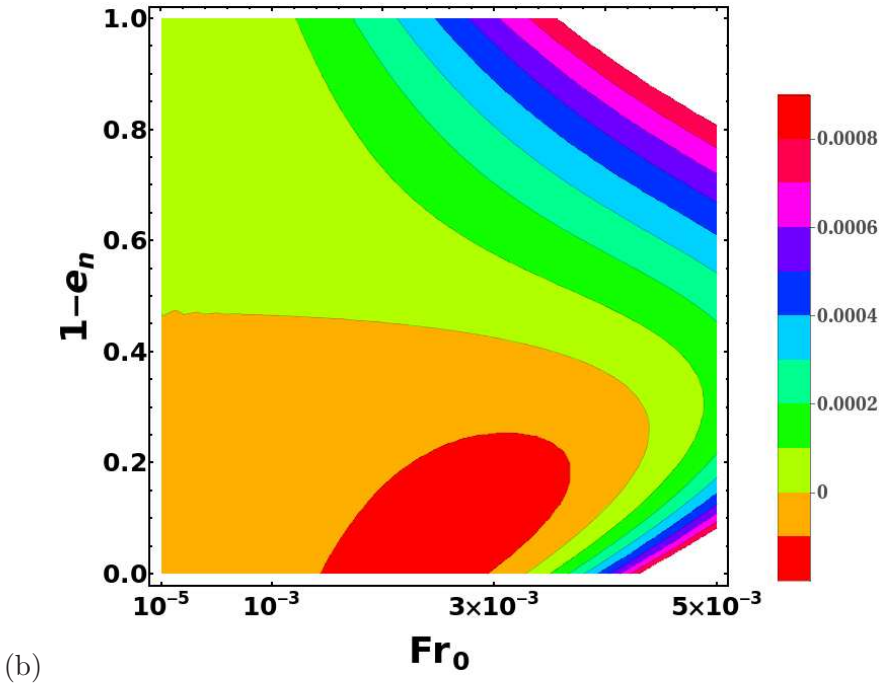

(b)

Figure 4.11: Contour plots of (a) $\mathcal{N}_1(0)$ and (b) derivative of $\mathcal{N}_1(0)$ w.r.to e_n in $(\mathrm{Fr}_0, 1-e_n)$-plane.

The transverse profiles for the first normal-stress difference $\mathcal{N}_1$ for a Froude number $\mathrm{Fr}_0 = 5 \times 10^{-3}$ with three different values of restitution coefficient $e_n = 0.5, 0.8$ and 1 are shown in Fig. 4.9. It is seen that $\mathcal{N}_1$ increases with distance from the channel centreline $y = 0$, with its minimum being located at $y = 0$. The dependence of $\mathcal{N}_1$ evaluated at the channel centreline $y = 0$ on e_n is illustrated in Fig. 4.10(a,b). We observe that the value of $\mathcal{N}_1(0)$ increases with increasing dissipation as it is evident from Fig. 4.9 and Fig. 4.10(b) at $\mathrm{Fr}_0 = 5 \times 10^{-3}$, while $\mathcal{N}_1(0)$ shows a non-monotonic dependence on the restitution coefficient e_n for the case of Froude number $\mathrm{Fr}_0 = 10^{-3}$ [Fig. 4.10(a)]. Fig. 4.10(c) shows the variation of $\mathcal{N}_1(0)$ with Fr_0 for e_n=1,

0.8 and 0.5. The transition from "non-monotonic" to "monotonic" dependence of $\mathcal{N}_1(0)$ with e_n can be understood from Fig. 4.11(b) which displays the contour-map of "$d\mathcal{N}_1(0)/de_n$" in the $(\mathrm{Fr}_0, 1-e_n)$-plane. In the lower left corner of Fig. 4.11(b), the first normal-stress difference decreases with increasing dissipation and increases elsewhere at any Fr_0.

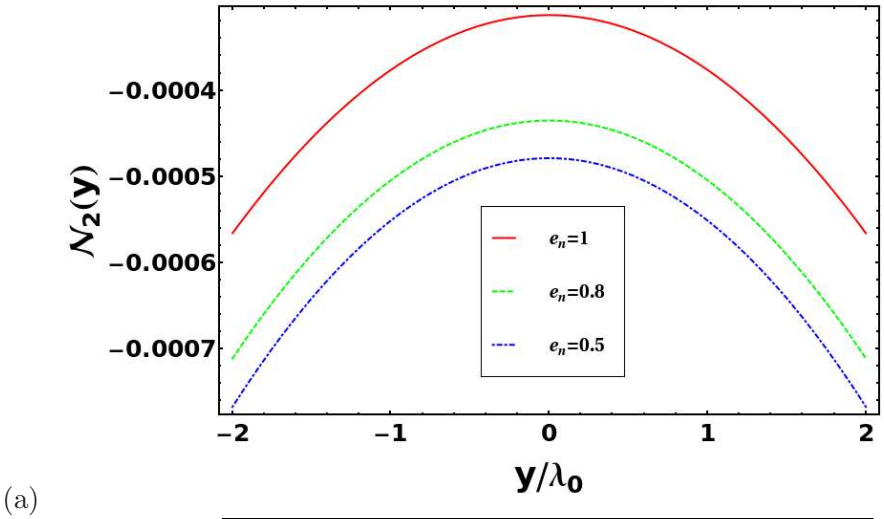

(a)

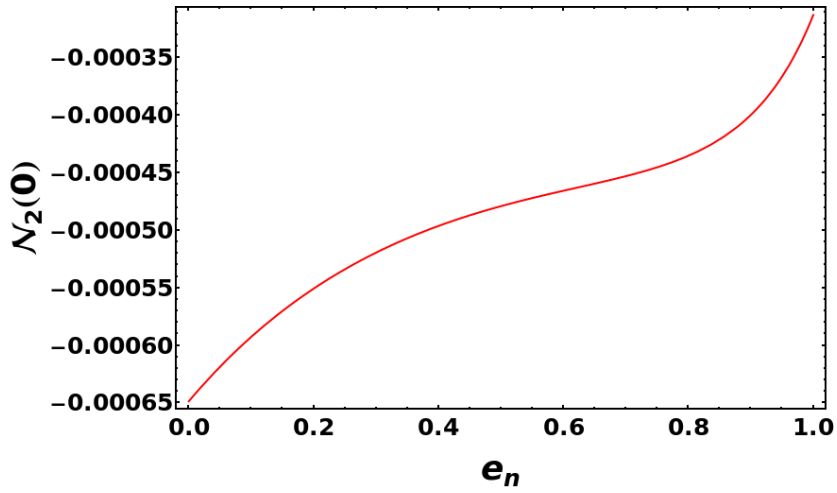

(b)

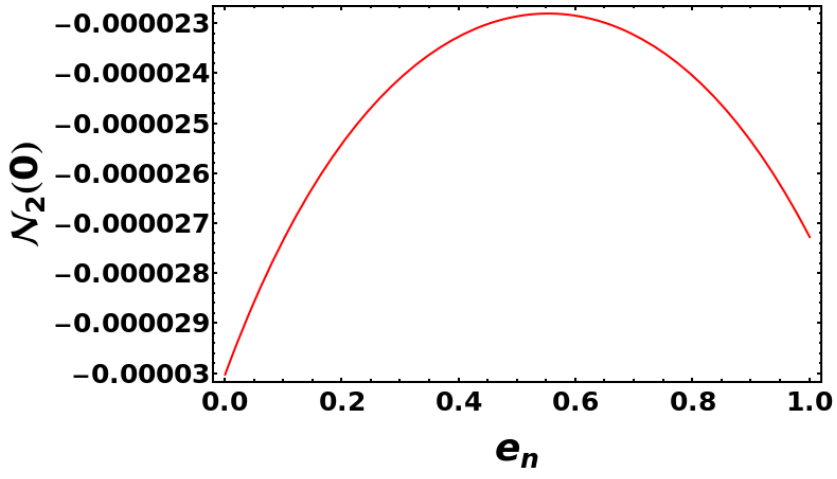

(c)

Figure 4.12: Profiles of (a) the second-normal stress difference $\mathcal{N}_2(y)$ for $\mathrm{Fr}_0 = 5\times10^{-3}$. Variation of $\mathcal{N}_2(0)$ against e_n for (b) $\mathrm{Fr}_0 = 5\times10^{-3}$ and (c) $\mathrm{Fr}_0 = 10^{-3}$.

The second normal-stress difference profiles for different e_n at $\mathrm{Fr}_0 = 5\times10^{-3}$ are illustrated in

Fig. 4.12(a) and the corresponding variations of its centreline value $\mathcal{N}_2(0)$ in Fig. 4.12(b,c). It is seen that the second normal-stress difference is negative and has its maximum at mid-layer of the channel $y = 0$ and decreases as one moves away from the channel center. The magnitude of the second normal-stress difference $\mathcal{N}_2(0)$ can vary non-monotonically with decreasing dissipation, which is evident from Fig. 4.12(b) and 4.12(c), depending on Fr_0. Fig. 4.13 summarizes the dependence of $\mathcal{N}_2(0)$ with Fr_0 and $(1 - e_n)$; while panel (a) displays the contours of $\mathcal{N}_2(0)$, the panel (b) shows the contours of $d\mathcal{N}_2(0)/de_n$. Similar to the variation of $\mathcal{N}_1(0)$ [see Fig. 4.11(b)], the second normal-stress difference $\mathcal{N}_2(0)$ increases with increasing $(1 - e_n)$ around the lower left corner of Fig. 4.13(b) and decreases with $(1-e_n)$ elsewhere. We conclude that, while $\mathcal{N}_2(0)$ varies non-monotonically with restitution coefficient at $\mathrm{Fr}_0 = \mathrm{Fr}_0^c \sim 3.8 \times 10^{-3}$, its magnitude increases monotonically with increasing dissipation at $\mathrm{Fr}_0 > \mathrm{Fr}_0^c$.

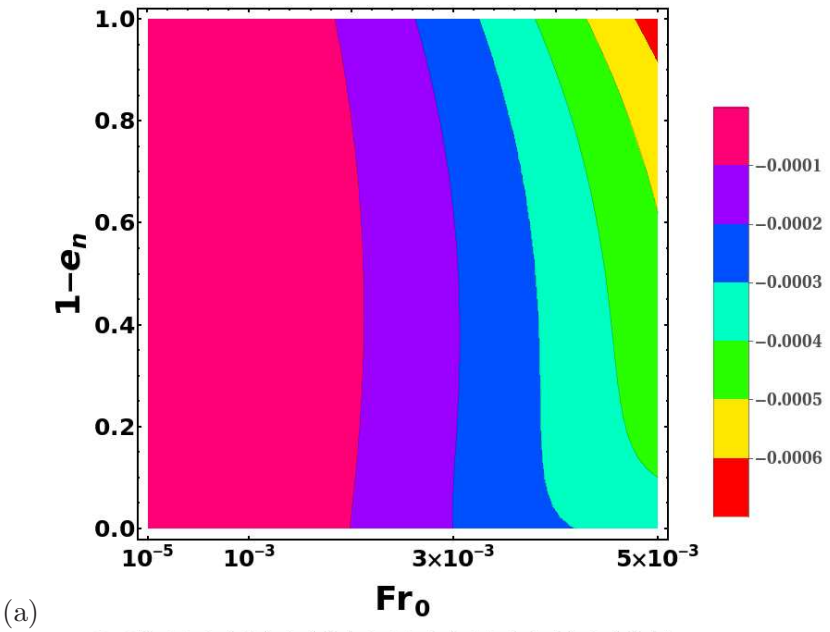

(a)

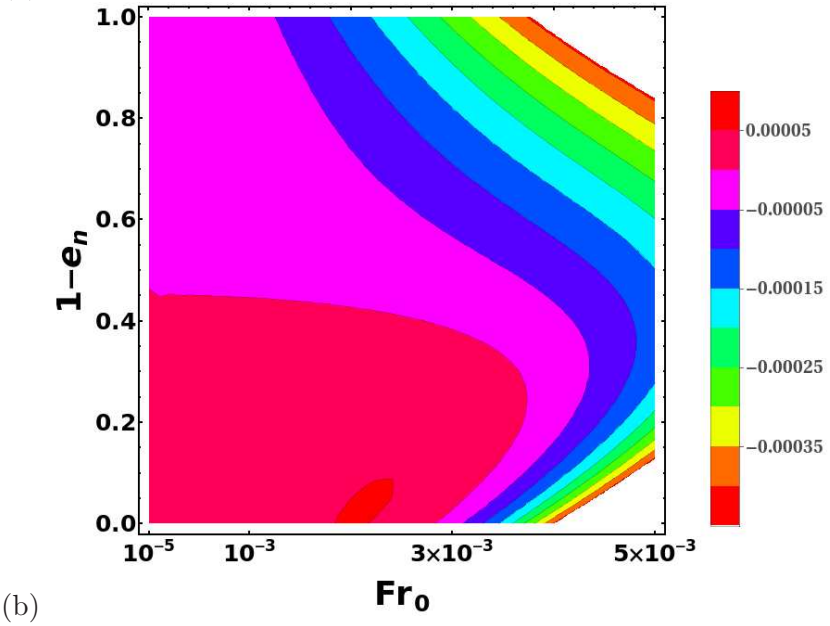

(b)

Figure 4.13: Contour plots of (a) $\mathcal{N}_2(0)$ and (b) the derivative of $\mathcal{N}_2(0)$ w.r.to e_n in $(\mathrm{Fr}_0, 1-e_n)$-plane.

4.6.2 Heat Flux: Tangential and Normal Components

Retaining terms up to fourth-order in gravitational acceleration (g), the longitudinal/tangential q_x and transverse/normal q_y components of the heat flux vector are expressed in real units as

$$
\begin{aligned}
q_x &= \underline{\left(\frac{2}{2+\zeta_0^*}\right)\eta_0 g} - \frac{2y^4\left(2+3\zeta_0^*+\zeta_0^{*2}\right)^3\left(114+257\zeta_0^*+58\zeta_0^{*2}\right)}{15(1+\zeta_0^*)^3(2+\zeta_0^*)^4(1+2\zeta_0^*)}\left(\frac{\rho_0^3 g^3}{8\eta_0 p_0}\right) \\
&\quad -\frac{1}{25(1+\zeta_0^*)^3(2+\zeta_0^*)^4(1+2\zeta_0^*)(2+3\zeta_0^*)^2}\Big(8(336144+1690880\zeta_0^*+3427496\zeta_0^{*2} \\
&\quad +3545632\zeta_0^{*3}+1930569\zeta_0^{*4}+495020\zeta_0^{*5}+35069\zeta_0^{*6}-942\zeta_0^{*7}+1152\zeta_0^{*8})\Big)\left(\frac{\rho_0\eta_0^3 g^3}{2p_0^3}\right) \\
&\quad +\frac{1}{25(1+\zeta_0^*)^3(2+\zeta_0^*)^4(1+2\zeta_0^*)(2+3\zeta_0^*)^2}\Big(4y^2(-50528-367408\zeta_0^*-1102144\zeta_0^{*2} \\
&\quad -1768792\zeta_0^{*3}-1631470\zeta_0^{*4}-839947\zeta_0^{*5}-186671\zeta_0^{*6}+22797\zeta_0^{*7}+20613\zeta_0^{*8} \\
&\quad +3150\zeta_0^{*9})\Big)\left(\frac{\rho_0^2\eta_0 g^3}{4p_0^2}\right)+O(g^5). \qquad (4.114)
\end{aligned}
$$

$$
\begin{aligned}
q_y &= \underline{\frac{\rho_0^2 g^2 y^3}{3\eta_0}} + \frac{12}{175}y^7(2+\zeta_0^*)\left(\frac{\rho_0^5 g^4}{32\eta_0^3 p_0}\right) \\
&\quad +\frac{8y^5\left(2668+10388\zeta_0^*+14179\zeta_0^{*2}+7782\zeta_0^{*3}+1323\zeta_0^{*4}\right)}{375(1+\zeta_0^*)^2(2+\zeta_0^*)(2+3\zeta_0^*)}\left(\frac{\rho_0^4 g^4}{16\eta_0 p_0^2}\right) \\
&\quad -\frac{64y^3\left(-10904-30784\zeta_0^*-29442\zeta_0^{*2}-10706\zeta_0^{*3}-799\zeta_0^{*4}+165\zeta_0^{*5}\right)}{75(1+\zeta_0^*)^2(2+\zeta_0^*)^3(2+3\zeta_0^*)}\left(\frac{\rho_0^3\eta_0 g^4}{8p_0^3}\right) \\
&\quad +O(g^6). \qquad (4.115)
\end{aligned}
$$

The underlined terms in each equation correspond to "second-order" solution as obtained by Tij & Santos (2004). In the following we present numerical results on the longitudinal q_x and transverse q_y components of heat flux based on the analytical expressions [see Eq. (4.114) and Eq. (4.115)], which are correct up to fourth-order in gravity g.

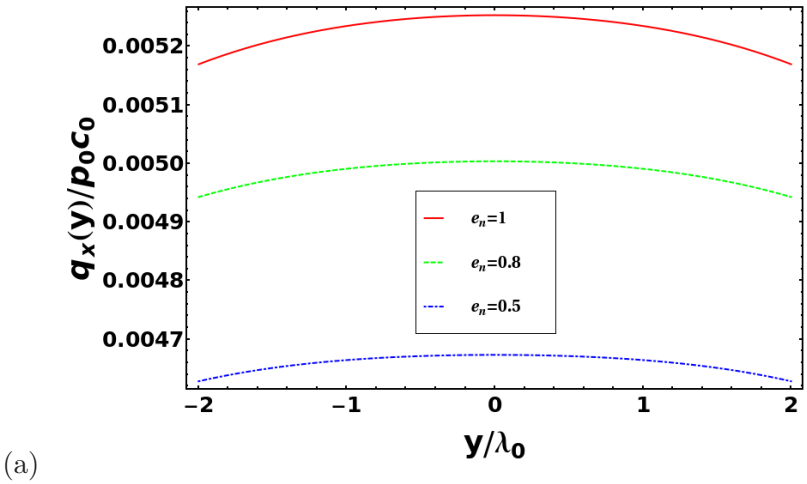

(a)

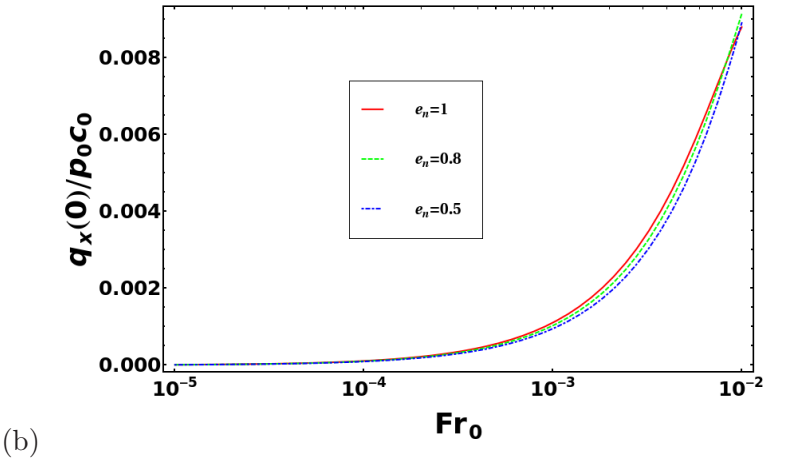

(b)

Figure 4.14: Profiles of dimensionless tangential heat flux ($q_x^* = q_x/p_0c_0$) for (a) $\mathrm{Fr}_0 = 5 \times 10^{-3}$ and (b) $q_x(0)/p_0c_0$ against Fr_0 with $e_n = 0.5$, $e_n = 0.8$, and $e_n = 1$, as predicted by the fourth-order solution in g.

Fig. 4.14(a) illustrates the profiles of dimensionless tangential heat flux $q_x(y)$ at a Froude number $\mathrm{Fr}_0 = 5 \times 10^{-3}$ for three values of restitution coefficient $e_n = 0.5, 0.8, 1$. It is seen that $q_x(y)$ is positive and has a maximum at channel centreline and decreases with distance from centreline $y = 0$. It is also evident from Fig. 4.14(a) that as dissipation increases the maximum value of centreline tangential heat flux q_x decreases but the variations are minor. Fig. 4.14(b) displays the dependence of $q_x(0)$ on the Froude number Fr_0; with increasing Froude number from 10^{-5} to 10^{-2}, the value of $q_x(0)$ is increases significantly.

Fig. 4.15 shows the transverse component of the heat flux $q_y(y)$ profile for $\mathrm{Fr}_0 = 5 \times 10^{-3}$ at different coefficient of restitution values. It is seen that $q_y(y)$ vanishes at channel centreline [see Eq. (4.115)] and it changes sign with distance from channel centreline $y = 0$ which is expected from Fourier's law of heat flux

$$q_y \propto \frac{dT}{dy}.$$

The variations of q_y for different values of restitution coefficient is found to be negligible, see Fig. 4.15. Simulation data on both q_x and q_y for "granular" Poiseuille flow are currently lacking – the present theoretical results can be compared when such data are available. On the other hand, the DSMC results for a molecular gas ($e_n = 1$) undergoing Poiseuille flow has been carried

out by Uribe & Garcia (1999) along with solutions of Burnett-order equations – their heat-flux profiles look similar to those in Fig. 4.14 and Fig. 4.15.

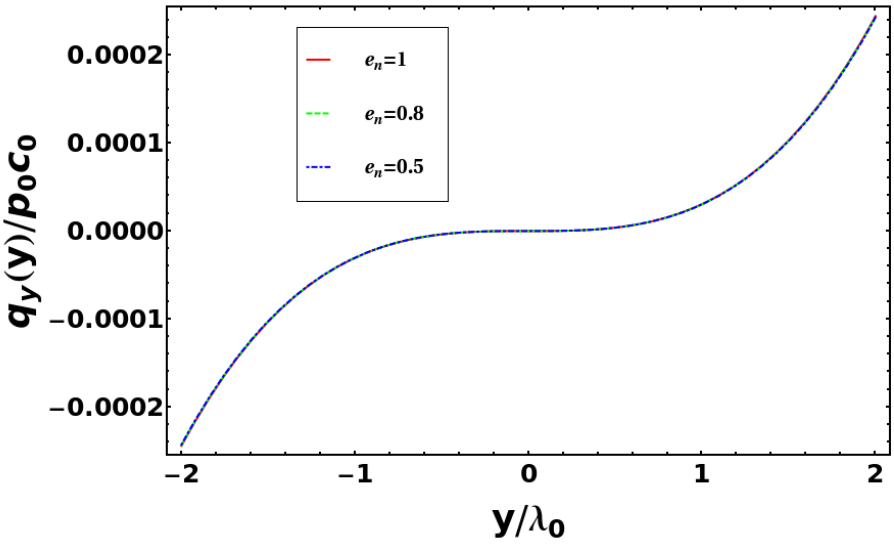

Figure 4.15: Profiles of dimensionless transverse component of heat flux ($q_y^* = q_y/p_0c_0$) for $\mathrm{Fr}_0 = 5 \times 10^{-3}$.

4.7 Summary and Discussion

4.7.1 Summary of Theoretical Predictions

The effect of inelastic dissipation on the gravity-driven flow of a "heated" granular gas (dubbed "granular Poiseuille flow") has been studied using the perturbation expansion of the velocity distribution function, following the previous work of Tij & Santos (2004). A BGK-like kinetic model with heating via white-noise, which compensates for collisional cooling due to inelasticity, has been employed. Neglecting wall-effects and focusing only on the bulk behaviour of the flow, the effect of gravity is incorporated perturbatively around a 'uniform' state (of constant temperature and density): the distribution function and all hydrodynamic and rheological fields are expanded in power-series in gravitational acceleration g, with the base state representing their respective values at the channel centreline.

The complexity of the problem allowed us to determine solutions only up to fourth-order in g; the related second-order solution has been obtained previously by Tij & Santos (2004). The fourth-order solutions are used to analyse the behaviour of (i) temperature bimodality ($\triangle T = (T_{\max} - T_0)/T_0$), (ii) normal stress differences and (iii) heat fluxes as functions of the restitution coefficient (e_n) and the Froude number Fr_0. The results exhibit that the non-Newtonian features such as temperature bimodality, normal stress differences and the existence of a non-zero longitudinal heat flux. It is shown that $\triangle T$ increases with increasing dissipation for $\mathrm{Fr}_0 \approx 5\times10^{-3}$; for small enough values of Fr_0 ($< 4\times10^{-3}$), however, a 'non-monotonic' behaviour of $\triangle T$ with e_n [i.e. $\triangle T$ decreases with decreasing e_n for $e_n \in (1, 0.5)$, but increases for $e_n < 0.5$] is observed. From the analyses of temperature profiles, we conclude that as the Froude number Fr_0 increases, the nature of the degree of bimodality switches from non-monotonic to monotonic

increasing behaviour with respect to increasing inelasticity. The first normal-stress difference (positive $\mathcal{N}_1$) increases with increasing dissipation and the second normal-stress difference (negative $\mathcal{N}_2$) decreases with increasing dissipation at $\mathrm{Fr}_0 = 5 \times 10^{-3}$, while the non-monotonic behaviour (similar to that of $\triangle T$) is seen in the profiles of first and second normal stress differences at $\mathrm{Fr}_0 = 10^{-3}$. The results presented in Figs. 4.9, 4.11 and 4.13 can be summarized as follows: there is a critical Froude number $\mathrm{Fr}_0^c \equiv \mathrm{Fr}_0(e_n)$ above and below which the excess temperature $\triangle T$, the first normal stress difference $\mathcal{N}_1$ and the second normal stress difference $\mathcal{N}_2$ vary non-monotonically and monotonically, respectively, with restitution coefficient.

4.7.2 Discussion: Comparison with Simulation

Here we discuss the present theoretical predictions in light with recent DSMC (direct simulation Monte Carlo) simulations of gravity-driven Poiseuille flow (Gupta & Alam (2017)); the schematic of the channel is depicted in Fig. 1.5 of Chapter 1. All simulations have been carried out in a channel of dimensionless width $W/\sigma = 1860$ (σ is the particle diameter). The average Knudsen number, defined as

$$\mathrm{Kn} = \frac{\lambda_{av}}{W} = \frac{(\sqrt{2}\pi n_{av}^*)^{-1}}{(W/\sigma)} \in (0.05, 10), \tag{4.116}$$

has been varied by varying the reduced density $n_{av}^* = n_{av}\sigma^3 \in (10^{-2}, 10^{-6})$; for example, the mean-free path is $\lambda_{av} = 186\sigma$ at a reduced density of $n_{av}^* = 1.21 \times 10^{-2}$. There is another dimensionless parameter to characterize the body force defined via

$$\widehat{g} = \frac{gW}{\frac{2k_B T_w}{m}} \tag{4.117}$$

where T_w is the wall-temperature (which is fixed at 1 for thermal-walls), m is the mass of a particle and k_B is the Boltzmann constant (set to unity in simulations).

Before making comparisons of theoretical results with simulation, let us first identify the parameter regime for which the DSMC simulation data exists currently. In the present analysis, we have a single control parameter $\mathrm{Fr}_0 = g\lambda_0/c_0^2$ (the Froude number defined at the channel centerline $y = 0$ and c_0 is the corresponding thermal velocity) which can be tied to two simulation control parameters via following relation:

$$\widehat{g} = \frac{g\lambda_0}{c_0^2}\frac{W}{\lambda_0}\frac{T_0}{T_w} \equiv \frac{\mathrm{Fr}_0}{\mathrm{Kn}_0}\left(\frac{T_0}{T_w}\right) \quad \Rightarrow \quad \mathrm{Fr}_0 = \widehat{g}\mathrm{Kn}_0\left(\frac{T_w}{T_0}\right). \tag{4.118}$$

Typically, for molecular gases ($e_n = 1$), $T_0 > T_w$ which can differ by a factor two or more at $\mathrm{Kn} \gg 1$; in contrast, $T_0 < T_w$ for a granular gas ($e_n < 1$); note further that the centerline Knudsen number Kn_0 can also differ significantly from its average value Kn (Eq. (4.116)) as confirmed by Gupta & Alam (2017). Assuming that $T_w \approx T_0$ and $\mathrm{Kn}_0 \approx \mathrm{Kn}$ for a nearly elastic gas ($e_n \sim 1$), we have

$$\mathrm{Fr}_0 \approx \widehat{g}\mathrm{Kn}. \tag{4.119}$$

All reported simulations of Gupta & Alam (2017) correspond to $\widehat{g} = 0.5$ and higher since the DSMC simulation data was found to be noisy for $\widehat{g} < 0.5$ and $\mathrm{Kn} < 0.01$ (this is a well-known

problem of DSMC method; people have suggested certain variance reduction methods to improve data quality at small Kn, see, for example, Baker and Hadjiconstantinou (2005)). Therefore, the DSMC data of Gupta & Alam (2017) correspond to

$$\mathrm{Fr}_0 \in (5 \times 10^{-3}, 5).$$

This range of Fr_0 should be contrasted with the convergence issues that we have encountered (see Section 3.6 in Chapter 3) for our asymptotic series solution; recall that our Padé-approximated solution holds for $\mathrm{Fr}_0 \leq 0.01$ – therefore, a quantitative comparison of our series solution with DSMC simulation of Gupta & Alam (2017) would not be fair. In the following we restrict to a qualitative comparison between theory and simulation.

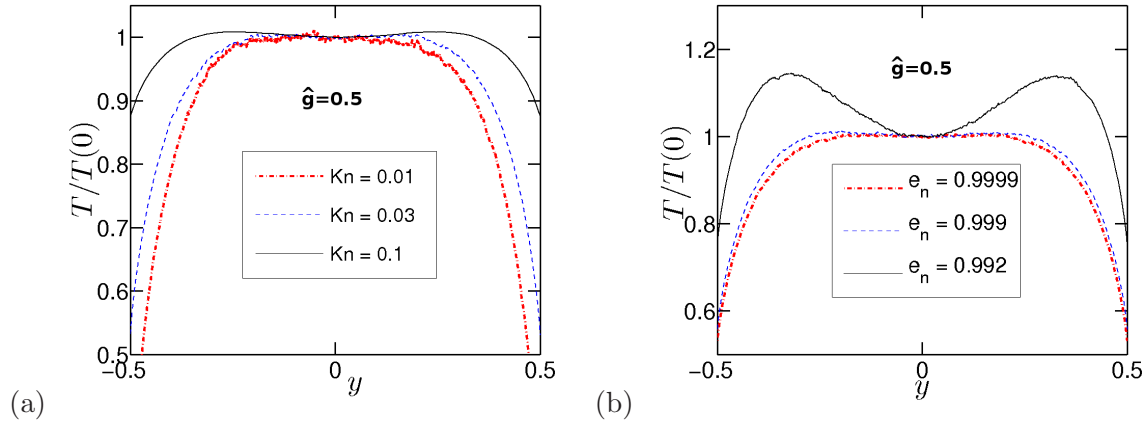

Figure 4.16: Temperature profiles from DSMC simulation of gravity-driven Poiseuille flow (Gupta & Alam 2017): (a) $e_n = 0.9999$ for different Knudsen number $\mathrm{Kn} = \lambda/W$ and (b) $\mathrm{Kn} = 0.03$ for different restitution coefficients. "Unimodal-to-bimodal" transitions in panels (a) and (b) are driven by "rarefaction" and "inelasticity", respectively.

Typical temperature profiles obtained from DSMC simulations are shown in Fig. 4.16 for a dimensionless acceleration of $\widehat{g} = 0.5$ (which is equivalent to a centerline Froude number of $\mathrm{Fr}_0 \approx 0.015$ at $\mathrm{Kn} = 0.03$). The observed "unimodal-to-bimodal" transitions in panels a and b are driven by "rarefaction" and "inelasticity", respectively. Therefore, the temperature bimodality can be driven by both (i) rarefaction (Tij and Santos 1994) and (ii) inelasticity (Alam *et al.* (2015); Gupta & Alam (2017)). The above transition is further clarified in Figs. 4.17(a) and 4.17(b) which display the variations of the excess temperature $[\Delta T = (T_{\max}/T_0 - 1)]$ with Kn and e_n, respectively. The continual increase of ΔT with decreasing e_n holds even at higher values of $\widehat{g}$ (i.e. at larger Fr_0), see Figs. 4.17(c). Our theoretical predictions (Figs. 4.6 and 4.8) suggest that ΔT increases with decreasing e_n for $\mathrm{Fr}_0 > \mathrm{Fr}_0^c \approx 3.8 \times 10^{-3}$, but decreases for $\mathrm{Fr}_0 < \mathrm{Fr}_0^c$. The latter non-monotonic variation (Fig. 4.8) remains unverified since we do not have simulation data at such small values of Fr_0.

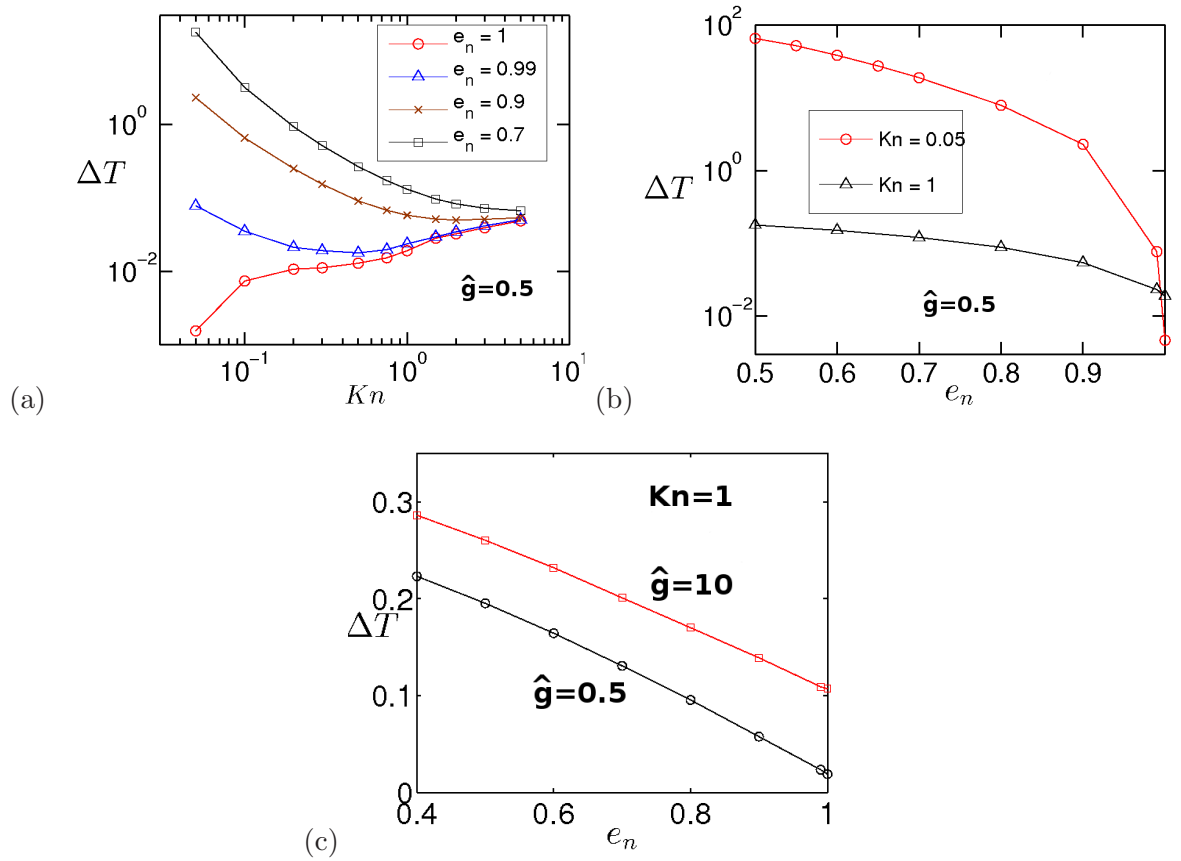

Figure 4.17: DSMC simulation results for the variation of excess temperature ΔT with (a) Kn for different e_n, (b) e_n for different Kn and (c) e_n for different $\widehat{g}$. See text for other details.

Next we consider the simulation results for first normal-stress difference, $\mathcal{N}_1 = (P_{xx} - P_{yy})/p$, see Fig. 4.18. Figs. 4.18(a) and 4.18(b) show the transverse profiles of $\mathcal{N}_1(y)$ at Knudsen numbers of Kn = 0.05 and 1, respectively; the gravitational acceleration is $\widehat{g} = 0.5$ (i.e. the centerline Froude number Fr_0 is 0.025 and 0.5 in panels a and b, respectively) – the simulation profiles look qualitatively similar to theoretical predictions in Fig. 4.9. The centerline value of first normal stress difference $\mathcal{N}_1(0)$ increases with increasing Kn (see panels c and d for $\widehat{g} = 0.5$ and 10, respectively) as well as with increasing dissipation (compare different symbols at Kn > 0.1). These results are found to be similar to our predictions in Fig. 4.10(b,c), but the non-monotonic variation of $\mathcal{N}_1(0)$ with e_n (Fig. 4.10(a) at very small values of Fr_0) remains unverified from simulation perspective.

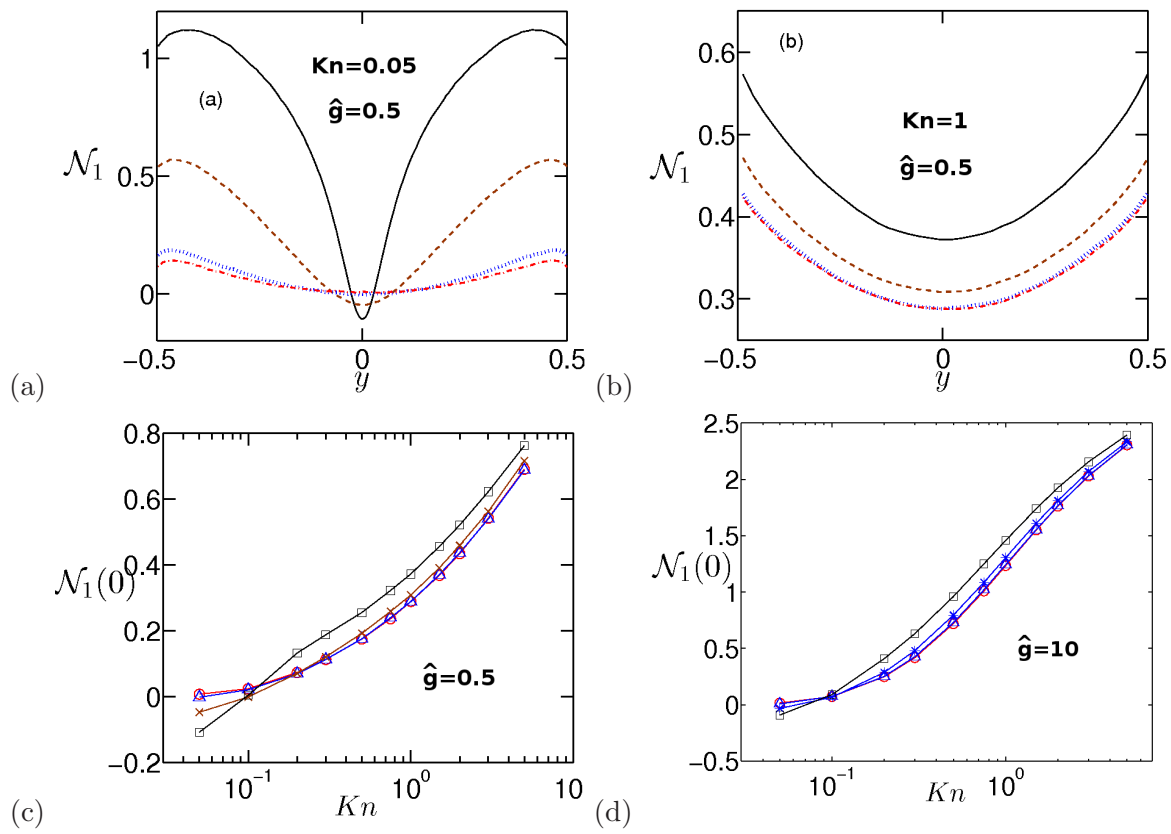

Figure 4.18: (a,b) Simulation profiles of the first normal stress difference: the black solid, red-dashed, blue-dotted and magenta dot-dashed lines correspond to restitution coefficients of $e_n = 0.7$, 0.9, 0.99 and 0.9, respectively. (c,d) Effect of gravitational strength $\widehat{g}$ on the centerline value of $\mathcal{N}_1(0)$ for different values of restitution coefficient [$e_n = 1$ (circles), $e_n = 0.99$ (triangles), $e_n = 0.99$ (crosses), and $e_n = 0.7$ (squares)].

From the above discussed simulation results, we find that both the temperature bimodality ΔT and the centreline first normal-stress difference $\mathcal{N}_1(0)$ increase with decreasing e_n at all studied values of gravitational strength $\widehat{g}$ (or, Fr_0), however, there exist no data for very small values of Fr_0 (for reasons mentioned above) at which the present theoretical predictions suggest a decreasing trend of both quantities with decreasing e_n.

The theoretical results (at small $\mathrm{Fr}_0 < \mathrm{Fr}_0^c$) can be reconciled if we analyse the differences between theoretical and simulation setup. It must be noted that there is no bulk-heating (via stochastic white-noise) source in the gravity-driven Poiseuille flows studied via (i) DSMC simulations (Gupta & Alam (2017)) and (ii) MD simulations (Alam *et al.* (2015)). The stochastic term in our theoretical analysis has been added for the convenience of generating a spatially "homogeneous/uniform" state (in which the collisional cooling is compensated via this bulk-heating mechanism) and the gravitational acceleration is then added as a small perturbation to further analyse the dynamics of the acceleration-driven Poiseuille flow of a "heated" granular gas. It is conceivable that for such a "heated" granular gas (with bulk heating via white-noise) there is indeed a threshold value for Froude number below which the "bulk-heating" via noise would dominate over gravitational acceleration, leading to different results for the variations of ΔT (and other quantities) compared to what is measured in simulations (Gupta & Alam (2017)) for a "purely" gravity-driven granular Poiseuille flow. On the other hand, at large enough val-

ues of $\widehat{g}$, or, Fr_0, the gravitational acceleration would dominate over stochastic heating and therefore the predicted results (at large $\mathrm{Fr}_0 > \mathrm{Fr}_0^c$) agree with both DSMC and MD results. Differences with theoretical predictions can also be reconciled if the simulations are carried out by incorporating the stochastic white-noise in gravity-driven granular Poiseuille flow.

Appendix 4A. Comparison of second- and fourth-order results with Padé approximation P[2,2]

Comparison of second- and fourth-order results with Padé approximation P[2,2] for $e_n = 1$

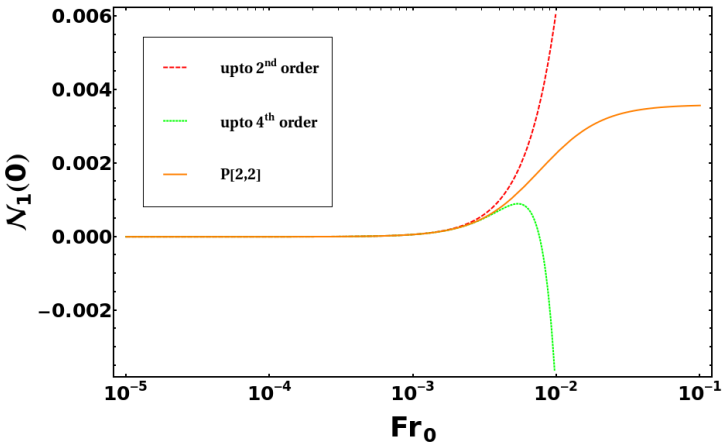

(a)

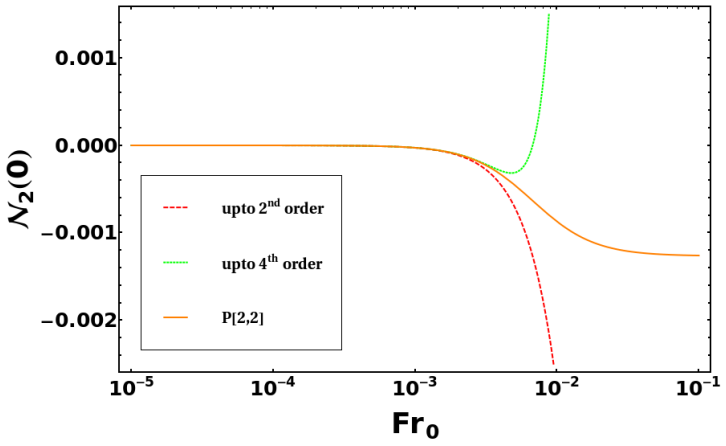

(b)

Figure 4.19: Comparison of second- and fourth-order results with Padé approximation P[2,2] for $e_n = 1$ (a) Variation of $\mathcal{N}_1(0)$ with Fr_0 and (b) Variation of $\mathcal{N}_2(0)$ with Fr_0.

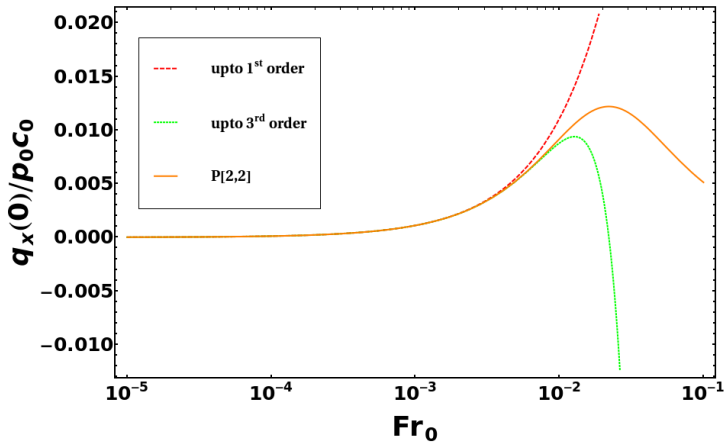

Figure 4.20: Variation of $q_x(0)/p_0c_0$ with Fr_0 for $e_n = 1$.

Comparison of second- and fourth-order results with Padé approximation P[2,2] for $e_n = 0.8$

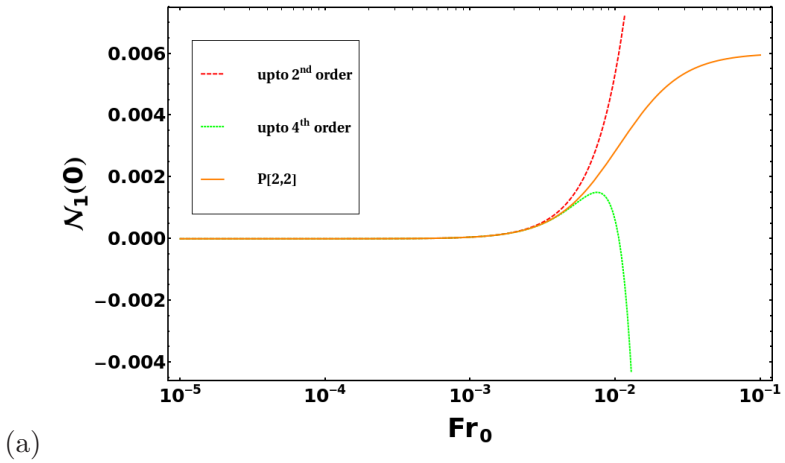

(a)

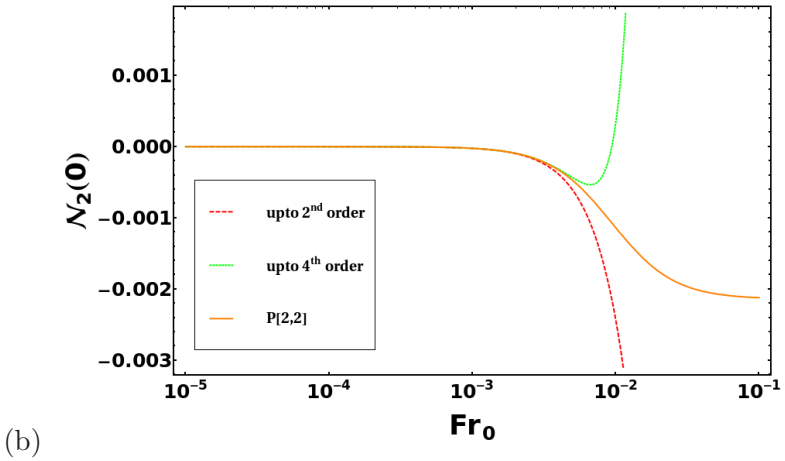

(b)

Figure 4.21: Comparison of second- and fourth-order results with Padé approximation P[2,2] for $e_n = 0.8$ (a) Variation of $\mathcal{N}_1(0)$ with Fr_0 and (b) Variation of $\mathcal{N}_2(0)$ with Fr_0.

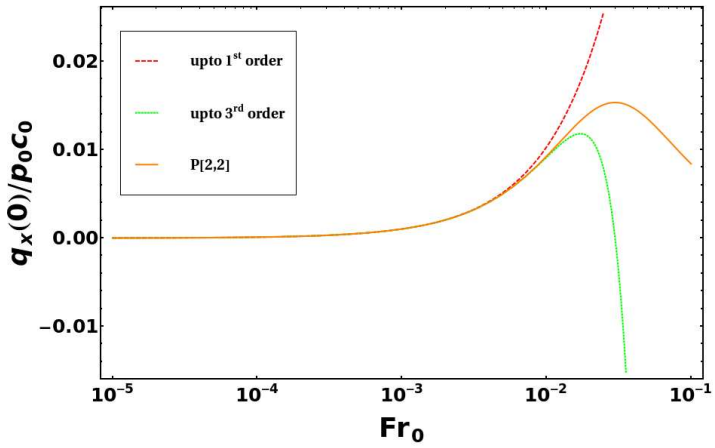

Figure 4.22: Variation of $q_x(0)/p_0c_0$ with Fr_0 for $e_n = 0.8$.

Chapter 5

Extended Hydrodynamic Equations for Binary Granular Mixtures via Grad's Method of Moments

5.1 Introduction

In reality, binary mixtures (A and B type particles) or polydisperse mixtures (having particles of different size and density) are confronted more often than a single gas. Due to different masses (m_A and m_B), diameters (σ_A and σ_B) and mean velocities ($\boldsymbol{u}_A$ and $\boldsymbol{u}_B$) of constituent particles, the state of a binary mixture consisting of two species can be described by two velocity distribution functions (one for each species), which are mastered by two Boltzmann equations. The Boltzmann collision operators for a binary mixture are mathematically more complicated than those for a simple (single) gas because the particles of a given constituent in a binary mixture collide with the particles of the same constituent as well as with those of other constituents.

It is commonly acknowledged that the description of a process in a gas through the infinite hierarchy of moment equations is equivalent to its description with the Boltzmann equation (Grad (1949*b*), Kogan (1969)). This chapter presents the derivation of moment equations for a binary granular mixture via Grad's moment method (Grad 1949*b*). As an application, the homogeneous cooling state (HCS) of a binary granular mixture is analysed in the end. The primary goal here is to derive a consistent set of "beyond-Navier-Stokes" hydrodynamic equations that can be used (with appropriate boundary conditions) to study "rarefied" flows such as those discussed in Chapters 3 and 4.

5.2 Boltzmann Equation for a Binary Mixture

5.2.1 Dynamics of Binary Collision

Consider a dilute mixture of two types (labelled A and B) of smooth inelastic hard spheres of masses m_A and m_B, and diameters σ_A and σ_B. The inelasticity of collisions among all pairs is characterized by three independent coefficients of normal restitution $e_{AA}, e_{AB} = e_{BA}$, and e_{BB}, where $e_{\alpha\beta}$ is the coefficient of normal restitution for collisions between particles of species $\alpha \in \{A, B\}$ and $\beta \in \{A, B\}$. The relation between pre- and post-collisional velocities due to a collision of a sphere of species α with a sphere of species β (Jenkins & Mancini (1987), Garzó & Dufty (2002), Serero *et al.* (2006), Kremer (2010)) is given by

$$\boldsymbol{c}'_\alpha = \boldsymbol{c}_\alpha - (1 + e_{\alpha\beta}) M^{\beta\alpha} (\boldsymbol{c}_{\alpha\beta} \cdot \hat{\boldsymbol{k}}) \hat{\boldsymbol{k}} \tag{5.1}$$

$$\boldsymbol{c}'_\beta = \boldsymbol{c}_\beta + (1+e_{\alpha\beta})M^{\alpha\beta}(\boldsymbol{c}_{\alpha\beta}\cdot\hat{\boldsymbol{k}})\hat{\boldsymbol{k}} \tag{5.2}$$

where $\{\boldsymbol{c}_\alpha, \boldsymbol{c}_\beta\}$ denote the precollisional velocities of the two colliding spheres, and $\{\boldsymbol{c}'_\alpha, \boldsymbol{c}'_\beta\}$ are the corresponding postcollisional velocities. $\hat{\boldsymbol{k}}$ is the unit contact vector between the centers of two colliding spheres,

$$M^{\alpha\beta} \equiv \frac{m_\alpha}{m_\alpha + m_\beta} \text{ and } \quad \boldsymbol{c}_{\alpha\beta} \equiv \boldsymbol{c}_\alpha - \boldsymbol{c}_\beta \tag{5.3}$$

is the precollisional relative velocity between two colliding spheres.

5.2.2 Boltzmann Equation

The basic kinetic equation is given by the Boltzmann equation. Actually, the description of a binary granular mixture consisting of two monatomic-inert-ideal gases in the phase space is provided by two velocity distribution functions of single gases in the mixture:

$$f_\alpha \equiv f_\alpha(\boldsymbol{x}, \boldsymbol{c}_\alpha, t) \quad \text{for} \quad \alpha = A, B. \tag{5.4}$$

Here, $\boldsymbol{x} \equiv (x,y,z)^T, \boldsymbol{c}_\alpha \equiv (c_x^{(\alpha)}, c_y^{(\alpha)}, c_z^{(\alpha)})^T$ and t denotes the position, instantaneous velocity of the species α and time, respectively. The velocity distribution function $f_\alpha(\boldsymbol{x}, \boldsymbol{c}_\alpha, t)$ is defined such that $f_\alpha(\boldsymbol{x}, \boldsymbol{c}_\alpha, t)d\boldsymbol{x}d\boldsymbol{c}_\alpha$ gives the number of particles of the species α at time t in a differential volume $d\boldsymbol{x}$ centred around the position $\boldsymbol{x}$ and differential volume $d\boldsymbol{c}_\alpha$ in velocity space located around $\boldsymbol{c}_\alpha$.

The two velocity distribution functions in a binary granular mixture are governed by two Boltzmann equations (Goldman & Sirovich (1967), Jenkins & Mancini (1987), Garzó & Dufty (2002), Serero *et al.* (2006))

$$\frac{\partial f_\alpha}{\partial t} + c_i^{(\alpha)}\frac{\partial f_\alpha}{\partial x_i} = \sum_{\beta=A,B} \mathfrak{B}_{\alpha\beta}(f_\alpha, f_\beta, e_{\alpha\beta}), \quad \alpha = A, B, \tag{5.5}$$

(or)

$$\frac{Df_\alpha}{Dt} + C_i^{(\alpha)}\frac{\partial f_\alpha}{\partial x_i} = \sum_{\beta=A,B} \mathfrak{B}_{\alpha\beta}(f_\alpha, f_\beta, e_{\alpha\beta}), \quad \alpha = A, B, \tag{5.6}$$

where the species Boltzmann collision operator is defined by:

$$\mathfrak{B}_{\alpha\beta}(f_\alpha, f_\beta, e_{\alpha\beta}) = \sigma_{\alpha\beta}^2 \int\int_{\boldsymbol{c}_{\alpha\beta}\cdot\hat{\boldsymbol{k}}>0} \left[\frac{f_\alpha(\boldsymbol{c}'_\alpha)f_\beta(\boldsymbol{c}'_\beta)}{e_{\alpha\beta}^2} - f_\alpha(\boldsymbol{c}_\alpha)f_\beta(\boldsymbol{c}_\beta)\right](\boldsymbol{c}_{\alpha\beta}\cdot\hat{\boldsymbol{k}})d\boldsymbol{c}_\beta d\hat{\boldsymbol{k}}. \tag{5.7}$$

In Eq. (5.7), $\sigma_{\alpha\beta} = \frac{\sigma_\alpha+\sigma_\beta}{2}$ and in Eq. (5.6), $\frac{D}{Dt} = \frac{\partial}{\partial t} + \boldsymbol{u}\cdot\boldsymbol{\nabla}$ is the material derivative, and the mixture velocity $\boldsymbol{u}$, and peculiar velocity $C_i^{(\alpha)}$ are defined in the next section.

5.3 Extended Hydrodynamic Fields and Moment Equations

In kinetic theory, for an arbitrary function $\Psi_\alpha \equiv \Psi_\alpha(\boldsymbol{x}, \boldsymbol{c}_\alpha, t)$, its average $\langle \Psi_\alpha \rangle$ is defined in terms of the velocity distribution function $f_\alpha(\boldsymbol{x}, \boldsymbol{c}_\alpha, t)$ as

$$n_\alpha \langle \Psi_\alpha \rangle = \int \Psi_\alpha f_\alpha(\boldsymbol{x}, \boldsymbol{c}_\alpha, t) d\boldsymbol{c}_\alpha. \tag{5.8}$$

The number density $n_\alpha(\boldsymbol{x}, t)$, mass density $\rho_\alpha(\boldsymbol{x}, t)$, macroscopic velocity $\boldsymbol{u}_\alpha(\boldsymbol{x}, t)$, granular temperature $T_\alpha(\boldsymbol{x}, t)$, stress tensor $\boldsymbol{\sigma}_\alpha(\boldsymbol{x}, t)$, heat flux vector $\boldsymbol{q}_\alpha(\boldsymbol{x}, t)$ and contracted fourth moment $p^{(\alpha)}_{iijj}(\boldsymbol{x}, t)$ of α-constituent are expressed in the form of moments on choosing Ψ_α as $\{1, m_\alpha, \boldsymbol{c}_\alpha, \frac{1}{2} m_\alpha C_\alpha^2, m_\alpha C^{(\alpha)}_{\langle i} C^{(\alpha)}_{j\rangle}, \frac{1}{2} m_\alpha C_\alpha^2 C_i^{(\alpha)}, m_\alpha C_\alpha^4\}$ in Eq. (5.8):

$$n_\alpha = \int f_\alpha d\boldsymbol{c}_\alpha, \tag{5.9}$$

$$\rho_\alpha = m_\alpha \int f_\alpha d\boldsymbol{c}_\alpha = m_\alpha n_\alpha, \tag{5.10}$$

$$n_\alpha \boldsymbol{u}_\alpha = \int \boldsymbol{c}_\alpha f_\alpha d\boldsymbol{c}_\alpha, \tag{5.11}$$

$$\frac{3}{2} n_\alpha T_\alpha = \frac{1}{2} m_\alpha \int C_\alpha^2 f_\alpha d\boldsymbol{c}_\alpha, \tag{5.12}$$

$$\sigma^{(\alpha)}_{ij} = m_\alpha \int C^{(\alpha)}_{\langle i} C^{(\alpha)}_{j\rangle} f_\alpha d\boldsymbol{c}_\alpha, \tag{5.13}$$

$$q_i^{(\alpha)} = \frac{1}{2} m_\alpha \int C_\alpha^2 C_i^{(\alpha)} f_\alpha d\boldsymbol{c}_\alpha, \tag{5.14}$$

$$p^{(\alpha)}_{iijj} = m_\alpha \int C_\alpha^4 f_\alpha d\boldsymbol{c}_\alpha, \tag{5.15}$$

where

$$\boldsymbol{C}_\alpha(\boldsymbol{x}, \boldsymbol{c}_\alpha, t) = \boldsymbol{c}_\alpha - \boldsymbol{u}(\boldsymbol{x}, t) \tag{5.16}$$

is the peculiar velocity of an α-species with respect to mixture velocity of the binary gas mixture and $\boldsymbol{u}(\boldsymbol{x}, t)$ is the mass-averaged mixture velocity (or, the barycentric velocity) of the binary gas mixture (defined below in Eq. (5.19)), and the angular brackets around the indices indicate the symmetric and trace-free tensor.

Denoting the total density, total pressure, total stress tensor, total heat flux and total contracted fourth moment for the binary mixture by $\rho, p, \boldsymbol{\sigma}, \boldsymbol{q}$ and p_{iijj}, respectively, and average

granular temperature for the binary mixture by T, we have

$$\begin{aligned}
\rho &= \sum_{\alpha=A}^{B} \rho_\alpha = \rho_A + \rho_B, \\
p &= nT = \sum_{\alpha=A}^{B} n_\alpha T_\alpha = n_A T_A + n_B T_B, \\
\sigma_{ij} &= \sum_{\alpha=A}^{B} \sigma_{ij}^{(\alpha)} = \sigma_{ij}^{(A)} + \sigma_{ij}^{(B)}, \\
q_i &= \sum_{\alpha=A}^{B} q_i^{(\alpha)} = q_i^{(A)} + q_i^{(B)}, \\
p_{iijj} &= \sum_{\alpha=A}^{B} p_{iijj}^{(\alpha)} = p_{iijj}^{(A)} + p_{iijj}^{(B)},
\end{aligned} \tag{5.17}$$

where

$$n = \sum_{\alpha=A}^{B} n_\alpha = n_A + n_B. \tag{5.18}$$

The mixture velocity (or the mass average velocity) $\boldsymbol{u}(\boldsymbol{x}, t)$ is defined as the ratio of total momentum density to total density

$$\boldsymbol{u}(\boldsymbol{x}, t) = \frac{1}{\rho} \sum_{\alpha=A}^{B} \rho_\alpha \boldsymbol{u}_\alpha = \frac{\rho_A \boldsymbol{u}_A + \rho_B \boldsymbol{u}_B}{\rho_A + \rho_B}. \tag{5.19}$$

In general, the mixture velocity $\boldsymbol{u}(\boldsymbol{x}, t)$ is different from the macroscopic velocity of each component $\boldsymbol{u}_\alpha$. In a binary gas mixture, this fact leads to a phenomenon called diffusion. The diffusion is described by the diffusion velocity of each component, which can be defined as the difference between macroscopic velocity of the component $\boldsymbol{u}_\alpha$ and mixture velocity $\boldsymbol{u}$. The diffusion velocity of the α-constituent is

$$\boldsymbol{v}_\alpha = \boldsymbol{u}_\alpha - \boldsymbol{u}. \tag{5.20}$$

Due to Eq. (5.19), the diffusion velocity $\boldsymbol{v}_\alpha$ satisfies the following condition

$$\sum_{\alpha=A}^{B} \rho_\alpha \boldsymbol{v}_\alpha = \rho_A \boldsymbol{v}_A + \rho_B \boldsymbol{v}_B = \boldsymbol{0}. \tag{5.21}$$

5.3.1 Moment Equations

To derive moment equations for the species α, we multiply the Boltzmann equation (5.5) by an arbitrary function Ψ_α and integrates over the velocity space, we get

$$\frac{\partial}{\partial t} \int \Psi_\alpha f_\alpha d\boldsymbol{c}_\alpha + \frac{\partial}{\partial x_k} \int \Psi_\alpha c_k^{(\alpha)} f_\alpha d\boldsymbol{c}_\alpha - \int \left(\frac{\partial \Psi_\alpha}{\partial t} + c_k^{(\alpha)} \frac{\partial \Psi_\alpha}{\partial x_k} \right) f_\alpha d\boldsymbol{c}_\alpha = \sum_{\beta=A,B} \int \Psi_\alpha \mathfrak{B}_{\alpha\beta} d\boldsymbol{c}_\alpha \tag{5.22}$$

(or)

$$\frac{D}{Dt}\int \Psi_\alpha f_\alpha d\boldsymbol{c}_\alpha + \frac{\partial u_k}{\partial x_k}\int \Psi_\alpha f_\alpha d\boldsymbol{c}_\alpha + \frac{\partial}{\partial x_k}\int \Psi_\alpha C_k^{(\alpha)} f_\alpha d\boldsymbol{c}_\alpha$$
$$-\int \left(\frac{D\Psi_\alpha}{Dt} + C_k^{(\alpha)}\frac{\partial \Psi_\alpha}{\partial x_k}\right) f_\alpha d\boldsymbol{c}_\alpha = \sum_{\beta=A,B}\int \Psi_\alpha \mathfrak{B}_{\alpha\beta} d\boldsymbol{c}_\alpha \tag{5.23}$$

The first 14-moment equations for the species α corresponding to 14 field variables $\{\rho_\alpha, u_i^{(\alpha)}, T_\alpha, \sigma_{ij}^{(\alpha)}, q_i^{(\alpha)}, p_{iijj}^{(\alpha)}\}$ are obtained by replacing Ψ_α in the transfer equation (5.22) with each element of $\Psi_\alpha = m_\alpha\{1, c_i^{(\alpha)}, C_\alpha^2, C_{\langle i}^{(\alpha)} C_{j\rangle}^{(\alpha)}, C_\alpha^2 C_i^{(\alpha)}, C_\alpha^4\}$.

The first 14 moment equations for the species α are

$$\frac{\partial \rho_\alpha}{\partial t} + \frac{\partial}{\partial x_k}(\rho_\alpha u_k^{(\alpha)}) = P_1^{(\alpha)}, \tag{5.24}$$

(or)

$$\frac{D\rho_\alpha}{Dt} + \rho_\alpha \frac{\partial u_k}{\partial x_k} + \frac{\partial}{\partial x_k}(\rho_\alpha v_k^{(\alpha)}) = P_1^{(\alpha)},$$
$$\frac{\partial}{\partial t}(\rho_\alpha u_i^{(\alpha)}) + \frac{\partial}{\partial x_k}(P_{ik}^{(\alpha)} + \rho_\alpha(u_i u_k^{(\alpha)} + u_k u_i^{(\alpha)} - u_i u_k)) = P_2^{(\alpha)}, \tag{5.25}$$

(or)

$$\frac{D(\rho_\alpha u_i^{(\alpha)})}{Dt} + \rho_\alpha u_i^{(\alpha)}\frac{\partial u_k}{\partial x_k} + \frac{\partial}{\partial x_k}(P_{ik}^{(\alpha)} + \rho_\alpha u_i v_k^{(\alpha)}) = P_2^{(\alpha)},$$
$$\frac{\partial}{\partial t}(3n_\alpha T_\alpha) + \frac{\partial}{\partial x_k}(2q_k^{(\alpha)} + 3u_k n_\alpha T_\alpha) + 2\frac{Du_i}{Dt}(\rho_\alpha u_i^{(\alpha)} - \rho_\alpha u_i) + 2\frac{\partial u_i}{\partial x_k}P_{ik}^{(\alpha)} = P_3^{(\alpha)}, \tag{5.26}$$

$$\frac{\partial}{\partial t}(\sigma_{ij}^{(\alpha)}) + \frac{\partial}{\partial x_k}(Q_{ijk}^{(\alpha)} + u_k P_{ij}^{(\alpha)} - \frac{1}{3}\delta_{ij}(2q_k^{(\alpha)} + 3u_k n_\alpha T_\alpha))$$
$$+\frac{Du_j}{Dt}(\rho_\alpha u_i^{(\alpha)} - \rho_\alpha u_i) + \frac{Du_i}{Dt}(\rho_\alpha u_j^{(\alpha)} - \rho_\alpha u_j) - \frac{2}{3}\delta_{ij}\frac{Du_m}{Dt}(\rho_\alpha u_m^{(\alpha)} - \rho_\alpha u_m)$$
$$+\frac{\partial u_i}{\partial x_k}P_{jk}^{(\alpha)} + \frac{\partial u_j}{\partial x_k}P_{ik}^{(\alpha)} - \frac{2}{3}\delta_{ij}\frac{\partial u_m}{\partial x_k}P_{km}^{(\alpha)} = P_4^{(\alpha)}, \tag{5.27}$$

$$\frac{\partial}{\partial t}(2q_i^{(\alpha)}) + \frac{\partial}{\partial x_k}(R_{rrik}^{(\alpha)} + 2u_k q_i^{(\alpha)}) + \frac{Du_i}{Dt}(3n_\alpha T_\alpha) + 2\frac{Du_m}{Dt}P_{im}^{(\alpha)}$$
$$+2\frac{\partial u_i}{\partial x_k}q_k^{(\alpha)} + 2\frac{\partial u_m}{\partial x_k}Q_{kim}^{(\alpha)} = P_5^{(\alpha)}, \tag{5.28}$$

$$\frac{\partial}{\partial t}(p_{iijj}^{(\alpha)}) + \frac{\partial}{\partial x_k}(p_{iijjk}^{(\alpha)} + u_k p_{iijj}^{(\alpha)}) + 8\frac{Du_i}{Dt}q_i^{(\alpha)} + 4\frac{\partial u_i}{\partial x_k}R_{rrik}^{(\alpha)} = P_6^{(\alpha)}, \tag{5.29}$$

where

$$P_{ij}^{(\alpha)} = m_\alpha \int f_\alpha C_i^{(\alpha)} C_j^{(\alpha)} d\boldsymbol{c}_\alpha \tag{5.30}$$

$$Q_{ijk}^{(\alpha)} = m_\alpha \int f_\alpha C_i^{(\alpha)} C_j^{(\alpha)} C_k^{(\alpha)} d\boldsymbol{c}_\alpha \tag{5.31}$$

$$R_{rrik}^{(\alpha)} = m_\alpha \int f_\alpha C_\alpha^2 C_i^{(\alpha)} C_k^{(\alpha)} d\boldsymbol{c}_\alpha \tag{5.32}$$

$$p^{(\alpha)}_{iijjk} = m_\alpha \int f_\alpha C^4_\alpha C^{(\alpha)}_k d\boldsymbol{c}_\alpha. \tag{5.33}$$

The integral expressions for production term $P^{(\alpha)}_i$ in Eqs. (5.24)-(5.29) can be obtained from the right-hand side of Eq. (5.22). The determination of $P^{(\alpha)}_i$ requires an expression for non-equilibrium distribution function which is considered in the next section.

5.3.2 Grad's Distribution Function for Species α

In order to determine Grad's distribution function for the species α, one can expand the distribution function f_α in series of the Hermite polynomials $H^{(\alpha)}_{i_1 i_2 \cdots i_N}(N = 0, 1, 2, \cdots)$ [Grad (1949*a*), Kremer (2010)]:

$$f_\alpha = f^{(\alpha)}_M \big(a^{(\alpha)} H^{(\alpha)} + a^{(\alpha)}_i H^{(\alpha)}_i + \frac{1}{2!} a^{(\alpha)}_{ij} H^{(\alpha)}_{ij} + \cdots + \frac{1}{N!} a^{(\alpha)}_{i_1 i_2 \cdots i_N} H^{(\alpha)}_{i_1 i_2 \cdots i_N} + \cdots \big), \tag{5.34}$$

where $a^{(\alpha)}_{i_1 i_2 \cdots i_N}(N = 0, 1, 2, \cdots)$ are coefficients that depend on $\boldsymbol{x}, t$ and

$$f^{(\alpha)}_M = n_\alpha \big(\frac{\beta_\alpha}{\pi}\big)^{3/2} \exp\left(-\beta_\alpha C^2_\alpha\right) = n_\alpha \big(\frac{m_\alpha}{T_\alpha}\big)^{3/2} \omega(\boldsymbol{\xi}^{(\alpha)}), \tag{5.35}$$

where

$$\beta_\alpha = \frac{m_\alpha}{2T_\alpha} \tag{5.36}$$

and the weight function $\omega(\boldsymbol{\xi}^{(\alpha)})$ is

$$\omega(\boldsymbol{\xi}^{(\alpha)}) = \frac{1}{(2\pi)^{3/2}} \exp\big(-\frac{{\xi^{(\alpha)}}^2}{2}\big), \quad \text{with} \quad \xi^{(\alpha)}_i = \sqrt{\frac{m_\alpha}{T_\alpha}} C^{(\alpha)}_i. \tag{5.37}$$

The Hermite polynomials are defined in terms of weight function (Grad (1949*b*)),

$$H^{(\alpha)}_{i_1 i_2 \cdots i_N}(\boldsymbol{\xi}^{(\alpha)}) = \frac{(-1)^N}{\omega(\boldsymbol{\xi}^{(\alpha)})} \frac{\partial^N \omega(\boldsymbol{\xi}^{(\alpha)})}{\partial \xi^{(\alpha)}_{i_1} \partial \xi^{(\alpha)}_{i_2} \cdots \partial \xi^{(\alpha)}_{i_N}}, \tag{5.38}$$

and they satisfy the following orthogonality condition

$$\int \omega(\boldsymbol{\xi}^{(\alpha)}) H^{(\alpha)}_{i_1 i_2 \cdots i_N}(\boldsymbol{\xi}^{(\alpha)}) H^{(\alpha)}_{j_1 j_2 \cdots j_M}(\boldsymbol{\xi}^{(\alpha)})\, d\boldsymbol{\xi}^{(\alpha)} = \delta_{MN} \Delta_{i_1 j_1 i_2 j_2 \cdots i_N j_N}, \tag{5.39}$$

where δ_{MN} is the Kronecker delta and

$$\Delta_{i_1 j_1 i_2 j_2 \cdots i_N j_N} = \delta_{i_1 j_1} \delta_{i_2 j_2} \cdots \delta_{i_N j_N} + (\text{all permutations of the } j\text{'s indices}). \tag{5.40}$$

From Eq. (5.38), we obtained the first five Hermite polynomials:

$$H^{(\alpha)}(\boldsymbol{\xi}^{(\alpha)}) = 1, \quad H^{(\alpha)}_i(\boldsymbol{\xi}^{(\alpha)}) = \xi^{(\alpha)}_i, \quad H^{(\alpha)}_{ij}(\boldsymbol{\xi}^{(\alpha)}) = \xi^{(\alpha)}_i \xi^{(\alpha)}_j - \delta_{ij}, \tag{5.41}$$

$$H^{(\alpha)}_{ijk}(\boldsymbol{\xi}^{(\alpha)}) = \xi^{(\alpha)}_i \xi^{(\alpha)}_j \xi^{(\alpha)}_k - (\xi^{(\alpha)}_i \delta_{jk} + \xi^{(\alpha)}_j \delta_{ik} + \xi^{(\alpha)}_k \delta_{ij}), \tag{5.42}$$

$$H^{(\alpha)}_{ijkl}(\boldsymbol{\xi}^{(\alpha)}) = \xi^{(\alpha)}_i\xi^{(\alpha)}_j\xi^{(\alpha)}_k\xi^{(\alpha)}_l - (\xi^{(\alpha)}_i\xi^{(\alpha)}_j\delta_{kl} + \xi^{(\alpha)}_i\xi^{(\alpha)}_k\delta_{jl} + \xi^{(\alpha)}_i\xi^{(\alpha)}_l\delta_{jk} + \xi^{(\alpha)}_j\xi^{(\alpha)}_k\delta_{il} + \xi^{(\alpha)}_j\xi^{(\alpha)}_l\delta_{ik} + \xi^{(\alpha)}_k\xi^{(\alpha)}_l\delta_{ij}) + (\delta_{ij}\delta_{kl} + \delta_{ik}\delta_{jl} + \delta_{il}\delta_{jk}). \quad (5.43)$$

The basic hydrodynamic fields of this 14-moment theory are the following 2×14 scalar fields:

$$\int f_\alpha d\boldsymbol{c}_\alpha = n_\alpha, \quad (5.44)$$

$$\int f_\alpha c^{(\alpha)}_i d\boldsymbol{c}_\alpha = n_\alpha u^{(\alpha)}_i, \quad (5.45)$$

$$\int f_\alpha m_\alpha C^2_\alpha d\boldsymbol{c}_\alpha = 3n_\alpha T_\alpha, \quad (5.46)$$

$$\int f_\alpha m_\alpha C^{(\alpha)}_{\langle i} C^{(\alpha)}_{j\rangle} d\boldsymbol{c}_\alpha = \sigma^{(\alpha)}_{ij}, \quad (5.47)$$

$$\int f_\alpha \frac{m_\alpha}{2} C^2_\alpha C^{(\alpha)}_i d\boldsymbol{c}_\alpha = q^{(\alpha)}_i, \quad (5.48)$$

$$\int f_\alpha m_\alpha C^4_\alpha d\boldsymbol{c}_\alpha = p^{(\alpha)}_{iijj}. \quad (5.49)$$

The above moments of the distribution function can be written in terms of Hermite polynomials as

$$n_\alpha = \int f_\alpha \left(\frac{T_\alpha}{m_\alpha}\right)^{\frac{3}{2}} H^{(\alpha)} d\boldsymbol{\xi}^{(\alpha)}, \quad (5.50)$$

$$n_\alpha(u^{(\alpha)}_i - u_i) = \int f_\alpha \left(\frac{T_\alpha}{m_\alpha}\right)^{2} H^{(\alpha)}_i d\boldsymbol{\xi}^{(\alpha)}, \quad (5.51)$$

$$3n_\alpha T_\alpha = \int f_\alpha m_\alpha \left(\frac{T_\alpha}{m_\alpha}\right)^{\frac{5}{2}} (H^{(\alpha)}_{ii} + 3H^{(\alpha)}) d\boldsymbol{\xi}^{(\alpha)}, \quad (5.52)$$

$$\sigma^{(\alpha)}_{ij} = \int f_\alpha m_\alpha \left(\frac{T_\alpha}{m_\alpha}\right)^{\frac{5}{2}} (H^{(\alpha)}_{ij} - \frac{H^{(\alpha)}_{rr}}{3}\delta_{ij}) d\boldsymbol{\xi}^{(\alpha)}, \quad (5.53)$$

$$2q^{(\alpha)}_i = \int f_\alpha m_\alpha \left(\frac{T_\alpha}{m_\alpha}\right)^{3} (H^{(\alpha)}_{ijj} + 5H^{(\alpha)}_i) d\boldsymbol{\xi}^{(\alpha)}, \quad (5.54)$$

$$p^{(\alpha)}_{iijj} = \int f_\alpha m_\alpha \left(\frac{T_\alpha}{m_\alpha}\right)^{\frac{7}{2}} (H^{(\alpha)}_{iijj} + 7H^{(\alpha)}_{ii} + 3H^{(\alpha)}_{jj} + 15H^{(\alpha)}) d\boldsymbol{\xi}^{(\alpha)}. \quad (5.55)$$

The coefficients $a^{(\alpha)}_{i_1 i_2 \cdots i_N}$ in Eq. (5.34) can be determined from the definition of the moments of the distribution function. For 2×14 moment theory, the distribution function (5.34) is written as

$$f_\alpha = f^{(\alpha)}_M \big(a^{(\alpha)} H^{(\alpha)} + a^{(\alpha)}_i H^{(\alpha)}_i + \frac{1}{2} a^{(\alpha)}_{ij} H^{(\alpha)}_{ij} + \frac{1}{10} a^{(\alpha)}_{rri} H^{(\alpha)}_{ssi} + \frac{1}{120} a^{(\alpha)}_{mmnn} H^{(\alpha)}_{rrss}\big), \quad (5.56)$$

where $a^{(\alpha)}, a^{(\alpha)}_i, a^{(\alpha)}_{ij}, a^{(\alpha)}_{rri}$ and $a^{(\alpha)}_{mmnn}$ are the coefficients to be determined.

Substitute the distribution function (5.56) into the definitions of the moments of the distribution function (5.50)-(5.55) and by using the orthogonality condition (5.39), we get the

coefficients

$$a^{(\alpha)}=1,\quad a_i^{(\alpha)}=\frac{(u_i^{(\alpha)}-u_i)}{\left(\frac{T_\alpha}{m_\alpha}\right)^{\frac{1}{2}}},\quad a_{rr}^{(\alpha)}=0,\quad a_{\langle ij\rangle}^{(\alpha)}=\frac{2\beta_\alpha}{\rho_\alpha}\sigma_{ij}^{(\alpha)}, \tag{5.57}$$

$$a_{rri}^{(\alpha)}=\frac{2q_i^{(\alpha)}}{\rho_\alpha\left(\frac{T_\alpha}{m_\alpha}\right)^{\frac{3}{2}}}-5\frac{(u_i^{(\alpha)}-u_i)}{\left(\frac{T_\alpha}{m_\alpha}\right)^{\frac{1}{2}}}, \tag{5.58}$$

$$a_{mmnn}^{(\alpha)}=\frac{p_{mmnn}^{(\alpha)}}{\rho_\alpha\left(\frac{T_\alpha}{m_\alpha}\right)^2}-15. \tag{5.59}$$

Now substituting the coefficients (5.57)-(5.59) and Hermite polynomials (5.41)-(5.43) in Eq. (5.56), we get Grad's distribution function

$$\begin{aligned} f_\alpha &= f_M^{(\alpha)}\Bigg[1+2\beta_\alpha(u_i^{(\alpha)}-u_i)C_i^{(\alpha)}\left(\frac{7}{2}-\beta_\alpha C_\alpha^2\right)+\frac{2\beta_\alpha^2}{\rho_\alpha}\sigma_{ij}^{(\alpha)}C_i^{(\alpha)}C_j^{(\alpha)} \\ &\quad+\frac{8}{5}\frac{\beta_\alpha^2}{\rho_\alpha}q_i^{(\alpha)}C_i^{(\alpha)}\left(\beta_\alpha C_\alpha^2-\frac{5}{2}\right)+\Delta_\alpha\left(\frac{\beta_\alpha^2C_\alpha^4}{2}-\frac{5\beta_\alpha C_\alpha^2}{2}+\frac{15}{8}\right)\Bigg], \end{aligned} \tag{5.60}$$

where

$$\Delta_\alpha=\frac{p_{iijj}^{(\alpha)}-p_{iijj}^{M(\alpha)}}{p_{iijj}^{M(\alpha)}} \tag{5.61}$$

is the dimensionless non-equilibrium part of the contracted fourth-order moment and

$$p_{iijj}^{M(\alpha)}=m_\alpha\int C_\alpha^4 f_M^{(\alpha)}d\boldsymbol{c}_\alpha=\rho_\alpha\left(\frac{15}{4\beta_\alpha^2}\right) \tag{5.62}$$

being the contracted fourth-order moment evaluated for a Maxwellian distribution function.

5.3.3 Production Terms in 2 × G14 System

Using Grad's distribution function (5.60), we can determine the full linear and non-linear production terms $P_i^{(\alpha)}$ (that appear on the right-hand side of Eqs. (5.24)-(5.29)). Here, we restrict ourselves to the linear production terms for the sake of simplicity. They are given by:

$$P_1^{(\alpha)}=0, \tag{5.63}$$

$$\begin{aligned} P_2^{(\alpha)} &= \sum_{\beta=A}^{B}\Bigg[\frac{4\sqrt{2\pi}\,(1+e_{\alpha\beta})\,T_\alpha\sqrt{\frac{m_\alpha}{T_\alpha}+\frac{m_\beta}{T_\beta}}\sqrt{\frac{m_\alpha m_\beta}{T_\alpha T_\beta}}T_\beta\sigma_{\alpha\beta}^2}{15\,(m_\alpha+m_\beta)\,(m_\beta T_\alpha+m_\alpha T_\beta)}(\rho_\alpha q_i^{(\beta)}-\rho_\beta q_i^{(\alpha)}) \\ &\quad-\frac{2\sqrt{2\pi}\,(1+e_{\alpha\beta})\,n_\alpha n_\beta T_\alpha\sqrt{\frac{m_\alpha}{T_\alpha}+\frac{m_\beta}{T_\beta}}\sqrt{\frac{m_\alpha m_\beta}{T_\alpha T_\beta}}T_\beta\sigma_{\alpha\beta}^2}{3\,(m_\alpha+m_\beta)\,(m_\beta T_\alpha+m_\alpha T_\beta)}\Bigg((m_\beta T_\alpha+m_\alpha T_\beta)(u_i^{(\alpha)}-u_i^{(\beta)}) \\ &\quad+(m_\alpha T_\beta(u_i^{(\alpha)}-u_i)-m_\beta T_\alpha(u_i^{(\beta)}-u_i))\Bigg)\Bigg], \end{aligned} \tag{5.64}$$

$$
\begin{aligned}
P_3^{(\alpha)} &= \sum_{\beta=A}^{B} \frac{\sqrt{\frac{\pi}{2}} m_\beta n_\alpha n_\beta \sqrt{\frac{m_\alpha}{T_\alpha}+\frac{m_\beta}{T_\beta}}\,(1+e_{\alpha\beta})\,\sigma_{\alpha\beta}^2}{(m_\alpha+m_\beta)^2\sqrt{\frac{m_\alpha m_\beta}{T_\alpha T_\beta}}\,(m_\beta T_\alpha+m_\alpha T_\beta)^2}\Big((8+3\Delta_\alpha)m_\beta^3 T_\alpha^3\,(-1+e_{\alpha\beta}) \\
&\quad +m_\alpha^3 T_\beta^2(2(-8+\Delta_\beta)T_\alpha+(8+3\Delta_\beta)T_\beta\,(1+e_{\alpha\beta})) \\
&\quad -m_\alpha m_\beta^2 T_\alpha^2\,(2(8+3\Delta_\alpha)T_\alpha+T_\beta\,(8+5\Delta_\alpha-3(8+\Delta_\alpha)e_{\alpha\beta})) \\
&\quad +m_\alpha^2 m_\beta T_\alpha T_\beta\,(-8(4+\Delta_\alpha)T_\alpha+T_\beta\,(8+5\Delta_\beta+3(8+\Delta_\beta)e_{\alpha\beta}))\Big), \qquad (5.65)
\end{aligned}
$$

$$
\begin{aligned}
P_4^{(\alpha)} &= \sum_{\beta=A}^{B} \frac{\sqrt{\frac{\pi}{2}} m_\beta \sqrt{\frac{m_\alpha}{T_\alpha}+\frac{m_\beta}{T_\beta}}\,(1+e_{\alpha\beta})\,\sigma_{\alpha\beta}^2}{15\,(m_\alpha+m_\beta)^2\sqrt{\frac{m_\alpha m_\beta}{T_\alpha T_\beta}}\,(m_\beta T_\alpha+m_\alpha T_\beta)^2}\Big[\Big(-80m_\alpha^3 n_\beta T_\beta^2-16m_\alpha m_\beta^2 n_\beta \\
&\quad \times T_\alpha(6T_\alpha+T_\beta\,(8-3e_{\alpha\beta}))+24m_\beta^3 n_\beta T_\alpha^2\,(-3+e_{\alpha\beta})+8m_\alpha^2 m_\beta n_\beta T_\beta(-22T_\alpha \\
&\quad +T_\beta\,(-7+3e_{\alpha\beta}))\Big)\sigma_{ij}^{(\alpha)}+\Big(8m_\alpha m_\beta^2 n_\alpha T_\alpha^2\,(1+3e_{\alpha\beta})+8m_\alpha^3 n_\alpha T_\beta(-2T_\alpha \\
&\quad +3T_\beta\,(1+e_{\alpha\beta}))-16m_\alpha^2 m_\beta n_\alpha T_\alpha\,(T_\alpha-T_\beta\,(2+3e_{\alpha\beta}))\Big)\sigma_{ij}^{(\beta)}\Big], \qquad (5.66)
\end{aligned}
$$

$$
\begin{aligned}
P_5^{(\alpha)} &= \sum_{\beta=A}^{B} \frac{2\sqrt{2\pi} m_\beta \sqrt{\frac{m_\alpha}{T_\alpha}+\frac{m_\beta}{T_\beta}}\,(1+e_{\alpha\beta})\,\sigma_{\alpha\beta}^2}{15\,(m_\alpha+m_\beta)^3\sqrt{\frac{m_\alpha m_\beta}{T_\alpha T_\beta}}\,(m_\beta T_\alpha+m_\alpha T_\beta)^2}\Big[\Big(-108m_\alpha^2 m_\beta^2 n_\beta T_\alpha^2 \\
&\quad -174m_\alpha^3 m_\beta n_\beta T_\alpha T_\beta-60m_\alpha^4 n_\beta T_\beta^2-6m_\alpha^3 m_\beta n_\beta T_\beta^2\,(9-11e_{\alpha\beta}) \\
&\quad +12m_\alpha m_\beta^3 n_\beta T_\alpha^2\,(-11+7e_{\alpha\beta})+6m_\alpha^2 m_\beta^2 n_\beta T_\alpha T_\beta\,(-33+25e_{\alpha\beta}) \\
&\quad -12m_\beta^4 n_\beta T_\alpha^2\,(4-3e_{\alpha\beta}+2e_{\alpha\beta}^2)-6m_\alpha^2 m_\beta^2 n_\beta T_\beta^2\,(3-3e_{\alpha\beta}+4e_{\alpha\beta}^2) \\
&\quad -6m_\alpha m_\beta^3 n_\beta T_\alpha T_\beta\,(12-9e_{\alpha\beta}+8e_{\alpha\beta}^2)\Big)q_i^{(\alpha)}+\Big(4m_\alpha^3 m_\beta n_\alpha T_\alpha^2+10m_\alpha^4 n_\alpha T_\alpha T_\beta \\
&\quad +24m_\alpha^3 m_\beta n_\alpha T_\beta^2\,(1+e_{\alpha\beta})^2-2m_\alpha^3 m_\beta n_\alpha T_\alpha T_\beta\,(-1+9e_{\alpha\beta}) \\
&\quad -2m_\alpha^2 m_\beta^2 n_\alpha T_\alpha^2\,(5+9e_{\alpha\beta})+2m_\alpha m_\beta^3 n_\alpha T_\alpha^2\,(5+15e_{\alpha\beta}+12e_{\alpha\beta}^2) \\
&\quad +2m_\alpha^2 m_\beta^2 n_\alpha T_\alpha T_\beta\,(20+39e_{\alpha\beta}+24e_{\alpha\beta}^2)\Big)q_i^{(\beta)} \\
&\quad +5n_\alpha n_\beta\Big(\Big(m_\alpha m_\beta^3 T_\alpha^2(T_\alpha(22-14e_{\alpha\beta})+3T_\beta(4-3e_{\alpha\beta}))+10m_\alpha^4 T_\beta^3(1+e_{\alpha\beta}) \\
&\quad +2m_\beta^4 T_\alpha^3(4-3e_{\alpha\beta}+2e_{\alpha\beta}^2)+3m_\alpha^2 m_\beta^2 T_\alpha(6T_\alpha^2+T_\alpha T_\beta(11-3e_{\alpha\beta}) \\
&\quad +T_\beta^2(1-3e_{\alpha\beta}-4e_{\alpha\beta}^2))+m_\alpha^3 m_\beta T_\beta(21T_\alpha^2+15T_\alpha T_\beta(1+e_{\alpha\beta}) \\
&\quad -2T_\beta^2(-1+3e_{\alpha\beta}+4e_{\alpha\beta}^2))\Big)(u_i^{(\alpha)}-u_i) \\
&\quad +\Big(5m_\alpha^4 T_\alpha T_\beta^2+2m_\beta^4 T_\alpha^3(3-e_{\alpha\beta}+4e_{\alpha\beta}^2)+m_\alpha^3 m_\beta T_\beta(24T_\alpha^2+T_\alpha T_\beta(1-9e_{\alpha\beta}) \\
&\quad -4T_\beta^2(1+e_{\alpha\beta})^2)+m_\alpha^2 m_\beta^2 T_\alpha(16T_\alpha^2-3T_\alpha T_\beta(-7+9e_{\alpha\beta})-T_\beta^2(4+9e_{\alpha\beta})) \\
&\quad +m_\alpha m_\beta^3 T_\alpha^2(-2T_\alpha(-7+9e_{\alpha\beta})+3T_\beta(3-e_{\alpha\beta}+4e_{\alpha\beta}^2))\Big)(u_i^{(\beta)}-u_i)\Big)\Big], \qquad (5.67)
\end{aligned}
$$

$$
\begin{aligned}
P_6^{(\alpha)} \;=\; & \sum_{\beta=A}^{B} \frac{-\sqrt{2\pi} n_\alpha n_\beta \sqrt{\frac{m_\alpha m_\beta}{T_\alpha T_\beta}}\,(1+e_{\alpha\beta})\,\sigma_{\alpha\beta}^2}{m_\alpha^2\,(m_\alpha+m_\beta)^{\,4}\sqrt{\frac{m_\alpha}{T_\alpha}+\frac{m_\beta}{T_\beta}}\,(m_\beta T_\alpha + m_\alpha T_\beta)^{\,2}}\Big(-2(8+15\Delta_\alpha) m_\beta^6 T_\alpha^5 \\
& \times\left(-2+2e_{\alpha\beta}-e_{\alpha\beta}^2+e_{\alpha\beta}^3\right)+5m_\alpha^6 T_\alpha T_\beta^3(2(8+8\Delta_\alpha-\Delta_\beta)T_\alpha \\
& -(8+3\Delta_\beta)T_\beta\,(1+e_{\alpha\beta}))-m_\alpha^5 m_\beta T_\beta^2(-4(64+92\Delta_\alpha-\Delta_\beta)T_\alpha^3 \\
& +2(8+15\Delta_\beta)T_\beta^3\,(1+e_{\alpha\beta})^{\,3}+T_\alpha^2 T_\beta(-8-108\Delta_\alpha+51\Delta_\beta \\
& +(232+132\Delta_\alpha+21\Delta_\beta)e_{\alpha\beta})-2(8+3\Delta_\beta)T_\alpha T_\beta^2\left(-1+3e_{\alpha\beta}+4e_{\alpha\beta}^2\right)) \\
& +m_\alpha^4 m_\beta^2 T_\alpha T_\beta((272+462\Delta_\alpha)T_\alpha^3-3T_\alpha^2 T_\beta(-104-207\Delta_\alpha+6\Delta_\beta \\
& +(161\Delta_\alpha+2(76+\Delta_\beta))e_{\alpha\beta})+2T_\alpha T_\beta^2(4(4+9\Delta_\alpha-3\Delta_\beta) \\
& +(24-36\Delta_\alpha+27\Delta_\beta)e_{\alpha\beta}+8(16+6\Delta_\alpha+3\Delta_\beta)e_{\alpha\beta}^2) \\
& -T_\beta^3\,(1+e_{\alpha\beta})\,(56+81\Delta_\beta+12(8+13\Delta_\beta)e_{\alpha\beta}+10(8+9\Delta_\beta)e_{\alpha\beta}^2)) \\
& +m_\alpha m_\beta^5 T_\alpha^4(4(8+15\Delta_\alpha)T_\alpha(4-3e_{\alpha\beta}+2e_{\alpha\beta}^2)+T_\beta(72+147\Delta_\alpha \\
& -(104+159\Delta_\alpha)e_{\alpha\beta}+2(8+33\Delta_\alpha)e_{\alpha\beta}^2-10(8+9\Delta_\alpha)e_{\alpha\beta}^3)) \\
& -m_\alpha^2 m_\beta^4 T_\alpha^3(2(8+15\Delta_\alpha)T_\alpha^2\,(-11+7e_{\alpha\beta})-2T_\alpha T_\beta(20(8+15\Delta_\alpha) \\
& -15(8+15\Delta_\alpha)e_{\alpha\beta}+8(16+21\Delta_\alpha)e_{\alpha\beta}^2)+T_\beta^2(-24-107\Delta_\alpha+16\Delta_\beta \\
& +3(56+43\Delta_\alpha+16\Delta_\beta)e_{\alpha\beta}+(96-42\Delta_\alpha+66\Delta_\beta)e_{\alpha\beta}^2 \\
& +10(16+9\Delta_\alpha+3\Delta_\beta)e_{\alpha\beta}^3))+m_\alpha^3 m_\beta^3 T_\alpha^2(12(8+15\Delta_\alpha)T_\alpha^3 \\
& +T_\alpha^2 T_\beta(55(8+15\Delta_\alpha)-(376+561\Delta_\alpha)e_{\alpha\beta})+6T_\alpha T_\beta^2(40+75\Delta_\alpha \\
& -3(8+19\Delta_\alpha-2\Delta_\beta)e_{\alpha\beta}+4(16+13\Delta_\alpha+\Delta_\beta)e_{\alpha\beta}^2) \\
& -T_\beta^3(56-14\Delta_\alpha+73\Delta_\beta+5(40+6\Delta_\alpha+39\Delta_\beta)e_{\alpha\beta} \\
& +(224-6\Delta_\alpha+222\Delta_\beta)e_{\alpha\beta}^2+10(16+3\Delta_\alpha+9\Delta_\beta)e_{\alpha\beta}^3))\Big). \qquad (5.68)
\end{aligned}
$$

In other words,

$$
\begin{aligned}
P_6^{(\alpha)} \;=\; & \sum_{\beta=A}^{B} \frac{-\sqrt{2\pi} n_\alpha n_\beta \sqrt{\frac{m_\alpha m_\beta}{T_\alpha T_\beta}} \left(1+e_{\alpha\beta}\right) \sigma_{\alpha\beta}^2}{m_\alpha^2 \left(m_\alpha+m_\beta\right)^4 \sqrt{\frac{m_\alpha}{T_\alpha}+\frac{m_\beta}{T_\beta}} \left(m_\beta T_\alpha + m_\alpha T_\beta\right)^2} \Bigg[\Bigg(96 m_\alpha^3 m_\beta^3 T_\alpha^5 + 272 m_\alpha^4 m_\beta^2 T_\alpha^4 T_\beta \\
& + 440 m_\alpha^3 m_\beta^3 T_\alpha^4 T_\beta + 320 m_\alpha^2 m_\beta^4 T_\alpha^4 T_\beta + 72 m_\alpha m_\beta^5 T_\alpha^4 T_\beta + 256 m_\alpha^5 m_\beta T_\alpha^3 T_\beta^2 \\
& + 312 m_\alpha^4 m_\beta^2 T_\alpha^3 T_\beta^2 + 240 m_\alpha^3 m_\beta^3 T_\alpha^3 T_\beta^2 + 24 m_\alpha^2 m_\beta^4 T_\alpha^3 T_\beta^2 + 80 m_\alpha^6 T_\alpha^2 T_\beta^3 + 8 m_\alpha^5 m_\beta T_\alpha^2 T_\beta^3 \\
& + 32 m_\alpha^4 m_\beta^2 T_\alpha^2 T_\beta^3 - 56 m_\alpha^3 m_\beta^3 T_\alpha^2 T_\beta^3 - 376 m_\alpha^3 m_\beta^3 T_\alpha^4 T_\beta e_{\alpha\beta} - 240 m_\alpha^2 m_\beta^4 T_\alpha^4 T_\beta e_{\alpha\beta} \\
& - 104 m_\alpha m_\beta^5 T_\alpha^4 T_\beta e_{\alpha\beta} - 456 m_\alpha^4 m_\beta^2 T_\alpha^3 T_\beta^2 e_{\alpha\beta} - 144 m_\alpha^3 m_\beta^3 T_\alpha^3 T_\beta^2 e_{\alpha\beta} \\
& - 168 m_\alpha^2 m_\beta^4 T_\alpha^3 T_\beta^2 e_{\alpha\beta} - 232 m_\alpha^5 m_\beta T_\alpha^2 T_\beta^3 e_{\alpha\beta} + 48 m_\alpha^4 m_\beta^2 T_\alpha^2 T_\beta^3 e_{\alpha\beta} \\
& - 200 m_\alpha^3 m_\beta^3 T_\alpha^2 T_\beta^3 e_{\alpha\beta} + 256 m_\alpha^2 m_\beta^4 T_\alpha^4 T_\beta e_{\alpha\beta}^2 + 16 m_\alpha m_\beta^5 T_\alpha^4 T_\beta e_{\alpha\beta}^2 \\
& + 384 m_\alpha^3 m_\beta^3 T_\alpha^3 T_\beta^2 e_{\alpha\beta}^2 - 96 m_\alpha^2 m_\beta^4 T_\alpha^3 T_\beta^2 e_{\alpha\beta}^2 + 256 m_\alpha^4 m_\beta^2 T_\alpha^2 T_\beta^3 e_{\alpha\beta}^2 \\
& - 224 m_\alpha^3 m_\beta^3 T_\alpha^2 T_\beta^3 e_{\alpha\beta}^2 - 80 m_\alpha m_\beta^5 T_\alpha^4 T_\beta e_{\alpha\beta}^3 - 160 m_\alpha^2 m_\beta^4 T_\alpha^3 T_\beta^2 e_{\alpha\beta}^3 \\
& - 160 m_\alpha^3 m_\beta^3 T_\alpha^2 T_\beta^3 e_{\alpha\beta}^3 - 40 m_\alpha^6 T_\alpha T_\beta^4 \left(1+e_{\alpha\beta}\right) - 56 m_\alpha^4 m_\beta^2 T_\alpha T_\beta^4 \left(1+e_{\alpha\beta}\right) \\
& - 96 m_\alpha^4 m_\beta^2 T_\alpha T_\beta^4 e_{\alpha\beta} \left(1+e_{\alpha\beta}\right) - 80 m_\alpha^4 m_\beta^2 T_\alpha T_\beta^4 e_{\alpha\beta}^2 \left(1+e_{\alpha\beta}\right) \\
& - 16 m_\alpha^5 m_\beta T_\beta^5 \left(1+e_{\alpha\beta}\right)^3 - 16 m_\alpha^2 m_\beta^4 T_\alpha^5 \left(-11+7e_{\alpha\beta}\right) \\
& + 32 m_\alpha m_\beta^5 T_\alpha^5 \left(4-3e_{\alpha\beta}+2e_{\alpha\beta}^2\right) + 16 m_\alpha^5 m_\beta T_\alpha T_\beta^4 \left(-1+3e_{\alpha\beta}+4e_{\alpha\beta}^2\right) \\
& - 16 m_\beta^6 T_\alpha^5 \left(-2+2e_{\alpha\beta}-e_{\alpha\beta}^2+e_{\alpha\beta}^3\right) \Bigg) + \Bigg(180 m_\alpha^3 m_\beta^3 T_\alpha^5 + 462 m_\alpha^4 m_\beta^2 T_\alpha^4 T_\beta \\
& + 825 m_\alpha^3 m_\beta^3 T_\alpha^4 T_\beta + 600 m_\alpha^2 m_\beta^4 T_\alpha^4 T_\beta + 147 m_\alpha m_\beta^5 T_\alpha^4 T_\beta + 368 m_\alpha^5 m_\beta T_\alpha^3 T_\beta^2 \\
& + 621 m_\alpha^4 m_\beta^2 T_\alpha^3 T_\beta^2 + 450 m_\alpha^3 m_\beta^3 T_\alpha^3 T_\beta^2 + 107 m_\alpha^2 m_\beta^4 T_\alpha^3 T_\beta^2 + 80 m_\alpha^6 T_\alpha^2 T_\beta^3 \\
& + 108 m_\alpha^5 m_\beta T_\alpha^2 T_\beta^3 + 72 m_\alpha^4 m_\beta^2 T_\alpha^2 T_\beta^3 + 14 m_\alpha^3 m_\beta^3 T_\alpha^2 T_\beta^3 - 561 m_\alpha^3 m_\beta^3 T_\alpha^4 T_\beta e_{\alpha\beta} \\
& - 450 m_\alpha^2 m_\beta^4 T_\alpha^4 T_\beta e_{\alpha\beta} - 159 m_\alpha m_\beta^5 T_\alpha^4 T_\beta e_{\alpha\beta} - 483 m_\alpha^4 m_\beta^2 T_\alpha^3 T_\beta^2 e_{\alpha\beta} \\
& - 342 m_\alpha^3 m_\beta^3 T_\alpha^3 T_\beta^2 e_{\alpha\beta} - 129 m_\alpha^2 m_\beta^4 T_\alpha^3 T_\beta^2 e_{\alpha\beta} - 132 m_\alpha^5 m_\beta T_\alpha^2 T_\beta^3 e_{\alpha\beta} \\
& - 72 m_\alpha^4 m_\beta^2 T_\alpha^2 T_\beta^3 e_{\alpha\beta} - 30 m_\alpha^3 m_\beta^3 T_\alpha^2 T_\beta^3 e_{\alpha\beta} + 336 m_\alpha^2 m_\beta^4 T_\alpha^4 T_\beta e_{\alpha\beta}^2 \\
& + 66 m_\alpha m_\beta^5 T_\alpha^4 T_\beta e_{\alpha\beta}^2 + 312 m_\alpha^3 m_\beta^3 T_\alpha^3 T_\beta^2 e_{\alpha\beta}^2 + 42 m_\alpha^2 m_\beta^4 T_\alpha^3 T_\beta^2 e_{\alpha\beta}^2 \\
& + 96 m_\alpha^4 m_\beta^2 T_\alpha^2 T_\beta^3 e_{\alpha\beta}^2 + 6 m_\alpha^3 m_\beta^3 T_\alpha^2 T_\beta^3 e_{\alpha\beta}^2 - 90 m_\alpha m_\beta^5 T_\alpha^4 T_\beta e_{\alpha\beta}^3 \\
& - 90 m_\alpha^2 m_\beta^4 T_\alpha^3 T_\beta^2 e_{\alpha\beta}^3 - 30 m_\alpha^3 m_\beta^3 T_\alpha^2 T_\beta^3 e_{\alpha\beta}^3 - 30 m_\alpha^2 m_\beta^4 T_\alpha^5 \left(-11+7e_{\alpha\beta}\right) \\
& + 60 m_\alpha m_\beta^5 T_\alpha^5 \left(4-3e_{\alpha\beta}+2e_{\alpha\beta}^2\right) - 30 m_\beta^6 T_\alpha^5 \left(-2+2e_{\alpha\beta}-e_{\alpha\beta}^2+e_{\alpha\beta}^3\right) \Bigg) \Delta_\alpha \\
& + \Bigg(- 4 m_\alpha^5 m_\beta T_\alpha^3 T_\beta^2 - 18 m_\alpha^4 m_\beta^2 T_\alpha^3 T_\beta^2 - 16 m_\alpha^2 m_\beta^4 T_\alpha^3 T_\beta^2 - 10 m_\alpha^6 T_\alpha^2 T_\beta^3 \\
& - 51 m_\alpha^5 m_\beta T_\alpha^2 T_\beta^3 - 24 m_\alpha^4 m_\beta^2 T_\alpha^2 T_\beta^3 - 73 m_\alpha^3 m_\beta^3 T_\alpha^2 T_\beta^3 - 6 m_\alpha^4 m_\beta^2 T_\alpha^3 T_\beta^2 e_{\alpha\beta} \\
& + 36 m_\alpha^3 m_\beta^3 T_\alpha^3 T_\beta^2 e_{\alpha\beta} - 48 m_\alpha^2 m_\beta^4 T_\alpha^3 T_\beta^2 e_{\alpha\beta} - 21 m_\alpha^5 m_\beta T_\alpha^2 T_\beta^3 e_{\alpha\beta} \\
& + 54 m_\alpha^4 m_\beta^2 T_\alpha^2 T_\beta^3 e_{\alpha\beta} - 195 m_\alpha^3 m_\beta^3 T_\alpha^2 T_\beta^3 e_{\alpha\beta} + 24 m_\alpha^3 m_\beta^3 T_\alpha^3 T_\beta^2 e_{\alpha\beta}^2 \\
& - 66 m_\alpha^2 m_\beta^4 T_\alpha^3 T_\beta^2 e_{\alpha\beta}^2 + 48 m_\alpha^4 m_\beta^2 T_\alpha^2 T_\beta^3 e_{\alpha\beta}^2 - 222 m_\alpha^3 m_\beta^3 T_\alpha^2 T_\beta^3 e_{\alpha\beta}^2 \\
& - 30 m_\alpha^2 m_\beta^4 T_\alpha^3 T_\beta^2 e_{\alpha\beta}^3 - 90 m_\alpha^3 m_\beta^3 T_\alpha^2 T_\beta^3 e_{\alpha\beta}^3 - 15 m_\alpha^6 T_\alpha T_\beta^4 \left(1+e_{\alpha\beta}\right) \\
& - 81 m_\alpha^4 m_\beta^2 T_\alpha T_\beta^4 \left(1+e_{\alpha\beta}\right) - 156 m_\alpha^4 m_\beta^2 T_\alpha T_\beta^4 e_{\alpha\beta} \left(1+e_{\alpha\beta}\right) \\
& - 90 m_\alpha^4 m_\beta^2 T_\alpha T_\beta^4 e_{\alpha\beta}^2 \left(1+e_{\alpha\beta}\right) - 30 m_\alpha^5 m_\beta T_\beta^5 \left(1+e_{\alpha\beta}\right)^3 \\
& + 6 m_\alpha^5 m_\beta T_\alpha T_\beta^4 \left(-1+3e_{\alpha\beta}+4e_{\alpha\beta}^2\right) \Bigg) \Delta_\beta \Bigg]. \qquad (5.69)
\end{aligned}
$$

5.4 Homogeneous Cooling State of a Binary Granular Mixture

5.4.1 Monodisperse Case and the Contracted Fourth Moment

One can obtain the production terms for a monodisperse gas by ignoring the summation and replacing β with α in equations (5.63)-(5.69) and substitute $m_A = m_B = m$, $n_A = n_B = n$, $\sigma_{AA} = \sigma_{BB} = \sigma_{AB} = \sigma$, $e_{AA} = e_{BB} = e_{AB} = e$, $\sigma_{ij}^{(A)} = \sigma_{ij}^{(B)} = \sigma_{ij}$, $q_i^{(A)} = q_i^{(B)} = q_i$ and $\Delta_A = \Delta_B = \Delta$. The collisional production terms (source terms) for monodisperse case become

$$P_1 = P_1^{(M)} = 0, \quad P_2 = P_2^{(M)} = 0, \tag{5.70}$$

$$P_3 = P_3^{(M)} = -\frac{4\sigma^2}{m}\sqrt{\pi}(1-e^2)\left(1+\frac{3\Delta}{16}\right)\rho^2\left(\frac{T}{m}\right)^{3/2}, \tag{5.71}$$

$$P_4 = P_4^{(M)} = -\frac{4}{5}\frac{\sigma^2}{m}\sqrt{\pi}(1+e)(3-e)\rho\left(\frac{T}{m}\right)^{1/2}\sigma_{ij}, \tag{5.72}$$

$$P_5 = P_5^{(M)} = -\frac{2}{15}\frac{\sigma^2}{m}\sqrt{\pi}(1+e)(49-33e)\rho\left(\frac{T}{m}\right)^{1/2}q_i, \tag{5.73}$$

$$P_6 = P_6^{(M)} = -\frac{4\sigma^2}{m}\sqrt{\pi}(1+e)\left[(2e^2+9)(1-e)+(271-207e+30e^2-30e^3)\frac{\Delta}{16}\right]\rho^2\left(\frac{T}{m}\right)^{5/2}. \tag{5.74}$$

We have verified that the above production terms for monodisperse case are same as in Kremer & Marques Jr (2011).

The moment equation of contracted fourth moment (Δ) for a spatially homogeneous system becomes

$$15\rho\left(\frac{T}{m}\right)^2\frac{d}{dt}(\Delta) = P_6^{(M)} - 10P_3^{(M)}(1+\Delta)\left(\frac{T}{m}\right). \tag{5.75}$$

The steady-state contracted fourth moment (Δ^∞) is defined in the following way

$$\Delta^\infty = \lim_{t\to\infty}\Delta. \tag{5.76}$$

For the steady-state contracted fourth moment (Δ^∞), Eq. (5.75) becomes

$$P_6^{(M)} - 10P_3^{(M)}(1+\Delta^\infty)\left(\frac{T}{m}\right) = 0. \tag{5.77}$$

Substituting the expressions for $P_6^{(M)}$ and $P_3^{(M)}$ in the above equation and neglecting products of Δ^∞, we obtain

$$\Delta^\infty = \frac{16(1-2e^2)(1-e)}{81-17e+30e^2(1-e)}. \tag{5.78}$$

This expression for Δ^∞ agrees with that of van Noije & Ernst (1998). The variation of Δ^∞ with restitution coefficient is shown in Fig. 5.1. Note that Δ^∞ is negative for $e \sim 1$ but becomes positive for highly dissipative particles ($e \leq 0.7$).

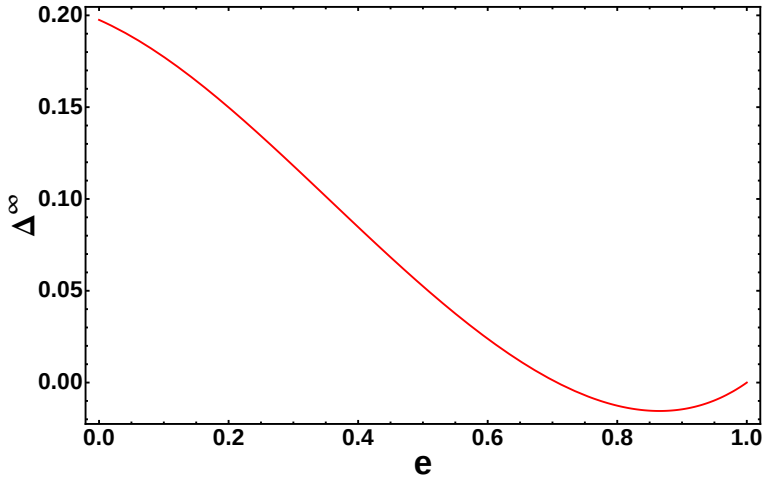

Figure 5.1: Steady-state contracted fourth moment (Δ^{∞}) versus coefficient of restitution (e) for a monatomic gas.

5.4.2 Homogeneous Cooling State and Energy Non-equipartition

For a spatially homogeneous system, all the field variables depend only on time. For the spatially homogeneous solution, the moment equations reduce to the following system of equations

$$\frac{d\rho_\alpha}{dt} = 0, \tag{5.79}$$

$$3n_\alpha \frac{d}{dt}(T_\alpha) = P_3^{(\alpha)}, \tag{5.80}$$

$$15\rho_\alpha \left(\frac{T_\alpha}{m_\alpha}\right)^2 \frac{d}{dt}(\Delta_\alpha) = P_6^{(\alpha)} - 10P_3^{(\alpha)}(1+\Delta_\alpha)\left(\frac{T_\alpha}{m_\alpha}\right). \tag{5.81}$$

Due to the presence of $P_3^{(\alpha)}, P_6^{(\alpha)}$ terms (RHS of the above equations), the above equations are nonlinear coupled differential equations. Due to the complexity of the equations, we solve the differential equations for $T_\alpha(t)$ and $\Delta_\alpha(t)$ numerically by considering initial conditions $T_\alpha(0) = 1$ and $\Delta_\alpha(0) = 1$ for $\alpha = A, B$.

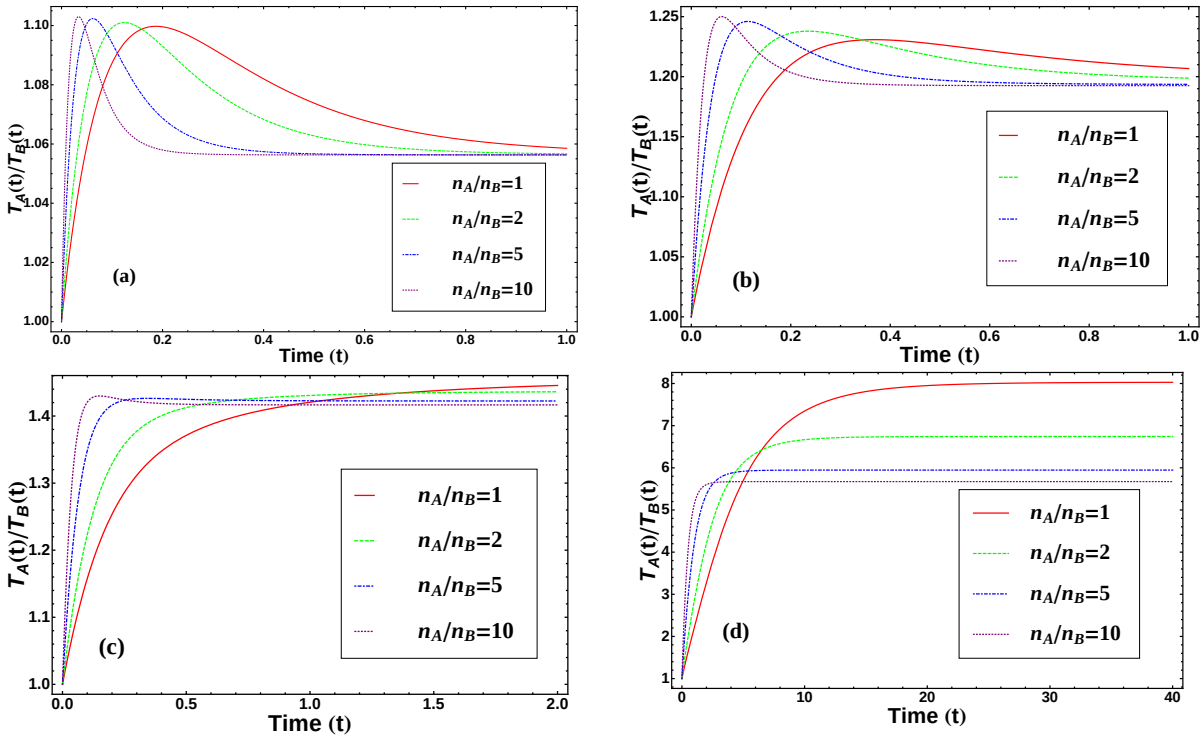

Figure 5.2: Temperature ratio $(T_A(t)/T_B(t))$ versus time for the value of coefficient of restitution $(e_{AA} = e_{AB} = e_{BB} = 0.9)$ for size ratio $(\sigma_A/\sigma_B) = 1$ and (a) mass ratio $(m_A/m_B) = 2$, (b) $m_A/m_B = 5$, (c) $m_A/m_B = 10$, (d) $m_A/m_B = 100$.

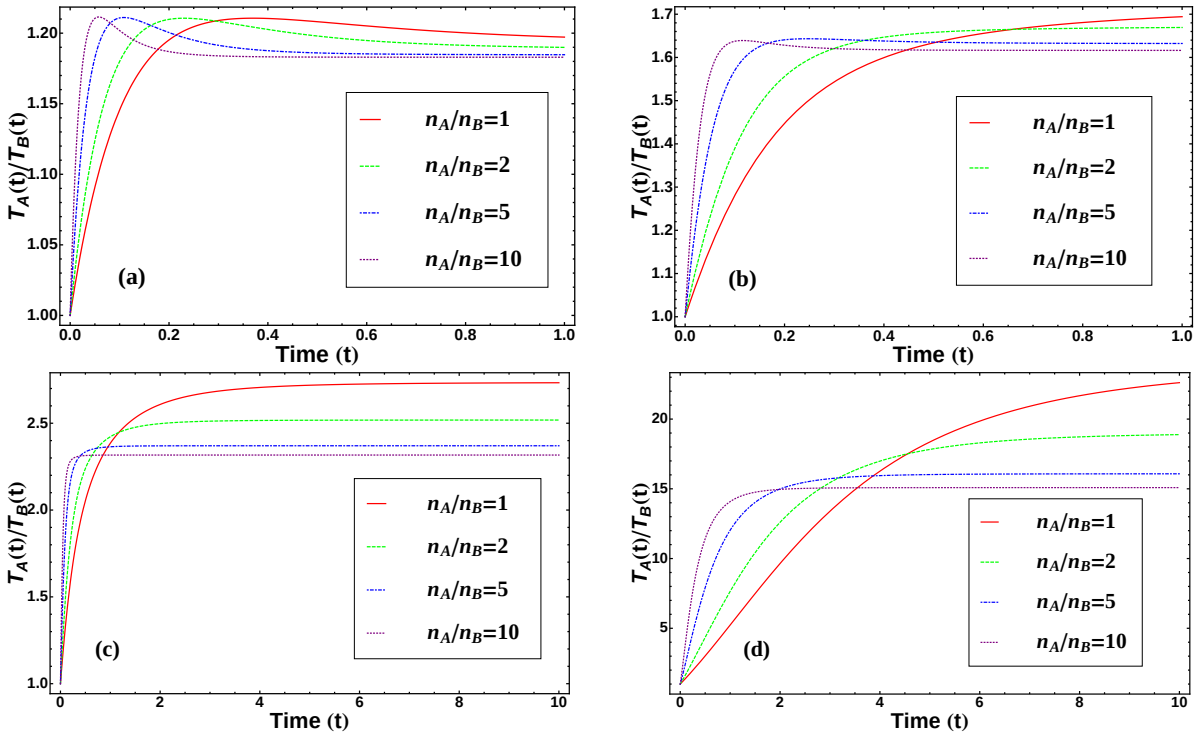

Figure 5.3: Same as Fig. 5.2 but for a coefficient of restitution of $e_{AA} = e_{AB} = e_{BB} = 0.7$.

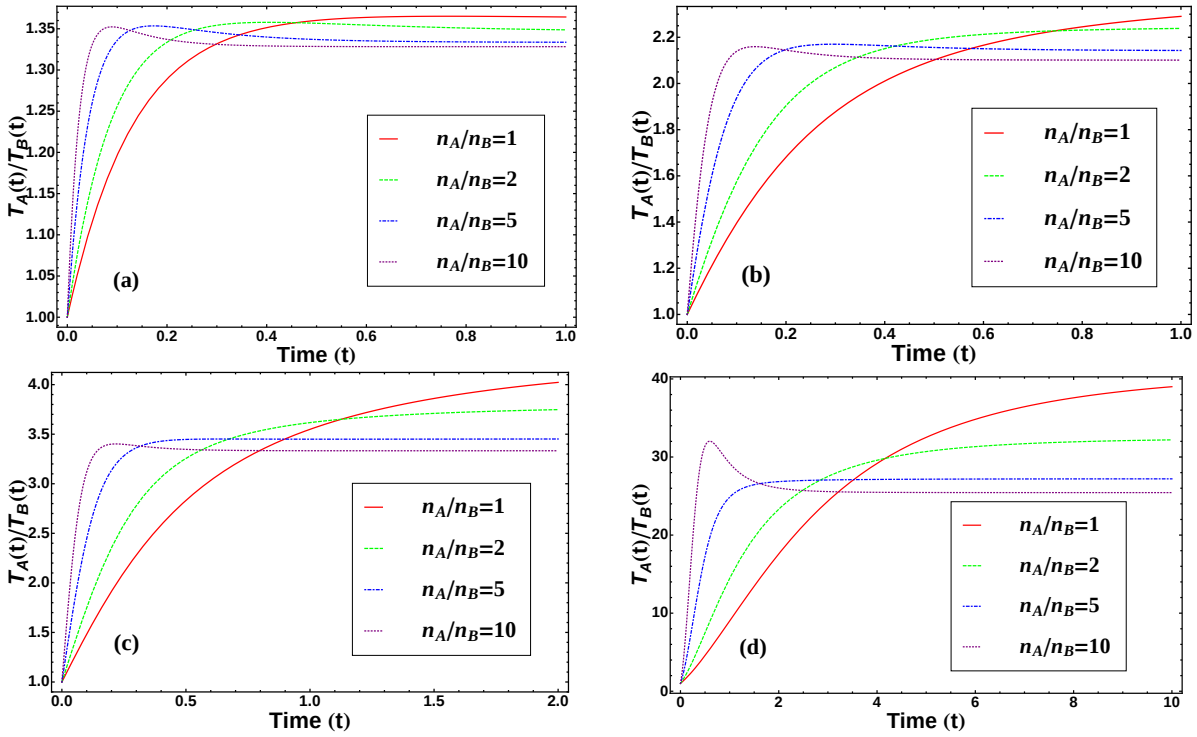

Figure 5.4: Same as Fig. 5.2 but for a coefficient of restitution of $e_{AA} = e_{AB} = e_{BB} = 0.5$.

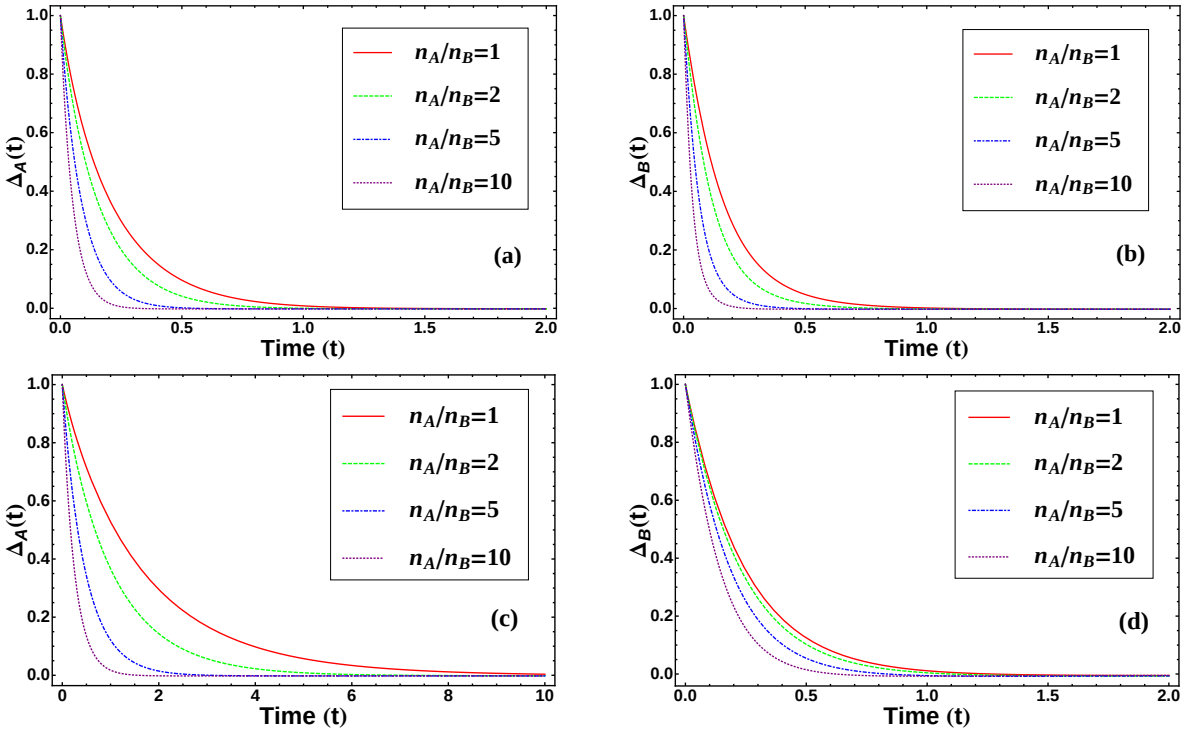

Figure 5.5: Contracted fourth moment ($\Delta_\alpha, \alpha = A, B$) versus time for the value of coefficient of restitution ($e_{AA} = e_{AB} = e_{BB} = 0.99$) for size ratio ($\sigma_A/\sigma_B$) = 1 and (a,b) mass ratio (m_A/m_B) = 5, (c,d) mass ratio (m_A/m_B) = 100.

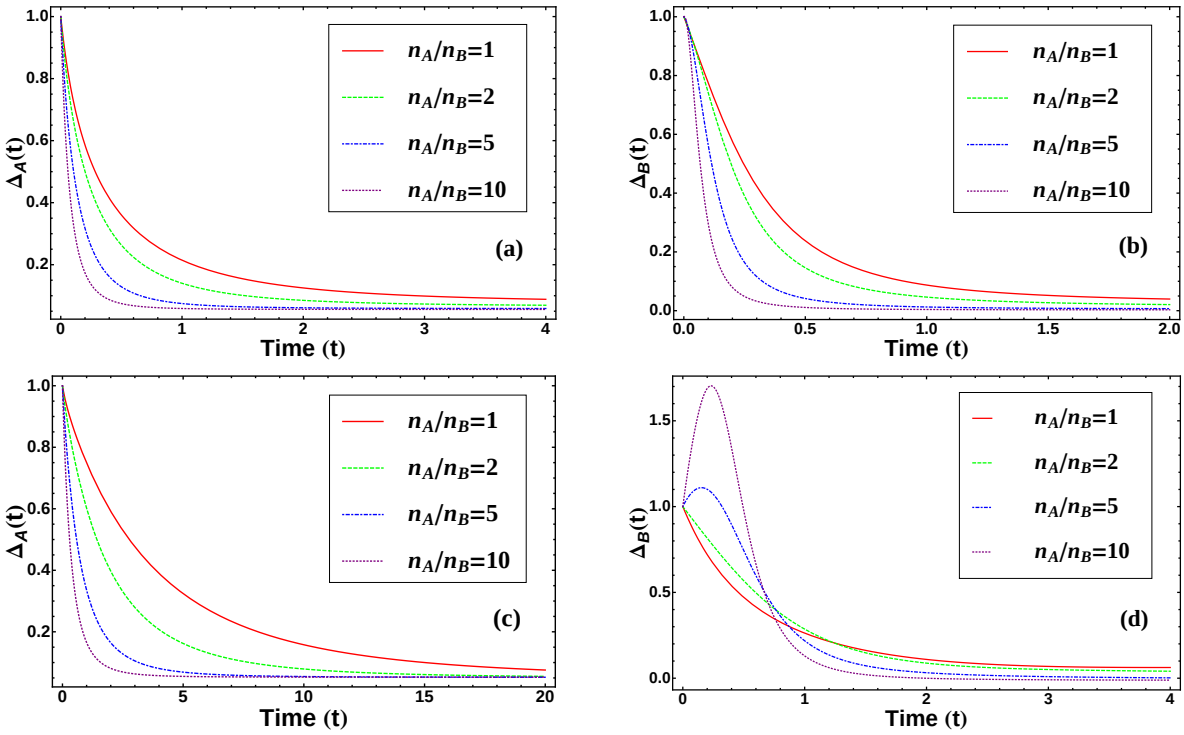

Figure 5.6: Same as Fig. 5.5 but for a coefficient of restitution of $e_{AA} = e_{AB} = e_{BB} = 0.5$.

Fig. 5.2 shows the time evolution of the temperature ratio $(T_A(t)/T_B(t))$, for the value of coefficient of restitution $(e_{AA} = e_{AB} = e_{BB} = 0.9)$ and (a) mass ratio (m_A/m_B) is 2, (b) mass ratio (m_A/m_B) is 5, (c) mass ratio (m_A/m_B) is 10, (d) mass ratio (m_A/m_B) is 100. Figs. 5.3 and 5.4 show the same as in Fig. 5.2, but for the different values of coefficient of restitution $(e_{AA} = e_{AB} = e_{BB} = 0.7, 0.5)$, respectively. In each figure we find $T_A/T_B(t \to \infty) > 1$, i.e. the energy is unequally partitioned between two species. The temporal variations of contracted fourth moments Δ_A and Δ_B are displayed in Figs. 5.5 and 5.6. In each case it is seen that the steady-state values of Δ_A and Δ_B attain a small non-zero value.

From the above figures, one can notice that the temperature ratio initially increases and reaches a steady state at large times. Let us define the steady-state temperature ratio (γ) and steady-state contracted fourth moment $(\Delta_\alpha^\infty, \alpha = A, B)$ in the following way:

$$\gamma = \lim_{t\to\infty} \frac{T_A}{T_B}, \tag{5.82}$$

and

$$\Delta_\alpha^\infty = \lim_{t\to\infty} \Delta_\alpha. \tag{5.83}$$

The moment equations (Eq. (5.80) - Eq. (5.81)) for the steady-state become

$$P_3^{(\alpha)} = 0, \tag{5.84}$$

$$P_6^{(\alpha)} = 0. \tag{5.85}$$

Solving these equations numerically gives T_A, T_B, Δ_A and Δ_B as functions of $n_A/n_B, m_A/m_B$

and $e_{\alpha\beta}$.

Fig. 5.7(a,b,c) shows the variations of steady-state temperature ratio with mass-ratio for the values of restitution coefficient ($e_{AA} = e_{AB} = e_{BB} =$) 0.9, 0.7, 0.5, respectively. Fig. 5.7(d) shows the variation of steady-state temperature ratio with restitution coefficient for a mass ratio of $m_A/m_B = 10$ and a number density ratio of $n_A/n_B = 2$. Theoretical results (circles) compare well with DSMC simulation data (denoted by triangles) of Montanero & Garzó (2002).

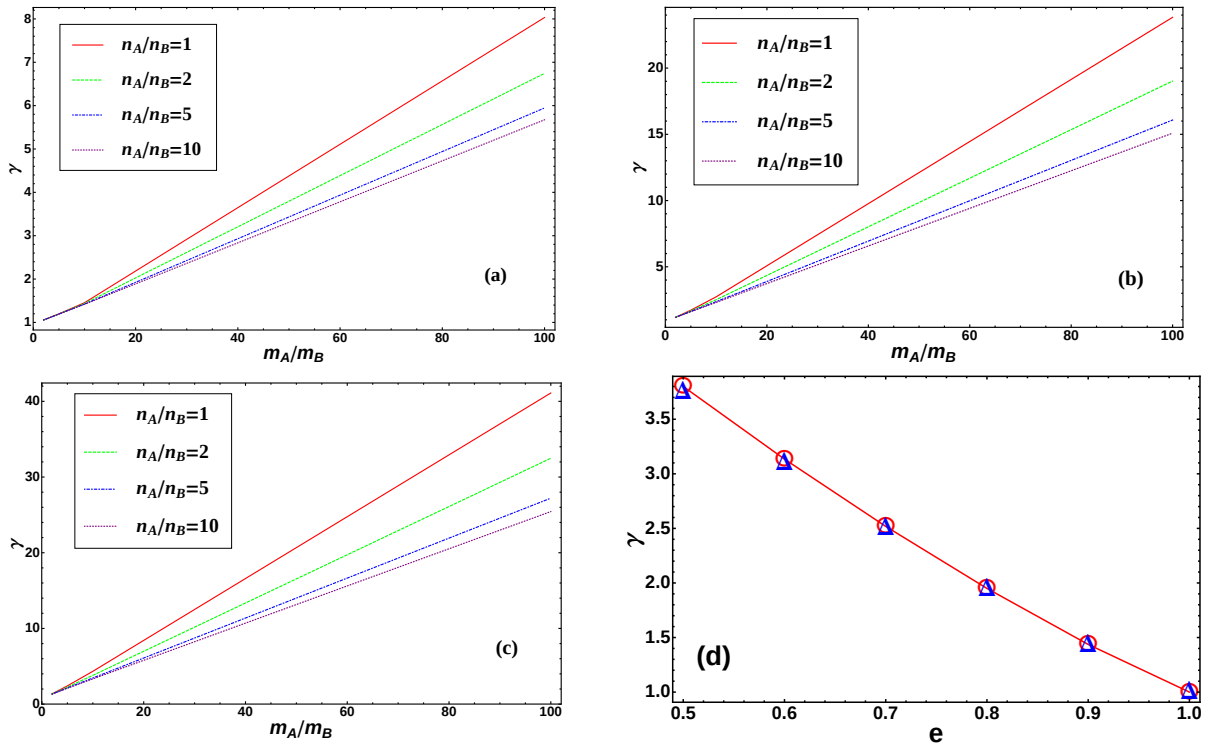

Figure 5.7: Steady-state temperature ratio (γ) versus mass ratio (m_A/m_B) for size ratio (σ_A/σ_B) = 1 and (a) $e_{AA} = e_{AB} = e_{BB} = 0.9$, (b) $e_{AA} = e_{AB} = e_{BB} = 0.7$, (c) $e_{AA} = e_{AB} = e_{BB} = 0.5$. (d) Variation of steady-state temperature ratio with restitution coefficient for a mass ratio of $m_A/m_B = 10$ and a number density ratio of $n_A/n_B = 2$; here red solid line and circles represent present theory, and the blue triangles represent simulation results of Montanero & Garzó (2002).

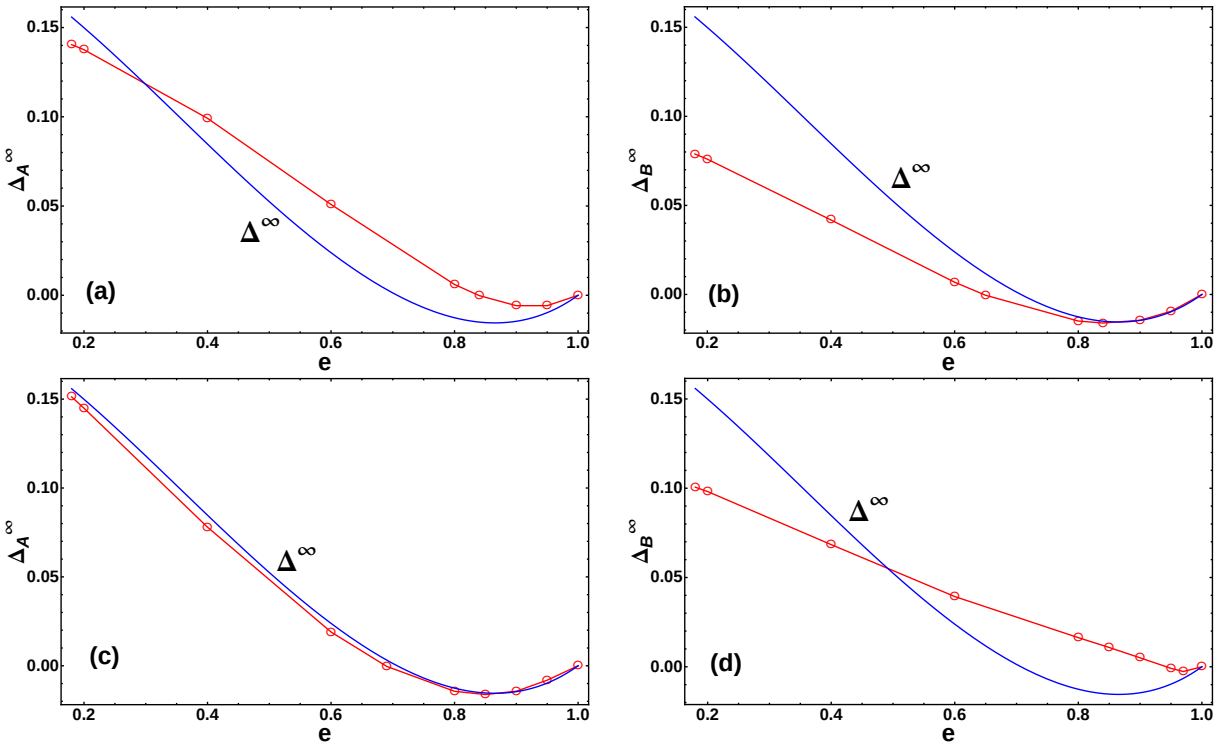

Figure 5.8: Steady-state contracted fourth moment ($\Delta_\alpha^\infty, \alpha = A, B$) versus coefficient of restitution ($e_{AA} = e_{AB} = e_{BB} = e$) for a size ratio $\sigma_A/\sigma_B = 1$, number-density ratio n_A/n_B=1 and (a,b) mass ratio $(m_A/m_B) = 5$, (c,d) mass ratio $(m_A/m_B) = 100$. The blue solid line in each panel is a reference for steady-state contracted fourth moment (Δ^∞) of a monodisperse gas.

Fig. 5.8 shows the dependence of steady-state contracted fourth-moment of each species (Δ_A^∞ and Δ_B^∞) with restitution coefficient for mass-ratios of $m_A/m_B = 5$ (upper panels) and $m_A/m_B = 100$ (lower panels). In each panel, the corresponding monodisperse value of Δ^∞ [Eq. 5.78] is superimposed for a comparison. Depending on the mass-ratio, the numerical values of Δ_A^∞ and Δ_B^∞ can differ significantly from its monodisperse limit.

5.5 Summary

A detailed derivation of the 2×14-moment equations for a dilute binary granular mixture is presented. We have derived the non-equilibrium distribution function in terms of 14 hydrodynamic fields for the species α via Grad's moment method. To close the hydrodynamic equations, all production terms have been calculated by using this non-equilibrium distribution function as functions of (i) the restitution coefficient ($e_{\alpha\beta}$), (ii) the mass and size ratios of two species and (iii) the number density ratio of each species. In the mono-disperse limit, the calculated "linear" production terms agree with previous work (Kremer & Marques Jr 2011). In future, the "nonlinear" versions of production terms should be determined so that the resulting equations can be used to study the Burnett/rarefied regime of binary granular mixtures.

We have applied these equations to analyse homogeneous cooling state and discussed about temperature ratio and contracted fourth moment for different restitution coefficients, mass ratios and number density ratios. At large times, both temperature ratio and contracted fourth

moment reach a steady-state. The variation of steady-state temperature ratio with restitution coefficient for a mass ratio of $m_A/m_B = 10$ and number density ratio of $n_A/n_B = 2$ has been compared with simulation results of Montanero & Garzó (2002) and the agreement is good.

To apply the presently derived extended hydrodynamic equations to wall-bounded flows such as acceleration-driven Poiseuille flow (Chapters 3 and 4), we need to derive boundary conditions on higher-order fields. These can be done by assuming Maxwell-type accommodation models for particle-wall collisions (Cercignani 2000). This is left for a future work.

Chapter 6

Summary and Outlook

Certain rarefaction effects in molecular and granular gases are analysed in this thesis from Boltzmann's kinetic theory. After a brief introduction about granular and rarefied gases and the related theoretical issues in Chapter 1, the remaining chapters (2, 3, 4 and 5) dealt with three independent problems in the kinetic theory of rarefied molecular and granular gases: (i) the analysis of higher-order effects on orientational correlation in the homogeneous-cooling state (HCS) of a granular gas of rough inelastic hard spheres (Chapter 2); (ii-a) the bulk hydrodynamics and rheology of the gravity-driven Poiseuille flow of a dilute gas of hard spheres and Maxwell molecules (Chapter 3), with a focus to understand certain rarefied effects (e.g. the bimodal-shape of the temperature profile, the normal stress differences, tangential heat flux, etc) and analyse the radius of convergence of the underlying series solutions, (ii-b) the bulk hydrodynamics and rheology of dilute granular Poiseuille flow (Chapter 4), and finally (iii) the derivation of extended hydrodynamic equations for binary granular mixtures following Grad's moment method (Chapter 5).

6.1 Summary of Present Work

Chapter 2 is devoted to investigate the HCS of a rough granular gas by focusing on a special kind of correlation: the "orientational" or "directional" correlation (Brilliantov *et al.* (2007); Gayen & Alam (2008)) between the direction of the angular velocity ($\boldsymbol{\omega}$) of a granular particle and the direction of its translational velocity ($\mathbf{c}$); this is defined as the mean square of the cosine of the angle between $\mathbf{c}$ and $\boldsymbol{\omega}$:

$$\left\langle \cos^2\theta \right\rangle = \frac{1}{N}\sum_{i=1}^{N}\frac{(\boldsymbol{c}_i\cdot\boldsymbol{\omega}_i)^2}{\boldsymbol{c}_i^2\boldsymbol{\omega}_i^2} \equiv \frac{1}{3}\int_c\int_\omega [P_0(\cos\theta)+2P_2(\cos\theta)][P_0(\cos\theta)+b_{112}(t)\boldsymbol{c}^2\boldsymbol{\omega}^2P_2(\cos\theta) +b_{122}(t)\boldsymbol{c}^2\boldsymbol{\omega}^4P_2(\cos\theta)+b_{212}(t)\boldsymbol{c}^4\boldsymbol{\omega}^2P_2(\cos\theta)]. \tag{6.1}$$

The dynamical equations are derived using pseudo-Liouville operator technique, with an approximate form of the single-particle distribution function that incorporates angular correlations. To assess the effects of higher-order angular corrections, both quadratic- and quartic-order terms (in translational and rotational velocities of particles) are retained in the perturbation expansion of distribution function. It is shown that higher-order corrections can markedly affect steady-state orientational correlation when the normal restitution coefficient is moderate or small and this effect is more prominent for nearly smooth particles. The transient evolution of orientational correlation is found to be significantly affected by higher-order terms. In particular, the higher-order orientational correlations can dominate over its leading-order contribution during short times even in the quasi-elastic limit although the steady correlation remains unaffected by such

corrections in the same limit. The building-up of correlations during transient stage seems to be closely tied to the evolution of the ratio between the rotational and translational temperatures. Finally, it is demonstrated that the transient dynamics of the temperature ratio (the ratio between rotational and translational temperatures) and its steady state remain insensitive to higher-order angular correlation.

In Chapter 3, the gravity-driven Poiseuille flow of hard spheres flowing through a channel is analysed using a perturbation expansion of the velocity distribution function in powers of the strength of gravitational acceleration (the Froude number $\mathrm{Fr}_0 = g\lambda/v_{th}^2$, where λ is the mean-free path and v_{th} is the thermal velocity, both evaluated at the center of the channel) by retaining terms up to tenth-order in Fr_0. The resulting solution holds only around the channel centerline since the wall-effects are not considered in the present analysis. A BGK kinetic model is adopted and the related problem for Maxwell molecules was originally analysed by Tij & Santos (1994) by retaining terms up to sixth-order in Froude number as detailed in section 3.7 of Chapter 3. The present high-order expansion (for both hard spheres and Maxwell molecules) helped to assess the asymptotic nature of the perturbation expansion and the related convergence issues for the resulting hydrodynamic (temperature, velocity and pressure) and rheological (stress tensor and heat flux) fields for which analytical expressions have been derived. Rarefaction effects (e.g. the bimodal shape of the temperature profile, tangential heat flux, normal stress differences, etc) are analysed using presently obtained high-order series solutions. It is found that the temperature bimodality,

$$\triangle T = \frac{T_{\max} - T_0}{T_0}, \tag{6.2}$$

where T_0 is the temperature at the channel centerline and $T_{\max}$ is the maximum temperature that occurs away from the channel center, and all transport coefficients show oscillating behaviour for Froude number greater than 10^{-3}. Therefore, adding further higher-order terms does not help to obtain converged solution – both indicates the asymptotic nature of the adopted series expansion. Subsequently, the Shanks transformation and the Padé approximations have been used to further analyse the convergence of series expansion. The present analysis indicates that the "diagonal" Padé approximation of the 10th-order series solution yields accurate/converged solution for a much larger range of Froude numbers up to $\mathrm{Fr}_0 \approx 10^{-1}$; it is concluded that further higher-order terms would be needed to obtain accurate solution for a larger range of Fr_0. These overall findings hold for both hard spheres and Maxwell molecules for the present problem of gravity-driven Poiseuille flow of molecular gases.

In Chapter 4, the effect of inelastic dissipation on the gravity-driven flow of a "heated" granular gas (dubbed "granular Poiseuille flow") is studied using the same perturbation expansion of the velocity distribution function. Again a BGK-type kinetic model (Brey *et al.* 1999*b*) with heating via white-noise (that compensates for collisional cooling due to inelasticity) is employed. Neglecting wall-effects and focusing only on the bulk behaviour of the flow, the effect of gravity is incorporated perturbatively around a 'uniform' state (of constant temperature and density): the distribution function and all hydrodynamic and rheological fields are expanded in power-series in Froude number Fr_0, with the base state representing their respective values at the channel centerline. The complexity of the problem allowed us to determine solutions only up to fourth-order in Fr_0; the related second-order solution has been obtained previously by Tij

& Santos (2004). The present fourth-order solutions are used to analyse the behaviour of (i) temperature bimodality ($\triangle T$), (ii) normal stress differences and (iii) heat fluxes as functions of the restitution coefficient (e_n) and the Froude number Fr_0. It is found that $\triangle T$ increases with increasing dissipation for $\mathrm{Fr}_0 \geq 4\times10^{-3}$; for small enough values of Fr_0 ($< 4\times10^{-3}$), however, a 'non-monotonic' behaviour of $\triangle T$ with e_n [i.e. $\triangle T$ decreases with decreasing e_n for $e_n \in (1, 0.5)$, but increases for $e_n < 0.5$] is recovered. A phase-diagram is constructed in the $(\mathrm{Fr}_0, 1-e_n)$-plane that demarcates two regions by identifying a critical Froude number $\mathrm{Fr}^c \equiv \mathrm{Fr}(e_n)$, above and below which the dependence of $\triangle T$ on e_n is monotonic and non-monotonic, respectively. Similarly, the first normal-stress difference (positive $\mathcal{N}_1$) increases with increasing dissipation and the second normal-stress difference (negative $\mathcal{N}_2$) decreases with increasing dissipation at $\mathrm{Fr}_0 > \mathrm{Fr}_0^c$; the non-monotonic behaviour (similar to that of $\triangle T$) of both $\mathcal{N}_1$ and $\mathcal{N}_2$ is seen at $\mathrm{Fr}_0 < \mathrm{Fr}_0^c$. The dependence of tangential heat flux q_x on dissipation is found to be similar to that of normal stress differences. Overall, it is concluded that the inelastic dissipation plays a "dual" role of decreasing (at $\mathrm{Fr}_0 < \mathrm{Fr}_0^c$) and increasing (at $\mathrm{Fr}_0 > \mathrm{Fr}_0^c$) the values of $\triangle T$, $\mathcal{N}_1$ and $\mathcal{N}_2$ with decreasing restitution coefficient e_n from the elastic limit. The results on temperature bimodality are compared qualitatively with recent MD simulations (Alam *et al.* 2015) and DSMC simulations (Gupta & Alam 2017) on gravity-driven granular Poiseuille flow, and the underlying differences are critically examined. It is concluded that the observed differences at small $\mathrm{Fr}_0 (\leq \mathrm{Fr}_0^c \approx 4\times10^{-3})$ might be related to the fact that a "heated" granular gas under acceleration could be fundamentally different from gravity-driven Poiseuille flow of inelastic particles. The latter issue requires further analysis.

In Chapter 5, the derivation of 2×14-moment equations for a dilute binary granular mixture is outlined for the first time – such higher-order moment equations are deemed to be appropriate for rarefied molecular gases beyond the Navier-Stokes regime of Knudsen number ($\mathrm{Kn} > 0.01$). Instead of using the approximate kinetic model as in Chapters 3 and 4, the Boltzmann equation for a binary mixture with exact collision term is employed in the present Chapter to derive the extended hydrodynamic equations. The non-equilibrium distribution function in terms of 14 hydrodynamic fields is obtained following the well-known Hermite expansion around the species Maxwellian. To close the hydrodynamic equations, all source/production terms have been calculated as functions of (i) the restitution coefficient ($e_{\alpha\beta}$), (ii) the mass and size ratios of two species and (iii) the number fraction of each species. In the mono-disperse limit, the calculated source terms agree with previous work (Kremer & Marques Jr 2011). The application of the resulting of hydrodynamic equations to analyse the homogeneous cooling state of binary granular mixtures is discussed briefly in the end.

6.2 Future Work

In Chapter 3, although we have determined terms up to 10th-order (in gravitational acceleration), it is found that the radius of convergence of obtained solution is very small ($\mathrm{Fr}_0 < 5\times10^{-2}$). Since the Knudsen and Froude numbers are related [$\mathrm{Fr}_0 = \widehat{g}\mathrm{Kn}_0(T_0/T_w)$], we may conclude that the radius of convergence of our 10th-order Padé-approximated solution (Chapter 3) belongs to the regime of slip flow (i.e. $\mathrm{Kn}_0 \leq 10^{-1}$). To apply these solutions in the transition regime ($\mathrm{Kn}_0 \geq 0.1$), one must calculate further higher-order terms which is a difficult task even with

Mathematica.

For inelastic particles discussed in Chapter 4, the situation is also difficult as we could determine solution up to fourth-order, although in principle it would be possible to calculate higher-order terms for granular flow too. Extending the Padé-approximated solution to the granular case, we can obtain converged solution for $\mathrm{Fr}_0 \leq 10^{-1}$ if we have 10 or more terms at our disposal. For a one-to-one comparison with simulation data [Alam *et al.* (2015); Gupta & Alam (2017)], it is required to have converged theoretical solution for $\mathrm{Kn}_0 > 0.01$ since the MD and DSMC simulations are known for $\mathrm{Kn}_0 > 0.01$. The standard DSMC-algorithm is not suitable for small Knudsen numbers ($\mathrm{Kn}_0 \leq 0.01$) and/or very small Froude numbers — other techniques may be needed to solve the underlying kinetic equation numerically [for example, low-deviation DSMC of Baker & Hadjiconstantinou (2005)].

To overcome above difficulties, it is recommended to solve the extended hydrodynamic equations (as derived in Chapter 5) for the granular Poiseuille flow. This requires derivation of boundary conditions on higher-order fields— Maxwell-type accommodation models (Cercignani 2000) can be employed to derive such boundary conditions. In the immediate future, the boundary-value problems such as Poiseuille flow with extended nonlinear hydrodynamic equations and boundary conditions should be solved to resolve differences with simulation data for Poiseuille flow.

References

Alam, M. 2012 Non-modal stability and optimal perturbations in unbounded granular shear flow: Three-dimensionality and particle spin. *Prog. Theor. Phys. Suppl.* **195**, 78–100.

Alam, M. & Luding, S. 2005 Non-Newtonian granular fluid: simulation and theory. *Powders and Grains* pp. 1141–1145.

Alam, M., Mahajan, A. & Shivanna, D. 2015 On knudsen-minimum effect and temperature bimodality in a dilute granular Poiseuille flow. *J. Fluid Mech.* **782**, 99–126.

Alam, M. & Nott, P. R. 1997 The influence of friction on the stability of unbounded granular shear flow. *J. Fluid Mech.* **343**, 267–301.

Alaoui, M. & Santos, A. 1992 Poiseuille flow driven by an external force. *Phys. Fluids. A* **4**, 1273–1282.

Andreotti, B., Forterre, Y. & Pouliquen, O. 2013 *Granular Media: Between Fluid and Solid*. Cambridge University Press, Cambridge.

Aoki, K., Takata, S. & Nakanishi, T. 2002 A Poiseuille-type flow of a rarefied gas between two parallel plates driven by a uniform external force. *Phys. Rev. E* **65**, 026315.

Aranson, I. S. & Tsimring, L. S. 2006 Patterns and collective behavior in granular media: Theoretical concepts. *Rev. Mod. Phys.* **78** (2), 641.

Araújo, A. D., Parteli, E. J. R., Pöschel, T., Andrade, J. S. & Herrmann, H. J. 2013 Numerical modeling of the wind flow over a transverse dune. *Scientific reports* **3**.

Baker, L. L. & Hadjiconstantinou, N. G. 2005 Variance reduction for monte carlo solutions of the boltzmann equation. *Phys. Fluids* **17** (051703).

Baker, G. A. Jr & Graves-Morris, P. 1996 *Padé Approximants*. Cambridge University Press, New York.

Bender, C. M. & Orszag, S. A. 1999 *Advanced Mathematical Methods for Scientists and Engineers: Asymptotic Methods and Perturbation Theory*. Springer, New York.

Bhatnagar, P. L., Gross, E. P. & Krook, M. 1954 A model for collision processes in gases. i. small amplitude processes in charged and neutral one-component systems. *Phys. Rev* **94**, 511–525.

Bird, G. A. 1994 *Molecular Gas Dynamics and the Direct Simulation of Gas Flows*. Clarendon Press, Oxford.

Bobylev, A. V. 1982 The Chapman-Enskog and Grad methods for solving the Boltzmann equation. *Sov. Phys. Dokl.* **27**, 29–31.

Bobylev, A. V. 2006 Instabilities in the Chapman-Enskog expansion and hyperbolic Burnett equations. *J. Stat. Phys.* **124**, 371–399.

Brey, J. J., Cubero, D. & Ruiz-Montero, M. J. 1999*a* High energy tail in the velocity distribution of a granular gas. *Phys. Rev. E* **59**, 1256–1258.

Brey, J. J., Dufty, J. W. & Santos, A. 1997*a* Dissipative dynamics for hard spheres. *J. Stat. Phys.* **87** (5-6), 1051–1066.

Brey, J. J., Dufty, J. W. & Santos, A. 1999*b* Kinetic models for granular flow. *J. Stat. Phys.* **97**, 281–322.

Brey, J. J., Ruiz-Montero, M. & Moreno, F. 1997*b* Steady uniform shear flow in a low density granular gas. *Phys. Rev. E* **55** (3), 2846.

Brilliantov, N. V. & Pöschel, T. 2004 *Kinetic theory of granular gases*. Oxford University Press, Oxford.

Brilliantov, N. V. & Pöschel, T. 2006 Breakdown of the sonine expansion for the velocity distribution of granular gases. *Europhys. Lett.* **74** (3).

Brilliantov, N. V., Pöschel, T., Kranz, W. T. & Zippelius, A. 2007 Translations and rotations are correlated in granular gases. *Phys. Rev. Lett.* **98**, 128001.

Burnett, D. 1936 The distribution of molecular velocities and the mean motion in a non-uniform gas. *Proceedings of the London Mathematical Society* **2** (1), 382–435.

Cafiero, R., Luding, S. & Herrmann, H. J. 2002 Rotationally driven gas of inelastic rough spheres. *Europhys. Lett.* **60** (6), 854.

Campbell, C. S. 1990 Rapid granular flows. *Annu. Rev. Fluid Mech.* **22** (1), 57–90.

Cercignani, C. 1969 *Mathematical Methods in Kinetic Theory*. Plenum, New York.

Cercignani, C. 1975 *Theory and Application of the Boltzmann Equation*. Scottish Academic, Edinburgh.

Cercignani, C. 1988 *The Boltzmann Equation and Its Applications*. Springer, New York.

Cercignani, C. 2000 *Rarefied Gas Dynamics: From Basic Concepts to Actual Calculations*. Cambridge University Press, Cambridge.

Cercignani, C. & Daneri, A. 1963 Flow of a rarefied gas between two parallel plates. *J. Appl. Phys* **34**, 3509–3513.

Chapman, S. 1918 On the kinetic theory of a gas. part ii: a composite monatomic gas: diffusion, viscosity, and thermal conduction. *Philosophical Transactions of the Royal Society of London. Series A, Containing Papers of a Mathematical or Physical Character* **217**, 115–197.

Chapman, S. & Cowling, T. G. 1970 *The Mathematical Theory of Non-Uniform Gases*. Cambridge University Press, Cambridge.

Corwin, E. I., Jaeger, H. M. & Nagel, S. R. 2005 Structural signature of jamming in granular media. *Nature* **435**, 1075–1078.

Enskog, D. 1917 Theorie der Vorgänge in Massing Verdumten Gasen. PhD thesis, Ph. D thesis, University of Uppsala, Sweden.

Ernst, M., Dorfman, J., Hoegy, W. & Leeuwen, J. V. 1969 Hard-sphere dynamics and binary-collision operators. *Physica* **45** (1), 127 – 146.

Esipov, S. E. & Pöschel, T. 1997 The granular phase diagram. *J. Stat. Phys.* **86** (5), 1385–1395.

Ferziger, J. H. & Kaper, H. G. 1972 *Mathematical Theory of Transport Processes in Gases*. North-Holland Pub. Co., Amsterdam, London.

Forterre, Y. & Pouliquen, O. 2008 Flows of dense granular media. *Annu. Rev. Fluid Mech.* **40**, 1–24.

Garzó, V. & Dufty, J. W. 1999 Dense fluid transport for inelastic hard spheres. *Phys. Rev. E* **59** (5), 5895.

Garzó, V. & Dufty, J. W. 2002 Hydrodynamics for a granular binary mixture at low density. *Phys. Fluids* **14**, 1476–1490.

Garzó, V. & Santos, A. 2003 *Kinetic Theory of Gases in Shear Flows. Nonlinear Transport*. Springer Science and Business Media.

Garzó, V., Santos, A. & Brey, J. 1989 A kinetic model for a multicomponent gas. *Phys. Fluids A: Fluid Dyn.* **1** (2), 380–383.

Gayen, B. & Alam, M. 2006 Algebraic and exponential instabilities in a sheared micropolar granular fluid. *J. Fluid Mech.* **567**, 195–233.

Gayen, B. & Alam, M. 2008 Orientational correlation and velocity distributions in uniform shear flow of a dilute granular gas. *Phys. Rev. Lett.* **100**, 068002.

Gayen, B. & Alam, M. 2011 Effect of coulomb friction on orientational correlation and velocity distribution functions in a sheared dilute granular gas. *Phys. Rev. E* **84**, 021304.

Goldhirsch, I. 2003 Rapid granular flows. *Annu. Rev. Fluid Mech.* **35** (1), 267–293.

Goldhirsch, I., Noskowicz, S. H. & Bar-Lev, O. 2005 Nearly smooth granular gases. *Phys. Rev. Lett.* **95**, 068002.

Goldhirsch, I. & Zanetti, G. 1993 Clustering instability in dissipative gases. *Phys. Rev. Lett.* **70**, 1619–1622.

Goldman, E. & Sirovich, L. 1967 Equations for gas mixtures. *Phys. Fluids* **10**, 1928–1940.

Goldshtein, A. & Shapiro, M. 1995 Mechanics of collisional motion of granular materials. part 1. general hydrodynamic equations. *J. Fluid Mech.* **282**, 75–114.

Gombosi, T. I. 1994 *Gaskinetic Theory*. Cambridge University Press, Cambridge.

Grad, H. 1949*a* Note on N-dimensional hermite polynomials. *Commun. Pure Appl. Math* **2**, 325–330.

Grad, H. 1949*b* On the kinetic theory of rarefied gases. *Commun. Pure Appl. Math* **2**, 331–407.

Grad, H. 1958 Principles of the kinetic theory of gases. *Thermodynamik der Gase, Handbuch der Physik* **3/12**, 205–294.

Gupta, R. & Alam, M. 2017 Hydrodynamics, wall-slip, and normal-stress differences in rarefied granular Poiseuille flow. *Phys. Rev. E* **95**, 022903.

Haff, P. K. 1983 Grain flow as a fluid-mechanical phenomenon. *J. Fluid Mech.* **134**, 401–430.

Hagen, G. 1839 Uber die bewegung des wassers in engen cylindrischen rohren. *Annalen der Physik* **122** (3), 423–442.

Herbst, O., Cafiero, R., Zippelius, A., Herrmann, H. J. & Luding, S. 2005 A driven two-dimensional granular gas with coulomb friction. *Phys. Fluids* **17** (107102), 1–16.

Hess, S. & Mansour, M. M. 1999 Temperature profile of a dilute gas undergoing a plane Poiseuille flow. *Physica A* **272**, 481–496.

Holway, L. H. 1966 New statistical models for kinetic theory: Methods of construction. *Phys. Fluids* **9**, 1658–1673.

Hsiau, S. S., Wu, M. H. & Chen, C. H. 1998 Arching phenomena in a vibrated granular bed. *Powder Tech.* **99** (2), 185–193.

Huthmann, M. & Zippelius, A. 1997 Dynamics of inelastically colliding rough spheres: Relaxation of translational and rotational energy. *Phys. Rev. E* **56**, R6275–R6278.

Jaeger, H. M., Nagel, S. R. & Behringer, R. P. 1996 Granular solids, liquids, and gases. *Rev. Mod. Phys.* **68** (4), 1259–1273.

Jenkins, J. T. & Mancini, F. 1987 Balance laws and constitutive relations for plane flows of a dense, binary mixture of smooth, nearly elastic, circular disks. *J. Appl. Mech* **54**, 27–34.

Jenkins, J. T. & Richman, M. W. 1985 Kinetic theory for plane flows of a dense gas of identical, rough, inelastic, circular disks. *Phys. Fluids* **28** (12), 3485–3494.

Jenkins, J. T. & Zhang, C. 2002 Kinetic theory for identical, frictional, nearly elastic spheres. *Phys. Fluids* **14** (3), 1228–1235.

Kadanoff, L. P. 1999 Built upon sand: Theoretical ideas inspired by granular flows. *Rev. Mod. Phys.* **71**, 435–444.

Knudsen, M. 1909 Die gesetze der molekularstromung und der inneren reibungsstromung der gase durch rohren. *Ann. Phys* **28**, 75–130.

Kogan, M. N. 1969 *Rarefied Gas Dynamics*. Plenum, New York.

Kranz, W., Brilliantov, N., Pöschel, T. & Zippelius, A. 2009 Correlation of spin and velocity in the homogeneous cooling state of a granular gas of rough particles. *The European Physical Journal Special Topics* **179** (1), 91–111.

Kremer, G. M. 2010 *An Introduction to the Boltzmann Equation and Transport Processes in Gases*. Springer, Berlin.

Kremer, G. M. & Marques Jr, W. 2011 Fourteen moment theory for granular gases. *Kinetic and Related Models* **4**, 317–331.

Kudrolli, A., Wolpert, M. & Gollub, J. P. 1997 Cluster formation due to collisions in granular material. *Phys. Rev. Lett.* **78**, 1383–1386.

Luding, S. & Herrmann, H. J. 1999 Cluster-growth in freely cooling granular media. *Chaos* **9** (3), 673–681.

Luding, S., Huthmann, M., McNamara, S. & Zippelius, A. 1998 Homogeneous cooling of rough, dissipative particles: Theory and simulations. *Phys. Rev. E* **58**, 3416–3425.

Maass, C. C., Isert, N., Maret, G. & Aegerter, C. M. 2008 Experimental investigation of the freely cooling granular gas. *Phys. Rev. Lett.* **100**, 248001.

Mansour, M. M., Baras, F. & Garcia, A. L. 1997 On the validity of hydrodynamics in plane Poiseuille flows. *Physica A* **240**, 255–267.

Maw, N., Barber, J. & Fawcett, J. 1976 The oblique impact of elastic spheres. *Wear* **38** (1), 101 – 114.

McCormack, F. J. & Williams, A. M. 1972 Anisotropic relaxation in binary mixture of maxwell molecules. *The Phys. Fluids* **15** (6), 995–998.

McNamara, S. & Young, W. R. 1996 Dynamics of a freely evolving, two-dimensional granular medium. *Phys. Rev. E* **53**, 5089–5100.

Mitarai, N., Hayakawa, H. & Nakanishi, H. 2002 Collisional granular flow as a micropolar fluid. *Phys. Rev. Lett.* **88**, 174301.

Montanero, J., Garzó, V., Santos, A. & Brey, J. 1999 Kinetic theory of simple granular shear flows of smooth hard spheres. *J. Fluid Mech.* **389**, 391–411.

Montanero, J. M. & Garzó, V. 2002 Monte carlo simulation of the homogeneous cooling state for a granular mixture. *Gran. Matt.* **4** (1), 17–24.

Montanero, M. J. & Santos, A. 2000 Computer simulation of uniformly heated granular fluids. *Gran. Matt.* **2** (2), 53–64.

Müller, I. & Ruggeri, T. 1998 *Rational Extended Thermodynamics*. Springer, New York.

Nie, X., Ben-Naim, E. & Chen, S. 2002 Dynamics of freely cooling granular gases. *Phys. Rev. Lett.* **89**, 204301.

van Noije, T. & Ernst, M. 1998 Velocity distributions in homogeneous granular fluids: the free and the heated case. *Gran. Matt.* **1** (2), 57–64.

Ohwada, T., Sone, Y. & Aoki, K. 1989*a* Numerical analysis of the poiseuille and thermal transpiration flows between two parallel plates on the basis of the boltzmann equation for hard-sphere molecules. *Phys. Fluids A: Fluid Dyn.* **1** (12), 2042–2049.

Ohwada, T., Sone, Y. & Aoki, K. 1989*b* Numerical analysis of the shear and thermal creep flows of a rarefied gas over a plane wall on the basis of the linearized boltzmann equation for hard-sphere molecules. *Phys. Fluids A: Fluid Dyn.* **1** (9), 1588–1599.

Ottino, J. M. & Khakhar, D. V. 2000 Mixing and segregation of granular materials. *Annu. Rev. Fluid Mech.* **32**, 55–91.

Padé, H. 1892 Sur la representation approchée d'une fonction par des fractions rationelles. *Ann. de l'Ecole Normale Superieure suppl* pp. 1–93.

Pareschi, L., Russo, G. & Toscani, G. 2006 *(Eds.) Modelling and Numerics of Kinetic Dissipative Systems*. Nova Science Publishers, New York.

Pidduck, F. B. 1922 The kinetic theory of a special type of rigid molecule. *Proceedings of the Royal Society of London A: Mathematical, Physical and Engineering Sciences* **101** (708), 101–112.

Poiseuille, J. L. M. 1847 *Recherches expérimentales sur le mouvement des liquides de nature différente dans les tubes de très petits diamètres*. Bachelier.

Pöschel, T. & Brilliantov, N. V. 2003 *(Eds.) Granular Gas Dynamics*. Springer, Berlin.

Pöschel, T. & Luding, S. 2001 *(Eds.) Granular Gases*. Springer Science & Business Media.

Pozzi, A. 1994 *Applications of Padé Approximation theory in Fluid Dynamics*. World Scientific Publishing, Singapore.

Pulvirenti, A. & Toscani, G. 1996 The theory of the nonlinear boltzmann equation for maxwell molecules in fourier representation. *Annali di Matematica Pura ed Applicata* **171** (1), 181–204.

Rao, K. K. & Nott, P. R. 2008 *An Introduction to Granular Flow*. Cambridge University Press.

Reitebuch, D. & Weiss, W. 1999 Application of high moment theory to the plane Couette flow. *Continuum Mech. Thermodyn.* **11**, 217–225.

Reyes, F. V., Lasanta, A., Santos, A. & Garzó, V. 2017 Energy nonequipartition in gas mixtures of inelastic rough hard spheres: The tracer limit. *Phys. Rev. E* **96** (052901).

Reyes, F. V. & Santos, A. 2015 Steady state in a gas of inelastic rough spheres heated by a uniform stochastic force. *Phys. Fluids* **27** (113301).

Reyes, F. V., Santos, A. & Kremer, G. M. 2014 Role of roughness on the hydrodynamic homogeneous base state of inelastic spheres. *Phys. Rev. E* **89**, 020202.

Risso, D. & Cordero, P. 1998 Generalized hydrodynamics for a Poiseuille flow: theory and simulations. *Phys. Rev. E* **58**, 546–553.

Rongali, R. & Alam, M. 2014 Higher-order effects on orientational correlation and relaxation dynamics in homogeneous cooling of a rough granular gas. *Phys. Rev. E* **89**, 062201.

Sabbane, M., Tij, M. & Santos, A. 2003 Maxwellian gas undergoing a stationary Poiseuille flow in a pipe. *Physica A* **327**, 264–290.

Santos, A. 2003 Transport coefficients of d-dimensional inelastic maxwell models. *Physica A* **321**, 442–466.

Santos, A. 2008 Does the chapman–enskog expansion for sheared granular gases converge? *Phys. Rev. Lett.* **100** (7), 078003.

Santos, A. & Astillero, A. 2005 System of elastic hard spheres which mimics the transport properties of a granular gas. *Phys. Rev. E* **72** (3), 031308.

Santos, A., Brey, J. J. & Dufty, J. W. 1986 Divergence of the chapman-enskog expansion. *Phys. Rev. Lett.* **56** (15), 1571.

Santos, A., Kremer, G. M. & Garzó, V. 2010 Energy production rates in fluid mixtures of inelastic rough hard spheres. *Prog. Theor. Phys. Suppl.* **184**, 31–48.

Santos, A., Kremer, G. M. & dos Santos, M. 2011 Sonine approximation for collisional moments of granular gases of inelastic rough spheres. *Phys. Fluids* **23** (030604), 1–12.

Sela, N. & Goldhirsch, I. 1998 Hydrodynamic equations for rapid flows of smooth inelastic spheres, to burnett order. *J. Fluid Mech.* **361**, 41–74.

Serero, D., Goldhirsch, I., Noskowicz, S. H. & Tan, M.-L. 2006 Hydrodynamics of granular gases and granular gas mixtures. *J. Fluid Mech.* **554**, 237–258.

Shakhov, E. M. 1968 Generalization of the krook kinetic relaxation equation. *Fluid Dyn.* **3**, 95–96.

Shanks, D. 1955 Nonlinear transformation of divergent and slowly convergent sequences. *J. Math. Phys.* **34**, 1–42.

Sone, Y. 1966 Thermal creep in rarefied gas. *J. Phys. Soc. Jpn* **21**, 1836–1837.

Sone, Y. 1972 Flow induced by thermal stress in rarefied gas. *Phys. Fluids* **15**, 1418–1423.

Sone, Y. 2002 *Kinetic Theory and Fluid Dynamics*. Birkhauser, Boston.

Sone, Y., Ohwada, T. & Aoki, K. 1989 Temperature jump and knudsen layer in a rarefied gas over a plane wall: Numerical analysis of the linearized boltzmann equation for hard-sphere molecules. *Phys. Fluids A* **1**, 363–370.

Struchtrup, H. 2002 Heat transfer in the transition regime: Solution of boundary value problems for Grad's moment equations via kinetic schemes. *Phys. Rev. E* **65**, 041204.

Struchtrup, H. 2005 *Macroscopic Transport Equations for Rarefied Gas Flows*. Springer, Berlin.

Struchtrup, H. & Torrilhon, M. 2003 Regularization of grad's 13 moment equations: Derivation and linear analysis. *Phys. Fluids* **15**, 2668–2680.

Struchtrup, H. & Torrilhon, M. 2008 Higher-order effects in rarefied channel flows. *Phys. Rev. E* **78**, 046301.

Struchtrup, H. & Torrilhon, M. 2013 Regularized 13 moment equations for hard sphere molecules: Linear bulk equations. *Phys. Fluids* **25**, 052001.

Tatsumi, S., Murayama, Y., Hayakawa, H. & Sano, M. 2009 Experimental study on the kinetics of granular gases under microgravity. *J. Fluid Mech.* **641**, 521–539.

Tij, M., Sabbane, M. & Santos, A. 1998 Nonlinear Poiseuille flow in a gas. *Phys. Fluids* **10**, 1021–1027.

Tij, M. & Santos, A. 1994 Perturbation analysis of a stationary nonequilibrium flow generated by an external force. *J. Stat. Phys.* **76**, 1399–1414.

Tij, M. & Santos, A. 2001 Non-Newtonian Poiseuille flow of a gas in a pipe. *Physica A* **289**, 336–358.

Tij, M. & Santos, A. 2004 Poiseuille flow in a heated granular gas. *J. Stat. Phys.* **117**, 901–928.

Tij, M., Tahiri, E., Montanero, J., Garzó, V., Santos, A. & Dufty, J. 2001 Nonlinear couette flow in a low density granular gas. *J. Stat. Phys.* **103** (5-6), 1035–1068.

Todd, B. D. & Evans, D. J. 1997 Temperature profile for Poiseuille flow. *Phys. Rev. E* **55**, 2800–2807.

Travis, K. P., Todd, B. D. & Evans, D. J. 1997 Poiseuille flow of molecular fluids. *Physica A* **240**, 315–327.

Truesdell, C. & Muncaster, R. G. 1980 *Fundamentals of Maxwell's Kinetic Theory of a Simple Monatomic Gas*. Academic Press, New York.

Uribe, F. J. & Garcia, A. L. 1999 Burnett description for plane Poiseuille flow. *Phys. Rev. E* **60**, 4063–4078.

Weiss, W. 1995 Continuous shock structure in extended thermodynamics. *Phys. Rev. E* **52**, 5760–5763.

Appendix A

Supplementary Material to Chapter 2

A.1 Derivation of Evolution Equations for Dynamical Variables

In Chapter 2, we have outlined the procedure to derive the evolution equation for $T(t)$; the equation for $R(t)$ is derived following the same route. To derive evolution equations for the first three Legendre coefficients $b_{112}(t)$, $b_{122}(t)$ and $b_{212}(t)$, we define the following auxiliary variable

$$\left\langle \Delta^{(\alpha\beta 2)} \right\rangle \equiv \left\langle \frac{2}{3N} \sum_{i=1}^{N} \boldsymbol{c}_i^{2\alpha} \boldsymbol{\omega}_i^{2\beta} P_2(\cos\theta_i) \right\rangle, \tag{A.1}$$

which, with the aid of the definition of ensemble average of a dynamic variable (using Eq. (2.14)), simplify to:

$$\left\langle \Delta^{(112)} \right\rangle = 30\left(\frac{T^2R^2}{m^2\mathcal{I}^2}\right)\left[b_{112}(t) + \frac{7R(t)}{\mathcal{I}} b_{122}(t) + \frac{7T(t)}{m} b_{212}(t)\right], \tag{A.2}$$

$$\left\langle \Delta^{(122)} \right\rangle = 210\left(\frac{T^2R^2}{m^2\mathcal{I}^2}\right)\left(\frac{R}{\mathcal{I}}\right)\left[b_{112}(t) + \frac{9R(t)}{\mathcal{I}} b_{122}(t) + \frac{7T(t)}{m} b_{212}(t)\right], \tag{A.3}$$

$$\left\langle \Delta^{(212)} \right\rangle = 210\left(\frac{T^2R^2}{m^2\mathcal{I}^2}\right)\left(\frac{T}{m}\right)\left[b_{112}(t) + \frac{7R(t)}{\mathcal{I}} b_{122}(t) + \frac{9T(t)}{m} b_{212}(t)\right]. \tag{A.4}$$

Differentiating above equations (A.2)-(A.4), we have

$$\begin{aligned}\frac{\mathrm{d}}{\mathrm{d}t}\left\langle \Delta^{(112)} \right\rangle = \frac{30TR}{m^2\mathcal{I}^2}\Bigg[TR\left(\dot{b}_{112}(t) + \frac{7R}{\mathcal{I}}\dot{b}_{122}(t) + \frac{7}{\mathcal{I}} b_{122}(t)\dot{R} + \frac{7T}{m}\dot{b}_{212}(t) + \frac{7}{m} b_{212}(t)\dot{T}\right) \\ +2\left(b_{112}(t) + \frac{7R}{\mathcal{I}} b_{122}(t) + \frac{7T}{m} b_{212}(t)\right)(T\dot{R} + R\dot{T})\Bigg],\end{aligned} \tag{A.5}$$

$$\begin{aligned}\frac{\mathrm{d}}{\mathrm{d}t}\left\langle \Delta^{(122)} \right\rangle = \frac{210TR^2}{m^2\mathcal{I}^3}\Bigg[TR\left(\dot{b}_{112}(t) + \frac{9R}{\mathcal{I}}\dot{b}_{122}(t) + \frac{9}{\mathcal{I}} b_{122}(t)\dot{R} + \frac{7T}{m}\dot{b}_{212}(t) + \frac{7}{m} b_{212}(t)\dot{T}\right) \\ +\left(b_{112}(t) + \frac{9R}{\mathcal{I}} b_{122}(t) + \frac{7T}{m} b_{212}(t)\right)(3T\dot{R} + 2R\dot{T})\Bigg],\end{aligned} \tag{A.6}$$

$$\begin{aligned}\frac{\mathrm{d}}{\mathrm{d}t}\left\langle \Delta^{(212)} \right\rangle = \frac{210T^2R}{m^3\mathcal{I}^2}\Bigg[TR\left(\dot{b}_{112}(t) + \frac{7R}{\mathcal{I}}\dot{b}_{122}(t) + \frac{7}{\mathcal{I}} b_{122}(t)\dot{R} + \frac{9T}{m}\dot{b}_{212}(t) + \frac{9}{m} b_{212}(t)\dot{T}\right) \\ +\left(b_{112}(t) + \frac{7R}{\mathcal{I}} b_{122}(t) + \frac{9T}{m} b_{212}(t)\right)(2T\dot{R} + 3R\dot{T})\Bigg],\end{aligned} \tag{A.7}$$

where an over-dot refers to time derivative. From the master equation (Eqn. (2.15)), we have

$$\frac{\mathrm{d}}{\mathrm{d}t}\left\langle \Delta^{(112)} \right\rangle = \left\langle \mathcal{L}\Delta^{(112)} \right\rangle, \tag{A.8}$$

$$\frac{\mathrm{d}}{\mathrm{d}t}\left\langle \Delta^{(122)} \right\rangle = \left\langle \mathcal{L}\Delta^{(122)} \right\rangle, \tag{A.9}$$

$$\frac{\mathrm{d}}{\mathrm{d}t}\left\langle \Delta^{(212)} \right\rangle = \left\langle \mathcal{L}\Delta^{(212)} \right\rangle. \tag{A.10}$$

The right hand side of each of the above equations can decomposed into four parts (see below):

$$\begin{aligned}\left\langle \mathcal{L}\Delta^{(112)}\right\rangle &= \left\langle (\mathcal{B}_{12}-1)\Delta^{(112)}\right\rangle^{(0)} + b_{112}(t)\left\langle (\mathcal{B}_{12}-1)\Delta^{(112)}\right\rangle^{(1)} \\ &\quad + b_{122}(t)\left\langle (\mathcal{B}_{12}-1)\Delta^{(112)}\right\rangle^{(2)} + b_{212}(t)\left\langle (\mathcal{B}_{12}-1)\Delta^{(112)}\right\rangle^{(3)}, \end{aligned} \tag{A.11}$$

$$\begin{aligned}\left\langle \mathcal{L}\Delta^{(122)}\right\rangle &= \left\langle (\mathcal{B}_{12}-1)\Delta^{(122)}\right\rangle^{(0)} + b_{112}(t)\left\langle (\mathcal{B}_{12}-1)\Delta^{(122)}\right\rangle^{(1)} \\ &\quad + b_{122}(t)\left\langle (\mathcal{B}_{12}-1)\Delta^{(122)}\right\rangle^{(2)} + b_{212}(t)\left\langle (\mathcal{B}_{12}-1)\Delta^{(122)}\right\rangle^{(3)}, \end{aligned} \tag{A.12}$$

$$\begin{aligned}\left\langle \mathcal{L}\Delta^{(212)}\right\rangle &= \left\langle (\mathcal{B}_{12}-1)\Delta^{(212)}\right\rangle^{(0)} + b_{112}(t)\left\langle (\mathcal{B}_{12}-1)\Delta^{(212)}\right\rangle^{(1)} \\ &\quad + b_{122}(t)\left\langle (\mathcal{B}_{12}-1)\Delta^{(212)}\right\rangle^{(2)} + b_{212}(t)\left\langle (\mathcal{B}_{12}-1)\Delta^{(212)}\right\rangle^{(3)}. \end{aligned} \tag{A.13}$$

The evaluation of above average terms are taken in the next section.

A.2 Procedure to Evaluate Averages of the Form $\left\langle (\mathcal{B}_{12}-1)\Delta^{(\alpha\beta 2)}\right\rangle^{(k)}$

Adopting the assumption of molecular chaos and carrying out integrations over the spatial degrees of freedom, we can write

$$\begin{aligned}\left\langle \mathcal{L}\Delta^{(\alpha\beta 2)}\right\rangle &= \nu\, N \int_{c_1}\int_{c_2}\int_{\omega_1}\int_{\omega_2} (\hat{\boldsymbol{n}}\cdot\boldsymbol{c}_{12})\Theta(-\hat{\boldsymbol{n}}\cdot\boldsymbol{c}_{12}) \\ &\quad \times[1 + b_{112}(t)\boldsymbol{c}_1^2\boldsymbol{\omega}_1^2 P_2(\cos\theta_1) + b_{122}(t)\boldsymbol{c}_1^2\boldsymbol{\omega}_1^4 P_2(\cos\theta_1) + b_{212}(t)\boldsymbol{c}_1^4\boldsymbol{\omega}_1^2 P_2(\cos\theta_1)] \\ &\quad \times[1 + b_{112}(t)\boldsymbol{c}_2^2\boldsymbol{\omega}_2^2 P_2(\cos\theta_2) + b_{122}(t)\boldsymbol{c}_2^2\boldsymbol{\omega}_2^4 P_2(\cos\theta_2) + b_{212}(t)\boldsymbol{c}_2^4\boldsymbol{\omega}_2^2 P_2(\cos\theta_2)] \\ &\quad \times(\mathcal{B}_{12}-1)\Delta^{(\alpha\beta 2)}. \end{aligned} \tag{A.14}$$

In the above, $\hat{\boldsymbol{n}}$ is an arbitrary fixed unit vector, $\nu = -8\pi n a^2 g_2(2a)$ and the following shorthand notations have been used:

$$\int_{c_i} \equiv \left(\frac{m}{2\pi T}\right)^{\frac{3}{2}} \int d^3c_i \exp\left(-\frac{m\boldsymbol{c}_i^2}{2T}\right) \quad \text{and} \quad \int_{\omega_i} \equiv \left(\frac{\mathcal{I}}{2\pi R}\right)^{\frac{3}{2}} \int d^3\omega_i \exp\left(-\frac{\mathcal{I}\boldsymbol{\omega}_i^2}{2R}\right). \tag{A.15}$$

To arrive at Eq. (A.14), we have integrated over the spatial degrees of freedom (since the HCS is spatially homogeneous) and used the definition of the pair correlation function

$$g_2(r_{12}) = \frac{N(N-1)}{n^2}\int g_N(\boldsymbol{r}_1,\ldots,\boldsymbol{r}_N)\Pi_{i=3}^N d\boldsymbol{r}_i, \tag{A.16}$$

where n is the number density of the particles.

Neglecting quadratic nonlinearities in Eq. (A.14), it is now clear that the term $\langle \mathcal{L}\Delta^{(\alpha\beta 2)}\rangle$ can be decomposed into four parts:

$$\begin{aligned}\left\langle \mathcal{L}\Delta^{(\alpha\beta 2)}\right\rangle &= \left\langle (\mathcal{B}_{12}-1)\Delta^{(\alpha\beta 2)}\right\rangle^{(0)} + b_{112}(t)\left\langle (\mathcal{B}_{12}-1)\Delta^{(\alpha\beta 2)}\right\rangle^{(1)} \\ &\quad + b_{122}(t)\left\langle (\mathcal{B}_{12}-1)\Delta^{(\alpha\beta 2)}\right\rangle^{(2)} + b_{212}(t)\left\langle (\mathcal{B}_{12}-1)\Delta^{(\alpha\beta 2)}\right\rangle^{(3)} + O\left(b_{\alpha\beta 2}^2\right). \end{aligned} \tag{A.17}$$

Each average term (denoted by superscripts 0, 1, 2, 3), for any function $\mathcal{F}$, is defined as

$$\begin{aligned}\langle \mathcal{F}\rangle^{(0)} &= \nu\int_{c_1}\int_{c_2}\int_{\omega_1}\int_{\omega_2} (\hat{\boldsymbol{n}}\cdot\boldsymbol{c}_{12})\Theta(-\hat{\boldsymbol{n}}\cdot\boldsymbol{c}_{12})\mathcal{F} \\ &= \sqrt{2}\,\nu\int_v\int_V\int_\omega\int_\Omega (\hat{\boldsymbol{n}}\cdot\boldsymbol{v})\Theta(-\hat{\boldsymbol{n}}\cdot\boldsymbol{v})\ \mathcal{F}, \end{aligned} \tag{A.18}$$

$$\begin{aligned}\langle\mathcal{F}\rangle^{(1)} &= \nu\int_{c_1}\int_{c_2}\int_{\omega_1}\int_{\omega_2}(\hat{\boldsymbol{n}}\cdot\boldsymbol{c}_{12})\Theta(-\hat{\boldsymbol{n}}\cdot\boldsymbol{c}_{12})[\boldsymbol{c}_1^2\boldsymbol{\omega}_1^2P_2(\cos\theta_1)+\boldsymbol{c}_2^2\boldsymbol{\omega}_2^2P_2(\cos\theta_2)]\;\mathcal{F}\\ &= \frac{3\sqrt{2}}{4}\,\nu\int_v\int_V\int_\omega\int_\Omega(\hat{\boldsymbol{n}}\cdot\boldsymbol{v})\Theta(-\hat{\boldsymbol{n}}\cdot\boldsymbol{v})\Big[(\boldsymbol{v}\cdot\boldsymbol{\omega})^2+(\boldsymbol{v}\cdot\boldsymbol{\Omega})^2+(\boldsymbol{V}\cdot\boldsymbol{\omega})^2+(\boldsymbol{V}\cdot\boldsymbol{\Omega})^2\\ &\quad -\frac{1}{3}(\boldsymbol{v}^2+\boldsymbol{V}^2)(\boldsymbol{\omega}^2+\boldsymbol{\Omega}^2)+2(\boldsymbol{v}\cdot\boldsymbol{\Omega})(\boldsymbol{V}\cdot\boldsymbol{\omega})+2(\boldsymbol{v}\cdot\boldsymbol{\omega})(\boldsymbol{V}\cdot\boldsymbol{\Omega})-\frac{4}{3}(\boldsymbol{v}\cdot\boldsymbol{V})(\boldsymbol{\omega}\cdot\boldsymbol{\Omega})\Big]\;\mathcal{F},\end{aligned}\tag{A.19}$$

$$\begin{aligned}\langle\mathcal{F}\rangle^{(2)} &= \nu\int_{c_1}\int_{c_2}\int_{\omega_1}\int_{\omega_2}(\hat{\boldsymbol{n}}\cdot\boldsymbol{c}_{12})\Theta(-\hat{\boldsymbol{n}}\cdot\boldsymbol{c}_{12})[\boldsymbol{c}_1^2\boldsymbol{\omega}_1^4P_2(\cos\theta_1)+\boldsymbol{c}_2^2\boldsymbol{\omega}_2^4P_2(\cos\theta_2)]\;\mathcal{F}\\ &= \frac{3\sqrt{2}}{8}\,\nu\int_v\int_V\int_\omega\int_\Omega(\hat{\boldsymbol{n}}\cdot\boldsymbol{v})\Theta(-\hat{\boldsymbol{n}}\cdot\boldsymbol{v})\Big[(\boldsymbol{\omega}^2+\boldsymbol{\Omega}^2)\Big((\boldsymbol{v}\cdot\boldsymbol{\omega})^2+(\boldsymbol{v}\cdot\boldsymbol{\Omega})^2+(\boldsymbol{V}\cdot\boldsymbol{\omega})^2\\ &\quad +(\boldsymbol{V}\cdot\boldsymbol{\Omega})^2-\frac{1}{3}(\boldsymbol{v}^2+\boldsymbol{V}^2)(\boldsymbol{\omega}^2+\boldsymbol{\Omega}^2)+2(\boldsymbol{v}\cdot\boldsymbol{\Omega})(\boldsymbol{V}\cdot\boldsymbol{\omega})+2(\boldsymbol{v}\cdot\boldsymbol{\omega})(\boldsymbol{V}\cdot\boldsymbol{\Omega})\Big)\\ &\quad +4(\boldsymbol{\omega}\cdot\boldsymbol{\Omega})\Big((\boldsymbol{v}\cdot\boldsymbol{\omega})(\boldsymbol{v}\cdot\boldsymbol{\Omega})+(\boldsymbol{V}\cdot\boldsymbol{\Omega})(\boldsymbol{V}\cdot\boldsymbol{\omega})+(\boldsymbol{v}\cdot\boldsymbol{\omega})(\boldsymbol{V}\cdot\boldsymbol{\omega})+(\boldsymbol{v}\cdot\boldsymbol{\Omega})(\boldsymbol{V}\cdot\boldsymbol{\Omega})\\ &\quad -\frac{1}{3}(\boldsymbol{v}^2+\boldsymbol{V}^2)(\boldsymbol{\omega}\cdot\boldsymbol{\Omega})-\frac{2}{3}(\boldsymbol{\omega}^2+\boldsymbol{\Omega}^2)(\boldsymbol{v}\cdot\boldsymbol{V})\Big)\Big]\;\mathcal{F},\end{aligned}\tag{A.20}$$

$$\begin{aligned}\langle\mathcal{F}\rangle^{(3)} &= \nu\int_{c_1}\int_{c_2}\int_{\omega_1}\int_{\omega_2}(\hat{\boldsymbol{n}}\cdot\boldsymbol{c}_{12})\Theta(-\hat{\boldsymbol{n}}\cdot\boldsymbol{c}_{12})[\boldsymbol{c}_1^4\boldsymbol{\omega}_1^2P_2(\cos\theta_1)+\boldsymbol{c}_2^4\boldsymbol{\omega}_2^2P_2(\cos\theta_2)]\;\mathcal{F}\\ &= \frac{3\sqrt{2}}{8}\,\nu\int_v\int_V\int_\omega\int_\Omega(\hat{\boldsymbol{n}}\cdot\boldsymbol{v})\Theta(-\hat{\boldsymbol{n}}\cdot\boldsymbol{v})\Big[(\boldsymbol{v}^2+\boldsymbol{V}^2)\Big((\boldsymbol{v}\cdot\boldsymbol{\omega})^2+(\boldsymbol{v}\cdot\boldsymbol{\Omega})^2+(\boldsymbol{V}\cdot\boldsymbol{\omega})^2\\ &\quad +(\boldsymbol{V}\cdot\boldsymbol{\Omega})^2-\frac{1}{3}(\boldsymbol{v}^2+\boldsymbol{V}^2)(\boldsymbol{\omega}^2+\boldsymbol{\Omega}^2)+2(\boldsymbol{v}\cdot\boldsymbol{\Omega})(\boldsymbol{V}\cdot\boldsymbol{\omega})+2(\boldsymbol{v}\cdot\boldsymbol{\omega})(\boldsymbol{V}\cdot\boldsymbol{\Omega})\Big)\\ &\quad +4(\boldsymbol{v}\cdot\boldsymbol{V})\Big((\boldsymbol{v}\cdot\boldsymbol{\omega})(\boldsymbol{v}\cdot\boldsymbol{\Omega})+(\boldsymbol{V}\cdot\boldsymbol{\Omega})(\boldsymbol{V}\cdot\boldsymbol{\omega})+(\boldsymbol{v}\cdot\boldsymbol{\omega})(\boldsymbol{V}\cdot\boldsymbol{\omega})+(\boldsymbol{v}\cdot\boldsymbol{\Omega})(\boldsymbol{V}\cdot\boldsymbol{\Omega})\\ &\quad -\frac{2}{3}(\boldsymbol{v}^2+\boldsymbol{V}^2)(\boldsymbol{\omega}\cdot\boldsymbol{\Omega})-\frac{1}{3}(\boldsymbol{\omega}^2+\boldsymbol{\Omega}^2)(\boldsymbol{v}\cdot\boldsymbol{V})\Big)\Big]\;\mathcal{F}.\end{aligned}\tag{A.21}$$

In the second line of each integral above, we have introduced new integration variables:

$$\boldsymbol{v}\equiv\frac{\boldsymbol{c}_1-\boldsymbol{c}_2}{\sqrt{2}}=\frac{\boldsymbol{c}_{12}}{\sqrt{2}},\quad \boldsymbol{V}\equiv\frac{(\boldsymbol{c}_1+\boldsymbol{c}_2)}{\sqrt{2}},\quad \boldsymbol{\omega}\equiv\frac{\boldsymbol{\omega}_1-\boldsymbol{\omega}_2}{\sqrt{2}}=\frac{\boldsymbol{\omega}_{12}}{\sqrt{2}},\quad \boldsymbol{\Omega}\equiv\frac{(\boldsymbol{\omega}_1+\boldsymbol{\omega}_2)}{\sqrt{2}}.\tag{A.22}$$

Let us define

$$\Delta^{(\alpha\beta 2)}=\Delta_A^{(\alpha\beta 2)}-\frac{\Delta_B^{(\alpha\beta 2)}}{3},\tag{A.23}$$

where

$$\Delta_A^{(\alpha\beta 2)}\equiv\sum_i(\boldsymbol{c}_i\cdot\boldsymbol{\omega}_i)^2\left((\alpha-1)\boldsymbol{c}_i^2+(\beta-1)\boldsymbol{\omega}_i^2+\delta_{\alpha\beta}\right)\quad\text{and}\quad\Delta_B^{(\alpha\beta 2)}\equiv\sum_i\boldsymbol{c}_i^{2\alpha}\boldsymbol{\omega}_i^{2\beta}.\tag{A.24}$$

Applying the collision rule to $\Delta_A^{(112)}$ and $\Delta_B^{(112)}$ we obtain

$$\begin{aligned}(\mathcal{B}_{12}-1)\Delta_A^{(112)} &= (\boldsymbol{\delta}\cdot\boldsymbol{\omega})^2+(\boldsymbol{\delta}\cdot\boldsymbol{\Omega})^2+\frac{1}{q^2a^2}[(\hat{\boldsymbol{n}}\times\boldsymbol{\delta})\cdot\boldsymbol{v}]^2+\frac{1}{q^2a^2}[(\hat{\boldsymbol{n}}\times\boldsymbol{\delta})\cdot\boldsymbol{V}]^2-\sqrt{2}(\boldsymbol{\delta}\cdot\boldsymbol{\Omega})(\boldsymbol{v}\cdot\boldsymbol{\Omega})\\ &\quad -\sqrt{2}\;(\boldsymbol{\delta}\cdot\boldsymbol{\Omega})(\boldsymbol{V}\cdot\boldsymbol{\omega})-\sqrt{2}\;(\boldsymbol{\delta}\cdot\boldsymbol{\omega})(\boldsymbol{v}\cdot\boldsymbol{\omega})-\sqrt{2}(\boldsymbol{\delta}\cdot\boldsymbol{\omega})(\boldsymbol{V}\cdot\boldsymbol{\Omega})\\ &\quad +\frac{\sqrt{2}}{qa}(\boldsymbol{v}\cdot\boldsymbol{\Omega})((\hat{\boldsymbol{n}}\times\boldsymbol{\delta})\cdot\boldsymbol{v})+\frac{\sqrt{2}}{qa}(\boldsymbol{V}\cdot\boldsymbol{\omega})((\hat{\boldsymbol{n}}\times\boldsymbol{\delta})\cdot\boldsymbol{v})+\frac{\sqrt{2}}{qa}(\boldsymbol{v}\cdot\boldsymbol{\omega})((\hat{\boldsymbol{n}}\times\boldsymbol{\delta})\cdot\boldsymbol{V})\\ &\quad +\frac{\sqrt{2}}{qa}(\boldsymbol{V}\cdot\boldsymbol{\Omega})((\hat{\boldsymbol{n}}\times\boldsymbol{\delta})\cdot\boldsymbol{V})-\frac{2}{qa}(\boldsymbol{\delta}\cdot\boldsymbol{\Omega})((\hat{\boldsymbol{n}}\times\boldsymbol{\delta})\cdot\boldsymbol{v})-\frac{2}{qa}(\boldsymbol{\delta}\cdot\boldsymbol{\omega})((\hat{\boldsymbol{n}}\times\boldsymbol{\delta})\cdot\boldsymbol{V})\end{aligned}\tag{A.25}$$

$$\begin{aligned}(\mathcal{B}_{12}-1)\Delta_B^{(112)} &= \frac{1}{q^2a^2}(\hat{\boldsymbol{n}}\times\boldsymbol{\delta})^2(\boldsymbol{v}^2+\boldsymbol{V}^2)+\frac{\sqrt{2}}{qa}[2((\hat{\boldsymbol{n}}\times\boldsymbol{\delta})\cdot\boldsymbol{\omega})(\boldsymbol{v}\cdot\boldsymbol{V})+((\hat{\boldsymbol{n}}\times\boldsymbol{\delta})\cdot\boldsymbol{\Omega})(\boldsymbol{v}^2+\boldsymbol{V}^2)]\\ &\quad +\boldsymbol{\delta}^2(\boldsymbol{\omega}^2+\boldsymbol{\Omega}^2)+\frac{2\boldsymbol{\delta}^2}{q^2a^2}(\hat{\boldsymbol{n}}\times\boldsymbol{\delta})^2+\frac{2\sqrt{2}}{qa}\boldsymbol{\delta}^2((\hat{\boldsymbol{n}}\times\boldsymbol{\delta})\cdot\boldsymbol{\Omega})-2\sqrt{2}(\boldsymbol{\delta}\cdot\boldsymbol{V})(\boldsymbol{\omega}\cdot\boldsymbol{\Omega})-\sqrt{2}(\boldsymbol{\delta}\cdot\boldsymbol{v})(\boldsymbol{\omega}^2+\boldsymbol{\Omega}^2)\\ &\quad -\frac{2\sqrt{2}}{q^2a^2}(\hat{\boldsymbol{n}}\times\boldsymbol{\delta})^2(\boldsymbol{\delta}\cdot\boldsymbol{v})-\frac{4}{qa}[((\hat{\boldsymbol{n}}\times\boldsymbol{\delta})\cdot\boldsymbol{\omega})(\boldsymbol{\delta}\cdot\boldsymbol{V})+((\hat{\boldsymbol{n}}\times\boldsymbol{\delta})\cdot\boldsymbol{\Omega})(\boldsymbol{\delta}\cdot\boldsymbol{v})].\end{aligned}\tag{A.26}$$

Applying the collision rule to $\Delta_A^{(122)}$ and $\Delta_B^{(122)}$ we obtain

$$
\begin{aligned}
(\mathcal{B}_{12}-1)\Delta_A^{(122)} \;=\;& \frac{1}{q^2a^2}(\hat{\boldsymbol{n}}\times\boldsymbol{\delta})^2[(\boldsymbol{c}_1\cdot\boldsymbol{\omega}_1)^2+(\boldsymbol{c}_2\cdot\boldsymbol{\omega}_2)^2]+\frac{2}{qa}[(\boldsymbol{c}_1\cdot\boldsymbol{\omega}_1)^2((\hat{\boldsymbol{n}}\times\boldsymbol{\delta})\cdot\boldsymbol{\omega}_1)+(\boldsymbol{c}_2\cdot\boldsymbol{\omega}_2)^2((\hat{\boldsymbol{n}}\times\boldsymbol{\delta})\cdot\boldsymbol{\omega}_2)]\\
&+[(\boldsymbol{\delta}\cdot\boldsymbol{\omega}_1)^2\boldsymbol{\omega}_1^2+(\boldsymbol{\delta}\cdot\boldsymbol{\omega}_2)^2\boldsymbol{\omega}_2^2]+\frac{1}{q^2a^2}(\hat{\boldsymbol{n}}\times\boldsymbol{\delta})^2[(\boldsymbol{\delta}\cdot\boldsymbol{\omega}_1)^2+(\boldsymbol{\delta}\cdot\boldsymbol{\omega}_2)^2]\\
&+\frac{2}{qa}[(\boldsymbol{\delta}\cdot\boldsymbol{\omega}_1)^2((\hat{\boldsymbol{n}}\times\boldsymbol{\delta})\cdot\boldsymbol{\omega}_1)+(\boldsymbol{\delta}\cdot\boldsymbol{\omega}_2)^2((\hat{\boldsymbol{n}}\times\boldsymbol{\delta})\cdot\boldsymbol{\omega}_2)]+\frac{1}{q^2a^2}[((\hat{\boldsymbol{n}}\times\boldsymbol{\delta})\cdot\boldsymbol{c}_1)^2\boldsymbol{\omega}_1^2+((\hat{\boldsymbol{n}}\times\boldsymbol{\delta})\cdot\boldsymbol{c}_2)^2\boldsymbol{\omega}_2^2]\\
&+\frac{1}{q^4a^4}(\hat{\boldsymbol{n}}\times\boldsymbol{\delta})^2[((\hat{\boldsymbol{n}}\times\boldsymbol{\delta})\cdot\boldsymbol{c}_1)^2+((\hat{\boldsymbol{n}}\times\boldsymbol{\delta})\cdot\boldsymbol{c}_2)^2]\\
&+\frac{2}{q^3a^3}[((\hat{\boldsymbol{n}}\times\boldsymbol{\delta})\cdot\boldsymbol{c}_1)^2((\hat{\boldsymbol{n}}\times\boldsymbol{\delta})\cdot\boldsymbol{\omega}_1)+((\hat{\boldsymbol{n}}\times\boldsymbol{\delta})\cdot\boldsymbol{c}_2)^2((\hat{\boldsymbol{n}}\times\boldsymbol{\delta})\cdot\boldsymbol{\omega}_2)]\\
&+2[(\boldsymbol{c}_2\cdot\boldsymbol{\omega}_2)(\boldsymbol{\delta}\cdot\boldsymbol{\omega}_2)\boldsymbol{\omega}_2^2-(\boldsymbol{c}_1\cdot\boldsymbol{\omega}_1)(\boldsymbol{\delta}\cdot\boldsymbol{\omega}_1)\boldsymbol{\omega}_1^2]+\frac{2}{q^2a^2}(\hat{\boldsymbol{n}}\times\boldsymbol{\delta})^2[(\boldsymbol{c}_2\cdot\boldsymbol{\omega}_2)(\boldsymbol{\delta}\cdot\boldsymbol{\omega}_2)-(\boldsymbol{c}_1\cdot\boldsymbol{\omega}_1)(\boldsymbol{\delta}\cdot\boldsymbol{\omega}_1)]\\
&+\frac{4}{qa}[(\boldsymbol{c}_2\cdot\boldsymbol{\omega}_2)(\boldsymbol{\delta}\cdot\boldsymbol{\omega}_2)((\hat{\boldsymbol{n}}\times\boldsymbol{\delta})\cdot\boldsymbol{\omega}_2)-(\boldsymbol{c}_1\cdot\boldsymbol{\omega}_1)(\boldsymbol{\delta}\cdot\boldsymbol{\omega}_1)((\hat{\boldsymbol{n}}\times\boldsymbol{\delta})\cdot\boldsymbol{\omega}_1)]\\
&+\frac{2}{qa}[(\boldsymbol{\delta}\cdot\boldsymbol{\omega}_2)((\hat{\boldsymbol{n}}\times\boldsymbol{\delta})\cdot\boldsymbol{c}_2)\boldsymbol{\omega}_2^2-(\boldsymbol{\delta}\cdot\boldsymbol{\omega}_1)((\hat{\boldsymbol{n}}\times\boldsymbol{\delta})\cdot\boldsymbol{c}_1)\boldsymbol{\omega}_1^2]\\
&+\frac{2}{q^3a^3}(\hat{\boldsymbol{n}}\times\boldsymbol{\delta})^2[(\boldsymbol{\delta}\cdot\boldsymbol{\omega}_2)((\hat{\boldsymbol{n}}\times\boldsymbol{\delta})\cdot\boldsymbol{c}_2)-(\boldsymbol{\delta}\cdot\boldsymbol{\omega}_1)((\hat{\boldsymbol{n}}\times\boldsymbol{\delta})\cdot\boldsymbol{c}_1)]\\
&+\frac{4}{q^2a^2}[(\boldsymbol{\delta}\cdot\boldsymbol{\omega}_2)((\hat{\boldsymbol{n}}\times\boldsymbol{\delta})\cdot\boldsymbol{c}_2)((\hat{\boldsymbol{n}}\times\boldsymbol{\delta})\cdot\boldsymbol{\omega}_2)-(\boldsymbol{\delta}\cdot\boldsymbol{\omega}_1)((\hat{\boldsymbol{n}}\times\boldsymbol{\delta})\cdot\boldsymbol{c}_1)((\hat{\boldsymbol{n}}\times\boldsymbol{\delta})\cdot\boldsymbol{\omega}_1)]\\
&+\frac{2}{qa}[(\boldsymbol{c}_1\cdot\boldsymbol{\omega}_1)((\hat{\boldsymbol{n}}\times\boldsymbol{\delta})\cdot\boldsymbol{c}_1)\boldsymbol{\omega}_1^2+(\boldsymbol{c}_2\cdot\boldsymbol{\omega}_2)((\hat{\boldsymbol{n}}\times\boldsymbol{\delta})\cdot\boldsymbol{c}_2)\boldsymbol{\omega}_2^2]\\
&+\frac{2}{q^3a^3}(\hat{\boldsymbol{n}}\times\boldsymbol{\delta})^2[(\boldsymbol{c}_1\cdot\boldsymbol{\omega}_1)((\hat{\boldsymbol{n}}\times\boldsymbol{\delta})\cdot\boldsymbol{c}_1)+(\boldsymbol{c}_2\cdot\boldsymbol{\omega}_2)((\hat{\boldsymbol{n}}\times\boldsymbol{\delta})\cdot\boldsymbol{c}_2)]\\
&+\frac{4}{q^2a^2}[(\boldsymbol{c}_1\cdot\boldsymbol{\omega}_1)((\hat{\boldsymbol{n}}\times\boldsymbol{\delta})\cdot\boldsymbol{c}_1)((\hat{\boldsymbol{n}}\times\boldsymbol{\delta})\cdot\boldsymbol{\omega}_1)+(\boldsymbol{c}_2\cdot\boldsymbol{\omega}_2)((\hat{\boldsymbol{n}}\times\boldsymbol{\delta})\cdot\boldsymbol{c}_2)((\hat{\boldsymbol{n}}\times\boldsymbol{\delta})\cdot\boldsymbol{\omega}_2)]. \qquad \text{(A.27)}
\end{aligned}
$$

$$
\begin{aligned}
(\mathcal{B}_{12}-1)\Delta_B^{(122)} \;=\;& \frac{1}{q^4a^4}(\hat{\boldsymbol{n}}\times\boldsymbol{\delta})^4[\boldsymbol{c}_1^2+\boldsymbol{c}_2^2]+\frac{4}{q^2a^2}[\boldsymbol{c}_1^2((\hat{\boldsymbol{n}}\times\boldsymbol{\delta})\cdot\boldsymbol{\omega}_1)^2+\boldsymbol{c}_2^2((\hat{\boldsymbol{n}}\times\boldsymbol{\delta})\cdot\boldsymbol{\omega}_2)^2]\\
&+\frac{2}{q^2a^2}(\hat{\boldsymbol{n}}\times\boldsymbol{\delta})^2[\boldsymbol{c}_1^2\boldsymbol{\omega}_1^2+\boldsymbol{c}_2^2\boldsymbol{\omega}_2^2]+\frac{4}{q^3a^3}(\hat{\boldsymbol{n}}\times\boldsymbol{\delta})^2[\boldsymbol{c}_1^2((\hat{\boldsymbol{n}}\times\boldsymbol{\delta})\cdot\boldsymbol{\omega}_1)+\boldsymbol{c}_2^2((\hat{\boldsymbol{n}}\times\boldsymbol{\delta})\cdot\boldsymbol{\omega}_2)]\\
&+\frac{4}{qa}[\boldsymbol{c}_1^2\boldsymbol{\omega}_1^2((\hat{\boldsymbol{n}}\times\boldsymbol{\delta})\cdot\boldsymbol{\omega}_1)+\boldsymbol{c}_2^2\boldsymbol{\omega}_2^2((\hat{\boldsymbol{n}}\times\boldsymbol{\delta})\cdot\boldsymbol{\omega}_2)]+\boldsymbol{\delta}^2[\boldsymbol{\omega}_1^4+\boldsymbol{\omega}_2^4]+\frac{2}{q^4a^4}[\boldsymbol{\delta}^2(\hat{\boldsymbol{n}}\times\boldsymbol{\delta})^4]\\
&+\frac{4}{q^2a^2}\boldsymbol{\delta}^2[((\hat{\boldsymbol{n}}\times\boldsymbol{\delta})\cdot\boldsymbol{\omega}_1)^2+((\hat{\boldsymbol{n}}\times\boldsymbol{\delta})\cdot\boldsymbol{\omega}_2)^2]+\frac{2}{q^2a^2}\boldsymbol{\delta}^2(\hat{\boldsymbol{n}}\times\boldsymbol{\delta})^2[\boldsymbol{\omega}_1^2+\boldsymbol{\omega}_2^2]\\
&+\frac{4}{q^3a^3}\boldsymbol{\delta}^2(\hat{\boldsymbol{n}}\times\boldsymbol{\delta})^2[((\hat{\boldsymbol{n}}\times\boldsymbol{\delta})\cdot\boldsymbol{\omega}_1)+((\hat{\boldsymbol{n}}\times\boldsymbol{\delta})\cdot\boldsymbol{\omega}_2)]+\frac{4}{qa}\boldsymbol{\delta}^2[\boldsymbol{\omega}_1^2((\hat{\boldsymbol{n}}\times\boldsymbol{\delta})\cdot\boldsymbol{\omega}_1)+\boldsymbol{\omega}_2^2((\hat{\boldsymbol{n}}\times\boldsymbol{\delta})\cdot\boldsymbol{\omega}_2)]\\
&+2[(\boldsymbol{c}_2\cdot\boldsymbol{\delta})\boldsymbol{\omega}_2^4-(\boldsymbol{c}_1\cdot\boldsymbol{\delta})\boldsymbol{\omega}_1^4]+\frac{2}{q^4a^4}(\hat{\boldsymbol{n}}\times\boldsymbol{\delta})^4[(\boldsymbol{c}_2\cdot\boldsymbol{\delta})-(\boldsymbol{c}_1\cdot\boldsymbol{\delta})]\\
&+\frac{8}{q^2a^2}[(\boldsymbol{c}_2\cdot\boldsymbol{\delta})((\hat{\boldsymbol{n}}\times\boldsymbol{\delta})\cdot\boldsymbol{\omega}_2)^2-(\boldsymbol{c}_1\cdot\boldsymbol{\delta})((\hat{\boldsymbol{n}}\times\boldsymbol{\delta})\cdot\boldsymbol{\omega}_1)^2]+\frac{4}{q^2a^2}(\hat{\boldsymbol{n}}\times\boldsymbol{\delta})^2[(\boldsymbol{c}_2\cdot\boldsymbol{\delta})\boldsymbol{\omega}_2^2-(\boldsymbol{c}_1\cdot\boldsymbol{\delta})\boldsymbol{\omega}_1^2]\\
&+\frac{8}{q^3a^3}(\hat{\boldsymbol{n}}\times\boldsymbol{\delta})^2[(\boldsymbol{c}_2\cdot\boldsymbol{\delta})((\hat{\boldsymbol{n}}\times\boldsymbol{\delta})\cdot\boldsymbol{\omega}_2)-(\boldsymbol{c}_1\cdot\boldsymbol{\delta})((\hat{\boldsymbol{n}}\times\boldsymbol{\delta})\cdot\boldsymbol{\omega}_1)]\\
&+\frac{8}{qa}[(\boldsymbol{c}_2\cdot\boldsymbol{\delta})((\hat{\boldsymbol{n}}\times\boldsymbol{\delta})\cdot\boldsymbol{\omega}_2)\boldsymbol{\omega}_2^2-(\boldsymbol{c}_1\cdot\boldsymbol{\delta})((\hat{\boldsymbol{n}}\times\boldsymbol{\delta})\cdot\boldsymbol{\omega}_1)\boldsymbol{\omega}_1^2]. \qquad \text{(A.28)}
\end{aligned}
$$

Applying the collision rule to $\Delta_A^{(212)}$ and $\Delta_B^{(212)}$ we obtain

$$
\begin{aligned}
(\mathcal{B}_{12}-1)\Delta_A^{(212)} &= \boldsymbol{\delta}^2[(\boldsymbol{c}_1\cdot\boldsymbol{\omega}_1)^2+(\boldsymbol{c}_2\cdot\boldsymbol{\omega}_2)^2]+2[(\boldsymbol{c}_2\cdot\boldsymbol{\omega}_2)^2(\boldsymbol{c}_2\cdot\boldsymbol{\delta})-(\boldsymbol{c}_1\cdot\boldsymbol{\omega}_1)^2(\boldsymbol{c}_1\cdot\boldsymbol{\delta})]\\
&+[(\boldsymbol{\delta}\cdot\boldsymbol{\omega}_1)^2\boldsymbol{c}_1^2+(\boldsymbol{\delta}\cdot\boldsymbol{\omega}_2)^2\boldsymbol{c}_2^2]+\boldsymbol{\delta}^2[(\boldsymbol{\delta}\cdot\boldsymbol{\omega}_1)^2+(\boldsymbol{\delta}\cdot\boldsymbol{\omega}_2)^2]+2[(\boldsymbol{\delta}\cdot\boldsymbol{\omega}_2)^2(\boldsymbol{c}_2\cdot\boldsymbol{\delta})-(\boldsymbol{\delta}\cdot\boldsymbol{\omega}_1)^2(\boldsymbol{c}_1\cdot\boldsymbol{\delta})]\\
&+\frac{1}{q^2a^2}[((\hat{\boldsymbol{n}}\times\boldsymbol{\delta})\cdot\boldsymbol{c}_1)^2\boldsymbol{c}_1^2+((\hat{\boldsymbol{n}}\times\boldsymbol{\delta})\cdot\boldsymbol{c}_2)^2\boldsymbol{c}_2^2]+\frac{1}{q^2a^2}\boldsymbol{\delta}^2[((\hat{\boldsymbol{n}}\times\boldsymbol{\delta})\cdot\boldsymbol{c}_1)^2+((\hat{\boldsymbol{n}}\times\boldsymbol{\delta})\cdot\boldsymbol{c}_2)^2]\\
&+\frac{2}{q^2a^2}[((\hat{\boldsymbol{n}}\times\boldsymbol{\delta})\cdot\boldsymbol{c}_2)^2(\boldsymbol{c}_2\cdot\boldsymbol{\delta})-((\hat{\boldsymbol{n}}\times\boldsymbol{\delta})\cdot\boldsymbol{c}_1)^2(\boldsymbol{c}_1\cdot\boldsymbol{\delta})]+2[(\boldsymbol{c}_2\cdot\boldsymbol{\omega}_2)(\boldsymbol{\delta}\cdot\boldsymbol{\omega}_2)\boldsymbol{c}_2^2-(\boldsymbol{c}_1\cdot\boldsymbol{\omega}_1)(\boldsymbol{\delta}\cdot\boldsymbol{\omega}_1)\boldsymbol{c}_1^2]\\
&+2\boldsymbol{\delta}^2[(\boldsymbol{c}_2\cdot\boldsymbol{\omega}_2)(\boldsymbol{\delta}\cdot\boldsymbol{\omega}_2)-(\boldsymbol{c}_1\cdot\boldsymbol{\omega}_1)(\boldsymbol{\delta}\cdot\boldsymbol{\omega}_1)]+4[(\boldsymbol{c}_1\cdot\boldsymbol{\omega}_1)(\boldsymbol{\delta}\cdot\boldsymbol{\omega}_1)(\boldsymbol{c}_1\cdot\boldsymbol{\delta})+(\boldsymbol{c}_2\cdot\boldsymbol{\omega}_2)(\boldsymbol{\delta}\cdot\boldsymbol{\omega}_2)(\boldsymbol{c}_2\cdot\boldsymbol{\delta})]\\
&+\frac{2}{qa}[(\boldsymbol{\delta}\cdot\boldsymbol{\omega}_2)((\hat{\boldsymbol{n}}\times\boldsymbol{\delta})\cdot\boldsymbol{c}_2)\boldsymbol{c}_2^2-(\boldsymbol{\delta}\cdot\boldsymbol{\omega}_1)((\hat{\boldsymbol{n}}\times\boldsymbol{\delta})\cdot\boldsymbol{c}_1)\boldsymbol{c}_1^2]\\
&+\frac{2}{qa}\boldsymbol{\delta}^2[(\boldsymbol{\delta}\cdot\boldsymbol{\omega}_2)((\hat{\boldsymbol{n}}\times\boldsymbol{\delta})\cdot\boldsymbol{c}_2)-(\boldsymbol{\delta}\cdot\boldsymbol{\omega}_1)((\hat{\boldsymbol{n}}\times\boldsymbol{\delta})\cdot\boldsymbol{c}_1)]\\
&+\frac{4}{qa}[(\boldsymbol{\delta}\cdot\boldsymbol{\omega}_1)((\hat{\boldsymbol{n}}\times\boldsymbol{\delta})\cdot\boldsymbol{c}_1)(\boldsymbol{c}_1\cdot\boldsymbol{\delta})+(\boldsymbol{\delta}\cdot\boldsymbol{\omega}_2)((\hat{\boldsymbol{n}}\times\boldsymbol{\delta})\cdot\boldsymbol{c}_2)(\boldsymbol{c}_2\cdot\boldsymbol{\delta})]\\
&+\frac{2}{qa}[(\boldsymbol{c}_1\cdot\boldsymbol{\omega}_1)((\hat{\boldsymbol{n}}\times\boldsymbol{\delta})\cdot\boldsymbol{c}_1)\boldsymbol{c}_1^2+(\boldsymbol{c}_2\cdot\boldsymbol{\omega}_2)((\hat{\boldsymbol{n}}\times\boldsymbol{\delta})\cdot\boldsymbol{c}_2)\boldsymbol{c}_2^2]+\frac{2}{qa}\boldsymbol{\delta}^2[(\boldsymbol{c}_1\cdot\boldsymbol{\omega}_1)((\hat{\boldsymbol{n}}\times\boldsymbol{\delta})\cdot\boldsymbol{c}_1)\\
&+(\boldsymbol{c}_2\cdot\boldsymbol{\omega}_2)((\hat{\boldsymbol{n}}\times\boldsymbol{\delta})\cdot\boldsymbol{c}_2)]+\frac{4}{qa}[(\boldsymbol{c}_2\cdot\boldsymbol{\omega}_2)((\hat{\boldsymbol{n}}\times\boldsymbol{\delta})\cdot\boldsymbol{c}_2)(\boldsymbol{c}_2\cdot\boldsymbol{\delta})-(\boldsymbol{c}_1\cdot\boldsymbol{\omega}_1)((\hat{\boldsymbol{n}}\times\boldsymbol{\delta})\cdot\boldsymbol{c}_1)(\boldsymbol{c}_1\cdot\boldsymbol{\delta})]. \qquad (A.29)
\end{aligned}
$$

$$
\begin{aligned}
(\mathcal{B}_{12}-1)\Delta_B^{(212)} &= \frac{1}{q^2a^2}(\hat{\boldsymbol{n}}\times\boldsymbol{\delta})^2[\boldsymbol{c}_1^4+\boldsymbol{c}_2^4]+\frac{2}{qa}[\boldsymbol{c}_1^4((\hat{\boldsymbol{n}}\times\boldsymbol{\delta})\cdot\boldsymbol{\omega}_1)+\boldsymbol{c}_2^4((\hat{\boldsymbol{n}}\times\boldsymbol{\delta})\cdot\boldsymbol{\omega}_2)]\\
&+\boldsymbol{\delta}^4[\boldsymbol{\omega}_1^2+\boldsymbol{\omega}_2^2]+\frac{2}{q^2a^2}[(\hat{\boldsymbol{n}}\times\boldsymbol{\delta})^2\boldsymbol{\delta}^4]+\frac{2}{qa}\boldsymbol{\delta}^4[((\hat{\boldsymbol{n}}\times\boldsymbol{\delta})\cdot\boldsymbol{\omega}_1)+((\hat{\boldsymbol{n}}\times\boldsymbol{\delta})\cdot\boldsymbol{\omega}_2)]\\
&+4[\boldsymbol{\omega}_1^2(\boldsymbol{c}_1\cdot\boldsymbol{\delta})^2+\boldsymbol{\omega}_2^2(\boldsymbol{c}_2\cdot\boldsymbol{\delta})^2]+\frac{4}{q^2a^2}(\hat{\boldsymbol{n}}\times\boldsymbol{\delta})^2[(\boldsymbol{c}_1\cdot\boldsymbol{\delta})^2+(\boldsymbol{c}_2\cdot\boldsymbol{\delta})^2]\\
&+\frac{8}{qa}[((\hat{\boldsymbol{n}}\times\boldsymbol{\delta})\cdot\boldsymbol{\omega}_1)(\boldsymbol{c}_1\cdot\boldsymbol{\delta})^2+((\hat{\boldsymbol{n}}\times\boldsymbol{\delta})\cdot\boldsymbol{\omega}_2)(\boldsymbol{c}_2\cdot\boldsymbol{\delta})^2]+2\boldsymbol{\delta}^2[\boldsymbol{c}_1^2\boldsymbol{\omega}_1^2+\boldsymbol{c}_2^2\boldsymbol{\omega}_2^2]\\
&+\frac{2}{q^2a^2}\boldsymbol{\delta}^2(\hat{\boldsymbol{n}}\times\boldsymbol{\delta})^2[\boldsymbol{c}_1^2+\boldsymbol{c}_2^2]\\
&+\frac{4}{qa}\boldsymbol{\delta}^2[\boldsymbol{c}_1^2((\hat{\boldsymbol{n}}\times\boldsymbol{\delta})\cdot\boldsymbol{\omega}_1)+\boldsymbol{c}_2^2((\hat{\boldsymbol{n}}\times\boldsymbol{\delta})\cdot\boldsymbol{\omega}_2)]+4\boldsymbol{\delta}^2[(\boldsymbol{c}_2\cdot\boldsymbol{\delta})\boldsymbol{\omega}_2^2-(\boldsymbol{c}_1\cdot\boldsymbol{\delta})\boldsymbol{\omega}_1^2]\\
&+\frac{4}{q^2a^2}\boldsymbol{\delta}^2(\hat{\boldsymbol{n}}\times\boldsymbol{\delta})^2[(\boldsymbol{c}_2\cdot\boldsymbol{\delta})-(\boldsymbol{c}_1\cdot\boldsymbol{\delta})]+\frac{8}{qa}\boldsymbol{\delta}^2[(\boldsymbol{c}_2\cdot\boldsymbol{\delta})((\hat{\boldsymbol{n}}\times\boldsymbol{\delta})\cdot\boldsymbol{\omega}_2)-(\boldsymbol{c}_1\cdot\boldsymbol{\delta})((\hat{\boldsymbol{n}}\times\boldsymbol{\delta})\cdot\boldsymbol{\omega}_1)]\\
&+4[(\boldsymbol{c}_2\cdot\boldsymbol{\delta})\boldsymbol{c}_2^2\boldsymbol{\omega}_2^2-(\boldsymbol{c}_1\cdot\boldsymbol{\delta})\boldsymbol{c}_1^2\boldsymbol{\omega}_1^2]+\frac{4}{q^2a^2}(\hat{\boldsymbol{n}}\times\boldsymbol{\delta})^2[(\boldsymbol{c}_2\cdot\boldsymbol{\delta})\boldsymbol{c}_2^2-(\boldsymbol{c}_1\cdot\boldsymbol{\delta})\boldsymbol{c}_1^2]\\
&+\frac{8}{qa}[(\boldsymbol{c}_2\cdot\boldsymbol{\delta})((\hat{\boldsymbol{n}}\times\boldsymbol{\delta})\cdot\boldsymbol{\omega}_2)\boldsymbol{c}_2^2-(\boldsymbol{c}_1\cdot\boldsymbol{\delta})((\hat{\boldsymbol{n}}\times\boldsymbol{\delta})\cdot\boldsymbol{\omega}_1)\boldsymbol{c}_1^2]. \qquad (A.30)
\end{aligned}
$$

Where

$$
\boldsymbol{c}_1=\frac{\boldsymbol{v}+\boldsymbol{V}}{\sqrt{2}},\quad \boldsymbol{c}_2=\frac{\boldsymbol{V}-\boldsymbol{v}}{\sqrt{2}},\quad \boldsymbol{\omega}_1=\frac{\boldsymbol{\omega}+\boldsymbol{\Omega}}{\sqrt{2}},\quad \boldsymbol{\omega}_2=\frac{\boldsymbol{\Omega}-\boldsymbol{\omega}}{\sqrt{2}}, \qquad (A.31)
$$

$$
\boldsymbol{\delta}=\sqrt{2}[\eta_t\boldsymbol{v}+\eta_t a(\hat{\boldsymbol{n}}\times\boldsymbol{\Omega})+(\eta_n-\eta_t)(\hat{\boldsymbol{n}}\cdot\boldsymbol{v})\hat{\boldsymbol{n}}]. \qquad (A.32)
$$

To determine the averages of the type $\langle(\mathcal{B}_{12}-1)\Delta^{(112)}\rangle^{(i)}$, $\langle(\mathcal{B}_{12}-1)\Delta^{(122)}\rangle^{(j)}$, $\langle(\mathcal{B}_{12}-1)\Delta^{(212)}\rangle^{(k)}$, where $i,j,k=0,1,2,3$, we need to evaluate the following averages for which we used Mathematica. For convenience we introduce the following abbreviations:

$$
\tilde{\nu}\equiv\nu\sqrt{\frac{T}{m\pi}},\quad \tilde{T}\equiv\frac{T}{m},\quad \tilde{R}\equiv\frac{R}{\mathcal{I}}. \qquad (A.33)
$$

The averages of the type $\langle(\mathcal{B}_{12}-1)\Delta^{(\alpha\beta 2)}\rangle^{(0)}$, with $\alpha,\beta=1,2$, contain the following terms:

$$
\langle(\boldsymbol{v}\cdot\boldsymbol{\omega})^2\rangle^{(0)}=-4\tilde{\nu}\tilde{T}\tilde{R},\quad \langle(\boldsymbol{V}\cdot\boldsymbol{\omega})^2\rangle^{(0)}=-3\tilde{\nu}\tilde{T}\tilde{R},\quad \langle(\hat{\boldsymbol{n}}\cdot\boldsymbol{v})^2(\hat{\boldsymbol{n}}\cdot\boldsymbol{\omega})^2\rangle^{(0)}=-2\tilde{\nu}\tilde{T}\tilde{R}
$$

$$
\langle(\hat{\boldsymbol{n}}\cdot\boldsymbol{V})^2(\hat{\boldsymbol{n}}\cdot\boldsymbol{\omega})^2\rangle^{(0)}=-\tilde{\nu}\tilde{T}\tilde{R},\quad \langle[((\hat{\boldsymbol{n}}\times\boldsymbol{\Omega})\cdot\boldsymbol{\omega})]^2\rangle^{(0)}=-2\tilde{\nu}\tilde{R}^2,\quad \langle[((\hat{\boldsymbol{n}}\times\boldsymbol{v})\cdot\boldsymbol{V})]^2\rangle^{(0)}=-2\tilde{\nu}\tilde{T}^2
$$

$$
\langle(\hat{\boldsymbol{n}}\cdot\boldsymbol{v})(\hat{\boldsymbol{n}}\cdot\boldsymbol{\omega})(\boldsymbol{v}\cdot\boldsymbol{\omega})\rangle^{(0)}=-2\tilde{\nu}\tilde{T}\tilde{R},\quad \langle(\hat{\boldsymbol{n}}\cdot\boldsymbol{V})(\hat{\boldsymbol{n}}\cdot\boldsymbol{\omega})(\boldsymbol{V}\cdot\boldsymbol{\omega})\rangle^{(0)}=-\tilde{\nu}\tilde{T}\tilde{R},\quad \langle\boldsymbol{v}^2(\hat{\boldsymbol{n}}\times\boldsymbol{\Omega})^2\rangle^{(0)}=-8\tilde{\nu}\tilde{T}\tilde{R}
$$

$$
\langle\boldsymbol{V}^2(\hat{\boldsymbol{n}}\times\boldsymbol{\Omega})^2\rangle^{(0)}=-6\tilde{\nu}\tilde{T}\tilde{R},\quad \langle\boldsymbol{v}^2(\hat{\boldsymbol{n}}\times\boldsymbol{v})^2\rangle^{(0)}=-12\tilde{\nu}\tilde{T}^2,\quad \langle\boldsymbol{V}^2(\hat{\boldsymbol{n}}\times\boldsymbol{v})^2\rangle^{(0)}=-6\tilde{\nu}\tilde{T}^2
$$

$$
\langle\boldsymbol{v}^2\boldsymbol{\omega}^2\rangle^{(0)}=-12\tilde{\nu}\tilde{T}\tilde{R},\quad \langle(\hat{\boldsymbol{n}}\cdot\boldsymbol{v})^2\boldsymbol{\omega}^2\rangle^{(0)}=-6\tilde{\nu}\tilde{T}\tilde{R},\quad \langle(\hat{\boldsymbol{n}}\cdot\boldsymbol{v})^2(\hat{\boldsymbol{n}}\times\boldsymbol{\Omega})^2\rangle^{(0)}=-4\tilde{\nu}\tilde{T}\tilde{R}
$$

$$\langle[(\hat{\boldsymbol{n}}\times\boldsymbol{v})\cdot\boldsymbol{\Omega})]^2\rangle^{(0)}=-2\tilde{\nu}\tilde{T}\tilde{R}\quad\langle(\hat{\boldsymbol{n}}\cdot\boldsymbol{v})^2(\hat{\boldsymbol{n}}\times\boldsymbol{v})^2\rangle^{(0)}=-4\tilde{\nu}\tilde{T}^2\quad\langle\boldsymbol{\omega}^2(\hat{\boldsymbol{n}}\times\boldsymbol{\Omega})^2\rangle^{(0)}=-6\tilde{\nu}\tilde{R}^2$$

$$\langle\boldsymbol{\Omega}^2(\hat{\boldsymbol{n}}\times\boldsymbol{\Omega})^2\rangle^{(0)}=-10\tilde{\nu}\tilde{R}^2,\quad\langle(\hat{\boldsymbol{n}}\times\boldsymbol{\Omega})^4\rangle^{(0)}=-8\tilde{\nu}\tilde{R}^2,\quad\langle(\hat{\boldsymbol{n}}\times\boldsymbol{\Omega})^2(\hat{\boldsymbol{n}}\times\boldsymbol{v})^2\rangle^{(0)}=-4\tilde{\nu}\tilde{T}\tilde{R}$$

$$\langle(\hat{\boldsymbol{n}}\times\boldsymbol{v})^2\rangle^{(0)}=-2\tilde{\nu}\tilde{T},\quad\langle(\hat{\boldsymbol{n}}\cdot\boldsymbol{v})^2\rangle^{(0)}=-2\tilde{\nu}\tilde{T},\quad\langle(\hat{\boldsymbol{n}}\times\boldsymbol{\Omega})^2\rangle^{(0)}=-2\tilde{\nu}\tilde{R},\quad\langle((\hat{\boldsymbol{n}}\times\boldsymbol{v})\cdot\boldsymbol{\Omega})\rangle^{(0)}=0$$

Note that these integrals match with those evaluated by Kranz *et al.* (2009) who considered leading-order behavior of orientational correlation. To go beyond the leading-order, we need to evaluate $\langle(\mathcal{B}_{12}-1)\Delta^{(\alpha\beta 2)}\rangle^{(1)}$, $\langle(\mathcal{B}_{12}-1)\Delta^{(\alpha\beta 2)}\rangle^{(2)}$ and $\langle(\mathcal{B}_{12}-1)\Delta^{(\alpha\beta 2)}\rangle^{(3)}$ which are detailed below.

The averages of the type $\langle(\mathcal{B}_{12}-1)\Delta^{(\alpha\beta 2)}\rangle^{(1)}$, with $\alpha,\beta=1,2$, contain the following terms:

$$\langle(\boldsymbol{v}\cdot\boldsymbol{\omega})^2\rangle^{(1)}=-24\tilde{\nu}\tilde{T}^2\tilde{R}^2,\quad\langle(\boldsymbol{V}\cdot\boldsymbol{\omega})^2\rangle^{(1)}=-15\tilde{\nu}\tilde{T}^2\tilde{R}^2,\quad\langle(\hat{\boldsymbol{n}}\cdot\boldsymbol{v})^2(\hat{\boldsymbol{n}}\cdot\boldsymbol{\omega})^2\rangle^{(1)}=-6\tilde{\nu}\tilde{T}^2\tilde{R}^2$$

$$\langle(\hat{\boldsymbol{n}}\cdot\boldsymbol{V})^2(\hat{\boldsymbol{n}}\cdot\boldsymbol{\omega})^2\rangle^{(1)}=-3\tilde{\nu}\tilde{T}^2\tilde{R}^2,\quad\langle[((\hat{\boldsymbol{n}}\times\boldsymbol{\Omega})\cdot\boldsymbol{\omega})]^2\rangle^{(1)}=2\tilde{\nu}\tilde{T}\tilde{R}^3,\quad\langle(\hat{\boldsymbol{n}}\cdot\boldsymbol{v})(\hat{\boldsymbol{n}}\cdot\boldsymbol{\omega})(\boldsymbol{v}\cdot\boldsymbol{\omega})\rangle^{(1)}=-12\tilde{\nu}\tilde{T}^2\tilde{R}^2$$

$$\langle(\hat{\boldsymbol{n}}\cdot\boldsymbol{V})(\hat{\boldsymbol{n}}\cdot\boldsymbol{\omega})(\boldsymbol{V}\cdot\boldsymbol{\omega})\rangle^{(1)}=-6\tilde{\nu}\tilde{T}^2\tilde{R}^2,\quad\langle\boldsymbol{v}^2(\hat{\boldsymbol{n}}\times\boldsymbol{\Omega})^2\rangle^{(1)}=6\tilde{\nu}\tilde{T}^2\tilde{R}^2,\quad\langle\boldsymbol{V}^2(\hat{\boldsymbol{n}}\times\boldsymbol{\Omega})^2\rangle^{(1)}=3\tilde{\nu}\tilde{T}^2\tilde{R}^2$$

$$\langle(\hat{\boldsymbol{n}}\cdot\boldsymbol{v})^2(\hat{\boldsymbol{n}}\times\boldsymbol{\Omega})^2\rangle^{(1)}=6\tilde{\nu}\tilde{T}^2\tilde{R}^2,\quad\langle[((\hat{\boldsymbol{n}}\times\boldsymbol{v})\cdot\boldsymbol{\Omega})]^2\rangle^{(1)}=6\tilde{\nu}\tilde{T}^2\tilde{R}^2,\quad\langle\boldsymbol{\omega}^2(\hat{\boldsymbol{n}}\times\boldsymbol{\Omega})^2\rangle^{(1)}=3\tilde{\nu}\tilde{T}\tilde{R}^3$$

$$\langle\boldsymbol{\Omega}^2(\hat{\boldsymbol{n}}\times\boldsymbol{\Omega})^2\rangle^{(1)}=7\tilde{\nu}\tilde{T}\tilde{R}^3,\quad\langle(\hat{\boldsymbol{n}}\times\boldsymbol{\Omega})^4\rangle^{(1)}=8\tilde{\nu}\tilde{T}\tilde{R}^3,\quad\langle(\hat{\boldsymbol{n}}\times\boldsymbol{\Omega})^2(\hat{\boldsymbol{n}}\times\boldsymbol{v})^2\rangle^{(1)}=0$$

$$\langle(\boldsymbol{v}\cdot\boldsymbol{\omega})(\boldsymbol{V}\cdot\boldsymbol{\Omega})\rangle^{(1)}=-20\tilde{\nu}\tilde{T}^2\tilde{R}^2,\quad\langle(\hat{\boldsymbol{n}}\cdot\boldsymbol{v})(\hat{\boldsymbol{n}}\cdot\boldsymbol{\omega})(\boldsymbol{V}\cdot\boldsymbol{\Omega})\rangle^{(1)}=-10\tilde{\nu}\tilde{T}^2\tilde{R}^2,\quad\langle(\hat{\boldsymbol{n}}\cdot\boldsymbol{V})(\hat{\boldsymbol{n}}\cdot\boldsymbol{\Omega})(\boldsymbol{v}\cdot\boldsymbol{\omega})\rangle^{(1)}=-7\tilde{\nu}\tilde{T}^2\tilde{R}^2$$

$$\langle(\hat{\boldsymbol{n}}\cdot\boldsymbol{v})(\hat{\boldsymbol{n}}\cdot\boldsymbol{V})(\hat{\boldsymbol{n}}\cdot\boldsymbol{\omega})(\hat{\boldsymbol{n}}\cdot\boldsymbol{\Omega})\rangle^{(1)}=-4\tilde{\nu}\tilde{T}^2\tilde{R}^2,\quad\langle[((\hat{\boldsymbol{n}}\times\boldsymbol{v})\cdot\boldsymbol{V})][((\hat{\boldsymbol{n}}\times\boldsymbol{\Omega})\cdot\boldsymbol{\omega})]\rangle^{(1)}=0,\quad\langle(\hat{\boldsymbol{n}}\cdot\boldsymbol{\omega})(\hat{\boldsymbol{n}}\cdot\boldsymbol{\Omega})(\boldsymbol{v}\cdot\boldsymbol{V})\rangle^{(1)}=-2\tilde{\nu}\tilde{T}^2\tilde{R}^2$$

$$\langle[((\hat{\boldsymbol{n}}\times\boldsymbol{v})\cdot\boldsymbol{\omega})][((\hat{\boldsymbol{n}}\times\boldsymbol{\Omega})\cdot\boldsymbol{V})]\rangle^{(1)}=-5\tilde{\nu}\tilde{T}^2\tilde{R}^2,\quad\langle(\hat{\boldsymbol{n}}\times\boldsymbol{v})^2\rangle^{(1)}=0,\quad\langle(\hat{\boldsymbol{n}}\cdot\boldsymbol{v})^2\rangle^{(1)}=0$$

$$\langle((\hat{\boldsymbol{n}}\times\boldsymbol{v})\cdot\boldsymbol{\Omega})\rangle^{(1)}=0,\quad\langle(\hat{\boldsymbol{n}}\times\boldsymbol{\Omega})^2\rangle^{(1)}=\tilde{\nu}\tilde{T}\tilde{R}^2$$

There seems to be a printing mistake in the work of Kranz *et al.* [Brilliantov *et al.* (2007); Kranz *et al.* (2009)] regarding a "prefactor" $(2\to 1)$ in the last term above.

The averages of the type $\langle(\mathcal{B}_{12}-1)\Delta^{(\alpha\beta 2)}\rangle^{(2)}$, with $\alpha,\beta=1,2$, contain the following terms:

$$\langle(\boldsymbol{v}\cdot\boldsymbol{\omega})^2\rangle^{(2)}=-168\tilde{\nu}\tilde{T}^2\tilde{R}^3,\quad\langle[((\hat{\boldsymbol{n}}\times\boldsymbol{\Omega})\cdot\boldsymbol{\omega})]^2\rangle^{(2)}=14\tilde{\nu}\tilde{T}\tilde{R}^4,\quad\langle(\hat{\boldsymbol{n}}\cdot\boldsymbol{v})^2(\hat{\boldsymbol{n}}\cdot\boldsymbol{\omega})^2\rangle^{(2)}=-42\tilde{\nu}\tilde{T}^2\tilde{R}^3$$

$$\langle(\hat{\boldsymbol{n}}\cdot\boldsymbol{v})(\hat{\boldsymbol{n}}\cdot\boldsymbol{\omega})(\boldsymbol{v}\cdot\boldsymbol{\omega})\rangle^{(2)}=-84\tilde{\nu}\tilde{T}^2\tilde{R}^3,\quad\langle(\boldsymbol{V}\cdot\boldsymbol{\Omega})^2\rangle^{(2)}=-105\tilde{\nu}\tilde{T}^2\tilde{R}^3,\quad\langle(\hat{\boldsymbol{n}}\cdot\boldsymbol{v})(\hat{\boldsymbol{n}}\cdot\boldsymbol{\Omega})(\boldsymbol{V}\cdot\boldsymbol{\omega})\rangle^{(2)}=-70\tilde{\nu}\tilde{T}^2\tilde{R}^3$$

$$\langle(\boldsymbol{v}\cdot\boldsymbol{\omega})(\boldsymbol{V}\cdot\boldsymbol{\Omega})\rangle^{(2)}=-140\tilde{\nu}\tilde{T}^2\tilde{R}^3,\quad\langle(\hat{\boldsymbol{n}}\cdot\boldsymbol{V})(\hat{\boldsymbol{n}}\cdot\boldsymbol{\Omega})(\boldsymbol{v}\cdot\boldsymbol{\omega})\rangle^{(2)}=-49\tilde{\nu}\tilde{T}^2\tilde{R}^3,\quad\langle(\hat{\boldsymbol{n}}\cdot\boldsymbol{v})(\hat{\boldsymbol{n}}\cdot\boldsymbol{\omega})(\hat{\boldsymbol{n}}\cdot\boldsymbol{V})(\hat{\boldsymbol{n}}\cdot\boldsymbol{\Omega})\rangle^{(2)}=-28\tilde{\nu}\tilde{T}^2\tilde{R}^3$$

$$\langle\boldsymbol{v}^2(\hat{\boldsymbol{n}}\times\boldsymbol{\Omega})^2\rangle^{(2)}=42\tilde{\nu}\tilde{T}^2\tilde{R}^3,\quad\langle\boldsymbol{V}^2(\hat{\boldsymbol{n}}\times\boldsymbol{\Omega})^2\rangle^{(2)}=21\tilde{\nu}\tilde{T}^2\tilde{R}^3,\quad\langle\boldsymbol{v}^2\boldsymbol{\omega}^2\rangle^{(2)}=0$$

$$\langle\boldsymbol{\omega}^2(\hat{\boldsymbol{n}}\times\boldsymbol{\Omega})^2\rangle^{(2)}=28\tilde{\nu}\tilde{T}\tilde{R}^4,\quad\langle\boldsymbol{\Omega}^2(\hat{\boldsymbol{n}}\times\boldsymbol{\Omega})^2\rangle^{(2)}=56\tilde{\nu}\tilde{T}\tilde{R}^4,\quad\langle\boldsymbol{\omega}^2(\hat{\boldsymbol{n}}\cdot\boldsymbol{v})^2\rangle^{(2)}=0$$

$$\langle(\hat{\boldsymbol{n}}\times\boldsymbol{\Omega})^4\rangle^{(2)}=64\tilde{\nu}\tilde{T}\tilde{R}^4,\quad\langle((\hat{\boldsymbol{n}}\times\boldsymbol{v})\cdot\boldsymbol{\Omega})^2\rangle^{(2)}=42\tilde{\nu}\tilde{T}^2\tilde{R}^3,\quad\langle((\hat{\boldsymbol{n}}\times\boldsymbol{\Omega})\cdot\boldsymbol{V})((\hat{\boldsymbol{n}}\times\boldsymbol{v})\cdot\boldsymbol{\omega})\rangle^{(2)}=-35\tilde{\nu}\tilde{T}^2\tilde{R}^3$$

$$\langle(\hat{\boldsymbol{n}}\times\boldsymbol{v})^2\rangle^{(2)}=0,\quad\langle(\hat{\boldsymbol{n}}\cdot\boldsymbol{v})^2\rangle^{(2)}=0,\quad\langle(\hat{\boldsymbol{n}}\times\boldsymbol{\Omega})^2\rangle^{(2)}=7\tilde{\nu}\tilde{T}\tilde{R}^3,\quad\langle((\hat{\boldsymbol{n}}\times\boldsymbol{v})\cdot\boldsymbol{\Omega})\rangle^{(2)}=0$$

$$\langle(\hat{\boldsymbol{n}}\times\boldsymbol{v})^2(\boldsymbol{V}\cdot\boldsymbol{\omega})^2\rangle^{(2)}=-210\tilde{\nu}\tilde{T}^3\tilde{R}^3,\quad\langle((\hat{\boldsymbol{n}}\times\boldsymbol{v})\cdot\boldsymbol{\omega})(\boldsymbol{V}\cdot\boldsymbol{\omega})((\hat{\boldsymbol{n}}\times\boldsymbol{\Omega})\cdot\boldsymbol{\omega})\rangle^{(2)}=-105\tilde{\nu}\tilde{T}^2\tilde{R}^4$$

$$\langle(\boldsymbol{V}\cdot\boldsymbol{\omega})((\hat{\boldsymbol{n}}\times\boldsymbol{\Omega})\cdot\boldsymbol{\omega})(\hat{\boldsymbol{n}}\cdot\boldsymbol{\omega})(\hat{\boldsymbol{n}}\cdot\boldsymbol{\Omega})\rangle^{(2)}=0,\quad\langle((\hat{\boldsymbol{n}}\times\boldsymbol{v})\cdot\boldsymbol{\omega})(\boldsymbol{V}\cdot\boldsymbol{\omega})((\hat{\boldsymbol{n}}\times\boldsymbol{v})\cdot\boldsymbol{V})\rangle^{(2)}=-28\tilde{\nu}\tilde{T}^3\tilde{R}^3$$

$$\langle(\boldsymbol{V}\cdot\boldsymbol{\omega})(\hat{\boldsymbol{n}}\cdot\boldsymbol{\omega})(\hat{\boldsymbol{n}}\cdot\boldsymbol{\Omega})((\hat{\boldsymbol{n}}\times\boldsymbol{v})\cdot\boldsymbol{V})\rangle^{(2)}=0,\quad\langle(\boldsymbol{V}\cdot\boldsymbol{\omega})(\hat{\boldsymbol{n}}\cdot\boldsymbol{\omega})(\hat{\boldsymbol{n}}\cdot\boldsymbol{\Omega})^2(\hat{\boldsymbol{n}}\cdot\boldsymbol{V})\rangle^{(2)}=-90\tilde{\nu}\tilde{T}^2\tilde{R}^4$$

$$\langle((\hat{\boldsymbol{n}}\times\boldsymbol{\Omega})\cdot\boldsymbol{\omega})^2\boldsymbol{\omega}^2\rangle^{(2)}=98\tilde{\nu}\tilde{T}\tilde{R}^5,\quad\langle((\hat{\boldsymbol{n}}\times\boldsymbol{\Omega})\cdot\boldsymbol{\omega})((\hat{\boldsymbol{n}}\times\boldsymbol{v})\cdot\boldsymbol{V})\boldsymbol{\omega}^2\rangle^{(2)}=0$$

$$\langle((\hat{\boldsymbol{n}}\times\boldsymbol{v})\cdot\boldsymbol{V})^2\boldsymbol{\omega}^2\rangle^{(2)}=0,\quad\langle(\hat{\boldsymbol{n}}\cdot\boldsymbol{\Omega})^2(\hat{\boldsymbol{n}}\cdot\boldsymbol{V})^2\boldsymbol{\omega}^2\rangle^{(2)}=-84\tilde{\nu}\tilde{T}^2\tilde{R}^4$$

$$\langle(\hat{\boldsymbol{n}}\cdot\boldsymbol{\Omega})^2(\hat{\boldsymbol{n}}\cdot\boldsymbol{V})^2\boldsymbol{\Omega}^2\rangle^{(2)}=-168\tilde{\nu}\tilde{T}^2\tilde{R}^4,\quad\langle(\hat{\boldsymbol{n}}\times\boldsymbol{v})^2(\hat{\boldsymbol{n}}\cdot\boldsymbol{\Omega})^2(\hat{\boldsymbol{n}}\cdot\boldsymbol{V})^2\rangle^{(2)}=-28\tilde{\nu}\tilde{T}^3\tilde{R}^3$$

$$\langle(\boldsymbol{v}\cdot\boldsymbol{\Omega})(\boldsymbol{V}\cdot\boldsymbol{\omega})\boldsymbol{\omega}^2\rangle^{(2)}=-840\tilde{\nu}\tilde{T}^2\tilde{R}^4,\quad\langle(\boldsymbol{V}\cdot\boldsymbol{\omega})(\hat{\boldsymbol{n}}\cdot\boldsymbol{v})(\hat{\boldsymbol{n}}\cdot\boldsymbol{\Omega})\boldsymbol{\omega}^2\rangle^{(2)}=-420\tilde{\nu}\tilde{T}^2\tilde{R}^4$$

$$\langle(\boldsymbol{v}\cdot\boldsymbol{\omega})(\hat{\boldsymbol{n}}\cdot\boldsymbol{v})(\hat{\boldsymbol{n}}\cdot\boldsymbol{\omega})\boldsymbol{\omega}^2\rangle^{(2)}=-672\tilde{\nu}\tilde{T}^2\tilde{R}^4,\quad\langle(\boldsymbol{v}\cdot\boldsymbol{\omega})(\hat{\boldsymbol{n}}\cdot\boldsymbol{v})(\hat{\boldsymbol{n}}\cdot\boldsymbol{\omega})\boldsymbol{\Omega}^2\rangle^{(2)}=-336\tilde{\nu}\tilde{T}^2\tilde{R}^4$$

$$\langle(\boldsymbol{v}\cdot\boldsymbol{\omega})^2\boldsymbol{\omega}^2\rangle^{(2)}=-1344\tilde{\nu}\tilde{T}^2\tilde{R}^4,\quad\langle(\boldsymbol{v}\cdot\boldsymbol{\omega})^2\boldsymbol{\Omega}^2\rangle^{(2)}=-672\tilde{\nu}\tilde{T}^2\tilde{R}^4$$

$$\langle(\hat{\boldsymbol{n}}\cdot\boldsymbol{v})^2(\hat{\boldsymbol{n}}\cdot\boldsymbol{\omega})^2\boldsymbol{\omega}^2\rangle^{(2)}=-336\tilde{\nu}\tilde{T}^2\tilde{R}^4,\quad\langle(\hat{\boldsymbol{n}}\cdot\boldsymbol{v})^2(\hat{\boldsymbol{n}}\cdot\boldsymbol{\omega})^2\boldsymbol{\Omega}^2\rangle^{(2)}=-168\tilde{\nu}\tilde{T}^2\tilde{R}^4$$

$$\langle(\boldsymbol{V}\cdot\boldsymbol{\omega})(\boldsymbol{V}\cdot\boldsymbol{\Omega})(\hat{\boldsymbol{n}}\cdot\boldsymbol{\omega})(\hat{\boldsymbol{n}}\cdot\boldsymbol{\Omega})\rangle^{(2)}=-126\tilde{\nu}\tilde{T}^2\tilde{R}^4,\quad\langle(\hat{\boldsymbol{n}}\times\boldsymbol{\Omega})^2(\boldsymbol{V}\cdot\boldsymbol{\omega})^2\rangle^{(2)}=-252\tilde{\nu}\tilde{T}^2\tilde{R}^4$$

$$\langle(\boldsymbol{V}\cdot\boldsymbol{\Omega})^2\boldsymbol{\omega}^2\rangle^{(2)}=-420\tilde{\nu}\tilde{T}^2\tilde{R}^4,\quad\langle(\boldsymbol{V}\cdot\boldsymbol{\Omega})^2\boldsymbol{\Omega}^2\rangle^{(2)}=-840\tilde{\nu}\tilde{T}^2\tilde{R}^4,\quad\langle(\boldsymbol{V}\cdot\boldsymbol{\omega})(\boldsymbol{V}\cdot\boldsymbol{\Omega})(\boldsymbol{\omega}\cdot\boldsymbol{\Omega})\rangle^{(2)}=-315\tilde{\nu}\tilde{T}^2\tilde{R}^4$$

$$\langle((\hat{\boldsymbol{n}}\times\boldsymbol{v})\cdot\boldsymbol{\omega})(\boldsymbol{V}\cdot\boldsymbol{\omega})(\boldsymbol{V}\cdot\boldsymbol{\Omega})\rangle^{(2)}=0,\quad \langle(\boldsymbol{v}\cdot\boldsymbol{\omega})(\boldsymbol{V}\cdot\boldsymbol{\omega})(\hat{\boldsymbol{n}}\cdot\boldsymbol{\omega})(\hat{\boldsymbol{n}}\cdot\boldsymbol{\Omega})\rangle^{(2)}=-189\tilde{\nu}\tilde{T}^2\tilde{R}^4,$$

$$\langle(\boldsymbol{V}\cdot\boldsymbol{\omega})(\boldsymbol{\omega}\cdot\boldsymbol{\Omega})(\hat{\boldsymbol{n}}\cdot\boldsymbol{v})(\hat{\boldsymbol{n}}\cdot\boldsymbol{\omega})\rangle^{(2)}=-210\tilde{\nu}\tilde{T}^2\tilde{R}^4,\quad \langle(\boldsymbol{v}\cdot\boldsymbol{\omega})(\hat{\boldsymbol{n}}\cdot\boldsymbol{\Omega})(\hat{\boldsymbol{n}}\cdot\boldsymbol{V})\boldsymbol{\omega}^2\rangle^{(2)}=-294\tilde{\nu}\tilde{T}^2\tilde{R}^4,$$

$$\langle(\hat{\boldsymbol{n}}\cdot\boldsymbol{v})(\hat{\boldsymbol{n}}\cdot\boldsymbol{\omega})(\hat{\boldsymbol{n}}\cdot\boldsymbol{\Omega})(\hat{\boldsymbol{n}}\cdot\boldsymbol{V})\boldsymbol{\omega}^2\rangle^{(2)}=-168\tilde{\nu}\tilde{T}^2\tilde{R}^4,\quad \langle(\boldsymbol{v}\cdot\boldsymbol{\omega})(\boldsymbol{V}\cdot\boldsymbol{\omega})(\boldsymbol{\omega}\cdot\boldsymbol{\Omega})\rangle^{(2)}=-420\tilde{\nu}\tilde{T}^2\tilde{R}^4$$

$$\langle(\boldsymbol{V}\cdot\boldsymbol{\Omega})((\hat{\boldsymbol{n}}\times\boldsymbol{\Omega})\cdot\boldsymbol{\omega})\boldsymbol{\omega}^2\rangle^{(2)}=0,\quad \langle(\hat{\boldsymbol{n}}\times\boldsymbol{\Omega})^2(\boldsymbol{v}\cdot\boldsymbol{\Omega})(\boldsymbol{V}\cdot\boldsymbol{\omega})\rangle^{(2)}=-504\tilde{\nu}\tilde{T}^2\tilde{R}^4$$

$$\langle(\boldsymbol{v}\cdot\boldsymbol{\Omega})(\boldsymbol{\omega}\cdot\boldsymbol{\Omega})(\hat{\boldsymbol{n}}\cdot\boldsymbol{\Omega})(\hat{\boldsymbol{n}}\cdot\boldsymbol{V})\rangle^{(2)}=-147\tilde{\nu}\tilde{T}^2\tilde{R}^4,\quad \langle(\hat{\boldsymbol{n}}\cdot\boldsymbol{v})(\hat{\boldsymbol{n}}\cdot\boldsymbol{\omega})(\hat{\boldsymbol{n}}\cdot\boldsymbol{\Omega})^3(\hat{\boldsymbol{n}}\cdot\boldsymbol{V})\rangle^{(2)}=-108\tilde{\nu}\tilde{T}^2\tilde{R}^4$$

$$\langle(\boldsymbol{v}\cdot\boldsymbol{\omega})(\boldsymbol{v}\cdot\boldsymbol{\Omega})(\boldsymbol{\omega}\cdot\boldsymbol{\Omega})\rangle^{(2)}=-504\tilde{\nu}\tilde{T}^2\tilde{R}^4,\quad \langle(\boldsymbol{v}\cdot\boldsymbol{\Omega})(\boldsymbol{\omega}\cdot\boldsymbol{\Omega})(\hat{\boldsymbol{n}}\cdot\boldsymbol{v})(\hat{\boldsymbol{n}}\cdot\boldsymbol{\omega})\rangle^{(2)}=-252\tilde{\nu}\tilde{T}^2\tilde{R}^4$$

$$\langle(\hat{\boldsymbol{n}}\times\boldsymbol{\Omega})^2(\boldsymbol{V}\cdot\boldsymbol{\Omega})(\hat{\boldsymbol{n}}\cdot\boldsymbol{\Omega})(\hat{\boldsymbol{n}}\cdot\boldsymbol{V})\rangle^{(2)}=-120\tilde{\nu}\tilde{T}^2\tilde{R}^4,\quad \langle(\hat{\boldsymbol{n}}\times\boldsymbol{\Omega})^2(\boldsymbol{V}\cdot\boldsymbol{\Omega})^2\rangle^{(2)}=-504\tilde{\nu}\tilde{T}^2\tilde{R}^4,$$

$$\langle(\hat{\boldsymbol{n}}\times\boldsymbol{\Omega})^2(\hat{\boldsymbol{n}}\cdot\boldsymbol{\Omega})^2(\hat{\boldsymbol{n}}\cdot\boldsymbol{V})^2\rangle^{(2)}=-24\tilde{\nu}\tilde{T}^2\tilde{R}^4,\quad \langle((\hat{\boldsymbol{n}}\times\boldsymbol{v})\cdot\boldsymbol{\Omega})(\hat{\boldsymbol{n}}\cdot\boldsymbol{\Omega})((\hat{\boldsymbol{n}}\times\boldsymbol{v})\cdot\boldsymbol{V})(\hat{\boldsymbol{n}}\cdot\boldsymbol{V})\rangle^{(2)}=-21\tilde{\nu}\tilde{T}^3\tilde{R}^3,$$

$$\langle(\hat{\boldsymbol{n}}\times\boldsymbol{v})^2(\boldsymbol{V}\cdot\boldsymbol{\Omega})(\hat{\boldsymbol{n}}\cdot\boldsymbol{\Omega})(\hat{\boldsymbol{n}}\cdot\boldsymbol{V})\rangle^{(2)}=-70\tilde{\nu}\tilde{T}^3\tilde{R}^3,\quad \langle(\hat{\boldsymbol{n}}\times\boldsymbol{\Omega})^2((\hat{\boldsymbol{n}}\times\boldsymbol{v})\cdot\boldsymbol{V})^2\rangle^{(2)}=-14\tilde{\nu}\tilde{T}^3\tilde{R}^3,$$

$$\langle(\hat{\boldsymbol{n}}\times\boldsymbol{v})^2(\boldsymbol{V}\cdot\boldsymbol{\Omega})^2\rangle^{(2)}=-210\tilde{\nu}\tilde{T}^3\tilde{R}^3,\quad \langle((\hat{\boldsymbol{n}}\times\boldsymbol{v})\cdot\boldsymbol{\Omega})(\boldsymbol{V}\cdot\boldsymbol{\Omega})((\hat{\boldsymbol{n}}\times\boldsymbol{v})\cdot\boldsymbol{V})\rangle^{(2)}=-28\tilde{\nu}\tilde{T}^3\tilde{R}^3,$$

$$\langle((\hat{\boldsymbol{n}}\times\boldsymbol{v})\cdot\boldsymbol{\Omega})(\boldsymbol{V}\cdot\boldsymbol{\Omega})((\hat{\boldsymbol{n}}\times\boldsymbol{\Omega})\cdot\boldsymbol{\omega})\rangle^{(2)}=105\tilde{\nu}\tilde{T}^2\tilde{R}^4,\quad \langle(\hat{\boldsymbol{n}}\times\boldsymbol{\Omega})^2(\boldsymbol{v}\cdot\boldsymbol{\omega})(\hat{\boldsymbol{n}}\cdot\boldsymbol{\Omega})(\hat{\boldsymbol{n}}\cdot\boldsymbol{V})\rangle^{(2)}=-114\tilde{\nu}\tilde{T}^2\tilde{R}^4,$$

$$\langle(\hat{\boldsymbol{n}}\times\boldsymbol{\Omega})^2(\boldsymbol{V}\cdot\boldsymbol{\Omega})(\hat{\boldsymbol{n}}\cdot\boldsymbol{v})(\hat{\boldsymbol{n}}\cdot\boldsymbol{\omega})\rangle^{(2)}=-252\tilde{\nu}\tilde{T}^2\tilde{R}^4,\quad \langle(\hat{\boldsymbol{n}}\times\boldsymbol{\Omega})^2(\boldsymbol{v}\cdot\boldsymbol{\omega})(\boldsymbol{V}\cdot\boldsymbol{\Omega})\rangle^{(2)}=-546\tilde{\nu}\tilde{T}^2\tilde{R}^4,$$

$$\langle(\hat{\boldsymbol{n}}\times\boldsymbol{\Omega})^2(\hat{\boldsymbol{n}}\cdot\boldsymbol{v})(\hat{\boldsymbol{n}}\cdot\boldsymbol{\omega})(\hat{\boldsymbol{n}}\cdot\boldsymbol{\Omega})(\hat{\boldsymbol{n}}\cdot\boldsymbol{V})\rangle^{(2)}=-60\tilde{\nu}\tilde{T}^2\tilde{R}^4,\quad \langle((\hat{\boldsymbol{n}}\times\boldsymbol{v})\cdot\boldsymbol{\Omega})((\hat{\boldsymbol{n}}\times\boldsymbol{\Omega})\cdot\boldsymbol{\omega})(\hat{\boldsymbol{n}}\cdot\boldsymbol{\Omega})(\hat{\boldsymbol{n}}\cdot\boldsymbol{V})\rangle^{(2)}=21\tilde{\nu}\tilde{T}^2\tilde{R}^4,$$

$$\langle((\hat{\boldsymbol{n}}\times\boldsymbol{v})\cdot\boldsymbol{\Omega})(\hat{\boldsymbol{n}}\cdot\boldsymbol{v})(\hat{\boldsymbol{n}}\cdot\boldsymbol{\omega})((\hat{\boldsymbol{n}}\times\boldsymbol{v})\cdot\boldsymbol{V})\rangle^{(2)}=-42\tilde{\nu}\tilde{T}^3\tilde{R}^3,\quad \langle(\hat{\boldsymbol{n}}\times\boldsymbol{v})^2(\boldsymbol{v}\cdot\boldsymbol{\omega})(\hat{\boldsymbol{n}}\cdot\boldsymbol{\Omega})(\hat{\boldsymbol{n}}\cdot\boldsymbol{V})\rangle^{(2)}=-140\tilde{\nu}\tilde{T}^3\tilde{R}^3,$$

$$\langle(\hat{\boldsymbol{n}}\times\boldsymbol{v})^2(\hat{\boldsymbol{n}}\cdot\boldsymbol{v})(\hat{\boldsymbol{n}}\cdot\boldsymbol{\omega})(\hat{\boldsymbol{n}}\cdot\boldsymbol{\Omega})(\hat{\boldsymbol{n}}\cdot\boldsymbol{V})\rangle^{(2)}=-56\tilde{\nu}\tilde{T}^3\tilde{R}^3,\quad \langle(\hat{\boldsymbol{n}}\times\boldsymbol{\Omega})^2(\boldsymbol{v}\cdot\boldsymbol{\omega})(\hat{\boldsymbol{n}}\cdot\boldsymbol{v})(\hat{\boldsymbol{n}}\cdot\boldsymbol{\omega})\rangle^{(2)}=-156\tilde{\nu}\tilde{T}^2\tilde{R}^4,$$

$$\langle(\hat{\boldsymbol{n}}\times\boldsymbol{\Omega})^2(\boldsymbol{v}\cdot\boldsymbol{\Omega})(\hat{\boldsymbol{n}}\cdot\boldsymbol{v})(\hat{\boldsymbol{n}}\cdot\boldsymbol{\Omega})\rangle^{(2)}=-240\tilde{\nu}\tilde{T}^2\tilde{R}^4,\quad \langle(\hat{\boldsymbol{n}}\times\boldsymbol{\Omega})^2(\boldsymbol{v}\cdot\boldsymbol{\omega})^2\rangle^{(2)}=-384\tilde{\nu}\tilde{T}^2\tilde{R}^4,$$

$$\langle(\hat{\boldsymbol{n}}\times\boldsymbol{\Omega})^2(\hat{\boldsymbol{n}}\cdot\boldsymbol{v})^2(\hat{\boldsymbol{n}}\cdot\boldsymbol{\omega})^2\rangle^{(2)}=-48\tilde{\nu}\tilde{T}^2\tilde{R}^4$$

$$\langle(\hat{\boldsymbol{n}}\times\boldsymbol{\Omega})^2(\boldsymbol{v}\cdot\boldsymbol{\Omega})^2\rangle^{(2)}=-720\tilde{\nu}\tilde{T}^2\tilde{R}^4,\quad \langle(\hat{\boldsymbol{n}}\times\boldsymbol{v})^2(\boldsymbol{v}\cdot\boldsymbol{\omega})(\hat{\boldsymbol{n}}\cdot\boldsymbol{v})(\hat{\boldsymbol{n}}\cdot\boldsymbol{\omega})\rangle^{(2)}=-224\tilde{\nu}\tilde{T}^3\tilde{R}^3$$

$$\langle(\hat{\boldsymbol{n}}\times\boldsymbol{v})^2(\boldsymbol{v}\cdot\boldsymbol{\Omega})(\hat{\boldsymbol{n}}\cdot\boldsymbol{v})(\hat{\boldsymbol{n}}\cdot\boldsymbol{\Omega})\rangle^{(2)}=-176\tilde{\nu}\tilde{T}^3\tilde{R}^3,\quad \langle(\hat{\boldsymbol{n}}\times\boldsymbol{v})^2(\boldsymbol{v}\cdot\boldsymbol{\omega})^2\rangle^{(2)}=-672\tilde{\nu}\tilde{T}^3\tilde{R}^3,$$

$$\langle(\hat{\boldsymbol{n}}\times\boldsymbol{v})^2(\hat{\boldsymbol{n}}\cdot\boldsymbol{v})^2(\hat{\boldsymbol{n}}\cdot\boldsymbol{\omega})^2\rangle^{(2)}=-56\tilde{\nu}\tilde{T}^3\tilde{R}^3,\quad \langle(\hat{\boldsymbol{n}}\times\boldsymbol{\Omega})^2((\hat{\boldsymbol{n}}\times\boldsymbol{\Omega})\cdot\boldsymbol{\omega})^2\rangle^{(2)}=100\tilde{\nu}\tilde{T}\tilde{R}^5$$

$$\langle((\hat{\boldsymbol{n}}\times\boldsymbol{v})\cdot\boldsymbol{\omega})(\boldsymbol{\omega}\cdot\boldsymbol{\Omega})\boldsymbol{V}^2\rangle^{(2)}=0,\quad \langle(\hat{\boldsymbol{n}}\times\boldsymbol{\Omega})^2(\boldsymbol{\omega}\cdot\boldsymbol{\Omega})^2\rangle^{(2)}=105\tilde{\nu}\tilde{T}\tilde{R}^5$$

$$\langle((\hat{\boldsymbol{n}}\times\boldsymbol{\Omega})\cdot\boldsymbol{V})((\hat{\boldsymbol{n}}\times\boldsymbol{v})\cdot\boldsymbol{\Omega})(\boldsymbol{\omega}\cdot\boldsymbol{\Omega})\rangle^{(2)}=-105\tilde{\nu}\tilde{T}^2\tilde{R}^4,\quad \langle((\hat{\boldsymbol{n}}\times\boldsymbol{v})\cdot\boldsymbol{\omega})^2\boldsymbol{V}^2\rangle^{(2)}=126\tilde{\nu}\tilde{T}^3\tilde{R}^3$$

$$\langle((\hat{\boldsymbol{n}}\times\boldsymbol{\Omega})\cdot\boldsymbol{V})((\hat{\boldsymbol{n}}\times\boldsymbol{v})\cdot\boldsymbol{\omega})\boldsymbol{\omega}^2\rangle^{(2)}=-210\tilde{\nu}\tilde{T}^2\tilde{R}^4,\quad \langle(\hat{\boldsymbol{n}}\times\boldsymbol{v})^2\boldsymbol{V}^2\boldsymbol{\omega}^2\rangle^{(2)}=0,\quad \langle(\hat{\boldsymbol{n}}\times\boldsymbol{\Omega})^2\boldsymbol{V}^2\boldsymbol{\omega}^2\rangle^{(2)}=84\tilde{\nu}\tilde{T}^2\tilde{R}^4$$

$$\langle((\hat{\boldsymbol{n}}\times\boldsymbol{v})\cdot\boldsymbol{\Omega})\boldsymbol{V}^2\boldsymbol{\omega}^2\rangle^{(2)}=0,\ \langle(\hat{\boldsymbol{n}}\times\boldsymbol{\Omega})^2\boldsymbol{\omega}^4\rangle^{(2)}=175\tilde{\nu}\tilde{T}\tilde{R}^5,\ \langle(\hat{\boldsymbol{n}}\times\boldsymbol{\Omega})^2\boldsymbol{\omega}^2\boldsymbol{\Omega}^2\rangle^{(2)}=217\tilde{\nu}\tilde{T}\tilde{R}^5,\ \langle(\hat{\boldsymbol{n}}\times\boldsymbol{\Omega})^2\boldsymbol{\Omega}^4\rangle^{(2)}=567\tilde{\nu}\tilde{T}\tilde{R}^5$$

$$\langle((\hat{\boldsymbol{n}}\times\boldsymbol{\Omega})\cdot\boldsymbol{V})(\hat{\boldsymbol{n}}\times\boldsymbol{v})^2((\hat{\boldsymbol{n}}\times\boldsymbol{v})\cdot\boldsymbol{\omega})\rangle^{(2)}=-140\tilde{\nu}\tilde{T}^3\tilde{R}^3,\quad \langle((\hat{\boldsymbol{n}}\times\boldsymbol{\Omega})\cdot\boldsymbol{V})(\hat{\boldsymbol{n}}\times\boldsymbol{\Omega})^2((\hat{\boldsymbol{n}}\times\boldsymbol{v})\cdot\boldsymbol{\omega})\rangle^{(2)}=-168\tilde{\nu}\tilde{T}^2\tilde{R}^4$$

$$\langle(\hat{\boldsymbol{n}}\times\boldsymbol{\Omega})^2((\hat{\boldsymbol{n}}\times\boldsymbol{v})\cdot\boldsymbol{\omega})^2\rangle^{(2)}=120\tilde{\nu}\tilde{T}^2\tilde{R}^4,\quad \langle(\hat{\boldsymbol{n}}\times\boldsymbol{\Omega})^4\boldsymbol{V}^2\rangle^{(2)}=192\tilde{\nu}\tilde{T}^2\tilde{R}^4,\quad \langle(\hat{\boldsymbol{n}}\times\boldsymbol{\Omega})^4\boldsymbol{\omega}^2\rangle^{(2)}=248\tilde{\nu}\tilde{T}\tilde{R}^5$$

$$\langle(\hat{\boldsymbol{n}}\times\boldsymbol{\Omega})^4\boldsymbol{\Omega}^2\rangle^{(2)}=648\tilde{\nu}\tilde{T}\tilde{R}^5,\quad \langle(\hat{\boldsymbol{n}}\times\boldsymbol{v})^4(\hat{\boldsymbol{n}}\times\boldsymbol{\Omega})^2\rangle^{(2)}=-56\tilde{\nu}\tilde{T}^3\tilde{R}^3,\quad \langle(\hat{\boldsymbol{n}}\times\boldsymbol{v})^2(\hat{\boldsymbol{n}}\times\boldsymbol{\Omega})^4\rangle^{(2)}=0$$

$$\langle(\hat{\boldsymbol{n}}\times\boldsymbol{\Omega})^6\rangle^{(2)}=648\tilde{\nu}\tilde{T}\tilde{R}^5,\quad \langle(\hat{\boldsymbol{n}}\times\boldsymbol{\Omega})^2(\boldsymbol{\omega}\cdot\boldsymbol{\Omega})(\boldsymbol{v}\cdot\boldsymbol{V})\rangle^{(2)}=42\tilde{\nu}\tilde{T}^2\tilde{R}^4,\quad \langle(\hat{\boldsymbol{n}}\times\boldsymbol{\Omega})^2(\boldsymbol{\omega}\cdot\boldsymbol{\Omega})(\hat{\boldsymbol{n}}\cdot\boldsymbol{v})(\hat{\boldsymbol{n}}\cdot\boldsymbol{V})\rangle^{(2)}=84\tilde{\nu}\tilde{T}^2\tilde{R}^4,$$

$$\langle((\hat{\boldsymbol{n}}\times\boldsymbol{v})\cdot\boldsymbol{\omega})((\hat{\boldsymbol{n}}\times\boldsymbol{v})\cdot\boldsymbol{\Omega})(\boldsymbol{v}\cdot\boldsymbol{V})\rangle^{(2)}=84\tilde{\nu}\tilde{T}^3\tilde{R}^3,\quad \langle((\hat{\boldsymbol{n}}\times\boldsymbol{v})\cdot\boldsymbol{\omega})((\hat{\boldsymbol{n}}\times\boldsymbol{v})\cdot\boldsymbol{\Omega})(\hat{\boldsymbol{n}}\cdot\boldsymbol{v})(\hat{\boldsymbol{n}}\cdot\boldsymbol{V})\rangle^{(2)}=28\tilde{\nu}\tilde{T}^3\tilde{R}^3,$$

$$\langle((\hat{\boldsymbol{n}}\times\boldsymbol{v})\cdot\boldsymbol{\omega})((\hat{\boldsymbol{n}}\times\boldsymbol{v})\cdot\boldsymbol{\Omega})(\boldsymbol{\omega}\cdot\boldsymbol{\Omega})\rangle^{(2)}=126\tilde{\nu}\tilde{T}^2\tilde{R}^4,\ \langle((\hat{\boldsymbol{n}}\times\boldsymbol{v})\cdot\boldsymbol{\Omega})^2\boldsymbol{\omega}^2\rangle^{(2)}=168\tilde{\nu}\tilde{T}^2\tilde{R}^4,\ \langle((\hat{\boldsymbol{n}}\times\boldsymbol{v})\cdot\boldsymbol{\omega})^2(\hat{\boldsymbol{n}}\cdot\boldsymbol{v})^2\rangle^{(2)}=112\tilde{\nu}\tilde{T}^3\tilde{R}^3$$

$$\langle((\hat{\boldsymbol{n}}\times\boldsymbol{v})\cdot\boldsymbol{\omega})^2\boldsymbol{v}^2\rangle^{(2)}=336\tilde{\nu}\tilde{T}^3\tilde{R}^3,\quad \langle((\hat{\boldsymbol{n}}\times\boldsymbol{v})\cdot\boldsymbol{\omega})^2((\hat{\boldsymbol{n}}\times\boldsymbol{v})\cdot\boldsymbol{\Omega})\rangle^{(2)}=0,\quad \langle((\hat{\boldsymbol{n}}\times\boldsymbol{v})\cdot\boldsymbol{\Omega})^3\rangle^{(2)}=0$$

$$\langle(\hat{\boldsymbol{n}}\times\boldsymbol{\Omega})^2((\hat{\boldsymbol{n}}\times\boldsymbol{v})\cdot\boldsymbol{\Omega})^2\rangle^{(2)}=288\tilde{\nu}\tilde{T}^2\tilde{R}^4,\quad \langle(\hat{\boldsymbol{n}}\times\boldsymbol{v})^2((\hat{\boldsymbol{n}}\times\boldsymbol{v})\cdot\boldsymbol{\Omega})^2\rangle^{(2)}=224\tilde{\nu}\tilde{T}^3\tilde{R}^3,\quad \langle(\hat{\boldsymbol{n}}\times\boldsymbol{\Omega})^4(\hat{\boldsymbol{n}}\cdot\boldsymbol{v})^2\rangle^{(2)}=384\tilde{\nu}\tilde{T}^2\tilde{R}^4$$

$$\langle(\hat{\boldsymbol{n}}\times\boldsymbol{v})^2(\hat{\boldsymbol{n}}\times\boldsymbol{\Omega})^2(\hat{\boldsymbol{n}}\cdot\boldsymbol{v})^2\rangle^{(2)}=56\tilde{\nu}\tilde{T}^3\tilde{R}^3,\quad \langle(\hat{\boldsymbol{n}}\times\boldsymbol{v})^2(\hat{\boldsymbol{n}}\times\boldsymbol{\Omega})^2\boldsymbol{v}^2\rangle^{(2)}=0,\quad \langle(\hat{\boldsymbol{n}}\times\boldsymbol{v})^2(\hat{\boldsymbol{n}}\times\boldsymbol{\Omega})^2((\hat{\boldsymbol{n}}\times\boldsymbol{v})\cdot\boldsymbol{\Omega})\rangle^{(2)}=0$$

$$\langle(\hat{\boldsymbol{n}}\times\boldsymbol{\Omega})^4((\hat{\boldsymbol{n}}\times\boldsymbol{v})\cdot\boldsymbol{\Omega})\rangle^{(2)}=0$$

The averages of the type $\langle(\mathcal{B}_{12}-1)\Delta^{(\alpha\beta 2)}\rangle^{(3)}$, with $\alpha,\beta=1,2$, contain the following terms:

$$\langle(\boldsymbol{v}\cdot\boldsymbol{\omega})^2\rangle^{(3)}=-180\tilde{\nu}\tilde{T}^3\tilde{R}^2,\quad \langle[((\hat{\boldsymbol{n}}\times\boldsymbol{\Omega})\cdot\boldsymbol{\omega})]^2\rangle^{(3)}=13\tilde{\nu}\tilde{T}^2\tilde{R}^3,\quad \langle(\hat{\boldsymbol{n}}\cdot\boldsymbol{v})^2(\hat{\boldsymbol{n}}\cdot\boldsymbol{\omega})^2\rangle^{(3)}=-45\tilde{\nu}\tilde{T}^3\tilde{R}^2$$

$$\langle(\hat{\boldsymbol{n}}\cdot\boldsymbol{v})(\hat{\boldsymbol{n}}\cdot\boldsymbol{\omega})(\boldsymbol{v}\cdot\boldsymbol{\omega})\rangle^{(3)}=-90\tilde{\nu}\tilde{T}^3\tilde{R}^2,\quad \langle(\hat{\boldsymbol{n}}\cdot\boldsymbol{V})^2(\hat{\boldsymbol{n}}\cdot\boldsymbol{\Omega})^2\rangle^{(3)}=-\frac{53}{2}\tilde{\nu}\tilde{T}^3\tilde{R}^2,\quad \langle(\boldsymbol{V}\cdot\boldsymbol{\Omega})^2\rangle^{(3)}=-\frac{245}{2}\tilde{\nu}\tilde{T}^3\tilde{R}^2$$

$$\langle(\hat{\boldsymbol{n}}\cdot\boldsymbol{V})(\hat{\boldsymbol{n}}\cdot\boldsymbol{\Omega})(\boldsymbol{V}\cdot\boldsymbol{\Omega})\rangle^{(3)}=-52\tilde{\nu}\tilde{T}^3\tilde{R}^2,\quad \langle(\boldsymbol{v}\cdot\boldsymbol{\Omega})(\boldsymbol{V}\cdot\boldsymbol{\omega})\rangle^{(3)}=-154\tilde{\nu}\tilde{T}^3\tilde{R}^2,\quad \langle(\hat{\boldsymbol{n}}\cdot\boldsymbol{v})(\hat{\boldsymbol{n}}\cdot\boldsymbol{\Omega})(\boldsymbol{V}\cdot\boldsymbol{\omega})\rangle^{(3)}=-77\tilde{\nu}\tilde{T}^3\tilde{R}^2$$

$$\langle(\hat{\boldsymbol{n}}\cdot\boldsymbol{V})(\hat{\boldsymbol{n}}\cdot\boldsymbol{\Omega})(\boldsymbol{v}\cdot\boldsymbol{\omega})\rangle^{(3)}=-\frac{115}{2}\tilde{\nu}\tilde{T}^3\tilde{R}^2,\quad \langle(\hat{\boldsymbol{n}}\cdot\boldsymbol{v})(\hat{\boldsymbol{n}}\cdot\boldsymbol{\omega})(\hat{\boldsymbol{n}}\cdot\boldsymbol{V})(\hat{\boldsymbol{n}}\cdot\boldsymbol{\Omega})\rangle^{(3)}=-32\tilde{\nu}\tilde{T}^3\tilde{R}^2,\quad \langle\boldsymbol{v}^2(\hat{\boldsymbol{n}}\times\boldsymbol{\Omega})^2\rangle^{(3)}=45\tilde{\nu}\tilde{T}^3\tilde{R}^2$$

$$\langle\boldsymbol{V}^2(\hat{\boldsymbol{n}}\times\boldsymbol{\Omega})^2\rangle^{(3)}=\frac{53}{2}\tilde{\nu}\tilde{T}^3\tilde{R}^2,\quad \langle\boldsymbol{v}^2\boldsymbol{\omega}^2\rangle^{(3)}=0,\quad \langle\boldsymbol{\omega}^2(\hat{\boldsymbol{n}}\times\boldsymbol{\Omega})^2\rangle^{(3)}=\frac{39}{2}\tilde{\nu}\tilde{T}^2\tilde{R}^3$$

$$\langle\boldsymbol{\Omega}^2(\hat{\boldsymbol{n}}\times\boldsymbol{\Omega})^2\rangle^{(3)}=\frac{91}{2}\tilde{\nu}\tilde{T}^2\tilde{R}^3,\quad \langle\boldsymbol{\omega}^2(\hat{\boldsymbol{n}}\cdot\boldsymbol{v})^2\rangle^{(3)}=0,\quad \langle(\hat{\boldsymbol{n}}\times\boldsymbol{\Omega})^4\rangle^{(3)}=52\tilde{\nu}\tilde{T}^2\tilde{R}^3$$

$$\langle((\hat{\boldsymbol{n}}\times\boldsymbol{v})\cdot\boldsymbol{\Omega})^2\rangle^{(3)}=45\tilde{\nu}\tilde{T}^3\tilde{R}^2,\quad \langle((\hat{\boldsymbol{n}}\times\boldsymbol{\Omega})\cdot\boldsymbol{V})((\hat{\boldsymbol{n}}\times\boldsymbol{v})\cdot\boldsymbol{\omega})\rangle^{(3)}=-\frac{77}{2}\tilde{\nu}\tilde{T}^3\tilde{R}^2,\quad \langle(\hat{\boldsymbol{n}}\times\boldsymbol{v})^2\rangle^{(3)}=0$$

$$\langle(\hat{\boldsymbol{n}}\cdot\boldsymbol{v})^2\rangle^{(3)}=0,\quad \langle(\hat{\boldsymbol{n}}\times\boldsymbol{\Omega})^2\rangle^{(3)}=\frac{13}{2}\tilde{\nu}\tilde{T}^2\tilde{R}^2,\quad \langle((\hat{\boldsymbol{n}}\times\boldsymbol{v})\cdot\boldsymbol{\Omega})\rangle^{(3)}=0$$

There are a few more terms (that run thro' about ten additional pages) that are not shown, but can be obtained from the authors. All these expressions are needed to calculate average terms of the form $\langle(\mathcal{B}_{12}-1)\Delta^{(\alpha\beta 2)}\rangle^{(k)}$ which are given below in Appendix A.3.

A.3 Expressions for Average Terms of the Form $\left\langle(\mathcal{B}_{12}-1)\Delta^{(\alpha\beta 2)}\right\rangle^{(k)}$

The expressions for various terms of the form $\langle(\mathcal{B}_{12}-1)\Delta^{(\alpha\beta 2)}\rangle^{(k)}$ as defined in Eq. (A.17) of Appendix-A.2 are given below.

$$\left\langle(\mathcal{B}_{12}-1)\Delta^{(112)}\right\rangle^{(0)}=-\frac{1}{3a^2m^2q^4}G\sqrt{T}\eta_t\Big[-q^2RT+q(RT+q(5R^2+6RT+6T^2))\eta_t-16q(R+T)(R+qT)\eta_t^2$$
$$+16(R+qT)^2\eta_t^3-8qT\eta_n(-qR+(R+qT)\eta_t)+8qT\eta_n^2(-qR+(R+qT)\eta_t)\Big],\tag{A.34}$$

$$\left\langle(\mathcal{B}_{12}-1)\Delta^{(112)}\right\rangle^{(1)}=\frac{1}{6a^4m^4q^5}GR^2T^{3/2}\Big[4qT\eta_n(-33q^2+2q(14+9q)\eta_t-6\eta_t^2)+12qT\eta_n^2(3q^2-2q\eta_t+2\eta_t^2)$$
$$+\eta_t\Big(-q^2(145+132q)T+q(4qR+45T+114qT+36q^2T)\eta_t-16q(2R+3(1+q)T)\eta_t^2+32(R+3qT)\eta_t^3\Big)\Big],\tag{A.35}$$

$$\left\langle(\mathcal{B}_{12}-1)\Delta^{(112)}\right\rangle^{(2)}=\frac{1}{6a^6m^5q^6}GR^3T^{3/2}\Big[28qT\eta_n(-33q^2+2q(14+9q)\eta_t-6\eta_t^2)+84qT\eta_n^2(3q^2-2q\eta_t+2\eta_t^2)$$
$$+\eta_t\Big(-7q^2(145+132q)T+21q(15T+12q^2T+2q(R+19T))\eta_t-16q(16R+21(1+q)T)\eta_t^2$$
$$+32(8R+21qT)\eta_t^3\Big)\Big],\tag{A.36}$$

$$\left\langle(\mathcal{B}_{12}-1)\Delta^{(112)}\right\rangle^{(3)}=\frac{1}{12a^4m^5q^5}GR^2T^{5/2}\Big[4qT\eta_n(-501q^2+2q(212+135q)\eta_t-90\eta_t^2)$$
$$+180qT\eta_n^2(3q^2-2q\eta_t+2\eta_t^2)+\eta_t\Big(-3q^2(741+668q)T+q(52qR+683T+1722qT+540q^2T)\eta_t$$
$$-16q(26R+45(1+q)T)\eta_t^2+32(13R+45qT)\eta_t^3\Big)\Big],\tag{A.37}$$

and

$$\Big\langle(\mathcal{B}_{12}-1)\Delta^{(122)}\Big\rangle^{(0)} = -\frac{1}{3a^4m^3q^7}G\sqrt{T}\eta_t\Big[-7q^4R^2T+q^3R(15RT+7q(5R^2+6RT+6T^2))\eta_t$$
$$-8q^2R(2RT+14q^2T(R+T)+3q(7R^2+8RT+3T^2))\eta_t^2+8q(R^2T+14q^3RT^2+q^2T(59R^2+34RT+8T^2)$$
$$+qR(45R^2+34RT+9T^2))\eta_t^3-192q(2R+T)(R+qT)^2\eta_t^4+192(R+qT)^3\eta_t^5-8qT\eta_n(-7q^3R^2+q^2R(15R+7qT)\eta_t$$
$$-16qR(R+qT)\eta_t^2+8(R+qT)^2\eta_t^3)+8qT\eta_n^2\Big(-7q^3R^2+q^2R(15R+7qT)\eta_t$$
$$-16qR(R+qT)\eta_t^2+8(R+qT)^2\eta_t^3\Big)\Big], \tag{A.38}$$

$$\Big\langle(\mathcal{B}_{12}-1)\Delta^{(122)}\Big\rangle^{(1)} = \frac{1}{6a^6m^5q^8}GR^2T^{3/2}\Big[4qT\eta_n(-231q^4R+2q^3(220+63q)R\eta_t$$
$$-2q^2((295+72q)R+136qT)\eta_t^2+16q((25+9q)R$$
$$+q(23+9q)T)\eta_t^3-32(3R+5qT)\eta_t^4)+4qT\eta_n^2(63q^4R-102q^3R\eta_t+22q^2(9R+4qT)\eta_t^2-32q(6R+5qT)\eta_t^3$$
$$+32(3R+5qT)\eta_t^4)+\eta_t\Big(-q^4(2069+924q)RT+q^3(2969RT+252q^2RT+6q(7R^2+407RT+227T^2))\eta_t$$
$$-8q^2(272RT+2q^2T(69R+136T)+q(51R^2+518RT+267T^2))\eta_t^2+8q(72RT+124q^3T^2+2q^2T(198R+185T)$$
$$+q(123R^2+404RT+111T^2))\eta_t^3-384q(3R^2+5q(1+q)T^2+3R(T+4qT))\eta_t^4$$
$$+576(R^2+6qRT+5q^2T^2)\eta_t^5\Big)\Big], \tag{A.39}$$

$$\Big\langle(\mathcal{B}_{12}-1)\Delta^{(122)}\Big\rangle^{(2)} = \frac{1}{6a^8m^6q^9}GR^3T^{3/2}\Big[4qT\eta_n(-2079q^4R+18q^3(220+63q)R\eta_t$$
$$-4q^2(3(421+108q)R+458qT)\eta_t^2+32q(6(17+6q)R$$
$$+q(76+27q)T)\eta_t^3-32(24R+35qT)\eta_t^4)+4qT\eta_n^2(567q^4R-918q^3R\eta_t+56q^2(30R+11qT)\eta_t^2$$
$$-32q(48R+35qT)\eta_t^3+32(24R+35qT)\eta_t^4)+\eta_t\Big(-9q^4(2069+924q)RT+6q^3(4279RT+378q^2RT+q(84R^2$$
$$+3663RT+1589T^2))\eta_t-8q^2(2250RT+2q^2T(621R+970T)+q(517R^2+4404RT+1905T^2))\eta_t^2+8q(576RT$$
$$+940q^3T^2+2q^2T(1677R+1367T)+q(1169R^2+3300RT+849T^2))\eta_t^3-384q(27R^2+35q(1+q)T^2$$
$$+24R(T+4qT))\eta_t^4+576(9R^2+48qRT+35q^2T^2)\eta_t^5\Big)\Big], \tag{A.40}$$

$$\Big\langle(\mathcal{B}_{12}-1)\Delta^{(122)}\Big\rangle^{(3)} = \frac{1}{12a^6m^6q^8}GR^2T^{5/2}\Big[4qT\eta_n(-3507q^4R+2q^3(3334+945q)R\eta_t$$
$$-2q^2((4477+1080q)R+2360qT)\eta_t^2+16q((379+135q)R+q(403+153q)T)\eta_t^3-160(9R+17qT)\eta_t^4)$$
$$+4qT\eta_n^2(945q^4R-1530q^3R\eta_t+22q^2(135R+68qT)\eta_t^2$$
$$-160q(18R+17qT)\eta_t^3+160(9R+17qT)\eta_t^4)+\eta_t\Big(-3q^4(10593+4676q)RT+q^3(45479RT+3780q^2RT+6q(91R^2$$
$$+6163RT+4039T^2))\eta_t-8q^2(4156RT+10q^2T(207R+472T)+q(663R^2+7850RT+4755T^2))\eta_t^2+8q(1096RT$$
$$+2108q^3T^2+2q^2T(2970R+3247T)+q(1599R^2+6128RT+1959T^2))\eta_t^3-384q(39R^2+85q(1+q)T^2$$
$$+45R(T+4qT))\eta_t^4+576(13R^2+90qRT+85q^2T^2)\eta_t^5\Big)\Big], \tag{A.41}$$

and

$$\Big\langle(\mathcal{B}_{12}-1)\Delta^{(212)}\Big\rangle^{(0)}=-\frac{1}{6a^2m^3q^5}G\sqrt{T}\eta_t\Big[-13q^3RT^2+q^2T(13RT+q(77R^2+102RT+90T^2))\eta_t$$
$$-16q^2T((16+7q)R^2+2(8+13q)RT+23qT^2)\eta_t^2+16q(16R^2T+q^2T(7R^2+34RT+47T^2)+qR(7R^2$$
$$+34RT+63T^2))\eta_t^3-384q(R+2T)(R+qT)^2\eta_t^4$$
$$+384(R+qT)^3\eta_t^5-256q^2T^2\eta_n^3(-qR+(R+qT)\eta_t)+128q^2T^2\eta_n^4(-qR+(R+qT)\eta_t)-8qT\eta_n(-16q^2RT+q(16RT$$
$$+q(7R^2+18RT+23T^2))\eta_t-32q(R+T)(R+qT)\eta_t^2+32(R+qT)^2\eta_t^3)+8qT\eta_n^2\Big(-32q^2RT+q(32RT+q(7R^2$$
$$+18RT+39T^2))\eta_t-32q(R+T)(R+qT)\eta_t^2+32(R+qT)^2\eta_t^3\Big)\Big], \tag{A.42}$$

$$\Big\langle(\mathcal{B}_{12}-1)\Delta^{(212)}\Big\rangle^{(1)}=\frac{1}{12a^4m^5q^6}GR^2T^{3/2}\Big[128q^2T^2\eta_n^3(-30q^2+q(23+9q)\eta_t-10\eta_t^2)$$
$$+320q^2T^2\eta_n^4(3q^2-2q\eta_t+2\eta_t^2)+8qT\eta_n(-501q^3T+q^2(469+495q)T\eta_t$$
$$-2q(55T+174q^2T+61q(2R+3T))\eta_t^2+16q((25+9q)R$$
$$+(10+23q+9q^2)T)\eta_t^3-64(3R+5qT)\eta_t^4)+16qT\eta_n^2(339q^3T-q^2(295+174q)T\eta_t+q(30qR+95T+93qT$$
$$+24q^2T)\eta_t^2-16q(6R+5(1+q)T)\eta_t^3+32(3R+5qT)\eta_t^4)+\eta_t\Big(-3q^3(741+1336q)T^2+q^2T(683T+5424q^2T$$
$$+6q(454R+861T))\eta_t-32q^2T((159+122q)R+(73+262q+120q^2)T)\eta_t^2+16q(162RT+60q^3T^2$$
$$+2q^2T(48R+185T)+q(15R^2+404RT+381T^2))\eta_t^3-384q(3R^2+12(1+q)RT+5q(4+q)T^2)\eta_t^4$$
$$+1152(R^2+6qRT+5q^2T^2)\eta_t^5\Big)\Big], \tag{A.43}$$

$$\Big\langle(\mathcal{B}_{12}-1)\Delta^{(212)}\Big\rangle^{(2)}=\frac{1}{12a^6m^6q^5}GR^3T^{3/2}\Big[\frac{16R^2\eta_t^4(149q^2-648q\eta_t+648\eta_t^2)}{q^2}$$
$$+\frac{1}{q}6RT\eta_t^2\Big(3765q^2-16q(430+337q)\eta_t+16(216+550q+135q^2)\eta_t^2-6144(1+q)\eta_t^3+9216\eta_t^4$$
$$+8\eta_n(-337q^2+32q(17+6q)\eta_t-256\eta_t^2)+8\eta_n^2(87q^2-256q\eta_t+256\eta_t^2)\Big)$$
$$+7T^2\Big(128\eta_n^3(-30q^2+q(23+9q)\eta_t-10\eta_t^2)+320\eta_n^4(3q^2-2q\eta_t+2\eta_t^2)+8\eta_n(-501q^2$$
$$+q(469+495q)\eta_t-2(55+183q+174q^2)\eta_t^2+16(10+23q+9q^2)\eta_t^3-320\eta_t^4)+16\eta_n^2(339q^2-q(295+174q)\eta_t$$
$$+(95+93q+24q^2)\eta_t^2-80(1+q)\eta_t^3+160\eta_t^4)+\eta_t\Big(-3q(741+1336q)+(683+5166q+5424q^2)\eta_t$$
$$-32(73+262q+120q^2)\eta_t^2+16(381+370q+60q^2)\eta_t^3-1920(4+q)\eta_t^4+5760\eta_t^5\Big)\Big)\Big], \tag{A.44}$$

$$\Big\langle(\mathcal{B}_{12}-1)\Delta^{(212)}\Big\rangle^{(3)}=\frac{1}{24a^4m^6q^6}GR^2T^{5/2}\Big[128q^2T^2\eta_n^3(-528q^2+q(403+153q)\eta_t-170\eta_t^2)$$
$$+5440q^2T^2\eta_n^4(3q^2-2q\eta_t+2\eta_t^2)+8qT\eta_n(-9675q^3T$$
$$+3q^2(3011+3157q)T\eta_t-2q(1045T+3138q^2T+5q(370R+699T))\eta_t^2+16q((379+135q)R$$
$$+(186+403q+153q^2)T)\eta_t^3-320(9R+17qT)\eta_t^4)+16qT\eta_n^2(6258q^3T-q^2(5399+3138q)T\eta_t+q(450qR+1687T$$
$$+1635qT+408q^2T)\eta_t^2-80q(18R+17(1+q)T)\eta_t^3+160(9R+17qT)\eta_t^4)+\eta_t\Big(-3q^3(14413+25800q)T^2$$
$$+q^2T(41788qR+13195T+99378qT+100128q^2T)\eta_t-32q^2T((2437+1850q)R+(1387+4766q+2112q^2)T)\eta_t^2$$
$$+16q(2462RT+1020q^3T^2+2q^2T(720R+3247T)+q(195R^2+6128RT+6757T^2))\eta_t^3$$
$$-384q(39R^2+180(1+q)RT+85q(4+q)T^2)\eta_t^4+1152(13R^2+90qRT+85q^2T^2)\eta_t^5\Big)\Big]. \tag{A.45}$$

Now we have explicit expressions for $\langle(\mathcal{B}_{12}-1)\Delta^{(\alpha\beta2)}\rangle^{(k)}$ in terms of T, R and other parameters. These are substituted into Eqs. (A.11)-(A.13) to obtain evolution equations for b_{112}, b_{122} and b_{212} as detailed below.

A.4 Evolution Equations for $T(t)$, $R(t)$, $b_{112}(t)$, $b_{122}(t)$ and $b_{212}(t)$

The results of above calculations are five first order differential equations for $T(t)$, $R(t)$, $b_{112}(t)$, $b_{122}(t)$ and $b_{212}(t)$:

$$\frac{3}{2}\frac{\mathrm{d}T}{\mathrm{d}t} = -\alpha_1 G T(t)^{3/2} + \alpha_2 G T(t)^{1/2}\left[1 - \frac{b_{112}(t)}{2}\frac{T(t)R(t)}{qm^2a^2} - \frac{7b_{122}(t)}{2}\frac{T(t)R^2(t)}{q^2m^3a^4} - \frac{13b_{212}(t)}{4}\frac{T^2(t)R(t)}{qm^3a^2}\right]R(t), \tag{A.46}$$

$$\frac{3}{2}\frac{\mathrm{d}R}{\mathrm{d}t} = \alpha_2 G T(t)^{3/2} - \alpha_3 G T(t)^{1/2}\left[1 - \frac{b_{112}(t)}{2}\frac{T(t)R(t)}{qm^2a^2} - \frac{7b_{122}(t)}{2}\frac{T(t)R^2(t)}{q^2m^3a^4} - \frac{13b_{212}(t)}{4}\frac{T^2(t)R(t)}{qm^3a^2}\right]R(t), \tag{A.47}$$

$$\begin{aligned}\frac{30R^2T^2}{a^4m^4q^2}\frac{\mathrm{d}b_{112}(t)}{\mathrm{d}t} &+ \frac{210R^3T^2}{a^6m^5q^3}\frac{\mathrm{d}b_{122}(t)}{\mathrm{d}t} + \frac{210R^2T^3}{a^4m^5q^2}\frac{\mathrm{d}b_{212}(t)}{\mathrm{d}t} = A_1 - b_{112}(t)\left[\frac{60TR}{a^4m^4q^2}\left(T\frac{\mathrm{d}R}{\mathrm{d}t} + R\frac{\mathrm{d}T}{\mathrm{d}t}\right) - B_1\right]\\ &- b_{122}(t)\left[\frac{210TR^2}{a^6m^5q^3}\left(3T\frac{\mathrm{d}R}{\mathrm{d}t} + 2R\frac{\mathrm{d}T}{\mathrm{d}t}\right) - C_1\right] - b_{212}(t)\left[\frac{210RT^2}{a^4m^5q^2}\left(2T\frac{\mathrm{d}R}{\mathrm{d}t} + 3R\frac{\mathrm{d}T}{\mathrm{d}t}\right) - D_1\right],\end{aligned} \tag{A.48}$$

$$\begin{aligned}\frac{210R^3T^2}{a^6m^5q^3}\frac{\mathrm{d}b_{112}(t)}{\mathrm{d}t} &+ \frac{1890R^4T^2}{a^8m^6q^4}\frac{\mathrm{d}b_{122}(t)}{\mathrm{d}t} + \frac{1470R^3T^3}{a^6m^6q^3}\frac{\mathrm{d}b_{212}(t)}{\mathrm{d}t} = A_3 - b_{112}(t)\left[\frac{210TR^2}{a^6m^5q^3}\left(3T\frac{\mathrm{d}R}{\mathrm{d}t} + 2R\frac{\mathrm{d}T}{\mathrm{d}t}\right) - B_3\right]\\ &- b_{122}(t)\left[\frac{3780TR^3}{a^8m^6q^4}\left(2T\frac{\mathrm{d}R}{\mathrm{d}t} + R\frac{\mathrm{d}T}{\mathrm{d}t}\right) - C_3\right] - b_{212}(t)\left[\frac{4410T^2R^2}{a^6m^6q^3}\left(T\frac{\mathrm{d}R}{\mathrm{d}t} + R\frac{\mathrm{d}T}{\mathrm{d}t}\right) - D_3\right],\end{aligned} \tag{A.49}$$

$$\begin{aligned}\frac{210R^2T^3}{a^4m^5q^2}\frac{\mathrm{d}b_{112}(t)}{\mathrm{d}t} &+ \frac{1470R^3T^3}{a^6m^6q^3}\frac{\mathrm{d}b_{122}(t)}{\mathrm{d}t} + \frac{1890R^2T^4}{a^4m^6q^2}\frac{\mathrm{d}b_{212}(t)}{\mathrm{d}t} = A_5 - b_{112}(t)\left[\frac{210T^2R}{a^4m^5q^2}\left(2T\frac{\mathrm{d}R}{\mathrm{d}t} + 3R\frac{\mathrm{d}T}{\mathrm{d}t}\right) - B_5\right]\\ &- b_{122}(t)\left[\frac{4410T^2R^2}{a^6m^6q^3}\left(T\frac{\mathrm{d}R}{\mathrm{d}t} + R\frac{\mathrm{d}T}{\mathrm{d}t}\right) - C_5\right] - b_{212}(t)\left[\frac{3780T^3R}{a^4m^6q^2}\left(T\frac{\mathrm{d}R}{\mathrm{d}t} + 2R\frac{\mathrm{d}T}{\mathrm{d}t}\right) - D_5\right],\end{aligned} \tag{A.50}$$

where

$$\alpha_1 \equiv \eta_n(1-\eta_n) + \eta_t(1-\eta_t),\ \alpha_2 \equiv \frac{\eta_t^2}{q},\ \alpha_3 \equiv \frac{\eta_t}{q}\left(1-\frac{\eta_t}{q}\right),\ G = 32na^2\sqrt{\frac{\pi}{m}}g_2(2a) \tag{A.51}$$

and the expressions for A_1, B_1, ..., are given below.

$$\begin{aligned}A_1 = &-\frac{1}{3a^2m^2q^4}G\sqrt{T}\eta_t\Big[-q^2RT + q(RT + q(5R^2 + 6RT + 6T^2))\eta_t - 16q(R+T)(R+qT)\eta_t^2\\ &+16(R+qT)^2\eta_t^3 - 8qT\eta_n(-qR + (R+qT)\eta_t) + 8qT\eta_n^2(-qR + (R+qT)\eta_t)\Big],\end{aligned} \tag{A.52}$$

$$\begin{aligned}B_1 = &\frac{1}{6a^4m^4q^5}GR^2T^{3/2}\Big[4qT\eta_n(-33q^2 + 2q(14+9q)\eta_t - 6\eta_t^2) + 12qT\eta_n^2(3q^2 - 2q\eta_t + 2\eta_t^2) + \eta_t\Big(-q^2(145+132q)T\\ &+q(4qR + 45T + 114qT + 36q^2T)\eta_t - 16q(2R + 3(1+q)T)\eta_t^2 + 32(R+3qT)\eta_t^3\Big)\Big],\end{aligned} \tag{A.53}$$

$$\begin{aligned}C_1 = &\frac{1}{6a^6m^5q^6}GR^3T^{3/2}\Big[28qT\eta_n(-33q^2 + 2q(14+9q)\eta_t - 6\eta_t^2) + 84qT\eta_n^2(3q^2 - 2q\eta_t + 2\eta_t^2)\\ &+\eta_t\Big(-7q^2(145+132q)T + 21q(15T + 12q^2T + 2q(R+19T))\eta_t\\ &-16q(16R + 21(1+q)T)\eta_t^2 + 32(8R + 21qT)\eta_t^3\Big)\Big],\end{aligned} \tag{A.54}$$

$$
\begin{aligned}
D_1 \;=\; & \frac{1}{12a^4m^5q^5}GR^2T^{5/2}\Big[4qT\eta_n(-501q^2+2q(212+135q)\eta_t-90\eta_t^2)+180qT\eta_n^2(3q^2-2q\eta_t+2\eta_t^2)\\
& +\eta_t\Big(-3q^2(741+668q)T+q(52qR+683T+1722qT+540q^2T)\eta_t\\
& -16q(26R+45(1+q)T)\eta_t^2+32(13R+45qT)\eta_t^3\Big)\Big], \qquad \text{(A.55)}
\end{aligned}
$$

$$
\begin{aligned}
A_3 \;=\; & -\frac{1}{3a^4m^3q^7}G\sqrt{T}\eta_t\Big[-7q^4R^2T+q^3R(15RT+7q(5R^2+6RT+6T^2))\eta_t-8q^2R(2RT+14q^2T(R+T)\\
& +3q(7R^2+8RT+3T^2))\eta_t^2+8q(R^2T+14q^3RT^2+q^2T(59R^2+34RT+8T^2)+qR(45R^2+34RT+9T^2))\eta_t^3\\
& -192q(2R+T)(R+qT)^2\eta_t^4+192(R+qT)^3\eta_t^5-8qT\eta_n(-7q^3R^2+q^2R(15R+7qT)\eta_t\\
& +8qT\eta_n^2\Big(-7q^3R^2+q^2R(15R+7qT)\eta_t-16qR(R+qT)\eta_t^2+8(R+qT)^2\eta_t^3\Big)\Big], \qquad \text{(A.56)}
\end{aligned}
$$

$$
\begin{aligned}
B_3 \;=\; & \frac{1}{6a^6m^5q^8}GR^2T^{3/2}\Big[4qT\eta_n(-231q^4R+2q^3(220+63q)R\eta_t-2q^2((295+72q)R+136qT)\eta_t^2+16q((25+9q)R\\
& +q(23+9q)T)\eta_t^3-32(3R+5qT)\eta_t^4)+4qT\eta_n^2(63q^4R-102q^3R\eta_t+22q^2(9R+4qT)\eta_t^2-32q(6R+5qT)\eta_t^3\\
& +32(3R+5qT)\eta_t^4)+\eta_t\Big(-q^4(2069+924q)RT+q^3(2969RT+252q^2RT+6q(7R^2+407RT+227T^2))\eta_t\\
& -8q^2(272RT+2q^2T(69R+136T)+q(51R^2+518RT+267T^2))\eta_t^2\\
& +8q(72RT+124q^3T^2+2q^2T(198R+185T)+q(123R^2+404RT+111T^2))\eta_t^3-384q(3R^2+5q(1+q)T^2\\
& +3R(T+4qT))\eta_t^4+576(R^2+6qRT+5q^2T^2)\eta_t^5\Big)\Big], \qquad \text{(A.57)}
\end{aligned}
$$

$$
\begin{aligned}
C_3 \;=\; & \frac{1}{6a^8m^6q^9}GR^3T^{3/2}\Big[4qT\eta_n(-2079q^4R+18q^3(220+63q)R\eta_t\\
& -4q^2(3(421+108q)R+458qT)\eta_t^2+32q(6(17+6q)R\\
& +q(76+27q)T)\eta_t^3-32(24R+35qT)\eta_t^4)+4qT\eta_n^2(567q^4R\\
& -918q^3R\eta_t+56q^2(30R+11qT)\eta_t^2-32q(48R+35qT)\eta_t^3\\
& +32(24R+35qT)\eta_t^4)+\eta_t\Big(-9q^4(2069+924q)RT\\
& +6q^3(4279RT+378q^2RT+q(84R^2+3663RT+1589T^2))\eta_t\\
& -8q^2(2250RT+2q^2T(621R+970T)+q(517R^2+4404RT\\
& +1905T^2))\eta_t^2+8q(576RT+940q^3T^2\\
& +2q^2T(1677R+1367T)+q(1169R^2+3300RT+849T^2))\eta_t^3\\
& -384q(27R^2+35q(1+q)T^2+24R(T+4qT))\eta_t^4+576(9R^2+48qRT+35q^2T^2)\eta_t^5\Big)\Big], \qquad \text{(A.58)}
\end{aligned}
$$

$$
\begin{aligned}
D_3 \;=\; & \frac{1}{12a^6m^6q^8}GR^2T^{5/2}\Big[4qT\eta_n(-3507q^4R+2q^3(3334+945q)R\eta_t \\
& -2q^2((4477+1080q)R+2360qT)\eta_t^2+16q((379+135q)R \\
& +q(403+153q)T)\eta_t^3-160(9R+17qT)\eta_t^4)+4qT\eta_n^2(945q^4R-1530q^3R\eta_t \\
& +22q^2(135R+68qT)\eta_t^2-160q(18R+17qT)\eta_t^3+160(9R+17qT)\eta_t^4) \\
& +\eta_t\Big(-3q^4(10593+4676q)RT+q^3(45479RT+3780q^2RT+6q(91R^2+6163RT+4039T^2))\eta_t \\
& -8q^2(4156RT+10q^2T(207R+472T)+q(663R^2+7850RT+4755T^2))\eta_t^2 \\
& +8q(1096RT+2108q^3T^2+2q^2T(2970R+3247T) \\
& +q(1599R^2+6128RT+1959T^2))\eta_t^3-384q(39R^2+85q(1+q)T^2 \\
& +45R(T+4qT))\eta_t^4+576(13R^2+90qRT+85q^2T^2)\eta_t^5\Big)\Big], \qquad \text{(A.59)}
\end{aligned}
$$

$$
\begin{aligned}
A_5 \;=\; & -\frac{1}{6a^2m^3q^5}G\sqrt{T}\eta_t\Big[-13q^3RT^2+q^2T(13RT+q(77R^2+102RT+90T^2))\eta_t \\
& -16q^2T((16+7q)R^2+2(8+13q)RT \\
& +23qT^2)\eta_t^2+16q(16R^2T+q^2T(7R^2+34RT+47T^2) \\
& +qR(7R^2+34RT+63T^2))\eta_t^3-384q(R+2T)(R+qT)^2\eta_t^4 \\
& +384(R+qT)^3\eta_t^5-256q^2T^2\eta_n^3(-qR+(R+qT)\eta_t) \\
& +128q^2T^2\eta_n^4(-qR+(R+qT)\eta_t)-8qT\eta_n(-16q^2RT \\
& +q(16RT+q(7R^2+18RT+23T^2))\eta_t-32q(R+T)(R+qT)\eta_t^2+32(R+qT)^2\eta_t^3) \\
& +8qT\eta_n^2\Big(-32q^2RT+q(32RT+q(7R^2+18RT+39T^2))\eta_t \\
& -32q(R+T)(R+qT)\eta_t^2+32(R+qT)^2\eta_t^3\Big)\Big], \qquad \text{(A.60)}
\end{aligned}
$$

$$
\begin{aligned}
B_5 \;=\; & \frac{1}{12a^4m^5q^6}GR^2T^{3/2}\Big[128q^2T^2\eta_n^3(-30q^2+q(23+9q)\eta_t-10\eta_t^2) \\
& +320q^2T^2\eta_n^4(3q^2-2q\eta_t+2\eta_t^2)+8qT\eta_n(-501q^3T \\
& +q^2(469+495q)T\eta_t-2q(55T+174q^2T+61q(2R+3T))\eta_t^2 \\
& +16q((25+9q)R+(10+23q+9q^2)T)\eta_t^3-64(3R+5qT)\eta_t^4) \\
& +16qT\eta_n^2(339q^3T-q^2(295+174q)T\eta_t+q(30qR+95T+93qT+24q^2T)\eta_t^2 \\
& -16q(6R+5(1+q)T)\eta_t^3+32(3R+5qT)\eta_t^4)+\eta_t\Big(-3q^3(741+1336q)T^2 \\
& +q^2T(683T+5424q^2T+6q(454R+861T))\eta_t-32q^2T((159+122q)R \\
& +(73+262q+120q^2)T)\eta_t^2+16q(162RT+60q^3T^2 \\
& +2q^2T(48R+185T)+q(15R^2+404RT+381T^2))\eta_t^3 \\
& -384q(3R^2+12(1+q)RT+5q(4+q)T^2)\eta_t^4+1152(R^2+6qRT+5q^2T^2)\eta_t^5\Big)\Big], \qquad \text{(A.61)}
\end{aligned}
$$

$$
\begin{aligned}
C_5 \;=\; & \frac{1}{12a^6m^6q^5}GR^3T^{3/2}\Big[\frac{16R^2\eta_t^4(149q^2-648q\eta_t+648\eta_t^2)}{q^2}+\frac{1}{q}6RT\eta_t^2(3765q^2-16q(430+337q)\eta_t \\
& +16(216+550q+135q^2)\eta_t^2-6144(1+q)\eta_t^3+9216\eta_t^4+8\eta_n(-337q^2+32q(17+6q)\eta_t-256\eta_t^2) \\
& +8\eta_n^2(87q^2-256q\eta_t+256\eta_t^2))+7T^2\Big(128\eta_n^3(-30q^2+q(23+9q)\eta_t-10\eta_t^2) \\
& +320\eta_n^4(3q^2-2q\eta_t+2\eta_t^2)+8\eta_n(-501q^2+q(469+495q)\eta_t \\
& -2(55+183q+174q^2)\eta_t^2+16(10+23q+9q^2)\eta_t^3-320\eta_t^4) \\
& +16\eta_n^2(339q^2-q(295+174q)\eta_t+(95+93q+24q^2)\eta_t^2-80(1+q)\eta_t^3+160\eta_t^4)+\eta_t(-3q(741+1336q) \\
& +(683+5166q+5424q^2)\eta_t-32(73+262q+120q^2)\eta_t^2 \\
& +16(381+370q+60q^2)\eta_t^3-1920(4+q)\eta_t^4+5760\eta_t^5)\Big)\Big], \qquad \text{(A.62)}
\end{aligned}
$$

$$
\begin{aligned}
D_5 \;=\; & \frac{1}{24a^4m^6q^6}GR^2T^{5/2}\Big[128q^2T^2\eta_n^3(-528q^2+q(403+153q)\eta_t-170\eta_t^2) \\
& +5440q^2T^2\eta_n^4(3q^2-2q\eta_t+2\eta_t^2)+8qT\eta_n(-9675q^3T \\
& +3q^2(3011+3157q)T\eta_t-2q(1045T+3138q^2T+5q(370R+699T))\eta_t^2 \\
& +16q((379+135q)R+(186+403q+153q^2)T)\eta_t^3 \\
& -320(9R+17qT)\eta_t^4)+16qT\eta_n^2(6258q^3T-q^2(5399+3138q)T\eta_t \\
& +q(450qR+1687T+1635qT+408q^2T)\eta_t^2 \\
& -80q(18R+17(1+q)T)\eta_t^3+160(9R+17qT)\eta_t^4) \\
& +\eta_t\Big(-3q^3(14413+25800q)T^2+q^2T(41788qR+13195T+99378qT \\
& +100128q^2T)\eta_t-32q^2T((2437+1850q)R+(1387+4766q+2112q^2)T)\eta_t^2 \\
& +16q(2462RT+1020q^3T^2+2q^2T(720R+3247T) \\
& +q(195R^2+6128RT+6757T^2))\eta_t^3-384q(39R^2+180(1+q)RT+85q(4+q)T^2)\eta_t^4 \\
& +1152(13R^2+90qRT+85q^2T^2)\eta_t^5\Big)\Big]. \qquad \text{(A.63)}
\end{aligned}
$$

A.5 Rescaled Evolution Equations for $b_{112}(\tau)$, $b_{122}(\tau)$ and $b_{212}(\tau)$

Let us define a dimensionless time τ via

$$\frac{\mathrm{d}}{\mathrm{d}\tau}=\tau_f\frac{\mathrm{d}}{\mathrm{d}t}, \qquad \text{(A.64)}$$

where τ_f is the mean free time given by

$$\tau_f^{-1}=16\Big(\frac{\pi T}{m}\Big)^{1/2}na^2g_2(2a)=\frac{1}{2}GT^{1/2}. \qquad \text{(A.65)}$$

With the above rescaling, the evolution equations [Eqs. (A.46)-(A.50), see Appendix A.4] transform into:

$$\frac{3}{4}\frac{dT}{d\tau}=-\alpha_1T(\tau)+\alpha_2\Big[1-\frac{b_{112}(\tau)}{2}\frac{T(\tau)R(\tau)}{qm^2a^2}-\frac{7\ b_{122}(\tau)}{2}\frac{T(\tau)R^2(\tau)}{q^2m^3a^4}-\frac{13b_{212}(\tau)}{4}\frac{T^2(\tau)R(\tau)}{qm^3a^2}\Big]R(\tau), \qquad \text{(A.66)}$$

$$\frac{3}{4}\frac{dR}{d\tau}=\alpha_2T(\tau)-\alpha_3\Big[1-\frac{b_{112}(\tau)}{2}\frac{T(\tau)R(\tau)}{qm^2a^2}-\frac{7\ b_{122}(\tau)}{2}\frac{T(\tau)R^2(\tau)}{q^2m^3a^4}-\frac{13b_{212}(\tau)}{4}\frac{T^2(\tau)R(\tau)}{qm^3a^2}\Big]R(\tau), \qquad \text{(A.67)}$$

$$\begin{aligned}
\frac{15GR^2T^{5/2}}{a^4m^4q^2}\frac{db_{112}(\tau)}{d\tau} \quad + \quad & \frac{105GR^3T^{5/2}}{a^6m^5q^3}\frac{db_{122}(\tau)}{d\tau}+\frac{105GR^2T^{7/2}}{a^4m^5q^2}\frac{db_{212}(\tau)}{d\tau}=A_1-b_{112}(\tau)(-B_1+B_2)\\
&-b_{122}(\tau)(-C_1+C_2)-b_{212}(\tau)(-D_1+D_2)+b_{112}^2(\tau)\Big(\frac{20GR^3T^{5/2}(\alpha_2R-\alpha_3T)}{a^6m^6q^3}\Big)\\
&+b_{122}^2(\tau)\Big(\frac{490GR^5T^{5/2}(2\alpha_2R-3\alpha_3T)}{a^{10}m^8q^5}\Big)+b_{212}^2(\tau)\Big(\frac{455GR^3T^{9/2}(3\alpha_2R-2\alpha_3T)}{a^6m^8q^3}\Big)\\
&+b_{112}(\tau)b_{122}(\tau)\Big(\frac{70GR^4T^{5/2}(4\alpha_2R-5\alpha_3T)}{a^8m^7q^4}\Big)\\
&+b_{112}(\tau)b_{212}(\tau)\Big(\frac{10GR^3T^{7/2}(34\alpha_2R-27\alpha_3T)}{a^6m^7q^3}\Big)\\
&+b_{122}(\tau)b_{212}(\tau)\Big(\frac{35GR^4T^{7/2}(68\alpha_2R-67\alpha_3T)}{a^8m^8q^4}\Big),
\end{aligned}\tag{A.68}$$

$$\begin{aligned}
\frac{105GR^3T^{5/2}}{a^6m^5q^3}\frac{db_{112}(\tau)}{d\tau} \quad + \quad & \frac{945GR^4T^{5/2}}{a^8m^6q^4}\frac{db_{122}(\tau)}{d\tau}+\frac{735GR^3T^{7/2}}{a^6m^6q^3}\frac{db_{212}(\tau)}{d\tau}=A_3-b_{112}(\tau)(-B_3+C_2)\\
&-b_{122}(\tau)(-C_3+B_4)-b_{212}(\tau)(-D_3+D_4)+b_{112}^2(\tau)\Big(\frac{70GR^4T^{5/2}(2\alpha_2R-3\alpha_3T)}{a^8m^7q^4}\Big)\\
&+b_{122}^2(\tau)\Big(\frac{8820GR^6T^{5/2}(\alpha_2R-2\alpha_3T)}{a^{12}m^9q^6}\Big)+b_{212}^2(\tau)\Big(\frac{9555GR^4T^{9/2}(\alpha_2R-\alpha_3T)}{a^8m^9q^4}\Big)\\
&+b_{112}(\tau)b_{122}(\tau)\Big(\frac{70GR^5T^{5/2}(32\alpha_2R-57\alpha_3T)}{a^{10}m^8q^5}\Big)\\
&+b_{112}(\tau)b_{212}(\tau)\Big(\frac{35GR^4T^{7/2}(68\alpha_2R-81\alpha_3T)}{a^8m^8q^4}\Big)\\
&+b_{122}(\tau)b_{212}(\tau)\Big(\frac{210GR^5T^{7/2}(88\alpha_2R-127\alpha_3T)}{a^{10}m^9q^5}\Big),
\end{aligned}\tag{A.69}$$

and

$$\begin{aligned}
\frac{105GR^2T^{7/2}}{a^4m^5q^2}\frac{db_{112}(\tau)}{d\tau} \quad + \quad & \frac{735GR^3T^{7/2}}{a^6m^6q^3}\frac{db_{122}(\tau)}{d\tau}+\frac{945GR^2T^{9/2}}{a^4m^6q^2}\frac{db_{212}(\tau)}{d\tau}=A_5-b_{112}(\tau)(-B_5+D_2)\\
&-b_{122}(\tau)(-C_5+D_4)-b_{212}(\tau)(-D_5+D_6)+b_{112}^2(\tau)\Big(\frac{70GR^3T^{7/2}(3\alpha_2R-2\alpha_3T)}{a^6m^7q^3}\Big)\\
&+b_{122}^2(\tau)\Big(\frac{10290GR^5T^{7/2}(\alpha_2R-\alpha_3T)}{a^{10}m^9q^5}\Big)+b_{212}^2(\tau)\Big(\frac{8190GR^3T^{11/2}(2\alpha_2R-\alpha_3T)}{a^6m^9q^3}\Big)\\
&+b_{112}(\tau)b_{122}(\tau)\Big(\frac{490GR^4T^{7/2}(6\alpha_2R-5\alpha_3T)}{a^8m^8q^4}\Big)\\
&+b_{112}(\tau)b_{212}(\tau)\Big(\frac{35GR^3T^{9/2}(111\alpha_2R-62\alpha_3T)}{a^6m^8q^3}\Big)\\
&+b_{122}(\tau)b_{212}(\tau)\Big(\frac{735GR^4T^{9/2}(37\alpha_2R-25\alpha_3T)}{a^8m^9q^4}\Big),
\end{aligned}\tag{A.70}$$

where

$$\left.\begin{aligned}
B_2 &= \tfrac{40GRT^{3/2}(-(\alpha_1+\alpha_3)RT+\alpha_2(R^2+T^2))}{a^4m^4q^2}\\
C_2 &= \tfrac{140GR^2T^{3/2}(2\alpha_2R^2-2\alpha_1RT-3\alpha_3RT+3\alpha_2T^2)}{a^6m^5q^3}\\
D_2 &= \tfrac{140GRT^{5/2}(3\alpha_2R^2-3\alpha_1RT-2\alpha_3RT+2\alpha_2T^2)}{a^4m^5q^2}\\
B_4 &= \tfrac{2520GR^3T^{3/2}(-(\alpha_1+2\alpha_3)RT+\alpha_2(R^2+2T^2))}{a^8m^6q^4}\\
D_4 &= \tfrac{2940GR^2T^{5/2}(-(\alpha_1+\alpha_3)RT+\alpha_2(R^2+T^2))}{a^6m^6q^3}\\
D_6 &= \tfrac{2520GRT^{7/2}(-(2\alpha_1+\alpha_3)RT+\alpha_2(2R^2+T^2))}{a^4m^6q^2}
\end{aligned}\right\}\tag{A.71}$$

and

$$\alpha_1\equiv\eta_n(1-\eta_n)+\eta_t(1-\eta_t),\quad \alpha_2\equiv\frac{\eta_t^2}{q},\quad \alpha_3\equiv\frac{\eta_t}{q}\Big(1-\frac{\eta_t}{q}\Big),\quad G=32na^2\sqrt{\frac{\pi}{m}}g_2(2a)\tag{A.72}$$

and the expressions for A_1, $B_1,\ldots$, are already given in Appendix A.4.

The above three evolution equations can be solved to yield separate evolution equations for $b_{112}(\tau), b_{122}(\tau), b_{212}(\tau)$

$$\begin{aligned}\dot{b}_{112}(\tau) &= A_0^{(1)}\frac{R}{T^3}+A_0^{(2)}\frac{1}{T^2}+A_0^{(3)}\frac{T}{R^3}+A_0^{(4)}\frac{1}{RT}+A_0^{(5)}\frac{1}{R^2}+b_{122}(\tau)\Big(A_1^{(1)}\frac{R^3}{T^2}+A_1^{(2)}\frac{R^2}{T}+A_1^{(3)}T+A_1^{(4)}R\Big)\\ &+b_{212}(\tau)\Big(A_2^{(1)}\frac{R^2}{T}+A_2^{(2)}R+A_2^{(3)}\frac{T^2}{R}+A_2^{(4)}T\Big)+b_{112}(\tau)\Big(A_3^{(1)}\frac{R^2}{T^2}+A_3^{(2)}\frac{R}{T}+A_3^{(3)}\frac{T}{R}+A_3^{(4)}\Big)\\ &+\frac{b_{112}(\tau)b_{122}(\tau)}{a^4m^3q^2}\Big(-\frac{70}{3}\alpha_2R^3+28\alpha_3R^2T\Big)+\frac{b_{112}(\tau)b_{212}(\tau)}{a^2m^3q}\Big(-\frac{55}{2}\alpha_2R^2T+\frac{137}{6}\alpha_3RT^2\Big)\\ &+\frac{b_{122}(\tau)b_{212}(\tau)}{a^4m^4q^2}\Big(-\frac{1519}{6}\alpha_2R^3T+\frac{1505}{6}\alpha_3R^2T^2\Big)+\frac{b_{112}^2(\tau)}{a^2m^2q}\Big(-\alpha_2R^2+\alpha_3RT\Big)\\ &+\frac{b_{122}^2(\tau)}{a^6m^4q^3}\Big(-\frac{343}{3}\alpha_2R^4+147\alpha_3R^3T\Big)+\frac{b_{212}^2(\tau)}{a^2m^4q}\Big(-\frac{273}{2}\alpha_2R^2T^2+\frac{637}{6}\alpha_3RT^3\Big),\end{aligned}\tag{A.73}$$

$$\begin{aligned}\dot{b}_{122}(\tau) &= B_0^{(1)}\frac{1}{RT^2}+B_0^{(2)}\frac{1}{R^2T}+B_0^{(3)}\frac{1}{R^3}+B_0^{(4)}\frac{T}{R^4}+b_{122}(\tau)\Big(B_1^{(1)}\frac{R}{T}+B_1^{(2)}+B_1^{(3)}\frac{T}{R}\Big)\\ &+b_{212}(\tau)\Big(B_2^{(1)}+B_2^{(2)}\frac{T}{R}+B_2^{(3)}\frac{T^2}{R^2}\Big)+b_{112}(\tau)\Big(B_3^{(1)}\frac{1}{T}+B_3^{(2)}\frac{1}{R}+B_3^{(3)}\frac{T}{R^2}\Big)\\ &+\frac{b_{112}(\tau)b_{122}(\tau)}{a^2m^2q}\Big(\frac{4}{3}\alpha_2R^2-\frac{22}{3}\alpha_3RT\Big)+\frac{b_{112}(\tau)b_{212}(\tau)}{m^2}\Big(-\frac{9}{2}\alpha_3T^2\Big)\\ &+\frac{b_{122}(\tau)b_{212}(\tau)}{a^2m^3q}\Big(\frac{26}{3}\alpha_2R^2T-\frac{293}{6}\alpha_3RT^2\Big)+\frac{b_{112}^2(\tau)}{m}\Big(-\frac{1}{3}\alpha_3T\Big)\\ &+\frac{b_{122}^2(\tau)}{a^4m^3q^2}\Big(\frac{28}{3}\alpha_2R^3-35\alpha_3R^2T\Big)+\frac{b_{212}^2(\tau)}{m^3}\Big(-\frac{91}{6}\alpha_3T^3\Big),\end{aligned}\tag{A.74}$$

$$\begin{aligned}\dot{b}_{212}(\tau) &= C_0^{(1)}\frac{R}{T^4}+C_0^{(2)}\frac{1}{T^3}+C_0^{(3)}\frac{1}{RT^2}+C_0^{(4)}\frac{1}{R^2T}+b_{122}(\tau)\Big(C_1^{(1)}\frac{R^3}{T^3}+C_1^{(2)}\frac{R^2}{T^2}+C_1^{(3)}\frac{R}{T}\Big)\\ &+b_{212}(\tau)\Big(C_2^{(1)}\frac{T}{R}+C_2^{(2)}\frac{R^2}{T^2}+C_2^{(3)}\frac{R}{T}+C_2^{(4)}\Big)+b_{112}(\tau)\Big(C_3^{(1)}\frac{R^2}{T^3}+C_3^{(2)}\frac{R}{T^2}+C_3^{(3)}\frac{1}{T}\Big)\\ &+\frac{b_{112}(\tau)b_{122}(\tau)}{a^4m^2q^2}\Big(\frac{14}{3}\frac{\alpha_2R^3}{T}\Big)+\frac{b_{112}(\tau)b_{212}(\tau)}{a^2m^2q}\Big(\frac{43}{6}\alpha_2R^2-\frac{4}{3}\alpha_3RT\Big)\\ &+\frac{b_{122}(\tau)b_{212}(\tau)}{a^4m^3q^2}\Big(\frac{301}{6}\alpha_2R^3-\frac{28}{3}\alpha_3R^2T\Big)+\frac{b_{112}^2(\tau)}{a^2mq}\Big(\frac{\alpha_2R^2}{3T}\Big)\\ &+\frac{b_{122}^2(\tau)}{a^6m^3q^3}\Big(\frac{49}{3}\frac{\alpha_2R^4}{T}\Big)+\frac{b_{212}^2(\tau)}{a^2m^3q}\Big(\frac{65}{2}\alpha_2R^2T-\frac{26}{3}\alpha_3RT^2\Big),\end{aligned}\tag{A.75}$$

where the coefficients have following form:

$$A_0^{(k)}=qm^2a^2A_{0k},\quad A_1^{(k)}=A_{1k}/qma^2,\quad A_2^{(k)}=A_{2k}/m,\quad A_3^{(k)}=A_{3k},\tag{A.76}$$

$$B_0^{(k)}=q^2m^3a^4B_{0k},\quad B_1^{(k)}=B_{1k},\quad B_2^{(k)}=qa^2B_{2k},\quad B_3^{(k)}=qma^2B_{3k},\tag{A.77}$$

$$C_0^{(k)}=qm^3a^2C_{0k},\quad C_1^{(k)}=C_{1k}/qa^2,\quad C_2^{(k)}=C_{2k},\quad C_3^{(k)}=mC_{3k},\tag{A.78}$$

The coefficients A_{ik}, B_{ik} and C_{ik} are dimensionless whose expressions are given in Appendix A.6.

A.5.1 Rescaled evolution equations for lower-order theory

The evolution equations for the lower-order theory as given by Kranz *et al.* (2009) are recovered from Eqs. (A.66)-(A.68) by removing all terms originating from higher-order Legendre coefficients (b_{122} and b_{212}):

$$\frac{3}{4}\frac{\mathrm{d}T}{\mathrm{d}\tau}=-\alpha_1T(\tau)+\alpha_2\Big[1-\frac{b_{112}(\tau)}{2}\frac{T(\tau)R(\tau)}{qm^2a^2}\Big]R(\tau),\tag{A.79}$$

$$\frac{3}{4}\frac{\mathrm{d}R}{\mathrm{d}\tau}=\alpha_2T(\tau)-\alpha_3\Big[1-\frac{b_{112}(\tau)}{2}\frac{T(\tau)R(\tau)}{qm^2a^2}\Big]R(\tau),\tag{A.80}$$

$$15\frac{\mathrm{d}b_{112}}{\mathrm{d}\tau}=-b_{112}(\tau)\Big(A_{L1}+B_{L1}\frac{R(\tau)}{T(\tau)}+\frac{30}{T(\tau)}\frac{\mathrm{d}T}{\mathrm{d}\tau}+\frac{30}{R(\tau)}\frac{\mathrm{d}R}{\mathrm{d}\tau}\Big)-\frac{qm^2a^2}{T(\tau)R(\tau)}\Big(A_{L0}+B_{L0}\frac{R(\tau)}{T(\tau)}+C_{L0}\frac{T(\tau)}{R(\tau)}\Big)\tag{A.81}$$

The coefficients of the time-derivatives on the left-hand side of above equations are incorrectly given in Kranz *et al.* (2009) as 1, 1 and 20, respectively; moreover, the coefficient of two time-derivatives on the right-hand side in the last equation is incorrectly given as 40. In above equations, the coefficients are given by

$$\alpha_1 = \eta_n(1-\eta_n) + \eta_t(1-\eta_t),\ \alpha_2 = \frac{\eta_t^2}{q},\ \alpha_3 = \frac{\eta_t}{q}\left(1-\frac{\eta_t}{q}\right) \tag{A.82}$$

and

$$A_{L0} = \frac{16}{3}\frac{\eta_t^3}{q}\left(\frac{2\eta_t}{q}-1\right) - \frac{2}{3}\frac{\eta_t^2}{q}\left(\frac{8\eta_t}{q}-3\right) + \frac{1}{3}\frac{\eta_t}{q}\left(\frac{\eta_t}{q}-1\right) + \frac{8}{3}\frac{\eta_t}{q}\left(\frac{\eta_t}{q}-1\right)\eta_n(\eta_n-1), \tag{A.83}$$

$$B_{L0} = \frac{1}{3}\frac{\eta_t^2}{q}\left[\frac{16\eta_t}{q}\left(\frac{\eta_t}{q}-1\right)+5\right], \tag{A.84}$$

$$C_{L0} = \frac{2}{3}\frac{\eta_t^2}{q}[8\eta_t(\eta_t-1) + 4\eta_n(\eta_n-1)+3], \tag{A.85}$$

$$\begin{aligned} A_{L1} &= -\frac{8\eta_t^3}{q}\left(\frac{2\eta_t}{q}-1\right) + \frac{1}{3}\frac{\eta_t^2}{q}\left(\frac{24\eta_t}{q}-\underline{57}\right) - \frac{5}{6}\frac{\eta_t}{q}\left(\frac{9\eta_t}{q}-29\right) - \frac{4\eta_t\eta_n^2}{q}\left(\frac{\eta_t}{q}-1\right) \\ &\quad + \frac{4\eta_t\eta_n}{3q}\left(\frac{3\eta_t}{q}-14\right) - 12\eta_t\eta_n + 22(\eta_t+\eta_n) - 6(\eta_t^2+\eta_n^2), \end{aligned} \tag{A.86}$$

$$B_{L1} = -\frac{2}{3}\frac{\eta_t^2}{q}\left[\frac{8\eta_t}{q}\left(\frac{\eta_t}{q}-1\right)+1\right]. \tag{A.87}$$

The underlined number on the second term in Eq. (A.86) is given as 37 in Kranz *et al.* (2009).

The above three equations can be transformed into a set of two coupled equations for the temperature ratio $R_T = R(\tau)/T(\tau)$ and the (dimensionless) leading Legendre coefficient $x(\tau) = b_{112}(\tau)/(\frac{qm^2a^2}{T(\tau)R(\tau)})$:

$$\frac{3}{4}\frac{\mathrm{d}R_T}{\mathrm{d}\tau} = (\alpha_2 + \alpha_1 R_T(\tau)) - \left(\alpha_3 R_T(\tau) + \alpha_2 R_T^2(\tau)\right)\left(1-\frac{x(\tau)}{2}\right), \tag{A.88}$$

$$\begin{aligned} 15\frac{\mathrm{d}x}{\mathrm{d}\tau} &= -x(\tau)\left(A_{L1} + B_{L1}R_T(\tau) - 20(\alpha_1-\alpha_3) + 20\alpha_2\left(R_T(\tau)+\frac{1}{R_T(\tau)}\right) + 10x(\tau)\left(\alpha_3 - \alpha_2 R_T(\tau)\right)\right) \\ &\quad - \left(A_{L0} + B_{L0}R_T(\tau) + \frac{C_{L0}}{R_T(\tau)}\right). \end{aligned} \tag{A.89}$$

The expression for steady state orientational correlation is:

$$\Psi_\theta^L = \langle\cos^2\theta\rangle_\infty - \frac{1}{3} \approx -\frac{6}{5}\left(\frac{A_{L0} + B_{L0}R_T^{(0)} + C_{L0}/R_T^{(0)}}{A_{L1} + B_{L1}R_T^{(0)} + 40\alpha_2/R_T^{(0)} - 40\alpha_3}\right). \tag{A.90}$$

A.6 Dimensionless Coefficients in Equations (2.39), (2.40) and (2.41)

The dimensionless coefficients, A_{ij}, B_{ij} and C_{ij}, in Eqs. (2.39)-(2.41) of the Chapter 2 are given by:

$$A_{01} = \frac{4\eta_t^4\left(7q^2 - 24q\eta_t + 24\eta_t^2\right)}{45q^4}, \tag{A.91}$$

$$\begin{aligned} A_{02} &= \frac{1}{180q^5}\eta_t^2\Big(-13q^4 - 16q^3(5+7q)\eta_t + 16q^2(29+34q+7q^2)\eta_t^2 - 768q(1+q+q^2)\eta_t^3 \\ &\quad + 384(1+3q^2)\eta_t^4 - 8q^2\eta_n(7q^2 - 32q\eta_t + 32\eta_t^2) + 8q^2\eta_n^2(7q^2 - 32q\eta_t + 32\eta_t^2)\Big), \end{aligned} \tag{A.92}$$

$$A_{03} = \frac{32\eta_t^4\left(1-\eta_n+\eta_n^2-3\eta_t+3\eta_t^2\right)}{45q^2}, \tag{A.93}$$

$$
\begin{aligned}
A_{04} &= \frac{1}{180q^4}\eta_t\Big(5q^3+256q^2\eta_n^3(q-\eta_t)-128q^2\eta_n^4(q-\eta_t)+(11-6q)q^2\eta_t-32q(1+2q)^2\eta_t^2 \\
&\quad +16(1+34q+58q^2+34q^3)\eta_t^3-384(1+4q+4q^2+q^3)\eta_t^4+1152(1+q^2)\eta_t^5-16\eta_n^2(7q^3-3q^2(5+3q)\eta_t \\
&\quad +16q(1+q+q^2)\eta_t^2-8(1+4q^2)\eta_t^3)+16\eta_n(-q^3-q^2(7+9q)\eta_t+16q(1+q+q^2)\eta_t^2-8(1+4q^2)\eta_t^3)\Big), \qquad \text{(A.94)}
\end{aligned}
$$

$$
\begin{aligned}
A_{05} &= \frac{1}{90q^3}\eta_t^2\Big(-9q^2-128q^2\eta_n^3+64q^2\eta_n^4-8q(9+5q)\eta_t+8(9+34q+29q^2)\eta_t^2-384(1+q+q^2)\eta_t^3+192(3+q^2)\eta_t^4 \\
&\quad -4\eta_n(5q^2-32q(1+q)\eta_t+32(1+q^2)\eta_t^2)+4\eta_n^2(21q^2-32q(1+q)\eta_t+32(1+q^2)\eta_t^2)\Big), \qquad \text{(A.95)}
\end{aligned}
$$

$$
A_{11} = -\frac{2\eta_t^4\left(149q^2-648q\eta_t+648\eta_t^2\right)}{45q^4}, \qquad \text{(A.96)}
$$

$$
\begin{aligned}
A_{12} &= -\frac{1}{180q^5}\eta_t^2\Big(5247q^4-8q^3(2585+2022q)\eta_t+24q^2(651+1100q+270q^2)\eta_t^2-1152q(9+16q+16q^2)\eta_t^3 \\
&\quad +1728(3+16q^2)\eta_t^4+24q^2\eta_n(-337q^2+32q(17+6q)\eta_t-256\eta_t^2)+24q^2\eta_n^2(87q^2-256q\eta_t+256\eta_t^2)\Big), \qquad \text{(A.97)}
\end{aligned}
$$

$$
\begin{aligned}
A_{13} &= -\frac{1}{90q^3}\eta_t^2\Big(987q^2-20q(381+388q)\eta_t+4(849+2734q+940q^2)\eta_t^2-6720(1+q)\eta_t^3+10080\eta_t^4 \\
&\quad +16\eta_n(-229q^2+4q(76+27q)\eta_t-140\eta_t^2)+112\eta_n^2(11q^2-20q\eta_t+20\eta_t^2)\Big), \qquad \text{(A.98)}
\end{aligned}
$$

$$
\begin{aligned}
A_{14} &= -\frac{1}{360q^4}\Big(896q^2\eta_n^3(-30q^2+q(23+9q)\eta_t-10\eta_t^2)+2240q^2\eta_n^4(3q^2-2q\eta_t+2\eta_t^2) \\
&\quad +8\eta_n(-420q^4+3q^3(1369+861q)\eta_t-2q^2(2575+1929q+1218q^2)\eta_t^2 \\
&\quad +16q(204+142q+161q^2+63q^3)\eta_t^3-64(12+35q^2)\eta_t^4) \\
&\quad +8\eta_n^2(2835q^4-4q^3(1094+609q)\eta_t+14q^2(167+93q+24q^2)\eta_t^2-32q(48+35q+35q^2)\eta_t^3 \\
&\quad +64(12+35q^2)\eta_t^4)+\eta_t\Big(-q^3(5203+3360q)+q^2(30929+54582q+22680q^2)\eta_t \\
&\quad -32q(1125+2377q+2119q^2+840q^3)\eta_t^2+16(576+3300q+4677q^2+2590q^3+420q^4)\eta_t^3 \\
&\quad -384(48+192q+140q^2+35q^3)\eta_t^4+1152(48+35q^2)\eta_t^5\Big)\Big), \qquad \text{(A.99)}
\end{aligned}
$$

$$
A_{21} = -\frac{13\eta_t^4\left(5q^2-24q\eta_t+24\eta_t^2\right)}{15q^4}, \qquad \text{(A.100)}
$$

$$
\begin{aligned}
A_{22} &= -\frac{1}{45q^5}\eta_t^2\Big(686q^4-5q^3(941+740q)\eta_t+q^2(3229+6128q+1440q^2)\eta_t^2-144q(13+30q+30q^2)\eta_t^3 \\
&\quad +72(13+90q^2)\eta_t^4+2q^2\eta_n(-925q^2+4q(379+135q)\eta_t-720\eta_t^2)+90q^2\eta_n^2(5q^2-16q\eta_t+16\eta_t^2)\Big), \qquad \text{(A.101)}
\end{aligned}
$$

$$
\begin{aligned}
A_{23} &= -\frac{1}{180q^3}\eta_t^2\Big(6237q^2-20q(951+944q)\eta_t+4(1959+6494q+2108q^2)\eta_t^2-16320(1+q)\eta_t^3+24480\eta_t^4 \\
&\quad +32\eta_n(-295q^2+q(403+153q)\eta_t-170\eta_t^2)+272\eta_n^2(11q^2-20q\eta_t+20\eta_t^2)\Big), \qquad \text{(A.102)}
\end{aligned}
$$

$$\begin{aligned}A_{24} &= -\frac{1}{720q^4}\Big(128q^2\eta_n^3(-528q^2+q(403+153q)\eta_t-170\eta_t^2)+5440q^2\eta_n^4(3q^2-2q\eta_t\\ &+2\eta_t^2)+8\eta_n(-1386q^4+q^3(8917+7041q)\eta_t-2q^2(4802+4575q+3138q^2)\eta_t^2\\ &+16q(379+321q+403q^2+153q^3)\eta_t^3-160(9+34q^2)\eta_t^4)+8\eta_n^2(7521q^4\\ &-4q^3(2722+1569q)\eta_t+2q^2(2452+1635q+408q^2)\eta_t^2-160q(18+17q+17q^2)\eta_t^3\\ &+160(9+34q^2)\eta_t^4)+\eta_t\Big(-9q^3(1349+1232q)+q^2(58777+118230q\\ &+60168q^2)\eta_t-32q(2078+4592q+5081q^2+2112q^3)\eta_t^2+16(1096+6128q\\ &+9817q^2+6494q^3+1020q^4)\eta_t^3-1920(18+72q+68q^2+17q^3)\eta_t^4+5760(18+17q^2)\eta_t^5\Big)\Big),\end{aligned} \tag{A.103}$$

$$A_{31} = -\frac{2\eta_t^4\left(5q^2-24q\eta_t+24\eta_t^2\right)}{15q^4}, \tag{A.104}$$

$$\begin{aligned}A_{32} &= -\frac{1}{45q^5}\eta_t^2\Big(245q^4-122q^3(5+4q)\eta_t+2q^2(221+404q+96q^2)\eta_t^2-288q(1+2q+2q^2)\eta_t^3\\ &+144(1+6q^2)\eta_t^4+4q^2\eta_n(-61q^2+4q(25+9q)\eta_t-48\eta_t^2)+12q^2\eta_n^2(5q^2-16q\eta_t+16\eta_t^2)\Big),\end{aligned} \tag{A.105}$$

$$\begin{aligned}A_{33} &= -\frac{1}{90q^3}\eta_t^2\Big(501q^2-4q(267+272q)\eta_t+4(111+370q+124q^2)\eta_t^2-960(1+q)\eta_t^3+1440\eta_t^4\\ &+32\eta_n(-17q^2+q(23+9q)\eta_t-10\eta_t^2)+16\eta_n^2(11q^2-20q\eta_t+20\eta_t^2)\Big),\end{aligned} \tag{A.106}$$

$$\begin{aligned}A_{34} &= -\frac{1}{360q^4}\Big(128q^2\eta_n^3(-30q^2+q(23+9q)\eta_t-10\eta_t^2)+320q^2\eta_n^4(3q^2-2q\eta_t+2\eta_t^2)\\ &+8\eta_n(-114q^4+q^3(461+333q)\eta_t-2q^2(302+255q+174q^2)\eta_t^2+16q(25+19q\\ &+23q^2+9q^3)\eta_t^3-32(3+10q^2)\eta_t^4)+8\eta_n^2(507q^4-4q^3(149+87q)\eta_t\\ &+2q^2(146+93q+24q^2)\eta_t^2-32q(6+5q+5q^2)\eta_t^3+32(3+10q^2)\eta_t^4)\\ &+\eta_t\Big(-q^3(1001+912q)+3q^2(1487+2134q+1352q^2)\eta_t-32q(136+284q+283q^2+120q^3)\eta_t^2\\ &+16(72+404q+585q^2+370q^3+60q^4)\eta_t^3-384(6+24q+20q^2+5q^3)\eta_t^4+1152(6+5q^2)\eta_t^5\Big)\Big),\end{aligned} \tag{A.107}$$

$$B_{01} = \frac{4\eta_t^3\left(7q^3-31q^2\eta_t+48q\eta_t^2-24\eta_t^3\right)}{315q^5}, \tag{A.108}$$

$$\begin{aligned}B_{02} &= -\frac{4}{315q^4}\eta_t^2\Big(q^2-8\eta_n(q-\eta_t)^2+8\eta_n^2(q-\eta_t)^2-2q(1+5q)\eta_t\\ &+(1+34q+31q^2)\eta_t^2-24(1+4q)\eta_t^3+72\eta_t^4\Big),\end{aligned} \tag{A.109}$$

$$B_{03} = \frac{4}{315q^3}\eta_t^3\Big(9q-16\eta_n(q-\eta_t)+16\eta_n^2(q-\eta_t)-(9+34q)\eta_t+48(1+q)\eta_t^2-72\eta_t^3\Big), \tag{A.110}$$

$$B_{04} = -\frac{32}{315q^2}\eta_t^4\left(1-\eta_n+\eta_n^2-3\eta_t+3\eta_t^2\right), \tag{A.111}$$

$$B_{11} = -\frac{\eta_t^2\left(1575q^4+1172q^3\eta_t-3780q^2\eta_t^2+5184q\eta_t^3-2592\eta_t^4\right)}{630q^5}, \tag{A.112}$$

$$B_{12} = \frac{1}{1260q^4}\Big(8\eta_n(189q^4+2q^3(647+63q)\eta_t-3q^2(793+216q)\eta_t^2+96q(17+6q)\eta_t^3 -384\eta_t^4)-24\eta_n^2(119q^4+104q^3\eta_t-231q^2\eta_t^2+256q\eta_t^3-128\eta_t^4)+\eta_t\Big(4q^3(271 +378q)-3q^2(-3623-5464q+952q^2)\eta_t-48q(375+685q+158q^2)\eta_t^2 +48(96+550q+461q^2)\eta_t^3-9216(1+4q)\eta_t^4+27648\eta_t^5\Big)\Big), \quad (A.113)$$

$$B_{13} = \frac{1}{630q^3}\eta_t^2\Big(-1533q^2-20q(381+388q)\eta_t+4(849+2734q+940q^2)\eta_t^2-6720(1+q)\eta_t^3+10080\eta_t^4 +16\eta_n(-229q^2+4q(76+27q)\eta_t-140\eta_t^2)+112\eta_n^2(11q^2-20q\eta_t+20\eta_t^2)\Big), \quad (A.114)$$

$$B_{21} = \frac{13\eta_t^2\left(7q^4-92q^3\eta_t+380q^2\eta_t^2-576q\eta_t^3+288\eta_t^4\right)}{1260q^5}, \quad (A.115)$$

$$B_{22} = \frac{1}{1260q^4}\eta_t\Big(-2229q^3+3q^2(4823+4154q)\eta_t-16q(1039+1805q+360q^2)\eta_t^2 +32(137+766q+585q^2)\eta_t^3-8640(1+4q)\eta_t^4 +25920\eta_t^5-360\eta_n^2(5q^3-13q^2\eta_t+16q\eta_t^2-8\eta_t^3) -8\eta_n\Big(-925q^3+q^2(2081+540q)\eta_t-4q(379+135q)\eta_t^2+360\eta_t^3\Big)\Big), \quad (A.116)$$

$$B_{23} = \frac{1}{1260q^3}\eta_t^2\Big(6237q^2-20q(951+944q)\eta_t+4(1959+6494q+2108q^2)\eta_t^2-16320(1+q)\eta_t^3+24480\eta_t^4 +32\eta_n(-295q^2+q(403+153q)\eta_t-170\eta_t^2)+272\eta_n^2(11q^2-20q\eta_t+20\eta_t^2)\Big), \quad (A.117)$$

$$B_{31} = \frac{\eta_t^2\left(7q^4-92q^3\eta_t+380q^2\eta_t^2-576q\eta_t^3+288\eta_t^4\right)}{630q^5}, \quad (A.118)$$

$$B_{32} = \frac{1}{630q^4}\eta_t\Big(-107q^3+q^2(907+822q)\eta_t-16q(68+119q+24q^2)\eta_t^2 +16(18+101q+78q^2)\eta_t^3-576(1+4q)\eta_t^4+1728\eta_t^5-24\eta_n^2(5q^3-13q^2\eta_t +16q\eta_t^2-8\eta_t^3)-8\eta_n(-61q^3+q^2(137+36q)\eta_t-4q(25+9q)\eta_t^2+24\eta_t^3)\Big), \quad (A.119)$$

$$B_{33} = \frac{1}{630q^3}\eta_t^2\Big(261q^2-4q(267+272q)\eta_t+4(111+370q+124q^2)\eta_t^2-960(1+q)\eta_t^3 +1440\eta_t^4+32\eta_n(-17q^2+q(23+9q)\eta_t-10\eta_t^2)+16\eta_n^2(11q^2-20q\eta_t+20\eta_t^2)\Big), \quad (A.120)$$

$$C_{01} = -\frac{4\eta_t^4\left(7q^2-24q\eta_t+24\eta_t^2\right)}{315q^4}, \quad (A.121)$$

$$C_{02} = -\frac{1}{1260q^3}\eta_t^2\Big(7q^2-16q(2+7q)\eta_t+16(2+34q+7q^2)\eta_t^2-768(1+q)\eta_t^3 +1152\eta_t^4-8\eta_n(7q^2-32q\eta_t+32\eta_t^2)+8\eta_n^2(7q^2-32q\eta_t+32\eta_t^2)\Big), \quad (A.122)$$

$$C_{03} = \frac{1}{1260q^2}\eta_t\Big(-q - 256\eta_n^3(q-\eta_t) + 128\eta_n^4(q-\eta_t) + (1-18q)\eta_t + 32(1+6q)\eta_t^2 - 16(35+34q)\eta_t^3 + 384(4+q)\eta_t^4 - 1152\eta_t^5 + 16\eta_n^2(9q - 9(1+q)\eta_t + 16(1+q)\eta_t^2 - 32\eta_t^3) - 16\eta_n(q-(1+9q)\eta_t + 16(1+q)\eta_t^2 - 32\eta_t^3)\Big), \quad (A.123)$$

$$C_{04} = \frac{1}{630q}\eta_t^2\Big(128\eta_n^3 - 64\eta_n^4 + 4\eta_n(9 - 32\eta_t + 32\eta_t^2) - 4\eta_n^2(25 - 32\eta_t + 32\eta_t^2) - 3(1 - 24\eta_t + 88\eta_t^2 - 128\eta_t^3 + 64\eta_t^4)\Big), \quad (A.124)$$

$$C_{11} = \frac{2\eta_t^4\left(149q^2 - 648q\eta_t + 648\eta_t^2\right)}{315q^4}, \quad (A.125)$$

$$C_{12} = \frac{1}{1260q^3}\eta_t^2\Big(5121q^2 - 16q(1178+1011q)\eta_t + 16(536+1650q+405q^2)\eta_t^2 - 18432(1+q)\eta_t^3 + 27648\eta_t^4 + 24\eta_n(-337q^2 + 32q(17+6q)\eta_t - 256\eta_t^2) + 24\eta_n^2(87q^2 - 256q\eta_t + 256\eta_t^2)\Big), \quad (A.126)$$

$$C_{13} = \frac{1}{360q^2}\Big(128\eta_n^3(-30q^2 + q(23+9q)\eta_t - 10\eta_t^2) + 320\eta_n^4(3q^2 - 2q\eta_t + 2\eta_t^2) + 8\eta_n(-60q^2 + 3q(91+123q)\eta_t - 2(34+183q+174q^2)\eta_t^2 + 16(10+23q+9q^2)\eta_t^3 - 320\eta_t^4) + 8\eta_n^2(405q^2 - 4q(137+87q)\eta_t + 2(74+93q+24q^2)\eta_t^2 - 160(1+q)\eta_t^3 + 320\eta_t^4) + \eta_t(-q(193+480q) + (53+3570q+3240q^2)\eta_t - 32(52+241q+120q^2)\eta_t^2 + 16(297+370q+60q^2)\eta_t^3 - 1920(4+q)\eta_t^4 + 5760\eta_t^5)\Big), \quad (A.127)$$

$$C_{21} = -\frac{8\eta_t^2}{3q}, \quad (A.128)$$

$$C_{22} = \frac{13\eta_t^4\left(5q^2 - 24q\eta_t + 24\eta_t^2\right)}{105q^4}, \quad (A.129)$$

$$C_{23} = \frac{1}{1260q^3}\eta_t^2\Big(-2335q^2 - 40q(451+370q)\eta_t + 8(1049+3064q+720q^2)\eta_t^2 - 17280(1+q)\eta_t^3 + 25920\eta_t^4 + 8\eta_n(-925q^2 + 4q(379+135q)\eta_t - 720\eta_t^2) + 360\eta_n^2(5q^2 - 16q\eta_t + 16\eta_t^2)\Big), \quad (A.130)$$

$$C_{24} = \frac{1}{5040q^2}\Big(128\eta_n^3(-528q^2 + q(403+153q)\eta_t - 170\eta_t^2) + 5440\eta_n^4(3q^2 - 2q\eta_t + 2\eta_t^2) + 8\eta_n(132q^2 + q(6065+7581q)\eta_t - 2(730+3495q+3138q^2)\eta_t^2 + 16(186+403q + 153q^2)\eta_t^3 - 5440\eta_t^4) + 8\eta_n^2(5271q^2 - 4q(2542+1569q)\eta_t + (2744+3270q + 816q^2)\eta_t^2 - 2720(1+q)\eta_t^3 + 5440\eta_t^4) + \eta_t\Big(3q(441+352q) + (-9807+75270q + 42168q^2)\eta_t - 32(1072+4451q+2112q^2)\eta_t^2 + 16(5497+6494q+1020q^2)\eta_t^3 - 32640(4+q)\eta_t^4 + 97920\eta_t^5\Big)\Big), \quad (A.131)$$

$$C_{31} = \frac{2\eta_t^4\left(5q^2-24q\eta_t+24\eta_t^2\right)}{105q^4}, \tag{A.132}$$

$$\begin{aligned} C_{32} = \frac{1}{630q^3}\eta_t^2\Big(&247q^2-8q(145+122q)\eta_t+8(67+202q+48q^2)\eta_t^2-1152(1+q)\eta_t^3\\ &+1728\eta_t^4+8\eta_n(-61q^2+4q(25+9q)\eta_t-48\eta_t^2)+24\eta_n^2(5q^2-16q\eta_t+16\eta_t^2)\Big), \end{aligned} \tag{A.133}$$

$$\begin{aligned} C_{33} = \frac{1}{2520q^2}\Big(&128\eta_n^3(-30q^2+q(23+9q)\eta_t-10\eta_t^2)+320\eta_n^4(3q^2-2q\eta_t+2\eta_t^2)\\ &+8\eta_n(-60q^2+3q(91+123q)\eta_t-2(34+183q+174q^2)\eta_t^2+16(10+23q+9q^2)\eta_t^3\\ &-320\eta_t^4)+8\eta_n^2(405q^2-4q(137+87q)\eta_t+2(74+93q+24q^2)\eta_t^2-160(1+q)\eta_t^3\\ &+320\eta_t^4)+\eta_t\Big(-q(193+480q)+(53+3570q+3240q^2)\eta_t-32(52+241q\\ &+120q^2)\eta_t^2+16(297+370q+60q^2)\eta_t^3-1920(4+q)\eta_t^4+5760\eta_t^5\Big)\Big). \end{aligned} \tag{A.134}$$

Appendix B

Supplementary Material to Chapter 3

B.1 Detailed derivation of Eq. (3.20)

The Eq. (3.10) is

$$\Big(- g\frac{\partial}{\partial c_x} + c_y\frac{\partial}{\partial y}\Big) f = J[f,f], \tag{B.1}$$

since we assumed that $J[f,f] \to -\nu(f - f_l)$, then the above equation becomes

$$\Big(- g\frac{\partial}{\partial c_x} + c_y\frac{\partial}{\partial y}\Big) f = -\nu(f - f_l).$$

Substitute $f = f_l(1+\Phi)$ in the above equation, we get

$$\Big(- g\frac{\partial}{\partial c_x} + c_y\frac{\partial}{\partial y}\Big)\{f_l(1+\Phi)\} = -\nu f_l\Phi. \tag{B.2}$$

First, we will simplify LHS:

$$\begin{aligned}
\Big(- g\frac{\partial}{\partial c_x} + c_y\frac{\partial}{\partial y}\Big)\{f_l(1+\Phi)\} &= f_l\Big(- g\frac{\partial}{\partial c_x} + c_y\frac{\partial}{\partial y}\Big)\Phi + (1+\Phi)\Big(- g\frac{\partial}{\partial c_x} + c_y\frac{\partial}{\partial y}\Big) f_l \\
&= f_l\Big\{\Big(- g\frac{\partial}{\partial c_x} + c_y\frac{\partial}{\partial y}\Big)\Phi + (1+\Phi)\Big(- g\frac{\partial}{\partial c_x} + c_y\frac{\partial}{\partial y}\Big)\log f_l\Big\} \\
&= f_l\Big\{\Big(- g\frac{\partial}{\partial C_x} + C_y\frac{\partial}{\partial y}\Big)\Phi + (1+\Phi)\Big(- g\frac{\partial}{\partial C_x} + C_y\frac{\partial}{\partial y}\Big)\log f_l\Big\}
\end{aligned}$$

($\because \boldsymbol{C} = \boldsymbol{c} - \boldsymbol{u} \Rightarrow C_y = c_y - u_y$, but $u_y = 0 \Rightarrow c_y = C_y$ & $\frac{\partial}{\partial c_x} = \frac{\partial}{\partial C_x}$)

$$\begin{aligned}
\Big(- g\frac{\partial}{\partial c_x} + c_y\frac{\partial}{\partial y}\Big)\{f_l(1+\Phi)\} &= f_l\Big\{\Big(- g\frac{\partial}{\partial C_x} + C_y\frac{\partial}{\partial y}\Big)\Phi + (1+\Phi)\Big(- g\frac{\partial}{\partial C_x} + C_y\frac{\partial}{\partial y}\Big)\log f_l\Big\} \\
&= f_l\Big\{(1+\Phi)\Big[- \Big(g + C_y\frac{\partial u_x}{\partial y}\Big)\frac{\partial}{\partial C_x}\log f_l + C_y\frac{\partial u_x}{\partial y}\frac{\partial}{\partial C_x}\log f_l \\
&\quad + C_y\frac{\partial}{\partial y}\log f_l\Big] - \Big(g + C_y\frac{\partial u_x}{\partial y}\Big)\frac{\partial\Phi}{\partial C_x} + C_y\frac{\partial u_x}{\partial y}\frac{\partial\Phi}{\partial C_x} + C_y\frac{\partial\Phi}{\partial y}\Big\} \\
&= f_l\Big\{(1+\Phi)\Big[C_y\Big(\frac{\partial}{\partial y} + \frac{\partial u_x}{\partial y}\frac{\partial}{\partial C_x}\Big)\log f_l - \Big(g + C_y\frac{\partial u_x}{\partial y}\Big)\frac{\partial}{\partial C_x}\log f_l\Big] \\
&\quad - \Big(g + C_y\frac{\partial u_x}{\partial y}\Big)\frac{\partial\Phi}{\partial C_x} + C_y\Big(\frac{\partial}{\partial y} + \frac{\partial u_x}{\partial y}\frac{\partial}{\partial C_x}\Big)\Phi\Big\} \\
&= f_l\Big\{(1+\Phi)\Big[C_y\tilde{\partial}_y\log f_l - \Big(g + C_y\frac{\partial u_x}{\partial y}\Big)\frac{\partial}{\partial C_x}\log f_l\Big] \\
&\quad - \Big(g + C_y\frac{\partial u_x}{\partial y}\Big)\frac{\partial\Phi}{\partial C_x} + C_y\tilde{\partial}_y\Phi\Big\}. \quad \Big(\because \tilde{\partial}_y = \frac{\partial}{\partial y} + \frac{\partial u_x}{\partial y}\frac{\partial}{\partial C_x}\Big)
\end{aligned}$$

Substitute the above expression into Eq. (B.2), we get

$$(1+\Phi)\Big[C_y\tilde{\partial}_y\log f_l - \Big(g + C_y\frac{\partial u_x}{\partial y}\Big)\frac{\partial}{\partial C_x}\log f_l\Big] = \Big(g + C_y\frac{\partial u_x}{\partial y}\Big)\frac{\partial}{\partial C_x}\Phi - C_y\tilde{\partial}_y\Phi - \nu\Phi. \tag{B.3}$$

B.2 Explicit expressions of the Boltzmann equation at fifth and higher orders

Here, we list the explicit expressions of the Boltzmann equation at 5th order and beyond. They are

1. The equation for $\Phi^{(5)}$ is

$$
\begin{aligned}
(1-\mathscr{A})\Phi^{(5)} \quad = \quad & \frac{\partial \Phi^{(4)}}{\partial c_x} - \nu^{(4)}\Phi^{(1)} - \nu^{(2)}\Phi^{(3)} - \Big(\Phi^{(3)}(-2u^{(1)} + \frac{\partial p^{(2)}}{\partial y}c_y \\
& -2u^{(1)}\frac{\partial u^{(1)}}{\partial y}c_y - \frac{1}{2}\frac{\partial T^{(2)}}{\partial y}\left(5-2c^2\right)c_y) + \Phi^{(1)}(2T^{(2)}u^{(1)} - 2u^{(3)} \\
& +2T^{(2)}u^{(1)}\frac{\partial u^{(1)}}{\partial y}c_y - 2\frac{\partial u^{(1)}}{\partial y}u^{(3)}c_y - 2u^{(1)}\frac{\partial u^{(3)}}{\partial y}c_y \\
& +\frac{1}{2}(2(p_y^{42}) - (T_y^{42})(5-2c^2) + 2\frac{\partial T^{(2)}}{\partial y}({u^{(1)}}^2 - T^{(2)}c^2))c_y) \\
& +2({T^{(2)}}^2 - T^{(4)})c_x + 2({T^{(2)}}^2 - T^{(4)})\frac{\partial u^{(1)}}{\partial y}c_y c_x - 2(-T^{(2)}\frac{\partial T^{(2)}}{\partial y}u^{(1)} \\
& +(T_y^{42})u^{(1)} + \frac{\partial T^{(2)}}{\partial y}u^{(3)})c_y c_x - 2T^{(2)}\frac{\partial u^{(3)}}{\partial y}c_y c_x + 2\frac{\partial u^{(5)}}{\partial y}c_y c_x \\
& +\Phi^{(4)}(2c_x + 2\frac{\partial u^{(1)}}{\partial y}c_y c_x) + \Phi^{(2)}(-2T^{(2)}c_x - 2\frac{\partial T^{(2)}}{\partial y}u^{(1)}c_y c_x \\
& -2T^{(2)}\frac{\partial u^{(1)}}{\partial y}c_y c_x + 2\frac{\partial u^{(3)}}{\partial y}c_y c_x)\Big),
\end{aligned}
\tag{B.4}
$$

where

$$
p_y^{42} = \frac{\partial}{\partial y}\left(-\frac{{p^{(2)}}^2}{2} + p^{(4)}\right), \tag{B.5}
$$

$$
T_y^{42} = \frac{\partial}{\partial y}\left(-\frac{{T^{(2)}}^2}{2} + T^{(4)}\right). \tag{B.6}
$$

2. The equation for $\Phi^{(6)}$ is

$$
\begin{aligned}
(1-\mathscr{A})\Phi^{(6)} \quad = \quad & \frac{\partial \Phi^{(5)}}{\partial c_x} - \nu^{(4)}\Phi^{(2)} - \nu^{(2)}\Phi^{(4)} - \Big(-2({T^{(2)}}^2 - T^{(4)})u^{(1)} + 2T^{(2)}u^{(3)} - 2u^{(5)} \\
& -2({T^{(2)}}^2 - T^{(4)})u^{(1)}\frac{\partial u^{(1)}}{\partial y}c_y + 2T^{(2)}\frac{\partial u^{(1)}}{\partial y}u^{(3)}c_y + 2T^{(2)}u^{(1)}\frac{\partial u^{(3)}}{\partial y}c_y - 2u^{(3)}\frac{\partial u^{(3)}}{\partial y}c_y \\
& -2\frac{\partial u^{(1)}}{\partial y}u^{(5)}c_y - 2u^{(1)}\frac{\partial u^{(5)}}{\partial y}c_y + \frac{1}{2}(2(p_y^{642}) - (T_y^{642})(5-2c^2) - 2(T^{(2)}\frac{\partial T^{(2)}}{\partial y}{u^{(1)}}^2 \\
& -(T_y^{42}){u^{(1)}}^2 - 2\frac{\partial T^{(2)}}{\partial y}u^{(1)}u^{(3)} - {T^{(2)}}^2\frac{\partial T^{(2)}}{\partial y}c^2 + \frac{\partial T^{(2)}}{\partial y}T^{(4)}c^2 + T^{(2)}(T_y^{42})c^2))c_y \\
& +\Phi^{(4)}(-2u^{(1)} + \frac{\partial p^{(2)}}{\partial y}c_y - 2u^{(1)}\frac{\partial u^{(1)}}{\partial y}c_y - \frac{1}{2}\frac{\partial T^{(2)}}{\partial y}(5-2c^2)c_y) \\
& +\Phi^{(2)}(2T^{(2)}u^{(1)} - 2u^{(3)} + 2T^{(2)}u^{(1)}\frac{\partial u^{(1)}}{\partial y}c_y - 2\frac{\partial u^{(1)}}{\partial y}u^{(3)}c_y - 2u^{(1)}\frac{\partial u^{(3)}}{\partial y}c_y \\
& +\frac{1}{2}(2(p_y^{42}) - (T_y^{42})(5-2c^2) + 2\frac{\partial T^{(2)}}{\partial y}({u^{(1)}}^2 - T^{(2)}c^2))c_y) + \Phi^{(5)}(1 + \frac{\partial u^{(1)}}{\partial y}c_y)2c_x \\
& +\Phi^{(3)}(-2T^{(2)}c_x - 2\frac{\partial T^{(2)}}{\partial y}u^{(1)}c_y c_x - 2T^{(2)}\frac{\partial u^{(1)}}{\partial y}c_y c_x + 2\frac{\partial u^{(3)}}{\partial y}c_y c_x) \\
& +\Phi^{(1)}(2({T^{(2)}}^2 - T^{(4)})c_x + 2({T^{(2)}}^2 - T^{(4)})\frac{\partial u^{(1)}}{\partial y}c_y c_x - 2(-T^{(2)}\frac{\partial T^{(2)}}{\partial y}u^{(1)} \\
& +(T_y^{42})u^{(1)} + \frac{\partial T^{(2)}}{\partial y}u^{(3)} - T^{(2)}\frac{\partial u^{(3)}}{\partial y} + \frac{\partial u^{(5)}}{\partial y})c_y c_x)\Big),
\end{aligned}
\tag{B.7}
$$

where

$$
p_y^{642} = \frac{\partial}{\partial y}\left(\frac{{p^{(2)}}^3}{3} - p^{(2)}p^{(4)} + p^{(6)}\right), \tag{B.8}
$$

$$
T_y^{642} = \frac{\partial}{\partial y}\left(\frac{{T^{(2)}}^3}{3} - T^{(2)}T^{(4)} + T^{(6)}\right). \tag{B.9}
$$

3. The equation for $\Phi^{(7)}$ is

$$
\begin{aligned}
(1-\mathscr{A})\Phi^{(7)} \quad = \quad & \frac{\partial\Phi^{(6)}}{\partial c_x} - \nu^{(6)}\Phi^{(1)} - \nu^{(4)}\Phi^{(3)} - \nu^{(2)}\Phi^{(5)} - \Big(\Phi^{(5)}(-2u^{(1)} + \frac{\partial p^{(2)}}{\partial y}c_y \\
& -2u^{(1)}\frac{\partial u^{(1)}}{\partial y}c_y - \frac{1}{2}\frac{\partial T^{(2)}}{\partial y}(5-2c^2)c_y) + \Phi^{(3)}(2T^{(2)}u^{(1)} - 2u^{(3)} + 2T^{(2)}u^{(1)}\frac{\partial u^{(1)}}{\partial y}c_y \\
& -2\frac{\partial u^{(1)}}{\partial y}u^{(3)}c_y - 2u^{(1)}\frac{\partial u^{(3)}}{\partial y}c_y + \frac{1}{2}(2(p_y^{42}) - (T_y^{42})(5-2c^2) \\
& +2\frac{\partial T^{(2)}}{\partial y}({u^{(1)}}^2 - T^{(2)}c^2))c_y) + \Phi^{(1)}(-2({T^{(2)}}^2 - T^{(4)})u^{(1)} + 2T^{(2)}u^{(3)} - 2u^{(5)} \\
& -2({T^{(2)}}^2 - T^{(4)})u^{(1)}\frac{\partial u^{(1)}}{\partial y}c_y + 2T^{(2)}\frac{\partial u^{(1)}}{\partial y}u^{(3)}c_y + 2T^{(2)}u^{(1)}\frac{\partial u^{(3)}}{\partial y}c_y - 2u^{(3)}\frac{\partial u^{(3)}}{\partial y}c_y \\
& -2\frac{\partial u^{(1)}}{\partial y}u^{(5)}c_y - 2u^{(1)}\frac{\partial u^{(5)}}{\partial y}c_y + \frac{1}{2}(2(p_y^{642}) - (T_y^{642})(5-2c^2) - 2(T^{(2)}\frac{\partial T^{(2)}}{\partial y}{u^{(1)}}^2 \\
& -(T_y^{42}){u^{(1)}}^2 - 2\frac{\partial T^{(2)}}{\partial y}u^{(1)}u^{(3)} - {T^{(2)}}^2\frac{\partial T^{(2)}}{\partial y}c^2 + \frac{\partial T^{(2)}}{\partial y}T^{(4)}c^2 + T^{(2)}(T_y^{42})c^2))c_y) \\
& -2({T^{(2)}}^3 - 2T^{(2)}T^{(4)} + T^{(6)})c_x - 2({T^{(2)}}^3 - 2T^{(2)}T^{(4)} + T^{(6)})\frac{\partial u^{(1)}}{\partial y}c_yc_x \\
& +2({T^{(2)}}^2 - T^{(4)})\frac{\partial u^{(3)}}{\partial y}c_yc_x - 2({T^{(2)}}^2\frac{\partial T^{(2)}}{\partial y}u^{(1)} + (T_y^{642})u^{(1)} + (T_y^{42})u^{(3)} \\
& -T^{(2)}((T_y^{42})u^{(1)} + \frac{\partial T^{(2)}}{\partial y}u^{(3)}) + \frac{\partial T^{(2)}}{\partial y}(-T^{(4)}u^{(1)} + u^{(5)}))c_yc_x - 2T^{(2)}\frac{\partial u^{(5)}}{\partial y}c_yc_x \\
& +2\frac{\partial u^{(7)}}{\partial y}c_yc_x + \Phi^{(6)}(2c_x + 2\frac{\partial u^{(1)}}{\partial y}c_yc_x) + \Phi^{(4)}(-2T^{(2)}c_x - 2\frac{\partial T^{(2)}}{\partial y}u^{(1)}c_yc_x \\
& -2T^{(2)}\frac{\partial u^{(1)}}{\partial y}c_yc_x + 2\frac{\partial u^{(3)}}{\partial y}c_yc_x) + \Phi^{(2)}(2({T^{(2)}}^2 - T^{(4)})c_x + 2({T^{(2)}}^2 - T^{(4)})\frac{\partial u^{(1)}}{\partial y}c_yc_x \\
& -2(-T^{(2)}\frac{\partial T^{(2)}}{\partial y}u^{(1)} + (T_y^{42})u^{(1)} + \frac{\partial T^{(2)}}{\partial y}u^{(3)} - T^{(2)}\frac{\partial u^{(3)}}{\partial y} + \frac{\partial u^{(5)}}{\partial y})c_yc_x)\Big). \qquad \text{(B.10)}
\end{aligned}
$$

4. The equation for $\Phi^{(8)}$ is

$$
\begin{aligned}
(1-\not{\alpha})\Phi^{(8)} \quad = \quad & \frac{\partial \Phi^{(7)}}{\partial c_x} - \nu^{(6)}\Phi^{(2)} - \nu^{(4)}\Phi^{(4)} - \nu^{(2)}\Phi^{(6)} - \Big(2({T^{(2)}}^3 - 2T^{(2)}T^{(4)} + T^{(6)})u^{(1)} \\
& -2({T^{(2)}}^2 - T^{(4)})u^{(3)} + 2T^{(2)}u^{(5)} - 2u^{(7)} + 2({T^{(2)}}^3 - 2T^{(2)}T^{(4)} + T^{(6)})u^{(1)}\frac{\partial u^{(1)}}{\partial y}c_y \\
& -2({T^{(2)}}^2 - T^{(4)})\frac{\partial u^{(1)}}{\partial y}u^{(3)}c_y - 2({T^{(2)}}^2 - T^{(4)})u^{(1)}\frac{\partial u^{(3)}}{\partial y}c_y + 2T^{(2)}u^{(3)}\frac{\partial u^{(3)}}{\partial y}c_y \\
& +2T^{(2)}\frac{\partial u^{(1)}}{\partial y}u^{(5)}c_y - 2\frac{\partial u^{(3)}}{\partial y}u^{(5)}c_y + 2T^{(2)}u^{(1)}\frac{\partial u^{(5)}}{\partial y}c_y - 2u^{(3)}\frac{\partial u^{(5)}}{\partial y}c_y \\
& -2\frac{\partial u^{(1)}}{\partial y}u^{(7)}c_y - 2u^{(1)}\frac{\partial u^{(7)}}{\partial y}c_y + \frac{1}{2}(2(p_y^{8642}) - (T_y^{8642})(5-2c^2) \\
& -2(-(T_y^{642})u^{(1)^2} - 2(T_y^{42})u^{(1)}u^{(3)} + {T^{(2)}}^3\frac{\partial T^{(2)}}{\partial y}c^2 + T^{(4)}(T_y^{42})c^2 \\
& -{T^{(2)}}^2(\frac{\partial T^{(2)}}{\partial y}u^{(1)^2} + (T_y^{42})c^2) + \frac{\partial T^{(2)}}{\partial y}(T^{(4)}u^{(1)^2} - u^{(3)^2} - 2u^{(1)}u^{(5)} + T^{(6)}c^2) \\
& +T^{(2)}((T_y^{42})u^{(1)^2} + 2\frac{\partial T^{(2)}}{\partial y}u^{(1)}u^{(3)} - 2\frac{\partial T^{(2)}}{\partial y}T^{(4)}c^2 + (T_y^{642})c^2)))c_y \\
& +\Phi^{(6)}(-2u^{(1)} + \frac{\partial p^{(2)}}{\partial y}c_y - 2u^{(1)}\frac{\partial u^{(1)}}{\partial y}c_y - \frac{1}{2}\frac{\partial T^{(2)}}{\partial y}(5-2c^2)c_y) \\
& +\Phi^{(4)}(2T^{(2)}u^{(1)} - 2u^{(3)} + 2T^{(2)}u^{(1)}\frac{\partial u^{(1)}}{\partial y}c_y - 2\frac{\partial u^{(1)}}{\partial y}u^{(3)}c_y - 2u^{(1)}\frac{\partial u^{(3)}}{\partial y}c_y \\
& +\frac{1}{2}(2(p_y^{42}) - (T_y^{42})(5-2c^2) + 2\frac{\partial T^{(2)}}{\partial y}(u^{(1)^2} - T^{(2)}c^2))c_y) \\
& +\Phi^{(2)}(-2({T^{(2)}}^2 - T^{(4)})u^{(1)} + 2T^{(2)}u^{(3)} - 2u^{(5)} - 2({T^{(2)}}^2 - T^{(4)})u^{(1)}\frac{\partial u^{(1)}}{\partial y}c_y \\
& +2T^{(2)}\frac{\partial u^{(1)}}{\partial y}u^{(3)}c_y + 2T^{(2)}u^{(1)}\frac{\partial u^{(3)}}{\partial y}c_y - 2u^{(3)}\frac{\partial u^{(3)}}{\partial y}c_y - 2\frac{\partial u^{(1)}}{\partial y}u^{(5)}c_y - 2u^{(1)}\frac{\partial u^{(5)}}{\partial y}c_y \\
& +\frac{1}{2}(2(p_y^{642}) - (T_y^{642})(5-2c^2) - 2(T^{(2)}\frac{\partial T^{(2)}}{\partial y}u^{(1)^2} - (T_y^{42})u^{(1)^2} - 2\frac{\partial T^{(2)}}{\partial y}u^{(1)}u^{(3)} \\
& -{T^{(2)}}^2\frac{\partial T^{(2)}}{\partial y}c^2 + \frac{\partial T^{(2)}}{\partial y}T^{(4)}c^2 + T^{(2)}(T_y^{42})c^2))c_y) + \Phi^{(7)}(2c_x + 2\frac{\partial u^{(1)}}{\partial y}c_yc_x) \\
& +\Phi^{(5)}(-2T^{(2)}c_x - 2\frac{\partial T^{(2)}}{\partial y}u^{(1)}c_yc_x - 2T^{(2)}\frac{\partial u^{(1)}}{\partial y}c_yc_x + 2\frac{\partial u^{(3)}}{\partial y}c_yc_x) \\
& +\Phi^{(3)}(2({T^{(2)}}^2 - T^{(4)})c_x + 2({T^{(2)}}^2 - T^{(4)})\frac{\partial u^{(1)}}{\partial y}c_yc_x - 2(-T^{(2)}\frac{\partial T^{(2)}}{\partial y}u^{(1)} \\
& +(T_y^{42})u^{(1)} + \frac{\partial T^{(2)}}{\partial y}u^{(3)})c_yc_x - 2T^{(2)}\frac{\partial u^{(3)}}{\partial y}c_yc_x + 2\frac{\partial u^{(5)}}{\partial y}c_yc_x) \\
& +\Phi^{(1)}(-2({T^{(2)}}^3 - 2T^{(2)}T^{(4)} + T^{(6)})c_x - 2({T^{(2)}}^3 - 2T^{(2)}T^{(4)} + T^{(6)})\frac{\partial u^{(1)}}{\partial y}c_yc_x \\
& +2({T^{(2)}}^2 - T^{(4)})\frac{\partial u^{(3)}}{\partial y}c_yc_x - 2({T^{(2)}}^2\frac{\partial T^{(2)}}{\partial y}u^{(1)} + (T_y^{642})u^{(1)} + (T_y^{42})u^{(3)} \\
& -T^{(2)}((T_y^{42})u^{(1)} + \frac{\partial T^{(2)}}{\partial y}u^{(3)}) + \frac{\partial T^{(2)}}{\partial y}(-T^{(4)}u^{(1)} + u^{(5)}))c_yc_x \\
& -2T^{(2)}\frac{\partial u^{(5)}}{\partial y}c_yc_x + 2\frac{\partial u^{(7)}}{\partial y}c_yc_x)\Big), \qquad \text{(B.11)}
\end{aligned}
$$

where

$$p_y^{8642} = \frac{\partial}{\partial y}\left(-\frac{{p^{(2)}}^4}{4} + {p^{(2)}}^2p^{(4)} - \frac{{p^{(4)}}^2}{2} - p^{(2)}p^{(6)} + p^{(8)}\right), \qquad \text{(B.12)}$$

$$T_y^{8642} = \frac{\partial}{\partial y}\left(-\frac{{T^{(2)}}^4}{4} + {T^{(2)}}^2T^{(4)} - \frac{{T^{(4)}}^2}{2} - T^{(2)}T^{(6)} + T^{(8)}\right). \qquad \text{(B.13)}$$

5. The equation for $\Phi^{(9)}$ is

$$
\begin{aligned}
(1-\mathscr{A})\Phi^{(9)} \quad = \quad & \frac{\partial\Phi^{(8)}}{\partial c_x} - \nu^{(8)}\Phi^{(1)} - \nu^{(6)}\Phi^{(3)} - \nu^{(4)}\Phi^{(5)} - \nu^{(2)}\Phi^{(7)} \\
& -\Big(\Phi^{(7)}(-2u^{(1)} + \frac{\partial p^{(2)}}{\partial y}c_y + \frac{1}{2}(-5)\frac{\partial T^{(2)}}{\partial y}c_y - 2u^{(1)}\frac{\partial u^{(1)}}{\partial y}c_y + \frac{\partial T^{(2)}}{\partial y}c^2 c_y) \\
& +\Phi^{(5)}(2T^{(2)}u^{(1)} - 2u^{(3)} + 2T^{(2)}u^{(1)}\frac{\partial u^{(1)}}{\partial y}c_y - 2\frac{\partial u^{(1)}}{\partial y}u^{(3)}c_y - 2u^{(1)}\frac{\partial u^{(3)}}{\partial y}c_y \\
& +((p_y^{42}) + (T_y^{42})(-\frac{5}{2} + c^2) + \frac{\partial T^{(2)}}{\partial y}({u^{(1)}}^2 - T^{(2)}c^2))c_y) + \Phi^{(3)}(-2({T^{(2)}}^2 - T^{(4)})u^{(1)} \\
& +2T^{(2)}u^{(3)} - 2u^{(5)} - 2({T^{(2)}}^2 - T^{(4)})u^{(1)}\frac{\partial u^{(1)}}{\partial y}c_y + 2T^{(2)}\frac{\partial u^{(1)}}{\partial y}u^{(3)}c_y + 2T^{(2)}u^{(1)}\frac{\partial u^{(3)}}{\partial y}c_y \\
& -2u^{(3)}\frac{\partial u^{(3)}}{\partial y}c_y - 2\frac{\partial u^{(1)}}{\partial y}u^{(5)}c_y - 2u^{(1)}\frac{\partial u^{(5)}}{\partial y}c_y + ((p_y^{642}) - \frac{5}{2}(T_y^{642}) + (T_y^{642})c^2 \\
& +(T_y^{42})({u^{(1)}}^2 - T^{(2)}c^2) + \frac{\partial T^{(2)}}{\partial y}(-T^{(2)}{u^{(1)}}^2 + 2u^{(1)}u^{(3)} + ({T^{(2)}}^2 - T^{(4)})c^2))c_y) \\
& +\Phi^{(1)}(2({T^{(2)}}^3 - 2T^{(2)}T^{(4)} + T^{(6)})u^{(1)} - 2({T^{(2)}}^2 - T^{(4)})u^{(3)} + 2T^{(2)}u^{(5)} - 2u^{(7)} \\
& +2({T^{(2)}}^3 - 2T^{(2)}T^{(4)} + T^{(6)})u^{(1)}\frac{\partial u^{(1)}}{\partial y}c_y - 2({T^{(2)}}^2 - T^{(4)})\frac{\partial u^{(1)}}{\partial y}u^{(3)}c_y \\
& -2({T^{(2)}}^2 - T^{(4)})u^{(1)}\frac{\partial u^{(3)}}{\partial y}c_y + 2T^{(2)}u^{(3)}\frac{\partial u^{(3)}}{\partial y}c_y + 2T^{(2)}\frac{\partial u^{(1)}}{\partial y}u^{(5)}c_y - 2\frac{\partial u^{(3)}}{\partial y}u^{(5)}c_y \\
& +2T^{(2)}u^{(1)}\frac{\partial u^{(5)}}{\partial y}c_y - 2u^{(3)}\frac{\partial u^{(5)}}{\partial y}c_y - 2\frac{\partial u^{(1)}}{\partial y}u^{(7)}c_y - 2u^{(1)}\frac{\partial u^{(7)}}{\partial y}c_y \\
& +((p_y^{8642}) - \frac{5}{2}(T_y^{8642}) + (T_y^{8642})c^2 + (T_y^{642})({u^{(1)}}^2 - T^{(2)}c^2) + (T_y^{42})(-T^{(2)}{u^{(1)}}^2 \\
& +2u^{(1)}u^{(3)} + ({T^{(2)}}^2 - T^{(4)})c^2) + \frac{\partial T^{(2)}}{\partial y}(({T^{(2)}}^2 - T^{(4)}){u^{(1)}}^2 - 2T^{(2)}u^{(1)}u^{(3)} + {u^{(3)}}^2 \\
& +2u^{(1)}u^{(5)} - ({T^{(2)}}^3 - 2T^{(2)}T^{(4)} + T^{(6)})c^2))c_y) + 2({T^{(2)}}^4 - 3{T^{(2)}}^2T^{(4)} + {T^{(4)}}^2 \\
& +2T^{(2)}T^{(6)} - T^{(8)})c_x + 2({T^{(2)}}^4 - 3{T^{(2)}}^2T^{(4)} + {T^{(4)}}^2 + 2T^{(2)}T^{(6)} - T^{(8)})\frac{\partial u^{(1)}}{\partial y}c_y c_x \\
& -2({T^{(2)}}^3 - 2T^{(2)}T^{(4)} + T^{(6)})\frac{\partial u^{(3)}}{\partial y}c_y c_x + 2({T^{(2)}}^2 - T^{(4)})\frac{\partial u^{(5)}}{\partial y}c_y c_x + 2({T^{(2)}}^3\frac{\partial T^{(2)}}{\partial y}u^{(1)} \\
& +T^{(4)}(T_y^{42})u^{(1)} + \frac{\partial T^{(2)}}{\partial y}T^{(6)}u^{(1)} - (T_y^{8642})u^{(1)} + \frac{\partial T^{(2)}}{\partial y}T^{(4)}u^{(3)} - (T_y^{642})u^{(3)} \\
& -{T^{(2)}}^2((T_y^{42})u^{(1)} + \frac{\partial T^{(2)}}{\partial y}u^{(3)}) - (T_y^{42})u^{(5)} + T^{(2)}((T_y^{642})u^{(1)} + (T_y^{42})u^{(3)} \\
& +\frac{\partial T^{(2)}}{\partial y}(-2T^{(4)}u^{(1)} + u^{(5)})) - \frac{\partial T^{(2)}}{\partial y}u^{(7)})c_y c_x - 2T^{(2)}\frac{\partial u^{(7)}}{\partial y}c_y c_x + 2\frac{\partial u^{(9)}}{\partial y}c_y c_x \\
& +\Phi^{(8)}(2c_x + 2\frac{\partial u^{(1)}}{\partial y}c_y c_x) + \Phi^{(6)}(-2T^{(2)}c_x - 2\frac{\partial T^{(2)}}{\partial y}u^{(1)}c_y c_x - 2T^{(2)}\frac{\partial u^{(1)}}{\partial y}c_y c_x \\
& +2\frac{\partial u^{(3)}}{\partial y}c_y c_x) + \Phi^{(4)}(2({T^{(2)}}^2 - T^{(4)})c_x + 2({T^{(2)}}^2 - T^{(4)})\frac{\partial u^{(1)}}{\partial y}c_y c_x - 2(-T^{(2)}\frac{\partial T^{(2)}}{\partial y}u^{(1)} \\
& +(T_y^{42})u^{(1)} + \frac{\partial T^{(2)}}{\partial y}u^{(3)})c_y c_x - 2T^{(2)}\frac{\partial u^{(3)}}{\partial y}c_y c_x + 2\frac{\partial u^{(5)}}{\partial y}c_y c_x) \\
& +\Phi^{(2)}(-2({T^{(2)}}^3 - 2T^{(2)}T^{(4)} + T^{(6)})c_x - 2({T^{(2)}}^3 - 2T^{(2)}T^{(4)} + T^{(6)})\frac{\partial u^{(1)}}{\partial y}c_y c_x \\
& +2({T^{(2)}}^2 - T^{(4)})\frac{\partial u^{(3)}}{\partial y}c_y c_x - 2({T^{(2)}}^2\frac{\partial T^{(2)}}{\partial y}u^{(1)} + (T_y^{642})u^{(1)} + (T_y^{42})u^{(3)} \\
& -T^{(2)}((T_y^{42})u^{(1)} + \frac{\partial T^{(2)}}{\partial y}u^{(3)}) + \frac{\partial T^{(2)}}{\partial y}(-T^{(4)}u^{(1)} + u^{(5)}))c_y c_x \\
& -2T^{(2)}\frac{\partial u^{(5)}}{\partial y}c_y c_x + 2\frac{\partial u^{(7)}}{\partial y}c_y c_x)\Big). \qquad \text{(B.14)}
\end{aligned}
$$

6. The equation for $\Phi^{(10)}$ is

$$
\begin{aligned}
(1-\mathscr{A})\Phi^{(10)} \quad = \quad & \frac{\partial \Phi^{(9)}}{\partial c_x} - \nu^{(8)}\Phi^{(2)} - \nu^{(6)}\Phi^{(4)} - \nu^{(4)}\Phi^{(6)} - \nu^{(2)}\Phi^{(8)} \\
& -\Big(- 2({T^{(2)}}^4 - 3{T^{(2)}}^2 T^{(4)} + {T^{(4)}}^2 + 2T^{(2)}T^{(6)} - T^{(8)})u^{(1)} \\
& +2({T^{(2)}}^3 - 2T^{(2)}T^{(4)} + T^{(6)})u^{(3)} - 2({T^{(2)}}^2 - T^{(4)})u^{(5)} + 2T^{(2)}u^{(7)} - 2u^{(9)} \\
& -2({T^{(2)}}^4 - 3{T^{(2)}}^2 T^{(4)} + {T^{(4)}}^2 + 2T^{(2)}T^{(6)} - T^{(8)})u^{(1)}\frac{\partial u^{(1)}}{\partial y}c_y \\
& +2({T^{(2)}}^3 - 2T^{(2)}T^{(4)} + T^{(6)})\frac{\partial u^{(1)}}{\partial y}u^{(3)}c_y + 2({T^{(2)}}^3 - 2T^{(2)}T^{(4)} + T^{(6)})u^{(1)}\frac{\partial u^{(3)}}{\partial y}c_y \\
& -2({T^{(2)}}^2 - T^{(4)})u^{(3)}\frac{\partial u^{(3)}}{\partial y}c_y - 2({T^{(2)}}^2 - T^{(4)})\frac{\partial u^{(1)}}{\partial y}u^{(5)}c_y + 2T^{(2)}\frac{\partial u^{(3)}}{\partial y}u^{(5)}c_y \\
& -2({T^{(2)}}^2 - T^{(4)})u^{(1)}\frac{\partial u^{(5)}}{\partial y}c_y + 2T^{(2)}u^{(3)}\frac{\partial u^{(5)}}{\partial y}c_y - 2u^{(5)}\frac{\partial u^{(5)}}{\partial y}c_y + 2T^{(2)}\frac{\partial u^{(1)}}{\partial y}u^{(7)}c_y \\
& -2\frac{\partial u^{(3)}}{\partial y}u^{(7)}c_y + 2T^{(2)}u^{(1)}\frac{\partial u^{(7)}}{\partial y}c_y - 2u^{(3)}\frac{\partial u^{(7)}}{\partial y}c_y - 2\frac{\partial u^{(1)}}{\partial y}u^{(9)}c_y - 2u^{(1)}\frac{\partial u^{(9)}}{\partial y}c_y \\
& +((p_y^{108642}) - \frac{5}{2}(T_y^{108642}) + (T_y^{108642})c^2 + (T_y^{8642})({u^{(1)}}^2 - T^{(2)}c^2) \\
& +(T_y^{642})(-T^{(2)}{u^{(1)}}^2 + 2u^{(1)}u^{(3)} + ({T^{(2)}}^2 - T^{(4)})c^2) + (T_y^{42})(({T^{(2)}}^2 - T^{(4)}){u^{(1)}}^2 \\
& -2T^{(2)}u^{(1)}u^{(3)} + {u^{(3)}}^2 + 2u^{(1)}u^{(5)} - ({T^{(2)}}^3 - 2T^{(2)}T^{(4)} + T^{(6)})c^2) \\
& +\frac{\partial T^{(2)}}{\partial y}((-{T^{(2)}}^3 + 2T^{(2)}T^{(4)} - T^{(6)}){u^{(1)}}^2 + 2({T^{(2)}}^2 - T^{(4)})u^{(1)}u^{(3)} \\
& -T^{(2)}({u^{(3)}}^2 + 2u^{(1)}u^{(5)}) + 2(u^{(3)}u^{(5)} + u^{(1)}u^{(7)}) + ({T^{(2)}}^4 - 3{T^{(2)}}^2 T^{(4)} + {T^{(4)}}^2 \\
& +2T^{(2)}T^{(6)} - T^{(8)})c^2))c_y + \Phi^{(8)}(-2u^{(1)} + \frac{\partial p^{(2)}}{\partial y}c_y + \frac{1}{2}(-5)\frac{\partial T^{(2)}}{\partial y}c_y - 2u^{(1)}\frac{\partial u^{(1)}}{\partial y}c_y \\
& +\frac{\partial T^{(2)}}{\partial y}c^2 c_y) + \Phi^{(6)}(2T^{(2)}u^{(1)} - 2u^{(3)} + 2T^{(2)}u^{(1)}\frac{\partial u^{(1)}}{\partial y}c_y - 2\frac{\partial u^{(1)}}{\partial y}u^{(3)}c_y \\
& -2u^{(1)}\frac{\partial u^{(3)}}{\partial y}c_y + ((p_y^{42}) + (T_y^{42})(-\frac{5}{2} + c^2) + \frac{\partial T^{(2)}}{\partial y}({u^{(1)}}^2 - T^{(2)}c^2))c_y) \\
& +\Phi^{(4)}(-2({T^{(2)}}^2 - T^{(4)})u^{(1)} + 2T^{(2)}u^{(3)} - 2u^{(5)} - 2({T^{(2)}}^2 - T^{(4)})u^{(1)}\frac{\partial u^{(1)}}{\partial y}c_y \\
& +2T^{(2)}\frac{\partial u^{(1)}}{\partial y}u^{(3)}c_y + 2T^{(2)}u^{(1)}\frac{\partial u^{(3)}}{\partial y}c_y - 2u^{(3)}\frac{\partial u^{(3)}}{\partial y}c_y - 2\frac{\partial u^{(1)}}{\partial y}u^{(5)}c_y - 2u^{(1)}\frac{\partial u^{(5)}}{\partial y}c_y \\
& +((p_y^{642}) - \frac{5}{2}(T_y^{642}) + (T_y^{642})c^2 + (T_y^{42})({u^{(1)}}^2 - T^{(2)}c^2) \\
& +\frac{\partial T^{(2)}}{\partial y}(-T^{(2)}{u^{(1)}}^2 + 2u^{(1)}u^{(3)} + ({T^{(2)}}^2 - T^{(4)})c^2))c_y) \\
& +\Phi^{(2)}(2({T^{(2)}}^3 - 2T^{(2)}T^{(4)} + T^{(6)})u^{(1)} - 2({T^{(2)}}^2 - T^{(4)})u^{(3)} + 2T^{(2)}u^{(5)} - 2u^{(7)} \\
& +2({T^{(2)}}^3 - 2T^{(2)}T^{(4)} + T^{(6)})u^{(1)}\frac{\partial u^{(1)}}{\partial y}c_y - 2({T^{(2)}}^2 - T^{(4)})\frac{\partial u^{(1)}}{\partial y}u^{(3)}c_y \\
& -2({T^{(2)}}^2 - T^{(4)})u^{(1)}\frac{\partial u^{(3)}}{\partial y}c_y + 2T^{(2)}u^{(3)}\frac{\partial u^{(3)}}{\partial y}c_y + 2T^{(2)}\frac{\partial u^{(1)}}{\partial y}u^{(5)}c_y - 2\frac{\partial u^{(3)}}{\partial y}u^{(5)}c_y \\
& +2T^{(2)}u^{(1)}\frac{\partial u^{(5)}}{\partial y}c_y - 2u^{(3)}\frac{\partial u^{(5)}}{\partial y}c_y - 2\frac{\partial u^{(1)}}{\partial y}u^{(7)}c_y - 2u^{(1)}\frac{\partial u^{(7)}}{\partial y}c_y
\end{aligned}
$$

$$
\begin{aligned}
&+((p_y^{8642}) - \frac{5}{2}(T_y^{8642}) + (T_y^{8642})c^2 + (T_y^{642})({u^{(1)}}^2 - T^{(2)}c^2) + (T_y^{42})(-T^{(2)}{u^{(1)}}^2 \\
&+2u^{(1)}u^{(3)} + ({T^{(2)}}^2 - T^{(4)})c^2) + \frac{\partial T^{(2)}}{\partial y}(({T^{(2)}}^2 - T^{(4)}){u^{(1)}}^2 - 2T^{(2)}u^{(1)}u^{(3)} + {u^{(3)}}^2 \\
&+2u^{(1)}u^{(5)} - ({T^{(2)}}^3 - 2T^{(2)}T^{(4)} + T^{(6)})c^2))c_y) + \Phi^{(9)}(2c_x + 2\frac{\partial u^{(1)}}{\partial y}c_yc_x) \\
&+\Phi^{(7)}(-2T^{(2)}c_x - 2\frac{\partial T^{(2)}}{\partial y}u^{(1)}c_yc_x - 2T^{(2)}\frac{\partial u^{(1)}}{\partial y}c_yc_x + 2\frac{\partial u^{(3)}}{\partial y}c_yc_x) \\
&+\Phi^{(5)}(2({T^{(2)}}^2 - T^{(4)})c_x + 2({T^{(2)}}^2 - T^{(4)})\frac{\partial u^{(1)}}{\partial y}c_yc_x - 2(-T^{(2)}\frac{\partial T^{(2)}}{\partial y}u^{(1)} + (T_y^{42})u^{(1)} + \frac{\partial T^{(2)}}{\partial y}u^{(3)})c_yc_x \\
&-2T^{(2)}\frac{\partial u^{(3)}}{\partial y}c_yc_x + 2\frac{\partial u^{(5)}}{\partial y}c_yc_x) + \Phi^{(3)}(-2({T^{(2)}}^3 - 2T^{(2)}T^{(4)} + T^{(6)})c_x(1 + \frac{\partial u^{(1)}}{\partial y}c_y) \\
&+2({T^{(2)}}^2 - T^{(4)})\frac{\partial u^{(3)}}{\partial y}c_yc_x - 2({T^{(2)}}^2\frac{\partial T^{(2)}}{\partial y}u^{(1)} + (T_y^{642})u^{(1)} + (T_y^{42})u^{(3)} - T^{(2)}((T_y^{42})u^{(1)} \\
&+\frac{\partial T^{(2)}}{\partial y}u^{(3)}) + \frac{\partial T^{(2)}}{\partial y}(-T^{(4)}u^{(1)} + u^{(5)}))c_yc_x - 2T^{(2)}\frac{\partial u^{(5)}}{\partial y}c_yc_x + 2\frac{\partial u^{(7)}}{\partial y}c_yc_x) \\
&+\Phi^{(1)}(2({T^{(2)}}^4 - 3{T^{(2)}}^2T^{(4)} + {T^{(4)}}^2 + 2T^{(2)}T^{(6)} - T^{(8)})c_x(1 + \frac{\partial u^{(1)}}{\partial y}c_y) \\
&-2({T^{(2)}}^3 - 2T^{(2)}T^{(4)} + T^{(6)})\frac{\partial u^{(3)}}{\partial y}c_yc_x + 2({T^{(2)}}^2 - T^{(4)})\frac{\partial u^{(5)}}{\partial y}c_yc_x + 2({T^{(2)}}^3\frac{\partial T^{(2)}}{\partial y}u^{(1)} + T^{(4)}(T_y^{42})u^{(1)} \\
&+\frac{\partial T^{(2)}}{\partial y}T^{(6)}u^{(1)} - (T_y^{8642})u^{(1)} + \frac{\partial T^{(2)}}{\partial y}T^{(4)}u^{(3)} - (T_y^{642})u^{(3)} - {T^{(2)}}^2((T_y^{42})u^{(1)} + \frac{\partial T^{(2)}}{\partial y}u^{(3)}) \\
&-(T_y^{42})u^{(5)} + T^{(2)}((T_y^{642})u^{(1)} + (T_y^{42})u^{(3)} + \frac{\partial T^{(2)}}{\partial y}(-2T^{(4)}u^{(1)} + u^{(5)})) - \frac{\partial T^{(2)}}{\partial y}u^{(7)})c_yc_x \\
&-2T^{(2)}\frac{\partial u^{(7)}}{\partial y}c_yc_x + 2\frac{\partial u^{(9)}}{\partial y}c_yc_x)\Big),
\end{aligned}
\tag{B.15}
$$

where

$$
p_y^{108642} = \frac{\partial}{\partial y}\left(p^{(10)} + \frac{{p^{(2)}}^5}{5} - {p^{(2)}}^3p^{(4)} + p^{(2)}{p^{(4)}}^2 + {p^{(2)}}^2p^{(6)} - p^{(4)}p^{(6)} - p^{(2)}p^{(8)}\right), \tag{B.16}
$$

$$
T_y^{108642} = \frac{\partial}{\partial y}\left(T^{(10)} + \frac{{T^{(2)}}^5}{5} - {T^{(2)}}^3T^{(4)} + T^{(2)}{T^{(4)}}^2 + {T^{(2)}}^2T^{(6)} - T^{(4)}T^{(6)} - T^{(2)}T^{(8)}\right). \tag{B.17}
$$

B.3 Solutions of Boltzmann equation at fourth and higher orders

Here, we list the explicit expressions of the solutions of Boltzmann equation at 4th order and beyond.

1. The solution of Boltzmann equation at 4th order ($\Phi^{(4)}$) is

$$
\begin{aligned}
\Phi^{(4)}(y,\boldsymbol{c}) \quad = \quad & \frac{1}{196875}2(141120000c_y^{12} - 141120000c_y^{11}y - 336000c_y^9 y(3 + 840c_z^2 - 5460c_x^2 + 70y^2) \\
& +1008000c_y^{10}(1 + 280c_z^2 - 1820c_x^2 + 70y^2) - 3360c_y^7 y(-301251 + 42000c_z^4 + 199500c_x^4 \\
& +620y^2 + 300y^4 + c_x^2(760950 - 68500y^2) - 2800c_z^2(6 + 195c_x^2 - 5y^2)) + 3360c_y^8(-312501 \\
& +42000c_z^4 + 199500c_x^4 + 720y^2 + 1700y^4 - 8400c_z^2(2 + 65c_x^2 - 5y^2) - 150c_x^2(-5223 + 1670y^2)) \\
& +875(1350 + 1800c_x^4 + 98946y^2 + 963y^4 + 44y^6 + 12c_x^2(-450 - 249y^2 + 10y^4)) \\
& +2c_y y(63000c_x^4(43 + 10y^2) + 4c_x^2(1659513681 + 35547540y^2 + 550305y^4 + 8350y^6) \\
& +5(-2785657392 - 29204490y^2 - 30975y^4 + 15850y^6) + 4c_z^2(1574778681 + 34106415y^2 + 356055y^4 \\
& +8350y^6 + 15750c_x^2(-57 + 10y^2))) - 1680c_y^5 y(-905076 - 94035y^2 + 30y^4 - 100c_x^4(1827 + 10y^2) \\
& +200c_z^4(-171 + 70y^2) + c_x^2(798846 + 219030y^2 - 1800y^4) - 2c_z^2(141627 + 1660y^2 - 600y^4 \\
& +50c_x^2(-4581 + 1370y^2))) + 560c_y^6(-2692953 - 872127y^2 + 1320y^4 + 200y^6 + 1800c_z^4(-57 + 70y^2) \\
& +1800c_x^4(-417 + 220y^2) + c_x^2(2655738 + 2151990y^2 - 69600y^4) - 6c_z^2(152877 + 7260y^2 - 3400y^4 \\
& +150c_x^2(-1677 + 1670y^2))) + 8c_y^3 y(1347378606 + 32300415y^2 + 938805y^4 + 8350y^6 \\
& -1260c_z^4(1083 - 760y^2 + 100y^4) + 1260c_x^4(-5933 - 1090y^2 + 400y^4) \\
& -210c_x^2(1312299 + 67565y^2 + 10305y^4) + 1260c_z^2(159646 + 6985y^2 - 5y^4 + 2c_x^2(5867 - 2665y^2 \\
& +150y^4))) + 56c_y^4(-191615283 - 13719915y^2 - 681675y^4 - 2600y^6 - 480c_x^4(-4203 + 2085y^2 \\
& +725y^4) + 60c_z^4(3249 - 7980y^2 + 1700y^4) + 10c_x^2(3620997 + 924021y^2 + 151290y^4 + 400y^6) \\
& -40c_z^2(709182 + 99126y^2 + 240y^4 - 100y^6 + 3c_x^2(23751 - 43920y^2 + 5800y^4))) \\
& +14c_y^2(80c_z^4 y^2(57 - 10y^2)^2 + 15(133439652 + 4238880y^2 + 14125y^4 - 4200y^6) \\
& +80c_x^4(-15300 + 4599y^2 + 3360y^4 + 100y^6) + 4c_x^2(-242679258 + 8694585y^2 + 188700y^4 \\
& +45400y^6) + 4c_z^2(-225032508 - 14545665y^2 - 286050y^4 - 2600y^6 \\
& +20c_x^2(12825 - 25902y^2 + 2220y^4 + 200y^6)))). \qquad \text{(B.18)}
\end{aligned}
$$

2. The solution of Boltzmann equation at 5th order ($\Phi^{(5)}$) is

$$
\begin{aligned}
\Phi^{(5)}(y,\boldsymbol{c}) \quad = \quad & -\frac{1}{1771875}4c_x(-114307200000c_y^{14}+114307200000c_y^{13}y+36288000c_y^{11}y(-6283+6300c_z^2 \\
& -9450c_x^2+490y^2)-72576000c_y^{12}(-3159+3150c_z^2-4725c_x^2+770y^2)-1814400c_y^{10}(-419221 \\
& +63000c_z^4-15750c_x^4-62200y^2+2250y^4+c_x^2(568530-85400y^2)-20c_z^2(7431+9450c_x^2-3080y^2)) \\
& +1209600c_y^9y(-615174+94500c_z^4-23625c_x^4-30645y^2+575y^4+c_x^2(839145-33600y^2) \\
& -30c_z^2(7361+9450c_x^2-980y^2))+9(5906250+1575000c_x^4+5312485962y^2+48442065y^4 \\
& +260470y^6+4175y^8+31500c_x^2(-250-137y^2+5y^4))+4c_yy(-12500204674419 \\
& -121967313678y^2+568343034y^4+14949450y^6+221800y^8+94500c_x^4(147+40y^2) \\
& +36c_x^2(1638022806+34718355y^2+454755y^4+10100y^6)+36c_z^2(1575227556+34350855y^2 \\
& +289380y^4+10100y^6+10500c_x^2(-57+10y^2)))+30240c_y^7y(-3415821-3644782y^2 \\
& -60780y^4+200y^6+117600c_z^4(-11+5y^2)-4200c_x^4(38+85y^2)-40c_x^2(5931-116070y^2+350y^4) \\
& -20c_z^2(438537+69660y^2-2300y^4+420c_x^2(-577+160y^2)))-60480c_y^8(-1159935-5869611y^2 \\
& -151225y^4+1400y^6+4200c_z^4(-159+220y^2)-1050c_x^4(171+320y^2)-15c_x^2(20723 \\
& -523930y^2+7000y^4)-30c_z^2(154999+72060y^2-4500y^4+280c_x^2(-321+305y^2))) \\
& +432c_y^5y(-1420698447-27637610y^2-9987565y^4-114400y^6-2800c_x^4(-3483 \\
& -2640y^2+550y^4)+700c_z^4(20007-16740y^2+2300y^4)+140c_x^2(-169311-142982y^2 \\
& +74995y^4+200y^6)-70c_z^2(15530997+1179514y^2+64260y^4-400y^6+20c_x^2(42093 \\
& -19410y^2+700y^4)))-1008c_y^6(-582127308-51755445y^2-24721950y^4-316900y^6 \\
& -1800c_x^4(-4407-1990y^2+2000y^4)+900c_z^4(7239-19720y^2+4500y^4) \\
& +30c_x^2(-1031445-350259y^2+965925y^4+1600y^6)-60c_z^2(7563285+1999317y^2 \\
& +166875y^4-2800y^6+15c_x^2(36447-63010y^2+7000y^4)))+72c_y^3y(5(677588877+274559964y^2 \\
& +6498681y^4-140590y^6)+840c_z^4(-6498+7809y^2-1740y^4+100y^6)+840c_x^4(-12498-5541y^2 \\
& +1260y^4+100y^6)+12c_x^2(-1638638946-38494155y^2-1198820y^4+26800y^6) \\
& +12c_z^2(-1475686821-75294905y^2-1330070y^4-57200y^6+140c_x^2(18627-8241y^2 \\
& -240y^4+100y^6)))+18c_y^2(2798629443666+27408005604y^2-1062123405y^4-20860630y^6 \\
& +155825y^8+1680c_z^4y^2(57-10y^2)^2+840c_x^4(-13875+2298y^2+3720y^4+200y^6) \\
& +4c_x^2(-4970516418+6362578089y^2+158718315y^4+2638860y^6+78200y^8) \\
& +4c_z^2(-4727478168+5862499839y^2+151378815y^4+1552110y^6+78200y^8 \\
& +420c_x^2(7125-14352y^2+720y^4+200y^6)))-72c_y^4(4982721156-1538058879y^2+18852435y^4 \\
& -7970410y^6-78200y^8-14c_x^2(1420635213+31470615y^2+3606375y^4-515600y^6) \\
& -1680c_x^4(14655-597y^2-7250y^4+300y^6)+420c_z^4(-16245+78888y^2-31300y^4+2800y^6) \\
& +28c_z^2(-626057919-111120120y^2-3738000y^4-159950y^6 \\
& +30c_x^2(61005-128112y^2+17600y^4+800y^6)))). \qquad \text{(B.19)}
\end{aligned}
$$

3. The solution of Boltzmann equation at 6th order ($\Phi^{(6)}$) is

$$
\begin{aligned}
\Phi^{(6)}(y,\boldsymbol{c}) \;=\; & \frac{1}{2436328125}2(-1844156160000000c_y^{18}+77962500000c_x^6+1844156160000000c_y^{17}y\\
&+3991680000000c_y^{15}y(-1278+1386c_z^2-9009c_x^2+77y^2)-11975040000000c_y^{16}(-426\\
&+462c_z^2-3003c_x^2+77y^2)+519750000c_x^4(-1125-573y^2+20y^4)+49500c_x^2(17718750\\
&+10544205924y^2+97721085y^4+369040y^6+10100y^8)+9625(-15187500\\
&-7051731599124y^2-35914554522y^4+63685566y^6+1294425y^8+15920y^{10})\\
&-1330560000c_y^{14}(-22739949+4158000c_z^4+19750500c_x^4-1913010y^2+57400y^4\\
&-2700c_z^2(2973+20020c_x^2-770y^2)-16200c_x^2(-7317+805y^2))+1330560000c_y^{13}y(-22503699\\
&+4158000c_z^4+19750500c_x^4-635010y^2+11200y^4-900c_z^2(8919+60060c_x^2-770y^2)\\
&-900c_x^2(-131181+4480y^2))+22176000c_y^{11}y(384194547+83160000c_z^6+550935000c_x^6\\
&-220616880y^2-1905600y^4+13000y^6-108000c_z^4(2529+15015c_x^2-385y^2)\\
&+27000c_x^4(-274446+4165y^2)-90c_x^2(-60998847-12352880y^2+96600y^4)\\
&+180c_z^2(-9247749+6583500c_x^4-441960y^2+11200y^4-300c_x^2(-141219+8960y^2)))\\
&-66528000c_y^{12}(137541849+27720000c_z^6+183645000c_x^6-222747420y^2-3163900y^4+35000y^6\\
&-108000c_z^4(843+5005c_x^2-385y^2)+27000c_x^4(-92532+6265y^2)-90c_x^2(-20594849-12844360y^2\\
&+197400y^4)+60c_z^2(-9405249+6583500c_x^4-1333860y^2+57400y^4-900c_x^2(-47423+9660y^2)))\\
&+211200c_y^9y(64881613440+5556059649y^2-1124215785y^4-5185200y^6+7000y^8\\
&+13230000c_z^6(-171+110y^2)+3307500c_x^6(-5499+2690y^2)-9450c_x^4(-26166357+10632095y^2\\
&+23100y^4)-630c_x^2(981965589-119171155y^2-8067200y^4+13500y^6)-37800c_z^4(865677\\
&+124455y^2-5600y^4+2100c_x^2(-717+320y^2))+1260c_z^2(-9917682-22390810y^2-328525y^4\\
&+3250y^6+55125c_x^4(-1017+170y^2)-15c_x^2(-10691637-6555980y^2+96600y^4)))\\
&-13305600c_y^{10}(1187074755+293629488y^2-90875300y^4-541850y^6+2000y^8+630000c_z^6(-57+110y^2)\\
&+630000c_x^6(-477+710y^2)+450c_x^4(9735294-12624565y^2+33600y^4)-30c_x^2(359122263\\
&-140451030y^2-14563200y^4+57500y^6)-600c_z^4(905052+377355y^2-28700y^4\\
&+3150c_x^2(-503+690y^2))+20c_z^2(-7131057-68221455y^2-1646075y^4+26250y^6\\
&+23625c_x^4(-2673+1790y^2)-45c_x^2(-3676279-6873960y^2+197400y^4)))\\
&+2c_yy(5197500000c_x^6(33+10y^2)+594000c_x^4(1630696431+34268920y^2+387205y^4+11850y^6)\\
&+4c_x^2(-10220190022113591366-1223258101590363 30y^2-403381781295570y^4-11269976850y^6\\
&+7123782875y^8+57434750y^{10})+5(19047251759486773284+202384768450164300y^2\\
&+576537292755270y^4+909573276150y^6+7405220625y^8+127424750y^{10})\\
&+4c_z^2(-10151461302474396366-1217785294007043 30y^2-407691633794445y^4-91556873100y^6\\
&+5523351625y^8+57434750y^{10}+1299375000c_x^4(-57+10y^2)+445500c_x^2(525275352+11523015y^2\\
&+74235y^4+3950y^6)))+31680c_y^7y(-10078037877411+66291805650y^2+1870910685y^4\\
&-162034550y^6-607500y^8+588000c_z^6(3249-3990y^2+800y^4)+294000c_x^6(34713-63255y^2\\
&+6100y^4)-2100c_x^4(-349797792-101312725y^2+7346475y^4+42000y^6)+10c_x^2(-244174086135\\
&-59174059077y^2+1106863905y^4+62477850y^6+14000y^8)-2100c_z^4(119542683+15905150y^2\\
&+722600y^4-13000y^6+420c_x^2(64347-54220y^2+6900y^4))-20c_z^2(50143579605+1162914501y^2\\
&+450248610y^4+3496700y^6-7000y^8+44100c_x^4(-113808+39205y^2+1650y^4)\\
&+210c_x^2(-439400367-40659100y^2-8345150y^4+27000y^6)))-31680c_y^8(-10071948218661\\
&+199076335290y^2+8629240200y^4-1207996650y^6-4826000y^8+588000c_z^6(3249-12540y^2\\
&+4100y^4)+147000c_x^6(56601-402960y^2+88400y^4)-2100c_x^4(-350487942-346932495y^2\\
&+59579900y^4+270000y^6)-210c_x^2(11662020810+9013279947y^2-448243850y^4-24189900y^6\\
&+8000y^8)-2100c_z^4(117873183+49716030y^2+3676900y^4-105000y^6+1260c_x^2(24099-64540y^2\\
&+14100y^4))+420c_z^2(-2329664880-131054661y^2-110010050y^4-1110300y^6+6000y^8\\
&+75600c_x^4(4053-5630y^2+200y^4)-60c_x^2(-69610657-24180695y^2-7642350y^4+57500y^6)))
\end{aligned}
$$

$$
\begin{aligned}
&+2640c_y^6(1941104325318228 + 61011142987284y^2 - 230900398785y^4 - 5180001330y^6\\
&+214987800y^8 + 668000y^{10} - 50400c_x^6(475497 + 1526385y^2 - 879000y^4 + 17500y^6)\\
&-25200c_z^6(-61731 + 422370y^2 - 256500y^4 + 35000y^6) + 2520c_x^4(-14257592955 - 1824421278y^2\\
&-217220000y^4 + 4676600y^6 + 28000y^8) - 6c_x^2(-9261559840554 - 2796114852090y^2\\
&-287327766075y^4 + 646251900y^6 + 120496000y^8) + 7560c_z^4(660127590 + 202780699y^2 + 12684300y^4\\
&+396700y^6 - 4000y^8 + 20c_x^2(-452922 + 1817915y^2 - 721500y^4 + 57500y^6)) + 24c_z^2(5772933417951\\
&+242288105535y^2 + 3199222425y^4 + 717260775y^6 + 4826000y^8 + 3150c_x^4(2694081 - 5115970y^2 + 370000y^4\\
&+90000y^6) + 105c_x^2(-9512166435 - 4155216681y^2 - 155167100y^4 - 24608300y^6 + 16000y^8)))\\
&+880c_y^5y(-5825146676974884 - 62003466454230y^2 + 195900595065y^4 + 3693688200y^6 - 53730250y^8\\
&-100800c_x^6(-217458 - 775935y^2 + 130650y^4 + 8000y^6) + 25200c_z^6(-185193 + 357390y^2 - 131100y^4 + 13000y^6)\\
&+360c_x^4(300298011930 + 14198855223y^2 + 746625705y^4 + 6949850y^6 + 14000y^8) + 18c_x^2(-9074060541504\\
&-1181614758450y^2 - 58200736335y^4 - 394038950y^6 + 6795000y^8) - 360c_z^4(41531031045 + 4341821127y^2\\
&+150565170y^4 + 3616400y^6 - 14000y^8 + 630c_x^2(-724869 + 846970y^2 - 185300y^4 + 9000y^6))\\
&-36c_z^2(11585574082152 + 146078273250y^2 + 968866605y^4 + 188128850y^6 + 1215000y^8\\
&+12600c_x^4(891453 - 385340y^2 - 33400y^4 + 7000y^6) - 10c_x^2(206835884010 + 23973955971y^2 + 416116785y^4\\
&+62658450y^6 + 28000y^8))) + 8c_y^3y(-8632861264899861066 - 106733410395942330y^2 - 350174446509195y^4\\
&+563993159400y^6 + 10146411000y^8 + 57434750y^{10} + 184800c_z^6y^2(-57 + 10y^2)^3 + 92400c_x^6(-7225875\\
&-5254686y^2 + 842940y^4 + 145800y^6 + 2000y^8) + 11880c_x^4(-260856585822 + 49697279625y^2 + 1385514445y^4\\
&+19070650y^6 + 1335000y^8) - 110c_x^2(2932262303107284 + 161829826773330y^2 + 774767287035y^4\\
&+17579301300y^6 + 323165875y^8) + 3960c_z^4(140c_x^2(-1218375 + 1644507y^2 - 357030y^4 + 12900y^6 + 1000y^8)\\
&-3(-59852961378 + 18411690675y^2 + 640478055y^4 + 8698100y^6 + 202500y^8)) + 220c_z^2(2520c_x^4(4960125\\
&-1982043y^2 - 249030y^4 + 42900y^6 + 1000y^8) + 108c_x^2(-90296796597 + 11650781975y^2 + 351190070y^4\\
&-3651225y^6 + 566250y^8) - 7(475094403467856 + 5177977478820y^2 + 4851313290y^4 - 175776300y^6\\
&+3837875y^8))) + 88c_y^4(784816780658952006 + 29128500114559020y^2 + 156402688848525y^4\\
&-327693132900y^6 - 5778891000y^8 + 25024000y^{10} - 302400c_z^6y^2(57 - 10y^2)^2(-19 + 10y^2)\\
&+75600c_x^6(2268375 + 1118424y^2 - 1741800y^4 - 24800y^6 + 16000y^8) - 360c_x^4(-1030411532241\\
&+1145555496540y^2 + 35860622700y^4 + 910432600y^6 + 31474000y^8) + 30c_x^2(972198358608078\\
&+22757976671598y^2 + 1978813086705y^4 + 57607835040y^6 + 673637100y^8 + 1336000y^{10})\\
&+360c_z^4(-179601527259 + 193547629485y^2 + 10736991300y^4 + 226524900y^6 + 4826000y^8\\
&+210c_x^2(1218375 - 7125228y^2 + 3487500y^4 - 418400y^6 + 8000y^8)) + 120c_z^2(553948123638357\\
&+17651291757687y^2 + 83498911020y^4 - 109201365y^6 + 59653650y^8 + 334000y^{10} + 2520c_x^4(-1589250\\
&+3358443y^2 - 212550y^4 - 124100y^6 + 7000y^8) - 6c_x^2(-380930939991 + 386839738215y^2 + 19397840700y^4\\
&+130772600y^6 + 30124000y^8))) + 22c_y^2(15120000c_x^6(-4500 + 249y^2 + 1360y^4 + 100y^6)\\
&+240c_x^4(-739149100200 + 1058756447007y^2 + 90667142370y^4 + 1751292060y^6 + 30983400y^8 + 334000y^{10})\\
&-5(1732827725021174544 + 55223110494502020y^2 + 270076108869000y^4 + 660979534950y^6 + 5892010875y^8\\
&+62141000y^{10}) + 4c_x^2(932290192938454056 + 20970335514557520y^2 + 59468393276775y^4 + 778241658600y^6\\
&+14205879000y^8 + 408104000y^{10}) + 480c_z^4y^2(-57 + 10y^2)(3149557362 + 68362455y^2 + 685860y^4 + 16700y^6\\
&+31500c_x^2(-57 + 10y^2)) + 4c_z^2(922870755232641306 + 33253494806797020y^2 + 182857241632275y^4\\
&+99355753350y^6 - 3488616000y^8 + 25024000y^{10} + 945000c_x^4(21375 - 42258y^2 + 880y^4 + 800y^6)\\
&+120c_x^2(-354729190725 + 312132302307y^2 + 72600947370y^4\\
&+1432764060y^6 + 21398400y^8 + 334000y^{10})))).
\end{aligned}
\tag{B.20}
$$

4. The solution of Boltzmann equation at 7th order ($\Phi^{(7)}$) is

$$
\begin{aligned}
\Phi^{(7)}(y,\boldsymbol{c}) \quad = \quad & -\frac{1}{95016796875}8c_x(6544910211840000000c_y^{20} - 654491021184000000c_y^{19}y \\
& +107883135360000000c_y^{18}(-3559 + 1820c_z^2 - 2730c_x^2 + 300y^2) \\
& -11987015040000000c_y^{17}y(-32001 + 16380c_z^2 - 24570c_x^2 + 880y^2) \\
& +7783776000000c_y^{16}(-82185129 + 25225200c_z^4 - 6306300c_x^4 - 24477900y^2 \\
& +326200y^4 - 9240c_z^2(10913 + 8190c_x^2 - 1350y^2) - 18480c_x^2(-15446 + 975y^2)) \\
& -2335132800000c_y^{15}y(-27137343 + 8408400c_z^4 - 2102100c_x^4 - 2686140y^2 \\
& +20440y^4 - 6160c_z^2(5449 + 4095c_x^2 - 220y^2) - 1540c_x^2(-61589 + 1170y^2)) \\
& +13(-1534886718750 + 116943750000c_x^6 - 402796155200847449 58y^2 \\
& -237107581028158995y^4 - 477200687881995y^6 + 27833733675y^8 \\
& +3575874225y^{10} + 28717375y^{12} + 3898125000c_x^4(-315 - 147y^2 + 5y^4) \\
& +74250c_x^2(41343750 + 15784289136y^2 + 148600935y^4 + 364210y^6 + 17775y^8)) \\
& -2594592000c_y^{13}y(64601136777 + 2522520000c_z^6 + 1846845000c_x^6 - 3780016080y^2 \\
& -115590200y^4 + 336000y^6 - 1386000c_z^4(11591 + 8190c_x^2 - 880y^2) \\
& -346500c_x^4(48089 + 1480y^2) - 750c_x^2(65315379 - 17265544y^2 + 68376y^4) \\
& -1500c_z^2(20409579 + 1261260c_x^4 + 3286648y^2 - 36792y^4 + 924c_x^2(-64613 + 2340y^2))) \\
& +7783776000c_y^{14}(22004630089 + 840840000c_z^6 + 615615000c_x^6 - 3959649960y^2 \\
& -197707700y^4 + 924000y^6 - 462000c_z^4(11621 + 8190c_x^2 - 2700y^2) \\
& -115500c_x^4(48659 + 3300y^2) - 750c_x^2(22123057 - 18379336y^2 + 150920y^4) \\
& -1500c_z^2(6905475 + 420420c_x^4 + 3331732y^2 - 65240y^4 + 308c_x^2(-65003 + 7800y^2))) \\
& -144144000c_y^{11}y(394303136517 + 184085732574y^2 - 2851682940y^4 - 45798000y^6 \\
& +40000y^8 + 182952000c_z^6(-63 + 40y^2) + 45738000c_x^6(-387 + 85y^2) \\
& -2700c_x^4(-113019939 + 9919790y^2 + 270480y^4) - 36c_x^2(32547014562 + 4389898845y^2 \\
& -255124200y^4 + 161000y^6) - 21600c_z^4(5094927 + 2172805y^2 - 45990y^4 \\
& +20790c_x^2(-168 + 65y^2)) - 108c_z^2(-3766634171 + 782715240y^2 + 39131600y^4 \\
& -168000y^6 + 115500c_x^4(1197 + 740y^2) + 100c_x^2(6987213 - 22433480y^2 + 170940y^4))) \\
& +864864000c_y^{12}(68291181261 + 94552282116y^2 - 2642475180y^4 - 55857700y^6 + 96000y^8 \\
& +16632000c_z^6(-118 + 225y^2) + 1039500c_x^6(-3103 + 2400y^2) - 1350c_x^4(-41061423 \\
& +15544790y^2 + 376600y^4) - 3c_x^2(68519161329 + 24992099640y^2 - 2935625700y^4 \\
& +5404000y^6) - 10800c_z^4(1760739 + 2209855y^2 - 81550y^4 + 1155c_x^2(-1073 + 1300y^2)) \\
& -36c_z^2(-2013531958 + 1234765095y^2 + 100627650y^4 - 693000y^6 + 346500c_x^4(247 + 275y^2) \\
& +300c_x^2(1410483 - 12003265y^2 + 188650y^4))) + 2c_y y(5732098174652792635733 04 \\
& +456383392271140815280 8y^2 + 2758079087789775750y^4 - 33628021624222740y^6 \\
& -120103207116 75y^8 + 786623336850y^{10} + 6431396000y^{12} + 60810750000c_x^6(61 + 20y^2) \\
& +7722000c_x^4(3253751487 + 67789470y^2 + 653310y^4 + 27200y^6) \\
& +156c_x^2(-10203195720306714741 - 122233035486800700y^2 - 394618709185470y^4 \\
& +80120007000y^6 + 7466329750y^8 + 78101000y^{10}) + 156c_z^2(-10151578307559054366 \\
& -121914403269050700y^2 - 398772819636345y^4 + 23165678250y^6 + 5948123500y^8 \\
& +78101000y^{10} + 779625000c_x^4(-57 + 10y^2) + 99000c_x^2(1576574181 + 34760985y^2 \\
& +156030y^4 + 13600y^6))) - 2059200c_y^9 y(-159342001410249 + 4290147440208y^2 \\
& +613467830430y^4 - 3044108400y^6 - 37996000y^8 + 1323000c_x^6(165843 - 100300y^2 + 720y^4) \\
& +5292000c_z^6(18297 - 22600y^2 + 4380y^4) - 5040c_x^4(-990926469 - 491189940y^2 \\
& -10890975y^4 + 203000y^6) + 210c_x^2(-189080847999 - 53306710560y^2 - 3071539950y^4 \\
& +45371600y^6 + 20000y^8) - 22680c_z^4(292144143 + 50352680y^2 + 6822700y^4 - 56000y^6 \\
& +350c_x^2(106401 - 81100y^2 + 8140y^4)) - 840c_z^2(7570820871 - 4894820535y^2 + 293994075y^4 \\
& +7698100y^6 - 10000y^8 + 9450c_x^4(-63729 - 4450y^2 + 6440y^4) + 3c_x^2(-3247845651 \\
& +343580490y^2 - 261239400y^4 + 322000y^6))) + 2059200c_y^{10}(-160849054983519
\end{aligned}
$$

$$
\begin{aligned}
&+13281635470950y^2+3135935430684y^4-28180640460y^6-377057700y^8+112000y^{10}\\
&+10584000c_z^6(9576-36435y^2+11650y^4)+1323000c_x^6(194463-396780y^2+30200y^4)\\
&-1260c_x^4(-3435464646-7316061885y^2+88721175y^4+6944000y^6)+210c_x^2(-177359588505\\
&-179435419488y^2-14171753640y^4+419553200y^6+36000y^8)-22680c_z^4(283845803+161295930y^2\\
&+35316350y^4-462000y^6+350c_x^2(121491-294960y^2+53900y^4))-840c_z^2(7053130035-15789726153y^2\\
&+1636889385y^4+56554450y^6-144000y^8+4725c_x^4(-167553+63930y^2+53800y^4)+42c_x^2(-211150989\\
&+69645285y^2-108251925y^4+386000y^6)))+617760c_y^8(-3979243279659060-254654996292522y^2\\
&+3497076969015y^4+336990774470y^6-725053775y^8-10386000y^{10}+705600c_z^6(-34656+207765y^2\\
&-126700y^4+16500y^6)-29400c_x^6(2109969-10044360y^2+2290800y^4+124000y^6)-700c_x^4(-46978961634\\
&-12439967553y^2-2173917675y^4-97333600y^6+324000y^8)+10c_x^2(-37915634941821-6723862337745y^2\\
&-805698804141y^4-38568325110y^6+257509800y^8+112000y^{10})-700c_z^4(29399943951+15859424322y^2\\
&+1250982600y^4+117289400y^6-576000y^8+84c_x^2(-5411709+19353960y^2-6816300y^4+386000y^6))\\
&-20c_z^2(33572989257948+471818541285y^2-160652442867y^4+5814149180y^6+126215100y^8-56000y^{10}\\
&+5880c_x^4(3414483-4243770y^2-1064400y^4+248000y^6)-70c_x^2(-703075221+9039233178y^2-586320900y^4\\
&+212715100y^6+36000y^8)))+205920c_y^7y(-352800c_z^6(-191691+354540y^2-128900y^4+12000y^6)\\
&+50400c_x^6(3197187-4253655y^2+235550y^4+57250y^6)-4200c_x^4(23997383415+1994117298y^2\\
&+140000670y^4+9463850y^6)+10c_x^2(114923226943413+6533016532686y^2+400981091490y^4\\
&+17393721900y^6-36152000y^8)+3(3986866203507621+78383042289342y^2-689839192245y^4\\
&-48294530830y^6+1765300y^8+558000y^{10})+16800c_z^4(3707808660+647802513y^2+27981120y^4\\
&+1973350y^6-5000y^8+21c_x^2(-2163627+2339505y^2-436800y^4+11500y^6))+40c_z^2(8820c_x^4(2320173\\
&-444870y^2-307050y^4+29000y^6)-105c_x^2(366072525+2185774746y^2-135195060y^4+22769200y^6\\
&+20000y^8)+4(12641108118093+39351480021y^2-11625301485y^4+236723400y^6+4753000y^8)))\\
&+156c_y^3y(739200c_z^6y^2(-57+10y^2)^3+184800c_x^6(-4357125-4584897y^2+524880y^4+156600y^6+4000y^8)\\
&+11880c_x^4(-556482298113+91714855414y^2+23892875160y^4+518078140y^6+9427600y^8+186000y^{10})\\
&+4c_x^2(30029357134282559823+651040265005071480y^2+2778201026931330y^4+653972200200y^6\\
&-69631628000y^8+2569494000y^{10})-5(-11249339069248500528+1065345605210901168y^2\\
&+8282541873612006y^4+15057515849310y^6+12793911625y^8+3345086400y^{10})+15840c_z^4(70c_x^2(-1218375\\
&+1702989y^2-345060y^4+3300y^6+2000y^8)+3(59867175753-48024399759y^2+3852565290y^4\\
&+107575785y^6+731900y^8+46500y^{10}))+8c_z^2(14809765817579052474+373540703773496490y^2\\
&+19201596061066665y^4-2448084545775y^6-100946122750y^8-960738000y^{10}+69300c_x^4(7923375\\
&-2797272y^2-645120y^4+81600y^6+4000y^8)+8910c_x^2(-46069453871-20151452062y^2+6540897720y^4\\
&+150334380y^6+2059200y^8+62000y^{10})))+3432c_y^6(-3577188270578865516-329229366317906040y^2\\
&-3087364292867925y^4+20029616482050y^6+1097777017125y^8+1774736500y^{10}-378000c_x^6(768033\\
&+10807434y^2-4836360y^4-325000y^6+56000y^8)+378000c_z^6(432117-4438134y^2+3874860y^4-929000y^6\\
&+64000y^8)+3600c_x^4(-783150790464+6685334428 50y^2+29170334067y^4+790981170y^6+88562400y^8\\
&+56000y^{10})-90c_x^2(8267690939287500+374297416121538y^2+9759203558265y^4+342920762870y^6\\
&+14589272975y^8+7984000y^{10})+1800c_z^4(824734026522-966183471225y^2-85327406241y^4\\
&-2225526660y^6-127802700y^8+112000y^{10}+630c_x^2(-3039183+14228766y^2-6742140y^4+653000y^6\\
&+4000y^8))-180c_z^2(5636703737448000+328696146672894y^2+102726439095y^4-104776589190y^6\\
&+924772675y^8+20772000y^{10}+6300c_x^4(-6404517+11519334y^2+1171640y^4-896000y^6+36000y^8)\\
&-10c_x^2(-502410498156-107105460525y^2+30712205643y^4-3527258070y^6+256434600y^8+224000y^{10})))\\
&+26c_y^2(-44297552321992743603984-5095288934552315559 06y^2+4690371669970625100y^4\\
&+32560227869438115y^6+38047359168225y^8-166009637475y^{10}+6154778875y^{12}\\
&+103950000c_x^6(-13545-504y^2+4440y^4+400y^6)+11880c_x^4(-408787107750+583133231457y^2\\
&+78789545835y^4+1553284810y^6+24110400y^8+369000y^{10})+2c_x^2(91987677719246064294\\
&-11933293323678798733 32y^2-150178814057578955y^4-5088865178094390y^6+7609074608025y^8\\
&+220227800100y^{10}+2723249000y^{12})+23760c_z^4y^2(-57+10y^2)(3150155862+68580645y^2+619185y^4\\
&+18450y^6+17500c_x^2(-57+10y^2))+2c_z^2(91365609495626760294-11811065701983777583 2y^2
\end{aligned}
$$

$$
\begin{aligned}
&-14907068658257287 05y^4 - 5169188871679140y^6 + 5965501481775y^8 + 176383298850y^{10} + 2723249000y^{12} \\
&+51975000c_x^4(17955 - 34758y^2 - 120y^4 + 800y^6) + 11880c_x^2(-197183991375 + 91063676907y^2 + 66927680085y^4 \\
&+1375311560y^6 + 17195400y^8 + 369000y^{10}))) + 624c_y^5y(19830092122901439918 + 493713221343706980y^2 \\
&+2711277847129005y^4 - 13297414959675y^6 - 657398780500y^8 - 1921476000y^{10} + 231000c_x^6(-1646649 \\
&+23415408y^2 - 2371680y^4 - 712800y^6 + 20000y^8) - 462000c_z^6(1666737 - 4698054y^2 + 2349540y^4 - 390600y^6 \\
&+20000y^8) - 3300c_x^4(-3802473765279 + 620225032014y^2 + 19154760660y^4 + 38475600y^6 + 48892000y^8) \\
&+330c_x^2(12433393315815381 + 177157668013452y^2 + 2148571653480y^4 + 46020514020y^6 + 2254150550y^8 \\
&+3348000y^{10}) - 6600c_z^4(105c_x^2(-19200051 + 24990792y^2 - 5729220y^4 + 166800y^6 + 20000y^8) \\
&-2(-586931479974 + 203424627609y^2 + 11115919710y^4 + 185627100y^6 + 9527000y^8)) \\
&-330c_z^2(25200c_x^4(2782827 - 931859y^2 - 345210y^4 + 55400y^6) + 10c_x^2(-897781382883 - 472670972172y^2 \\
&-12745143180y^4 - 1563982800y^6 + 35984000y^8) - 3(5650247159235252 + 103383878814384y^2 - 94438452465y^4 \\
&-15952277410y^6 + 10548100y^8 + 1116000y^{10}))) + 52c_y^4(-143803608652004088942 - 6364742323413471505 2y^2 \\
&-795872322440176905y^4 - 3196422089562240y^6 + 14002377577650y^8 + 741765830850y^{10} + 2723249000y^{12} \\
&+1108800c_z^6y^2(57 - 10y^2)^2(855 - 678y^2 + 40y^4) + 277200c_x^6(29129625 + 31672080y^2 - 29144088y^4 - 2256480y^6 \\
&+446400y^8 + 16000y^{10}) + 23760c_x^4(1349214675165 - 1821868698636y^2 - 67285404480y^4 - 1421344890y^6 \\
&-99243700y^8 + 3197000y^{10}) - 462c_x^2(777953012585226768 + 52502734700736030y^2 + 359763606829575y^4 \\
&+13422738586 50y^6 + 12139745625y^8 + 1516328000y^{10}) + 11880c_z^4(-898263495045 + 3100534641603y^2 \\
&-486110147985y^4 - 18240764780y^6 - 199718900y^8 - 10386000y^{10} + 70c_x^2(8528625 - 53697420y^2 + 27149412y^4 \\
&-2616480y^6 - 153600y^8 + 16000y^{10})) + 264c_z^2(-133806740898266 4969 - 11882155416800949 0y^2 \\
&-1047929851502100y^4 + 1574733224925y^6 + 95105536875y^8 + 451986625y^{10} + 6300c_x^4(-17458875 + 35640540y^2 \\
&+991956y^4 - 2343240y^6 + 73200y^8 + 8000y^{10}) - 90c_x^2(-796890994830 - 909551853y^2 + 349013455035y^4 \\
&+10061352280y^6 + 286384400y^8 + 1996000y^{10})))). \qquad \text{(B.21)}
\end{aligned}
$$

5. The solution of Boltzmann equation at 8th order ($\Phi^{(8)}$) is

$$
\begin{aligned}
\Phi^{(8)}(y,\boldsymbol{c}) \quad = \quad & \frac{1}{249419091796875}2(54977245779456000000000c_y^{24} - 54977245779456000000000c_y^{23}y \\
&-26179640847360000000c_y^{21}y(-16179 + 8400c_z^2 - 54600c_x^2 + 350y^2) \\
&+78538922542080000000c_y^{22}(-5393 + 2800c_z^2 - 18200c_x^2 + 350y^2) \\
&-26153487360000000c_y^{19}y(-375939777 + 126126000c_z^4 + 599098500c_x^4 - 26970020y^2 \\
&+173250y^4 - 80080c_z^2(6117 + 20475c_x^2 - 175y^2) - 5005c_x^2(-1031883 + 17150y^2)) \\
&+26153487360000000c_y^{20}(-378567402 + 126126000c_z^4 + 599098500c_x^4 - 80953950y^2 \\
&+873950y^4 - 240240c_z^2(2039 + 6825c_x^2 - 175y^2) - 15015c_x^2(-344311 + 17850y^2)) \\
&+375(558698765625000 + 85135050000000c_x^8 + 15916047034793257572115896y^2 \\
&+66980699178964376593788y^4 + 5730541538737973958 0y^6 - 138067490368452645y^8 \\
&-503767766201 70y^{10} + 2130275524650y^{12} + 15454024000y^{14} + 1702701000000c_x^6(-700 \\
&-299y^2 + 10y^4) + 54054000c_x^4(82687500 + 21035287098y^2 + 201002865y^4 + 245980y^6 \\
&+27200y^8) + 364c_x^2(-12279093750000 - 160917490171840195332y^2 \\
&-949093398289020600y^4 - 1874390848621830y^6 + 480553759125y^8 + 14572199400y^{10} \\
&+156202000y^{12})) - 6538371840000000c_y^{17}y(67422271059 + 3363360000c_z^6 + 22282260000c_x^6 \\
&-2474782580y^2 - 53728580y^4 + 154000y^6 - 2402400c_z^4(8289 + 27300c_x^2 - 350y^2) \\
&+300300c_x^4(-1115127 + 10150y^2) - 220c_x^2(518981823 - 150509765y^2 + 665000y^4) \\
&+20c_z^2(-1653552213 + 2396394000c_x^4 - 163107560y^2 + 1386000y^4 - 30030c_x^2(-697743 \\
&+17150y^2))) + 217945728000000c_y^{18}(204116603427 + 10090080000c_z^6 + 66846780000c_x^6 \\
&-22408439220y^2 - 808092000y^4 + 3388000y^6 - 21621600c_z^4(2763 + 9100c_x^2 - 350y^2) \\
&+2702700c_x^4(-372759 + 12250y^2) - 660c_x^2(518137623 - 463349775y^2 + 3658900y^4)
\end{aligned}
$$

$$
\begin{aligned}
&+60c_z^2(-1669317963+2396394000c_x^4-489673800y^2+6991600y^4-90090c_x^2(-232931\\
&+17850y^2)))-484323840000c_y^{15}y(93988153004031+1135134000000c_z^8+1287160875000c_x^8\\
&+14877889830630y^2-163306854000y^4-1704550500y^6+2275000y^8-4324320000c_z^6(2172\\
&+6825c_x^2-175y^2)+67567500c_x^6(-1334073+71050y^2)+202500c_x^4(4501641797\\
&-322585802y^2+358050y^4)-675c_x^2(1689348134253+42065705730y^2-3008868460y^4\\
&+4942000y^6)+405000c_z^4(-70047683+79879800c_x^4-11045496y^2+138600y^4\\
&-2002c_x^2(-363603+17150y^2))+5400c_z^2(20918862654+5570565000c_x^6-1354405085y^2\\
&-40587705y^4+154000y^6+150150c_x^4(-578217+10150y^2)-825c_x^2(28229897-20323548y^2\\
&+133000y^4)))+1452971520000c_y^{16}(31791675685302+378378000000c_z^8+429053625000c_x^8\\
&+15025932196560y^2-276224119200y^4-4009632000y^6+7945000y^8-4324320000c_z^6(724\\
&+2275c_x^2-175y^2)+67567500c_x^6(-445741+73150y^2)+135000c_x^4(2275921551-532773010y^2\\
&+1790635y^4)-75c_x^2(5144596640109+354885949710y^2-47731126200y^4+127246000y^6)\\
&+135000c_z^4(-71098733+79879800c_x^4-33171600y^2+699160y^4-18018c_x^2(-40517+5950y^2))\\
&+600c_z^2(63701926587+16711695000c_x^6-12290851620y^2-610717350y^4+3388000y^6\\
&+1351350c_x^4(-193789+12250y^2)-2475c_x^2(28133857-62620390y^2+731780y^4)))\\
&-17297280000c_y^{13}y(-3414304503853110+427356377409591y^2+20463082433640y^4\\
&-99723683700y^6-642908000y^8+280000y^{10}+105945840000c_z^8(-57+50y^2)\\
&+1891890000c_x^8(21903+6250y^2)+14553000c_x^6(-62615979-32327495y^2+388500y^4)\\
&-18900c_x^4(-205004286057-211881131895y^2+3265463410y^4+2394000y^6)\\
&-14c_x^2(-270822449842263+354413729788335y^2+3449843316900y^4-81040581000y^6\\
&+42700000y^8)-58212000c_z^6(1925871+750680y^2-18000y^4+910c_x^2(-4209+2450y^2))\\
&+37800c_z^4(14493175881-3408618640y^2-164680980y^4+924000y^6+2102100c_x^4(-5901+1450y^2)\\
&-4620c_x^2(-4391369-7532245y^2+95000y^4))+14c_z^2(77547795355413+36453542373540y^2\\
&-712294443900y^4-10284759000y^6+18200000y^8+945945000c_x^6(-15819+10150y^2)\\
&+3118500c_x^4(84903811-43112820y^2+93000y^4)-1350c_x^2(635859047931+35981978510y^2\\
&-6079534880y^4+14826000y^6)))+121080960000c_y^{14}(-502610911574805+185418260313201y^2\\
&+14734743843510y^4-105669129000y^6-841992000y^8+700000y^{10}+45405360000c_z^8(-19+50y^2)\\
&+1621620000c_x^8(4163+2100y^2)+2079000c_x^6(-67664529-90111825y^2+2181200y^4)-2700c_x^4(-203733282807\\
&-659411322795y^2+20685178800y^4+623000y^6)-6c_x^2(-100825090520571+369495778816395y^2\\
&+5168557286100y^4-209213199000y^6+205240000y^8)-8316000c_z^6(1994121+2256600y^2-90800y^4\\
&+2730c_x^2(-1453+2550y^2))+5400c_z^4(15164288631-10359887340y^2-826685400y^4+6776000y^6\\
&+6306300c_x^4(-2117+1750y^2)-4620c_x^2(-4407969-23264875y^2+522700y^4))+6c_z^2(27014564024721\\
&+37062698707980y^2-1206961473600y^4-24215796000y^6+63560000y^8+10405395000c_x^6(-493+950y^2)\\
&+1039500c_x^4(91745361-143025100y^2+930200y^4)-450c_x^2(663561693681+98292936510y^2-32191175400y^4\\
&+127246000y^6)))-576576000c_y^{11}y(-399313093445460369-16105709872981260y^2+627848878062420y^4\\
&+14613112060200y^6-30472993250y^8-158085000y^{10}+1746360000c_z^8(9747-16720y^2+4500y^4)\\
&+436590000c_x^8(-1057257+143570y^2+76000y^4)+2835000c_x^6(-685651311-821173957y^2-286893393y^4\\
&+700000y^6)-1260c_x^4(-47343944154924-10953752511645y^2-4215128436225y^4+13618898250y^6+25550000y^8)\\
&-30c_x^2(-13569887561441715-547583214124989y^2+218896786143315y^4+1473616422300y^6-11362421000y^8\\
&+280000y^{10})-11340000c_z^6(176086791+46350658y^2+5722382y^4-61600y^6+154c_x^2(473517-547670y^2\\
&+95000y^4))+1260c_z^4(-3171694923801+1957971022020y^2-148171928400y^4-3466557000y^6+9100000y^8\\
&+1039500c_x^4(2078631-1218560y^2+46500y^4)-9000c_x^2(-2252574234-294982026y^2-156623219y^4+741300y^6))\\
&+60c_z^2(-2321762588432595+83968636237857y^2+12367468655955y^4-108422969400y^6-967022000y^8\\
&+560000y^{10}+14553000c_x^6(265221-1197335y^2+194250y^4)-94500c_x^4(169187418-2672461077y^2+331775257y^4\\
&+478800y^6)-42c_x^2(16800454077876+21001172731605y^2+526476382650y^4-27189738000y^6+21350000y^8)))\\
&+576576000c_y^{12}(-400388679550321119-497275786830217 50y^2+3170407636710153y^4+101905983356940y^6\\
&-335710252800y^8-1866984000y^{10}+280000y^{12}+1746360000c_z^8(9747-51300y^2+22700y^4)
\end{aligned}
$$

$$+873180000c_x^8(-644991+503100y^2+145900y^4)+945000c_x^6(167126427-11563836597y^2-4058086230y^4$$
$$+23690800y^6)-3780c_x^4(-12913483163208-13840394403315y^2-7543975332825y^4+57132798000y^6$$
$$+72520000y^8)-210c_x^2(-1995049477006470-248692544152659y^2+167653523732040y^4+1296741676500y^6$$
$$-17677950000y^8+3800000y^{10})-3780000c_z^6(520082973+430286148y^2+86387220y^4-1355200y^6$$
$$+462c_x^2(508917-1800900y^2+522700y^4))+3780c_z^4(-977998386267+2067973228440y^2-252039607800y^4$$
$$-8177268000y^6+31780000y^8+346500c_x^4(2400531-4642500y^2+465100y^4)-3000c_x^2(-2143982889$$
$$-967575912y^2-832561230y^4+6362300y^6))+420c_z^2(-334398637919385+37247289940242y^2+8964151508880y^4$$
$$-115043553000y^6-1268460000y^8+1400000y^{10}+2079000c_x^6(154071-3583800y^2+1090600y^4)$$
$$-54000c_x^4(52755912-2233139586y^2+529225785y^4+31150y^6)-36c_x^2(2601456981546+11263298272530y^2$$
$$+381100607025y^4-35167633500y^6+51310000y^8)))+5241600c_y^9y(642745905682810302450$$
$$+7319252906651418579y^2+82419093160772445y^4-1610800167499380y^6-23445585739675y^8$$
$$+4617880250y^{10}+55110000y^{12}-1746360000c_z^8(-61731+162450y^2-83220y^4+11000y^6)$$
$$-62370000c_x^8(108562167-58234750y^2-9688560y^4+1544000y^6)+46200c_x^6(10967413444947$$
$$+1237529427210y^2-69685731675y^4+41812917750y^6+22750000y^8)+4950c_x^4(-8653008712164390$$
$$-212126499552954y^2-3702442689855y^4-2221146494450y^6-2174249000y^8+1680000y^{10})$$
$$-110c_x^2(567289039655682981+53508801862729395y^2+819473689549305y^4-129176894871000y^6$$
$$-783186949750y^8+1416645000y^{10})+92400c_z^6(1640946525561+412080385230y^2+29301535350y^4$$
$$+1790734500y^6-9100000y^8+9450c_x^2(-7656867+13149050y^2-4414140y^4+353000y^6))$$
$$+19800c_z^4(474969215722050+3899718495099y^2-614734448895y^4+22414072950y^6+324114000y^8$$
$$-280000y^{10}+132300c_x^4(12038709-10963150y^2+1244980y^4+57000y^6)+14c_x^2(-5250570164739$$
$$-1627914513645y^2-47311736400y^4-13859185500y^6+21350000y^8))-110c_z^2(-862796981247453819$$
$$-22973961133664730y^2+241461580995180y^4+17503200121500y^6-66143056000y^8-474255000y^{10}$$
$$+3969000c_x^6(20528469+22532550y^2-11265120y^4+500000y^6)-1260c_x^4(-14159910354453$$
$$-574887959415y^2-456681825675y^4+13484120250y^6+51100000y^8)-90c_x^2(-6036620627130345$$
$$+98116776404346y^2+24683003059470y^4+477339899300y^6-7589834000y^8+280000y^{10})))$$
$$+57657600c_y^{10}(-58371127575545753325-1994670100691743419y^2-39026237017571055y^4$$
$$+1036374476617620y^6+18566208138150y^8-20031698000y^{10}-109960000y^{12}+52920000c_z^8(-185193$$
$$+1559520y^2-1328100y^4+242000y^6)+26460000c_x^8(30555684-63186885y^2-2767200y^4+2396500y^6)$$
$$+12600c_x^6(-3451743497574-1242180063945y^2-165692042100y^4-107485041000y^6+55160000y^8)$$
$$-3150c_x^4(-1224699523828020-99729341953164y^2-7093686589455y^4-2548196838000y^6+1634152000y^8$$
$$+7400000y^{10})+10c_x^2(559415480810349681+187131414997158975y^2+4008696333887637y^4$$
$$-1004742742634190y^6-6277405678200y^8+25570164000y^{10}+1120000y^{12})-25200c_z^6(548490395187$$
$$+403638803910y^2+50573089800y^4+4246638000y^6-31780000y^8+1050c_x^2(-25843401+139470390y^2$$
$$-79376700y^4+9089000y^6))-12600c_z^4(67661149186125+1654574837634y^2-462538062495y^4+23851390500y^6$$
$$+426468000y^8-700000y^{10}+6300c_x^4(45227952-137144655y^2+34560900y^4+44500y^6)+6c_x^2(-1700675873613$$
$$-1698281517465y^2-96485222700y^4-36063934500y^6+102620000y^8))+70c_z^2(-123224972521621617$$
$$-9888667846601850y^2+175203525541716y^4+17499028478580y^6-104163492600y^8-801048000y^{10}+160000y^{12}$$
$$+1512000c_x^6(12410604+18295065y^2-23917575y^4+2115250y^6)-540c_x^4(-4834788813576-103440268305y^2$$
$$-884022564150y^4+57475686000y^6+145040000y^8)-90c_x^2(-860338811070135+37157782408686y^2$$
$$+19343008151220y^4+408603214500y^6-11835088000y^8+3800000y^{10})))+2c_yy(425675250000000c_x^8(201+70y^2)$$
$$+405405000000c_x^6(1624428981+33534900y^2+268905y^4+15350y^6)+1638000c_x^4(-30593099824215449598$$
$$-366758602891737210y^2-1155971663964810y^4+561674812050y^6+23490842375y^8+304964250y^{10})$$
$$+4c_x^2(32489148633653329088218091384 04+29890926277369912550813177160y^2$$

$$
\begin{aligned}
&+7872837697527763062963861 0y^4 + 7780059975644371855440 0y^6 - 3715401363231182625y^8 \\
&-12118774428306000y^{10} + 564612955593750y^{12} + 3107531282500y^{14}) + 5(-6226113241492693728891955811568 \\
&-549375387062423531749489350 00y^2 - 13729070946362988087201330 0y^4 - 1406504183009031107001 00y^6 \\
&-67331013574390941375y^8 + 2791149132394350 0y^{10} + 867659206863750y^{12} + 7427813807500y^{14}) \\
&+8c_z^2(162144948074945366390986596670 2 + 1492423757105645431093659633 0y^2 \\
&+39366101157249793892520555y^4 + 3910862985315324696157 5y^6 - 1852234059787736625y^8 \\
&-10900983240181125y^{10} + 233742361453125y^{12} + 1553765641250y^{14} + 372465843750000c_x^6(-57 + 10y^2) \\
&+50675625000c_x^4(1577471931 + 34926675y^2 + 89355y^4 + 15350y^6) + 614250c_x^2(-10151734388402973366 \\
&-1220511780902383 20y^2 - 389865074801895y^4 + 141432776100y^6 + 6169326625y^8 + 101654750y^{10}))) \\
&+524160c_y^7y(-3234000c_z^8(10556001 - 44446320y^2 + 33139800y^4 - 8208000y^6 + 650000y^8) \\
&-462000c_x^8(-9051377643 + 9987013260y^2 + 509714100y^4 - 415791000y^6 + 6650000y^8) \\
&+231000c_x^6(-17184251286855 + 85514077188y^2 - 26276034060y^4 - 13396331850y^6 + 544664000y^8 + 440000y^{10}) \\
&-550c_x^4(5093819175405946608 + 115485222724595640y^2 + 345166317066375y^4 - 20130425390700y^6 \\
&+1640910257375y^8 + 4223340000y^{10}) + 2(6377764434682765184260 2 + 5126860585135151928 45y^2 \\
&+1545284529603207855y^4 + 7930445520786525y^6 - 106126264341625y^8 - 1172859458500y^{10} - 1443503125y^{12}) \\
&+55c_x^2(71652899391146797500 - 35809716391579116y^2 - 27509255271901305y^4 - 495125299135980y^6 \\
&+25786493406825y^8 + 1606852052 50y^{10} + 30060000y^{12}) + 924000c_z^6(-506291894010 + 253631813247y^2 \\
&+20841139035y^4 + 618778350y^6 + 23531000y^8 - 40000y^{10} + 14c_x^2(232144299 - 537488055y^2 + 254092950y^4 \\
&-37759500y^6 + 1525000y^8)) + 1100c_z^4(448150408705614321 + 144099171841328 55y^2 + 30190080965625y^4 \\
&-2539203370650y^6 + 40867132250y^8 + 474255000y^{10} + 17640c_x^4(-1045390401 + 1225527570y^2 - 215675550y^4 \\
&-9627000y^6 + 1825000y^8) + 630c_x^2(9441118596105 - 2672470013112y^2 - 242417651010y^4 - 1947044600y^6 \\
&-545321000y^8 + 40000y^{10})) + 10c_z^2(855489267998218299600 + 158864897098747113 12y^2 \\
&+122294031927394635y^4 - 639888199840890y^6 - 28124739768400y^8 + 10841969500y^{10} + 165330000y^{12} \\
&+1293600c_x^6(1130746149 + 131774445y^2 - 376282800y^4 + 35399250y^6 + 812500y^8) \\
&+138600c_x^4(3221074299375 - 2075072660856y^2 - 90379269705y^4 - 7022469425y^6 - 80101750y^8 + 120000y^{10}) \\
&-220c_x^2(1349242743633937929 + 38460401817230295y^2 - 277080725541375y^4 - 21259922212350y^6 \\
&-394955491625y^8 + 1416645000y^{10}))) + 87360c_y^8(-7650362733484171369062 24 - 1901403571581978072 8400y^2 \\
&-10650584343937650730 50y^4 - 769570771723261200y^6 + 11882163077247375y^8 + 147554006490000y^{10} \\
&+86560120000y^{12} + 58212000c_z^8(3518667 - 51854040y^2 + 65629800y^4 - 22572000y^6 + 2270000y^8) \\
&+16632000c_x^8(-2062429803 + 8450802360y^2 - 1175983200y^4 - 515592000y^6 + 31420000y^8) \\
&-1386000c_x^6(-20730935817630 + 7668512288631y^2 + 361061299350y^4 - 67665480000y^6 + 8193024000y^8 \\
&+8000000y^{10}) + 9900c_x^4(1691019182151149886 + 125486502689520000y^2 + 1192657296143187y^4 \\
&-14392510501740y^6 + 6803407756800y^8 + 13668264000y^{10} + 1120000y^{12}) + 330c_x^2(-73187628331136082750 \\
&+38460604010469330 06y^2 + 2082051302339272 95y^4 + 296739056388537 0y^6 - 281852204246100y^8 \\
&-1710901463000y^{10} + 747840000y^{12}) - 11088000c_z^6(-253309696605 + 399887260182y^2 + 52306165350y^4 \\
&+2328985500y^6 + 109353000y^8 - 350000y^{10} + 21c_x^2(92976633 - 712900710y^2 + 587095200y^4 - 128043000y^6 \\
&+7330000y^8)) - 19800c_z^4(149306294715666732 + 143169167478629 25y^2 + 56502354726594y^4 \\
&-5933125732380y^6 + 150367851600y^8 + 1873368000y^{10} - 560000y^{12} + 141120c_x^4(-60469524 + 244241505y^2 \\
&-95025600y^4 + 3061500y^6 + 647500y^8) + 420c_x^2(5096582039115 - 4888617884847y^2 - 734762663550y^4 \\
&-11576464500y^6 - 2996113000y^8 + 1900000y^{10})) + 660c_z^2(-77696212410371280600 \\
&-43207445007543438 72y^2 - 5696356416176821 5y^4 + 401825767840560y^6 + 22227214133700y^8 \\
&-43605724000y^{10} - 329880000y^{12} + 705600c_x^6(-316500804 + 213667605y^2 + 355296150y^4 - 78313500y^6 \\
&+985000y^8) - 25200c_x^4(1610362572075 - 3351688238961y^2 - 151569659250y^4 - 31570585500y^6 \\
&+189356000y^8 + 1850000y^{10}) + 60c_x^2(447235143734331918 + 43058475106578225y^2 - 417244751512344y^4 \\
&-55712995337370y^6 - 1039348011600y^8 + 8526132000y^{10} + 560000y^{12})))
\end{aligned}
$$

$$
\begin{aligned}
&+5040c_y^5y(25126623390806664314612824 8+22268284941309680220948 00y^2+44024357503700728654 50y^4\\
&-9823941849590797 50y^6+2758134098916625y^8-147816214445250y^{10}-1447199247500y^{12}\\
&-96096000c_z^8y^2(-57+10y^2)^3(-19+10y^2)+24024000c_x^8(-315067725+1190310282y^2-37550160y^4\\
&-56624400y^6+340000y^8+160000y^{10})-343200c_x^6(-247862624829057+22254029326305y^2\\
&+13782056347080y^4+362450105700y^6+10939531000y^8+178980000y^{10})\\
&+520c_x^4(-1863018373003642770300-7520148516773649972 6y^2-453543509697086655y^4\\
&+1258629525279720y^6+61769383863825y^8-66203872250y^{10}+330660000y^{12})\\
&+26c_x^2(4129963040556308732404 32+56263117786983537784 20y^2+44487840165374743830y^4\\
&+21721902264696150y^6-2357675681931625y^8+19110523947750y^{10}+131317575000y^{12})\\
&+343200c_z^6(15355201383207-18541544082705y^2+2760485330295y^4+116961563550y^6+1732356500y^8\\
&+52695000y^{10}+70c_x^2(-291678975+951053778y^2-535151340y^4+101255400y^6-6380000y^8+40000y^{10}))\\
&+520c_z^4(282221216574447565800+16500905828218847574y^2+157289624134449345y^4+56000756446470y^6\\
&-8954266888050y^8+15660596500y^{10}+330660000y^{12}+138600c_x^4(1135743525-1526306886y^2\\
&+312837780y^4+14452200y^6-4900000y^8+120000y^{10})-1980c_x^2(86486449506093-58950472986720y^2\\
&+2860037115705y^4+143634582450y^6-748281500y^8+157405000y^{10}))\\
&+104c_z^2(1418330517323595661551 80+13336571322393733329 30y^2+68121493703248570 20y^4\\
&+22440866013759600y^6-87159770674625y^8-2756339076500y^{10}-5774012500y^{12}\\
&+231000c_x^6(-4589595675+961886178y^2+978429960y^4-119721600y^6-7220000y^8+440000y^{10})\\
&-9900c_x^4(21431420524143-66117059780520y^2+9000962674830y^4+280624597200y^6+4775056000y^8\\
&+234630000y^{10})+55c_x^2(-139585290620388259500-6456499225732295082y^2-45599251798550835y^4\\
&+254729612124540y^6+8006010739275y^8+162628719250y^{10}+60120000y^{12})))\\
&+3120c_y^6(-40585029209619785303165121 6-10742812785066817855716624y^2\\
&-40521926945578482807480y^4-53969592559174115670y^6-231819667318926225y^8\\
&+3293511280082100y^{10}+33740355152000y^{12}+50570200000y^{14}+77616000c_z^8y^2(57-10y^2)^2(9747\\
&-14820y^2+3500y^4)-77616000c_x^8(-71130150+3092048397y^2-1055136240y^4-236281500y^6\\
&+29052000y^8+700000y^{10})+184800c_x^6(-1095878716738596+1060523798098275y^2+144479050145262y^4\\
&+5146356267360y^6+368747893800y^8-2363136000y^{10}+1120000y^{12})+18480c_x^4(83761348534070274900\\
&+11928519275499705438y^2+12577063917910558 5y^4-84464700987240y^6-20398811514300y^8\\
&+446691181000y^{10}+1077720000y^{12})-154c_x^2(11300451315060195065433 6+29478650635487243232 00y^2\\
&+26753347324362087450y^4-12002262421691745 0y^6-4619055628135125y^8+112007593290000y^{10}\\
&+733820320000y^{12})-184800c_z^6(46075812913746-197329967208675y^2+48753182534238y^4\\
&+2788046212140y^6+57614776200y^8+1886136000y^{10}-1120000y^{12}+840c_x^2(-97226325+1185254694y^2\\
&-1243106730y^4+368311500y^6-37341000y^8+950000y^{10}))-9240c_z^4(25658329885600362300\\
&+44886568113351876 24y^2+72269099568976905y^4+75806037937980y^6-6665899635900y^8+54232708000y^{10}\\
&+659760000y^{12}+50400c_x^4(454889925-2275561053y^2+1092025260y^4-60356250y^6-14913000y^8+925000y^{10})\\
&-60c_x^2(321529802602554-805205299854375y^2+95131630142262y^4+5981924101860y^6+13511413800y^8\\
&+8534364000y^{10}+1120000y^{12}))-28c_z^2(85057978514165188293484 8+25120354058701088487300y^2\\
&+23202474277340753010 0y^4+114114703172313690 0y^6-4877460459964125y^8-176850952410000y^{10}\\
&-173120240000y^{12}+2772000c_x^6(-4456322325+6970098438y^2+2726865540y^4-1128033000y^6+19728000y^8\\
&+4000000y^{10})-19800c_x^4(25856940640104-665435242109925y^2+190972719993762y^4+7210154178360y^6\\
&+253368928800y^8+6863364000y^{10}+1120000y^{12})-330c_x^2(13705216520939921 2500+24502365810130698252y^2\\
&+31601276450764051 5y^4-1929630951906210y^6-91542684017700y^8-1737146471000y^{10}+1495680000y^{12})))\\
&+16c_y^3y(14153955779748220574635254778 02+13190247270854291401876942830y^2
\end{aligned}
$$

$$
\begin{aligned}
&+3534245801349079207571680 5y^4 + 34721675999924156067825y^6 - 2547471769166449125y^8\\
&+37235170131090750y^{10} + 148242183140625y^{12} + 1553765641250y^{14} + 94594500000c_x^8(-1998675 - 2877822y^2\\
&+227880y^4 + 111600y^6 + 4000y^8) + 10810800c_x^6(-222161816890125 + 23969759521113y^2 + 16214485367115y^4\\
&+682125058890y^6 + 12376025900y^8 + 226573000y^{10} + 1670000y^{12}) + 16380c_x^4(4849502109540193451808\\
&-1005735689906020012170y^2 - 117797220719020007 55y^4 - 37093550333038650y^6 + 166610360142875y^8\\
&+3471104979750y^{10} + 71432800000y^{12}) - 8190c_x^2(-87491219548289284945504 98 - 668119220780690938297 50y^2\\
&-233726451845457723075y^4 - 712624234297251375y^6 + 357876526104625y^8 + 26115101107750y^{10}\\
&+164663938125y^{12}) + 21621600c_z^6y^2(57 - 10y^2)^2(1574828556 + 34197415y^2 + 338555y^4 + 8350y^6\\
&+17500c_x^2(-57 + 10y^2)) + 16380c_z^4(-11806665475873118655 42 + 37625651415669611448 0y^2\\
&+710567038568249824 5y^4 + 309182723107731 00y^6 - 9506802685875y^8 - 821240319000y^{10} - 5774012500y^{12}\\
&+17325000c_x^4(-1705725 + 2405628y^2 - 451620y^4 - 8400y^6 + 4000y^8) + 3960c_x^2(22456587376125\\
&-19559836235331y^2 + 770152587120y^4 + 186872323695y^6 + 3461095450y^8 + 53986500y^{10} + 835000y^{12}))\\
&+630c_z^2(14218173915490394137180292 4 + 12425981419007868025314 00y^2 + 25132580734184011588 50y^4\\
&-302166517407183000y^6 - 5358233203483875y^8 - 18105672750750y^{10} - 723599623750y^{12}\\
&+900900000c_x^6(2357775 - 728361y^2 - 252810y^4 + 25800y^6 + 2000y^8) + 102960c_x^4(-11932736988375\\
&-18831794352231y^2 + 4034987154870y^4 + 257051723445y^6 + 4503460450y^8 + 83636500y^{10} + 835000y^{12})\\
&+52c_x^2(1808748976007505058758 - 3048746172028246582 20y^2 - 2238899160116470005y^4\\
&-3787576211526525y^6 + 65332648525375y^8 + 829088767875y^{10} + 32829393750y^{12})))\\
&+48c_y^4(336336000c_z^8y^4(57 - 10y^2)^4 + 336336000c_x^8(733556250 + 1282392000y^2 - 883508499y^4 - 126477720y^6\\
&+16799400y^8 + 1272000y^{10} + 10000y^{12}) + 1201200c_x^6(1273096797635250 - 1694474829154359y^2\\
&-284718034289430y^4 + 36093477523320y^6 + 844972484400y^8 + 13627152000y^{10} + 593840000y^{12})\\
&-3640c_x^4(95210933840982874765 62 - 10876824697497026187150y^2 - 20598995467084510822 5y^4\\
&-8330579613026401 50y^6 + 2914437911368500y^8 + 86559143055000y^{10} + 896979940000y^{12})\\
&+65c_x^2(-36732476086264065144967 2216 - 85528051157836869479916 48y^2 - 74168600514707077720110y^4\\
&-43452290095446682989 0y^6 - 44244633658528957 5y^8 + 12098639034682200y^{10} + 15758479674000y^{12}\\
&+101140400000y^{14}) + 7(-67399555746508419420190015812 - 18845770245437235965248484 10y^2\\
&-83723331916510827776235 00y^4 - 11214226612374548387625y^6 + 1510026314321596500y^8\\
&-9240629711044875y^{10} + 102620363007500y^{12} + 1159666600000y^{14})\\
&+4804800c_z^6y^2(-57 + 10y^2)(808014978603 - 301603190175y^2 - 8795501190y^4 - 104227500y^6 - 2749000y^8\\
&+70c_x^2(-10965375 + 11827728y^2 - 2332620y^4 + 81600y^6 + 4000y^8)) + 1820c_z^4(3542066338826442687876\\
&-3950841469906638187650y^2 - 1205605531741486664 25y^4 - 749756695800350700y^6 + 87633464935500y^8\\
&+29296945920000y^{10} + 86560120000y^{12} + 277200c_x^4(639646875 - 4158891000y^2 + 2065707504y^4\\
&-128270880y^6 - 30002400y^8 + 2088000y^{10} + 40000y^{12}) + 1980c_x^2(-202176449307000 + 833558484994641y^2\\
&-194725512639630y^4 - 1309299570180y^6 + 48122501400y^8 - 4374168000y^{10} + 124640000y^{12}))\\
&+260c_z^2(-11482364233115635671221 8104 - 29900829633339325439976 12y^2 - 12711631866392729311965y^4\\
&-31232474647931312910y^6 - 64727850870473175y^8 + 320115753093675y^{10} + 9521589406000y^{12}\\
&+25285100000y^{14} + 1293600c_x^6(-3290371875 + 6379185375y^2 + 794599254y^4 - 577528380y^6 + 1722600y^8\\
&+3588000y^{10} + 40000y^{12}) + 27720c_x^4(95794183311750 + 213049625080383y^2 - 170782453691640y^4\\
&+7125637910160y^6 + 199189465200y^8 + 674496000y^{10} + 179620000y^{12}) - 154c_x^2(6940121423664819159784\\
&-7886931351601032769 50y^2 - 1480021274621427457 5y^4 - 62686191574509300y^6 + 341145985662000y^8\\
&+7430722020000y^{10} + 183455080000y^{12}))) + 6c_y^2(56756700000000c_x^8(-2760 - 321y^2 + 960y^4 + 100y^6)\\
&+1081080000c_x^6(-611425914750 + 849764698839y^2 + 149658927600y^4 + 2965446120y^6 + 42294800y^8\\
&+808000y^{10}) + 1040c_x^4(32160283344077437602900 - 46484470330370849411712y^2\\
&-34240920390462130225 65y^4 - 35786886489548804610y^6 - 103117404255049800y^8 + 163840109848800y^{10}\\
&+3849328336000y^{12} + 25285100000y^{14}) - 5(-20757741882236947102641148 58256
\end{aligned}
$$

$$
\begin{aligned}
&-5494570790813856899644521024 0y^2 - 230462017952655347563805100y^4 - 348109492626144507258000y^6\\
&-261111595154343058125y^8 + 18189642245024250y^{10} + 2656887756818750y^{12} + 7121442600000y^{14})\\
&+28c_x^2(-154855095513729615676402154424 - 37000086677344304091115738 20y^2\\
&-14107084849336112267634000y^4 - 231112784532500097727 50y^6 - 365616469723613501 25y^8\\
&+46523897115481500y^{10} + 1510305535115000y^{12} + 18900297200000y^{14}) + 2080c_z^4y^2(826454136925279257179 4\\
&-131690481127058945322 0y^2 - 165775397589910543 05y^4 - 53785686792429900y^6 + 27663688529400y^8\\
&+1086500618000y^{10} + 12642550000y^{12} + 27286875000c_x^4(57 - 10y^2)^2 + 2079000c_x^2(-179601527259\\
&+27589002525y^2 + 656232780y^4 + 4373700y^6 + 202000y^8)) + 4c_z^2(28378350000000c_x^6(1995 - 3786y^2 - 90y^4\\
&+100y^6) + 270270000c_x^4(-591944739750 + 68809039803y^2 + 260213781450y^4 + 5425002240y^6 + 59789600y^8\\
&+1616000y^{10}) + 520c_x^2(15989289120873234520200 - 14763050756596987984062y^2 - 30271962593889883285 65y^4\\
&-3448714938218066286 0y^6 - 105609833950767300y^8 + 100806811828800y^{10} + 3011164786000y^{12}\\
&+25285100000y^{14}) + 7(-15442405700960740020695819 0424 - 42653172992776895181691258 20y^2\\
&-18679479743540179353289500y^4 - 25496436915444838092750y^6 + 1889079752751852375y^8\\
&+25451708281535250y^{10} - 24901059235000y^{12} + 2319333200000y^{14}))))).
\end{aligned}
\tag{B.22}
$$

6. The solution of Boltzmann equation at 9th order ($\Phi^{(9)}$) is

$$
\begin{aligned}
\Phi^{(9)}(y,\boldsymbol{c}) \;=\; & \frac{1}{4240124560546875}4c_x(28599163254473011200000000000c_y^{26} - 28599163254473011200000000000c_y^{25}y\\
&-53406467328614400000000c_y^{23}y(-63451 + 21420c_z^2 - 32130c_x^2 + 875y^2)\\
&+26703233664307200000000c_y^{24}(-126937 + 42840c_z^2 - 64260c_x^2 + 5320y^2)\\
&-5779920706560000000c_y^{21}y(3442257603 + 2968812000c_z^4 - 742203000c_x^4 - 963841340y^2\\
&+3826900y^4 - 92400c_z^2(191431 + 96390c_x^2 - 3500y^2) - 46200c_x^2(-910453 + 9800y^2))\\
&+5779920706560000000c_y^{22}(3412673433 + 2968812000c_z^4 - 742203000c_x^4 - 2917862640y^2\\
&+19781300y^4 - 92400c_z^2(191501 + 96390c_x^2 - 10640y^2) - 46200c_x^2(-911363 + 31220y^2))\\
&-17(1885608333984375000 + 31925643750000000c_x^8 + 78081093527599183565411367580 08y^2\\
&+35859473987546277430464162060y^4 + 61456998282685664909189940y^6\\
&+42362177631815059343325y^8 - 3748782310121148300y^{10} - 4229317933590750y^{12}\\
&+142407869212500y^{14} + 776882820625y^{16} + 212837625000000c_x^6(-2700 - 1059y^2 + 35y^4)\\
&+101351250000c_x^4(29767500 + 5259950262y^2 + 50969625y^4 + 2870y^6 + 7675y^8)\\
&+819000c_x^2(-6139546875000 - 4021326110486438245 8y^2 - 237614058942709680y^4\\
&-459726026839695y^6 + 222804467325y^8 + 3646507975y^{10} + 50827375y^{12}))\\
&-14820309504000000 0c_y^{19}y(2264799848955 + 77189112000c_z^6 + 56513457000c_x^6 + 23801516436y^2\\
&-1815683100y^4 + 3133900y^6 - 10810800c_z^4(64529 + 32130c_x^2 - 1750y^2) - 2702700c_x^4(161981 + 2450y^2)\\
&-39c_x^2(105557910603 - 6598123840y^2 + 17840900y^4) - 624c_z^2(-365231532 + 92775375c_x^4\\
&+181685735y^2 - 956725y^4 + 34650c_x^2(-153421 + 2450y^2)))\\
&+44460928512000000 0c_y^{20}(760481680052 + 25729704000c_z^6 + 18837819000c_x^6 + 22918429575y^2\\
&-3088526595y^4 + 7884800y^6 - 7207200c_z^4(32282 + 16065c_x^2 - 2660y^2) - 1801800c_x^4(81323 + 3010y^2)\\
&-26c_x^2(52931710404 - 10305844395y^2 + 51393650y^4) - 208c_z^2(-359703702 + 92775375c_x^4\\
&+550123035y^2 - 4945325y^4 + 17325c_x^2(-307297 + 15610y^2)))\\
&-1852538688000000c_y^{17}y(-37326392134947 + 1543782240000c_z^8 + 1199187990000c_x^8\\
&+29348543547620y^2 + 107659816248y^4 - 3232321440y^6 + 2634800y^8\\
&-1441440000c_z^6(13337 + 6426c_x^2 - 700y^2) + 180180000c_x^6(-188299 + 3440y^2)\\
&-2340c_x^4(-104765778879 + 1617528220y^2 + 17086300y^4) - 4c_x^2(68893395094677 + 13463903401560y^2\\
&-221123456400y^4 + 202048000y^6) - 37440c_z^4(-114182589 + 61850250c_x^4 + 244822270y^2\\
&-1913450y^4 + 57750c_x^2(-63383 + 1960y^2)) + 16c_z^2(14036003003112 + 282567285000c_x^6\\
&+206772200685y^2 - 27365622900y^4 + 62678000y^6 - 67567500c_x^4(33407 + 980y^2)
\end{aligned}
$$

$$
\begin{aligned}
&-221123456400y^4 + 202048000y^6) - 37440c_z^4(-114182589 + 61850250c_x^4 + 244822270y^2\\
&-1913450y^4 + 57750c_x^2(-63383 + 1960y^2)) + 16c_z^2(14036003003112 + 282567285000c_x^6\\
&+206772200685y^2 - 27365622900y^4 + 62678000y^6 - 67567500c_x^4(33407 + 980y^2)\\
&-585c_x^2(36342404403 - 4441646440y^2 + 17840900y^4)))\\
&+5557616064000000c_y^{18}(-12806189001387 + 514594080000c_z^8 + 399729330000c_x^8\\
&+29838488334500y^2 + 167234785460y^4 - 7842985200y^6 + 9338000y^8 - 480480000c_z^6(13351\\
&+6426c_x^2 - 2128y^2) + 60060000c_x^6(-189041 + 11804y^2) - 780c_x^4(-105798254169\\
&+6593876520y^2 + 70555100y^4) - 4c_x^2(23243288476129 + 13623295298730y^2 - 402741450650y^4\\
&+631246000y^6) - 24960c_z^4(-53431677 + 30925125c_x^4 + 370780410y^2 - 4945325y^4\\
&+28875c_x^2(-63565 + 6244y^2)) + 8c_z^2(9470605694173 + 188378190000c_x^6 + 393112687710y^2\\
&-93128431550y^4 + 315392000y^6 - 45045000c_x^4(33673 + 2408y^2) - 780c_x^2(18274996854\\
&-6942484395y^2 + 51393650y^4))) - 588107520000c_y^{15}y(-494349989265583857\\
&-19631433493203840y^2 + 4406885102144700y^4 + 9952429770000y^6 - 124651996000y^8\\
&+40180000y^{10} + 6356750400000c_z^8(-154 + 125y^2) + 56756700000c_x^8(-14428 + 10775y^2)\\
&+378378000c_x^6(58304277 - 43368710y^2 + 132100y^4) - 18900c_x^4(11475898561489\\
&-6005284965000y^2 - 3593274300y^4 + 189343000y^6) - 1260c_x^2(-656420140953651\\
&+99590092007450y^2 + 6471137338470y^4 - 39795414600y^6 + 8652000y^8)\\
&-3027024000c_z^6(3317211 + 3279820y^2 - 49700y^4 + 2100c_x^2(-1439 + 700y^2))\\
&-151200c_z^4(-866693206927 - 18930460275y^2 + 9208791900y^4 - 31339000y^6\\
&+63063000c_x^4(361 + 175y^2) + 15015c_x^2(15569589 - 29677520y^2 + 231700y^4))\\
&+1260c_z^2(-27953025771699 + 90050059084000y^2 + 482662481880y^4 - 24335894400y^6\\
&+26348000y^8 + 180180000c_x^6(-29623 + 8600y^2) - 900900c_x^4(-105024477 + 10683260y^2\\
&+221900y^4) - 120c_x^2(2921605412281 + 1154653645350y^2 - 37144095450y^4 + 50512000y^6)))\\
&+12350257920000c_y^{16}(-24375748526700471 - 2775182979205710y^2 + 1077344284113150y^4\\
&+2951611114200y^6 - 57460116000y^8 + 30800000y^{10} + 151351200000c_z^8(-313 + 760y^2)\\
&+1351350000c_x^8(-29491 + 65920y^2) + 9009000c_x^6(123675669 - 274649670y^2 + 2031400y^4)\\
&-900c_x^4(12359459060239 - 19550156645070y^2 + 77607349050y^4 + 1265418000y^6)\\
&-30c_x^2(-1379529853025847 + 655242382905330y^2 + 66196745989500y^4 - 653715676000y^6\\
&+325920000y^8) - 144144000c_z^6(3410271 + 9944820y^2 - 256900y^4 + 4200c_x^2(-752 + 1115y^2))\\
&-3600c_z^4(-1793471466779 - 99259473030y^2 + 94073698950y^4 - 473088000y^6\\
&+2711709000c_x^4(19 + 20y^2) + 60060c_x^2(8496927 - 46482135y^2 + 667450y^4))\\
&+60c_z^2(-30619690224939 + 276034198523160y^2 + 2211887452500y^4 - 177240037000y^6\\
&+280140000y^8 + 360360000c_x^6(-15739 + 14755y^2) - 900900c_x^4(-111951147 + 43925760y^2\\
&+916300y^4) - 60c_x^2(5994584902637 + 7020522890940y^2 - 406324460850y^4 + 946869000y^6)))\\
&-19603584000c_y^{13}y(-8935753335022796688 - 2256068025241483950y^2 - 31998381166369485y^4\\
&+2934061393757400y^6 + 5605694991000y^8 - 26503680000y^{10} + 1400000y^{12}\\
&+158918760000c_z^8(17727 - 28660y^2 + 7100y^4) + 11351340000c_x^8(-101157 - 393740y^2 + 70900y^4)\\
&-4158000c_x^6(-13971620124 - 26438170710y^2 + 4710487425y^4 + 2543000y^6)\\
&-18900c_x^4(8208461113704 + 51705229689410y^2 - 6607579527015y^4 - 29782492800y^6\\
&+59136000y^8) + 60c_x^2(72566831016923481 + 61214169801141630y^2 - 2200454397505980y^4\\
&-90585216318600y^6 + 209334643000y^8 + 21560000y^{10}) - 116424000c_z^6(1454993037 + 398746905y^2\\
&+122981100y^4 - 814000y^6 + 1365c_x^2(236127 - 238760y^2 + 33100y^4)) - 18900c_z^4(-9594935972721\\
&-31824391252540y^2 - 316563435840y^4 + 49045723200y^6 - 79044000y^8 + 6306300c_x^4(-348411\\
&+51380y^2 + 31700y^4) + 4620c_x^2(-5231114487 + 1749601320y^2 - 987393600y^4 + 2624000y^6))\\
&+30c_z^2(-293989386627767313 - 5074882377278490y^2 + 5354463694550040y^4 + 18535429018800y^6\\
&-374858764000y^8 + 160720000y^{10} + 378378000c_x^6(2681427 - 2314610y^2 + 132100y^4)\\
&-1455300c_x^4(-647189019 - 10652239710y^2 - 55817700y^4 + 4918000y^6)
\end{aligned}
$$

$$
\begin{aligned}
&-2520c_x^2(20743857583002 + 25464434292280y^2 + 3324544981605y^4 - 40002764400y^6 + 12978000y^8)))\\
&+58810752000c_y^{14}(-2939819794093160811 - 2369850309657506655y^2 - 50593173170480010y^4\\
&+7113647175209400y^6 + 14324320632750y^8 - 112617960000y^{10} + 18200000y^{12}\\
&+52972920000c_z^8(18297 - 89760y^2 + 36700y^4) + 7567560000c_x^8(-81801 - 557445y^2 + 193900y^4)\\
&+14553000c_x^6(1733895933 + 7443388635y^2 - 2581141725y^4 + 2104000y^6) - 18900c_x^4(4536345428553\\
&+54012413598275y^2 - 13231522292950y^4 - 39248834500y^6 + 221760000y^8)\\
&-210c_x^2(-6993661627522251 - 1861328468230582 5y^2 + 1294830577496625y^4 + 62808732556200y^6\\
&-240950781000y^8 + 5600000y^{10}) - 58212000c_z^6(940191303 + 832232910y^2 + 419521650y^4 - 4096000y^6\\
&+1820c_x^2(128961 - 400305y^2 + 95350y^4)) - 18900c_z^4(-3250317272397 - 33308592783100y^2\\
&-442257514700y^4 + 119190518000y^6 - 280140000y^8 + 2102100c_x^4(-411921 + 316680y^2 + 130900y^4)\\
&+4620c_x^2(-1641831039 + 1871466870y^2 - 1805512950y^4 + 8198000y^6))\\
&+420c_z^2(-7162555963751712 - 387832143521025y^2 + 657795553481625y^4 + 2695730679900y^6\\
&-86465967000y^8 + 61600000y^{10} + 31531500c_x^6(847467 - 2298810y^2 + 290200y^4)\\
&-207900c_x^4(158510541 - 6159178905y^2 + 166863425y^4 + 5478000y^6) - 45c_x^2(22221350469831\\
&+110695523876050y^2 + 22685562618600y^4 - 438709874000y^6 + 325920000y^8)))\\
&+9801792000c_y^{12}(-417916818914758000173 - 864885048272563689 0y^2 - 1065654452238303690y^4\\
&-11537375076629640y^6 + 700399259464500y^8 + 1330286590000y^{10} - 3511960000y^{12}\\
&+349272000c_z^8(-1003941 + 7623180y^2 - 6138100y^4 + 1024000y^6) + 174636000c_x^8(11864823\\
&-233190y^2 - 13336700y^4 + 1273000y^6) - 113400c_x^6(-887196257397 - 389241976905y^2\\
&-495069522725y^4 + 45846206000y^6 + 68840000y^8) - 3780c_x^4(-3437279523654903\\
&+34232439551655y^2 + 125384654372425y^4 - 8444501538150y^6 - 49393233000y^8 + 36400000y^{10})\\
&+6c_x^2(-11654169343676137278 + 652251406832232165y^2 + 286235321288065695y^4\\
&-5323314268133400y^6 - 214768101305250y^8 + 271463500000y^{10} + 44800000y^{12})\\
&-907200c_z^6(168429816441 + 190387617315y^2 + 24320520800y^4 + 5095083250y^6 - 23345000y^8\\
&+770c_x^2(-9895263 + 47267415y^2 - 23266300y^4 + 2049500y^6)) - 3780c_z^4(2976755961272247\\
&-49849176347220y^2 - 75618628312700y^4 - 643764821400y^6 + 58011702000y^8 - 61600000y^{10}\\
&+69300c_x^4(57637743 - 120616440y^2 - 2235700y^4 + 5478000y^6) + 180c_x^2(-107092467861\\
&-667361530040y^2 + 106012993450y^4 - 37284012000y^6 + 54320000y^8))\\
&+24c_z^2(-2333902800999535857 - 354228484666437990y^2 - 3006267968920545y^4\\
&+2150235137096025y^6 + 67987927383 75y^8 - 84594125000y^{10} + 18200000y^{12}\\
&+7276500c_x^6(-20204163 + 154663740y^2 - 60480800y^4 + 1052000y^6) - 28350c_x^4(-919522713411\\
&-143422975840y^2 - 281245718800y^4 - 6858403250y^6 + 73920000y^8) - 315c_x^2(-1439490885976953\\
&+240310138492530y^2 + 113605579772050y^4 + 10752637431600y^6 - 80602443000y^8 + 2800000y^{10})))\\
&-891072000c_y^{11}y(-4606097847829276479912 - 2919998563545851587 8y^2 - 2194734136867046775y^4\\
&-20193186627374310y^6 + 808312156289000y^8 + 1575621288000y^{10} - 2002000000y^{12}\\
&+2561328000c_z^8(-1432809 + 3502935y^2 - 1693200y^4 + 203500y^6) + 91476000c_x^8(181437228\\
&+47318355y^2 - 54623100y^4 + 2585500y^6) - 831600c_x^6(-1362682050633 - 175768729515y^2\\
&-147672765780y^4 + 6652677900y^6 + 15832000y^8) - 1980c_x^4(-72451420901955081 + 393210026768160y^2\\
&+512955424125585y^4 - 16900723040550y^6 - 129163048000y^8 + 22540000y^{10})\\
&+44c_x^2(-17400920401149829362 + 260183552223727755y^2 + 80065816985717955y^4 - 660083731279200y^6\\
&-33212408193000y^8 + 17627820000y^{10} + 2800000y^{12}) - 1663200c_z^6(1017702981621 + 383539538430y^2\\
&+27412923660y^4 + 4180627200y^6 - 13174000y^8 + 770c_x^2(-51737823 + 79334820y^2 - 22611900y^4\\
&+1312000y^6)) - 3960c_z^4(31333742037417897 - 191230515438795y^2 - 150233520527370y^4 - 1203402674400y^6\\
&+62777386000y^8 - 40180000y^{10} + 485100c_x^4(68452632 - 39230505y^2 - 4575900y^4 + 1229500y^6)\\
&+1890c_x^2(-133583471661 - 204910124130y^2 + 20164031140y^4 - 4513868200y^6 + 2884000y^8))\\
&-44c_z^2(140286951555885066 87 + 672868262798415495y^2 + 3507266787764670y^4 - 1765478202454800y^6\\
&-5415978177000y^8 + 39784080000y^{10} - 2800000y^{12} + 4158000c_x^6(204054984 - 464104935y^2 + 90377700y^4
\end{aligned}
$$

$$+1271500y^6) + 56700c_x^4(-2751513028983 - 243467055765y^2 - 130353175530y^4 - 5119837600y^6 + 19712000y^8)$$
$$-90c_x^2(30126694657203081 - 1848265510616910y^2 - 411203896722360y^4 - 31008869881200y^6$$
$$+139802278000y^8 + 21560000y^{10}))) - 8c_y y(-591227017520359529780708637706045 74$$
$$-39877806442977855692256177740278 8y^2 - 475245538304614298243126480376y^4$$
$$+693009196114576809234877110y^6 + 152550215206791437367832 5y^8 + 27364891362502300425y^{10}$$
$$-424870158236572125y^{12} + 13280328176925250y^{14} + 74805337240000y^{16} + 1809119812500000c_x^8(219 + 80y^2)$$
$$+2067565500000c_x^6(1622645556 + 33169115y^2 + 212555y^4 + 17100y^6) + 27846000c_x^4(-10195108778469288366$$
$$-1223014338153565 65y^2 - 375884077452345y^4 + 299637129825y^6 + 8063148500y^8 + 128096000y^{10})$$
$$+68c_x^2(162370995417448331028601381 4952 + 149415089570540526417441857 10y^2$$
$$+391351384504621485072928 80y^4 + 371482518497713235613 00y^6 - 627217826689992037 5y^8$$
$$-4749301170636750y^{10} + 342161162017500y^{12} + 2300754010000y^{14}) + 34c_z^2(324290519720175540434612199 8904$$
$$+298552295178543247978550614 20y^2 + 782976820422669311721882 60y^4 + 746547634607223587638 50y^6$$
$$-126467070570404313 75y^8 - 17727976303742250y^{10} + 584323676160000y^{12} + 4601508020000y^{14}$$
$$+425675250000000c_x^6(-57 + 10y^2) + 547296750000c_x^4(175391034 + 3896235y^2 + 2520y^4 + 1900y^6)$$
$$+819000c_x^2(-10151929600554434616 - 122188868115812190y^2 - 380963448672345y^4 + 263114482950y^6$$
$$+6186961000y^8 + 128096000y^{10}))) - 29702400c_y^9 y(-191049954372827644810 3002$$
$$-20744142157381545291312y^2 - 245803198289857881 75y^4 - 1319242465612416510y^6 - 11472056635382475y^8$$
$$+182677685085000y^{10} + 390341920000y^{12} - 74844000c_x^8(776832903 - 282403240y^2 - 194528040y^4$$
$$+28431200y^6 + 376000y^8) + 87318000c_z^8(47594601 - 164139480y^2 + 115821720y^4 - 26709600y^6 + 1882000y^8)$$
$$-277200c_x^6(-6870775516938 - 24861434309775y^2 - 1255220125155y^4 - 253325249100y^6 - 790414000y^8$$
$$+7420000y^{10}) + 1980c_x^4(9214533778582639647 + 30456196541776971 0y^2 - 1833611387721120y^4$$
$$-334236906784350y^6 - 250208793000y^8 + 27249600000y^{10} + 2800000y^{12}) - 60c_x^2(299018029582284595 0209$$
$$+674170358750950778 64y^2 - 862092554384338 20y^4 - 364186964102430 15y^6 - 127199194760000y^8$$
$$+4978730292000y^{10} + 1343100000y^{12}) - 277200c_z^6(-61535878015563 + 27749695055850y^2 + 3299888968920y^4$$
$$+96838277400y^6 + 9097166000y^8 - 11480000y^{10} + 3780c_x^2(97807383 - 199974290y^2 + 83896560y^4$$
$$-9873800y^6 + 206000y^8)) - 3960c_z^4(3341888818720370289 + 151163852726740770y^2 - 385256348694315y^4$$
$$-95078886509700y^6 - 807929908500y^8 + 13280400000y^{10} - 1400000y^{12} + 1058400c_x^4(-75885372$$
$$+69562785y^2 - 1860015y^4 - 2787300y^6 + 176000y^8) - 420c_x^2(-27869908483656 + 1282067206200y^2$$
$$+827129510865y^4 - 58574981700y^6 + 5019279500y^8 + 1540000y^{10})) - 30c_z^2(6278174211148974926253$$
$$+938451421116750243 78y^2 + 124488004776536 0160y^4 + 407758774646322 0y^6 - 964346904598000y^8$$
$$-3124662396000y^{10} + 6006000000y^{12} + 3326400c_x^6(285849459 + 1704749130y^2 - 719008920y^4 + 14427600y^6$$
$$+3958000y^8) + 27720c_x^4(91568861159562 - 31490996753025y^2 - 1693179835380y^4 - 119246237100y^6$$
$$-9343294000y^8 + 3220000y^{10}) - 132c_x^2(2297623977471442347 + 106313116186189710y^2$$
$$-2854011156041745y^4 - 188606953031850y^6 - 11351941113000y^8 + 11734800000y^{10} + 2800000y^{12})))$$
$$+89107200c_y^{10}(-636129563136538674282849 - 222841699094656425479 85y^2 - 613795394922568474 77y^4$$
$$-338400656359790409 0y^6 - 29009549063993850y^8 + 749110928868500y^{10} + 1526170746250y^{12}$$
$$-638000000y^{14} + 8316000c_x^8(-3399947649 + 6050745855y^2 + 2399394900y^4 - 862802500y^6 + 13260000y^8)$$
$$+29106000c_z^8(51298461 - 572733720y^2 + 684011400y^4 - 220820000y^6 + 20010000y^8)$$
$$-138600c_x^6(-8288928254466 - 43877804942655y^2 - 3132156778425y^4 - 1383754134300y^6 + 22636659000y^8$$
$$+90400000y^{10}) + 990c_x^4(6098708303452131318 + 68747028143344740 0y^2 - 3727449758377695y^4$$
$$-1652091205547650y^6 + 20267473612875y^8 + 249452840000y^{10} + 16800000y^{12})$$
$$+110c_x^2(-543456999475861597119 - 354016510316444853 99y^2 + 173166178404204090y^4$$
$$+497260004247304 20y^6 - 69400827944775y^8 - 11882086253500y^{10} + 319420000y^{12})$$
$$-554400c_z^6(-10543792652379 + 14834423108430y^2 + 2849459534550y^4 + 126337673550y^6 + 14778718500y^8$$
$$-30800000y^{10} + 105c_x^2(716061303 - 4687682310y^2 + 3449429700y^4 - 621305000y^6 + 23280000y^8))$$
$$-3960c_z^4(1111237657418483658 + 154979004547382400y^2 - 546428848006545y^4 - 236007773648150y^6$$
$$-1903752922125y^8 + 56570290000y^{10} - 18200000y^{12} + 44100c_x^4(-833222736 + 2692068345y^2 - 523068900y^4$$
$$-135827500y^6 + 15840000y^8) + 210c_x^2(20375593561917 - 5312211064515y^2 - 3847915898775y^4$$

$$+288336440100y^6 - 40729495500y^8 + 2800000y^{10})) - 220c_z^2(284669260922913364827 + 13626804225660990462y^2$$
$$+313277632061039730y^4 + 1189154847719790y^6 - 419599767915675y^8 - 1304466839500y^{10} + 5268640000y^{12}$$
$$+75600c_x^6(1440441198 + 10978251165y^2 - 10216632300y^4 + 916527500y^6 + 51630000y^8)$$
$$+1890c_x^4(65776447179684 - 75779102389905y^2 - 4944040936425y^4 - 919809898050y^6 - 50441721000y^8$$
$$+72800000y^{10}) - 9c_x^2(1503668071228542093 + 271514932771890150y^2 - 9657944553866070y^4$$
$$-1131839414731900y^6 - 73487947722750y^8 + 180977440000y^{10} + 44800000y^{12})))$$
$$-16320c_y^7y(-33853058396354390596676226954 - 513465731835801682474204668y^2$$
$$-1405044439536002464639440y^4 + 9156772425072274902290y^6 - 2550885254580745582 5y^8$$
$$-2908754325697447 50y^{10} + 1216532816646000y^{12} + 2393044420000y^{14} + 3531528000c_z^8(-42224004$$
$$+230565285y^2 - 214044120y^4 + 69870600y^6 - 9212000y^8 + 410000y^{10}) - 504504000c_x^8(-11229387372$$
$$+10363776255y^2 + 2109270240y^4 - 757595700y^6 - 10906000y^8 + 2380000y^{10}) + 33633600c_x^6(-166814275344966$$
$$-67513620735765y^2 + 18383402517570y^4 + 548644381650y^6 + 22709763000y^8 + 905370000y^{10} + 200000y^{12})$$
$$+109200c_x^4(547863549580507160385 + 37610192542769630784y^2 + 292101316466114925y^4 - 2261894019154605y^6$$
$$-115218768813500y^8 - 1860744879750y^{10} + 316800000y^{12}) - 1820c_x^2(2009557019237209674618078$$
$$+2896526105786639367486y^2 + 2105130112171446313 80y^4 + 98279658634674330y^6 - 26017039290743325y^8$$
$$-262685097864000y^{10} + 758664640000y^{12}) + 33633600c_z^6(-106538851119141 + 120553718365485y^2$$
$$-15438060812430y^4 - 943785863100y^6 - 13497507000y^8 - 952680000y^{10} + 200000y^{12} + 420c_x^2(427094046$$
$$-1106056215y^2 + 581830830y^4 - 95693400y^6 + 3763000y^8 + 110000y^{10})) - 109200c_z^4(374067666569648457945$$
$$+34508806794925180641y^2 + 445713465705371325y^4 - 846552485961270y^6 - 76060286054500y^8$$
$$-761230464000y^{10} + 3003000000y^{12} + 194040c_x^4(1369562904 - 1612047285y^2 + 188699220y^4 + 62170650y^6$$
$$-8383000y^8 + 115000y^{10}) - 924c_x^2(157788224498709 - 69219641993265y^2 - 4605036936930y^4$$
$$+20422031400y^6 - 20097417000y^8 + 417270000y^{10} + 200000y^{12})) - 3640c_z^2(120863019387783464 5473864$$
$$+1405853217623663947 2843y^2 + 48767885017928708940y^4 + 295226640261799290y^6 + 1333203579911775y^8$$
$$-107469831627000y^{10} - 390695680000y^{12} + 3880800c_x^6(-1041477021 - 601282035y^2 + 614034270y^4$$
$$-36113850y^6 - 6898000y^8 + 265000y^{10}) - 27720c_x^4(163755869314059 - 152093777839515y^2$$
$$+9162958110570y^4 + 384476029650y^6 - 1373389500y^8 + 973620000y^{10} + 200000y^{12})$$
$$+60c_x^2(-73172474707391163720 - 5310653461905512259y^2 - 25509983392953675y^4 + 1618573796917605y^6$$
$$+34051200804500y^8 + 2533280061000y^{10} + 1343100000y^{12}))) - 816c_y^5y(-49188967938151794 18284411418048$$
$$-865229745419573156487360896 40y^2 - 352402816168621468102392540y^4 - 413447512720514407235100y^6$$
$$+419396902960567657125y^8 - 416089682645889525 0y^{10} - 58921773322895000y^{12} - 67775986480000y^{14}$$
$$+3363360000c_z^8y^2(-57 + 10y^2)^3(342 - 237y^2 + 10y^4) + 3363360000c_x^8(-640766700 + 1595535894y^2$$
$$+59909031y^4 - 97742520y^6 - 2145600y^8 + 492000y^{10} + 10000y^{12}) + 24024000c_x^6(767720140631388$$
$$+588424632177 69y^2 - 103878228139245y^4 - 1124361797400y^6 - 22549614000y^8 - 1862400000y^{10}$$
$$+59900000y^{12}) - 36400c_x^4(119275593327311130115 56 - 225142377047280223007 4y^2$$
$$-2825673291241601377 5y^4 - 62377614492492420y^6 + 1035600678505800y^8 + 20524311108000y^{10}$$
$$+790694540000y^{12}) + 40c_x^2(-20246676831357898041262336194 - 276212798980508825723656368y^2$$
$$-1047503522103887843434440y^4 - 2808779605251308398710y^6 + 301082749790747925y^8$$
$$+1521877015540927 50y^{10} + 233405685285850 0y^{12} + 2393044420000y^{14}) + 24024000c_z^6(138227438741238$$
$$-288887362629831y^2 + 84845962067580y^4 - 4544178197400y^6 - 177917100000y^8 - 1208190000y^{10}$$
$$-91000000y^{12} + 280c_x^2(-291678975 + 1019575188y^2 - 595914138y^4 + 110465460y^6 - 4831200y^8$$
$$-366000y^{10} + 20000y^{12})) + 72800c_z^4(392104080558593037 1422 - 147257261237610345313 8y^2$$
$$-4071641222060958892 5y^4 - 236012206211925165y^6 + 408379725062100y^8 + 16139482888500y^{10}$$
$$+195878480000y^{12} + 69300c_x^4(3499339725 - 4702082724y^2 + 788821524y^4 + 133513920y^6 - 25052400y^8$$
$$+168000y^{10} + 40000y^{12}) - 990c_x^2(369365003637462 - 252839388665619y^2 - 8440084011555y^4$$
$$+4483342509900y^6 + 111131575500y^8 + 2661510000y^{10} + 40700000y^{12}))$$
$$+20c_z^2(-448652045263339265241452438 88 - 66090172882702708536340143 6y^2$$
$$-1857021647020557771884130y^4 + 1291815878854799598 30y^6 - 2093574538052272275y^8$$
$$-90394956131093250y^{10} + 1358072820342000y^{12} + 4786088840000y^{14} + 168168000c_x^6(-5771875725$$

$$
\begin{aligned}
&+413362926y^2+1714851324y^4-149203080y^6-24692400y^8+1068000y^{10}+40000y^{12})\\
&+10810800c_x^4(-67161143226429+134292355507023y^2-19278958286490y^4-1083910278300y^6\\
&-22123617000y^8-959860000y^{10}+3200000y^{12})-7280c_x^2(96146261584804782803\\
&+2024446189508272987 38y^2+1245391320359866 6800y^4+86002042669409790y^6\\
&+94275659570400y^8-4740293511000y^{10}+189135520000y^{12})))\\
&+212160c_y^8(-259889522461218989644482 6390-1287159052976210820252868 56y^2\\
&-64552582454521815259452 0y^4-1188904629463064583 30y^6-2049355982269530742 5y^8\\
&-196393970889616500y^{10}+1766160270890750y^{12}+3860769450000y^{14}\\
&+407484000c_z^8(-31668003+607433040y^2-985746600y^4+457869600y^6-78798000y^8+4400000y^{10})\\
&-116424000c_x^8(-5805558927+21102745860y^2+108183600y^4-2677071600y^6+133668000y^8\\
&+8800000y^{10})-1940400c_x^6(326568696034158+82855688672295y^2-136121974226595y^4\\
&-5174039143800y^6-470662818000y^8-9133140000y^{10}+1600000y^{12})\\
&+23100c_x^4(194176172371043004282+5068876346838471 1824y^2+741317697435521745y^4\\
&-5041689610501530y^6-452892227082975y^8-4294601584000y^{10}+15396840000y^{12})\\
&-210c_x^2(13377835429196108605770 42+5916941655393290014647 0y^2+7004774312002805939 37y^4\\
&+49057620108290640y^6-16954548062222677 5y^8-1217566922448250y^{10}+12242820935000y^{12}\\
&+3828000000y^{14})-7761600c_z^6(38065572432027-141204099379770y^2+30936295532070y^4\\
&+2545297105050y^6+51542688000y^8+4078065000y^{10}-2600000y^{12}+210c_x^2(-377705997\\
&+3304576710y^2-3150581400y^4+818807400y^6-61182000y^8+200000y^{10}))\\
&-46200c_z^4(67570805821885640694+1965868790703342216 3y^2+434393660550487365y^4\\
&-915800957755110y^6-133697032240950y^8-1227039508000y^{10}+10540080000y^{12}\\
&+846720c_x^4(87299883-367928190y^2+129019725y^4+12728025y^6-4680750y^8+162500y^{10})\\
&-252c_x^2(130878237462021-220326936728085y^2-4179344841765y^4+1439507628900y^6\\
&-136063243500y^8+6463670000y^{10}+3200000y^{12}))-420c_z^2(1108800c_x^6(-4645618677\\
&-1182882015y^2+10572625350y^4-1980638100y^6-89337000y^8+11300000y^{10})\\
&-166320c_x^4(20834724098016-65657712931785y^2+9456333768435y^4+440129787150y^6\\
&+10388444000y^8+1492970000y^{10}+200000y^{12})-220c_x^2(1195832276555013228 6\\
&+5609757920633102187y^2+9685793332361128 5y^4-2590362039338640y^6-993641982835 50y^8\\
&-6076439863250y^{10}+316620000y^{12})+3(26820120968461478461 0032+10108808775954771317820y^2\\
&+6931548956214579242 7y^4+592708358122185690y^6+2029410072956475y^8-296370034119500y^{10}\\
&-1015815277500y^{12}+638000000y^{14})))-272c_y^4(20961429390127048500713665778148\\
&+4380489185435839885462572537018y^2+3742102827992334590858661588 0y^4\\
&+1030698552422090116195681 05y^6+9939395046307435233525 0y^8-6123654709656283800 0y^{10}\\
&+1044629113500847875y^{12}+15051265330518750y^{14}+35847628085000y^{16}+5045040000c_z^8y^4(57-10y^2)^4\\
&+5045040000c_x^8(187839000+468157725y^2-261012699y^4-55292220y^6+5459400y^8+672000y^{10}\\
&+10000y^{12})+3603600c_x^6(2333486180544750-2857607560723545y^2-958385978730243y^4\\
&+104925982712040y^6+10236315522600y^8+202667700000y^{10}+4121560000y^{12}+58000000y^{14})\\
&+3120c_x^4(-877872212400566646613 35+1214290200480424805312 19y^2+2230240044266573089905y^4\\
&+8750824337441590519 5y^6+417989082439137825y^8+425061707272125y^{10}-10031541661750y^{12}\\
&+968401012500y^{14})-6c_x^2(-3180469452698048695428463943724-1921773866553278869643141830 20y^2\\
&-1246238704126061047128451725y^4-2435236255025064215299575y^6-1319587137495380754000y^8\\
&+7802866010984669625y^{10}+148616489928326875y^{12}+3087601887050000y^{14})\\
&+14414400c_z^6y^2(-57+10y^2)(4040842469265-2577963320919y^2+118982283525y^4+3580882800y^6\\
&+19391500y^8+1450000y^{10}+350c_x^2(-5117175+5774328y^2-1108620y^4+21600y^6+4000y^8))\\
&+780c_z^4(123975124024512889095660-435189594556251022130874y^2+745247797198022735451 45y^4\\
&+138774986717576081 1030y^6+591099733842466 1175y^8-961118920007400 0y^{10}-274892325914500y^{12}\\
&-3860769450000y^{14}+9702000c_x^4(230272875-1517377050y^2+727114104y^4-18299880y^6-16682400y^8
\end{aligned}
$$

$$
\begin{aligned}
&+888000y^{10}+40000y^{12})+13860c_x^2(-471924149508000+1987761992503455y^2-357177952993743y^4\\
&-72724990332960y^6+6007522070100y^8+139646100000y^{10}+1670560000y^{12}+58000000y^{14}))\\
&+12c_z^2(158274328146587470358864934811 2+10480405995940387245797559501 0y^2\\
&+732420564485964202692268425y^4+11803542111244205823501 00y^6-15937929006417961042 50y^8\\
&-2180288034763088250y^{10}+52977125360022500y^{12}-133629976993750y^{14}+420420000c_x^6(-1032962625\\
&+1887131925y^2+423179154y^4-211084380y^6-5297400y^8+1788000y^{10}+40000y^{12})\\
&+1801800c_x^4(125849644373250+767133716655915y^2-485082209020059y^4+3056518313520y^6\\
&+4003403976300y^8+80465325000y^{10}+1448030000y^{12}+29000000y^{14})+130c_x^2(-11169084916460385744984 0\\
&+2048961802600224973137 6y^2+42371029530479532866445y^4+87627309498254448153 0y^6\\
&+3743295817968785925y^8-4557768855024000y^{10}-201441800812000y^{12}+6417300000y^{14})))\\
&+816c_y^6(-48936477000055640836363403992368-31244033480841448991238967452 0y^2\\
&-22280987369870725223704977 00y^4-36638300391410749887355 50y^6+48894731217813502271 25y^8\\
&-43932186945441795000y^{10}-616051351224400000y^{12}+546261725725000y^{14}\\
&+5045040000c_z^8y^2(57-10y^2)^2(-68229+136230y^2-45020y^4+2600y^6)-5045040000c_x^8(498307950\\
&-6566901579y^2+1595368170y^4+777976380y^6-67165200y^8-6724000y^{10}+140000y^{12})\\
&+12012000c_x^6(2631438496653372-1900987055089479y^2-1308514640853735y^4+92630235313350y^6\\
&+2306532909600y^8+32552109000y^{10}+3865640000y^{12})-109200c_x^4(4897589584761667764432\\
&-4458491917022825166870y^2-1239306909233221229 94y^4-55859486297236083 0y^6+51049211694104 25y^8\\
&+162665117821250y^{10}+3769157530000y^{12}+1914000000y^{14})-780c_x^2(1036582910017897622687209980\\
&+4543484074019888485534754 4y^2+3183805679561827203010 05y^4+1480847900082379092495y^6\\
&+614757375080125200y^8-107456758435035625y^{10}-1353828121569875y^{12}+4278200000y^{14})\\
&+12012000c_z^6(322612360509222-2479738073758029y^2+1301880462649515y^4-106733542642650y^6\\
&-5103517041900y^8-51575661000y^{10}-3516160000y^{12}+840c_x^2(-291678975+3885778008y^2-4418433090y^4\\
&+1379327940y^6-135102600y^8+38000y^{10}+320000y^{12}))+54600c_z^4(5510508245859228832836\\
&-6967070626755322258560y^2-3179144176589605863 87y^4-26560515002279850 90y^6+47767074636822 75y^8\\
&+276944437880000y^{10}+3032758852500y^{12}-3828000000y^{14}+277200c_x^4(2076226425-10658631942y^2\\
&+4810011660y^4+111573540y^6-168141600y^8+9758000y^{10}+120000y^{12})+660c_x^2(-1061024024951478\\
&+2984270460413571y^2-363810489499485y^4-64038544545150y^6-1432828908900y^8-90263931000y^{10}\\
&+102740000y^{12}))-780c_z^2(1148299643317046101139661480+5458015525101294777999854 4y^2\\
&+2892641689601455590136 80y^4+42627667676996562237 0y^6+21135417177141555 75y^8\\
&+17624678688155000y^{10}-680350865601750y^{12}-2573846300000y^{14}+6468000c_x^6(8304239475-10451679966y^2\\
&-8902862820y^4+2801556720y^6+93661200y^8-28456000y^{10}+160000y^{12})-46200c_x^4(-426952144622178\\
&+3626997585480171y^2-1362660788323485y^4+9580368731850y^6+663274866600y^8-51361716000y^{10}\\
&+2563340000y^{12})+70c_x^2(4071439994901225821028-1539072704363466375180y^2+2908100666892387789 9y^4\\
&+7384833860493196 80y^6+9850180328151075y^8+56184074168750y^{10}+12353077895000y^{12}+7656000000y^{14})))\\
&-34c_y^2(139553683825020270561521592145759 44+16332843520603004762896849833411 36y^2\\
&-50181368059239909540272666442 0y^4-37308872500324285743418536 00y^6-56402334823012454332806 75y^8\\
&-12792065948134466994 00y^{10}+3662248700604516750y^{12}+17257063514407500y^{14}+439347981079375y^{16}\\
&+17027010000000c_x^8(-33075-6114y^2+12040y^4+1400y^6)+5405400000c_x^6(-512545888890+691727176539y^2\\
&+145689732405y^4+2886066120y^6+38323800y^8+878000y^{10})+9360c_x^4(17857306170192697015500\\
&-2556096264446042995261 2y^2-3161302210745224986825y^4-34916134994649922860y^6\\
&-102944187702816075y^8+146120500499050y^{10}+3512766551000y^{12}+30107225000y^{14})\\
&+8c_x^2(-48734234962641359655755805133 56+63637415546817056278328829214 38y^2\\
&+59975458855777284404234029380y^4+16095715306942261333808965 5y^6+13665616896340559312662 5y^8\\
&-12392641589975634487 5y^{10}+7296761730534412 5y^{12}+475279126526250 0y^{14}+35847628085000y^{16})\\
&+18720c_z^4y^2(8264665833111183058794-1316837149084453827600y^2-16597090656928182555y^4\\
&-53171197647148350y^6+381327786320 25y^8+1109336700500y^{10}+15053612500y^{12}
\end{aligned}
$$

$$
\begin{aligned}
&+12733875000c_x^4(57-10y^2)^2+1155000c_x^2(-179652699009+27588535695y^2+661690155y^4+3607200y^6\\
&+219500y^8))+8c_z^2(-4864370267448147387642108754356+6345857626980967481671559712438y^2\\
&+59839749014561301164160411630y^4+160934345001656920702413405y^6+13796553856254218461912 5y^8\\
&-12495536046914407 9875y^{10}+2234750025556912 5y^{12}+4111250769731250y^{14}+35847628085000y^{16}\\
&+8513505000000c_x^6(12825-23907y^2-980y^4+700y^6)+675675000c_x^4(-497610636390-79022576997y^2\\
&+256529526435y^4+5385642990y^6+52752600y^8+1756000y^{10})+2340c_x^2(8883143509337453664000\\
&-4396201054043033073762y^2-2896614287701080078825y^4-34065319408958909610y^6\\
&-104775790256173575y^8+105665644037800y^{10}+2865719976000y^{12}+30107225000y^{14})))\\
&-136c_y^3y(378378000000c_x^8(-1096740-2106297y^2+106380y^4+89100y^6+4000y^8)\\
&+14414400c_x^6(-530605482954750+25848850200453y^2+50799268917180y^4+3068699980140y^6\\
&+56728472400y^8+963888000y^{10}+10720000y^{12})+3120c_x^4(108917966230617704704236\\
&-19550149637667290317368y^2-4441684425078444428115y^4-52010916748202217960y^6\\
&-155308937861777700y^8+420653286616500y^{10}+9049577796000y^{12}+92040170000y^{14})\\
&+24c_x^2(-15961864253230831994170 81802532-2853789714393965131580681886 0y^2\\
&-10849999012999135570271691 0y^4-13004967828956242954815 0y^6+36821373734280510375y^8\\
&+1954082337785077 50y^{10}+908287618420000y^{12}+66138952280000y^{14})-5(89220766929742041526019880112 32\\
&-22040254489805864755452102693 6y^2-15525944921825617439127207 24y^4-28634720801948874009797 40y^6\\
&-11826460790520876249 75y^8+2462451169487727600y^{10}+25415396432994750y^{12}+358985408818000y^{14})\\
&+57657600c_z^6y^2(57-10y^2)^2(4725233793+102784185y^2+948990y^4+26800y^6+26250c_x^2(-57+10y^2))\\
&+6240c_z^4(-24794464371785098815132+20272299186841820940591y^2-18193412526343327107 45y^4\\
&-24599387128593459105y^6-81816426216721350y^8+126916398015750y^{10}+2721923148000y^{12}\\
&+46020085000y^{14}+181912500c_x^4(-1364580+1922553y^2-334620y^4-15900y^6+4000y^8)\\
&+13860c_x^2(67392149769000-56674834385211y^2-725289331410y^4+974387888820y^6+19807936200y^8\\
&+246444000y^{10}+5360000y^{12}))+24c_z^2(-15901998710629489819351540870 32-29959254980014142294038136610y^2\\
&-12050592814524586488332166 0y^4-13599312138302852776815 0y^6+15165044541820585912 5y^8\\
&+85993368990813375y^{10}-4785383875711250y^{12}-16943996620000y^{14}+94594500000c_x^6(1666170-447561y^2\\
&-214560y^4+18300y^6+2000y^8)+1801800c_x^4(-29594808999000-133464603161547y^2+22256607908430y^4\\
&+2473782722640y^6+46147172400y^8+728388000y^{10}+10720000y^{12})+520c_x^2(14562136031912845109118\\
&+5379496818442818539391y^2-20188841273981471772 45y^4-25312835886577979355y^6\\
&-79896736610367600y^8+161471601443250y^{10}+3623356023000y^{12}+46020085000y^{14})))). \qquad \text{(B.23)}
\end{aligned}
$$

7. The solution of Boltzmann equation at 10th order ($\Phi^{(10)}$) is

$$
\begin{aligned}
\Phi^{(10)}(y,\boldsymbol{c}) \;=\; & \frac{1}{90632662481689453125}2(-123891575218377084518400000000000c_y^{30} \\
& +4640392319062500000000c_x^{10}+123891575218377084518400000000000c_y^{29}y \\
& +5899598819922718310400000000000c_y^{27}y(-3099+1050c_z^2-6825c_x^2+35y^2) \\
& -1769879645976815493120000000000c_y^{28}(-1033+350c_z^2-2275c_x^2+35y^2) \\
& +309359487937500000000c_x^8(-3375-1221y^2+40y^4)+29462808375000000c_x^6(248062500 \\
& +31580233272y^2+310057965y^4-330680y^6+51300y^8)+198402750000c_x^4(-92093203125000 \\
& -3216466350888906986 64y^2-1904001341829747930y^4-3606473456495910y^6+2648498383575y^8 \\
& +28230298800y^{10}+512384000y^{12})+1453500c_x^2(9428041669921875000 \\
& +15610285763348997277053543062016y^2+7171808266957884529772426634 0y^4 \\
& +12230770951898824631614308 0y^6+8080875482148639467797 5y^8-153842869903070848 50y^{10} \\
& -5350785622250250y^{12}+343149985320000y^{14}+2300754010000y^{16}) \\
& +2375(-576996150199218750000-42322259235784821987074407376857547 04y^2 \\
& -1503958893798433045061719270871431 2y^4-1617602735226918380295901059914 4y^6 \\
& +2330546938047722258666171370y^8+1297396095484677216551523 0y^{10}+4021271932719073032 00y^{12} \\
& -289568543705023950 0y^{14}+67700816693789625y^{16}+349806477920000y^{18}) \\
& -3953465763287040000000000c_y^{26}(3840234309+3133746000c_z^4+14885293500c_x^4 \\
& -2312103255y^2+13043800y^4-11191950c_z^2(1657+3640c_x^2-70y^2) \\
& -2356200c_x^2(-71934+2135y^2))+3953465763287040000000000c_y^{25}y(3871159434+3133746000c_z^4 \\
& +14885293500c_x^4-770598675y^2+2597980y^4-3730650c_z^2(4971+10920c_x^2-70y^2) \\
& -196350c_x^2(-862893+8330y^2))+5068545850368000000000c_y^{23}y(655238363895909 \\
& +24443218800000c_z^6+161936324550000c_x^6+5102146804170y^2-299725826400y^4 \\
& +467467000y^6-116396280000c_z^4(1872+4095c_x^2-35y^2)+10720710000c_x^4(-257427+1535y^2) \\
& -3900c_x^2(1027645845279-54961714500y^2+148656200y^4)+7800c_z^2(10635674013+44655880500c_x^4 \\
& -3090075450y^2+12989900y^4-392700c_x^2(-1300167+16660y^2))) \\
& -1520563755110400000000c_y^{24}(8147739600000c_z^6+53978774850000c_x^6 \\
& -116396280000c_z^4(624+1365c_x^2-35y^2)+10720710000c_x^4(-85899+1715y^2) \\
& -1300c_x^2(1027998663129-167893387200y^2+786401000y^4)+3(73121922497601 \\
& +1689754991730y^2-166854387700y^4+371371000y^6)+2600c_z^2(10511973513+44655880500c_x^4 \\
& -9271762500y^2+65219000y^4-1178100c_x^2(-433599+17080y^2))) \\
& +1689515283456000000 0c_y^{21}y(-6534926757181458+366648282000000c_z^8+415752962625000c_x^8 \\
& +3247326075368475y^2+7821043608150y^4-211179078000y^6+175945000y^8 \\
& -17459442000000c_z^6(2517+5460c_x^2-70y^2)+22972950000c_x^6(-1646583+34300y^2) \\
& +643500c_x^4(655042380213-19486596150y^2+23559200y^4)-39000c_x^2(5962669735140 \\
& +510638981541y^2-7711285890y^4+8816500y^6)+234000c_z^4(8683567857+44655880500c_x^4 \\
& -4654315050y^2+25979800y^4-40055400c_x^2(-12861+245y^2))+150c_z^2(284536328967387 \\
& +64774529820000c_x^6+2820941343870y^2-240347807700y^4+467467000y^6 \\
& +3216213000c_x^4(-346533+3070y^2)-3120c_x^2(512100683313-41393536800y^2+148656200y^4))) \\
& -1520563755110400000000c_y^{22}(-731648567348787+40738698000000c_z^8+46194773625000c_x^8 \\
& +1087256769758385y^2+4285287054300y^4-165734684500y^6+187495000y^8 \\
& -5819814000000c_z^6(839+1820c_x^2-70y^2)+15315300000c_x^6(-274588+17465y^2) \\
& +71500c_x^4(657040583763-62349532350y^2+159005000y^4)-22750c_x^2(1144281585141 \\
& +292978856040y^2-7636123660y^4+13090000y^6)+26000c_z^4(8498017107+44655880500c_x^4 \\
& -13966017450y^2+130438000y^4-3534300c_x^2(-145863+8540y^2))+50c_z^2(95420520492129 \\
& +21591509940000c_x^6+2794666235010y^2-401427726700y^4+1114113000y^6 \\
& +3216213000c_x^4(-115691+3430y^2)-1040c_x^2(512371623213-126468445950y^2+786401000y^4))) \\
& +120679663104000000c_y^{19}y(-79024399236940001733+102661518960000000c_z^{10}
\end{aligned}
$$

$$
\begin{aligned}
&-481684180477500000c_x^{10} - 149566809237226605 0y^2 + 225071488601019900y^4 + 281117404782000y^6 \\
&-3946082630000y^8 + 1729700000y^{10} - 12221609400000000c_z^8(129 + 273c_x^2 - 7y^2) + 8040532500000c_x^8(1304019 \\
&+19445y^2) + 40950000c_x^6(-640411257051 - 226448006400y^2 + 1231399400y^4) + 52500c_x^4(-6650711776947177 \\
&+1779491471646330y^2 - 13010011914900y^4 + 1850849000y^6) - 700c_x^2(-933911214203631717 \\
&+729914471630966 70y^2 + 1963996562079450y^4 - 12689975017500y^6 + 6735575000y^8) \\
&+327600000c_z^6(948253833 + 14885293500c_x^4 - 3128479200y^2 + 25979800y^4 - 392700c_x^2(-448929 + 16660y^2)) \\
&+2100000c_z^4(17535493102419 + 3238726491000c_x^6 + 234111296484y^2 - 36193957800y^4 + 93493400y^6 \\
&+643242600c_x^4(-89106 + 1535y^2) - 234c_x^2(338113478079 - 55650718200y^2 + 297312400y^4)) \\
&+2800c_z^2(-3534346756617957 + 207876481312500c_x^8 + 3513105010961145y^2 + 10875216355200y^4 \\
&-423251317500y^6 + 439862500y^8 + 11486475000c_x^6(-1689927 + 68600y^2) + 965250c_x^4(229885724907 \\
&-13099241400y^2 + 23559200y^4) - 1950c_x^2(78563375754363 + 10179808543440y^2 - 232198173900y^4 \\
&+352660000y^6))) - 84475764172800000c_y^{20}(-11460308269003128819 + 14665931280000000c_z^{10} \\
&-68812025782500000c_x^{10} - 647705440038763350y^2 + 161611875344938500y^4 + 267790702230000y^6 \\
&-5198923800000y^8 + 3180100000y^{10} - 5237832600000000c_z^8(43 + 91c_x^2 - 7y^2) + 3445942500000c_x^8(437133 \\
&+14525y^2) + 5850000c_x^6(-656754345351 - 657445819800y^2 + 6520283000y^4) + 22500c_x^4(-2237102025989139 \\
&+1840129904276430y^2 - 25153521292900y^4 + 13544531000y^6) - 300c_x^2(-315540965646589239 \\
&+75802343877168990y^2 + 3299298239642400y^4 - 31713299695000y^6 + 24734325000y^8) \\
&+46800000c_z^6(824553333 + 14885293500c_x^4 - 9388509900y^2 + 130438000y^4 - 1178100c_x^2(-149853 + 17080y^2)) \\
&+900000c_z^4(5903330075073 + 1079575497000c_x^6 + 230177618736y^2 - 60458458060y^4 + 222822600y^6 \\
&+31518887400c_x^4(-608 + 35y^2) - 78c_x^2(338491601979 - 170087009400y^2 + 1572802000y^4)) \\
&+3600c_z^2(-397381343305773 + 23097386812500c_x^8 + 1178309801514180y^2 + 5939709332550y^4 \\
&-332218425000y^6 + 468737500y^8 + 3828825000c_x^6(-563939 + 69860y^2) + 107250c_x^4(231232599807 \\
&-41941038300y^2 + 159005000y^4) - 650c_x^2(26492839001541 + 10219776586320y^2 - 402487269800y^4 \\
&+916300000y^6))) + 670442572800000c_y^{17}y(-228283419714417695565 - 230015520791523252261y^2 \\
&-1326637354276102680y^4 + 95073697519457400y^6 + 85403221714500y^8 - 588678510000y^{10} + 107800000y^{12} \\
&+30798455688000000c_z^{10}(-9 + 10y^2) - 14472958500000c_x^{10}(-330633 + 80270y^2) \\
&+28378350000c_x^8(-5569770759 + 814303725y^2 + 8715700y^4) + 12285000c_x^6(137777694828687 \\
&-1401896759970y^2 - 733703008500y^4 + 1343111000y^6) - 6300c_x^4(1000772416467665739 \\
&+173390667128958285y^2 - 11840873124715650y^4 + 28111185795000y^6 + 9929150000y^8) \\
&-90c_x^2(-44617142249951404203 - 21096906823633501980y^2 + 448935346845563550y^4 \\
&+64097149605735 00y^6 - 20091693370000y^8 + 4326700000y^{10}) - 454053600000c_z^8(12562299 + 10406775y^2 \\
&-168700y^4 + 89250c_x^2(-333 + 238y^2)) + 196560000c_z^6(409448206413 + 5807393070y^2 - 4676606550y^4 \\
&+17979500y^6 + 20616750c_x^4(-9891 + 3070y^2) - 2310c_x^2(-38597079 - 370316400y^2 + 3861200y^4)) \\
&+25200c_z^4(-329171797579311 + 4295473775177760y^2 + 18330690392100y^4 - 1274219760000y^6 \\
&+1759450000y^8 + 643242600000c_x^6(-1548 + 1225y^2) + 27027000c_x^4(834098379 - 479420475y^2 \\
&+1682800y^4) - 23400c_x^2(3088924578909 + 840404765835y^2 - 38986228050y^4 + 88165000y^6)) \\
&+90c_z^2(-9345219733566565947 - 319227430972349970y^2 + 97049786610092400y^4 + 158021429112000y^6 \\
&-3162122530000y^8 + 1729700000y^{10} + 804053250000c_x^8(159831 + 38890y^2) + 1261260000c_x^6(-1719819459 \\
&-1507512900y^2 + 15992200y^4) + 409500c_x^4(4359325260249 + 47793467109810y^2 - 671549825100y^4 \\
&+142373000y^6) - 140c_x^2(-350187203397157821 + 95624538706463310y^2 + 3917852336759850y^4 \\
&-38185893982500y^6 + 26942300000y^8))) - 670442572800000c_y^{18}(-223745226487051177440 \\
&-700542223327583789859y^2 - 6664226019803329950y^4 + 67093045935611220 0y^6 + 684596540016000y^8 \\
&-6844241250000y^{10} + 2038400000y^{12} + 92395367064000000c_z^{10}(-3 + 10y^2) - 347351004000000c_x^{10}(-14592 \\
&+11665y^2) + 28378350000c_x^8(-5898256884 + 3023750025y^2 + 33568000y^4) + 221130000c_x^6(8046178388544 \\
&-777756869955y^2 - 196593681900y^4 + 619041500y^6) - 56700c_x^4(114937932032249796 + 56061784590887615y^2 \\
&-7050232031962100y^4 + 29341989022500y^6 + 3811500000y^8) - 1260c_x^2(-3258181349433041202 \\
&-4598523056126584260y^2 + 172751190615860175y^4 + 3241763204418000y^6 - 14507623710000y^8 \\
&+5082700000y^{10}) - 454053600000c_z^8(12963924 + 31240275y^2 - 847000y^4 + 535500c_x^2(-57 + 122y^2))
\end{aligned}
$$

$$
\begin{aligned}
&+589680000c_z^6(140337836721+5305021200y^2-7813725150y^4+42850500y^6+20616750c_x^4(-3477+3430y^2)\\
&-770c_x^2(-35813079-1132949700y^2+20426000y^4))+226800c_z^4(-38658479578479+1446584768476740y^2\\
&+9929944361400y^4-1000400555000y^6+1874950000y^8+53603550000c_x^6(-2109+4990y^2)\\
&+3003000c_x^4(883780254-1538038875y^2+11357500y^4)-15600c_x^2(528319400079+421696237305y^2\\
&-33805735425y^4+114537500y^6))+630c_z^2(-1377649116133287921-139308854015673630y^2\\
&+69811562583108900y^4+149594813784000y^6-4167123030000y^8+3180100000y^{10}\\
&+344594250000c_x^8(58197+29050y^2)+180180000c_x^6(-1828516959-4379380800y^2+84679000y^4)\\
&+175500c_x^4(916570120923+49544952523830y^2-1299622916900y^4+1041887000y^6)\\
&-180c_x^2(-40452306867018519+331817542668778890y^2+2193006752249900y^4-31821505485000y^6\\
&+32979100000y^8)))+2031644160000c_y^{15}y(-12448890367261697364841 98-131198483961935107744 95y^2\\
&-368488764087198790404 6y^4-108477453230739004 50y^6+425174585585310000y^8+358782160927500y^{10}\\
&-1006247550000y^{12}+30800000y^{14}+2097727632000000c_z^{10}(3249-7125y^2+2410y^4)\\
&-187297110000 00c_x^{10}(12045342-11324025y^2+454580y^4)+44594550000c_x^8(34477212924\\
&-160354205025y^2+1993178775y^4+59342000y^6)+2079000c_x^6(-1351664503439436+377947713175624 35y^2\\
&+845023788029475y^4-33838994846250y^6+16497250000y^8)-148500c_x^4(-1113420667129232931\\
&+2049000242281044003y^2+133945658685854610y^4-3201117704622150y^6+1648012474500y^8\\
&+1771840000y^{10})-1650c_x^2(3500779402415487069 99-12104012324840665476 89y^2\\
&-18274665747094929837y^4+152717258503384470y^6+1554037947445950y^8-2298870630000y^{10}\\
&+98000000y^{12})-1248647400000c_z^8(574652979+237513930y^2+62151600y^4-467000y^6\\
&+4200c_x^2(87663-127830y^2+27580y^4))+8316000c_z^6(172592419841541+501615939519540y^2\\
&+2699910995400y^4-855434250000y^6+1759450000y^8+315315000c_x^4(851709-662310y^2+48080y^4)\\
&-600600c_x^2(-2623534569-188371290y^2-517478250y^4+2290000y^6))+148500c_z^4(-423651682668486069\\
&-2299221160929378y^2+11767992740796600y^4+27350296930800y^6-951264972000y^8+691880000y^{10}\\
&+44144100000c_x^6(13509-211836y^2+45692y^4)+6306300c_x^4(-13473274329+28406298030y^2\\
&-4445837700y^4+1849000y^6)-168c_x^2(1632889737435759+3682985555385885y^2+324047436165975y^4\\
&-6402971973750y^6+6735575000y^8))+3300c_z^2(-49545005973750909657-13149672434748768618y^2\\
&-1389284946671679 54y^4+204229206737627 40y^6+24466651887150y^8-235700430000y^{10}+53900000y^{12}\\
&+28378350000c_x^8(-13080696+3849045y^2+871570y^4)+945945000c_x^6(2185318125-2114255022y^2\\
&-974529480y^4+3488600y^6)-3780c_x^4(-410365391461257-391027409831130y^2-2057691479025300y^4\\
&+9406017967500y^6+4964575000y^8)-90c_x^2(-1930147635230447031-748997172524317122y^2\\
&+587644694674312 80y^4+1280136699893400y^6-6040175148000y^8+1730680000y^{10})))\\
&+67044257280000c_y^{16}(37531951184175559138881+11658451689852604915 95y^2\\
&+566512229103407761230y^4+22294437961804060 50y^6-11759215600759500 0y^8-99515061720000y^{10}\\
&+451333400000y^{12}-42000000y^{14}-63567504000000c_z^{10}(3249-21660y^2+12100y^4)\\
&+283783500000c_x^{10}(26302509-77144160y^2+7765600y^4)-28378350000c_x^8(2359682514-25618875855y^2\\
&+1340587000y^4+17654000y^6)-567000c_x^6(-567495847917954+13872886512647015y^2\\
&+171705078370400y^4-26906959502500y^6+27319600000y^8)+31500c_x^4(-193657434542332713\\
&+947597006775283155y^2+90690174103214790y^4-3602606763400950y^6+4538119644000y^8+2705360000y^{10})\\
&+50c_x^2(377311136694100736589-385429261786852079097y^2-9318865640200484508 0y^4\\
&+121966183225898550 0y^6+14227116929982000y^8-31043160540000y^{10}+3547600000y^{12})\\
&+113513400000c_z^8(188264493+243962430y^2+103917500y^4-1113000y^6+2800c_x^2(46179-203490y^2\\
&+72950y^4))-2268000c_z^6(20883776173449+17233571545566 0y^2+1366191636600y^4-671927410000y^6\\
&+1874950000y^8+35035000c_x^4(941949-2293980y^2+324500y^4)-800800c_x^2(-208443042-48863865y^2\\
&-224682625y^4+1487500y^6))-31500c_z^4(-621357932727419 67-11831092252717 50y^2+850065776413326 0y^4\\
&+25493806177200y^6-1254128904000y^8+1272040000y^{10}+6306300000c_x^6(-1197-630012y^2+241940y^4)\\
&+2702700c_x^4(-4745183523+31021290450y^2-8628046500y^4+13531000y^6)-72c_x^2(480322588640028\\
&+3867759481792645y^2+543545627755450y^4-16018958532500y^6+24734325000y^8))\\
&-100c_z^2(-49400327937438072882-40734561470153087439y^2-704669970142090260y^4
\end{aligned}
$$

$$+144388450892769300y^6 + 194061880296000y^8 - 2741383260000y^{10} + 1019200000y^{12}$$
$$+454053600000c_x^8(-935586 + 1043505y^2 + 209800y^4) + 5675670000c_x^6(565198308 - 1452189423y^2$$
$$-784524400y^4 + 4823700y^6) - 11340c_x^4(373059090337056 - 681193338874085y^2 - 3683783481526100y^4$$
$$+29499047847500y^6 + 5717250000y^8) - 1260c_x^2(-141684385363339149 - 167889970199776680y^2$$
$$+22604130035577945y^4 + 647013237176400y^6 - 4363646013000y^8 + 2033080000y^{10})))$$
$$+507911040000c_y^{13}y(-59099270323864515798547494 - 83367383536062404267781 6y^2$$
$$-267744025403998328839 5y^4 - 34175481585619292028 0y^6 - 719558905041276300y^8 + 14761696716139500y^{10}$$
$$+13844080880000y^{12} - 10524800000y^{14} + 998917920000c_z^{10}(-1296351 + 4321170y^2 - 2832900y^4 + 467000y^6)$$
$$+71351280000c_x^{10}(317247021 - 1764626220y^2 + 371928900y^4 + 8548000y^6) + 91476000c_x^8(-85602948255594$$
$$+3521166865965y^2 - 10989688614975y^4 - 289817838750y^6 + 1433950000y^8) - 59400c_x^6(8179040446446411738$$
$$-1283168254060381 50y^2 - 2009645432882225 25y^4 - 6588064435928250y^6 + 51791306945000y^8 + 4900000000y^{10})$$
$$-3300c_x^4(-2065963064539763740806 - 2464998908510079408 6y^2 + 14790614291250629139y^4$$
$$+638607166905572460y^6 - 5606151219709650y^8 - 2267981940000y^{10} + 921200000y^{12})$$
$$+c_x^2(263986742726699422600474 92 - 3619492585823524904386 20y^2 + 3338733808327799190771 0y^4$$
$$+275968958257825441300y^6 - 9055781177907717000y^8 - 87826214268180000y^{10} + 47752782000000y^{12}$$
$$+616000000y^{14}) - 182952000c_z^8(5818421711907 + 2723588299530y^2 + 308315706300y^4 + 39695340000y^6$$
$$-159950000y^8 + 54600c_x^2(-11602521 + 25726680y^2 - 11163600y^4 + 1145000y^6))$$
$$+118800c_z^6(-900455721163265169 + 7168513919247450y^2 + 6587697115175400y^4 + 24360688854000y^6$$
$$-3188404660000y^8 + 3459400000y^{10} + 52552500c_x^4(-133267617 + 169903566y^2 - 34049820y^4 + 369800y^6)$$
$$-1540c_x^2(-73638632440107 - 48732921525330y^2 - 818320724550y^4 - 1185261982500y^6 + 2449300000y^8))$$
$$+6600c_z^4(-111704021146765749177 - 6051663642031045857y^2 - 4983974094975372y^4 + 24556988379616920y^6$$
$$+44319738728700y^8 - 708246420000y^{10} + 215600000y^{12} + 189189000c_x^6(385571529 + 221579190y^2$$
$$-216684300y^4 + 17443000y^6) - 291060c_x^4(-13625284124781 + 2950840535085y^2 - 2202418461150y^4$$
$$+123543975000y^6 + 128950000y^8) - 54c_x^2(-3920621948839322181 + 92936057333821800y^2$$
$$+45105305466919250y^4 + 2124903618404500y^6 - 20218364740000y^8 + 8653400000y^{10}))$$
$$+4c_z^2(-3030914676363107227944327 - 2752892655476433534603 0y^2 - 2031040765893667855635y^4$$
$$-11224775866503419550y^6 + 909945255075293250y^8 + 1051608025192500y^{10} - 4025868000000y^{12}$$
$$+154000000y^{14} + 178378200000c_x^8(796504212 - 711344025y^2 - 7843500y^4 + 14835500y^6)$$
$$+22869000c_x^6(-179847669767346 + 2529728588835y^2 - 1119496261275y^4 - 3130338333750y^6$$
$$+2999500000y^8) - 89100c_x^4(-1143975444051569031 - 56219243956180200y^2 + 5423794194175525y^4$$
$$-5538214125985750y^6 + 5477218635000y^8 + 8859200000y^{10}) - 1650c_x^2(-59498396221623326226$$
$$-50911674578922212811y^2 - 61187256378398818 71y^4 + 201741098167238310y^6 + 3109001376572100y^8$$
$$-6903165150000y^{10} + 392000000y^{12}))) - 507911040000c_y^{14}(-59084718215883754652533044$$
$$-24977772959144593966200 90y^2 - 1336338271295047753078 5y^4 - 24227627184840631374 90y^6$$
$$-57962888150178478 50y^8 + 166864332072768000y^{10} + 146475109120000y^{12} - 232056000000y^{14}$$
$$+20977276320000c_z^{10}(-61731 + 638970y^2 - 697300y^4 + 159000y^6) - 1498376880000c_x^{10}(-11016951$$
$$+276984645y^2 - 117707800y^4 + 591500y^6) + 274428000c_x^8(-27523528191873 + 7213491423180y^2$$
$$-224565258792 00y^4 - 227098445000y^6 + 4881300000y^8) + 415800c_x^6(-1172578487227939134$$
$$+21009024242454510y^2 + 167288599504366875y^4 + 4735609538905500y^6 - 781972185600 00y^8$$
$$+10704400000y^{10}) - 3300c_x^4(-2071012098329600146686 - 8426326959825493332 6y^2$$
$$+835667375115064580 55y^4 + 424742093253621675 0y^6 - 61796125878381000y^8 - 737310420000y^{10}$$
$$+21246400000y^{12}) + 198c_x^2(133069496580419150647854 - 556472147155659808227 0y^2$$
$$+932054960457762729525y^4 + 995062080241323654 00y^6 - 531943056759189000y^8 - 5059218248000000y^{10}$$
$$+4797184000000y^{12}) - 11525976000c_z^8(92772156939 + 126969122010y^2 + 25096374600y^4 + 4460445000y^6$$
$$-24350000y^8 + 9100c_x^2(-1196487 + 8132160y^2 - 5902700y^4 + 850000y^6)) + 831600c_z^6(-128310755308262667$$
$$+3222366365817630y^2 + 4861338054646500y^4 + 204196144140 00y^6 - 4207042980000y^8 + 6360200000y^{10}$$
$$+157657500c_x^4(-7377765 + 29504526y^2 - 10796380y^4 + 386600y^6) - 4620c_x^2(-3418382378817$$
$$-6979178976030y^2 - 224938683300y^4 - 424508465000y^6 + 1284900000y^8))$$

$$
\begin{aligned}
&+6600c_z^4(-111750094394101976652 - 185906170638125562 87y^2 - 38755882346877990y^4\\
&+1743457362493644 00y^6 + 342904340304000y^8 - 8242583580000y^{10} + 4076800000y^{12}\\
&+7945938000c_x^6(12269682 + 9199095y^2 - 26535700y^4 + 3445500y^6) - 873180c_x^4(-4717752010152\\
&+3834467501445y^2 - 4156727454300y^4 + 389223692500y^6 + 148500000y^8) - 756c_x^2(-279739640973549204\\
&+18163749755634060y^2 + 17331063246010125y^4 + 1071910849048000y^6 - 14621212710000y^8\\
&+10165400000y^{10})) + 132c_z^2(-91733089027301432594919 - 24880674789265940070 30y^2\\
&-31823545544084295540 0y^4 - 2315772748371571650y^6 + 252134779581504000y^8 + 288423779250000y^{10}\\
&-1806371000000y^{12} + 210000000y^{14} + 198648450000c_x^8(25910919 - 76741950y^2 + 6492800y^4 + 2522000y^6)\\
&+43659000c_x^6(-2945981057967 + 1144111237095y^2 - 630190354800y^4 - 356618812500y^6 + 709600000y^8)\\
&-37800c_x^4(-80947885953421179 - 8138880005619315y^2 + 287016431932875y^4 - 3123403961806375y^6\\
&+75753893400 00y^8 + 6763400000y^{10}) - 50c_x^2(-55930948893189310941 - 165001274213077268001y^2\\
&-32138013362153286420y^4 + 160085498736149910 0y^6 + 28436838110208000y^8 - 93272436180000y^{10}\\
&+14190400000y^{12}))) + 14511744000c_y^{12}(28964635002500466217642482789 + 10350843674124580588554827 85y^2\\
&+72674855718065994553658 19y^4 + 150908258315484750638 25y^6 + 147915354557821940397 0y^8\\
&+29562013375547383 50y^{10} - 41266270813082000y^{12} - 41802651360000y^{14} + 10287200000y^{16}\\
&-403409160000c_z^{10}(3518667 - 54323280y^2 + 88589400y^4 - 38912000y^6 + 4870000y^8)\\
&-115259760000c_x^{10}(2857152207 + 4835885670y^2 - 8346443350y^4 + 826063000y^6 + 48870000y^8)\\
&-29106000c_x^8(3592004847951681 - 4542099145294860y^2 - 4732863864300y^4 - 150228981489000y^6\\
&-6316624170000y^8 + 11155600000y^{10}) + 115500c_x^6(385983615660445127808 + 67293594857717867142y^2\\
&-92307808112321182 5y^4 - 4960029881178918 00y^6 - 18363681988933500y^8 + 70001696520000y^{10}\\
&+16542400000y^{12}) + 6930c_x^4(-23136337448515953345 4236 - 16637126099034881518470y^2\\
&-94173983729993189925y^4 + 35391821335222157400y^6 + 13861815618114360 00y^8 - 70563964838000 00y^{10}\\
&-5059936000000y^{12} + 280000000y^{14}) - 315c_x^2(23605065306530533900612692 + 13871264800625098980470 28y^2\\
&-10268082487308245503365y^4 + 5455140591671071754 0y^6 + 37622398013667574800y^8\\
&-66836909494718000y^{10} - 765863808980000y^{12} + 186164000000y^{14}) + 58212000c_z^8(-157411228810878\\
&+314915304611205y^2 + 76407682604400y^4 + 5489655462000y^6 + 535860360000y^8 - 1590050000y^{10}\\
&+17325c_x^2(188516727 - 1791772200y^2 + 1953198200y^4 - 562108000y^6 + 42830000y^8))\\
&+924000c_z^6(10697800183184688651 + 203334900937027479 9y^2 - 7895488377358575y^4\\
&-4776248084879250y^6 - 17290884348000y^8 + 1379908530000y^{10} - 1019200000y^{12}\\
&+4365900c_x^4(-526662456 + 2948651595y^2 - 1774729150y^4 + 203972500y^6 + 2475000y^8)\\
&+126c_x^2(1976765641796169 - 1969420531698540y^2 - 649355941080450y^4 - 5939601666000y^6\\
&-7424195355000y^8 + 10165400000y^{10})) - 13860c_z^4(-19328936503217292734832 - 93156612908540832976 5y^2\\
&-24607378102037106600y^4 - 7172950359985200y^6 + 503214461699670 00y^8 + 89396991450000y^{10}\\
&-904050000000y^{12} + 140000000y^{14} + 72765000c_x^6(-3104582373 + 5254263540y^2 + 3267479100y^4\\
&-1435556000y^6 + 70960000y^8) - 6300c_x^4(152397769293063 - 5021885486082105y^2 + 337719911610600y^4\\
&-243673722874500y^6 + 7610959140000y^8 + 13526800000y^{10}) - 100c_x^2(-86864061213986878773\\
&-17226241255232190027y^2 + 225977786168154300y^4 + 62024201391675600y^6 + 2365667197938000y^8\\
&-15593057550000y^{10} + 3547600000y^{12})) - 420c_z^2(-10840732740005911546441176\\
&-50477651680013948484725 4y^2 - 22912041379064583507 30y^4 - 10885672460144108434 5y^6\\
&-5015565066128364 00y^8 + 2970377505588900 0y^{10} + 36123066790000y^{12} - 77352000000y^{14}\\
&+3430350000c_x^8(-864893547 + 5528499606y^2 - 2054421740y^4 - 168060200y^6 + 32542000y^8)\\
&+138600c_x^6(7690240273923837 - 4129304711024745y^2 - 169240720832100y^4 + 48030383367000y^6\\
&-19819303740000y^8 + 5352200000y^{10}) - 3300c_x^4(-50242248602609250348 - 56644207601340825 27y^2\\
&-13984041806176050 0y^4 + 15960324880191825y^6 - 5332797921404250y^8 - 151185510000y^{10}\\
&+5311600000y^{12}) + 66c_x^2(47425142071798844868018 + 14085808476011913973 5y^2\\
&+95269910014744718400y^4 + 8089080435037918050y^6 - 17796275295531300 0y^8 - 2532736773700000y^{10}\\
&+3599414000000y^{12}))) + 186048000c_y^{11}y(-22601827833504371286820032 96792
\end{aligned}
$$

$$
\begin{aligned}
&-269478232586685237280300235 10y^2 - 1116533423654849748688440 30y^4 - 151628446506222116531100y^6\\
&-127173357182531263353 75y^8 - 258240586053905910 00y^{10} + 230148216956805000y^{12}\\
&+249746893175000y^{14} + 3496212720000c_z^{10}(31668003 - 151858260y^2 + 146854800y^4 - 46398000y^6\\
&+4570000y^8) + 499458960000c_x^{10}(32741643501 + 36100372455y^2 - 24032707650y^4 + 710686500y^6\\
&+131965000y^8) + 2270268000c_x^8(3410885915300106 - 1349078749904655y^2 - 19073511150525y^4\\
&-13597862883750y^6 - 878281415000y^8 + 444800000y^{10}) - 9009000c_x^6(392304009862872459828\\
&+18264313746756994014y^2 - 241293901642198209y^4 - 54745781775808860y^6 - 2311084841235225y^8\\
&+3796751280000y^{10} + 1156400000y^{12}) + 60060c_x^4(208995091843348047536 4474\\
&+46576940765370170984010y^2 + 158171758612565760405y^4 - 3791549433706340 3100y^6\\
&-1421444272137729750y^8 + 3778912624758750y^{10} + 3790405500000y^{12} + 56000000y^{14})\\
&+2730c_x^2(21296208609523056516722 1378 + 367467647055921280147771 8y^2 - 195591284789536201000 05y^4\\
&+599716881648910068120y^6 + 369759580532971472 25y^8 - 22919093262783000y^{10} - 477639141825000y^{12}\\
&+20534800000y^{14}) - 4540536000c_z^8(-157237296032628 + 102081873002715y^2 + 15488503017750y^4\\
&+754626042000y^6 + 57874445000y^8 - 123550000y^{10} + 1925c_x^2(1515941163 - 4591821960y^2 + 2959115400y^4\\
&-602436000y^6 + 34990000y^8)) - 36036000c_z^6(21405150336961582002 + 1361824460508900591y^2\\
&-3197397894550146y^4 - 1317698469524340y^6 - 5082918484650y^8 + 236845560000y^{10} - 107800000y^{12}\\
&+485100c_x^4(-7698776868 + 13573624185y^2 - 4523266350y^4 + 277579500y^6 + 12895000y^8)\\
&+252c_x^2(1895829161453469 - 602281220541795y^2 - 121329662453775y^4 - 564980145750y^6\\
&-731132410000y^8 + 618100000y^{10})) + 10920c_z^4(-191588546718418856315743\\
&-30799074398240178340695y^2 - 472829351608916964585y^4 - 50783340592432800y^6\\
&+5426721353325195 00y^8 + 100214111693250 0y^{10} - 6040996500000y^{12} + 308000000y^{14}\\
&+1600830000c_x^6(-10080073026 + 3499627545y^2 + 3369178350y^4 - 772372500y^6 + 21425000y^8)\\
&-623700c_x^4(225553727267388 - 1607191510761165y^2 + 13565580421275y^4 - 29090902528500y^6\\
&+387767842500y^8 + 1265600000y^{10}) - 4950c_x^2(-174674908770166093401 - 109116051346057666 68y^2\\
&+96029081404289208y^4 + 15985270142693820y^6 + 518664685263450y^8 - 2305423890000y^{10}\\
&+196000000y^{12})) + 5460c_z^2(-650675020777653646836313 56 - 100678987588700749529901 6y^2\\
&-267866570552180387634 0y^4 - 896079961374056474 40y^6 - 378329587907775075y^8\\
&+15734597764761000y^{10} + 20633499600000y^{12} - 21049600000y^{14} + 2286900000c_x^8(-6511179654\\
&+12479300505y^2 - 1925406630y^4 - 351086100y^6 + 28679000y^8) - 831600c_x^6(-7057311143032287\\
&+888277771334385y^2 + 49580262491850y^4 - 136295691423 75y^6 + 1866822173750y^8 + 350000000y^{10})\\
&-9900c_x^4(-99707960291679029556 - 4429697827834883268y^2 - 49042554210142542y^4\\
&+6838235110574820y^6 - 964907833215675y^8 - 760716600000y^{10} + 460600000y^{12})\\
&+4c_x^2(47100086732 1892 6 9 0 3 7 3 8 0 7 - 29152670352970508986 95y^2 + 16304040864543525474 15y^4\\
&+109114330123741256325y^6 - 1554936491142923625y^8 - 22001531515830000y^{10} + 17908563750000y^{12}\\
&+308000000y^{14}))) + 93024000c_y^9y(-95575746503989787660188153944354\\
&-75494258345016665204158893 9852y^2 - 263166972342021556116185 9781y^4\\
&-47635743758919921346521 78y^6 - 201576126515708953008 0y^8 - 231065205236592829830y^{10}\\
&-566119742196372000y^{12} + 1406924399521000y^{14} + 1345050330000y^{16} + 6356750400c_z^{10}(-601692057\\
&+4750200450y^2 - 6259523400y^4 + 2865618000y^6 - 536370000y^8 + 35300000y^{10})\\
&+1816214400c_x^{10}(-2094348148137 + 246273750450y^2 + 934744746600y^4 - 105197922000y^6\\
&-10360920000y^8 + 491800000y^{10}) - 252252000c_x^8(3634514829009684 - 8700294590733807y^2\\
&+596405761492581y^4 + 9612080002890y^6 - 252934941600y^8 + 132916680000y^{10} + 39200000y^{12})\\
&+10920c_x^6(-592873163224136867358594 - 652492596616561833848 10y^2 - 453336951463567007760y^4\\
&+958178929089496455 0y^6 + 482770714409416125y^8 + 34243685828066250y^{10} + 11575294500000y^{12}\\
&+616000000y^{14}) + 8190c_x^4(27442973526434937205587 7452 + 45190183026331262837610 00y^2\\
&+24824337022700619236910y^4 + 405753969595594742 10y^6 - 451108159841250697 5y^8\\
&-183911980044012750y^{10} - 22314576795000y^{12} + 83168800000y^{14})\\
&-78c_x^2(-39399795874742955330039459714 - 184197525543013211261661321 0y^2
\end{aligned}
$$

$$
\begin{aligned}
&-74718745747776086693363 55y^4 + 37973661126973891842600y^6 - 367365787766023055625y^8\\
&-22671697536295358250y^{10} - 24567180609685000y^{12} + 90075378525000y^{14})\\
&-252252000c_z^8(530766105542379 - 855652021215957y^2 + 164389405185936y^4 + 12929055729840y^6\\
&+328221266400y^8 + 17081130000y^{10} - 15400000y^{12} + 126c_x^2(-22593731193 + 91791885150y^2 - 77533075800y^4\\
&+22892634000y^6 - 2585130000y^8 + 88300000y^{10})) - 43680c_z^6(4109651371023200263 9386\\
&+5908201786594877255640y^2 + 112525928159609750940y^4 - 145967394869361450y^6 - 28103395370477625y^8\\
&-142298404458750y^{10} + 2015128500000y^{12} - 154000000y^{14} + 2910600c_x^4(83255543091 - 186174886500y^2\\
&+84085033500y^4 - 9464787000y^6 - 247290000y^8 + 45200000y^{10}) + 11550c_x^2(-9110052242049402\\
&+8751520568746161y^2 - 722137691603493y^4 - 76335724450170y^6 + 81126546300y^8 - 165609315000y^{10}\\
&+28000000y^{12})) - 32760c_z^4(1178744294754542811241069 2 + 21151001590311039653745 0y^2\\
&+994834255270372378785y^4 + 6663630220164224010y^6 + 2400483472461525y^8 - 3103779903500250y^{10}\\
&-6789418720000y^{12} + 10524800000y^{14} + 7761600c_x^6(-94031549892 + 77272456275y^2 + 13902187950y^4\\
&-8894650500y^6 + 611880000y^8 + 6250000y^{10}) + 46200c_x^4(2942065948325094 + 1292694612729993y^2\\
&-640913983275429y^4 - 18432554133510y^6 - 2181809555100y^8 - 27674445000y^{10} + 32900000y^{12})\\
&-2c_x^2(3036353673638740558229 28 + 429955989426377403689 70y^2 + 731122950926461203495y^4\\
&-39470963229578083 50y^6 - 278328685851711000y^8 - 7378882032195000y^{10} + 11940736500000y^{12}\\
&+308000000y^{14})) + 12c_z^2(-6032256841181633379944680 14309 - 98921724737639303178775196 10y^2\\
&-44591553326524131592544880y^4 - 43802295817304068194150y^6 - 10140681975162538800 00y^8\\
&-47528548310471182 50y^{10} + 81245528213421250y^{12} + 124873446587500y^{14} + 756756000c_x^8(133502723613\\
&-1878192612450y^2 + 665906837400y^4 + 41217210000y^6 - 13524720000y^8 + 222400000y^{10})\\
&-21021000c_x^6(46469127490398306 - 24852042070465 03y^2 - 709821233204571y^4 - 4503421917990y^6\\
&-9848562098400y^8 + 270640020000y^{10} + 165200000y^{12}) + 30030c_x^4(4558823080455120103 2546\\
&+5680412757449310499290y^2 + 92285885956023304965y^4 + 3286920111405300y^6 - 44464199122450125y^8\\
&+1289872835066250y^{10} + 2528085000000y^{12} + 56000000y^{14}) + 2730c_x^2(6811776035586680915424 7296\\
&+8800376867165530267409 25y^2 - 205217170303567702549 5y^4 + 32037648568082959230y^6\\
&+18661220473638484 50y^8 - 699787725694200 0y^{10} - 159582408135000y^{12} + 10267400000y^{14})))\\
&+279072000c_y^{10}(3184989899945978213382 5423759268 + 75402178761766719703556248 5330y^2\\
&+44748165698314027025618612 07y^4 + 11956290154286613437005704y^6 + 99934285357539625642 65y^8\\
&+84457775137535236437 0y^{10} + 184446619447984075 0y^{12} - 9530913454290000y^{14} - 105773418400000y^{16}\\
&-2118916800c_z^{10}(-601692057 + 16361801550y^2 - 37223793000y^4 + 23880150000y^6 - 5702850000y^8\\
&+454300000y^{10}) - 9686476800c_x^{10}(-210583032282 + 268226357175y^2 + 329279044500y^4 - 93742621875y^6\\
&-2385787500y^8 + 463362500y^{10}) + 168168000c_x^8(1610101846811682 - 1437586464780261 9y^2\\
&+2410065955182465y^4 + 43192171499850y^6 + 6530966050500y^8 + 832669785000y^{10} + 64400000y^{12})\\
&+120120c_x^6(16594557917097775855968 + 85776673230868963152 60y^2 + 15463524620420113072 5y^4\\
&-22300178496909012 00y^6 - 237630246356763000y^8 - 12039425108100000y^{10} + 4692856000000y^{12}\\
&+1680000000y^{14}) - 30030c_x^4(2488008995767413491353873 2 + 13414014621502888408815 24y^2\\
&+13798680487510394437920y^4 + 31746356146216467630y^6 - 5023892589111485325y^8\\
&-189908783015151000y^{10} + 192036168880000y^{12} + 278316000000y^{14})\\
&+26c_x^2(-3882601375860878274374333 5014 - 6818497728722726105219120730y^2\\
&-52067273614953899285983923y^4 + 24739950386713262126580 0y^6 - 42992964799925521723 65y^8\\
&-25445545684171344270 0y^{10} - 78992267886336000y^{12} + 1973400729120000y^{14} + 82297600000y^{16})\\
&+84084000c_z^8(531008490770604 - 2741343247619613y^2 + 879533564158080y^4 + 92868040431000y^6\\
&+3212491968000y^8 + 199763190000y^{10} - 291200000y^{12} + 504c_x^2(-6610278942 + 87808529925y^2\\
&-127991448000y^4 + 54101205000y^6 - 8113500000y^8 + 363050000y^{10})) + 480480c_z^6(12455149650443356552 92\\
&+5358747125724686586 90y^2 + 17081940243710360025y^4 - 2809404925570530 0y^6 - 7946457818517000y^8\\
&-34590432375000y^{10} + 905779000000y^{12} - 210000000y^{14} + 44100c_x^4(220215683907 - 1605317471550y^2\\
&+1321828285500y^4 - 259372485000y^6 + 5081400000y^8 + 966200000y^{10}) + 350c_x^2(-10069143749733537
\end{aligned}
$$

$$+30964181466977649y^2 - 4638457597113540y^4 - 646842366878400y^6 - 1002873960000y^8 - 2248001730000y^{10}$$
$$+1013600000y^{12})) - 10920c_z^4(-1178194232114120661830359 2 - 6375249793048960132418 34y^2$$
$$-5109508952066938637295y^4 - 502542747682675345 80y^6 - 6999953641171425y^8 + 35294714871636000y^{10}$$
$$+70263291620000y^{12} - 232056000000y^{14} + 3880800c_x^6(281800657584 - 880982727975y^2 + 3405456000y^4$$
$$+151090245000y^6 - 19285650000y^8 + 191150000y^{10}) - 46200c_x^4(3878652545749359 + 2172193184537262y^2$$
$$-3458521330252245y^4 - 61526336331150y^6 - 26192945875500y^8 - 16863345000y^{10} + 758800000y^{12})$$
$$+198c_x^2(3011782945494080614122 + 1407476508486701189040y^2 + 418302789025428672 75y^4$$
$$-277152415226794800y^6 - 2943748810089450 0y^8 - 847398428800000y^{10} + 2401644000000y^{12}))$$
$$-52c_z^2(-4638553605157888159890954 9543 - 2279494477026273638025847260y^2$$
$$-1748253153335695181683685 1y^4 - 2879642968473716662140 0y^6 - 7469161027356575616 30y^8$$
$$-3175668336778048650y^{10} + 87749808213718000y^{12} + 125169460440000y^{14} - 41148800000y^{16}$$
$$+58212000c_x^8(-82563456087 - 7325489376450y^2 + 5837651127000y^4 - 189734580000y^6 - 138404700000y^8$$
$$+5577800000y^{10}) - 3234000c_x^6(27660861760506723 - 5243304202259547 6y^2 + 1149449177993310y^4$$
$$+107125358662800y^6 - 40668584382000y^8 + 2510059950000y^{10} + 1181600000y^{12})$$
$$-20790c_x^4(-51422690135833605910 44 - 1733429100854953351080y^2 - 4408479225997739 3925y^4$$
$$-166274628386761650y^6 + 37283729542434000y^8 - 2420556831800000y^{10} - 3380468000000y^{12}$$
$$+280000000y^{14}) + 210c_x^2(67950027526930334878551921 + 2977101036934062024882357y^2$$
$$-4879062109490449924890y^4 + 2968353192919035398 40y^6 + 1742140765474634002 5y^8$$
$$-1463592466835730 00y^{10} - 2303333166460000y^{12} + 837738000000y^{14})))$$
$$+2c_y y(1856156927625000000000c_x^{10}(79 + 30y^2) + 824958634500000000c_x^8(1621220931 + 32788680y^2$$
$$+157005y^4 + 18850y^6) + 11904165000000c_x^6(-10193703433622139816 - 122361941339578710y^2$$
$$-366373448657370y^4 + 415171097550y^6 + 8134435375y^8 + 157424750y^{10})$$
$$+17442000c_x^4(3246930156472975931812541591904 + 2988312145625968037247589 2180y^2$$
$$+7781708837160865648812771 0y^4 + 7072442854258332480930 0y^6 - 2123176575101594512 5y^8$$
$$-3351615058018500y^{10} + 816466927088750y^{12} + 6471610507500y^{14})$$
$$+25(5588872274345977683059018006714001925415760 + 4127602366930603491792193515753390564744 0y^2$$
$$+8826194267172055447845038958 0992804712y^4 + 8199204396298999399674449147180124 0y^6$$
$$+3631643420372342484052339931535 0y^8 + 6112408279561345779584726250y^{10} - 2333623720848436460965500y^{12}$$
$$+27560391510038287500y^{14} + 5064566807225514937 5y^{16} + 2905701310222562 50y^{18})$$
$$+4c_x^2(-1440070164591753803660674145070665544 89919608 - 1084336765004788338940418821304604649 05000y^2$$
$$-2376803155248416053866833440380701434 80y^4 - 2228112239023771243877841996127239 00y^6$$
$$-8188771899469011208229310238800 0y^8 + 1131126460398575794384952175 0y^{10}$$
$$+5469544730102791255627500y^{12} - 3135037998756190792500y^{14} + 1388692481709736406 25y^{16}$$
$$+581260562928781250y^{18}) + 4c_z^2(-1439059541200056130042659661486751907112 9608$$
$$-1083711754893235034062620864209127367710 00y^2 - 2376253480416159593446401341607720049 80y^4$$
$$-2229748910158155518981392661206089 00y^6 - 8217127754643942665603908197862 5y^8$$
$$+1134348894987161787273924675 0y^{10} + 5532488427278462298783750y^{12} - 6130539658346833980000y^{14}$$
$$+1191009078585094218 75y^{16} + 581260562928781250y^{18} + 139211769571875000000c_x^8(-57 + 10y^2)$$
$$+206239658625000000c_x^6(1579716306 + 35179305y^2 - 43995y^4 + 18850y^6)$$
$$+2976041250000c_x^4(-10152164010671375616 - 122327485648254810y^2 - 372062990628945y^4$$
$$+388080861300y^6 + 6001026625y^8 + 157424750y^{10}) + 26163000c_x^2(5404855852720163764046787504 84$$
$$+4977001513551027477181695030y^2 + 1297721841322457479619691 0y^4 + 1184700507776255562592 5y^6$$
$$-3573746932809928875y^8 - 189549860514787 5y^{10} + 116441069285625y^{12} + 1078601751250y^{14})))$$
$$+930240c_y^7 y(-2211212236757626283588851724655855 48 - 1562771428991631192251958936435540y^2$$
$$-3497540217208501697293386706380y^4 - 4969387309930322790781670400y^6 - 4583466706590282412526625y^8$$
$$-5724682075853231400 00y^{10} - 157663563085757688750y^{12} - 497011503445212500y^{14} - 269547868125000y^{16}$$
$$+70630560000c_z^{10}y^2(-57 + 10y^2)^3(3249 - 4560y^2 + 1100y^4) - 10090080000c_x^{10}(-1805854828050$$
$$+1371175843149y^2 + 562492996380y^4 - 142643027700y^6 - 9728019000y^8 + 1052940000y^{10} + 13300000y^{12})$$

$$
\begin{aligned}
&+168168000c_x^8(-88520786590849704 - 127710055411469685y^2 + 34438482900056655y^4 + 1210431336264000y^6\\
&+35494001482500y^8 + 2683414935000y^{10} - 27390750000y^{12} + 2000000y^{14})\\
&+1092000c_x^6(393986585525665040644428 - 20157530478242489406459y^2 + 947247135442212902220y^4\\
&+13484788419506151825y^6 + 1251815470347172 5y^8 - 2045379596653125y^{10} + 120398130242500y^{12}\\
&+72901400000y^{14}) - 1800c_x^4(-8397860974900366918649942 96172 - 178849572392415812 74040995740y^2\\
&-706858637796774056113720 20y^4 - 795363169713291217788 75y^6 - 43450855993964293875y^8\\
&+4089224442008865250y^{10} + 410260176775868125y^{12} + 535147132650000y^{14})\\
&+300c_x^2(-20541099421483521333946723704474 + 27321144363706421039505974 28y^2\\
&+60524847473932974408788912 4y^4 + 11142378474413098902959 97y^6 - 11132404320779124838455y^8\\
&+3358877648149580329 5y^{10} + 3447356058098091125y^{12} + 7743018859782250y^{14} + 1345050330000y^{16})\\
&-168168000c_z^8(-3501650943434196 + 10606289921371935y^2 - 4837501624558905y^4 + 445613643324000y^6\\
&+22009508325000y^8 + 320888790000y^{10} + 13113750000y^{12} - 2000000y^{14} + 2100c_x^2(2850120270 - 17732414943y^2\\
&+18514816380y^4 - 6845985000y^6 + 1072908000y^8 - 66870000y^{10} + 1000000y^{12}))\\
&-2184000c_z^6(-23844771400330239543954 + 12779594093188959736392y^2 + 57649798463720177 4840y^4\\
&+5085872634240471150y^6 - 5449175062385175y^8 - 471139779498750y^{10} - 3262087640000y^{12} + 10524800000y^{14}\\
&+323400c_x^4(-37393683210 + 102605073057y^2 - 55598540130y^4 + 8440201350y^6 + 60655500y^8 - 72285000y^{10}\\
&+2350000y^{12}) - 308c_x^2(-44483455915963029 + 70791768592083315y^2 - 17328544760858220y^4\\
&+425621246682375y^6 + 35532722486250y^8 - 293238202500y^{10} + 38785125000y^{12} + 2000000y^{14}))\\
&-600c_z^4(40837399766676638253162378030 84 + 10758200518523806231197844530y^2\\
&+55775546786811214264466565y^4 + 10022587787024956593450 0y^6 + 3414343287765981821 25y^8\\
&+6723676237230907 50y^{10} - 94833895896880000y^{12} - 249746893175000y^{14} + 1177176000c_x^6(140094917685\\
&-158709593943y^2 + 4074345360y^4 + 12596562450y^6 - 1398649500y^8 - 19875000y^{10} + 2950000y^{12})\\
&-1681680c_x^4(67862009051935371 - 13384043304880185y^2 - 15381798345465345y^4 + 1417321879920000y^6\\
&+45824936703750y^8 + 1078838010000y^{10} + 45205875000y^{12} + 2000000y^{14})\\
&-5460c_x^2(-228848223067340742810252 + 78245216401261690925991y^2 + 30143267469934450801 20y^4\\
&+2208958096481596845 0y^6 - 9357845086565002 5y^8 - 317999978057250 0y^{10} - 80345245357500y^{12}\\
&+10267400000y^{14})) - 100c_z^2(113124252792294355779545213587752 + 12091585532587033433470157007 36y^2\\
&+58075126188760492987138743 78y^4 + 11351543885093140182488034y^6 + 4503975449993400531 15y^8\\
&+9236126256392165949 0y^{10} + 663018506577021000y^{12} - 2919167308403000y^{14} - 4035150990000y^{16}\\
&+3531528000c_x^8(-100983373920 - 125415009693y^2 + 91515610350y^4 - 579881700y^6 - 2085957000y^8\\
&+63360000y^{10} + 2800000y^{12}) - 6726720c_x^6(141231647711895021 - 140787380076949935y^2\\
&+6523116261900030y^4 + 1760652404245125y^6 + 43166041796250y^8 + 2386195503750y^{10} + 18897562500y^{12}\\
&+2000000y^{14}) - 32760c_x^4(-1196814978209680344789 12 + 8331342842724504989601 6y^2\\
&+3576299572933448434920y^4 + 2635768104747452 4825y^6 - 7386307880082900y^8 - 4927428466914375y^{10}\\
&-5906188338750y^{12} + 41584400000y^{14}) + 312c_x^2(-44354884335636083557369337316\\
&-99025654056647133673028 2095y^2 - 27297237017799454949535 60y^4 + 1199885465879415990675 0y^6\\
&-15873611392881540375y^8 - 167809528116542550 0y^{10} - 5493405419989375y^{12} + 45037689262500y^{14})))\\
&+1860480c_y^8(110547942223661329753697417704141524 + 23745442638414795613852093863005 70y^2\\
&+9306861477433951204046270947950y^4 + 2061582120492115845731267 1600y^6 + 2610091369679775565433850 0y^8\\
&+3275103337176353933250y^{10} + 979195451282364736875y^{12} + 27481764521481750 00y^{14} - 1724263493200000y^{16}\\
&-141261120000c_z^{10}y^2(57 - 10y^2)^2(-185193 + 584820y^2 - 347700y^4 + 52000y^6) - 5045040000c_x^{10}(3112105586625\\
&-10030124928096y^2 - 1942013385900y^4 + 1988049268800y^6 - 27365256000y^8 - 19735200000y^{10} + 250600000y^{12})\\
&+1513512000c_x^8(9019523939075028 + 18948873104990685y^2 - 14904429482794050y^4 + 168190351512300y^6\\
&-1565662848000y^8 - 1219817200000y^{10} + 61738500000y^{12} + 15000000y^{14})\\
&-273000c_x^6(948247722494663644844406 - 45475135555839806599 9524y^2 - 12317209227501041192175y^4\\
&+3580244024087115000 0y^6 + 156088001460511890 0y^8 + 21222253724100000y^{10} + 4747678549480000y^{12}\\
&+3229776000000y^{14}) + 1950c_x^4(-38613284236710228155890 5045864 - 27492563738147221417704309540y^2\\
&-20546125713202577379757 0344y^4 - 60076802440285850180 1150y^6 - 6814381881752765500 95y^8
\end{aligned}
$$

$$+588892747324978404 00y^{10}+29525437559087120 00y^{12}+260516990736000 0y^{14}+24689280000 0y^{16})$$
$$+75c_x^2(4136527298608406928969064496 9748-693992014714248236696775157092y^2$$
$$-1586159088676077121411160755 8y^4-3830810570521834634839704 6y^6+2464453960585303619082 15y^8$$
$$-1323204529325295847230y^{10}-952207270607410090 00y^{12}-164781614504340000y^{14}$$
$$+1143653513600 00y^{16})+252252000c_z^8(-1167466366668357+12379123358978985y^2-9590927024904300y^4$$
$$+1231699878712800y^6+75549423942000y^8+1441626450000y^{10}+65069000000y^{12}-30000000y^{14}$$
$$+350c_x^2(7125300675-157193299944y^2+295018297200y^4-160130282400y^6+34239942000y^8$$
$$-2917440000y^{10}+72400000y^{12}))+2184000c_z^6(-11923045186207504639752+20087598676166975314053y^2$$
$$+14724547712097897539 25y^4+18488985004228575375y^6-20921939791775550y^8-2707250592337500y^{10}$$
$$-160786914350 00y^{12}+116028000000y^{14}+161700c_x^4(-54390453075+512606275578y^2-521134317000y^4$$
$$+137623590000y^6-7036416000y^8-866340000y^{10}+54200000y^{12})-1386c_x^2(-5897219958411831$$
$$+316293333588310 05y^2-14139042811383150y^4+671316423134400y^6+58649474001000y^8$$
$$-228800950000y^{10}+85991000000y^{12}))+3900c_z^4(3140948222193792651319129 0968$$
$$+2478228141862956677858613180y^2+21968325132761843101257453y^4+64523091325302676385550y^6$$
$$+30592454490571966839 0y^8+259810245555445200y^{10}-103329509028844000y^{12}-249384946320000y^{14}$$
$$+123446400000y^{16}+90552000c_x^6(234378791325-986780548872y^2+258130427400y^4+108774889200y^6$$
$$-26515458000y^8+714240000y^{10}+42200000y^{12})+4656960c_x^4(-2707628034993336+3612070462446405y^2$$
$$+1905050943942975y^4-380213345095350y^6-12245193016500y^8-610398125000y^{10}-15187500000y^{12}$$
$$+2500000y^{14})-420c_x^2(-247443799461143471084052+28261023969299861398843 8y^2$$
$$+188036396371102650005 25y^4+203005867289191659000y^6-94760513862935580 0y^8$$
$$-45818955679200000y^{10}-1160280347510000y^{12}+837738000000y^{14}))$$
$$+150c_z^2(3769710142456153361775195705218 4+120750617515777767419691339950 4y^2$$
$$+9860324293075098189700509156y^4+28552164272128357725466602y^6+13450353489488009739645y^8$$
$$+3739489471735299882 60y^{10}+2099614577858843500y^{12}-20042292585420000y^{14}-31732025520000y^{16}$$
$$+672672000c_x^8(-385773744825-608978286126y^2+1441102480650y^4-196848073800y^6-38822760000y^8$$
$$+3834360000y^{10}+16100000y^{12})+6726720c_x^6(-61067486175963057+21887845321855986 0y^2$$
$$-4260053996265555 0y^4-337932344614770 0y^6-78437410893000y^8-11429864850000y^{10}$$
$$+82673000000y^{12}+60000000y^{14})-240240c_x^4(-5142094454346152243346+1129189345102828269275 4y^2$$
$$+7802487601653502721 25y^4+841257432649356975 0y^6-15544236851015400y^8-2447542483650000y^{10}$$
$$+24365457920000y^{12}+69579000000y^{14})+156c_x^2(-2942842666219992242285310 8244$$
$$-2251884029430230248827644640y^2-1255436361659671728518034 9y^4+3957842946343616388135 0y^6$$
$$-1851064879552019138 70y^8-126727720076459078 50y^{10}-1004547935748000y^{12}+6587034345600 00y^{14}$$
$$+41148800000y^{16})))+13680c_y^5y(-3413995114614382345930153888027538967 84$$
$$-2512668082458393174516566492970002160y^2-4916796630431668605327166082941320y^4$$
$$-2888088094395251109260309911500y^6+1002535281705988737908326125y^8$$
$$+1136404638057591814070250y^{10}-1307427826550967607500y^{12}-5329475693043603500 0y^{14}$$
$$-180441250780493750y^{16}+45741696000c_z^{10}y^4(-57+10y^2)^5+45741696000c_x^{10}(-501520106250$$
$$+979241673375y^2+103561958943y^4-70621182450y^6-3634668000y^8+464490000y^{10}+19650000y^{12}$$
$$+100000y^{14})+816816000c_x^8(206166014618753700+59347317717351153y^2-43767159222523905y^4$$
$$-2004987879876870y^6+175485517182000y^8+3571005798000y^{10}+75969780000y^{12}+2368600000y^{14})$$
$$-884000c_x^6(6528956376794658351966036-7555729351571921197325 34y^2-3447858143944345207430 97y^4$$
$$-6154114152851666687070y^6-22989875349917044800y^8+84084901295377500y^{10}+2434884730383000y^{12}$$
$$+16209808280000y^{14})+6800c_x^4(5997731230126242110279395158739 2+1944131392114377296194856956464y^2$$
$$+1035436810958111363745648404 7y^4+1209803113312668537692129 1y^6-3100884384108180981811 5y^8$$
$$-1553596191562704061 5y^{10}+126526876135628587 5y^{12}-851599591911325 0y^{14}+403515099000 0y^{16})$$
$$+34c_x^2(-4176433771841315892230262870651040 32-3125318038823177364454210752388560y^2$$
$$-1102332533998070099650997993922 0y^4-2189102410168070928881960610 0y^6$$
$$-6767228751602285467375875y^8+4464566463830001165000y^{10}-1550250438379413487 50y^{12}$$

$$+6369937954297337500y^{14}+15317572736250000y^{16})+3267264000c_z^8y^2(57-10y^2)^2(359126296893$$
$$-145841412150y^2-3939899670y^4-43775700y^6-1196000y^8+70c_x^2(-5117175+4867857y^2-888030y^4$$
$$+27900y^6+1000y^8))+884000c_z^6(-432386668458828343559376+52453208223768705529037 4y^2$$
$$-83930889871948678588953y^4-188479501937336967588 0y^6-9323106640280970075y^8$$
$$+10399500149582250y^{10}+418103621029500y^{12}+3842259895000y^{14}+129360c_x^4(-196883308125$$
$$+713630991150y^2-419715236628y^4+72377728200y^6-920682000y^8-596340000y^{10}+24600000y^{12}$$
$$+400000y^{14})+924c_x^2(72587781114574950-178784024381487063y^2+62003252249311905y^4$$
$$-4416662650252230y^6-127053813991500y^8-537654753000y^{10}-100734780000y^{12}+933400000y^{14}))$$
$$+3400c_z^4(-184116080239637687012375747202 96-818816925584283007726454462352y^2$$
$$-6331434320356389242404311906y^4-14004844796873177777047518y^6-29911526368619786941 05y^8$$
$$-1910198838780987 30y^{10}-183766961175987000y^{12}+3235122836486000y^{14}+8070301980000y^{16}$$
$$+33633600c_x^6(1463626513125-1936444170150y^2+243231434172y^4+91294792200y^6-13130262000y^8$$
$$-250740000y^{10}+42600000y^{12}+400000y^{14})+720720c_x^4(-125079127252386300+6881079888360008 1y^2$$
$$+20948327990468865y^4-4973452762176990y^6+20879248282500y^8+1554606531000y^{10}-29776740000y^{12}$$
$$+1890200000y^{14})-2340c_x^2(-805612835718984566317968+5753433817889455692553 02y^2$$
$$-3901034209541944681067 4y^4-6727228056610043805 90y^6-2552498463124469475y^8$$
$$+10717110803925750y^{10}+172859961648500y^{12}+6005025235000y^{14}))$$
$$+68c_z^2(-24370299528601290692254705918400961 6-18247999987300080115432176911848 80y^2$$
$$-54813078220559711856691255968 60y^4-11170665514903134047812804800y^6$$
$$-11210804931378523288442625y^8+3280569168761694810000y^{10}-5942966408222988375 0y^{12}$$
$$-591730052286312500y^{14}-539095736250000y^{16}+3363360000c_x^8(-679638954375-49467291300y^2$$
$$+254353749993y^4-13717548450y^6-5204898000y^8+141840000y^{10}+15150000y^{12}+100000y^{14})$$
$$+12012000c_x^6(-279192829534230150+484054564278278637y^2-505918948518751 95y^4$$
$$-1165155238785573 0y^6+315555357159000y^8+7380594252000y^{10}+75317820000y^{12}+6627400000y^{14})$$
$$-234000c_x^4(-715952313639609059461 14+279653241554909496016281y^2-436116750818558294046 87y^4$$
$$-787036948838515502820y^6-3048047829524815425y^8+10525060671415500y^{10}+271525446493000y^{12}$$
$$+4116516405000y^{14})+300c_x^2(167909117748709446393725293332 48+548348917097130517025224162596y^2$$
$$+28520566021262456383758245 73y^4+17260485408348513080439 69y^6-19792590676075283476410y^8$$
$$+3575053769068018965y^{10}+96186008719732662 5y^{12}+7901977531043250y^{14}+2690100660000y^{16})))$$
$$+77520c_y^6(60244770469377038894929908021630592656+13280057844995285023503420944266439 52y^2$$
$$+45697140666660061247044128487534 80y^4+58521646115545517287376197604 40y^6$$
$$+44396386587158852328076244 25y^8+28403208923532552094986 00y^{10}+10087779651164847450 00y^{12}$$
$$+14133571757060548 5000y^{14}+489028501335300000y^{16}+547860524000000y^{18}$$
$$-363242880000c_z^{10}y^4(57-10y^2)^4(-19+10y^2)+363242880000c_x^{10}(17373740625-155055349575y^2$$
$$+23194422144y^4+24049282860y^6-1266325200y^8-330956000y^{10}+3320000y^{12}+400000y^{14})$$
$$-864864000c_x^8(67265756169944850-19846663284896154y^2-64745433478587015y^4+42125754110189 40y^6$$
$$+542160537907500y^8+12216307257000y^{10}+435396860000y^{12}+4129500000y^{14})$$
$$+93600c_x^6(160251267843364538648946 60-16557766906694137280568720y^2-16532675403031341889757 73y^4$$
$$-61692629460253001005950y^6-34839883249308222624 0y^8+92545929886497780 0y^{10}+47926010136564000y^{12}$$
$$-394161590880000y^{14}+82297600000y^{16})+3600c_x^4(-19790638026789810314998900400364$$
$$-23311472136431433652839040819 92y^2-22531688656833348642918272004y^4$$
$$-48961912923418986753019758y^6+28617173247220293280545y^8+45345477376340551410y^{10}$$
$$-1865775134847260000y^{12}+120119964968280000y^{14}+146097376880000y^{16})$$
$$-6c_x^2(-41819550403842428280274919231246923 2-72156050147782208511378857319537 60y^2$$
$$-24342544944105248785668399255600y^4-45576203310845541515784903300y^6$$
$$+40785945219363976508126 25y^8-29029269301390813680225 0y^{10}+29427874970937841125 0y^{12}$$
$$+12948140175604560000 0y^{14}+330474138905600000y^{16})+2594592000c_z^8y^2(-57+10y^2)(20473601844276$$
$$-23964470157285y^2+4107921085590y^4+144131815700y^6+1836173000y^8+58600000y^{10}$$

$$
\begin{aligned}
&-1400c_x^2(19445265 - 47422404y^2 + 24320760y^4 - 4154800y^6 + 218000y^8)) + 93600c_z^6(72066307829519998016946 0\\
&-30996551515242961633570 20y^2 + 82129504897806649802372 7y^4 + 25302651121335126820050y^6\\
&+16415650330111620126 0y^8 - 176607199966012200y^{10} - 10290335280036000y^{12} - 82174340880000y^{14}\\
&+82297600000y^{16} + 9702000c_x^4(7291974375 - 102161328570y^2 + 120276621576y^4 - 36948912480y^6\\
&+2727417600y^8 + 257488000y^{10} - 30760000y^{12} + 400000y^{14}) - 18480c_x^2(8067605984658675\\
&-75602519424648783y^2 + 52500033865814220y^4 - 7383753084266370y^6 + 30517815123000y^8\\
&+6476206734000y^{10} - 130546580000y^{12} + 6346500000y^{14})) + 5400c_z^4(20457592976973818484 8517586594944\\
&+27249222480016434593982453367 2y^2 + 35770867803175689555518825744y^4 + 11829071046072485811684078y^6\\
&+11057663826021463105455y^8 + 25682643972043498440y^{10} + 147310906825036500y^{12} - 7661229871980000y^{14}\\
&-21154683680000y^{16} + 336336000c_x^6(-31834215000 + 164231070885y^2 - 66620114712y^4 - 8841270420y^6\\
&+4025732400y^8 - 151608000y^{10} - 15040000y^{12} + 400000y^{14}) - 480480c_x^4(-34136571992452650\\
&+88880770782418167y^2 + 9250625137426470y^4 - 10214639073024120y^6 + 418214250049500y^8\\
&+13488153369000y^{10} + 120242270000y^{12} + 11596500000y^{14}) + 52c_x^2(-4992586944032610720899640\\
&+13023825611266353845156580y^2 - 19253281573193302298740 23y^4 - 48261372779875217296950y^6\\
&-25156127665373732874 0y^8 + 101407995037067800y^{10} + 2442764186066400 0y^{12} + 661413009120000y^{14}\\
&+82297600000y^{16})) + 24c_z^2(12183470376072294166204436204285980 8 + 27980929609213642200287825809532 40y^2\\
&+14847937148525207923486334444400y^4 + 45697880308205911290362307450y^6 + 62364797407172212505177625y^8\\
&-18074732818917734709750y^{10} + 35603486406635233312 5y^{12} + 32842156944591000 00y^{14} - 3448526986400000y^{16}\\
&+37837800000c_x^8(71727373125 - 65504211570y^2 - 109729738962y^4 + 27567261900y^6 + 2852946000y^8\\
&-467660000y^{10} - 7700000y^{12} + 600000y^{14}) - 108108000c_x^6(-20796751092894525 + 147964508021769453y^2\\
&-53803342943282520y^4 - 3084217615972080y^6 + 531668646909000y^8 + 12462890836000y^{10} + 337384080000y^{12}\\
&+8156000000y^{14}) + 11700c_x^4(-3573596963654194678740 + 882944108190284597244018 0y^2\\
&-28059082651884825172592 73y^4 - 7673148588327821686395 0y^6 - 400811657211071346240y^8\\
&+13097421233547728 00y^{10} + 5078006594536400 0y^{12} + 438660159120000y^{14} + 82297600000y^{16})\\
&+75c_x^2(-331341534143160325049 97961785896 - 418012673347928886066537194296 8y^2\\
&-41211796227562665017241204276y^4 - 56869204739604762973249782y^6 + 37561022275192029734620 5y^8\\
&-10558062587039278311 0y^{10} - 27778290274776223000y^{12} - 164761008439380000y^{14} + 228730702720000y^{16})))\\
&+8c_y^3y(-12842620502740589318875954680938692119329808 - 97297204412575068975203129236179187245000y^2\\
&-21546084588029355343277353738996521198 0y^4 - 20424181967551531927546231545492390 0y^6\\
&-74854531310792313680016789747375y^8 + 10162752069371924648055134250y^{10} + 21117230159903085307837 50y^{12}\\
&+92449789248176243325 00y^{14} - 83068686738469406250y^{16} + 581260562928781250y^{18}\\
&+27498621150000000 0c_x^{10}(-2308095 - 5868342y^2 + 154980y^4 + 264600y^6 + 14000y^8)\\
&+52378326000000c_x^8(-314474287689450 - 2110511945997y^2 + 35623945127295y^4 + 2731306607190y^6\\
&+51016424400y^8 + 819438000y^{10} + 11420000y^{12}) + 453492000c_x^6(19325807449102184470209 00\\
&-23078969109466347292399 8y^2 - 13839774270347864261322 9y^4 - 44914247996916264217 02y^6\\
&-38532820476012322845y^8 - 86061232844570970y^{10} + 445462499464500y^{12} + 6826640899000y^{14}\\
&+34488470000y^{16}) + 697680c_x^4(-25899843498779756555210600 6720328\\
&+54754326501911092950762472563960y^2 + 44935549269934538567076 6204045y^4\\
&+10175054604749196242692862 25y^6 + 29545459498340912213587 5y^8 - 26937534738392695462 50y^{10}\\
&+40904779680194893 75y^{12} + 121892338395256250y^{14} + 1321389039375000y^{16})\\
&-1710c_x^2(34508284867584197270707377310794332 9784 + 23654889107157000828037353376148823 60y^2\\
&+51935119320256170022062264634610 20y^4 + 66280823710635028256693596665 00y^6\\
&+49559049444165635934899088 75y^8 - 29316655192507519900927 50y^{10} - 18359299973367803362 50y^{12}\\
&+10257281691702633500 0y^{14} + 240148955127415625y^{16}) + 906984000c_z^6y^2(-57 + 10y^2)(842824772770769305902\\
&-13097888721703851080 4y^2 - 16431609217032625 77y^4 - 5056256194889130y^6 + 7255512796455y^8\\
&+144852943900y^{10} + 1724423500y^{12} + 4244625000c_x^4(57 - 10y^2)^2 + 231000c_x^2(-269389497951 + 41393172555y^2\\
&+979206795y^4 + 7195800y^6 + 285500y^8)) + 697680c_z^4(62030885359251476363482311597072\\
&-20457000966516087620825100312390y^2 - 29336798960159472747201994758 0y^4
\end{aligned}
$$

$$
\begin{aligned}
&-10316121024971228892180005 25y^6 - 11869458214852272738453 75y^8 + 433269153318727293750y^{10} \\
&+523637604418201875y^{12} - 15786424806850000y^{14} - 44924644687500y^{16} + 16554037500000c_x^6(-292410 \\
&+409887y^2 - 66330y^4 - 5100y^6 + 1000y^8) + 225225000c_x^4(94384829901600 - 74284103692197y^2 \\
&-5064270846705y^4 + 1850777956440y^6 + 39051081900y^8 + 421638000y^{10} + 11420000y^{12}) \\
&+1300c_x^2(-619875620122564445478300 + 548253108583211057959548y^2 - 27323683559366056920981y^4 \\
&-4643394708662484543153y^6 - 5166747607843374745 5y^8 - 146948702947895205y^{10} + 301491168494250y^{12} \\
&+6113795048500y^{14} + 51732705000y^{16})) + 3420c_z^2(-190143880716606781367561727258149051592 \\
&-13864912473587406653086487120789290 80y^2 - 269476582673817526655872996287516 0y^4 \\
&-16194914805388713502260772620 00y^6 + 5099496521984637467434740 00y^8 + 735815237219896571419500y^{10} \\
&-660436021762962585000y^{12} - 91069530719555800 00y^{14} - 90220625390246875y^{16} \\
&+482431950000000c_x^8(4529385 - 1051731y^2 - 665910y^4 + 48300y^6 + 7000y^8) \\
&+91891800000c_x^6(-1536069877650 - 50384640212361y^2 + 6796591651710y^4 + 1135191995595y^6 \\
&+21773673450y^8 + 310269000y^{10} + 5710000y^{12}) + 265200c_x^4(336938915091023057250900 \\
&+486170968837386203574588y^2 - 112371248790920564566506y^4 - 567343847773243189410 3y^6 \\
&-54796253687514986955y^8 - 139316005812203955y^{10} + 459923908064250y^{12} + 8176878198500y^{14} \\
&+51732705000y^{16}) + 408c_x^2(-98109029368326753351467701436628 + 17003354135223118183025461366410y^2 \\
&+76839585661788704906414182920y^4 - 72988979448177204952790 25y^6 - 43371648580391932901 1000y^8 \\
&-11465598562061704856 25y^{10} + 17161818733511112 50y^{12} + 43464624765140625y^{14} + 638232197343750y^{16})))) \\
&+152c_y^4(67592579133173530364268204703292018848 4832 + 153632688869073688363720050789194662636 80y^2 \\
&+56591064035183284758763112121746825700y^4 + 74290340271652185024073505190214800y^6 \\
&+335671246546555111397629688013 75y^8 - 778766844476640200527771 4250y^{10} \\
&-57428248712901365457112 50y^{12} + 46455629815571335875 00y^{14} + 260310263519250450000y^{16} \\
&+902451573712000000y^{18} + 578918340000000c_x^{10}(308154375 + 1030611600y^2 - 481986396y^4 - 137234880y^6 \\
&+10317600y^8 + 1888000y^{10} + 40000y^{12}) + 14702688000c_x^8(146425283748450000 - 1594446737914878 75y^2 \\
&-85098442702166964y^4 + 7114834403671050y^6 + 1397758310365680y^8 + 41701120880400y^{10} + 761352492000y^{12} \\
&+12948660000y^{14} + 66800000y^{16}) + 71604000c_x^6(-12295046106896829277617 00 + 16664685809112757102939 56y^2 \\
&+24928211472771156497016 3y^4 - 38249475135843279735504y^6 - 47488809564776915874 0y^8 \\
&-14115512847470003 20y^{10} + 5785477799836000y^{12} + 120325021440000y^{14} + 2008650240000y^{16}) \\
&-24480c_x^4(-50776953658490862716912864 8051392 + 58486156581770967313970593156 2690y^2 \\
&+84444168972799385070720869720 25y^4 + 28179235308504765375421856325y^6 + 19640428837821328193031375y^8 \\
&-67919415075288747345375y^{10} + 56311670811154736250y^{12} + 306554099643791 2500y^{14} + 13335901676600000y^{16}) \\
&+510c_x^2(60894674457031572096085576030840094856 + 12509517594759957906279591259539966 24y^2 \\
&+55344642543210182164663231991019 60y^4 + 15490603734405245450805242021580y^6 \\
&+24545753695017513662547568725y^8 + 64719462434189140702624 50y^{10} - 15703535729639257841250y^{12} \\
&+173790245369581020000y^{14} - 877201595153250000y^{16} + 1095721048000000y^{18}) \\
&+29405376000c_z^8y^4(-57 + 10y^2)^3(6299563599 + 136795785y^2 + 1345470y^4 + 33400y^6 + 78750c_x^2(-57 + 10y^2)) \\
&+95472000c_z^6y^2(144125696432441191921992 - 7947172200265513432 9254y^2 + 85131317330029704742 47y^4 \\
&+14525045676010179387 0y^6 + 565181900896064760y^8 - 657346598874000y^{10} - 18855109170000y^{12} \\
&-203410420000y^{14} + 48510000c_x^4(57 - 10y^2)^2(29925 - 29202y^2 + 1220y^4 + 200y^6) + 308c_x^2(-51835289527964250 \\
&+46643470575141447y^2 - 7969908470709150y^4 + 51752481043860y^6 + 30212386885800y^8 + 516144984000y^{10} \\
&+8797320000y^{12} + 133600000y^{14})) + 6120c_z^4(-37218652091296809718156255226 7432 \\
&+42959956958755567510898233399 2840y^2 + 99614557759284261475937271616 50y^4 \\
&+50038111969269978257631877950y^6 + 76744971570605069018912625y^8 - 26114051501138637036000y^{10} \\
&-75185040995208007500y^{12} + 107207848462185000 0y^{14} - 3448526986400000y^{16} + 567567000000c_x^6(127929375 \\
&-846398700y^2 + 388541304y^4 + 4767120y^6 - 11942400y^8 + 488000y^{10} + 40000y^{12}) \\
&+7207200c_x^4(-35409422870521875 + 144611503425655875y^2 - 12436865754333678y^4 - 1130806533627540 0y^6 \\
&+723482174106360y^8 + 44154429760800y^{10} + 707889984000y^{12} + 14497320000y^{14} + 133600000y^{16}) \\
&+3900c_x^2(18596759168830346930349 00 - 77675646882832218703596 96y^2 + 19391958891064860313052 07y^4
\end{aligned}
$$

$$
\begin{aligned}
&-19811933543127274200036y^6 - 1600931639316498627 60y^8 - 89960890949732880y^{10} + 5977234952766000y^{12}\\
&+792540960000y^{14} + 4398667360000y^{16})) + 2040c_z^2(167766890052239387123447139835123835 64\\
&+3660720157521167111710968540952600 56y^2 + 1308286277980553055968786658645990y^4\\
&+216051508737501898414183332102 0y^6 + 265400213340760419308339452 5y^8 + 193991378616189488927092 5y^{10}\\
&-5115997377633644775 00y^{12} + 13559479690481786250y^{14} + 141164009971125000y^{16} + 273930262000000y^{18}\\
&+567567000000c_x^8(-1028345625 + 1763766900y^2 + 575772408y^4 - 230117760y^6 - 12124800y^8 + 2376000y^{10}\\
&+80000y^{12}) + 14414400c_x^6(15117027739340625 + 208393242266797875y^2 - 114024196885408803y^4\\
&-4786040860779150y^6 + 1626238820668860y^8 + 60955131385800y^{10} + 1043409984000y^{12} + 20197320000y^{14}\\
&+133600000y^{16}) + 23400c_x^4(-8954149643649300100626 00 - 17282795824542741808641 48y^2\\
&+151245823043484570653198 1y^4 - 8420173461293352327676 8y^6 - 1083729303599505850980y^8\\
&-3301837305640621440y^{10} + 1227310595826000 0y^{12} + 218594020980000y^{14} + 5619129880000y^{16})\\
&-6c_x^2(-8260689353871797903099340186565 68 + 9482948433081729407264918895039 60y^2\\
&+1242764964269716867464782557260 0y^4 + 3613724714687567424886997055 0y^6 + 3584881445157975217129875y^8\\
&-1755384414225416514540 00y^{10} + 1808150309479168200 00y^{12} + 782679806904990000 0y^{14}\\
&+826185347264000 00y^{16}))) + 38c_y^2(3473510040000000000c_x^{10}(-14625 - 3582y^2 + 5520y^4 + 700y^6)\\
&+1240539300000000c_x^8(-227435082840 + 298509767577y^2 + 71648667930y^4 + 1415217860y^6 + 17567400y^8\\
&+474000y^{10}) + 238680000c_x^6(80333497973969964801000 - 11147900068886834234797 2y^2\\
&-1844273936146113458563 5y^4 - 2078403511025091234 60y^6 - 611372061511734600y^8 + 923239637350800y^{10}\\
&+20815062296000y^{12} + 212001600000y^{14}) + 4080c_x^4(-14615806445391221515399744858068 00\\
&+2136799538150224998329077007945736y^2 + 1498036780491128552479369767602 40y^4\\
&+1245596411040563123786573399070y^6 + 3146533976406475791464102775y^8 + 2708099899912794704867550y^{10}\\
&-1091983195646371665000y^{12} + 2173100697625455000y^{14} + 57913742316600000y^{16} + 273930262000000y^{18})\\
&+25(-2941725240476240535255547552622299814793 60 - 6517640117736926102069495954787639311856y^2\\
&-2328643631082508593602616271448035992 0y^4 - 3081536282372019972393194222813892 0y^6\\
&-1886635919482322946903062967870 0y^8 - 5196510330118932764250060750y^{10} + 1231095478949010358456500y^{12}\\
&+1455625772107105297500y^{14} - 189750447618308381 25y^{16} + 20284131251900000y^{18})\\
&+4c_x^2(7581996804456150089712183491515831322320 32 + 1606154582781065464966085034027528836 5680y^2\\
&+5527273791586989758253194808551170170 0y^4 + 7285295074937930644325825946532680 0y^6\\
&+5112785076633415982205284392012 5y^8 + 1987447031612562924687608325 0y^{10} - 2005071168318070582036125 0y^{12}\\
&+1026017156881805827500 0y^{14} + 7350979855560169500 00y^{16} + 56490519655520000 00y^{18})\\
&+8160c_z^4y^2(-3721843451713983585620400794344 32 + 6137108317302879721179288675762 0y^2\\
&+5867204694398591323855196721 60y^4 + 1544040872498237912882032950y^6 + 1385957521620383307871275y^8\\
&-5656934151568320075 00y^{10} - 3419507078552250 0y^{12} + 18906884637300000y^{14} + 136965131000000y^{16}\\
&+2979726750000000c_x^6(57 - 10y^2)^2 + 912161250000c_x^4(-59904133128 + 9197020455y^2 + 222295010y^4 + 946900y^6\\
&+79000y^8) + 351000c_x^2(8264821457261699605044 - 1316774252576632040730y^2 - 1661675818756697320 5y^4\\
&-5255912096515080 0y^6 + 48910680795900y^8 + 1116770858000y^{10} + 17666800000y^{12}))\\
&+4c_z^2(7574001306506707913846749764564522909250 32 + 1711278752432694533851701910493911557168 0y^2\\
&+6244437508326491040792516534791618070 0y^4 + 8132856232097768508933755979799980 0y^6\\
&+3734350326421748931444091057012 5y^8 - 8173467517723567473484570500y^{10} - 8278592198085038876523750y^{12}\\
&+8906259156700566712500y^{14} + 56195624007180450000y^{16} + 902451573712000000y^{18}\\
&+1085471887500000000c_x^8(192375 - 352962y^2 - 19680y^4 + 11200y^6) + 1240539300000000c_x^6(-55337202585\\
&-20960842329y^2 + 31797157665y^4 + 669974480y^6 + 5812200y^8 + 237000y^{10})\\
&+59670000c_x^4(7995044686010594716350 0 - 1122144237033256088744 4y^2 - 3423706645895010385564 5y^4\\
&-4073437772979572081 70y^6 - 1243113912009169200y^8 + 1454218451901600y^{10} + 34216312592000y^{12}\\
&+424003200000y^{14}) + 2040c_x^2(-7296578786047509412309933611534 00 + 6935265271114104011451099635259 36y^2\\
&+1362537656216931350195176927689 90y^4 + 1209522799756005938942900231070y^6\\
&+3117518159068284969048576525y^8 + 2739792539623453538023800y^{10} - 1119575495821509090000y^{12}\\
&+935900771064705000y^{14} + 47863755795600000y^{16} + 273930262000000y^{18}))))). \qquad \text{(B.24)}
\end{aligned}
$$

Appendix C

Supplementary Material to Chapter 4

C.1 Detailed derivation of Eq. (4.32)

The heating rate associated with the external driving $\mathscr{F}$ is

$$\gamma(\boldsymbol{x},t) = -\frac{m}{3n(\boldsymbol{x},t)T(\boldsymbol{x},t)}\int d\boldsymbol{c}\; C^2 \mathscr{F} f(\boldsymbol{x},\boldsymbol{c};t), \tag{C.1}$$

where $\mathscr{F} = -\frac{\xi^2}{2}\left(\frac{\partial}{\partial \boldsymbol{c}}\right)^2$, $\boldsymbol{C} = \boldsymbol{c} - \boldsymbol{u}, \Rightarrow d\boldsymbol{C} = d\boldsymbol{c}$ and $\frac{\partial}{\partial \boldsymbol{C}} = \frac{\partial}{\partial \boldsymbol{c}}$;

$$\begin{aligned}
\therefore \gamma(\boldsymbol{x},t) &= -\frac{m}{3n(\boldsymbol{x},t)T(\boldsymbol{x},t)}\int d\boldsymbol{C}\; C^2\left(-\frac{\xi^2}{2}\left(\frac{\partial^2}{\partial \boldsymbol{C}^2}\right)\right) f_l(\boldsymbol{x},\boldsymbol{c};t), \\
&= -\frac{m}{3n(\boldsymbol{x},t)T(\boldsymbol{x},t)}\left(-\frac{\xi^2}{2}\right)\int d\boldsymbol{C}\; C^2\left(\frac{\partial^2}{\partial \boldsymbol{C}^2}\right) f_l(\boldsymbol{x},\boldsymbol{c};t),
\end{aligned}$$

since we know that $f_l(\boldsymbol{x},\boldsymbol{c};t) = n(\boldsymbol{x},t)\left[\frac{m}{2\pi T(\boldsymbol{x},t)}\right]^{3/2}\exp\left[-\frac{mC^2}{2T(\boldsymbol{x},t)}\right]$, so substitute this value $f_l(\boldsymbol{x},\boldsymbol{c};t)$ into the above equation, we get

$$\gamma(\boldsymbol{x},t) = \frac{m}{3n(\boldsymbol{x},t)T(\boldsymbol{x},t)}\left(\frac{\xi^2}{2}\right) n(\boldsymbol{x},t)\left[\frac{m}{2\pi T(\boldsymbol{x},t)}\right]^{3/2}\int d\boldsymbol{C}\; C^2\left(\frac{\partial^2}{\partial \boldsymbol{C}^2}\right)\exp\left[-\frac{mC^2}{2T}\right].$$

After integration, we get the heating rate

$$\gamma(\boldsymbol{x},t) = \frac{m\xi^2}{T}. \tag{C.2}$$

For simplicity, we assume that the white-noise driving compensates locally for the collisional energy loss. This means that $\gamma = \zeta$,

$$\Rightarrow \xi^2 = \frac{\gamma T}{m} = \frac{\zeta T}{m}$$

$$\begin{aligned}
\therefore \mathscr{F} &= -\frac{1}{2}\left(\frac{\zeta T}{m}\right)\left(\frac{\partial}{\partial \boldsymbol{c}}\right)^2 \\
&= -\frac{\zeta T}{2m}\left(\frac{\partial}{\partial \boldsymbol{c}}\right)^2
\end{aligned}$$

$\therefore$ The Boltzmann equation (4.3) becomes,

$$\left(-\frac{\zeta T}{2m}\frac{\partial^2}{\partial \boldsymbol{c}^2} - g\frac{\partial}{\partial c_x} + c_y\frac{\partial}{\partial y}\right) f = J[f,f]. \tag{C.3}$$

Since we assumed that $J[f,f] \to -\beta(\alpha)\nu(f - f_l) + \frac{\zeta_l}{2}\frac{\partial}{\partial \boldsymbol{c}}\cdot[(\boldsymbol{c}-\boldsymbol{u})f]$, substitute this value $(J[f,f])$ into the above equation, we get

$$\left(-g\frac{\partial}{\partial c_x} + c_y\frac{\partial}{\partial y}\right) f = -\beta\nu(f - f_l) + \frac{\zeta_l}{2}\frac{\partial}{\partial \boldsymbol{c}}\cdot\left(\boldsymbol{C} + \frac{T}{m}\frac{\partial}{\partial \boldsymbol{c}}\right) f.$$

Substitute $f = f_l(1+\Phi)$ in the above equation, we get

$$\left(-g\frac{\partial}{\partial c_x} + c_y\frac{\partial}{\partial y}\right)\{f_l(1+\Phi)\} = -\beta\nu f_l\Phi + \frac{\zeta_l}{2}\frac{\partial}{\partial \boldsymbol{c}}\cdot\left\{\left(\boldsymbol{C} + \frac{T}{m}\frac{\partial}{\partial \boldsymbol{c}}\right)(f_l(1+\Phi))\right\}. \tag{C.4}$$

First, we will find $\frac{\partial f_l}{\partial \boldsymbol{c}}$:

$$\begin{aligned}
\frac{\partial f_l}{\partial \boldsymbol{c}} &= n\Big(\frac{m}{2\pi T}\Big)^{3/2}\sum_{i=1}^{3}\hat{\boldsymbol{\delta}}_{\boldsymbol{i}}\frac{\partial}{\partial c_i}\exp\Big[-\Big(\frac{m}{2T}\Big)\Big((c_1-u_1)^2+(c_2-u_2)^2+(c_3-u_3)^2\Big)\Big] \\
&= n\Big(\frac{m}{2\pi T}\Big)^{3/2}\sum_{i=1}^{3}\hat{\boldsymbol{\delta}}_{\boldsymbol{i}}\frac{\partial}{\partial c_i}\exp\Big[-\Big(\frac{m}{2T}\Big)\Big(\sum_{j=1}^{3}(c_j-u_j)^2\Big)\Big] \\
&= n\Big(\frac{m}{2\pi T}\Big)^{3/2}\exp\Big[-\frac{m(\boldsymbol{c}-\boldsymbol{u})^2}{2T}\Big]\sum_{i=1}^{3}\hat{\boldsymbol{\delta}}_{\boldsymbol{i}}\Big[-\Big(\frac{m}{T}\Big)\Big(\sum_{j=1}^{3}(c_j-u_j)\delta_{ji}\Big)\Big] \\
&= n\Big(\frac{m}{2\pi T}\Big)^{3/2}\exp\Big[-\frac{m(\boldsymbol{c}-\boldsymbol{u})^2}{2T}\Big]\sum_{i=1}^{3}\hat{\boldsymbol{\delta}}_{\boldsymbol{i}}\Big[-\Big(\frac{m}{T}\Big)\Big(c_i-u_i\Big)\Big] \\
&= f_l\Big[-\Big(\frac{m}{T}\Big)\Big(\boldsymbol{c}-\boldsymbol{u}\Big)\Big] \\
&= -\frac{m}{T}f_l\boldsymbol{C}. \quad (\because \boldsymbol{C}=\boldsymbol{c}-\boldsymbol{u})
\end{aligned}$$

Next, we will find $\frac{\partial}{\partial \boldsymbol{c}}\cdot\Big\{\Big(\boldsymbol{C}+\frac{T}{m}\frac{\partial}{\partial \boldsymbol{c}}\Big)(f_l(1+\Phi))\Big\}$:

$$\begin{aligned}
\frac{\partial}{\partial \boldsymbol{c}}\cdot\Big\{\Big(\boldsymbol{C}+\frac{T}{m}\frac{\partial}{\partial \boldsymbol{c}}\Big)(f_l(1+\Phi))\Big\} &= \frac{\partial}{\partial \boldsymbol{c}}\cdot\Big\{\boldsymbol{C}f_l(1+\Phi)+\frac{T}{m}\Big(f_l\frac{\partial\Phi}{\partial \boldsymbol{c}}+(1+\Phi)\frac{\partial f_l}{\partial \boldsymbol{c}}\Big)\Big\} \\
&= \frac{\partial}{\partial \boldsymbol{c}}\cdot\Big\{\boldsymbol{C}f_l(1+\Phi)+\frac{T}{m}\Big(f_l\frac{\partial\Phi}{\partial \boldsymbol{c}}+(1+\Phi)\Big(-\frac{m}{T}f_l\boldsymbol{C}\Big)\Big)\Big\} \\
&= \frac{\partial}{\partial \boldsymbol{c}}\cdot\Big\{\boldsymbol{C}f_l(1+\Phi)+\frac{T}{m}f_l\frac{\partial\Phi}{\partial \boldsymbol{c}}-(1+\Phi)f_l\boldsymbol{C}\Big\} \\
&= \frac{\partial}{\partial \boldsymbol{c}}\cdot\Big\{\frac{T}{m}f_l\frac{\partial\Phi}{\partial \boldsymbol{c}}\Big\} \\
&= \frac{T}{m}\Big[\frac{\partial}{\partial \boldsymbol{c}}\cdot\Big\{f_l\frac{\partial\Phi}{\partial \boldsymbol{c}}\Big\}\Big] \\
&= \frac{T}{m}\Big[f_l\frac{\partial}{\partial \boldsymbol{c}}\cdot\frac{\partial\Phi}{\partial \boldsymbol{c}}+\frac{\partial f_l}{\partial \boldsymbol{c}}\cdot\frac{\partial\Phi}{\partial \boldsymbol{c}}\Big] \\
&= \frac{T}{m}\Big[f_l\frac{\partial}{\partial \boldsymbol{c}}\cdot\frac{\partial\Phi}{\partial \boldsymbol{c}}+\Big(-\frac{m}{T}f_l\boldsymbol{C}\Big)\cdot\frac{\partial\Phi}{\partial \boldsymbol{c}}\Big] \\
&= f_l\Big[\frac{T}{m}\frac{\partial}{\partial \boldsymbol{C}}-\boldsymbol{C}\Big]\cdot\frac{\partial\Phi}{\partial \boldsymbol{C}}. \quad \Big(\because \frac{\partial}{\partial \boldsymbol{C}}=\frac{\partial}{\partial \boldsymbol{c}}\Big)
\end{aligned}$$

Then, Eq. (C.4) becomes

$$\Big(-g\frac{\partial}{\partial c_x}+c_y\frac{\partial}{\partial y}\Big)\{f_l(1+\Phi)\}=-\beta\nu f_l\Phi+\frac{\zeta_l f_l}{2}\Big[\frac{T}{m}\frac{\partial}{\partial \boldsymbol{C}}-\boldsymbol{C}\Big]\cdot\frac{\partial\Phi}{\partial \boldsymbol{C}}. \tag{C.5}$$

Now, we will simplify LHS:

$$\begin{aligned}
\Big(-g\frac{\partial}{\partial c_x}+c_y\frac{\partial}{\partial y}\Big)\{f_l(1+\Phi)\} &= f_l\Big(-g\frac{\partial}{\partial c_x}+c_y\frac{\partial}{\partial y}\Big)\Phi+(1+\Phi)\Big(-g\frac{\partial}{\partial c_x}+c_y\frac{\partial}{\partial y}\Big)f_l \\
&= f_l\Big\{\Big(-g\frac{\partial}{\partial c_x}+c_y\frac{\partial}{\partial y}\Big)\Phi+(1+\Phi)\Big(-g\frac{\partial}{\partial c_x}+c_y\frac{\partial}{\partial y}\Big)\log f_l\Big\} \\
&= f_l\Big\{\Big(-g\frac{\partial}{\partial C_x}+C_y\frac{\partial}{\partial y}\Big)\Phi+(1+\Phi)\Big(-g\frac{\partial}{\partial C_x}+C_y\frac{\partial}{\partial y}\Big)\log f_l\Big\}
\end{aligned}$$

($\because \boldsymbol{C} = \boldsymbol{c} - \boldsymbol{u} \Rightarrow C_y = c_y - u_y$, but $u_y = 0 \Rightarrow c_y = C_y$ & $\frac{\partial}{\partial c_x} = \frac{\partial}{\partial C_x}$)

$$\begin{aligned}
\Big(-g\frac{\partial}{\partial c_x} + c_y\frac{\partial}{\partial y}\Big)\{f_l(1+\Phi)\} &= f_l\Big\{\Big(-g\frac{\partial}{\partial C_x} + C_y\frac{\partial}{\partial y}\Big)\Phi + (1+\Phi)\Big(-g\frac{\partial}{\partial C_x} + C_y\frac{\partial}{\partial y}\Big)\log f_l\Big\} \\
&= f_l\Big\{(1+\Phi)\Big[-\Big(g + C_y\frac{\partial u_x}{\partial y}\Big)\frac{\partial}{\partial C_x}\log f_l + C_y\frac{\partial u_x}{\partial y}\frac{\partial}{\partial C_x}\log f_l \\
&\quad + C_y\frac{\partial}{\partial y}\log f_l\Big] - \Big(g + C_y\frac{\partial u_x}{\partial y}\Big)\frac{\partial\Phi}{\partial C_x} + C_y\frac{\partial u_x}{\partial y}\frac{\partial\Phi}{\partial C_x} + C_y\frac{\partial\Phi}{\partial y}\Big\} \\
&= f_l\Big\{(1+\Phi)\Big[C_y\Big(\frac{\partial}{\partial y} + \frac{\partial u_x}{\partial y}\frac{\partial}{\partial C_x}\Big)\log f_l - \Big(g + C_y\frac{\partial u_x}{\partial y}\Big)\frac{\partial}{\partial C_x}\log f_l\Big] \\
&\quad - \Big(g + C_y\frac{\partial u_x}{\partial y}\Big)\frac{\partial\Phi}{\partial C_x} + C_y\Big(\frac{\partial}{\partial y} + \frac{\partial u_x}{\partial y}\frac{\partial}{\partial C_x}\Big)\Phi\Big\} \\
&= f_l\Big\{(1+\Phi)\Big[C_y\tilde{\partial}_y\log f_l - \Big(g + C_y\frac{\partial u_x}{\partial y}\Big)\frac{\partial}{\partial C_x}\log f_l\Big] \\
&\quad - \Big(g + C_y\frac{\partial u_x}{\partial y}\Big)\frac{\partial\Phi}{\partial C_x} + C_y\tilde{\partial}_y\Phi\Big\}. \quad \Big(\because \tilde{\partial}_y = \frac{\partial}{\partial y} + \frac{\partial u_x}{\partial y}\frac{\partial}{\partial C_x}\Big)
\end{aligned}$$

Substitute the above expression into Eq. (C.5), we get

$$\begin{aligned}
&(1+\Phi)\Big[C_y\tilde{\partial}_y\log f_l - \Big(g + C_y\frac{\partial u_x}{\partial y}\Big)\frac{\partial}{\partial C_x}\log f_l\Big] = \Big(g + C_y\frac{\partial u_x}{\partial y}\Big)\frac{\partial}{\partial C_x}\Phi \\
&-C_y\tilde{\partial}_y\Phi - (\nu' - \zeta_l)\Phi + \frac{\zeta_l}{2}\Big[\Big(\frac{T}{m}\frac{\partial}{\partial \boldsymbol{C}} - \boldsymbol{C}\Big)\cdot\frac{\partial}{\partial \boldsymbol{C}}\Phi\Big],
\end{aligned} \tag{C.6}$$

where $\nu' - \zeta_l = \beta\nu$.

C.2 Expressions for the coefficients b_i in terms of ζ_0^*

$$b_0 = -\frac{4\left(10 + 39\zeta_0^* + 47{\zeta_0^*}^2 + 30{\zeta_0^*}^3\right)}{5(1+\zeta_0^*)^2\left(4 + 16\zeta_0^* + 19{\zeta_0^*}^2 + 6{\zeta_0^*}^3\right)}, \tag{C.7}$$

$$b_1 = -\frac{8\left(-160 - 622\zeta_0^* + 1051{\zeta_0^*}^2 + 2829{\zeta_0^*}^3 + 1696{\zeta_0^*}^4 + 276{\zeta_0^*}^5\right)}{25\left(2 + 3\zeta_0^* + {\zeta_0^*}^2\right)^2\left(2 + 7\zeta_0^* + 6{\zeta_0^*}^2\right)}, \tag{C.8}$$

$$b_2 = -\frac{48(1+3\zeta_0^*)}{5\left(4 + 12\zeta_0^* + 11{\zeta_0^*}^2 + 3{\zeta_0^*}^3\right)}, \tag{C.9}$$

$$b_3 = \frac{4}{2+\zeta_0^*}, \tag{C.10}$$

$$b_4 = -\frac{32\left(5 + 29\zeta_0^* + 12{\zeta_0^*}^2\right)}{5\left(4 + 20\zeta_0^* + 35{\zeta_0^*}^2 + 25{\zeta_0^*}^3 + 6{\zeta_0^*}^4\right)}, \tag{C.11}$$

$$b_5 = \frac{32\left(5 + 17\zeta_0^* + 6{\zeta_0^*}^2\right)}{5\left(4 + 12\zeta_0^* + 11{\zeta_0^*}^2 + 3{\zeta_0^*}^3\right)}, \tag{C.12}$$

$$b_6 = -\frac{8\left(5 + 9\zeta_0^* + 2{\zeta_0^*}^2\right)}{5\left(2 + 3\zeta_0^* + {\zeta_0^*}^2\right)}, \tag{C.13}$$

$$b_7 = \frac{4}{3}, \tag{C.14}$$

$$b_8 = \frac{8(4 + \zeta_0^*(12 + \zeta_0^*(113 + \zeta_0^*(176 + \zeta_0^*(79 + 6\zeta_0^*)))))}{(1+\zeta_0^*)^2(2+\zeta_0^*)^2(2 + \zeta_0^*(7 + 6\zeta_0^*))}, \tag{C.15}$$

$$b_9 = \frac{32(3 + 2\zeta_0^*)(-2 + \zeta_0^*(11 + 12\zeta_0^*))}{(1+\zeta_0^*)^2(2+\zeta_0^*)^2(2 + \zeta_0^*(7 + 6\zeta_0^*))}, \tag{C.16}$$

$$b_{10} = -\frac{16(-8 + \zeta_0^*(22 + \zeta_0^*(23 + 3\zeta_0^*)))}{(1+\zeta_0^*)(2+\zeta_0^*)^2(2 + 3\zeta_0^*)}, \tag{C.17}$$

$$b_{11} = \frac{8\zeta_0^*}{1+\zeta_0^*}, \tag{C.18}$$

$$b_{12} = \frac{64(3+2\zeta_0^*)}{4+20\zeta_0^*+35{\zeta_0^*}^2+25{\zeta_0^*}^3+6{\zeta_0^*}^4}, \tag{C.19}$$

$$b_{13} = -\frac{64(3+2\zeta_0^*)}{4+12\zeta_0^*+11{\zeta_0^*}^2+3{\zeta_0^*}^3}, \tag{C.20}$$

$$b_{14} = \frac{16}{1+\zeta_0^*}, \tag{C.21}$$

$$b_{15} = \frac{8\zeta_0^*\left(76-48\zeta_0^*-137{\zeta_0^*}^2+7{\zeta_0^*}^3+42{\zeta_0^*}^4\right)}{25\left(2+3\zeta_0^*+{\zeta_0^*}^2\right)^2\left(2+7\zeta_0^*+6{\zeta_0^*}^2\right)}, \tag{C.22}$$

$$b_{16} = \frac{16\left(76-48\zeta_0^*-137{\zeta_0^*}^2+7{\zeta_0^*}^3+42{\zeta_0^*}^4\right)}{25\left(2+3\zeta_0^*+{\zeta_0^*}^2\right)^2\left(2+7\zeta_0^*+6{\zeta_0^*}^2\right)}, \tag{C.23}$$

$$b_{17} = -\frac{16\left(76+40\zeta_0^*+23{\zeta_0^*}^2+21{\zeta_0^*}^3\right)}{25(2+\zeta_0^*)^2\left(2+5\zeta_0^*+3{\zeta_0^*}^2\right)}, \tag{C.24}$$

$$b_{18} = -\frac{8\zeta_0^*}{5+5\zeta_0^*}, \tag{C.25}$$

$$b_{19} = -\frac{64}{5\left(2+9\zeta_0^*+13{\zeta_0^*}^2+6{\zeta_0^*}^3\right)}, \tag{C.26}$$

$$b_{20} = \frac{64}{5\left(2+5\zeta_0^*+3{\zeta_0^*}^2\right)}, \tag{C.27}$$

$$b_{21} = -\frac{16}{5+5\zeta_0^*}, \tag{C.28}$$

$$b_{22} = \frac{16}{15}. \tag{C.29}$$

C.3 Expressions for the coefficients c_i in terms of ζ_0^*

$$c_0 = -\frac{512(6+\zeta_0^*)(5+7\zeta_0^*)}{5(1+\zeta_0^*)(1+2\zeta_0^*)(1+3\zeta_0^*)(2+3\zeta_0^*)(2+5\zeta_0^*)(2+7\zeta_0^*)}, \tag{C.30}$$

$$\begin{aligned} c_1 \;=\; & \frac{1}{(25(1+\zeta_0^*)^3(2+\zeta_0^*)^4(1+2\zeta_0^*)^2(1+3\zeta_0^*)(2+3\zeta_0^*)^3(2+5\zeta_0^*)^2(2+7\zeta_0^*))}(-(32(6400+\zeta_0^*(115456 \\ & +\zeta_0^*(1689856+\zeta_0^*(2003200+\zeta_0^*(-65560032+\zeta_0^*(-411549088+\zeta_0^*(-1127199552+\zeta_0^*(-1637392928 \\ & +\zeta_0^*(-1153603587+\zeta_0^*(-15402953+\zeta_0^*(629343301+3\zeta_0^*(164504451 \\ & +2\zeta_0^*(28914649+60\zeta_0^*(79847+5040\zeta_0^*)))))))))))))), \end{aligned} \tag{C.31}$$

$$\begin{aligned} c_2 \;=\; & \frac{1}{\left(25(2+\zeta_0^*)^4\left(2+5\zeta_0^*+3{\zeta_0^*}^2\right)^3\left(2+9\zeta_0^*+10{\zeta_0^*}^2\right)^2\left(2+13\zeta_0^*+21{\zeta_0^*}^2\right)\right)}(16(19200+1768960\zeta_0^* \\ & +37601152{\zeta_0^*}^2+400608960{\zeta_0^*}^3+2353838976{\zeta_0^*}^4+8319795184{\zeta_0^*}^5+18777868088{\zeta_0^*}^6+27958142676{\zeta_0^*}^7 \\ & +27725778301{\zeta_0^*}^8+18090525151{\zeta_0^*}^9+7481701685{\zeta_0^*}^{10} \\ & +1835506509{\zeta_0^*}^{11}+253573278{\zeta_0^*}^{12}+27690840{\zeta_0^*}^{13}+3628800{\zeta_0^*}^{14})), \end{aligned} \tag{C.32}$$

$$c_3 = -\frac{16}{75}(16+3\zeta_0^*), \tag{C.33}$$

$$c_4 = -\frac{512(-90+\zeta_0^*(-251+\zeta_0^*(-114+7\zeta_0^*)))}{5(1+\zeta_0^*)(2+\zeta_0^*)(1+2\zeta_0^*)(1+3\zeta_0^*)(2+3\zeta_0^*)(2+5\zeta_0^*)(2+7\zeta_0^*)}, \tag{C.34}$$

$$\begin{aligned} c_5 \;=\; & \frac{1}{25\left(2+13\zeta_0^*+21{\zeta_0^*}^2\right)\left(8+60\zeta_0^*+170{\zeta_0^*}^2+225{\zeta_0^*}^3+137{\zeta_0^*}^4+30{\zeta_0^*}^5\right)^2}(128(3168-266560\zeta_0^*-2431776{\zeta_0^*}^2 \\ & -8530992{\zeta_0^*}^3-15192058{\zeta_0^*}^4-14589440{\zeta_0^*}^5-7184789{\zeta_0^*}^6-1352088{\zeta_0^*}^7+124185{\zeta_0^*}^8+53550{\zeta_0^*}^9)), \end{aligned} \tag{C.35}$$

$$c_6 = -\frac{512(6+\zeta_0^*)(5+7\zeta_0^*)}{5(1+\zeta_0^*)(1+2\zeta_0^*)(1+3\zeta_0^*)(2+3\zeta_0^*)(2+5\zeta_0^*)(2+7\zeta_0^*)}, \tag{C.36}$$

$$c_7 = \frac{1}{(25(1+\zeta_0^*)^3(2+\zeta_0^*)^3(1+2\zeta_0^*)^2(1+3\zeta_0^*)(2+3\zeta_0^*)^3(2+5\zeta_0^*)^2(2+7\zeta_0^*))}(64(-7296+\zeta_0^*(66112 +\zeta_0^*(-3014944+\zeta_0^*(-37561072+\zeta_0^*(-175254680+\zeta_0^*(-435219604+\zeta_0^*(-633759158+\zeta_0^*(-542052413 +\zeta_0^*(-240321304+3\zeta_0^*(-5545966+\zeta_0^*(10905084+245\zeta_0^*(18181+2190\zeta_0^*)))))))))))), \quad (C.37)$$

$$c_8 = \frac{1}{25(1+\zeta_0^*)^2(2+\zeta_0^*)^2(1+2\zeta_0^*)^2(1+3\zeta_0^*)(2+3\zeta_0^*)^2(2+5\zeta_0^*)^2(2+7\zeta_0^*)}(128(5248+\zeta_0^*(-89280 +\zeta_0^*(-945296+\zeta_0^*(-3269392+\zeta_0^*(-5379048+\zeta_0^*(-4319520+\zeta_0^*(-1214339+\zeta_0^*(418732 +45\zeta_0^*(7333+1190\zeta_0^*)))))))))), \quad (C.38)$$

$$c_9 = \frac{1}{(25(1+\zeta_0^*)^3(2+\zeta_0^*)^4(1+2\zeta_0^*)^2(1+3\zeta_0^*)(2+3\zeta_0^*)^3(2+5\zeta_0^*)^2(2+7\zeta_0^*))}(-(32\zeta_0^*(19456+\zeta_0^*(-47744 +\zeta_0^*(6648000+\zeta_0^*(77547168+\zeta_0^*(355680112+\zeta_0^*(874577048+\zeta_0^*(1260636372+\zeta_0^*(1061148238 +\zeta_0^*(453618697+\zeta_0^*(19817351+3\zeta_0^*(-21226699+7\zeta_0^*(-1008061 +60\zeta_0^*(-533+315\zeta_0^*)))))))))))))), \quad (C.39)$$

$$c_{10} = \frac{1}{(25(1+\zeta_0^*)^3(2+\zeta_0^*)^3(1+2\zeta_0^*)^2(1+3\zeta_0^*)(2+3\zeta_0^*)^3(2+5\zeta_0^*)^2(2+7\zeta_0^*))}(64(11904+\zeta_0^*(-90688 +\zeta_0^*(4404256+\zeta_0^*(60671728+\zeta_0^*(311288120+\zeta_0^*(855958996+\zeta_0^*(1408881542+\zeta_0^*(1437673637 +\zeta_0^*(902419996+3\zeta_0^*(110703484+\zeta_0^*(21764684+5\zeta_0^*(444469+44310\zeta_0^*)))))))))))), \quad (C.40)$$

$$c_{11} = \frac{1}{\left(25(2+\zeta_0^*)^4\left(2+5\zeta_0^*+3{\zeta_0^*}^2\right)^3\left(2+9\zeta_0^*+10{\zeta_0^*}^2\right)^2\left(2+13\zeta_0^*+21{\zeta_0^*}^2\right)\right)}(64(673536+16203776\zeta_0^* +177130112{\zeta_0^*}^2+1002252288{\zeta_0^*}^3+3214870240{\zeta_0^*}^4+6053513456{\zeta_0^*}^5+6355376056{\zeta_0^*}^6+2489807928{\zeta_0^*}^7 -1958832265{\zeta_0^*}^8-2914409797{\zeta_0^*}^9-1339676673{\zeta_0^*}^{10} -144713706{\zeta_0^*}^{11}+72425724{\zeta_0^*}^{12}+20467395{\zeta_0^*}^{13}+1105650{\zeta_0^*}^{14})), \quad (C.41)$$

$$c_{12} = \frac{1}{25(1+\zeta_0^*)^2(2+\zeta_0^*)^2(1+2\zeta_0^*)^2(1+3\zeta_0^*)(2+3\zeta_0^*)^2(2+5\zeta_0^*)^2(2+7\zeta_0^*)}(128(-6752+\zeta_0^*(150720 +\zeta_0^*(1723904+\zeta_0^*(6740208+\zeta_0^*(13036002+\zeta_0^*(13528880+\zeta_0^*(7475661 +\zeta_0^*(2093482+45\zeta_0^*(7333+1190\zeta_0^*)))))))))), \quad (C.42)$$

$$c_{13} = \frac{1}{\left(25\left(2+9\zeta_0^*+10{\zeta_0^*}^2\right)^2\left(2+13\zeta_0^*+21{\zeta_0^*}^2\right)\left(4+12\zeta_0^*+11{\zeta_0^*}^2+3{\zeta_0^*}^3\right)^3\right)}(128(49344+1162944\zeta_0^* -939280{\zeta_0^*}^2-74478704{\zeta_0^*}^3-437041596{\zeta_0^*}^4-1253267676{\zeta_0^*}^5-2118157755{\zeta_0^*}^6-2223659601{\zeta_0^*}^7 -1441772678{\zeta_0^*}^8-540032443{\zeta_0^*}^9-93687255{\zeta_0^*}^{10}+216300{\zeta_0^*}^{11}+1499400{\zeta_0^*}^{12})), \quad (C.43)$$

$$c_{14} = -\frac{896\left(4+6\zeta_0^*+{\zeta_0^*}^2\right)}{5\left(4+28\zeta_0^*+71{\zeta_0^*}^2+77{\zeta_0^*}^3+30{\zeta_0^*}^4\right)}, \quad (C.44)$$

$$c_{15} = -\frac{8\left(-928-32240\zeta_0^*-294512{\zeta_0^*}^2-766056{\zeta_0^*}^3-807050{\zeta_0^*}^4-330907{\zeta_0^*}^5+524{\zeta_0^*}^6+31179{\zeta_0^*}^7+5910{\zeta_0^*}^8\right)}{25(2+\zeta_0^*)^3\left(2+5\zeta_0^*+3{\zeta_0^*}^2\right)^2\left(2+9\zeta_0^*+10{\zeta_0^*}^2\right)}, \quad (C.45)$$

$$c_{16} = -\frac{64\zeta_0^*(672+\zeta_0^*(-6656+\zeta_0^*(-42236+\zeta_0^*(-76360+\zeta_0^*(-55357+3\zeta_0^*(-4613+2\zeta_0^*(136+65\zeta_0^*)))))))}{25(1+\zeta_0^*)^2(2+\zeta_0^*)^3(1+2\zeta_0^*)(2+3\zeta_0^*)^2(2+5\zeta_0^*)}, \quad (C.46)$$

$$c_{17} = -\frac{128(-64+\zeta_0^*(-168+\zeta_0^*(-69+7\zeta_0^*)))}{5(1+\zeta_0^*)(2+\zeta_0^*)(1+2\zeta_0^*)(2+3\zeta_0^*)(2+5\zeta_0^*)}, \quad (C.47)$$

$$c_{18} = \frac{64\left(528-22384\zeta_0^*-98204{\zeta_0^*}^2-151240{\zeta_0^*}^3-101818{\zeta_0^*}^4-27001{\zeta_0^*}^5-441{\zeta_0^*}^6+510{\zeta_0^*}^7\right)}{25\left(2+9\zeta_0^*+10{\zeta_0^*}^2\right)\left(4+12\zeta_0^*+11{\zeta_0^*}^2+3{\zeta_0^*}^3\right)^2}, \quad (C.48)$$

$$c_{19} = -\frac{896\left(4+6\zeta_0^*+{\zeta_0^*}^2\right)}{5\left(4+28\zeta_0^*+71{\zeta_0^*}^2+77{\zeta_0^*}^3+30{\zeta_0^*}^4\right)}, \tag{C.49}$$

$$c_{20} = \frac{128(424+\zeta_0^*(-2052+\zeta_0^*(-12162+\zeta_0^*(-18295+\zeta_0^*(-9694+\zeta_0^*(-38+3\zeta_0^*(449+85\zeta_0^*)))))))}{25(1+\zeta_0^*)^2(2+\zeta_0^*)^2(1+2\zeta_0^*)(2+3\zeta_0^*)^2(2+5\zeta_0^*)}, \tag{C.50}$$

$$c_{21} = \frac{32\zeta_0^*(1856+\zeta_0^*(-6688+\zeta_0^*(-42728+\zeta_0^*(-60980+3\zeta_0^*(-8162+\zeta_0^*(3101+\zeta_0^*(2881+490\zeta_0^*)))))))}{25(1+\zeta_0^*)^2(2+\zeta_0^*)^3(1+2\zeta_0^*)(2+3\zeta_0^*)^2(2+5\zeta_0^*)}, \tag{C.51}$$

$$c_{22} = \frac{64(-352+\zeta_0^*(9696+\zeta_0^*(54076+\zeta_0^*(100760+\zeta_0^*(83937+\zeta_0^*(32749+6\zeta_0^*(949+85\zeta_0^*)))))))}{25(1+\zeta_0^*)^2(2+\zeta_0^*)^2(1+2\zeta_0^*)(2+3\zeta_0^*)^2(2+5\zeta_0^*)}, \tag{C.52}$$

$$c_{23} = -\frac{16\left(-16416-183952\zeta_0^*-197344{\zeta_0^*}^2+793888{\zeta_0^*}^3+1992834{\zeta_0^*}^4+1752789{\zeta_0^*}^5+700402{\zeta_0^*}^6+123969{\zeta_0^*}^7+8310{\zeta_0^*}^8\right)}{25(2+\zeta_0^*)^3\left(2+5\zeta_0^*+3{\zeta_0^*}^2\right)^2\left(2+9\zeta_0^*+10{\zeta_0^*}^2\right)}, \tag{C.53}$$

$$c_{24} = \frac{256(6+\zeta_0^*)(5+7\zeta_0^*)}{5\left(4+40\zeta_0^*+155{\zeta_0^*}^2+290{\zeta_0^*}^3+261{\zeta_0^*}^4+90{\zeta_0^*}^5\right)}, \tag{C.54}$$

$$c_{25} = -\frac{64(-2336+\zeta_0^*(44816+\zeta_0^*(378296+\zeta_0^*(1064928+\zeta_0^*(1414088+\zeta_0^*(946777+\zeta_0^*(315286+45\zeta_0^*(1219+170\zeta_0^*)))))))))}{25(1+\zeta_0^*)^2(2+\zeta_0^*)^2(1+2\zeta_0^*)^2(1+3\zeta_0^*)(2+3\zeta_0^*)^2(2+5\zeta_0^*)}, \tag{C.55}$$

$$\begin{aligned} c_{26} \;=\; & -\frac{1}{25\left(2+3\zeta_0^*+{\zeta_0^*}^2\right)^3\left(2+7\zeta_0^*+6{\zeta_0^*}^2\right)^2\left(2+11\zeta_0^*+15{\zeta_0^*}^2\right)}(32(20320+339888\zeta_0^*+127376{\zeta_0^*}^2-7288080{\zeta_0^*}^3 \\ & -28101030{\zeta_0^*}^4-47995043{\zeta_0^*}^5-44177189{\zeta_0^*}^6-22305427{\zeta_0^*}^7-5608693{\zeta_0^*}^8-471282{\zeta_0^*}^9+20520{\zeta_0^*}^{10})), \end{aligned} \tag{C.56}$$

$$c_{27} = \frac{256(6+\zeta_0^*)(5+7\zeta_0^*)}{5\left(4+40\zeta_0^*+155{\zeta_0^*}^2+290{\zeta_0^*}^3+261{\zeta_0^*}^4+90{\zeta_0^*}^5\right)}, \tag{C.57}$$

$$\begin{aligned} c_{28} \;=\; & -\frac{1}{25(1+\zeta_0^*)^3(2+\zeta_0^*)^3(1+3\zeta_0^*)(2+5\zeta_0^*)(2+\zeta_0^*(7+6\zeta_0^*))^2}(32(-1216+\zeta_0^*(1984+\zeta_0^*(-203760 \\ & +\zeta_0^*(-1516576+\zeta_0^*(-4206524+\zeta_0^*(-5743184+\zeta_0^*(-3923859+\zeta_0^*(-957325 \\ & +3\zeta_0^*(101087+\zeta_0^*(71263+10470\zeta_0^*)))))))))), \end{aligned} \tag{C.58}$$

$$\begin{aligned} c_{29} \;=\; & -\frac{1}{25(1+\zeta_0^*)^2(2+\zeta_0^*)^2(1+2\zeta_0^*)^2(1+3\zeta_0^*)(2+3\zeta_0^*)^2(2+5\zeta_0^*)}(64(2464+\zeta_0^*(-19584+\zeta_0^*(-163704 \\ & +\zeta_0^*(-383772+\zeta_0^*(-370412+\zeta_0^*(-102573+\zeta_0^*(63436+45\zeta_0^*(1019+170\zeta_0^*)))))))), \end{aligned} \tag{C.59}$$

$$c_{30} = \frac{256(-90+\zeta_0^*(-251+\zeta_0^*(-114+7\zeta_0^*)))}{5(1+\zeta_0^*)(2+\zeta_0^*)(1+2\zeta_0^*)(1+3\zeta_0^*)(2+3\zeta_0^*)(2+5\zeta_0^*)}, \tag{C.60}$$

$$c_{31} = -\frac{64\left(1424-81784\zeta_0^*-535924{\zeta_0^*}^2-1295222{\zeta_0^*}^3-1493132{\zeta_0^*}^4-825063{\zeta_0^*}^5-164444{\zeta_0^*}^6+18495{\zeta_0^*}^7+7650{\zeta_0^*}^8\right)}{25\left(2+11\zeta_0^*+15{\zeta_0^*}^2\right)\left(4+20\zeta_0^*+35{\zeta_0^*}^2+25{\zeta_0^*}^3+6{\zeta_0^*}^4\right)^2}, \tag{C.61}$$

$$\begin{aligned} c_{32} \;=\; & -\frac{1}{25(1+\zeta_0^*)^3(2+\zeta_0^*)^3(1+3\zeta_0^*)(2+5\zeta_0^*)(2+\zeta_0^*(7+6\zeta_0^*))^2}(32(1184+\zeta_0^*(-7616+\zeta_0^*(293040+\zeta_0^*(2666824 \\ & +\zeta_0^*(8710526+\zeta_0^*(14311166+\zeta_0^*(12917291+\zeta_0^*(6380525+3\zeta_0^*(523887+\zeta_0^*(49663+1470\zeta_0^*)))))))))), \end{aligned} \tag{C.62}$$

$$\begin{aligned} c_{33} \;=\; & \frac{1}{25\left(2+3\zeta_0^*+{\zeta_0^*}^2\right)^3\left(2+7\zeta_0^*+6{\zeta_0^*}^2\right)^2\left(2+11\zeta_0^*+15{\zeta_0^*}^2\right)}(16(-173248-2667152\zeta_0^*-18092304{\zeta_0^*}^2 \\ & -65176624{\zeta_0^*}^3-135704024{\zeta_0^*}^4-169568123{\zeta_0^*}^5-126274146{\zeta_0^*}^6-51959566{\zeta_0^*}^7 \\ & -8735508{\zeta_0^*}^8+705945{\zeta_0^*}^9+312750{\zeta_0^*}^{10})), \end{aligned} \tag{C.63}$$

$$c_{34} = \frac{64(4+\zeta_0^*)(6+7\zeta_0^*)}{15\left(2+9\zeta_0^*+13{\zeta_0^*}^2+6{\zeta_0^*}^3\right)}, \tag{C.64}$$

$$c_{35} = \frac{32(-8+\zeta_0^*(148+\zeta_0^*(358+\zeta_0^*(239+43\zeta_0^*))))}{15(1+\zeta_0^*)^2(2+\zeta_0^*)(1+2\zeta_0^*)(2+3\zeta_0^*)}, \tag{C.65}$$

$$c_{36} = \frac{64(4+\zeta_0^*)(6+7\zeta_0^*)}{15\left(2+9\zeta_0^*+13{\zeta_0^*}^2+6{\zeta_0^*}^3\right)}, \tag{C.66}$$

$$c_{37} = \frac{64(-2+\zeta_0^*)(3+7\zeta_0^*)}{15\left(2+9\zeta_0^*+13{\zeta_0^*}^2+6{\zeta_0^*}^3\right)}, \tag{C.67}$$

$$c_{38} = \frac{64\left(-6+272\zeta_0^*+573{\zeta_0^*}^2+331{\zeta_0^*}^3+42{\zeta_0^*}^4\right)}{15(1+\zeta_0^*)^2\left(4+16\zeta_0^*+19{\zeta_0^*}^2+6{\zeta_0^*}^3\right)}, \tag{C.68}$$

$$c_{39} = -\frac{32(8+\zeta_0^*(92+\zeta_0^*(242+\zeta_0^*(181+47\zeta_0^*))))}{15(1+\zeta_0^*)^2(2+\zeta_0^*)(1+2\zeta_0^*)(2+3\zeta_0^*)}, \tag{C.69}$$

$$c_{40} = \frac{16\left(-1856-12304\zeta_0^*-14458{\zeta_0^*}^2+1675{\zeta_0^*}^3+9816{\zeta_0^*}^4+4749{\zeta_0^*}^5+768{\zeta_0^*}^6\right)}{75\left(2+3\zeta_0^*+{\zeta_0^*}^2\right)^2\left(2+7\zeta_0^*+6{\zeta_0^*}^2\right)}, \tag{C.70}$$

$$c_{41} = -\frac{64(4+\zeta_0^*)}{30+45\zeta_0^*}, \tag{C.71}$$

$$c_{42} = -\frac{64\zeta_0^*(4+\zeta_0^*)}{15\left(4+8\zeta_0^*+3{\zeta_0^*}^2\right)}, \tag{C.72}$$

$$c_{43} = -\frac{4\left(4-20\zeta_0^*+115{\zeta_0^*}^2+91{\zeta_0^*}^3\right)}{15\left(4+12\zeta_0^*+11{\zeta_0^*}^2+3{\zeta_0^*}^3\right)}, \tag{C.73}$$

$$c_{44} = -\frac{64(4+\zeta_0^*)}{30+45\zeta_0^*}, \tag{C.74}$$

$$c_{45} = \frac{8\left(44-52\zeta_0^*-35{\zeta_0^*}^2+13{\zeta_0^*}^3\right)}{15\left(4+12\zeta_0^*+11{\zeta_0^*}^2+3{\zeta_0^*}^3\right)}, \tag{C.75}$$

$$c_{46} = -\frac{64(4+\zeta_0^*)}{30+45\zeta_0^*}, \tag{C.76}$$

$$c_{47} = -\frac{64\zeta_0^*(4+\zeta_0^*)}{15\left(4+8\zeta_0^*+3{\zeta_0^*}^2\right)}. \tag{C.77}$$

C.4 Expressions for the coefficients d_i in terms of ζ_0^*

$$\begin{aligned} d_1 \;=\; & \frac{1}{\left(625(1+\zeta_0^*)^5(2+\zeta_0^*)^4(1+2\zeta_0^*)^4(1+3\zeta_0^*)^3(2+3\zeta_0^*)^4(1+4\zeta_0^*)^2(1+5\zeta_0^*)(2+5\zeta_0^*)^3(2+7\zeta_0^*)^2(2+9\zeta_0^*)\right)} \\ & \times(64(2560000+\zeta_0^*(124416000+\zeta_0^*(3789895680+\zeta_0^*(46872549376+\zeta_0^*(731488077568+\zeta_0^*(19641993564416 \\ & +\zeta_0^*(347501242841600+\zeta_0^*(3808587581450752+\zeta_0^*(28228947568177904+\zeta_0^*(150556714695389456 \\ & +\zeta_0^*(600537733610080728+\zeta_0^*(1834491732714094488+\zeta_0^*(4351921325171795785 \\ & +\zeta_0^*(8073778385759994311+\zeta_0^*(11736172603428739981+\zeta_0^*(13351459880635132719+\zeta_0^*(11892358109744259971 \\ & +\zeta_0^*(8419308331050329821+\zeta_0^*(5030630180338161779+3\zeta_0^*(959971186933789695+4\zeta_0^*(143081953484253556 \\ & +3\zeta_0^*(26632461459398236+3\zeta_0^*(3909222837795229+30\zeta_0^*(40182928024567 \\ & +120\zeta_0^*(65928530257+210\zeta_0^*(34892047+1683360\zeta_0^*)))))))))))))))))))))))))), \end{aligned} \tag{C.78}$$

$$\begin{aligned} d_2 \;=\; & \frac{1}{\left(625(1+\zeta_0^*)^5(2+\zeta_0^*)^4(1+2\zeta_0^*)^4(1+3\zeta_0^*)^3(2+3\zeta_0^*)^4(1+4\zeta_0^*)^2(1+5\zeta_0^*)(2+5\zeta_0^*)^3(2+7\zeta_0^*)^2(2+9\zeta_0^*)\right)} \\ & \times(16(7680000+\zeta_0^*(92078866432+\zeta_0^*(4934981488640+\zeta_0^*(124603073317888+\zeta_0^*(1960434861994752 \\ & +\zeta_0^*(21476521959196928+\zeta_0^*(173756996049691392+\zeta_0^*(1076429403430753408+\zeta_0^*(5230755058642326672 \\ & +\zeta_0^*(20276017330415145888+\zeta_0^*(63447265941941536912+\zeta_0^*(161608434026449661308 \\ & +\zeta_0^*(336903703347727128097+\zeta_0^*(576561669853886333373+\zeta_0^*(810574156674474980587 \\ & +\zeta_0^*(934551747989787792923+\zeta_0^*(879574965199623014357+\zeta_0^*(670011929255231028093 \\ & +\zeta_0^*(407119142841727000697+\zeta_0^*(192555551980039586533+18\zeta_0^*(3771424628603511079 \\ & +\zeta_0^*(907875900125925877+12\zeta_0^*(9630308468886617+90\zeta_0^*(-3771333160599 \\ & +5\zeta_0^*(-685627994239+2520\zeta_0^*(-28437061+33390\zeta_0^*)))))))))))))))))))))))))), \end{aligned} \tag{C.79}$$

$$
\begin{aligned}
d_3 \;=\; & \frac{1}{\left(3125\left(2+3\zeta_0^*+\zeta_0^{*2}\right)^5\left(2+7\zeta_0^*+6\zeta_0^{*2}\right)^4\left(2+11\zeta_0^*+15\zeta_0^{*2}\right)^3\left(2+15\zeta_0^*+28\zeta_0^{*2}\right)^2\left(2+19\zeta_0^*+45\zeta_0^{*2}\right)\right)} \\
& \times(64(-76800000-117479882752\zeta_0^*-6282832805888{\zeta_0^*}^2-159472834932736{\zeta_0^*}^3-2489892812405248{\zeta_0^*}^4 \\
& -27376254733251584{\zeta_0^*}^5-233694634521558272{\zeta_0^*}^6-1658170928487026432{\zeta_0^*}^7-10089623150252015904{\zeta_0^*}^8 \\
& -52548938774346239040{\zeta_0^*}^9-230483333265799955936{\zeta_0^*}^{10}-838874364092895348688{\zeta_0^*}^{11} \\
& -2512246470524856478038{\zeta_0^*}^{12}-6167946949601438367436{\zeta_0^*}^{13}-12395316457940023967725{\zeta_0^*}^{14} \\
& -20359491877036361158589{\zeta_0^*}^{15}-27255419202421678052502{\zeta_0^*}^{16}-29585231132319260900787{\zeta_0^*}^{17} \\
& -25815819645256977545164{\zeta_0^*}^{18}-17861302581808108576325{\zeta_0^*}^{19}-9585183797775616093176{\zeta_0^*}^{20} \\
& -3843057501640383252501{\zeta_0^*}^{21}-1068599689872018175215{\zeta_0^*}^{22}-166396033462323023730{\zeta_0^*}^{23} \\
& +31620619545965698 68{\zeta_0^*}^{24}+7822373352114216600{\zeta_0^*}^{25}+167184374601568320 0{\zeta_0^*}^{26} \\
& +158078434220784000{\zeta_0^*}^{27}+5871366466560000{\zeta_0^*}^{28})),
\end{aligned}
\tag{C.80}
$$

$$
\begin{aligned}
d_5 \;=\; & \frac{4902912}{125(1+\zeta_0^*)^5}+\frac{2272376704}{3125(1+\zeta_0^*)^4}+\frac{3022095296}{625(1+\zeta_0^*)^3}+\frac{72724386976}{3125(1+\zeta_0^*)^2}+\frac{21471489328}{225(1+\zeta_0^*)}-\frac{294912}{25(2+\zeta_0^*)^5}+\frac{12189184}{375(2+\zeta_0^*)^4} \\
& +\frac{2836544}{25(2+\zeta_0^*)^3}+\frac{1626754648}{16875(2+\zeta_0^*)^2}-\frac{3333256529}{354375(2+\zeta_0^*)}-\frac{2328576}{5(1+2\zeta_0^*)^4}-\frac{2294770176}{125(1+2\zeta_0^*)^3}-\frac{3461263793408}{16875(1+2\zeta_0^*)^2} \\
& -\frac{56165002277504}{50625(1+2\zeta_0^*)}-\frac{47734272}{5(1+3\zeta_0^*)^3}-\frac{128647946304}{125(1+3\zeta_0^*)^2}+\frac{13188096}{5(2+3\zeta_0^*)^4}-\frac{15335136}{25(2+3\zeta_0^*)^3}+\frac{416904696}{125(2+3\zeta_0^*)^2} \\
& -\frac{637904456469}{1250(2+3\zeta_0^*)}-\frac{7144062976}{75(1+4\zeta_0^*)^2}-\frac{58218678575104}{2625(1+4\zeta_0^*)}+\frac{235558400}{(2+5\zeta_0^*)^3}+\frac{3018983696}{(2+5\zeta_0^*)^2}+\frac{781083690347}{45(2+5\zeta_0^*)} \\
& +\frac{56908569228}{25(2+7\zeta_0^*)^2}+\frac{231239033174611}{3750(2+7\zeta_0^*)}+\frac{410888844828}{25(2+9\zeta_0^*)}-\frac{11416160000}{9+45\zeta_0^*}-\frac{575927156016}{25+75\zeta_0^*},
\end{aligned}
\tag{C.81}
$$

$$
\begin{aligned}
d_9 \;=\; & \frac{1}{590625}\Bigg(-\frac{5283532800}{(1+\zeta_0^*)^5}-\frac{117061507584}{(1+\zeta_0^*)^4}-\frac{991137014784}{(1+\zeta_0^*)^3}-\frac{5472712049280}{(1+\zeta_0^*)^2}-\frac{24352371363040}{1+\zeta_0^*} \\
& +\frac{2322432000}{(2+\zeta_0^*)^5}-\frac{5692377600}{(2+\zeta_0^*)^4}-\frac{24054172800}{(2+\zeta_0^*)^3}-\frac{28231553560}{(2+\zeta_0^*)^2}-\frac{9350211425}{2+\zeta_0^*}+\frac{83825280000}{(1+2\zeta_0^*)^4} \\
& +\frac{4908616742400}{(1+2\zeta_0^*)^3}+\frac{70418487032320}{(1+2\zeta_0^*)^2}+\frac{520767079006720}{1+2\zeta_0^*}+\frac{5536006560000}{(1+3\zeta_0^*)^3} \\
& +\frac{628844630500800}{(1+3\zeta_0^*)^2}+\frac{16243205501023200}{1+3\zeta_0^*}-\frac{130636800000}{(2+3\zeta_0^*)^4}+\frac{4032526680000}{(2+3\zeta_0^*)^3} \\
& +\frac{13909922056800}{(2+3\zeta_0^*)^2}+\frac{175456504741770}{2+3\zeta_0^*}+\frac{100015792128000}{(1+4\zeta_0^*)^2}+\frac{21418823385907200}{1+4\zeta_0^*} \\
& +\frac{1610458500000000}{1+5\zeta_0^*}-\frac{92451240000000}{(2+5\zeta_0^*)^3}-\frac{1453459436100000}{(2+5\zeta_0^*)^2}-\frac{10228375718981875}{2+5\zeta_0^*} \\
& -\frac{1768776949044000}{(2+7\zeta_0^*)^2}-\frac{51082997768329170}{2+7\zeta_0^*}-\frac{18382144014927000}{2+9\zeta_0^*}\Bigg),
\end{aligned}
\tag{C.82}
$$

$$
\begin{aligned}
d_{13} \;=\; & \frac{1}{(625(1+\zeta_0^*)^3(2+\zeta_0^*)^3(1+2\zeta_0^*)^4(1+3\zeta_0^*)^3(2+3\zeta_0^*)^3(1+4\zeta_0^*)^2(1+5\zeta_0^*)(2+5\zeta_0^*)^3(2+7\zeta_0^*)^2(2+9\zeta_0^*))} \\
& \times(128\zeta_0^*(11089920+\zeta_0^*(-280623616+\zeta_0^*(34098428160+\zeta_0^*(1207112624128+\zeta_0^*(17430529970688 \\
& +\zeta_0^*(148418048610752+\zeta_0^*(846965391404832+\zeta_0^*(3446431066062784+\zeta_0^*(10335747606331128 \\
& +\zeta_0^*(23219774880984558+\zeta_0^*(39224289272804301+\zeta_0^*(49377135461168488+\zeta_0^*(45050883532802385 \\
& +\zeta_0^*(27791294941287132+\zeta_0^*(9185619714130947+\zeta_0^*(-940824130835800+9\zeta_0^*(-287144583277269 \\
& +2\zeta_0^*(-65035099616057+30\zeta_0^*(-359594313401 \\
& +630\zeta_0^*(58710441+560\zeta_0^*(59411+5355\zeta_0^*)))))))))))))))))))),
\end{aligned}
\tag{C.83}
$$

$$
\begin{aligned}
d_{40} \;=\; & \frac{1}{\left(125(1+\zeta_0^*)^4(2+\zeta_0^*)^4(1+3\zeta_0^*)^2(1+4\zeta_0^*)(2+5\zeta_0^*)^2(2+7\zeta_0^*)(2+\zeta_0^*(7+6\zeta_0^*))^3\right)}(-(16(-7036160 \\
& +\zeta_0^*(-271792640+\zeta_0^*(-4671710336+\zeta_0^*(-46454968768+\zeta_0^*(-297658382464+\zeta_0^*(-1310446572848 \\
& +\zeta_0^*(-4147641722024+\zeta_0^*(-9783078691924+\zeta_0^*(-17749369127195+\zeta_0^*(-25487976779879 \\
& +\zeta_0^*(-29593532113349+\zeta_0^*(-27921130892368+\zeta_0^*(-21001784205383+\zeta_0^*(-12053244493383 \\
& +\zeta_0^*(-4928381041391+6\zeta_0^*(-213908648015 \\
& +9\zeta_0^*(-3003888787+50\zeta_0^*(1144897+847644\zeta_0^*))))))))))))))))))), \qquad \text{(C.84)}
\end{aligned}
$$

$$
d_{134} \;=\; \frac{8(44+\zeta_0^*(-180+\zeta_0^*(-795+\zeta_0^*(55+516\zeta_0^*))))}{225(1+\zeta_0^*)(2+\zeta_0^*)(1+2\zeta_0^*)(2+3\zeta_0^*)}, \qquad \text{(C.85)}
$$

$$
\begin{aligned}
d_{148} \;=\; & \frac{1}{\left(75(1+\zeta_0^*)^3(2+\zeta_0^*)^3(1+3\zeta_0^*)(2+5\zeta_0^*)(2+\zeta_0^*(7+6\zeta_0^*))^2\right)}(4(10272+\zeta_0^*(185904+\zeta_0^*(471984 \\
& +\zeta_0^*(-3589848+\zeta_0^*(-21765022+\zeta_0^*(-47261285+\zeta_0^*(-48608788+\zeta_0^*(-19193642+\zeta_0^*(5942210 \\
& +\zeta_0^*(8429011+12\zeta_0^*(238862+28605\zeta_0^*)))))))))), \qquad \text{(C.86)}
\end{aligned}
$$

$$
d_0 \;=\; \frac{28672(2+\zeta_0^*)(10+\zeta_0^*(31+25\zeta_0^*))}{25(1+\zeta_0^*)(1+2\zeta_0^*)(1+3\zeta_0^*)(2+3\zeta_0^*)(1+4\zeta_0^*)(1+5\zeta_0^*)(2+5\zeta_0^*)(2+7\zeta_0^*)(2+9\zeta_0^*)}, \qquad \text{(C.87)}
$$

$$
\begin{aligned}
d_{12} \;=\; & \frac{1}{\left(625(1+\zeta_0^*)^4(2+\zeta_0^*)^3(1+2\zeta_0^*)^4(1+3\zeta_0^*)^3(2+3\zeta_0^*)^3(1+4\zeta_0^*)^2(1+5\zeta_0^*)(2+5\zeta_0^*)^3(2+7\zeta_0^*)^2(2+9\zeta_0^*)\right)} \\
& \times(64{\zeta_0^*}^2(11089920+\zeta_0^*(-280623616+\zeta_0^*(34098428160+\zeta_0^*(1207112624128+\zeta_0^*(17430529970688 \\
& +\zeta_0^*(148418048610752+\zeta_0^*(846965391404832+\zeta_0^*(3446431066062784+\zeta_0^*(10335747606331128 \\
& +\zeta_0^*(23219774880984558+\zeta_0^*(39224289272804301+\zeta_0^*(49377135461168488+\zeta_0^*(45050883532802385 \\
& +\zeta_0^*(27791294941287132+\zeta_0^*(9185619714130947+\zeta_0^*(-940824130835800+9\zeta_0^*(-287144583277269 \\
& +2\zeta_0^*(-65035099616057+30\zeta_0^*(-359594313401+630\zeta_0^*(58710441 \\
& +560\zeta_0^*(59411+5355\zeta_0^*)))))))))))))))))))), \qquad \text{(C.88)}
\end{aligned}
$$

$$
\begin{aligned}
d_{16} \;=\; & \frac{1}{\left(625(1+\zeta_0^*)^4(2+\zeta_0^*)^4(1+2\zeta_0^*)^4(1+4\zeta_0^*)^2(1+5\zeta_0^*)(2+5\zeta_0^*)^3(2+7\zeta_0^*)^2(2+9\zeta_0^*)(2+9\zeta_0^*(1+\zeta_0^*))^3\right)} \\
& \times(-(128(612796416+\zeta_0^*(48784497664+\zeta_0^*(1441117392896+\zeta_0^*(20482750941696+\zeta_0^*(149296489890304 \\
& +\zeta_0^*(345521028556160+\zeta_0^*(-3834227744208768+\zeta_0^*(-47174533402749184+\zeta_0^*(-281976551129783768 \\
& +\zeta_0^*(-1136872697028550724+\zeta_0^*(-3372315289610916792+\zeta_0^*(-7632927490937746674 \\
& +\zeta_0^*(-13408546114499816065+\zeta_0^*(-18397602384322986573+\zeta_0^*(-19688766341053817121 \\
& +\zeta_0^*(-16289087637088184659+\zeta_0^*(-10230021736770896137+\zeta_0^*(-4717444388507126267 \\
& +\zeta_0^*(-1496606307350450615+3\zeta_0^*(-92134560892802393+90\zeta_0^*(-30655936990125+2\zeta_0^*(16171402728881 \\
& +270\zeta_0^*(13281558973+2800\zeta_0^*(400222+13923\zeta_0^*)))))))))))))))))))))))))), \qquad \text{(C.89)}
\end{aligned}
$$

$$
\begin{aligned}
d_{19} \;=\; & \frac{1}{\left(125(1+\zeta_0^*)^2(2+\zeta_0^*)(1+2\zeta_0^*)^2(1+3\zeta_0^*)^2(2+3\zeta_0^*)(1+4\zeta_0^*)^2(1+5\zeta_0^*)(2+5\zeta_0^*)^2(2+7\zeta_0^*)^2(2+9\zeta_0^*)\right)} \\
& \times(-(1024(-160+\zeta_0^*(-2205872+\zeta_0^*(-40871184+\zeta_0^*(-322754616+\zeta_0^*(-1418282994+\zeta_0^*(-3798488367 \\
& +\zeta_0^*(-6379043696+\zeta_0^*(-6642957514+3\zeta_0^*(-1353621932 \\
& +\zeta_0^*(-420465797+10\zeta_0^*(-3588839+719460\zeta_0^*))))))))))))), \qquad \text{(C.90)}
\end{aligned}
$$

$$
\begin{aligned}
d_{22} \;=\; & \frac{1}{\left(625(1+\zeta_0^*)^3(2+\zeta_0^*)^3(1+2\zeta_0^*)^3(1+3\zeta_0^*)^3(2+3\zeta_0^*)^2(1+4\zeta_0^*)^2(1+5\zeta_0^*)(2+5\zeta_0^*)^3(2+7\zeta_0^*)^2(2+9\zeta_0^*)\right)} \\
& \times(-(256(53333504+\zeta_0^*(1906905600+\zeta_0^*(5306730368+\zeta_0^*(-425820087872+\zeta_0^*(-7430124176928 \\
& +\zeta_0^*(-64179698196048+\zeta_0^*(-354256626427656+\zeta_0^*(-1363989258706252+\zeta_0^*(-3817552024426292 \\
& +\zeta_0^*(-7925504490288529+\zeta_0^*(-12295852421828877+\zeta_0^*(-14216541816735720+\zeta_0^*(-12088232423695058 \\
& +\zeta_0^*(-7350720384507113+3\zeta_0^*(-1007843440145595+2\zeta_0^*(-122677105281951+2\zeta_0^*(-4636581984223 \\
& +30\zeta_0^*(55357494139+132300\zeta_0^*(112441+7584\zeta_0^*)))))))))))))))))))),
\end{aligned} \tag{C.91}
$$

$$
d_{25} \;=\; \frac{4(634+107\zeta_0^*)}{1575}, \tag{C.92}
$$

$$
\begin{aligned}
d_{29} \;=\; & \frac{1}{\left(3125\left(2+3\zeta_0^*+{\zeta_0^*}^2\right)^5\left(2+7\zeta_0^*+6{\zeta_0^*}^2\right)^4\left(2+11\zeta_0^*+15{\zeta_0^*}^2\right)^3\left(2+15\zeta_0^*+28{\zeta_0^*}^2\right)^2\left(2+19\zeta_0^*+45{\zeta_0^*}^2\right)\right)} \\
& \times(32\zeta_0^*(-204907413504-11315129675776\zeta_0^*-296299391209472{\zeta_0^*}^2-4895543023210496{\zeta_0^*}^3 \\
& -57049772738055168{\zeta_0^*}^4-496878952624716544{\zeta_0^*}^5-335145246557117286 4{\zeta_0^*}^6-1794058324129035980 8{\zeta_0^*}^7 \\
& -776227350951926380 80{\zeta_0^*}^8-275367915986412929872{\zeta_0^*}^9 \\
& -810300634794382191376{\zeta_0^*}^{10}-199665700903635876657 6{\zeta_0^*}^{11}-415129474524069115737 2{\zeta_0^*}^{12} \\
& -732389976682122905782 5{\zeta_0^*}^{13}-110019043951436505189 28{\zeta_0^*}^{14}-140829275068867550240 04{\zeta_0^*}^{15} \\
& -153249333874174137060 74{\zeta_0^*}^{16}-140944796983841035715 78{\zeta_0^*}^{17}-108507740909231584246 50{\zeta_0^*}^{18} \\
& -689676764552565703235 2{\zeta_0^*}^{19}-355228634272707093002{\zeta_0^*}^{20}-144612709213193168980 5{\zeta_0^*}^{21} \\
& -449636296476628315710{\zeta_0^*}^{22}-101604329486549731764{\zeta_0^*}^{23}-154240061489487918 00{\zeta_0^*}^{24} \\
& -136042504900623360 0{\zeta_0^*}^{25}-48002876640432000{\zeta_0^*}^{26}+323443653120000{\zeta_0^*}^{27})),
\end{aligned} \tag{C.93}
$$

$$
\begin{aligned}
d_{67} \;=\; & \frac{1}{\left(375(1+\zeta_0^*)^3(2+\zeta_0^*)^3(1+2\zeta_0^*)^2(1+3\zeta_0^*)(2+3\zeta_0^*)^3(2+5\zeta_0^*)^2(2+7\zeta_0^*)\right)}(-(16(35601664+\zeta_0^*(669605888 \\
& +\zeta_0^*(5139473792+\zeta_0^*(20238651264+\zeta_0^*(40581427904+\zeta_0^*(21175330880+\zeta_0^*(-87774271096 \\
& +\zeta_0^*(-234010861544+\zeta_0^*(-279095045633+\zeta_0^*(-186210848688+\zeta_0^*(-66981951116 \\
& +5\zeta_0^*(-1839337486+3\zeta_0^*(74103419+18\zeta_0^*(1311769+7560\zeta_0^*))))))))))))))),
\end{aligned} \tag{C.94}
$$

$$
\begin{aligned}
d_{97} \;=\; & -\frac{1}{375(1+\zeta_0^*)^2(2+\zeta_0^*)^2(1+2\zeta_0^*)(2+3\zeta_0^*)^2(2+5\zeta_0^*)}(4(9440+\zeta_0^*(-324496+\zeta_0^*(-2531456 \\
& +\zeta_0^*(-6038784+\zeta_0^*(-5823350+\zeta_0^*(-1618299+\zeta_0^*(844226+\zeta_0^*(555049+83610\zeta_0^*)))))))),
\end{aligned} \tag{C.95}
$$

$$
\begin{aligned}
d_{106} \;=\; & \frac{1}{\left(625\left(2+9\zeta_0^*+10{\zeta_0^*}^2\right)^3\left(2+13\zeta_0^*+21{\zeta_0^*}^2\right)^2\left(2+17\zeta_0^*+36{\zeta_0^*}^2\right)\left(4+12\zeta_0^*+11{\zeta_0^*}^2+3{\zeta_0^*}^3\right)^4\right)} \\
& \times(32(-90555973632-3596867837952\zeta_0^*-66399257382912{\zeta_0^*}^2-755333578386432{\zeta_0^*}^3 \\
& -59206656200560 64{\zeta_0^*}^4-339074465672465 92{\zeta_0^*}^5-146936321915571968{\zeta_0^*}^6 \\
& -492735036948185984{\zeta_0^*}^7-1297547161637900416{\zeta_0^*}^8-2708372735675709312{\zeta_0^*}^9 \\
& -450419892373184830 4{\zeta_0^*}^{10}-597736949493048671 6{\zeta_0^*}^{11}-631551533045631920 8{\zeta_0^*}^{12} \\
& -527620339975359966 7{\zeta_0^*}^{13}-343792799448620616 5{\zeta_0^*}^{14}-170318720372260063 8{\zeta_0^*}^{15} \\
& -610227847105413770{\zeta_0^*}^{16}-140374647407297427{\zeta_0^*}^{17}-12254315605514901{\zeta_0^*}^{18} \\
& +3416880432611520{\zeta_0^*}^{19}+1240672089143340{\zeta_0^*}^{20}+141592871599200{\zeta_0^*}^{21} \\
& +3978747864000{\zeta_0^*}^{22})),
\end{aligned} \tag{C.96}
$$

$$
\begin{aligned}
d_4 \;=\; & \frac{1}{\left(625(1+\zeta_0^*)^4(2+\zeta_0^*)^4(1+2\zeta_0^*)^4(1+3\zeta_0^*)^3(2+3\zeta_0^*)^4(1+4\zeta_0^*)^2(1+5\zeta_0^*)(2+5\zeta_0^*)^3(2+7\zeta_0^*)^2(2+9\zeta_0^*)\right)} \\
& \times(256(-6963200+\zeta_0^*(-23746560+\zeta_0^*(-9928026112+\zeta_0^*(-11669244416+\zeta_0^*(7160633412608 \\
& +\zeta_0^*(165436125964800+\zeta_0^*(1950885437803776+\zeta_0^*(14928662567311552 \\
& +\zeta_0^*(81261593065179328+\zeta_0^*(329912190269242664+\zeta_0^*(1026598359357200344+\zeta_0^*(2487630720503669230 \\
& +\zeta_0^*(4733078550200494268+\zeta_0^*(7087844647408736153+\zeta_0^*(8331005861513100972+\zeta_0^*(7626364400352423873 \\
& +\zeta_0^*(5368497642822154098+\zeta_0^*(2859255574904675477+3\zeta_0^*(379684369394872660+\zeta_0^*(116260185930145987 \\
& +18\zeta_0^*(1756534257203137+\zeta_0^*(514049313882379+30\zeta_0^*(4697556673067 \\
& +360\zeta_0^*(2417282369+70\zeta_0^*(3466747+171360\zeta_0^*)))))))))))))))))))))))))), \qquad \text{(C.97)}
\end{aligned}
$$

$$
\begin{aligned}
d_6 \;=\; & \frac{1}{\left(3125\left(2+3\zeta_0^*+{\zeta_0^*}^2\right)^5\left(2+7\zeta_0^*+6{\zeta_0^*}^2\right)^4\left(2+11\zeta_0^*+15{\zeta_0^*}^2\right)^3\left(2+15\zeta_0^*+28{\zeta_0^*}^2\right)^2\left(2+19\zeta_0^*+45{\zeta_0^*}^2\right)\right)} \\
& \times(64(-220892053504-11987115851776\zeta_0^*-304724606799872{\zeta_0^*}^2-4741564190539776{\zeta_0^*}^3 \\
& -51853006164763648{\zeta_0^*}^4-44089610814282854{\zeta_0^*}^5-31309814575365655{\zeta_0^*}^6 \\
& -19170943135875987968{\zeta_0^*}^7-10077332992802033248{\zeta_0^*}^8 \\
& -4461233055020516085{\zeta_0^*}^9-1636220694585862191856{\zeta_0^*}^{10} \\
& -492739134526039268736{\zeta_0^*}^{11}-121398168709591464769{\zeta_0^*}^{12}-24436978960944628218980{\zeta_0^*}^{13} \\
& -4013920180268581086172{\zeta_0^*}^{14}-536572436619639223045{\zeta_0^*}^{15}-58080197263743857624764{\zeta_0^*}^{16} \\
& -5047044408246083512684{\zeta_0^*}^{17}-347272814603229384183{\zeta_0^*}^{18}-18506251171326846824812{\zeta_0^*}^{19} \\
& -7354738037099373907412{\zeta_0^*}^{20}-2021520892242980902740{\zeta_0^*}^{21}-308852690742614775735{\zeta_0^*}^{22} \\
& +71120887823810658{\zeta_0^*}^{23}+14582690283842734500{\zeta_0^*}^{24}+3048352062185597400{\zeta_0^*}^{25} \\
& +283511942144928000{\zeta_0^*}^{26}+10485453751920000{\zeta_0^*}^{27})), \qquad \text{(C.98)}
\end{aligned}
$$

$$
\begin{aligned}
d_7 \;=\; & \frac{1}{\left(625(1+\zeta_0^*)^3(2+\zeta_0^*)^3(1+2\zeta_0^*)^3(1+3\zeta_0^*)^3(2+3\zeta_0^*)^3(1+4\zeta_0^*)^2(1+5\zeta_0^*)(2+5\zeta_0^*)^3(2+7\zeta_0^*)^2(2+9\zeta_0^*)\right)} \\
& \times(256(11476992+\zeta_0^*(-413199872+\zeta_0^*(9297169664+\zeta_0^*(631278411520+\zeta_0^*(11264231716352 \\
& +\zeta_0^*(110639524318400+\zeta_0^*(710041354879776+\zeta_0^*(3209384892110912+\zeta_0^*(10627957082173920 \\
& +\zeta_0^*(26343580041390514+\zeta_0^*(49382566813735801+\zeta_0^*(70166435900841001+\zeta_0^*(75245262955438776 \\
& +\zeta_0^*(60305389283435520+\zeta_0^*(35636683854377029+\zeta_0^*(15347944774323517+18\zeta_0^*(268813782988445 \\
& +4\zeta_0^*(16079758436929+180\zeta_0^*(16370781768+175\zeta_0^*(10145479+75348\zeta_0^*))))))))))))))))))), \qquad \text{(C.99)}
\end{aligned}
$$

$$
\begin{aligned}
d_8 \;=\; & \frac{1}{\left(625(1+\zeta_0^*)^4(2+\zeta_0^*)^4(1+2\zeta_0^*)^4(1+3\zeta_0^*)^3(2+3\zeta_0^*)^4(1+4\zeta_0^*)^2(1+5\zeta_0^*)(2+5\zeta_0^*)^3(2+7\zeta_0^*)^2(2+9\zeta_0^*)\right)} \\
& \times(-(128(-1647955968+\zeta_0^*(-115953342464+\zeta_0^*(-4695603817472+\zeta_0^*(-82176735579648 \\
& +\zeta_0^*(-668477335472640+\zeta_0^*(-1115391949201408+\zeta_0^*(31180020775510912+\zeta_0^*(374012306552728384 \\
& +\zeta_0^*(2392553252511252976+\zeta_0^*(10511894387264751720+\zeta_0^*(34268456205260423076 \\
& +\zeta_0^*(85807518800585021546+\zeta_0^*(167856000624632596072+\zeta_0^*(258297860535759493243 \\
& +\zeta_0^*(312454574299764781465+\zeta_0^*(294731220081962004873+\zeta_0^*(213026688441455359353 \\
& +\zeta_0^*(114153434042305183631+\zeta_0^*(42426679867082306779+3\zeta_0^*(3046338604857365915 \\
& +3\zeta_0^*(19919236657609523+6\zeta_0^*(-9155860817067893+90\zeta_0^*(-25727374046291 \\
& +210\zeta_0^*(-9204517919+560\zeta_0^*(442649+5355\zeta_0^*))))))))))))))))))))))))), \qquad \text{(C.100)}
\end{aligned}
$$

$$
d_{10} \;=\; \frac{28672(2+\zeta_0^*)\left(10+31\zeta_0^*+25{\zeta_0^*}^2\right)}{25(1+5\zeta_0^*)\left(4+40\zeta_0^*+123{\zeta_0^*}^2+108{\zeta_0^*}^3\right)\left(4+48\zeta_0^*+223{\zeta_0^*}^2+498{\zeta_0^*}^3+529{\zeta_0^*}^4+210{\zeta_0^*}^5\right)}, \qquad \text{(C.101)}
$$

$$
\begin{aligned}
d_{11} &= \frac{1}{\left(625(1+\zeta_0^*)^3(2+\zeta_0^*)^3(1+2\zeta_0^*)^3(1+3\zeta_0^*)^3(2+3\zeta_0^*)^2(1+4\zeta_0^*)^2(1+5\zeta_0^*)(2+5\zeta_0^*)^3(2+7\zeta_0^*)^2(2+9\zeta_0^*)\right)} \\
&\times(256(554496+\zeta_0^*(-25511680+\zeta_0^*(2349969152+\zeta_0^*(77480914432+\zeta_0^*(1023962248128+\zeta_0^*(7893209464608 \\
&+\zeta_0^*(40293194041376+\zeta_0^*(144633247670592+\zeta_0^*(376283997828222+\zeta_0^*(718352097920349 \\
&+\zeta_0^*(1003732905569427+\zeta_0^*(1005209132858760+\zeta_0^*(681839919547648+\zeta_0^*(262643734479013 \\
&+\zeta_0^*(3394101578995+2\zeta_0^*(-27685258845617+18\zeta_0^*(-804900623529 \\
&+10\zeta_0^*(-17061964709+2100\zeta_0^*(-287353+106848\zeta_0^*)))))))))))))))))))), \qquad \text{(C.102)}
\end{aligned}
$$

$$
\begin{aligned}
d_{14} &= \frac{1}{\left(125(1+\zeta_0^*)^2(2+\zeta_0^*)(1+2\zeta_0^*)^2(1+3\zeta_0^*)^2(2+3\zeta_0^*)(1+4\zeta_0^*)^2(1+5\zeta_0^*)(2+5\zeta_0^*)^2(2+7\zeta_0^*)^2(2+9\zeta_0^*)\right)} \\
&\times(-(1024(9120+\zeta_0^*(-677552+\zeta_0^*(-13923024+\zeta_0^*(-110631016+\zeta_0^*(-475070934+\zeta_0^*(-1215871827 \\
&+\zeta_0^*(-1889286156+\zeta_0^*(-1696188214+\zeta_0^*(-704052036 \\
&+\zeta_0^*(60458449+30\zeta_0^*(5388521+1425060\zeta_0^*))))))))))))), \qquad \text{(C.103)}
\end{aligned}
$$

$$
\begin{aligned}
d_{15} &= \frac{1}{\left(125(1+\zeta_0^*)^2(2+\zeta_0^*)^2(1+2\zeta_0^*)^2(1+3\zeta_0^*)^2(2+3\zeta_0^*)^2(1+4\zeta_0^*)^2(1+5\zeta_0^*)(2+5\zeta_0^*)^2(2+7\zeta_0^*)^2(2+9\zeta_0^*)\right)} \\
&\times(1024(-266880+\zeta_0^*(9750048+\zeta_0^*(317393552+\zeta_0^*(3569293312+\zeta_0^*(21880087136+\zeta_0^*(83147196978 \\
&+\zeta_0^*(206047103817+\zeta_0^*(338109999435+\zeta_0^*(364701737524+\zeta_0^*(252603401684+\zeta_0^*(109871237821 \\
&+27\zeta_0^*(1167462469+10\zeta_0^*(27166373+4522980\zeta_0^*))))))))))))), \qquad \text{(C.104)}
\end{aligned}
$$

$$
\begin{aligned}
d_{17} &= \frac{1}{\left(625(1+\zeta_0^*)^3(2+\zeta_0^*)^3(1+2\zeta_0^*)^3(1+3\zeta_0^*)^3(2+3\zeta_0^*)^3(1+4\zeta_0^*)^2(1+5\zeta_0^*)(2+5\zeta_0^*)^3(2+7\zeta_0^*)^2(2+9\zeta_0^*)\right)} \\
&\times(-(512(-75540992+\zeta_0^*(-8917233408+\zeta_0^*(-92102430464+\zeta_0^*(1243384747520+\zeta_0^*(35284985569088 \\
&+\zeta_0^*(373805552465760+\zeta_0^*(2411410108859584+\zeta_0^*(10716347534507408+\zeta_0^*(34620460341709670 \\
&+\zeta_0^*(83531802299673201+\zeta_0^*(152417050249922479+\zeta_0^*(210812165995273839+\zeta_0^*(219525139063997374 \\
&+\zeta_0^*(169139873773550665+\zeta_0^*(93283286454646431+\zeta_0^*(34564024023853033+6\zeta_0^*(1237827683611135 \\
&+9\zeta_0^*(8641443168733+10\zeta_0^*(-248688385877+8400\zeta_0^*(-4459492+100611\zeta_0^*))))))))))))))))))), \qquad \text{(C.105)}
\end{aligned}
$$

$$
d_{18} = -\frac{57344(130+\zeta_0^*(573+\zeta_0^*(624+125\zeta_0^*)))}{25(1+\zeta_0^*)(1+2\zeta_0^*)(1+3\zeta_0^*)(2+3\zeta_0^*)(1+4\zeta_0^*)(1+5\zeta_0^*)(2+5\zeta_0^*)(2+7\zeta_0^*)(2+9\zeta_0^*)}, \qquad \text{(C.106)}
$$

$$
d_{20} = -\frac{28672(-190+\zeta_0^*(-1409+\zeta_0^*(-2499+\zeta_0^*(-621+275\zeta_0^*))))}{25(1+\zeta_0^*)(2+\zeta_0^*)(1+2\zeta_0^*)(1+3\zeta_0^*)(2+3\zeta_0^*)(1+4\zeta_0^*)(1+5\zeta_0^*)(2+5\zeta_0^*)(2+7\zeta_0^*)(2+9\zeta_0^*)}, \qquad \text{(C.107)}
$$

$$
\begin{aligned}
d_{21} &= \frac{1}{\left(125(1+\zeta_0^*)^2(2+\zeta_0^*)(1+2\zeta_0^*)^2(1+3\zeta_0^*)^2(2+3\zeta_0^*)^2(1+4\zeta_0^*)^2(1+5\zeta_0^*)(2+5\zeta_0^*)^2(2+7\zeta_0^*)^2(2+9\zeta_0^*)\right)} \\
&\times(1024(835680+\zeta_0^*(-21114832+\zeta_0^*(-644868112+\zeta_0^*(-6442843512+\zeta_0^*(-34714943898+\zeta_0^*(-114987442053 \\
&+\zeta_0^*(-245365744314+\zeta_0^*(-339182138588+\zeta_0^*(-294639643352+3\zeta_0^*(-49117728865+4\zeta_0^*(-2711746787 \\
&+15\zeta_0^*(6777619+6424740\zeta_0^*))))))))))), \qquad \text{(C.108)}
\end{aligned}
$$

$$
d_{23} = \frac{2672(2+\zeta_0^*)}{7875}, \qquad \text{(C.109)}
$$

$$
d_{24} = \frac{2672(2+\zeta_0^*)}{7875}, \qquad \text{(C.110)}
$$

$$
d_{26} = \frac{2672(2+\zeta_0^*)}{7875}, \qquad \text{(C.111)}
$$

$$d_{27} = \frac{57344(2+\zeta_0^*)(10+\zeta_0^*(31+25\zeta_0^*))}{25(1+\zeta_0^*)(1+2\zeta_0^*)(1+3\zeta_0^*)(2+3\zeta_0^*)(1+4\zeta_0^*)(1+5\zeta_0^*)(2+5\zeta_0^*)(2+7\zeta_0^*)(2+9\zeta_0^*)}, \quad \text{(C.112)}$$

$$\begin{aligned} d_{28} = {} & \frac{1}{\left(625(1+\zeta_0^*)^5(2+\zeta_0^*)^4(1+2\zeta_0^*)^4(1+3\zeta_0^*)^3(2+3\zeta_0^*)^4(1+4\zeta_0^*)^2(1+5\zeta_0^*)(2+5\zeta_0^*)^3(2+7\zeta_0^*)^2(2+9\zeta_0^*)\right)} \\ & \times(64\zeta_0^*(19456000+\zeta_0^*(91535360+\zeta_0^*(38491773952+\zeta_0^*(-955097624064+\zeta_0^*(-55921917991168 \\ & +\zeta_0^*(-995702171347200+\zeta_0^*(-10135475211668096+\zeta_0^*(-69219587959353792+\zeta_0^*(-341148364362401088 \\ & +\zeta_0^*(-1262698192718115944+\zeta_0^*(-3591338268364291124+\zeta_0^*(-7945387860882373430 \\ & +\zeta_0^*(-13726133860600510353+\zeta_0^*(-18433894651160386388+\zeta_0^*(-18949525657713757612 \\ & +\zeta_0^*(-14390455297949381458+\zeta_0^*(-7390346243959007658+\zeta_0^*(-1798953547268848942 \\ & +\zeta_0^*(633319439028048220+9\zeta_0^*(91103896113800616+\zeta_0^*(41849730899288363 \\ & +6\zeta_0^*(1769747749931891+90\zeta_0^*(2884157474881 \\ & +10\zeta_0^*(35230991587+5040\zeta_0^*(1435748+179865\zeta_0^*)))))))))))))))))))))))), \end{aligned} \quad \text{(C.113)}$$

$$\begin{aligned} d_{31} = {} & \frac{1}{\left(625(1+\zeta_0^*)^4(2+\zeta_0^*)^4(1+2\zeta_0^*)^4(1+4\zeta_0^*)^2(1+5\zeta_0^*)(2+5\zeta_0^*)^3(2+7\zeta_0^*)^2(2+9\zeta_0^*)(2+9\zeta_0^*(1+\zeta_0^*))^3\right)} \\ & \times(-(256(322756608+\zeta_0^*(18578051072+\zeta_0^*(495161268224+\zeta_0^*(7173536778752+\zeta_0^*(61277447232512 \\ & +\zeta_0^*(304814071975680+\zeta_0^*(612018266340608+\zeta_0^*(-2836385541934016+\zeta_0^*(-29772451898209632 \\ & +\zeta_0^*(-135997926505694672+\zeta_0^*(-409595880581646648+\zeta_0^*(-887136264653691454 \\ & +\zeta_0^*(-1413181041975692676+\zeta_0^*(-1634374090163478519+\zeta_0^*(-1282941463139237099 \\ & +\zeta_0^*(-508747067328314502+\zeta_0^*(199733793798261310+\zeta_0^*(482525002436637049 \\ & +\zeta_0^*(389951270092404565+6\zeta_0^*(31775468849632495+18\zeta_0^*(557010257729191+10\zeta_0^*(11022661229233 \\ & +720\zeta_0^*(1738883296+35\zeta_0^*(2830739+85680\zeta_0^*)))))))))))))))))))))))), \end{aligned} \quad \text{(C.114)}$$

$$\begin{aligned} d_{33} = {} & \frac{1}{\left(3125\left(2+3\zeta_0^*+{\zeta_0^*}^2\right)^5\left(2+7\zeta_0^*+6{\zeta_0^*}^2\right)^4\left(2+11\zeta_0^*+15{\zeta_0^*}^2\right)^3\left(2+15\zeta_0^*+28{\zeta_0^*}^2\right)^2\left(2+19\zeta_0^*+45{\zeta_0^*}^2\right)\right)} \\ & \times(64(-204829589504-11312596811776\zeta_0^*-296233827663872{\zeta_0^*}^2-4894173021259776{\zeta_0^*}^3 \\ & -57016015833627648{\zeta_0^*}^4-49619393532572605 44{\zeta_0^*}^5-3342129970740341504{\zeta_0^*}^6-178538996678118919 68{\zeta_0^*}^7 \\ & -77044534603628596480{\zeta_0^*}^8-272491282594179976512{\zeta_0^*}^9-799330610227786661856{\zeta_0^*}^{10} \\ & -1964001120872720237736{\zeta_0^*}^{11}-4074549755702795637692{\zeta_0^*}^{12}-7180716916448822815230{\zeta_0^*}^{13} \\ & -10789796872371181398223{\zeta_0^*}^{14}-13834923249657637189014{\zeta_0^*}^{15}-15099378749164370604264{\zeta_0^*}^{16} \\ & -13939704662289711739848{\zeta_0^*}^{17}-10776084113836063608810{\zeta_0^*}^{18}-6876821879318446040312{\zeta_0^*}^{19} \\ & -3554567849948564663912{\zeta_0^*}^{20}-1451257089608825183490{\zeta_0^*}^{21}-4522763930098622887 35{\zeta_0^*}^{22} \\ & -1024156237930635911 94{\zeta_0^*}^{23}-1559384638725896550 0{\zeta_0^*}^{24}-1386386756315202600{\zeta_0^*}^{25} \\ & -508969965510720 00{\zeta_0^*}^{26}+146367511920000{\zeta_0^*}^{27})), \end{aligned} \quad \text{(C.115)}$$

$$\begin{aligned} d_{35} = {} & \frac{1}{\left(625(1+\zeta_0^*)^3(2+\zeta_0^*)^3(1+2\zeta_0^*)^3(1+3\zeta_0^*)^3(2+3\zeta_0^*)^2(1+4\zeta_0^*)^2(1+5\zeta_0^*)(2+5\zeta_0^*)^3(2+7\zeta_0^*)^2(2+9\zeta_0^*)\right)} \\ & \times(-(512(13045504+\zeta_0^*(589066240+\zeta_0^*(-155428992+\zeta_0^*(-195551394752+\zeta_0^*(-3177620417728 \\ & +\zeta_0^*(-26751079594928+\zeta_0^*(-144870452153816+\zeta_0^*(-547168249604372+\zeta_0^*(-1498221787707107 \\ & +\zeta_0^*(-3028925627105289+\zeta_0^*(-4543172925208502+\zeta_0^*(-5019462316397290 \\ & +\zeta_0^*(-3994266587963303+\zeta_0^*(-2176575772445213+4\zeta_0^*(-178020253292410+\zeta_0^*(-16834069352659 \\ & +24\zeta_0^*(489539942804+45\zeta_0^*(4785926827+1400\zeta_0^*(528421+23184\zeta_0^*))))))))))))))))))), \end{aligned} \quad \text{(C.116)}$$

$$
\begin{aligned}
d_{37} \;=\; & \frac{1}{\big(125(1+\zeta_0^*)^2(2+\zeta_0^*)(1+2\zeta_0^*)^2(1+3\zeta_0^*)^2(2+3\zeta_0^*)(1+4\zeta_0^*)^2(1+5\zeta_0^*)(2+5\zeta_0^*)^2(2+7\zeta_0^*)^2(2+9\zeta_0^*)\big)} \\
& \times(-(2048(4480+\zeta_0^*(-1441712+\zeta_0^*(-27397104+\zeta_0^*(-216692816+\zeta_0^*(-946676964+\zeta_0^*(-2507180097 \\
& +\zeta_0^*(-4134164926+\zeta_0^*(-4169572864+\zeta_0^*(-2382458916 \\
& +\zeta_0^*(-600469471+90\zeta_0^*(299947+357420\zeta_0^*)))))))))))),
\end{aligned} \tag{C.117}
$$

$$
\begin{aligned}
d_{38} \;=\; & \frac{1}{\big(625(1+\zeta_0^*)^4(2+\zeta_0^*)^3(1+2\zeta_0^*)^3(1+3\zeta_0^*)^2(2+3\zeta_0^*)^3(1+4\zeta_0^*)(2+5\zeta_0^*)^2(2+7\zeta_0^*)\big)}(128\zeta_0^*(199808 \\
& +\zeta_0^*(-2467200+\zeta_0^*(57396608+\zeta_0^*(2258072016+\zeta_0^*(24230323016+\zeta_0^*(136742046368+\zeta_0^*(477931957772 \\
& +\zeta_0^*(1107206848713+\zeta_0^*(1750736102314+\zeta_0^*(1903438219494+\zeta_0^*(1412397457327+\zeta_0^*(706700558131 \\
& +\zeta_0^*(244095554612+3\zeta_0^*(23050033496+9\zeta_0^*(746118509+70\zeta_0^*(2368991+202020\zeta_0^*))))))))))))))),
\end{aligned} \tag{C.118}
$$

$$
\begin{aligned}
d_{39} \;=\; & \frac{1}{\big(625(1+\zeta_0^*)^4(2+\zeta_0^*)^4(1+3\zeta_0^*)^2(1+4\zeta_0^*)(2+5\zeta_0^*)^2(2+7\zeta_0^*)(2+\zeta_0^*(7+6\zeta_0^*))^3\big)}(32(-531200+\zeta_0^*(23925760 \\
& +\zeta_0^*(1497348608+\zeta_0^*(38474339072+\zeta_0^*(410248104608+\zeta_0^*(2224728401728+\zeta_0^*(6179042589920 \\
& +\zeta_0^*(4029348381552+\zeta_0^*(-33085376270631+\zeta_0^*(-138553607443904+\zeta_0^*(-292213882186214 \\
& +\zeta_0^*(-396524555636860+\zeta_0^*(-365490353069247+4\zeta_0^*(-57118165530514+\zeta_0^*(-23071736572181 \\
& +3\zeta_0^*(-1721926257197+36\zeta_0^*(-2064895390+\zeta_0^*(1545287921 \\
& +180\zeta_0^*(1662111+66920\zeta_0^*))))))))))))))),
\end{aligned} \tag{C.119}
$$

$$
d_{41} \;=\; \frac{7168(2+\zeta_0^*)(10+\zeta_0^*(31+25\zeta_0^*))}{25(1+\zeta_0^*)(1+2\zeta_0^*)(1+3\zeta_0^*)(2+3\zeta_0^*)(1+4\zeta_0^*)(2+5\zeta_0^*)(2+7\zeta_0^*)}, \tag{C.120}
$$

$$
\begin{aligned}
d_{43} \;=\; & \frac{1}{\big(625(1+\zeta_0^*)^4(2+\zeta_0^*)^4(1+3\zeta_0^*)^2(1+4\zeta_0^*)(2+5\zeta_0^*)^2(2+7\zeta_0^*)(2+\zeta_0^*(7+6\zeta_0^*))^3\big)}(-(32(-180858880 \\
& +\zeta_0^*(-4849324800+\zeta_0^*(-50777642624+\zeta_0^*(-240424783936+\zeta_0^*(-246523515744+\zeta_0^*(2927865642416 \\
& +\zeta_0^*(16488397523880+\zeta_0^*(41035696904084+\zeta_0^*(46220266061238+\zeta_0^*(-23119820361968 \\
& +\zeta_0^*(-174410982696888+\zeta_0^*(-314884583552015+\zeta_0^*(-334488426802544 \\
& +\zeta_0^*(-233523622368692+\zeta_0^*(-108390906062938+3\zeta_0^*(-10694046185111+12\zeta_0^*(-148562559395 \\
& +3\zeta_0^*(-2883677057+420\zeta_0^*(587227+55440\zeta_0^*))))))))))))))),
\end{aligned} \tag{C.121}
$$

$$
\begin{aligned}
d_{47} \;=\; & \frac{1}{\big(625(1+\zeta_0^*)^4(2+\zeta_0^*)^4(1+3\zeta_0^*)^2(1+4\zeta_0^*)(2+5\zeta_0^*)^2(2+7\zeta_0^*)(2+\zeta_0^*(7+6\zeta_0^*))^3\big)}(64(-78051072 \\
& +\zeta_0^*(-3193813120+\zeta_0^*(-51933463616+\zeta_0^*(-437245085664+\zeta_0^*(-2139439330928+\zeta_0^*(-6200255021480 \\
& +\zeta_0^*(-8971894062556+\zeta_0^*(4162763459734+\zeta_0^*(50724635261818+\zeta_0^*(122744426337165 \\
& +\zeta_0^*(175343719885595+\zeta_0^*(167673948747764+\zeta_0^*(110223341652796 \\
& +\zeta_0^*(49181748429855+\zeta_0^*(14215712469277+6\zeta_0^*(402231102761 \\
& +3\zeta_0^*(11011747727+30\zeta_0^*(14126417+1733340\zeta_0^*))))))))))))))),
\end{aligned} \tag{C.122}
$$

$$
\begin{aligned}
d_{50} \;=\; & \frac{1}{\big(625(1+\zeta_0^*)^3(2+\zeta_0^*)^3(1+2\zeta_0^*)^3(1+4\zeta_0^*)(2+5\zeta_0^*)^2(2+7\zeta_0^*)(2+9\zeta_0^*(1+\zeta_0^*))^2\big)}(64\zeta_0^*(46208+\zeta_0^*(-419520 \\
& +\zeta_0^*(40494496+\zeta_0^*(640431056+\zeta_0^*(4008659832+\zeta_0^*(13773635004+\zeta_0^*(28781626414+\zeta_0^*(37515153447 \\
& +\zeta_0^*(29308327538+\zeta_0^*(11110656166+3\zeta_0^*(-350795040+\zeta_0^*(-978278031 \\
& +4\zeta_0^*(-93485024+15\zeta_0^*(-755513+28140\zeta_0^*))))))))))))))),
\end{aligned} \tag{C.123}
$$

$$d_{53} = \frac{1}{\big(125(1+\zeta_0^*)^2(2+\zeta_0^*)(1+2\zeta_0^*)^2(1+3\zeta_0^*)^2(2+3\zeta_0^*)(1+4\zeta_0^*)(2+5\zeta_0^*)^2(2+7\zeta_0^*)\big)}(-(512(-192+\zeta_0^*(-277176 +\zeta_0^*(-3056804+\zeta_0^*(-13733018+\zeta_0^*(-32265791+\zeta_0^*(-42399404+\zeta_0^*(-30763436+\zeta_0^*(-11128937 +6\zeta_0^*(-220907+22120\zeta_0^*)))))))))), \tag{C.124}$$

$$d_{56} = \frac{1}{\big(625(1+\zeta_0^*)^2(2+\zeta_0^*)^3(1+2\zeta_0^*)^3(1+3\zeta_0^*)^2(2+3\zeta_0^*)^2(1+4\zeta_0^*)(2+5\zeta_0^*)^2(2+7\zeta_0^*)\big)}(-(128(6201792 +\zeta_0^*(124303840+\zeta_0^*(344484064+\zeta_0^*(-5313228576+\zeta_0^*(-50211807572+\zeta_0^*(-204276310754 +\zeta_0^*(-486092324424+\zeta_0^*(-733387706917+\zeta_0^*(-715404405598 +\zeta_0^*(-443039612886+\zeta_0^*(-162365623030+\zeta_0^*(-27779875567 +12\zeta_0^*(78351874+45\zeta_0^*(1865071+172620\zeta_0^*)))))))))))))), \tag{C.125}$$

$$d_{58} = \frac{1}{\big(625(1+\zeta_0^*)^4(2+\zeta_0^*)^4(1+3\zeta_0^*)^2(1+4\zeta_0^*)(2+5\zeta_0^*)^2(2+7\zeta_0^*)(2+\zeta_0^*(7+6\zeta_0^*))^3\big)}(-(32\zeta_0^*(81699840 +\zeta_0^*(2618622592+\zeta_0^*(38520891328+\zeta_0^*(330693960992+\zeta_0^*(1849874439472+\zeta_0^*(7223530869080 +\zeta_0^*(20674147774148+\zeta_0^*(45048174054806+\zeta_0^*(77109869963429 +\zeta_0^*(106254235643014+\zeta_0^*(119479533066785+\zeta_0^*(109423480096522+\zeta_0^*(80099680961581 +3\zeta_0^*(15109618442908+3\zeta_0^*(2103548847121+2\zeta_0^*(304040565535 +48\zeta_0^*(1146990952+15\zeta_0^*(7177909+207480\zeta_0^*)))))))))))))))))), \tag{C.126}$$

$$d_{66} = -\frac{7168(2+\zeta_0^*)(10+\zeta_0^*(31+25\zeta_0^*))}{75(1+\zeta_0^*)(1+2\zeta_0^*)(1+3\zeta_0^*)(2+3\zeta_0^*)(2+5\zeta_0^*)(2+7\zeta_0^*)}, \tag{C.127}$$

$$d_{68} = \frac{1}{5625}8\Big(-\frac{468000}{(1+\zeta_0^*)^3}-\frac{9876624}{(1+\zeta_0^*)^2}-\frac{57181548}{1+\zeta_0^*}+\frac{691200}{(2+\zeta_0^*)^4}-\frac{5380800}{(2+\zeta_0^*)^3}-\frac{6468240}{(2+\zeta_0^*)^2} -\frac{821150}{2+\zeta_0^*}-\frac{158490000}{(1+2\zeta_0^*)^2}-\frac{527501480}{1+2\zeta_0^*}+\frac{1801764000}{1+3\zeta_0^*}+\frac{76488000}{(2+3\zeta_0^*)^3}+\frac{496652400}{(2+3\zeta_0^*)^2} +\frac{909838125}{2+3\zeta_0^*}+\frac{100170000}{(2+5\zeta_0^*)^2}-\frac{1902107700}{2+5\zeta_0^*}-\frac{1412379675}{2+7\zeta_0^*}\Big), \tag{C.128}$$

$$d_{69} = \frac{1}{\big(375(1+\zeta_0^*)^3(2+\zeta_0^*)^3(1+2\zeta_0^*)^2(1+3\zeta_0^*)(2+3\zeta_0^*)^3(2+5\zeta_0^*)^2(2+7\zeta_0^*)\big)}(-(128(-19200 +\zeta_0^*(-183552+\zeta_0^*(-428288+\zeta_0^*(38696256+\zeta_0^*(417590176+\zeta_0^*(1915915024 +\zeta_0^*(4904241936+\zeta_0^*(7667006028+\zeta_0^*(7549875473+\zeta_0^*(4677704268 +\zeta_0^*(1800879452+\zeta_0^*(459063866+3\zeta_0^*(37056817+90\zeta_0^*(104233+12040\zeta_0^*)))))))))))))), \tag{C.129}$$

$$d_{70} = \frac{1}{\big(375(1+\zeta_0^*)^2(2+\zeta_0^*)(1+2\zeta_0^*)^2(1+3\zeta_0^*)(2+3\zeta_0^*)^2(2+5\zeta_0^*)^2(2+7\zeta_0^*)\big)}(256\zeta_0^*(14592 +\zeta_0^*(-166944+\zeta_0^*(-1926688+\zeta_0^*(-6574104+\zeta_0^*(-9976732+\zeta_0^*(-5972196 +\zeta_0^*(1186013+3\zeta_0^*(1063613+20\zeta_0^*(23074+3045\zeta_0^*)))))))))), \tag{C.130}$$

$$d_{75} = \frac{1}{\big(375(1+\zeta_0^*)^2(2+\zeta_0^*)^2(1+2\zeta_0^*)^2(1+3\zeta_0^*)(2+3\zeta_0^*)^2(2+5\zeta_0^*)^2(2+7\zeta_0^*)\big)}(64(1203648 +\zeta_0^*(16555936+\zeta_0^*(34526720+\zeta_0^*(-246951024+\zeta_0^*(-1435127324+\zeta_0^*(-3173512730 +\zeta_0^*(-3644249520+\zeta_0^*(-2251058381+3\zeta_0^*(-228876628 +3\zeta_0^*(-7461639+10\zeta_0^*(86803+15960\zeta_0^*)))))))))))), \tag{C.131}$$

$$d_{76} = -\frac{1}{375(1+\zeta_0^*)^2(2+\zeta_0^*)(1+2\zeta_0^*)^2(1+3\zeta_0^*)(2+3\zeta_0^*)(2+5\zeta_0^*)^2(2+7\zeta_0^*)}(256(992+\zeta_0^*(369528 +\zeta_0^*(2943484+\zeta_0^*(9288874+\zeta_0^*(14683463+\zeta_0^*(12213942 +\zeta_0^*(5106631+869006\zeta_0^*+5040{\zeta_0^*}^2)))))))), \tag{C.132}$$

$$d_{79} = \frac{1}{\left(1875(1+\zeta_0^*)^3(2+\zeta_0^*)^4(1+2\zeta_0^*)^2(1+3\zeta_0^*)(2+3\zeta_0^*)^3(2+5\zeta_0^*)^2(2+7\zeta_0^*)\right)}(-(32(-157502976 +\zeta_0^*(-4263411712+\zeta_0^*(-46914044160+\zeta_0^*(-271355846272+\zeta_0^*(-925287607616 +\zeta_0^*(-1950658377248+\zeta_0^*(-2511100171360+\zeta_0^*(-1705704796296+\zeta_0^*(-21613367630 +\zeta_0^*(1052900022882+\zeta_0^*(975484772055+\zeta_0^*(455914816843 +\zeta_0^*(127368906947+3\zeta_0^*(8114588501+540\zeta_0^*(2313427+215565\zeta_0^*)))))))))))))))), \tag{C.133}$$

$$d_{82} = \frac{1}{5625}4\Big(-\frac{14400}{(1+\zeta_0^*)^3}+\frac{5283552}{(1+\zeta_0^*)^2}+\frac{25888104}{1+\zeta_0^*}-\frac{345600}{(2+\zeta_0^*)^4}+\frac{2366400}{(2+\zeta_0^*)^3}+\frac{1089720}{(2+\zeta_0^*)^2} -\frac{1080625}{2+\zeta_0^*}-\frac{55188000}{(1+2\zeta_0^*)^2}-\frac{688268560}{1+2\zeta_0^*}-\frac{1316952000}{1+3\zeta_0^*}+\frac{5088000}{(2+3\zeta_0^*)^3}+\frac{13312800}{(2+3\zeta_0^*)^2} +\frac{14857200}{2+3\zeta_0^*}+\frac{155400000}{(2+5\zeta_0^*)^2}+\frac{3270607725}{2+5\zeta_0^*}+\frac{695192400}{2+7\zeta_0^*}\Big), \tag{C.134}$$

$$d_{88} = -\frac{256(2+\zeta_0^*)(3+4\zeta_0^*)}{75\left(2+11\zeta_0^*+19{\zeta_0^*}^2+10{\zeta_0^*}^3\right)}, \tag{C.135}$$

$$d_{89} = -\frac{128\zeta_0^*(2+\zeta_0^*)\left(24+43\zeta_0^*+10{\zeta_0^*}^2\right)}{75\left(4+28\zeta_0^*+71{\zeta_0^*}^2+77{\zeta_0^*}^3+30{\zeta_0^*}^4\right)}, \tag{C.136}$$

$$d_{92} = -\frac{64(12+\zeta_0^*(2500+\zeta_0^*(4347+25\zeta_0^*(67+12\zeta_0^*))))}{375(1+\zeta_0^*)(1+2\zeta_0^*)(2+3\zeta_0^*)(2+5\zeta_0^*)}, \tag{C.137}$$

$$d_{95} = \frac{1}{1875(1+\zeta_0^*)^2(2+\zeta_0^*)^2(1+2\zeta_0^*)(2+3\zeta_0^*)^2(2+5\zeta_0^*)}(16(286112+\zeta_0^*(2268800+\zeta_0^*(5980296 +\zeta_0^*(7161932+\zeta_0^*(4711148+\zeta_0^*(2690865+\zeta_0^*(1630274+\zeta_0^*(545903+50670\zeta_0^*)))))))), \tag{C.138}$$

$$d_{96} = \frac{256\zeta_0^*(384+\zeta_0^*(1768+\zeta_0^*(2812+\zeta_0^*(1898+\zeta_0^*(533+60\zeta_0^*)))))}{75(1+\zeta_0^*)(2+\zeta_0^*)(1+2\zeta_0^*)(2+3\zeta_0^*)^2(2+5\zeta_0^*)}, \tag{C.139}$$

$$d_{98} = -\frac{1}{1875(1+\zeta_0^*)^2(2+\zeta_0^*)^2(1+2\zeta_0^*)(2+3\zeta_0^*)^2(2+5\zeta_0^*)}(32(-83856+\zeta_0^*(-227680+\zeta_0^*(-45328 +\zeta_0^*(-256236+\zeta_0^*(-1506499+\zeta_0^*(-1831215+2\zeta_0^*(-364466+11\zeta_0^*(823+1845\zeta_0^*)))))))), \tag{C.140}$$

$$d_{103} = \frac{1}{1875(1+\zeta_0^*)^2(2+\zeta_0^*)^2(1+2\zeta_0^*)(2+3\zeta_0^*)^2(2+5\zeta_0^*)}(16(108512+\zeta_0^*(1030160+\zeta_0^*(3351856 +\zeta_0^*(5373672+\zeta_0^*(4975198+\zeta_0^*(2963505+\zeta_0^*(1142414+\zeta_0^*(217213+2070\zeta_0^*)))))))), \tag{C.141}$$

$$d_{104} = -\frac{28672(2+\zeta_0^*)(10+\zeta_0^*(31+25\zeta_0^*))}{25(1+\zeta_0^*)(1+2\zeta_0^*)(1+3\zeta_0^*)(2+3\zeta_0^*)(1+4\zeta_0^*)(2+5\zeta_0^*)(2+7\zeta_0^*)(2+9\zeta_0^*)}, \tag{C.142}$$

$$
\begin{aligned}
d_{105} \;=\; & \frac{1}{\left(625(1+\zeta_0^*)^4(2+\zeta_0^*)^4(1+2\zeta_0^*)^3(1+3\zeta_0^*)^2(2+3\zeta_0^*)^4(1+4\zeta_0^*)(2+5\zeta_0^*)^3(2+7\zeta_0^*)^2(2+9\zeta_0^*)\right)} \\
& \times(-(128(-4403200+\zeta_0^*(-14102528+\zeta_0^*(-4278851584+\zeta_0^*(12859245568+\zeta_0^*(2309451527936 \\
& +\zeta_0^*(37956630839296+\zeta_0^*(324025489690112+\zeta_0^*(1773866140204672+\zeta_0^*(6772737883818672 \\
& +\zeta_0^*(18818420192082000+\zeta_0^*(38923509085389448+\zeta_0^*(60566012703658196+\zeta_0^*(71020258002950273 \\
& +\zeta_0^*(62414582823166174+\zeta_0^*(40667459018500579+\zeta_0^*(19464104989469720+3\zeta_0^*(2325063255897473 \\
& +3\zeta_0^*(234010530468862+\zeta_0^*(72928521617605+12\zeta_0^*(1837177435318+75\zeta_0^*(5216622269 \\
& +84\zeta_0^*(7143557+342720\zeta_0^*)))))))))))))))))))))))),
\end{aligned}
\tag{C.143}
$$

$$
\begin{aligned}
d_{107} \;=\; & \frac{1}{\left(3125(2+\zeta_0^*)^5\left(2+5\zeta_0^*+3{\zeta_0^*}^2\right)^4\left(2+9\zeta_0^*+10{\zeta_0^*}^2\right)^3\left(2+13\zeta_0^*+21{\zeta_0^*}^2\right)^2\left(2+17\zeta_0^*+36{\zeta_0^*}^2\right)\right)} \\
& \times(-(64(-215789461504-8746313420800\zeta_0^*-164759329415168{\zeta_0^*}^2-19006807797985 28{\zeta_0^*}^3 \\
& -15195367072711168{\zeta_0^*}^4-9104935745945 2672{\zeta_0^*}^5-4319621128350 62016{\zeta_0^*}^6-1680122418618996480{\zeta_0^*}^7 \\
& -543816321235765 0976{\zeta_0^*}^8-1463445045053 7802224{\zeta_0^*}^9-3243377870392 3443584{\zeta_0^*}^{10} \\
& -584980602635306 81752{\zeta_0^*}^{11}-8485610014512 3111614{\zeta_0^*}^{12}-9781668870692 4581381{\zeta_0^*}^{13} \\
& -883555963633536 44837{\zeta_0^*}^{14}-6135709548178 7863894{\zeta_0^*}^{15}-3181127985701 4067452{\zeta_0^*}^{16} \\
& -116947365611842 36453{\zeta_0^*}^{17}-2718068313297 897345{\zeta_0^*}^{18}-2492901141518 19096{\zeta_0^*}^{19} \\
& +549426184413164 64{\zeta_0^*}^{20}+2032146273655 7280{\zeta_0^*}^{21}+2375349932869200{\zeta_0^*}^{22} \\
& +90204669576000{\zeta_0^*}^{23}))),
\end{aligned}
\tag{C.144}
$$

$$
\begin{aligned}
d_{109} \;=\; & \frac{1}{\left(625(1+\zeta_0^*)^3(2+\zeta_0^*)^3(1+2\zeta_0^*)^3(1+3\zeta_0^*)^2(2+3\zeta_0^*)^3(1+4\zeta_0^*)(2+5\zeta_0^*)^3(2+7\zeta_0^*)^2(2+9\zeta_0^*)\right)} \\
& \times(-(128\zeta_0^*(4435968+\zeta_0^*(-37696000+\zeta_0^*(6601870080+\zeta_0^*(157325319168+\zeta_0^*(1552396569600 \\
& +\zeta_0^*(8849053528256+\zeta_0^*(32778492285024+\zeta_0^*(83163383846592+\zeta_0^*(147448219071216 \\
& +\zeta_0^*(181670538286518+\zeta_0^*(149240856824007+\zeta_0^*(71134840986292 \\
& +\zeta_0^*(6869447018016+\zeta_0^*(-13770724331024+3\zeta_0^*(-2800834163737+6\zeta_0^*(-88027477289 \\
& +7350\zeta_0^*(1966367+42\zeta_0^*(27191+3060\zeta_0^*)))))))))))))))))),
\end{aligned}
\tag{C.145}
$$

$$
\begin{aligned}
d_{114} \;=\; & \frac{1}{\left(625(1+\zeta_0^*)^4(2+\zeta_0^*)^4(1+3\zeta_0^*)^2(1+4\zeta_0^*)(2+5\zeta_0^*)^3(2+7\zeta_0^*)^2(2+9\zeta_0^*)(2+\zeta_0^*(7+6\zeta_0^*))^3\right)}(256(308932608 \\
& +\zeta_0^*(17675271680+\zeta_0^*(385601850624+\zeta_0^*(4156103862784+\zeta_0^*(24299555179776+\zeta_0^*(67146193809728 \\
& +\zeta_0^*(-68448186525216+\zeta_0^*(-1423666370052512+\zeta_0^*(-6526421213816736+\zeta_0^*(-18167501422069074 \\
& +\zeta_0^*(-35192004662033571+\zeta_0^*(-49572600082972748+\zeta_0^*(-51460384873603788 \\
& +\zeta_0^*(-39186323610021681+\zeta_0^*(-21406805038323606+\zeta_0^*(-7975667457919504+3\zeta_0^*(-596890100875270 \\
& +3\zeta_0^*(-15342448558517+9\zeta_0^*(461998263099+260\zeta_0^*(518483683 \\
& +105\zeta_0^*(484859+21420\zeta_0^*)))))))))))))))))))),
\end{aligned}
\tag{C.146}
$$

$$
\begin{aligned}
d_{116} \;=\; & \frac{1}{\left(625(1+\zeta_0^*)^3(2+\zeta_0^*)^3(1+2\zeta_0^*)^3(1+4\zeta_0^*)(2+5\zeta_0^*)^3(2+7\zeta_0^*)^2(2+9\zeta_0^*)(2+9\zeta_0^*(1+\zeta_0^*))^2\right)}(256(51413504 \\
& +\zeta_0^*(1434788864+\zeta_0^*(5070148992+\zeta_0^*(-143251974080+\zeta_0^*(-2007833685728+\zeta_0^*(-12952480296816 \\
& +\zeta_0^*(-51735504581272+\zeta_0^*(-140148728099604+\zeta_0^*(-267555037640556+\zeta_0^*(-365022431474905 \\
& +\zeta_0^*(-354792261500062+\zeta_0^*(-240552425045472+\zeta_0^*(-108127387512550 \\
& +\zeta_0^*(-28272082773143+12\zeta_0^*(-185215403834+3\zeta_0^*(24608393521 \\
& +8820\zeta_0^*(785749+56880\zeta_0^*)))))))))))))))))),
\end{aligned}
\tag{C.147}
$$

$$
\begin{aligned}
d_{120} \;=\; & \frac{1}{\left(3125(2+\zeta_0^*)^5\left(2+5\zeta_0^*+3{\zeta_0^*}^2\right)^4\left(2+9\zeta_0^*+10{\zeta_0^*}^2\right)^3\left(2+13\zeta_0^*+21{\zeta_0^*}^2\right)^2\left(2+17\zeta_0^*+36{\zeta_0^*}^2\right)\right)} \\
& \times(64(175201992704+7281169428480\zeta_0^*+145035829547008{\zeta_0^*}^2+1820761330843648{\zeta_0^*}^3 \\
& +15841952635844608{\zeta_0^*}^4+99881565208454912{\zeta_0^*}^5+468179247624925696{\zeta_0^*}^6+1657332549556271360{\zeta_0^*}^7 \\
& +4465681027226856256{\zeta_0^*}^8+9150349822599769424{\zeta_0^*}^9+14055830323747194704{\zeta_0^*}^{10} \\
& +15511507787385992192{\zeta_0^*}^{11}+10725276572323669584{\zeta_0^*}^{12}+14435160360927113 41{\zeta_0^*}^{13} \\
& -6673037413478440928{\zeta_0^*}^{14}-9306254122916015481{\zeta_0^*}^{15}-7086522134743291338{\zeta_0^*}^{16} \\
& -3559526587863482677{\zeta_0^*}^{17}-1204806001590191280{\zeta_0^*}^{18}-262784625419193219{\zeta_0^*}^{19} \\
& -31887940718066814{\zeta_0^*}^{20}-955552225663980{\zeta_0^*}^{21}+211893535639800{\zeta_0^*}^{22} \\
& +17886362004000{\zeta_0^*}^{23})),
\end{aligned}
\tag{C.148}
$$

$$
\begin{aligned}
d_{122} \;=\; & \frac{1}{\left(125(1+\zeta_0^*)^2(2+\zeta_0^*)(1+2\zeta_0^*)^2(1+3\zeta_0^*)^2(2+3\zeta_0^*)(1+4\zeta_0^*)(2+5\zeta_0^*)^2(2+7\zeta_0^*)^2(2+9\zeta_0^*)\right)} \\
& \times(1024(-160+\zeta_0^*(-1589072+\zeta_0^*(-23125824+\zeta_0^*(-140451896+\zeta_0^*(-461853514+\zeta_0^*(-891960497 \\
& +\zeta_0^*(-1024071411+\zeta_0^*(-669590259+\zeta_0^*(-216863701+6\zeta_0^*(-3022231+719460\zeta_0^*)))))))))),
\end{aligned}
\tag{C.149}
$$

$$
\begin{aligned}
d_{125} \;=\; & \frac{1}{\left(3125(2+\zeta_0^*)^5\left(2+5\zeta_0^*+3{\zeta_0^*}^2\right)^4\left(2+9\zeta_0^*+10{\zeta_0^*}^2\right)^3\left(2+13\zeta_0^*+21{\zeta_0^*}^2\right)^2\left(2+17\zeta_0^*+36{\zeta_0^*}^2\right)\right)} \\
& \times(-(64(-204771221504-8366824140800\zeta_0^*-159906061447168{\zeta_0^*}^2-1901124774166528{\zeta_0^*}^3 \\
& -15741498445383168{\zeta_0^*}^4-96304851251196672{\zeta_0^*}^5-451129332860278016{\zeta_0^*}^6-1656585623149332480{\zeta_0^*}^7 \\
& -4847523908653954976{\zeta_0^*}^8-11438409738676862224{\zeta_0^*}^9 \\
& -21951836190726981584{\zeta_0^*}^{10}-34466115640215222752{\zeta_0^*}^{11}-44420139945315668114{\zeta_0^*}^{12} \\
& -47017151694726326881{\zeta_0^*}^{13}-40750426249191234087{\zeta_0^*}^{14}-28705466907875919394{\zeta_0^*}^{15} \\
& -16216330743222333202{\zeta_0^*}^{16}-7192672975637794453{\zeta_0^*}^{17}-2425555545133259595{\zeta_0^*}^{18} \\
& -592101196586931096{\zeta_0^*}^{19}-96625519817262786{\zeta_0^*}^{20}-9087388027902720{\zeta_0^*}^{21} \\
& -333218748655800{\zeta_0^*}^{22}+3241895076000{\zeta_0^*}^{23}))),
\end{aligned}
\tag{C.150}
$$

$$
d_{132} \;=\; \frac{64\zeta_0^*(788+\zeta_0^*(2981+\zeta_0^*(3119+6\zeta_0^*(166+21\zeta_0^*))))}{1125(1+\zeta_0^*)(2+\zeta_0^*)(1+2\zeta_0^*)(2+3\zeta_0^*)},
\tag{C.151}
$$

$$
d_{133} \;=\; \frac{64\zeta_0^*(2+\zeta_0^*)}{225\left(1+3\zeta_0^*+2{\zeta_0^*}^2\right)},
\tag{C.152}
$$

$$
d_{135} \;=\; \frac{128(2+\zeta_0^*)}{225(1+2\zeta_0^*)},
\tag{C.153}
$$

$$
d_{137} \;=\; \frac{64\zeta_0^*(2+\zeta_0^*)}{225\left(1+3\zeta_0^*+2{\zeta_0^*}^2\right)},
\tag{C.154}
$$

$$
d_{139} \;=\; -\frac{64\left(52+53\zeta_0^*+87{\zeta_0^*}^2+93{\zeta_0^*}^3\right)}{1125\left(2+9\zeta_0^*+13{\zeta_0^*}^2+6{\zeta_0^*}^3\right)},
\tag{C.155}
$$

$$
d_{142} \;=\; -\frac{16(840+\zeta_0^*(3388+\zeta_0^*(3756+\zeta_0^*(2344+\zeta_0^*(1081+126\zeta_0^*)))))}{375(1+\zeta_0^*)(2+\zeta_0^*)(1+2\zeta_0^*)(2+3\zeta_0^*)},
\tag{C.156}
$$

$$d_{144} = -\frac{16\zeta_0^*(88+\zeta_0^*(-344+\zeta_0^*(-206+3\zeta_0^*(157+42\zeta_0^*))))}{1125(1+\zeta_0^*)(2+\zeta_0^*)(1+2\zeta_0^*)(2+3\zeta_0^*)}, \tag{C.157}$$

$$\begin{aligned} d_{149} = & -\frac{1}{375(1+\zeta_0^*)^3(2+\zeta_0^*)(1+3\zeta_0^*)(2+5\zeta_0^*)(2+\zeta_0^*(7+6\zeta_0^*))^2}(64\zeta_0^*(-2592+\zeta_0^*(13480 \\ & +\zeta_0^*(173024+\zeta_0^*(560058+\zeta_0^*(878482+\zeta_0^*(772355+3\zeta_0^*(128902+\zeta_0^*(32369+3660\zeta_0^*)))))))), \end{aligned} \tag{C.158}$$

$$\begin{aligned} d_{150} = & \frac{1}{\left(375(1+\zeta_0^*)^3(2+\zeta_0^*)^3(1+3\zeta_0^*)(2+5\zeta_0^*)(2+\zeta_0^*(7+6\zeta_0^*))^2\right)}(-(16(-1600+\zeta_0^*(-134080 \\ & +\zeta_0^*(-5226128+\zeta_0^*(-32240768+\zeta_0^*(-75367676+\zeta_0^*(-54908632+\zeta_0^*(71411849+\zeta_0^*(178754931 \\ & +\zeta_0^*(156107451+\zeta_0^*(71226877+12\zeta_0^*(1538327+3\zeta_0^*(80227+6480\zeta_0^*)))))))))))), \end{aligned} \tag{C.159}$$

$$d_{151} = \frac{256(2+\zeta_0^*)\left(34+103\zeta_0^*+80{\zeta_0^*}^2\right)}{75\left(4+40\zeta_0^*+155{\zeta_0^*}^2+290{\zeta_0^*}^3+261{\zeta_0^*}^4+90{\zeta_0^*}^5\right)}, \tag{C.160}$$

$$d_{154} = -\frac{64\zeta_0^*(304+\zeta_0^*(-3720+\zeta_0^*(-20744+\zeta_0^*(-32606+\zeta_0^*(-17303+\zeta_0^*(-631+1410\zeta_0^*))))))}{375(1+\zeta_0^*)^2(2+\zeta_0^*)(1+2\zeta_0^*)^2(1+3\zeta_0^*)(2+3\zeta_0^*)(2+5\zeta_0^*)}, \tag{C.161}$$

$$d_{156} = \frac{128(176+\zeta_0^*(27460+\zeta_0^*(120664+\zeta_0^*(181941+\zeta_0^*(111368+21\zeta_0^*(1331+90\zeta_0^*))))))}{375(1+\zeta_0^*)(2+\zeta_0^*)(1+2\zeta_0^*)^2(1+3\zeta_0^*)(2+3\zeta_0^*)(2+5\zeta_0^*)}, \tag{C.162}$$

$$\begin{aligned} d_{158} = & \frac{1}{\left(375(1+\zeta_0^*)^2(2+\zeta_0^*)^2(1+2\zeta_0^*)^2(1+3\zeta_0^*)(2+3\zeta_0^*)^2(2+5\zeta_0^*)\right)}(64(-72712+\zeta_0^*(-766132 \\ & +\zeta_0^*(-2031618+\zeta_0^*(464629+\zeta_0^*(9820677+\zeta_0^*(16407418+\zeta_0^*(11635237 \\ & +\zeta_0^*(3645572+388119\zeta_0^*+6660{\zeta_0^*}^2)))))))), \end{aligned} \tag{C.163}$$

$$\begin{aligned} d_{162} = & \frac{1}{\left(375(1+\zeta_0^*)^3(2+\zeta_0^*)^3(1+3\zeta_0^*)(2+5\zeta_0^*)(2+\zeta_0^*(7+6\zeta_0^*))^2\right)}(8(90400+\zeta_0^*(-3988080+\zeta_0^*(-50377392 \\ & +\zeta_0^*(-206158632+\zeta_0^*(-367354254+\zeta_0^*(-198317463+\zeta_0^*(311866346+3\zeta_0^*(211556878+\zeta_0^*(166643218 \\ & +\zeta_0^*(71281851+2\zeta_0^*(8838521+6\zeta_0^*(212233+14670\zeta_0^*)))))))))))), \end{aligned} \tag{C.164}$$

$$\begin{aligned} d_{164} = & \frac{1}{\left(375(1+\zeta_0^*)^3(2+\zeta_0^*)^3(1+3\zeta_0^*)(2+5\zeta_0^*)(2+\zeta_0^*(7+6\zeta_0^*))^2\right)}(-(16\zeta_0^*(141760+\zeta_0^*(2096192 \\ & +\zeta_0^*(10526432+\zeta_0^*(26719224+\zeta_0^*(40901688+\zeta_0^*(43983234+\zeta_0^*(38580881+\zeta_0^*(28146451 \\ & +\zeta_0^*(14789167+3\zeta_0^*(1558073+12\zeta_0^*(19777+855\zeta_0^*)))))))))))), \end{aligned} \tag{C.165}$$

$$d_{115} = \frac{28672(-190+\zeta_0^*(-1409+\zeta_0^*(-2499+\zeta_0^*(-621+275\zeta_0^*))))}{25(1+\zeta_0^*)(2+\zeta_0^*)(1+2\zeta_0^*)(1+3\zeta_0^*)(2+3\zeta_0^*)(1+4\zeta_0^*)(2+5\zeta_0^*)(2+7\zeta_0^*)(2+9\zeta_0^*)}, \tag{C.166}$$

$$\begin{aligned} d_{117} = & \frac{1}{\left(125(1+\zeta_0^*)^2(2+\zeta_0^*)(1+2\zeta_0^*)^2(1+3\zeta_0^*)^2(2+3\zeta_0^*)^2(1+4\zeta_0^*)(2+5\zeta_0^*)^2(2+7\zeta_0^*)^2(2+9\zeta_0^*)\right)}(-(1024(811680 \\ & +\zeta_0^*(-13114032+\zeta_0^*(-355035472+\zeta_0^*(-2884871592+\zeta_0^*(-12264120838+\zeta_0^*(-31073808243 \\ & +\zeta_0^*(-48687456004+3\zeta_0^*(-15482625926 \\ & +\zeta_0^*(-8299946604+\zeta_0^*(-1914735385+88204602\zeta_0^*+75773880{\zeta_0^*}^2)))))))))), \end{aligned} \tag{C.167}$$

$$
\begin{aligned}
d_{30} \;=\;& \frac{1}{\big(625(1+\zeta_0^*)^3(2+\zeta_0^*)^3(1+2\zeta_0^*)^3(1+3\zeta_0^*)^3(2+3\zeta_0^*)^3(1+4\zeta_0^*)^2(1+5\zeta_0^*)(2+5\zeta_0^*)^3(2+7\zeta_0^*)^2(2+9\zeta_0^*)\big)} \\
&\times(512(-8107008+\zeta_0^*(438320128+\zeta_0^*(-24725793536+\zeta_0^*(-996613326080+\zeta_0^*(-14893359522048 \\
&+\zeta_0^*(-128896500104000+\zeta_0^*(-742258069901824+\zeta_0^*(-3035752004511888+\zeta_0^*(-9129105513025180 \\
&+\zeta_0^*(-20547496525358936+\zeta_0^*(-34820466995767149+\zeta_0^*(-44211122390855974+\zeta_0^*(-41290605270954824 \\
&+\zeta_0^*(-27188331290083630+\zeta_0^*(-11343576009662721+2\zeta_0^*(-931469069607679+3\zeta_0^*(137548546693685 \\
&+3\zeta_0^*(33156416240341+30\zeta_0^*(282291997307+37800\zeta_0^*(770381+10122\zeta_0^*)))))))))))))))))))), \qquad \text{(C.168)}
\end{aligned}
$$

$$
\begin{aligned}
d_{32} \;=\;& \frac{1}{354375}16\Big(\frac{50803200}{(1+\zeta_0^*)^4}+\frac{87145632}{(1+\zeta_0^*)^3}-\frac{636301008}{(1+\zeta_0^*)^2}-\frac{2898216720}{1+\zeta_0^*}+\frac{1512000}{(2+\zeta_0^*)^4}-\frac{3931200}{(2+\zeta_0^*)^3}-\frac{8421315}{(2+\zeta_0^*)^2} \\
&-\frac{2123195}{2+\zeta_0^*}-\frac{2857680000}{(1+2\zeta_0^*)^4}-\frac{69439688640}{(1+2\zeta_0^*)^3}-\frac{446144721792}{(1+2\zeta_0^*)^2}-\frac{101219558048}{1+2\zeta_0^*}-\frac{7838208000}{(1+3\zeta_0^*)^3} \\
&+\frac{370426361760}{(1+3\zeta_0^*)^2}+\frac{56023135471800}{1+3\zeta_0^*}+\frac{8817984000}{(2+3\zeta_0^*)^4}+\frac{82313431200}{(2+3\zeta_0^*)^3}+\frac{247212997920}{(2+3\zeta_0^*)^2}+\frac{295919392797}{2+3\zeta_0^*} \\
&+\frac{1237972377600}{(1+4\zeta_0^*)^2}+\frac{146319038115840}{1+4\zeta_0^*}+\frac{16272900000000}{1+5\zeta_0^*}+\frac{940653000000}{(2+5\zeta_0^*)^3}+\frac{3393849729375}{(2+5\zeta_0^*)^2} \\
&-\frac{19839202566750}{2+5\zeta_0^*}-\frac{8119192788000}{(2+7\zeta_0^*)^2}-\frac{257650507801890}{2+7\zeta_0^*}-\frac{160009126061400}{2+9\zeta_0^*}\Big), \qquad \text{(C.169)}
\end{aligned}
$$

$$
\begin{aligned}
d_{34} \;=\;& \frac{1}{\big(125(1+\zeta_0^*)^2(2+\zeta_0^*)(1+2\zeta_0^*)^2(1+3\zeta_0^*)^2(2+3\zeta_0^*)^2(1+4\zeta_0^*)^2(1+5\zeta_0^*)(2+5\zeta_0^*)^2(2+7\zeta_0^*)^2(2+9\zeta_0^*)\big)} \\
&\times(1024(268320+\zeta_0^*(-16410512+\zeta_0^*(-399585392+\zeta_0^*(-3726575192+\zeta_0^*(-19186217118+\zeta_0^*(-60974480913 \\
&+\zeta_0^*(-124336914114+\zeta_0^*(-162207701308+\zeta_0^*(-128965278172+\zeta_0^*(-53623795255+12\zeta_0^*(-368485247 \\
&+1185\zeta_0^*(303941+76860\zeta_0^*)))))))))))), \qquad \text{(C.170)}
\end{aligned}
$$

$$
d_{36} \;=\; -\frac{57344(130+\zeta_0^*(573+\zeta_0^*(624+125\zeta_0^*)))}{25(1+\zeta_0^*)(1+2\zeta_0^*)(1+3\zeta_0^*)(2+3\zeta_0^*)(1+4\zeta_0^*)(1+5\zeta_0^*)(2+5\zeta_0^*)(2+7\zeta_0^*)(2+9\zeta_0^*)}, \qquad \text{(C.171)}
$$

$$
\begin{aligned}
d_{42} \;=\;& \frac{1}{\big(625(1+\zeta_0^*)^3(2+\zeta_0^*)^3(1+2\zeta_0^*)^3(1+3\zeta_0^*)^2(2+3\zeta_0^*)^3(1+4\zeta_0^*)(2+5\zeta_0^*)^2(2+7\zeta_0^*)\big)}(256(65408+\zeta_0^*(-4160000 \\
&+\zeta_0^*(66059808+\zeta_0^*(2590354016+\zeta_0^*(27517918216+\zeta_0^*(155422754768+\zeta_0^*(548553045422+\zeta_0^*(1295162956838 \\
&+\zeta_0^*(2111311713864+\zeta_0^*(2404437883594+\zeta_0^*(1911125268677+\zeta_0^*(1051934677756+\zeta_0^*(400141102262 \\
&+3\zeta_0^*(36252867346+3\zeta_0^*(2544259727+90\zeta_0^*(4369879+289380\zeta_0^*)))))))))))))))), \qquad \text{(C.172)}
\end{aligned}
$$

$$
\begin{aligned}
d_{44} \;=\;& \frac{1}{\big(625(1+\zeta_0^*)^4(2+\zeta_0^*)^4(1+3\zeta_0^*)^2(1+4\zeta_0^*)(2+5\zeta_0^*)^2(2+7\zeta_0^*)(2+\zeta_0^*(7+6\zeta_0^*))^3\big)}(64(49462528 \\
&+\zeta_0^*(1995171072+\zeta_0^*(44094124800+\zeta_0^*(450581938048+\zeta_0^*(2399697922592+\zeta_0^*(6519289098976 \\
&+\zeta_0^*(3355354219888+\zeta_0^*(-39770712677432+\zeta_0^*(-160806538962911 \\
&+\zeta_0^*(-337016698687303+\zeta_0^*(-457030555857806+\zeta_0^*(-422019454718275+\zeta_0^*(-265229551578671 \\
&+\zeta_0^*(-108900537528055+\zeta_0^*(-25967571426082+3\zeta_0^*(-728311895197+18\zeta_0^*(7422822453 \\
&+40\zeta_0^*(41184691+1248870\zeta_0^*)))))))))))))))))), \qquad \text{(C.173)}
\end{aligned}
$$

$$
\begin{aligned}
d_{45} \;=\;& \frac{1}{\big(625(1+\zeta_0^*)^3(2+\zeta_0^*)^3(1+2\zeta_0^*)^3(1+3\zeta_0^*)^2(2+3\zeta_0^*)^3(1+4\zeta_0^*)(2+5\zeta_0^*)^2(2+7\zeta_0^*)\big)}(128(13141632 \\
&+\zeta_0^*(905778560+\zeta_0^*(7735604512+\zeta_0^*(-5137213856+\zeta_0^*(-395164526536+\zeta_0^*(-2631514368168 \\
&+\zeta_0^*(-9400205932922+\zeta_0^*(-21505324729958+\zeta_0^*(-33389354469544 \\
&+\zeta_0^*(-35796456144499+\zeta_0^*(-26287578927662+\zeta_0^*(-12767644747746+\zeta_0^*(-3776761053802 \\
&+3\zeta_0^*(-180934232431+6\zeta_0^*(9212729+360\zeta_0^*(1084177+29190\zeta_0^*)))))))))))))))), \qquad \text{(C.174)}
\end{aligned}
$$

$$d_{46} = \frac{1}{\left(125(1+\zeta_0^*)^2(2+\zeta_0^*)^2(1+2\zeta_0^*)^2(1+3\zeta_0^*)^2(2+3\zeta_0^*)^2(1+4\zeta_0^*)(2+5\zeta_0^*)^2(2+7\zeta_0^*)\right)}(256(-35584+\zeta_0^*(1720320 +\zeta_0^*(35928960+\zeta_0^*(269042984+\zeta_0^*(1057464700+\zeta_0^*(2443005426+\zeta_0^*(3446160593+\zeta_0^*(2975917701 +\zeta_0^*(1556569429+\zeta_0^*(503759689+54\zeta_0^*(2106613+319620\zeta_0^*)))))))))), \quad \text{(C.175)}$$

$$d_{48} = \frac{1}{\left(125(1+\zeta_0^*)^2(2+\zeta_0^*)(1+2\zeta_0^*)^2(1+3\zeta_0^*)^2(2+3\zeta_0^*)(1+4\zeta_0^*)(2+5\zeta_0^*)^2(2+7\zeta_0^*)\right)}(-(512(2128 +\zeta_0^*(-57136+\zeta_0^*(-754144+\zeta_0^*(-3423748+\zeta_0^*(-7640661+\zeta_0^*(-8767264+\zeta_0^*(-4285366 +\zeta_0^*(501573+2\zeta_0^*(646769+183960\zeta_0^*)))))))))), \quad \text{(C.176)}$$

$$d_{49} = \frac{1}{\left(625(1+\zeta_0^*)^2(2+\zeta_0^*)^3(1+2\zeta_0^*)^3(1+3\zeta_0^*)^2(2+3\zeta_0^*)^2(1+4\zeta_0^*)(2+5\zeta_0^*)^2(2+7\zeta_0^*)\right)}(128(46208+\zeta_0^*(-419520 +\zeta_0^*(40494496+\zeta_0^*(640431056+\zeta_0^*(4008659832+\zeta_0^*(13773635004+\zeta_0^*(28781626414+\zeta_0^*(37515153447 +\zeta_0^*(29308327538+\zeta_0^*(11110656166+3\zeta_0^*(-350795040+\zeta_0^*(-978278031+4\zeta_0^*(-93485024 +15\zeta_0^*(-755513+28140\zeta_0^*)))))))))))))), \quad \text{(C.177)}$$

$$d_{51} = \frac{7168(2+\zeta_0^*)(10+\zeta_0^*(31+25\zeta_0^*))}{25(1+\zeta_0^*)(1+2\zeta_0^*)(1+3\zeta_0^*)(2+3\zeta_0^*)(1+4\zeta_0^*)(2+5\zeta_0^*)(2+7\zeta_0^*)}, \quad \text{(C.178)}$$

$$d_{52} = -\frac{1024(1670+\zeta_0^*(7187+\zeta_0^*(7761+1610\zeta_0^*)))}{25(1+\zeta_0^*)(1+2\zeta_0^*)(1+3\zeta_0^*)(2+3\zeta_0^*)(1+4\zeta_0^*)(2+5\zeta_0^*)(2+7\zeta_0^*)}, \quad \text{(C.179)}$$

$$d_{54} = -\frac{1024(-880+\zeta_0^*(-6808+\zeta_0^*(-11903+\zeta_0^*(-2102+1785\zeta_0^*))))}{25(1+\zeta_0^*)(2+\zeta_0^*)(1+2\zeta_0^*)(1+3\zeta_0^*)(2+3\zeta_0^*)(1+4\zeta_0^*)(2+5\zeta_0^*)(2+7\zeta_0^*)}, \quad \text{(C.180)}$$

$$d_{55} = \frac{1}{\left(125(1+\zeta_0^*)^2(2+\zeta_0^*)^2(1+2\zeta_0^*)^2(1+3\zeta_0^*)^2(2+3\zeta_0^*)^2(1+4\zeta_0^*)(2+5\zeta_0^*)^2(2+7\zeta_0^*)\right)}(256(765152 +\zeta_0^*(-5644000+\zeta_0^*(-163587840+\zeta_0^*(-1128219552+\zeta_0^*(-3932657210+\zeta_0^*(-8020869078+\zeta_0^*(-9965274409 +\zeta_0^*(-7427907953+\zeta_0^*(-3054411227+3\zeta_0^*(-170614559+2\zeta_0^*(6272639+2743860\zeta_0^*)))))))))), \quad \text{(C.181)}$$

$$d_{57} = \frac{1}{\left(625(1+\zeta_0^*)^4(2+\zeta_0^*)^3(1+2\zeta_0^*)^3(1+3\zeta_0^*)^2(2+3\zeta_0^*)^3(1+4\zeta_0^*)(2+5\zeta_0^*)^2(2+7\zeta_0^*)\right)}(-(64\zeta_0^*(1107968 +\zeta_0^*(-12857600+\zeta_0^*(794696768+\zeta_0^*(17211199936+\zeta_0^*(142225655536+\zeta_0^*(660409484928 +\zeta_0^*(1952062379612+\zeta_0^*(3869721872348+\zeta_0^*(5226921152569+\zeta_0^*(4737865071899 +\zeta_0^*(2697602482142+\zeta_0^*(752714002776+\zeta_0^*(-82589754073 +9\zeta_0^*(-15241630703+2\zeta_0^*(-2227937629+60\zeta_0^*(-3472787+66360\zeta_0^*)))))))))))))))), \quad \text{(C.182)}$$

$$d_{59} = \frac{14336(2+\zeta_0^*)(10+\zeta_0^*(31+25\zeta_0^*))}{25(1+\zeta_0^*)(1+2\zeta_0^*)(1+3\zeta_0^*)(2+3\zeta_0^*)(1+4\zeta_0^*)(2+5\zeta_0^*)(2+7\zeta_0^*)}, \quad \text{(C.183)}$$

$$d_{60} = \frac{1}{\left(625(1+\zeta_0^*)^2(2+\zeta_0^*)^3(1+2\zeta_0^*)^3(1+3\zeta_0^*)^2(2+3\zeta_0^*)^2(1+4\zeta_0^*)(2+5\zeta_0^*)^2(2+7\zeta_0^*)\right)}(-(256(1409792 +\zeta_0^*(36414080+\zeta_0^*(107088384+\zeta_0^*(-1703080416+\zeta_0^*(-16087322352+\zeta_0^*(-64666903704+\zeta_0^*(-150249991544 +\zeta_0^*(-217916952482+3\zeta_0^*(-66343500706+\zeta_0^*(-36292663367+\zeta_0^*(-9657613810+3\zeta_0^*(136506407 +4\zeta_0^*(82019808+5\zeta_0^*(3754963+244860\zeta_0^*)))))))))))))), \quad \text{(C.184)}$$

$$d_{63} = \frac{1}{\left(625(1+\zeta_0^*)^4(2+\zeta_0^*)^4(1+3\zeta_0^*)^2(1+4\zeta_0^*)(2+5\zeta_0^*)^2(2+7\zeta_0^*)(2+\zeta_0^*(7+6\zeta_0^*))^3\right)}(-(64(82748672 +\zeta_0^*(2640886528+\zeta_0^*(38750585600+\zeta_0^*(330812721152+\zeta_0^*(1830386015008+\zeta_0^*(7024112101024 +\zeta_0^*(19632431978112+\zeta_0^*(41613826334032+\zeta_0^*(69430063946961 +\zeta_0^*(94270235591203+\zeta_0^*(106395134331431+\zeta_0^*(99677533923725+\zeta_0^*(75545816648821 +\zeta_0^*(44400372924805+\zeta_0^*(19205563856557+3\zeta_0^*(1908695134697+42\zeta_0^*(8481062413 +240\zeta_0^*(3460781+113295\zeta_0^*)))))))))))))))))), \tag{C.185}$$

$$d_{65} = \frac{1}{\left(125(1+\zeta_0^*)^2(2+\zeta_0^*)(1+2\zeta_0^*)^2(1+3\zeta_0^*)^2(2+3\zeta_0^*)(1+4\zeta_0^*)(2+5\zeta_0^*)^2(2+7\zeta_0^*)\right)}(-(1024(968 +\zeta_0^*(-167156+\zeta_0^*(-1905474+\zeta_0^*(-8578383+\zeta_0^*(-19953226+\zeta_0^*(-25583334+\zeta_0^*(-17524401 +2\zeta_0^*(-2656841+8\zeta_0^*(-997+15645\zeta_0^*)))))))))), \tag{C.186}$$

$$d_{71} = \frac{1}{375(1+\zeta_0^*)^2(2+\zeta_0^*)(1+2\zeta_0^*)^2(1+3\zeta_0^*)(2+3\zeta_0^*)(2+5\zeta_0^*)^2(2+7\zeta_0^*)}(512(1824+\zeta_0^*(-28704 +\zeta_0^*(-291992+\zeta_0^*(-944972+\zeta_0^*(-1401904+\zeta_0^*(-927771+\zeta_0^*(-108243 +2\zeta_0^*(78271+28140\zeta_0^*)))))))), \tag{C.187}$$

$$d_{72} = -\frac{7168(2+\zeta_0^*)(10+\zeta_0^*(31+25\zeta_0^*))}{75(1+\zeta_0^*)(1+2\zeta_0^*)(1+3\zeta_0^*)(2+3\zeta_0^*)(2+5\zeta_0^*)(2+7\zeta_0^*)}, \tag{C.188}$$

$$d_{73} = \frac{2048(10+\zeta_0^*(-574+\zeta_0^*(-989+\zeta_0^*(909+770\zeta_0^*))))}{75(1+\zeta_0^*)(2+\zeta_0^*)(1+2\zeta_0^*)(1+3\zeta_0^*)(2+3\zeta_0^*)(2+5\zeta_0^*)(2+7\zeta_0^*)}, \tag{C.189}$$

$$d_{74} = \frac{1}{\left(375(1+\zeta_0^*)^2(2+\zeta_0^*)^2(1+2\zeta_0^*)^2(1+3\zeta_0^*)(2+3\zeta_0^*)^2(2+5\zeta_0^*)^2(2+7\zeta_0^*)\right)}(-(256(700896 +\zeta_0^*(-578064+\zeta_0^*(-53976048+\zeta_0^*(-311269336+\zeta_0^*(-829365698+\zeta_0^*(-1224784057 +\zeta_0^*(-1038861632+\zeta_0^*(-486084664+\zeta_0^*(-107146118-4885869\zeta_0^*+953190{\zeta_0^*}^2)))))))))), \tag{C.190}$$

$$d_{77} = \frac{1024(1370+\zeta_0^*(5667+\zeta_0^*(6046+1365\zeta_0^*)))}{75(1+\zeta_0^*)(1+2\zeta_0^*)(1+3\zeta_0^*)(2+3\zeta_0^*)(2+5\zeta_0^*)(2+7\zeta_0^*)}, \tag{C.191}$$

$$d_{78} = \frac{1}{\left(375(1+\zeta_0^*)^2(2+\zeta_0^*)^2(1+2\zeta_0^*)^2(1+3\zeta_0^*)(2+3\zeta_0^*)^2(2+5\zeta_0^*)^2(2+7\zeta_0^*)\right)}(-(256(20928 +\zeta_0^*(318688+\zeta_0^*(4660816+\zeta_0^*(30590312+\zeta_0^*(98867256+\zeta_0^*(172847524+\zeta_0^*(168533494 +\zeta_0^*(91192913+\zeta_0^*(27860356+9\zeta_0^*(639627+104230\zeta_0^*)))))))))), \tag{C.192}$$

$$d_{80} = \frac{1}{\left(375(1+\zeta_0^*)^3(2+\zeta_0^*)^3(1+2\zeta_0^*)^2(1+3\zeta_0^*)(2+3\zeta_0^*)^3(2+5\zeta_0^*)^2(2+7\zeta_0^*)\right)}(-(64(3459328 +\zeta_0^*(188148096+\zeta_0^*(1415604544+\zeta_0^*(2399569568+\zeta_0^*(-13860297872+\zeta_0^*(-84645614600 +\zeta_0^*(-215183028052+\zeta_0^*(-320198163618+\zeta_0^*(-300522327436 +\zeta_0^*(-179281457111+\zeta_0^*(-65624164357+5\zeta_0^*(-2692804229 +9\zeta_0^*(-27960719+6\zeta_0^*(-91137+8120\zeta_0^*)))))))))))))))), \tag{C.193}$$

$$d_{81} = -\frac{14336(2+\zeta_0^*)(10+\zeta_0^*(31+25\zeta_0^*))}{75(1+\zeta_0^*)(1+2\zeta_0^*)(1+3\zeta_0^*)(2+3\zeta_0^*)(2+5\zeta_0^*)(2+7\zeta_0^*)}, \tag{C.194}$$

$$d_{83} = \frac{1}{\left(375(1+\zeta_0^*)^3(2+\zeta_0^*)^3(1+2\zeta_0^*)^2(1+3\zeta_0^*)(2+3\zeta_0^*)^3(2+5\zeta_0^*)^2(2+7\zeta_0^*)\right)}(-(128(-19200 +\zeta_0^*(1502976+\zeta_0^*(-29294336+\zeta_0^*(-510120128+\zeta_0^*(-3019865568+\zeta_0^*(-9646144112 +\zeta_0^*(-18884945808+\zeta_0^*(-23700271764+\zeta_0^*(-19056974839+\zeta_0^*(-9306212584 +\zeta_0^*(-2250598956+\zeta_0^*(57065642+3\zeta_0^*(56732369+90\zeta_0^*(129211+7980\zeta_0^*)))))))))))))), \quad \text{(C.195)}$$

$$d_{85} = \frac{1}{\left(375(1+\zeta_0^*)^2(2+\zeta_0^*)(1+2\zeta_0^*)^2(1+3\zeta_0^*)(2+3\zeta_0^*)(2+5\zeta_0^*)^2(2+7\zeta_0^*)\right)}(256(2656+\zeta_0^*(-426936+\zeta_0^*(-3527468 +\zeta_0^*(-11178818+\zeta_0^*(-17487271+\zeta_0^*(-14069484+\zeta_0^*(-5323117+2\zeta_0^*(-277961+53760\zeta_0^*))))))))), \quad \text{(C.196)}$$

$$d_{87} = \frac{1}{\left(375(1+\zeta_0^*)^2(2+\zeta_0^*)^2(1+2\zeta_0^*)^2(1+3\zeta_0^*)(2+3\zeta_0^*)^2(2+5\zeta_0^*)^2(2+7\zeta_0^*)\right)}(64(536448+\zeta_0^*(9632832 +\zeta_0^*(28680576+\zeta_0^*(-92648624+\zeta_0^*(-676055448+\zeta_0^*(-1525765612+\zeta_0^*(-1688261776+\zeta_0^*(-931500111 +5\zeta_0^*(-38319160+3\zeta_0^*(2080467+2\zeta_0^*(607961+72240\zeta_0^*)))))))))), \quad \text{(C.197)}$$

$$d_{90} = -\frac{256(2+\zeta_0^*)(3+4\zeta_0^*)}{75\left(2+11\zeta_0^*+19{\zeta_0^*}^2+10{\zeta_0^*}^3\right)}, \quad \text{(C.198)}$$

$$d_{91} = \frac{256\left(36+130\zeta_0^*+123{\zeta_0^*}^2+26{\zeta_0^*}^3\right)}{75\left(4+28\zeta_0^*+71{\zeta_0^*}^2+77{\zeta_0^*}^3+30{\zeta_0^*}^4\right)}, \quad \text{(C.199)}$$

$$d_{93} = \frac{512\left(24+85\zeta_0^*+82{\zeta_0^*}^2+19{\zeta_0^*}^3\right)}{75\left(4+28\zeta_0^*+71{\zeta_0^*}^2+77{\zeta_0^*}^3+30{\zeta_0^*}^4\right)}, \quad \text{(C.200)}$$

$$d_{94} = \frac{64(-5496+\zeta_0^*(-26812+\zeta_0^*(-47498+\zeta_0^*(-41877+\zeta_0^*(-21682+5\zeta_0^*(-1041+20\zeta_0^*))))))}{125(1+\zeta_0^*)(2+\zeta_0^*)(1+2\zeta_0^*)(2+3\zeta_0^*)^2(2+5\zeta_0^*)}, \quad \text{(C.201)}$$

$$d_{99} = -\frac{512(2+\zeta_0^*)(3+4\zeta_0^*)}{75\left(2+11\zeta_0^*+19{\zeta_0^*}^2+10{\zeta_0^*}^3\right)}, \quad \text{(C.202)}$$

$$d_{101} = -\frac{64(12+\zeta_0^*(2980+\zeta_0^*(5447+5\zeta_0^*(461+80\zeta_0^*))))}{375(1+\zeta_0^*)(1+2\zeta_0^*)(2+3\zeta_0^*)(2+5\zeta_0^*)}, \quad \text{(C.203)}$$

$$d_{102} = \frac{128\zeta_0^*(576+\zeta_0^*(2712+\zeta_0^*(4348+\zeta_0^*(2922+\zeta_0^*(797+90\zeta_0^*)))))}{75(1+\zeta_0^*)(2+\zeta_0^*)(1+2\zeta_0^*)(2+3\zeta_0^*)^2(2+5\zeta_0^*)}, \quad \text{(C.204)}$$

$$d_{108} = -\frac{28672(2+\zeta_0^*)(10+\zeta_0^*(31+25\zeta_0^*))}{25(1+\zeta_0^*)(1+2\zeta_0^*)(1+3\zeta_0^*)(2+3\zeta_0^*)(1+4\zeta_0^*)(2+5\zeta_0^*)(2+7\zeta_0^*)(2+9\zeta_0^*)}, \quad \text{(C.205)}$$

$$d_{110} = \frac{1}{\left(625(1+\zeta_0^*)^3(2+\zeta_0^*)^3(1+2\zeta_0^*)^3(1+4\zeta_0^*)(2+5\zeta_0^*)^3(2+7\zeta_0^*)^2(2+9\zeta_0^*)(2+9\zeta_0^*(1+\zeta_0^*))^2\right)} \times(-(256(554496+\zeta_0^*(-8614144+\zeta_0^*(965385728+\zeta_0^*(23087669760+\zeta_0^*(224224046528 +\zeta_0^*(1251442757856+\zeta_0^*(4523126509312+\zeta_0^*(11162168580864+\zeta_0^*(19187692132606 +\zeta_0^*(22838849702715+\zeta_0^*(18037619508622+\zeta_0^*(8173812430212+\zeta_0^*(620760562100 +\zeta_0^*(-1598995387427+36\zeta_0^*(-26203869592+7\zeta_0^*(-819055093 +60\zeta_0^*(-202399+267120\zeta_0^*))))))))))))))))), \quad \text{(C.206)}$$

$$d_{111} = \frac{1}{\left(125(1+\zeta_0^*)^2(2+\zeta_0^*)(1+2\zeta_0^*)^2(1+3\zeta_0^*)^2(2+3\zeta_0^*)(1+4\zeta_0^*)(2+5\zeta_0^*)^2(2+7\zeta_0^*)^2(2+9\zeta_0^*)\right)}(1024(9120 +\zeta_0^*(-409552+\zeta_0^*(-6826304+\zeta_0^*(-41752616+\zeta_0^*(-132541774+\zeta_0^*(-236815037+\zeta_0^*(-230693011 +\zeta_0^*(-93806719+\zeta_0^*(21523999+18\zeta_0^*(1815503+475020\zeta_0^*))))))))))), \quad \text{(C.207)}$$

$$d_{112} = \frac{1}{\left(125(1+\zeta_0^*)^2(2+\zeta_0^*)^2(1+2\zeta_0^*)^2(1+3\zeta_0^*)^2(2+3\zeta_0^*)^2(1+4\zeta_0^*)(2+5\zeta_0^*)^2(2+7\zeta_0^*)^2(2+9\zeta_0^*)\right)} \times(-(6144(-32480+\zeta_0^*(1157808+\zeta_0^*(30738112+\zeta_0^*(283773192+\zeta_0^*(1404823506+\zeta_0^*(4216354823 +\zeta_0^*(8026916527+\zeta_0^*(9781279075+3\zeta_0^*(2511693373+2\zeta_0^*(601580909 +2\zeta_0^*(92536623+\zeta_0^*(21225439+3337110\zeta_0^*))))))))))))), \quad \text{(C.208)}$$

$$d_{113} = \frac{1}{\left(625(1+\zeta_0^*)^3(2+\zeta_0^*)^3(1+2\zeta_0^*)^3(1+3\zeta_0^*)^2(2+3\zeta_0^*)^3(1+4\zeta_0^*)(2+5\zeta_0^*)^3(2+7\zeta_0^*)^2(2+9\zeta_0^*)\right)} \times(256(-136336384+\zeta_0^*(-12093237760+\zeta_0^*(-114343874048+\zeta_0^*(624817568512+\zeta_0^*(17968436106368 +\zeta_0^*(150648901377088+\zeta_0^*(736641126140416+\zeta_0^*(2413644349419712+\zeta_0^*(5597373037024172 +\zeta_0^*(9406595100566774+\zeta_0^*(11523531098835622+\zeta_0^*(10203524256787205+3\zeta_0^*(2122335846902416 +\zeta_0^*(885168940600656+\zeta_0^*(21902322053737 0+27\zeta_0^*(776321953841 +4\zeta_0^*(-23930593996+35\zeta_0^*(-147894653+1346940\zeta_0^*))))))))))))))))), \quad \text{(C.209)}$$

$$d_{118} = \frac{1}{\left(625(1+\zeta_0^*)^3(2+\zeta_0^*)^3(1+2\zeta_0^*)^3(1+3\zeta_0^*)^2(2+3\zeta_0^*)^3(1+4\zeta_0^*)(2+5\zeta_0^*)^3(2+7\zeta_0^*)^2(2+9\zeta_0^*)\right)} \times(-(256(6075392+\zeta_0^*(-197196800+\zeta_0^*(4452858624+\zeta_0^*(215832360704+\zeta_0^*(2970900017536 +\zeta_0^*(22367010202496+\zeta_0^*(108353600376992+\zeta_0^*(362590783530464+\zeta_0^*(868737073869204 +\zeta_0^*(1516384470433348+\zeta_0^*(1938971075815739+\zeta_0^*(1810381838185315+\zeta_0^*(1222569487515086 +3\zeta_0^*(196842418547882+3\zeta_0^*(22647404948455+\zeta_0^*(5746869254263+36\zeta_0^*(30705088293 +35\zeta_0^*(108533849+3430980\zeta_0^*))))))))))))))))), \quad \text{(C.210)}$$

$$d_{119} = \frac{1}{\left(625(1+\zeta_0^*)^4(2+\zeta_0^*)^4(1+2\zeta_0^*)^3(1+3\zeta_0^*)^2(2+3\zeta_0^*)^4(1+4\zeta_0^*)(2+5\zeta_0^*)^3(2+7\zeta_0^*)^2(2+9\zeta_0^*)\right)} \times(256(-895862784+\zeta_0^*(-45372716032+\zeta_0^*(-1253289049600+\zeta_0^*(-16729070683904 +\zeta_0^*(-117857153228544+\zeta_0^*(-401132759704704+\zeta_0^*(196447555090496+\zeta_0^*(9075985878725152 +\zeta_0^*(49423096547799896+\zeta_0^*(159639380404352444+\zeta_0^*(357933522916464442+\zeta_0^*(585536483238032373 +\zeta_0^*(710154349696709566+\zeta_0^*(636507540592381152+\zeta_0^*(412316873110840778+\zeta_0^*(182830302622624464 +\zeta_0^*(47968209592453376+3\zeta_0^*(1005278649076730+3\zeta_0^*(-260537881680874 +15\zeta_0^*(-5365451627621+84\zeta_0^*(-5662821764+1785\zeta_0^*(52783+1260\zeta_0^*))))))))))))))))))), \quad \text{(C.211)}$$

$$d_{121} = \frac{57344(130+\zeta_0^*(573+\zeta_0^*(624+125\zeta_0^*)))}{25(1+\zeta_0^*)(1+2\zeta_0^*)(1+3\zeta_0^*)(2+3\zeta_0^*)(1+4\zeta_0^*)(2+5\zeta_0^*)(2+7\zeta_0^*)(2+9\zeta_0^*)}, \quad \text{(C.212)}$$

$$d_{123} = -\frac{57344(2+\zeta_0^*)(10+\zeta_0^*(31+25\zeta_0^*))}{25(1+\zeta_0^*)(1+2\zeta_0^*)(1+3\zeta_0^*)(2+3\zeta_0^*)(1+4\zeta_0^*)(2+5\zeta_0^*)(2+7\zeta_0^*)(2+9\zeta_0^*)}, \quad \text{(C.213)}$$

$$
\begin{aligned}
d_{124} &= \frac{1}{\left(625(1+\zeta_0^*)^4(2+\zeta_0^*)^4(1+2\zeta_0^*)^3(1+3\zeta_0^*)^2(2+3\zeta_0^*)^4(1+4\zeta_0^*)(2+5\zeta_0^*)^3(2+7\zeta_0^*)^2(2+9\zeta_0^*)\right)}(-(128(5836800\\
&+\zeta_0^*(1081344+\zeta_0^*(8097196032+\zeta_0^*(-201329470464+\zeta_0^*(-7918811062528+\zeta_0^*(-101637898289408\\
&+\zeta_0^*(-740886988600576+\zeta_0^*(-3564983738333056+\zeta_0^*(-12118306959735056+\zeta_0^*(-30132053855364000\\
&+\zeta_0^*(-55703026691457304+\zeta_0^*(-76703481088946908+\zeta_0^*(-77536218749564879\\
&+\zeta_0^*(-55030127987788877+\zeta_0^*(-23899302702513592+\zeta_0^*(-2180756073630360+\zeta_0^*(4888343177097113\\
&+3\zeta_0^*(1250772728044697+6\zeta_0^*(80680905510455+3\zeta_0^*(6337260501797\\
&+2700\zeta_0^*(349943331+7\zeta_0^*(4864751+278460\zeta_0^*)))))))))))))))))))))))), \qquad \text{(C.214)}
\end{aligned}
$$

$$
\begin{aligned}
d_{127} &= \frac{1}{\left(625(1+\zeta_0^*)^3(2+\zeta_0^*)^3(1+2\zeta_0^*)^3(1+4\zeta_0^*)(2+5\zeta_0^*)^3(2+7\zeta_0^*)^2(2+9\zeta_0^*)(2+9\zeta_0^*(1+\zeta_0^*))^2\right)}(512(12085504\\
&+\zeta_0^*(428597504+\zeta_0^*(1056360832+\zeta_0^*(-58301782720+\zeta_0^*(-767002537728+\zeta_0^*(-4833083885136\\
&+\zeta_0^*(-18906986857592+\zeta_0^*(-49982973821284+\zeta_0^*(-92464472714281+\zeta_0^*(-120811794254360\\
&+\zeta_0^*(-110127502888242+\zeta_0^*(-67037233351992+\zeta_0^*(-23980051960025\\
&+4\zeta_0^*(-594674649127+3\zeta_0^*(156545101721+144\zeta_0^*(504614132\\
&+35\zeta_0^*(2376641+115920\zeta_0^*)))))))))))))))))), \qquad \text{(C.215)}
\end{aligned}
$$

$$
\begin{aligned}
d_{129} &= \frac{1}{\left(625(1+\zeta_0^*)^4(2+\zeta_0^*)^4(1+3\zeta_0^*)^2(1+4\zeta_0^*)(2+5\zeta_0^*)^3(2+7\zeta_0^*)^2(2+9\zeta_0^*)(2+\zeta_0^*(7+6\zeta_0^*))^3\right)}(128(653910016\\
&+\zeta_0^*(27884038144+\zeta_0^*(549000080384+\zeta_0^*(6074478993920+\zeta_0^*(41815698872576+\zeta_0^*(189873881720832\\
&+\zeta_0^*(584314160011648+\zeta_0^*(1217809182863680+\zeta_0^*(1671075352472576+\zeta_0^*(1501449900187880\\
&+\zeta_0^*(1506126604169372+\zeta_0^*(3801563798667690+\zeta_0^*(8971715402578681\\
&+\zeta_0^*(13781645512800343+\zeta_0^*(14143753652370326+\zeta_0^*(9971029102763000+\zeta_0^*(4833832554325601\\
&+3\zeta_0^*(523926321032017+60\zeta_0^*(1802635735589+3\zeta_0^*(71641129949\\
&+420\zeta_0^*(10398221+342720\zeta_0^*)))))))))))))))))))), \qquad \text{(C.216)}
\end{aligned}
$$

$$
\begin{aligned}
d_{131} &= \frac{1}{\left(125(1+\zeta_0^*)^2(2+\zeta_0^*)(1+2\zeta_0^*)^2(1+3\zeta_0^*)^2(2+3\zeta_0^*)(1+4\zeta_0^*)(2+5\zeta_0^*)^2(2+7\zeta_0^*)^2(2+9\zeta_0^*)\right)}(2048(4480\\
&+\zeta_0^*(-999312+\zeta_0^*(-14976064+\zeta_0^*(-91102256+\zeta_0^*(-297197644+\zeta_0^*(-564387767+\zeta_0^*(-627382211\\
&+\zeta_0^*(-381698489-97669851\zeta_0^*+7272834{\zeta_0^*}^2+6433560{\zeta_0^*}^3))))))))), \qquad \text{(C.217)}
\end{aligned}
$$

$$
d_{136} = \frac{128(2+\zeta_0^*)}{225(1+2\zeta_0^*)}, \qquad \text{(C.218)}
$$

$$
d_{138} = \frac{256(2+\zeta_0^*)}{225(1+2\zeta_0^*)}, \qquad \text{(C.219)}
$$

$$
d_{140} = \frac{128(2+\zeta_0^*)}{225(1+2\zeta_0^*)}, \qquad \text{(C.220)}
$$

$$
d_{141} = \frac{64\left(908+3357\zeta_0^*+3313{\zeta_0^*}^2+762{\zeta_0^*}^3\right)}{1125\left(2+9\zeta_0^*+13{\zeta_0^*}^2+6{\zeta_0^*}^3\right)}, \qquad \text{(C.221)}
$$

$$
d_{143} = \frac{256(2+\zeta_0^*)}{225(1+2\zeta_0^*)}, \qquad \text{(C.222)}
$$

$$d_{145} = \frac{128\zeta_0^*(2+\zeta_0^*)}{225\left(1+3\zeta_0^*+2{\zeta_0^*}^2\right)}, \tag{C.223}$$

$$d_{147} = -\frac{64\left(52+33\zeta_0^*+47{\zeta_0^*}^2+78{\zeta_0^*}^3\right)}{1125\left(2+9\zeta_0^*+13{\zeta_0^*}^2+6{\zeta_0^*}^3\right)}, \tag{C.224}$$

$$d_{152} = \frac{256(2+\zeta_0^*)\left(34+103\zeta_0^*+80{\zeta_0^*}^2\right)}{75\left(4+40\zeta_0^*+155{\zeta_0^*}^2+290{\zeta_0^*}^3+261{\zeta_0^*}^4+90{\zeta_0^*}^5\right)}, \tag{C.225}$$

$$d_{153} = -\frac{128(304+\zeta_0^*(-3720+\zeta_0^*(-20744+\zeta_0^*(-32606+\zeta_0^*(-17303+\zeta_0^*(-631+1410\zeta_0^*))))))}{375(1+\zeta_0^*)(2+\zeta_0^*)(1+2\zeta_0^*)^2(1+3\zeta_0^*)(2+3\zeta_0^*)(2+5\zeta_0^*)}, \tag{C.226}$$

$$d_{155} = -\frac{256\left(464+1820\zeta_0^*+1899{\zeta_0^*}^2+465{\zeta_0^*}^3\right)}{75(1+\zeta_0^*)(2+3\zeta_0^*)\left(2+15\zeta_0^*+37{\zeta_0^*}^2+30{\zeta_0^*}^3\right)}, \tag{C.227}$$

$$d_{157} = -\frac{256\left(232+860\zeta_0^*+1037{\zeta_0^*}^2+545{\zeta_0^*}^3\right)}{75(1+\zeta_0^*)(2+3\zeta_0^*)\left(2+15\zeta_0^*+37{\zeta_0^*}^2+30{\zeta_0^*}^3\right)}, \tag{C.228}$$

$$\begin{aligned} d_{159} = & -\frac{1}{375(1+\zeta_0^*)^2(2+\zeta_0^*)(1+2\zeta_0^*)^2(1+3\zeta_0^*)(2+3\zeta_0^*)^2(2+5\zeta_0^*)}(128(-40344+\zeta_0^*(-136620 \\ & +\zeta_0^*(377168+\zeta_0^*(2469376+\zeta_0^*(4538349+\zeta_0^*(3754940+\zeta_0^*(1384417 \\ & +6\zeta_0^*(31334+2385\zeta_0^*))))))))), \end{aligned} \tag{C.229}$$

$$\begin{aligned} d_{160} = & -\frac{1}{375(1+\zeta_0^*)^2(2+\zeta_0^*)(1+2\zeta_0^*)^2(1+3\zeta_0^*)(2+3\zeta_0^*)^2(2+5\zeta_0^*)}(128(-1792+\zeta_0^*(24080 \\ & +\zeta_0^*(232224+\zeta_0^*(741208+\zeta_0^*(1208432+\zeta_0^*(1135005+\zeta_0^*(617756 \\ & +3\zeta_0^*(57569+6660\zeta_0^*))))))))), \end{aligned} \tag{C.230}$$

$$\begin{aligned} d_{161} = & \frac{1}{\left(375(1+\zeta_0^*)^3(2+\zeta_0^*)^2(1+2\zeta_0^*)^2(1+3\zeta_0^*)(2+3\zeta_0^*)^2(2+5\zeta_0^*)\right)}(-(64(-20128+\zeta_0^*(-1120320 \\ & +\zeta_0^*(-6723172+\zeta_0^*(-13480128+\zeta_0^*(-1494931+3\zeta_0^*(11016359+\zeta_0^*(17551484+\zeta_0^*(12257451 \\ & +\zeta_0^*(4266703+729406\zeta_0^*+66090{\zeta_0^*}^2))))))))))), \end{aligned} \tag{C.231}$$

$$\begin{aligned} d_{163} = & -\frac{1}{375(1+\zeta_0^*)^3(2+\zeta_0^*)(1+3\zeta_0^*)(2+5\zeta_0^*)(2+\zeta_0^*(7+6\zeta_0^*))^2}(128\zeta_0^*(-992+\zeta_0^*(33780+\zeta_0^*(296924 \\ & +\zeta_0^*(942983+\zeta_0^*(1482307+\zeta_0^*(1232755+\zeta_0^*(524981+3\zeta_0^*(33919+2535\zeta_0^*)))))))), \end{aligned} \tag{C.232}$$

$$d_{165} = \frac{512(2+\zeta_0^*)\left(34+103\zeta_0^*+80{\zeta_0^*}^2\right)}{75\left(4+40\zeta_0^*+155{\zeta_0^*}^2+290{\zeta_0^*}^3+261{\zeta_0^*}^4+90{\zeta_0^*}^5\right)}, \tag{C.233}$$

$$d_{167} = \frac{128\left(-128+\zeta_0^*\left(31180+\zeta_0^*\left(141408+\zeta_0^*\left(214547+\zeta_0^*\left(128671+28582\zeta_0^*+480{\zeta_0^*}^2\right)\right)\right)\right)\right)}{375(1+\zeta_0^*)(2+\zeta_0^*)(1+2\zeta_0^*)^2(1+3\zeta_0^*)(2+3\zeta_0^*)(2+5\zeta_0^*)}, \tag{C.234}$$

$$d_{169} = \frac{1}{\left(375(1+\zeta_0^*)^2(2+\zeta_0^*)^2(1+2\zeta_0^*)^2(1+3\zeta_0^*)(2+3\zeta_0^*)^2(2+5\zeta_0^*)\right)}(128(-15256+\zeta_0^*(-203324 +\zeta_0^*(-724750+\zeta_0^*(-773901+\zeta_0^*(668109+\zeta_0^*(2101655+\zeta_0^*(1660004 +3\zeta_0^*(175199+\zeta_0^*(21217+2955\zeta_0^*))))))))), \tag{C.235}$$

$$d_{126} = \frac{1}{\left(125(1+\zeta_0^*)^2(2+\zeta_0^*)(1+2\zeta_0^*)^2(1+3\zeta_0^*)^2(2+3\zeta_0^*)^2(1+4\zeta_0^*)(2+5\zeta_0^*)^2(2+7\zeta_0^*)^2(2+9\zeta_0^*)\right)} \times(-(1024(244320+\zeta_0^*(-10176112+\zeta_0^*(-207575472+\zeta_0^*(-1557067912+\zeta_0^*(-6278242058 +\zeta_0^*(-15128542783+\zeta_0^*(-22320639884+\zeta_0^*(-19455123858 +\zeta_0^*(-8617554632+3\zeta_0^*(-217190845+6\zeta_0^*(46295827+11923380\zeta_0^*))))))))))), \tag{C.236}$$

$$d_{130} = \frac{57344(130+\zeta_0^*(573+\zeta_0^*(624+125\zeta_0^*)))}{25(1+\zeta_0^*)(1+2\zeta_0^*)(1+3\zeta_0^*)(2+3\zeta_0^*)(1+4\zeta_0^*)(2+5\zeta_0^*)(2+7\zeta_0^*)(2+9\zeta_0^*)}, \tag{C.237}$$

$$d_{146} = \frac{256(2+\zeta_0^*)}{225(1+2\zeta_0^*)}, \tag{C.238}$$

$$d_{61} = \frac{1}{\left(125(1+\zeta_0^*)^2(2+\zeta_0^*)^2(1+2\zeta_0^*)^2(1+3\zeta_0^*)^2(2+3\zeta_0^*)^2(1+4\zeta_0^*)(2+5\zeta_0^*)^2(2+7\zeta_0^*)\right)}(256(187392 +\zeta_0^*(-5416640+\zeta_0^*(-94110480+\zeta_0^*(-580762912+\zeta_0^*(-1899935680+\zeta_0^*(-3671233648 +\zeta_0^*(-4290335539+\zeta_0^*(-2914686443+\zeta_0^*(-968129347 +3\zeta_0^*(-5830739+26019718\zeta_0^*+5017320{\zeta_0^*}^2))))))))), \tag{C.239}$$

$$d_{62} = \frac{1}{\left(625(1+\zeta_0^*)^3(2+\zeta_0^*)^3(1+2\zeta_0^*)^3(1+3\zeta_0^*)^2(2+3\zeta_0^*)^3(1+4\zeta_0^*)(2+5\zeta_0^*)^2(2+7\zeta_0^*)\right)}(128(-736768 +\zeta_0^*(19872000+\zeta_0^*(-751210368+\zeta_0^*(-17248775936+\zeta_0^*(-144417735136+\zeta_0^*(-675977368128 +\zeta_0^*(-2014178394312+\zeta_0^*(-4032870694848+\zeta_0^*(-5522030243844+\zeta_0^*(-5105735537449 +\zeta_0^*(-2999969940692+\zeta_0^*(-891989172276+\zeta_0^*(77765512498+3\zeta_0^*(57753228559 +18\zeta_0^*(1147102693+40\zeta_0^*(4347131+224070\zeta_0^*))))))))))))))), \tag{C.240}$$

$$d_{64} = -\frac{1024(1670+\zeta_0^*(7187+\zeta_0^*(7761+1610\zeta_0^*)))}{25(1+\zeta_0^*)(1+2\zeta_0^*)(1+3\zeta_0^*)(2+3\zeta_0^*)(1+4\zeta_0^*)(2+5\zeta_0^*)(2+7\zeta_0^*)}, \tag{C.241}$$

$$d_{84} = \frac{1024(1370+\zeta_0^*(5667+\zeta_0^*(6046+1365\zeta_0^*)))}{75(1+\zeta_0^*)(1+2\zeta_0^*)(1+3\zeta_0^*)(2+3\zeta_0^*)(2+5\zeta_0^*)(2+7\zeta_0^*)}, \tag{C.242}$$

$$d_{86} = \frac{1}{\left(375(1+\zeta_0^*)^2(2+\zeta_0^*)^2(1+2\zeta_0^*)^2(1+3\zeta_0^*)(2+3\zeta_0^*)^2(2+5\zeta_0^*)^2(2+7\zeta_0^*)\right)}(-(256(102336 +\zeta_0^*(-2672864+\zeta_0^*(-35502928+\zeta_0^*(-167776816+\zeta_0^*(-413023508+\zeta_0^*(-586273762 +\zeta_0^*(-488177177+\zeta_0^*(-227672909+\zeta_0^*(-50433223+3\zeta_0^*(-663113+200130\zeta_0^*))))))))))), \tag{C.243}$$

$$d_{100} = \frac{256\left(36+130\zeta_0^*+123{\zeta_0^*}^2+26{\zeta_0^*}^3\right)}{75\left(4+28\zeta_0^*+71{\zeta_0^*}^2+77{\zeta_0^*}^3+30{\zeta_0^*}^4\right)}, \tag{C.244}$$

$$
\begin{aligned}
d_{128} \quad = \quad & \frac{1}{\left(625(1+\zeta_0^*)^3(2+\zeta_0^*)^3(1+2\zeta_0^*)^3(1+3\zeta_0^*)^2(2+3\zeta_0^*)^3(1+4\zeta_0^*)(2+5\zeta_0^*)^3(2+7\zeta_0^*)^2(2+9\zeta_0^*)\right)} \\
& \times(-(256(-12015616+\zeta_0^*(401638400+\zeta_0^*(-19751332352+\zeta_0^*(-608306382592+\zeta_0^*(-6937696880128 \\
& +\zeta_0^*(-45181520222208+\zeta_0^*(-192280709730816+\zeta_0^*(-568452807839872+\zeta_0^*(-1201827679817992 \\
& +\zeta_0^*(-1833686364438404+\zeta_0^*(-2000835661447622+\zeta_0^*(-1507237236797145+\zeta_0^*(-709701874306328 \\
& +\zeta_0^*(-133356058233658+3\zeta_0^*(19739720142730+3\zeta_0^*(5362666546451+12\zeta_0^*(127325738758 \\
& +735\zeta_0^*(21115939+642780\zeta_0^*)))))))))))))))))))), \qquad \text{(C.245)}
\end{aligned}
$$

$$
d_{166} \quad = \quad -\frac{256\left(464+1820\zeta_0^*+1899{\zeta_0^*}^2+465{\zeta_0^*}^3\right)}{75(1+\zeta_0^*)(2+3\zeta_0^*)\left(2+15\zeta_0^*+37{\zeta_0^*}^2+30{\zeta_0^*}^3\right)}, \qquad \text{(C.246)}
$$

$$
\begin{aligned}
d_{168} \quad = \quad & -\frac{1}{375(1+\zeta_0^*)^2(2+\zeta_0^*)(1+2\zeta_0^*)^2(1+3\zeta_0^*)(2+3\zeta_0^*)^2(2+5\zeta_0^*)}(256(-592+\zeta_0^*(39080+\zeta_0^*(326524 \\
& +\zeta_0^*(1033558+3\zeta_0^*(549094+\zeta_0^*(471360+\zeta_0^*(213502+\zeta_0^*(46519+4035\zeta_0^*))))))))). \qquad \text{(C.247)}
\end{aligned}
$$